ICRP ref: 4853-0034-6317

Annals of the ICRP

ICRP PUBLICATION 1XX

Occupational Intakes of Radionuclides: Part 5

Editor-in-Chief
C.H. CLEMENT

Associate Editor
H. FUJITA

Authors on behalf of ICRP
F. Paquet, R.W. Leggett, E. Blanchardon, M.R. Bailey, D. Gregoratto,T. Smith, G. Ratia, E. Davesne, V. Berkovski, J.D. Harrison

PUBLISHED FOR

The International Commission on Radiological Protection

by

[Sage logo]

Please cite this issue as 'ICRP, 202Y. Occupational Intakes of Radionuclides: Part 5. ICRP Publication 1XX, Ann. ICRP XX (0).'

CONTENTS

247
248

OCCUPATIONAL INTAKES OF RADIONUCLIDES: PART 5

ICRP Publication 1XX

Approved by the Commission in Month Year

Abstract– This publication is the fifth and the last in a series dedicated to occupational intakes of radionuclides, that replaces the *Publication 30* series and *Publications 54*, *68* and *78* (ICRP, 1979a,b, 1980, 1981, 1988, 1989, 1997). The first publication of this new series (OIR Part 1) describes the assessment of internal occupational exposure to radionuclides, biokinetic and dosimetric models, methods of individual and workplace monitoring, and general aspects of retrospective dose assessment. The following publications of the series (Parts 2 to 5) provide data on individual elements and their radioisotopes, including information on chemical forms encountered in the workplace; a list of principal radioisotopes and their physical half-lives and decay modes; the parameter values of the reference biokinetic model; and data on monitoring techniques for the radioisotopes most commonly encountered in workplaces. For most of the elements, reviews of data on inhalation, ingestion and systemic biokinetics are also provided.

Dosimetric data provided in the printed publications of the series include tables of committed effective dose per intake (Sv per Bq intake) for inhalation and ingestion, tables of committed effective dose per content (Sv per Bq measurement) for inhalation, and graphs of retention and excretion data per Bq intake for inhalation. These data are provided for all absorption types and for the most common isotope(s) of each element section.

The electronic data that accompanies this series of publications contains a comprehensive set of committed effective and equivalent dose coefficients, committed effective dose per content functions, and reference bioassay functions. Data are provided for inhalation, ingestion and for direct input to the blood.

This publication provides the above data for the following elements: beryllium, fluorine, sodium, magnesium, aluminium, silicon, chlorine, potassium, scandium, titanium, vanadium, chromium, manganese, nickel, copper, gallium, germanium, arsenic, selenium, bromine, rubidium, rhodium, palladium, silver, cadmium, indium, tin, hafnium, tantalum, tungsten, rhenium, osmium, platinium, gold, mercury, thallium, astatine and francium. Additional dosimetric data for exposure from submersion in a cloud of gas are given in the annex for the noble gases neon, argon, krypton and xenon.

Keywords: Occupational exposure; Internal Dose Assessment; Biokinetic and Dosimetric models; Bioassays interpretation

MAIN POINTS

- **This publication is the fifth in a series of documents (OIR) replacing the *Publication 30* series and *Publications 54*, *68* and *78*. The OIR series provides dose coefficients and bioassay functions for radionuclides encountered in the workplace.**

- **This publication considers radioisotopes of the following elements: beryllium (Be), fluorine (F), sodium (Na), magnesium (Mg), aluminium (Al), silicon (Si), chlorine (Cl), potassium (K), scandium (Sc), titanium (Ti), vanadium (V), chromium (Cr), manganese (Mn), nickel (Ni), copper (Cu), gallium (Ga), germanium (Ge), arsenic (As), selenium (Se), bromine (Br), rubidium (Rb), rhodium (Rh), palladium (Pd), silver (Ag), cadmium (Cd), indium (In), tin (Sn), hafnium (Hf), tantalum (Ta), tungsten (W), rhenium (Re), osmium (Os), platinium (Pt), gold (Au), mercury (Hg), thallium (Tl), astatine (At) and francium (Fr).**

- **Sections on individual elements and their radioisotopes include information on (when available): a list of principal radioisotopes and their physical half-lives and decay modes; parameter values for reference biokinetic models; and data on monitoring techniques for the radioisotopes most commonly encountered in workplaces. Reviews of data on ingestion and systemic biokinetics are provided for all elements, but for inhalation only for some that were considered important for radiological protection.**

- **Dosimetric data provided in the printed publications of the series include tables of committed effective dose per intake (Sv per Bq intake) for inhalation and ingestion, tables of committed effective dose per content (Sv per Bq measurement) for inhalation, and graphs of retention and excretion per Bq intake for inhalation. These data are provided for all absorption types and for the most common isotope(s) of each element.**

- **The electronic viewer accompanied with this series of publications contains a comprehensive set of committed effective and equivalent dose coefficients, committed effective dose per content functions, and reference bioassay functions. Data are provided for inhalation, ingestion and for direct input to blood.**

- **In addition to these data given for radionuclide intakes by ingestion or by inhalation, dose coefficients for exposure by submersion in a cloud of noble gases are given in the annex.**

- **An analysis of the data shows that, for inhalation of reference forms of radionuclides (aerosols of 5µm, Type F, M or S) and for ingestion, the vast majority of new dose coefficients are lower (generally within a factor of 2 to 3) than those published in the ICRP *Publication 30* Series (ICRP, 1979a, 1980a, 1981, 1988b) and revised in ICRP *Publication 68* (1994). For ingestion of ^{59}Ni as metal and of ^{107}Pd the dose coefficient is even 20 and 50 times lower, respectively, than in *Publication 68*. In some very rare cases, (inhalation of ^{10}Be Type S; inhalation of ^{32}Si Type S; inhalation of ^{44}Ti Types F, M and S; inhalation of ^{68}Ge, Type F; ingestion of ^{68}Ge) the coefficients have increased by a factor 1.5 to 5, because of the revision of the biokinetic models and a better description of radionuclide retention and distribution in tissues.**

1. INTRODUCTION

(1) This publication is Part 5 of a series which provides revised dose coefficients for occupational intakes of radionuclides (OIR) by inhalation and ingestion. It also presents radionuclide-specific information for the design and planning of monitoring programmes and retrospective assessment of occupational internal doses.

(2) This OIR series replaces the *Publication 30* series (ICRP, 1979a,b, 1980, 1981, 1988), and *Publications 54*, *68* and *78* (ICRP, 1989, 1994a, 1997). The revised dose coefficients, dose per content values and reference bioassay functions have been calculated using the *Publication 100* Human Alimentary Tract Model (HATM) (ICRP, 2006) and a revision of the *Publication 66* Human Respiratory Tract Model (HRTM) (ICRP, 1994b) which takes account of more recent data. The revisions made to the HRTM are described in OIR Part 1(ICRP, 2015). Revisions have also been made to many models for the systemic biokinetics of radionuclides, making them more physiologically realistic representations of uptake and retention in organs and tissues and of excretion.

(3) OIR Parts 2 – 4 gave data for those elements for which intakes of radionuclides were considered to be of most importance for radiological protection of workers. In Part 4 all lanthanides were included because of the similarity in behaviour of the elements in that series. In Part 5 data are given for the remaining elements that were considered in the *Publication 30* Series. Data for noble gases are given in the annex A for exposure by submersion.

1.1. Methodology used in this publication series

(4) The general methodology for producing the biokinetic and dosimetric models is given in OIR Part 1 (ICRP, 2015). For each element, detailed reviews of the literature were carried out to identify experimental studies and human contamination cases that provide information to quantify absorption to blood from the respiratory and alimentary tracts, and the biokinetics following systemic uptake. These reviews, and the analyses of the data obtained from them, are summarised in each element section.

(5) In the case of inhalation, reviews were not carried out in Part 5 for most elements: default parameter values for Type F, M and S particulate materials were usually adopted. Reviews were conducted for seven elements (Al, Ni, Se, Ag, Cd, Hg, Au), for which it was considered there was probably sufficient evidence to support the provision of guidance to augment the use of default parameter values. For these elements, chemical forms are usually addressed in order of decreasing solubility in the lungs. Where information was available, HRTM absorption parameter values were derived from experimental data from both *in vivo* and *in vitro* studies. For *in vitro* studies, estimation of the dissolution parameter values (rapidly dissolved fraction, f_r, rapid and slow dissolution rates, s_r and s_s) was usually straightforward. For *in vivo* studies, however, simulation modelling was often needed to derive them from the data available: typically retention in organs and excretion in urine and faeces: for further information see Supporting Guidance 3 (ICRP, 2002b).

(6) In some recent publications, the authors derived HRTM parameter values: if so they are reported. In most cases, parameter values were derived by the ICRP Task Group (INDOS or IDC) members and their colleagues. This is indicated in the text by wording such as ‘analysis carried out here...’: the first such occurrence for each element is given as ‘analysis carried out here (i.e. by the Task Group)...’.

(7) Material-specific rates of absorption have been adopted (and dose coefficients and bioassay functions provided for them in the accompanying electronic annex) for a limited number of selected materials i.e. those for which:

- There are *in vivo* data from which specific parameter values can be derived;
- Results from different studies are consistent;
- It was considered that occupational exposure to the material is likely;
- The specific parameter values are sufficiently different from default Type F, M or S parameter values to justify providing additional specific dose coefficients and bioassay functions.

In Part 5, material-specific rates of absorption are adopted only for one material: elemental mercury vapour.

(8) Other materials were assigned to default HRTM absorption types, using the criteria described in *Publication 71* (ICRP, 1995b) and Supporting Guidance 3 (ICRP, 2002b) for making such assignments using experimental data. Type M is assumed for particulate forms of most elements 'by default' (i.e. in the absence of such information). A material is assigned to Type F if the amount absorbed into blood by 30 d after intake is greater than the amount absorbed over the same period from a hypothetical material with a constant absorption rate corresponding to a half-time of 10 d, under identical conditions. Similarly, a material is assigned to Type S if the amount absorbed into blood by 180 d is less than the amount absorbed over the same period from a hypothetical material with a constant rate of absorption to blood of 0.001 d^{-1} (extrapolation was used in some cases, as indicated in the text). For studies where it was possible to apply the criteria, a statement is made to the effect that results 'are consistent with' (or 'give') assignment to Type F (M or S). For studies where the results point towards a particular Type, but there was insufficient information to apply the criteria, a statement is made to the effect that the results 'indicate' or 'suggest' Type F (M or S) behaviour.

(9) Assignments are not made here on the basis of the known solubility of chemical forms in aqueous media, because this is not considered to be a reliable guide to absorption from the respiratory tract [Section E.2.2.1 in *Publication 66* (1994b)]. If it is considered appropriate in a particular situation, it would need to be carried out with caution. In practice, it might well be possible to assign a radionuclide, to which workers have been exposed, to an absorption type without knowing its chemical form (e.g. from environmental and/or bioassay measurements). These could include *in vitro* dissolution tests on air filters or swabs; *in vivo* measurements (chest compared to whole body); or excretion measurements (urine compared to faecal). Nevertheless, for each element, a default absorption type is recommended for use in the absence of information on which the exposure material can be assigned to Type F, M or S. For most elements Type M is recommended by default including all of those in Part 5 except the halogens (Type F) and aluminium (Type S).

(10) For soluble (Type F) forms of each element, estimates are made of the overall rate of absorption from the respiratory tract to blood, where information is available. In general this results from dissolution of the deposited material, and also transfer through lining fluids and epithelium into blood. Nevertheless, for simplicity this is usually represented by the rapid dissolution rate, s_r, (see Section 3.2.3 in OIR Part 1). Because of the wide range of the estimated values of s_r, element-specific values are adopted in this series of documents for those elements for which estimates could be made, and which were markedly different from the default value of 30 d^{-1}: only Ag and Ni in Part 5. Justification of the value chosen for an element is given in the subsection headed: 'Rapid dissolution rate for *element*'.

(11) For some elements, a significant fraction of the dissolved material is absorbed slowly. In some cases this can be represented by formation of particulate material (which is subject to clearance by particle transport). In others, some dissolved material appears to be attached to lung structural components, and removed only by absorption to blood. To represent the latter type of time-dependent uptake, it is assumed that a fraction, f_b, of the dissolved material is retained in the 'bound' state, from which it goes into blood at a rate s_b. Evidence for retention

in the bound state, rather than by transformation into particulate material may be in one or more forms (e.g. systemic uptake rather than faecal clearance of the retained material; slower clearance than for insoluble particles deposited in the same region of the respiratory tract; or autoradiography showing diffuse rather than focal retention of activity).

(12) The bound state was included in the HRTM mainly to take account of slow clearance of dissolved materials from the alveolar-interstitial region. Applying the same bound state parameter values in all regions could lead, unintentionally, to high calculated doses to the bronchial (BB) and bronchiolar (bb) regions. Hence in this series of documents it is assumed that for those elements for which a bound state is adopted ($f_b > 0$), it is applied in the alveolar-interstitial region by default, and in the conducting airways (ET_2, BB and bb regions) only if there is supporting experimental evidence. Justification of the values chosen for an element is given in the subsection headed: 'Extent of binding of *element* to the respiratory tract'. In Part 5, a bound state is adopted only for Hg.

1.2. Data presented in this publication series

(13) Data presented in this publication series are in a standard format for each element and its radioisotopes. Each element section provides information on principal radioisotopes, their physical half-lives and decay modes; reviews of data on inhalation (for some elements), ingestion and systemic biokinetics; the structure and parameter values for the systemic biokinetic model; monitoring techniques and detection limits typically achieved in a practical monitoring programme. The detection limits presented in this publication were derived from a compilation of data from laboratories in Europe, Asia, North America and South America that perform routine monitoring of the specified radionuclide. The sensitivity of the measurements depends on the technique, the counting time and other factors. For example *in vivo* detection limits depend on the detection system (type, quality and number of detectors), counting geometry, and shielding and design of the installation. Those details are outside the scope of this publication.

(14) Dosimetric data are provided in the printed publications of the series and in electronic annexes. The methodology for dose calculation is described in OIR Part 1 (ICRP, 2015). Due to the amount of data to be provided, the printed publications provide tables and graphs restricted to tables of committed effective dose per intake (Sv Bq^{-1}) for inhalation and ingestion; tables of committed effective dose per content (Sv Bq^{-1}) for inhalation, and graphs of retention and excretion data per Bq intake for inhalation.

(15) Data in the printed publications are provided for all absorption types of the most common isotope(s) and for an Activity Median Aerodynamic Diameter (AMAD) of 5 µm. In cases for which sufficient information is available (principally for actinide elements, and gas and vapour forms of others), lung absorption is specified for different chemical forms and dose coefficients and bioassay data are calculated accordingly. The dose coefficients and dose per content values presented in this publication series are given for a Reference Worker at light work (ICRP, 2015).

(16) The electronic annex accompanied with this series of publications contains a comprehensive set of committed effective and equivalent dose coefficients, dose per content functions, and reference bioassay functions for almost all radionuclides included in *Publication 107* (ICRP, 2008) that have half-lives equal to or greater than 10 min, and for other selected radionuclides. Data are provided for a range of physico-chemical forms and for aerosols with median sizes ranging from an Activity Median Thermodynamic Diameter (AMTD) of 0.001 µm to an AMAD of 20 µm. Data for ingestion and injection (i.e. direct entry to the blood) are

provided to allow the interpretation of bioassay data for cases of inadvertent ingestion (e.g. of material on contaminated skin) or rapid absorption through intact or damaged skin (injection).

(17) The dose coefficients and other radionuclide-specific data are provided as a set of data files which may be accessed by the user directly or by using the accompanying Data Viewer. The Data Viewer permits rapid navigation of the dataset and visualisation of the data in tabulated and graphical formats, such as graphs of the time series of dose per content coefficients or predicted activity content per unit dose (Bq Sv^{-1}) as a function of time after intake. Graphical presentations of decay chains and nuclear decay data from *Publication 107* (ICRP, 2008) are also included.

(18) Part 2 (ICRP, 2016) provided the data above on: hydrogen (H), carbon (C), phosphorus (P), sulphur (S), calcium (Ca), iron (Fe), cobalt (Co), zinc (Zn), strontium (Sr), yttrium (Y), zirconium (Zr), niobium (Nb), molybdenum (Mo) and technetium (Tc).

(19) Part 3 (ICRP, 2017) provided the data above on the following elements: ruthenium (Ru), antimony (Sb), tellurium (Te), iodine (I), caesium (Cs), barium (Ba), iridium (Ir), lead (Pb), bismuth (Bi), polonium (Po), radon (Rn), radium (Ra), thorium (Th) and uranium (U).

(20) Part 4 (ICRP, 2019) provided data on the actinides and lanthanide series (please note that Th and U data are given in Part 3). The elements included are: lanthanum (La), cerium (Ce), praseodymium (Pr), neodymium (Nd), promethium (Pm), samarium (Sm), europium (Eu), gadolinium (Gd), terbium (Tb), dysprosium (Dy), holmium (Ho), erbium (Er), thulium (Tm), ytterbium (Yb), lutetium (Lu), actinium (Ac), protactinium (Pa), neptunium (Np), plutonium (Pu), americium (Am), curium (Cm), berkelium (Bk), californium (Cf), einsteinium (Es) and fermium (Fm).

(21) Due to the similarities between the elements in a series, generic biokinetic models are provided for the lanthanides and the actinides. Specific individual data are given, when relevant, in the element sections.

(22) Part 5 provides data for the remaining elements.

2. BERYLLIUM (Z = 4)

2.1. Isotopes

Table 2.1. Isotopes of beryllium addressed in this publication.

Isotope	Physical half-life	Decay mode
^{7}Be*	53.22 d	EC
^{10}Be	1.51×10^{6} y	B-

EC, electron-capture decay; B-, beta-minus decay
*Dose coefficients and bioassay data for this radionuclide are given in the printed copy of this publication.

2.2. Routes of Intake

2.2.1. Inhalation

(23) For beryllium, default parameter values were adopted on absorption to blood from the respiratory tract (ICRP, 2015). Absorption parameter values and types, and associated f_A values for particulate forms of beryllium are given in Table 2.2.

Table 2.2. Absorption parameter values for inhaled and ingested beryllium.

	Absorption parameter values*			
Inhaled particulate materials	f_r	s_r (d^{-1})	s_s (d^{-1})	Absorption from the alimentary tract, f_A
Default parameter values†				
Absorption type				
F	1	30	–	0.005
M‡	0.2	3	0.005	0.001
S	0.01	3	1×10^{-4}	5×10^{-5}
Ingested materials§				
All forms	–	–	–	0.005

*It is assumed that the bound state can be neglected for beryllium (i.e. $f_b = 0$). The values of s_r for Type F, M and S forms of beryllium (30, 3 and 3 d^{-1} respectively) are the general default values.
†For inhaled material deposited in the respiratory tract and subsequently cleared by particle transport to the alimentary tract, the default f_A values for inhaled materials are applied [i.e. the product of f_r for the absorption type and the f_A value for ingested soluble forms of beryllium (0.005)].
‡Default Type M is recommended for use in the absence of specific information on which the exposure material can be assigned to an absorption type (e.g. if the form is unknown, or if the form is known but there is no information available on the absorption of that form from the respiratory tract). For guidance on the use of specific information, see Section 1.1.
§Activity transferred from systemic compartments into segments of the alimentary tract is assumed to be subject to reabsorption to blood. The default absorption fraction f_A for the secreted activity is the highest value for any form of the radionuclide ($f_A = 0.005$).

2.2.2. Ingestion

(24) Beryllium absorption studies were reviewed by the World Health Organisation (WHO, 1990) and by the United States Agency for Toxic Substances and Disease Registry (ATSDR, 1988, 2002). The mean fractional absorption of beryllium, administered as the chloride, from the gastrointestinal tract of four different mammalian species has been estimated as 0.006 (Furchner et al., 1973). In experiments on rats, Bugryshev et al. (1974) have estimated the

fractional gastrointestinal absorption of the element, again administered as the chloride, to be between 0.0014 and 0.0021 and a similar value is indicated from experiments on dairy cows (Mullen et al., 1972).

(25) The fractional absorption of beryllium, administered as beryllium sulphate, from the gastrointestinal tract of rats is also typically 0.01 or less, with oral absorption maybe reduced by the formation of beryllium phosphate precipitates in the alkaline environment of the intestine (Reeves, 1965). Bugryshev et al. (1984), as cited by ATSDR (1988), found that beryllium oxide was absorbed more readily in rats than was the hydroxide, and beryllium fluoride was absorbed more readily than were chloride, sulphate, nitrate and hydroxide. Watanabe et al. (1985), as cited by ATSDR (1988), observed better intestinal absorption of soluble beryllium sulphate than insoluble beryllium oxide and beryllium metal. After intragastric administration of soluble beryllium chloride and ^{7}Be-labelled carbon particles to mice, LeFevre and Joel (1986) found less than 0.1% of beryllium in tissues other than intestinal.

(26) In *Publications 30* and *68* (ICRP, 1981, 1994a) a fractional absorption of 0.005 was adopted. The same value of $f_A = 0.005$ is used in this publication for all forms of beryllium.

2.2.3. Systemic distribution, retention and excretion of beryllium

2.2.3.1 Biokinetic data

(27) Because of its light weight, strength, electrical conductivity, high melting point, and corrosion resistance, beryllium (Be) is used in many industries (Kolanz, 2001). Its small neutron cross-section makes it useful in the production of nuclear weapons and sealed neutron sources (Taylor et al., 2002). Beryllium is also used in plasma-facing components in experimental and future commercial fusion reactors with radiation safety concerns due to neutron-activated beryllium and tritiated beryllium (Scaffidi-Argentina et al., 2000).

(28) Prolonged inhalation of beryllium can result in the frequently fatal lung disease berylliosis. Beryllium is also classified as a carcinogen (Taylor et al., 2002; Kreiss et al., 2007). Acute inhalation of high levels of beryllium can result in a non-specific, potentially lethal chemical pneumonitis within hours or days and sometimes in specific lung damage appearing years later (Stiefel et al., 1980).

(29) Zhu et al. (2010) measured concentrations of beryllium in 17 tissues obtained from autopsies of up to 68 Chinese men from four areas of China. The subjects were considered healthy until the time of sudden accidental death. The beryllium concentration was also measured in blood of living subjects from the same areas. Based on median beryllium concentrations in tissues and reference tissue masses, about 36% of systemic beryllium (defined here as total-body beryllium minus beryllium in the lungs) was contained in bone, 30% in skeletal muscle, 17% in fat, 8% in blood, 3% in skin, 1.5% in liver, and 0.05% in kidneys. As a central estimate, the mass of beryllium in the total-body was ~20 μg, including ~1 μg in the lungs.

(30) Studies on rodents indicate that the systemic distribution of beryllium depends on the dosage, chemical form, and route of entry (Vacher and Stoner, 1968). The fractions of systemic beryllium retained in bone and excreted in urine tended to increase with decreasing mass of administered Be. Beryllium accumulated to a large extent in the liver when administered intravenously as sulfate or chloride but not when administered intravenously as citrate (Van Cleave and Kaylor, 1953). Following intratracheal installation, the skeleton was the main repository for all forms of administered beryllium (Van Cleave and Kaylor, 1955). Following oral intake of beryllium sulphate by rats, the skeleton contained >75% of the systemic content (Reeves, 1965).

(31) Scott et al. (1950) examined the effect of added carrier (beryllium sulphate) on the distribution and excretion of intravenously administered ^{7}Be in rabbits and rats. In all cases, the preponderance of excretion of ^{7}Be over the 7-d observation period was in urine and occurred during the first 24 h. The cumulative urinary to faecal excretion ratio over 7 d was 2.1 and 6.8, respectively, in rats injected with ^{7}Be with and without carrier, respectively, and 11 and 14 in rabbits injected with ^{7}Be with and without carrier, respectively. Activity was removed from blood more rapidly in the animals injected with ^{7}Be without carrier than in animals injected with ^{7}Be with carrier. At 7 d, the animals injected with ^{7}Be without carrier showed higher uptake by the skeleton and greater loss in urine than animals injected with ^{7}Be with carrier. The most pronounced effect of the added carrier was increased accumulation of activity in the liver.

(32) Vacher and Stoner (1968) studied the disappearance of beryllium from blood in rats following its injection as carrier-free ^{7}Be or beryllium sulphate ($BeSO_4$) labelled with ^{7}Be. Carrier-free ^{7}Be cleared rapidly from blood, with only a few percent retained after 2 h. Beryllium cleared much more slowly from blood when injected as $BeSO_4$ because only a small portion of the injected material remained in diffusible form. The residence time in blood increased with the mass of injected $BeSO_4$.

(33) Furchner et al. (1973) compared the biokinetics of ^{7}Be ($T_{1/2}$ = 53.2 d) in mice, rats, monkeys, and dogs after oral or parenteral administration, over observation periods up to 380 d. Cumulative urinary plus faecal excretion of ^{7}Be measured over the first week (6 days for dogs and monkeys) was about 51% of the administered amount for mice, 45% for rats, 55% for dogs, and 29% for monkeys. Urinary to faecal excretion ratios were 2.9 for mice, 9.7 for rats, 1.7 for monkeys, and 10.2 for dogs. For each of the four animal types, total-body retention following intravenous injection could be described as a sum of three exponential terms. The long-term component of retention represented about 40% of the injected amount for dogs, 46% for mice, 50% for rats, and 59% for monkeys. Assuming a physical half-life of 52 d for ^{7}Be, the investigators derived biological half-times of 1210 d for mice, 890 d for rats, 1270 d for dogs, and 1770 d for monkeys. The more recently estimated half-time of 53.22 d for ^{7}Be (ICRP, 2008) would yield higher estimated biological half-times, up to ~3900 for monkeys, due to the small difference between the effective long-term half-time in the animals and the physical half-life of ^{7}Be. The systemic distribution of ^{7}Be was determined for rats at 0.25-71 d post intraperitoneal injection. Bone was the dominant repository at all measurement times, containing about 64% of the retained activity at 1 d, 81% at 10 d, and 93% at 71 d. The liver contained about 8% of retained ^{7}Be at 1 d, 3% at 10 d, and 0.7% at 71 d. The kidneys contained about 6% at 1 d, 1% at 10 d, and 0.6% at 71 d.

(34) Finch et al. (1990) investigated the behaviour of inhaled ^{7}Be in dogs after inhalation of ^{7}BeO particles calcined at either 500 °C or 1000 °C. Faecal excretion was the dominant mode of excretion at early times after exposure, but urinary excretion dominated at later times. The distribution of activity in the body was determined at 8, 32, 64, and 180 d post exposure. Lung retention at 180 d was much higher for beryllium oxide (BeO) calcined at 1000 °C (62% of ILB) than for BeO calcined at 500 °C (14% of ILB). Most of the activity cleared from the lungs but not excreted was contained in the lymph nodes, skeleton, liver, and blood. On average, the skeleton contained about 8 times as much activity as the liver.

2.2.3.2. Biokinetic model for systemic beryllium

(35) The structure of the biokinetic model for systemic beryllium applied in this publication is shown in Fig. 2.1. Transfer coefficients are listed in Table 2.3. The transfer coefficients describing the short- and intermediate-term kinetics of beryllium were selected to yield reasonable reproductions of the distribution, retention, and excretion of beryllium observed

over the first ~1 y in laboratory animals administered low masses of soluble forms of Be. The transfer coefficients describing the long-term behaviour were selected to approximate the long-term distribution of beryllium indicated by human autopsy data. The return of beryllium from compartments with extended retention to a second blood compartment with relatively slow loss was a convenient way to model both the rapid blood clearance at early times after administration of beryllium to animals and the relatively large estimated portion of total-body beryllium in blood (8%) in environmentally exposed persons.

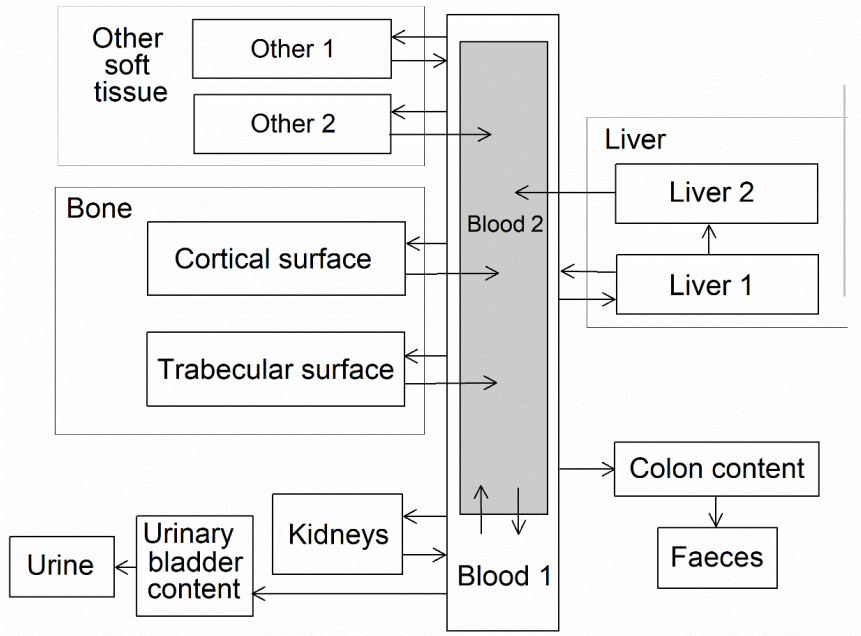

Fig. 2.1. Structure of the biokinetic model for systemic beryllium.

Table 2.3. Transfer coefficients in the biokinetic model for systemic beryllium.

From	To	Transfer coefficient (d^{-1})
Blood 1	Urinary bladder content	20
Blood 1	Right colon content	5.0
Blood 1	Trabecular bone surface	15
Blood 1	Cortical bone surface	15
Blood 1	Liver 1	5.0
Blood 1	Kidneys	3.0
Blood 1	Other 1	30
Blood 1	Other 2	5.0
Blood 1	Blood 2	2.0
Blood 2	Blood 1	0.014
Trabecular bone surface	Blood 2	0.0025
Cortical bone surface	Blood 2	0.0025
Liver 1	Blood 1	0.2
Liver 1	Liver 2	0.05
Liver 2	Blood 2	0.0019
Kidneys	Blood 1	0.15
Other 1	Blood 1	0.07
Other 2	Blood 2	0.00025

2.3. Individual monitoring

2.3.1. ^{7}Be

(36) Measurements of ^{7}Be may be performed by in vivo whole-body measurement technique and by gamma measurement in urine.

Table 2.4. Monitoring techniques for ^{7}Be.

Isotope	Monitoring Technique	Method of Measurement	Typical Detection Limit
^{7}Be	Urine Bioassay	γ-ray spectrometry[a]	9 Bq L^{-1}
^{7}Be	Whole-body monitoring	γ-ray spectrometry[a, b]	200Bq

[a] Measurement system comprised of Germanium Detectors
[b] Counting time of 20 minutes

2.4. Dosimetric data for beryllium

Table 2.5 Committed effective dose coefficients (Sv Bq^{-1}) for the inhalation or ingestion of ^{7}Be and ^{10}Be compounds.

Inhaled particulate materials (5 µm AMAD aerosols)	Effective dose coefficients (Sv Bq^{-1})	
	^{7}Be	^{10}Be
Type F, — NB: Type F should not be assumed without evidence	5.7E-11	1.6E-08
Type M, default	4.3E-11	5.9E-09
Type S	5.3E-11	4.7E-08
Ingested materials		
All compounds	2.1E-11	4.4E-10

AMAD, activity median aerodynamic diameter

Table 2.6 Dose per activity content of ^{7}Be in daily excretion of urine (Sv Bq^{-1}); 5µm activity median aerodynamic diameter aerosols inhaled by a reference worker at light work.

Time after intake (d)	Type F Urine	Type M Urine	Type S Urine
1	1.3E-09	1.3E-08	3.2E-07
2	1.6E-08	1.1E-07	2.9E-06
3	3.8E-08	2.6E-07	7.4E-06
4	4.8E-08	3.0E-07	8.9E-06
5	5.4E-08	3.2E-07	9.6E-06
6	5.9E-08	3.4E-07	1.0E-05
7	6.4E-08	3.6E-07	1.1E-05
8	6.9E-08	3.8E-07	1.2E-05
9	7.4E-08	4.0E-07	1.2E-05
10	8.0E-08	4.2E-07	1.3E-05
15	1.1E-07	5.1E-07	1.6E-05

30	2.6E-07	8.0E-07	2.8E-05
45	5.5E-07	1.2E-06	4.2E-05
60	1.0E-06	1.6E-06	5.7E-05
90	2.3E-06	2.9E-06	9.3E-05
180	8.4E-06	1.4E-05	3.2E-04
365	1.1E-04	2.5E-04	3.9E-03

642 Table 2.7 Dose per activity content of ^{10}Be in total body (Sv Bq^{-1}); 5μm activity median aerodynamic
643 diameter aerosols inhaled by a reference worker at light work.

Time after intake (d)	Type F Total body	Type M Total body	Type S Total body
1	2.7E-08	9.7E-09	7.6E-08
2	4.3E-08	1.8E-08	1.4E-07
3	6.9E-08	3.9E-08	3.0E-07
4	8.8E-08	6.9E-08	5.4E-07
5	9.7E-08	9.0E-08	7.1E-07
6	1.0E-07	9.8E-08	7.8E-07
7	1.0E-07	1.0E-07	8.1E-07
8	1.0E-07	1.0E-07	8.2E-07
9	1.0E-07	1.0E-07	8.3E-07
10	1.0E-07	1.1E-07	8.4E-07
15	1.1E-07	1.1E-07	8.7E-07
30	1.1E-07	1.2E-07	9.1E-07
45	1.2E-07	1.2E-07	9.3E-07
60	1.2E-07	1.3E-07	9.6E-07
90	1.2E-07	1.4E-07	1.0E-06
180	1.3E-07	1.7E-07	1.2E-06
365	1.5E-07	2.1E-07	1.5E-06

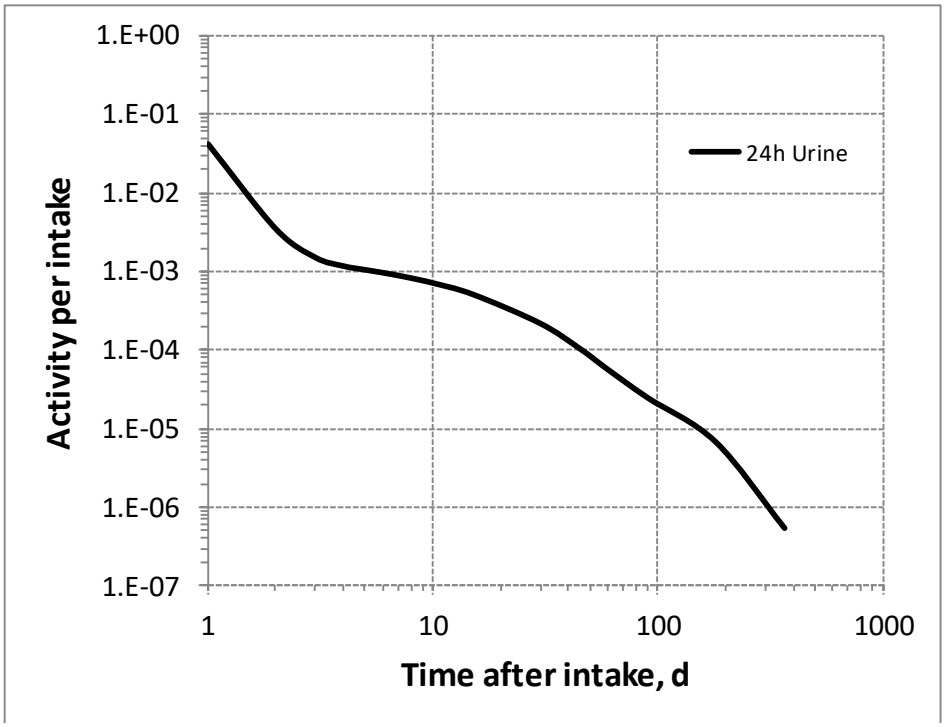

644

645 Fig. 2.2. Daily excretion of ^{7}Be following inhalation of 1 Bq Type F.

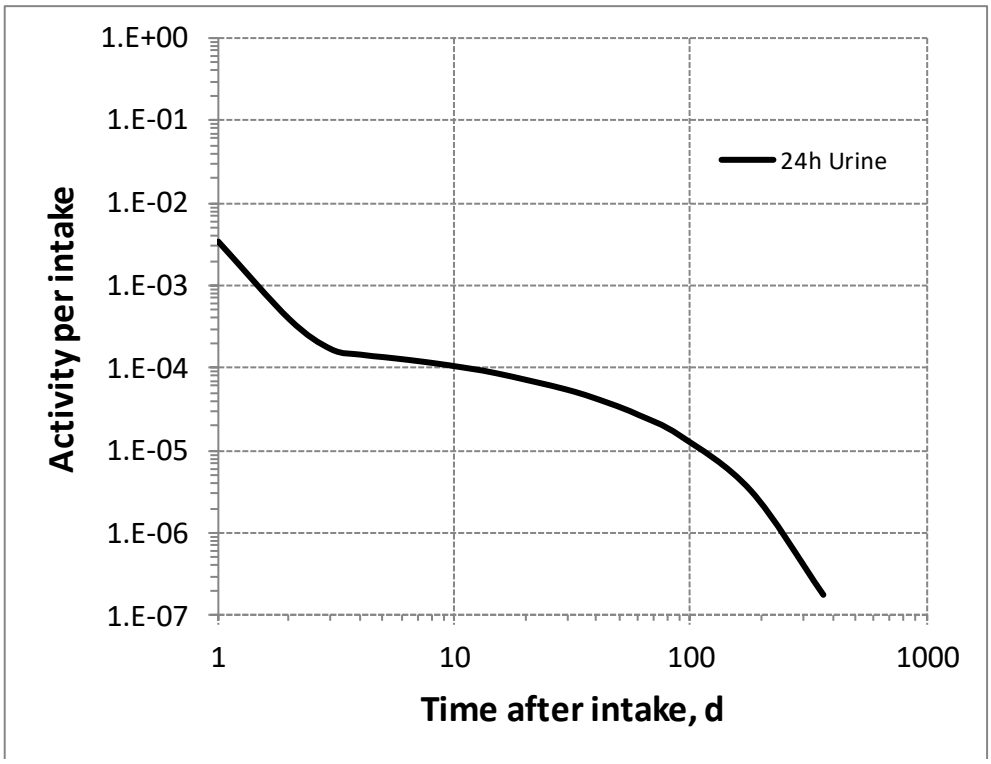

646

647 Fig. 2.3. Daily excretion of ^{7}Be following inhalation of 1 Bq Type M.

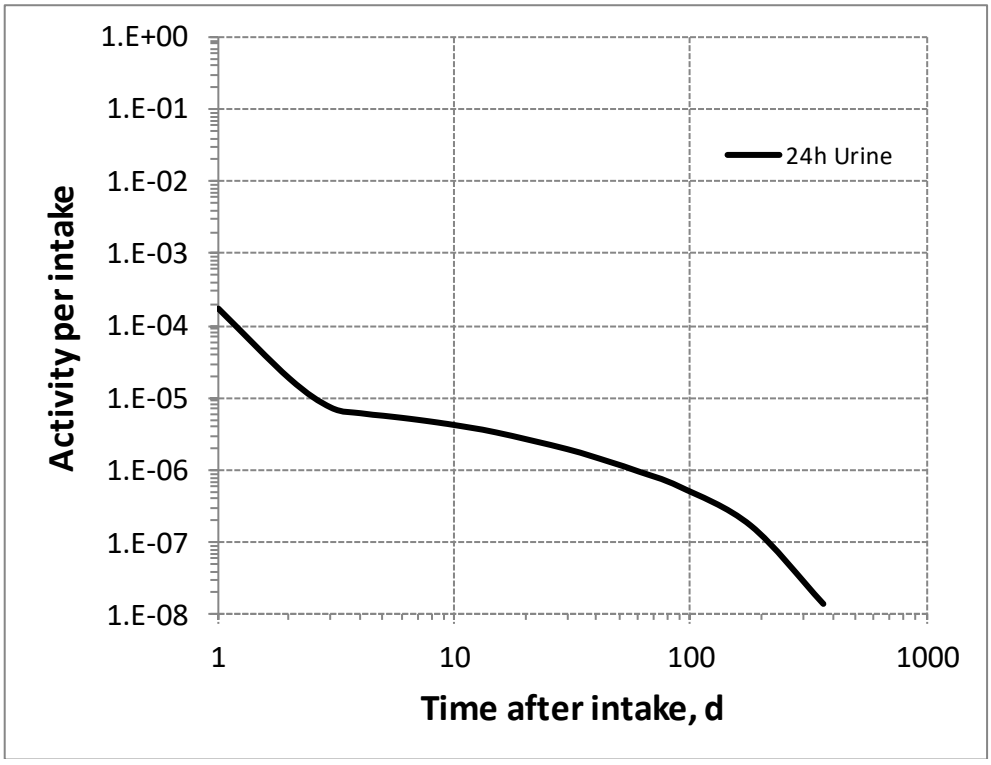

648

649 Fig. 2.4. Daily excretion of ^{7}Be following inhalation of 1 Bq Type S.

650

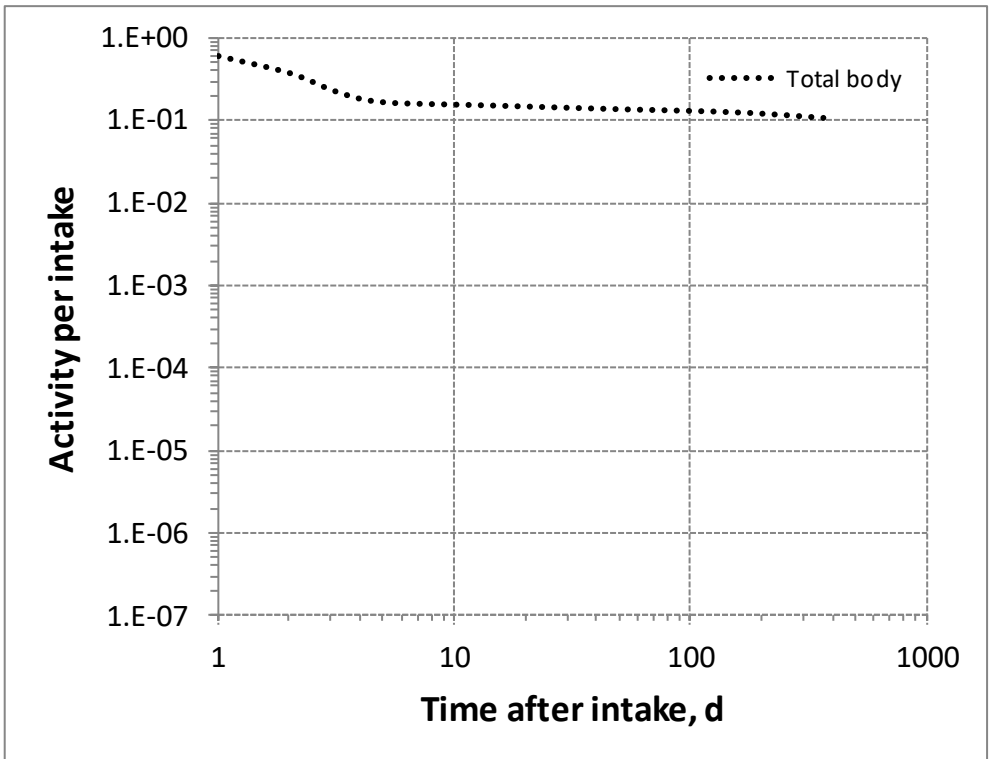

651

652 Fig. 2.5. Daily excretion of ^{10}Be following inhalation of 1 Bq Type F.

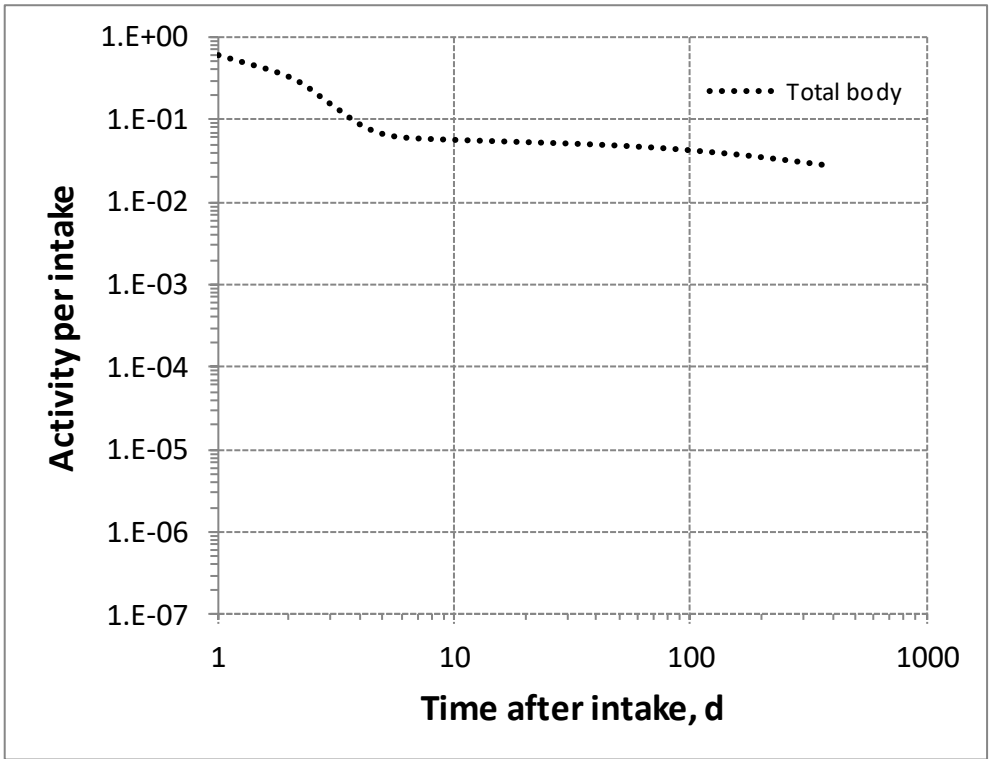

653

654 Fig. 2.6. Daily excretion of ^{10}Be following inhalation of 1 Bq Type M.

655

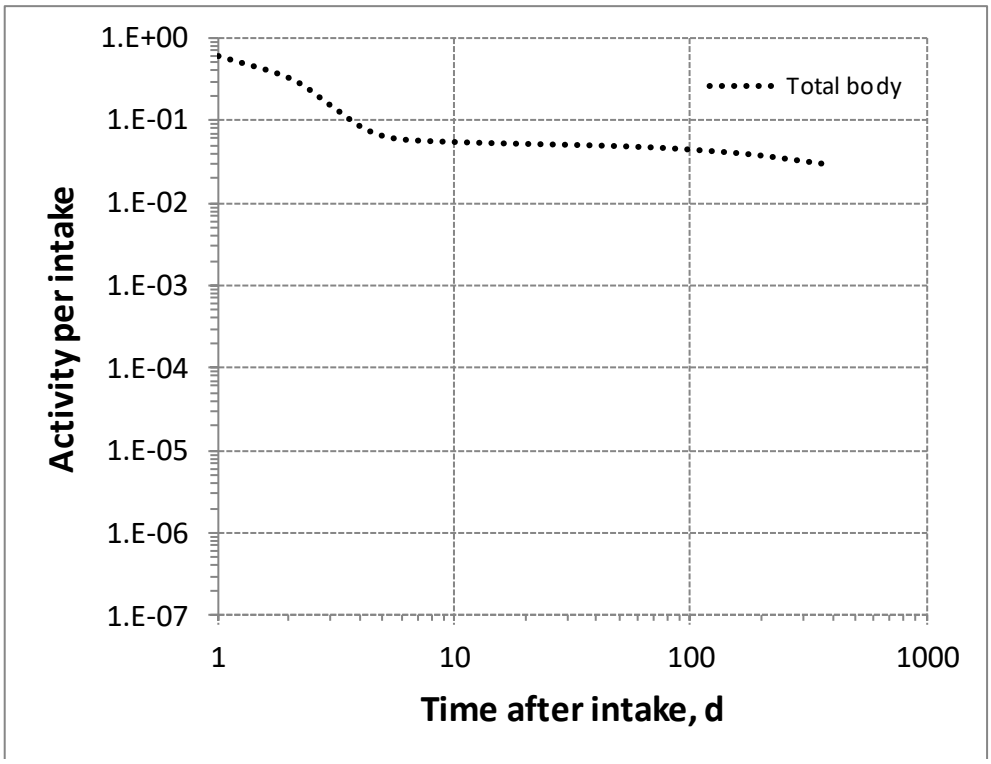

Fig. 2.7. Daily excretion of ^{10}Be following inhalation of 1 Bq Type S.

3. FLUORINE (Z = 9)

3.1. Isotopes

Table 3.1. Isotopes of fluorine addressed in this publication.

Isotope	Physical half-life	Decay mode
^{18}F*	109.77 min	EC, B+

EC, electron-capture decay; B+, beta-plus decay.
*Dose coefficients and bioassay data for this radionuclide are given in the printed copy of this publication.

3.2. Routes of Intake

3.2.1. Inhalation

(37) For fluorine, default parameter values were adopted for the absorption to blood from the respiratory tract (ICRP, 2015). For fluorine, and the other halogens, intakes could be in both particulate and gas and vapour forms, and it is therefore assumed that inhaled fluorine is 50% particulate and 50% gas/vapour in the absence of information (ICRP, 2002b). Absorption parameter values and types, and associated f_A values for gas and vapour forms of fluorine are given in Table 3.2 and for particulate forms in Table 3.3. By analogy with the halogen iodine, considered in detail in *Publication 137* (OIR P3) (ICRP, 2017), default Type F is recommended for particulate forms in the absence of specific information on which the exposure material can be assigned to an absorption type.

Table 3.2. Deposition and absorption for gas and vapour compounds of fluorine.

	Percentage deposited (%)*						Absorption†	
Chemical form/origin	Total	ET_1	ET_2	BB	bb	AI	Type	Absorption from the alimentary tract, f_A‡
Unspecified	100	0	20	10	20	50	F	1.0

ET_1, anterior nasal passage; ET_2, posterior nasal passage, pharynx and larynx; BB, bronchial; bb, bronchiolar; AI, alveolar-interstitial.
*Percentage deposited refers to how much of the material in the inhaled air remains in the body after exhalation. Almost all inhaled gas molecules contact airway surfaces, but usually return to the air unless they dissolve in, or react with, the surface lining. The default distribution between regions is assumed: 20% ET_2, 10% BB, 20% bb, and 50% AI.
†It is assumed that the bound state can be neglected for fluorine, i.e. $f_b = 0$.
‡For inhaled material deposited in the respiratory tract and subsequently cleared by particle transport to the alimentary tract, the default f_A values for inhaled materials are applied [i.e. the product of f_r for the absorption type (or specific value where given) and the f_A value for ingested soluble forms of fluorine (1)].

3.2.2. Ingestion

(38) The gastrointestinal absorption of fluoride is rapid and extensive (ICRP, 1975; Underwood, 1977; Patten et al., 1978). Exposure of the population to fluoride through the use of fluoridated toothpastes, mouthwashes, and topical gels is increasing. It has been shown that fluoride is absorbed readily from the mouth. However, the diffusible fluoride concentration within the mouth probably declines rapidly after ingestion due to binding by teeth, plaque, and micro-organisms (Patten et al., 1978). Absorption of carrier-free ^{18}F from the mouth has been investigated using rats: radiofluoride absorption was 6.8% after 2.5 h (Gabler, 1968; Patten et al., 1978). Wagner (1962) showed that 50% of a 29-µg dose of fluoride was absorbed from the ligated rat stomach within 1 h, and only 16% remained after 5 h.

(39) In *Publications 30* and *68* (ICRP, 1980, 1994a), f_1 was taken to be 1 for all compounds of fluorine. In the present publication, the value $f_A = 1$ is used for all chemical forms of fluorine.

Table 3.3. Absorption parameter values for inhaled and ingested fluorine.

Inhaled particulate materials	Absorption parameter values* f_r	s_r (d^{-1})	s_s (d^{-1})	Absorption from the alimentary tract, f_A
Default parameter values†				
Absorption type				
F‡	1	30	–	1
M	0.2	3	0.005	0.2
S	0.01	3	1×10^{-4}	0.01
Ingested materials§				
All forms	–	–	–	1

*It is assumed that the bound state can be neglected for fluorine (i.e. $f_b = 0$). The values of s_r for Type F, M and S forms of fluorine (30, 3 and 3 d^{-1} respectively) are the general default values.

†For inhaled material deposited in the respiratory tract and subsequently cleared by particle transport to the alimentary tract, the default f_A values for inhaled materials are applied [i.e. the product of f_r for the absorption type and the f_A value for ingested soluble forms of fluorine (1)].

‡Default Type F is recommended for use in the absence of specific information on which the exposure material can be assigned to an absorption type (e.g. if the form is unknown, or if the form is known but there is no information available on the absorption of that form from the respiratory tract). For guidance on the use of specific information, see Section 1.1.

§Activity transferred from systemic compartments into segments of the alimentary tract is assumed to be subject to reabsorption to blood. The default absorption fraction f_A for the secreted activity is the highest value for any form of the radionuclide ($f_A = 1$).

3.2.3. Systemic distribution, retention and excretion of fluorine

3.2.3.1. Biokinetic data

(40) Fluorine-18 has been widely used for skeletal imaging. Its systemic biokinetics has been studied in human subjects and laboratory animals (Suttie and Phillips, 1959; Costeas et al., 1970; Wootton, 1974; Hall et al., 1977; Charkes et al., 1978; Hawkins et al., 1992; Whitford, 1994; Schiepers et al., 1997).

(41) The fluoride ion is the most bioavailable form of fluorine. Fluoride entering blood deposits primarily in bone. Uptake by bone is rapid and thought to occur mainly by adsorption onto hydroxyapatite crystals, followed by exchange with hydroxyl groups in the hydroxyapatite. Uptake by bone marrow is negligible. Uptake by bone is correlated with calcium influx. The highest concentrations of fluoride in bone occur at sites of bone growth or remodeling (Neuman and Neuman, 1958; Whitford, 1994; Schiepers et al., 1997).

(42) Charkes et al. (1978) developed a biokinetic model for systemic fluoride (Fig. 3.1) based on results of several studies of the kinetics of ^{18}F in human subjects. Two compartments were used to describe kinetics of fluoride in bone: a ‘buffer’ compartment between blood and mineral bone, assumed to represent an extracellular fluid space of bone, and a compartment representing mineral bone. A portion of fluoride entering the buffer pool was assumed to return rapidly to blood. The remainder was assumed to enter a mineral bone compartment that returns fluoride to the buffer pool.

730 *3.2.3.2. Biokinetics of systemic fluorine*

731 (43) The biokinetic model for systemic fluoride used in this publication is based on the
732 model developed by Charkes et al. (1978), which consolidates results of several studies of the
733 kinetics of ^{18}F in human subjects. The structure of the model used here is shown in Fig. 3.2.
734 Parameter values are listed in Table 3.4. The model incorporates flow rates derived by Charkes
735 and coworkers but applies these rates within a modified model framework. In view of the
736 relatively short half-life of ^{18}F (~110 min), the only radioisotope of fluorine addressed in this
737 publication, all bone compartments are assumed to be part of bone surface. The compartment
738 called Bone ECF in the Charkes model is divided into compartments called Trabecular Surface
739 1 (TS1) and Cortical Surface 1 (CS1). The compartment called Bone in Charkes model is
740 divided into compartments called Trabecular Surface 2 (TS2) and Cortical Surface 2 (CS2).
741 The ratio of flow rates from Blood to TS1 and CS1 (~1.25) is the ratio applied to calcium in
742 *Publication 134* (2016). The sum of flow rates from Blood to TS1 and CS1 is the same as the
743 flow rate from Blood to Bone ECF in the Charkes model (with a small rounding difference).
744 The flow rates assigned to 'Tubular urine' in the Charkes model are assigned to the kidneys in
745 the present model. The kidneys are assumed to exchange fluoride with Blood and to lose
746 fluoride to the urinary bladder (UB) content. The rate of removal from the UB content is
747 assumed to be 12 d^{-1}, the ICRP's default value for workers and adult members of the public.

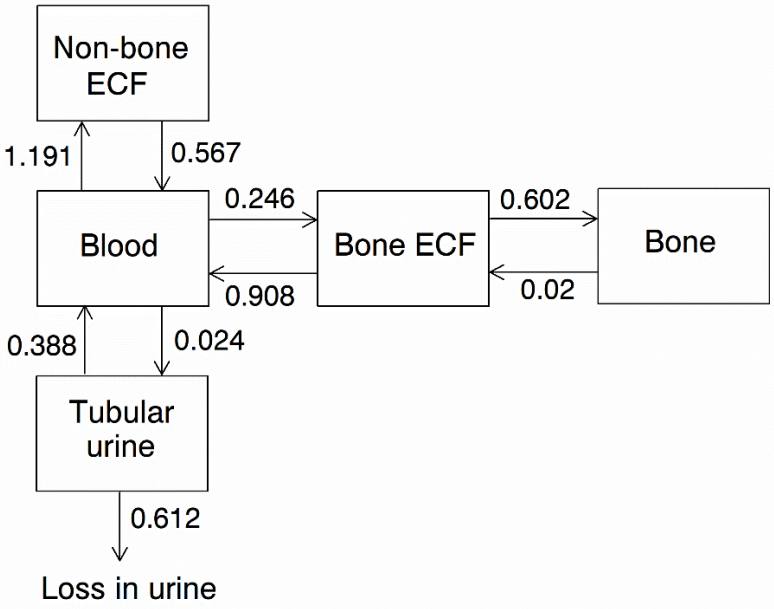

748
749 Fig. 3.1. Biokinetic model of Charkes et al. (1978) for systemic fluoride. Numbers next to arrows are
750 transfer coefficients (min-1). ECF = extracellular fluids.

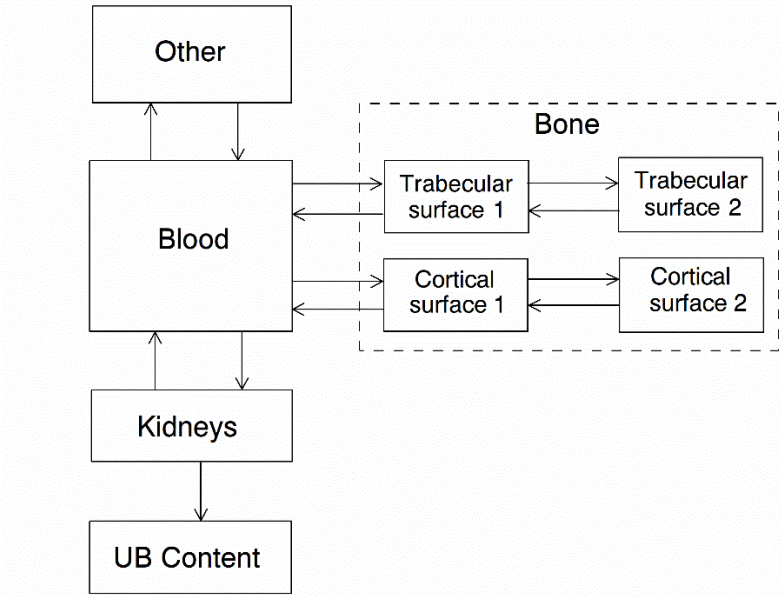

Fig. 3.2. Structure of the biokinetic model for systemic fluoride used in this publication UB = Urinary Bladder.

Table 3.4. Transfer coefficients in the biokinetic model for systemic fluorine.

From	To	Transfer coefficient (d^{-1})
Blood	Trabecular surface 1	197
Blood	Cortical surface 1	158
Blood	Other	1720
Blood	Kidneys	34.6
Trabecular surface 1	Blood	1310
Trabecular surface 1	Trabecular surface 2	867
Cortical surface 1	Blood	1310
Cortical surface 1	Cortical surface 2	867
Trabecular surface 2	Trabecular surface 1	28.8
Cortical surface 2	Cortical surface 1	28.8
Other	Blood	817
Kidneys	Blood	559
Kidneys	Urinary Bladder Content	881

3.3. Individual monitoring

(44) Information of detection limit for routine individual measurement is not available.

3.4. Dosimetric data for fluorine

759 Table 3.5. Committed effective dose coefficients (Sv Bq^{-1}) for the inhalation or ingestion of ^{18}F
760 compounds.

	Effective dose coefficients (Sv Bq^{-1})
Inhaled gases or vapours	^{18}F
Unspecified	7.8E-11
Inhaled particulate materials (5 μm AMAD aerosols)	
Type F, default	3.1E-11
Type M	5.0E-11
Type S	5.1E-11
Ingested materials	
All forms	4.8E-11

761 AMAD, activity median aerodynamic diameter
762

4. SODIUM (Z = 11)

4.1. Isotopes

Table 4.1. Isotopes of sodium addressed in this publication.

Isotope	Physical half-life	Decay mode
^{22}Na*	2.6019 y	EC, B+
^{24}Na*	14.9590 h	B^-

EC, electron-capture decay; B+, beta-plus decay; B- beta-minus decay

*Dose coefficients and bioassay data for this radionuclide are given in the printed copy of this publication. Data for other radionuclides listed in this table are given in the online electronic files on the ICRP website.

4.2. Routes of Intake

4.2.1. Inhalation

(45) For sodium, default parameter values were adopted on absorption to blood from the respiratory tract (ICRP, 2015). Absorption parameter values and types, and associated f_A values for particulate forms of sodium are given in Table 4.2.

Table 4.2. Absorption parameter values for inhaled and ingested sodium.

	Absorption parameter values*			
Inhaled particulate materials	f_r	s_r (d^{-1})	s_s (d^{-1})	Absorption from the alimentary tract, f_A
Default parameter values†				
Absorption type				
F	1	30	–	1
M‡	0.2	3	0.005	0.2
S	0.01	3	1×10^{-4}	0.01
Ingested materials§				
All forms				1

*It is assumed that the bound state can be neglected for sodium (i.e. $f_b = 0$). The values of s_r for Type F, M and S forms of sodium (30, 3 and 3 d^{-1} respectively) are the general default values.

†For inhaled material deposited in the respiratory tract and subsequently cleared by particle transport to the alimentary tract, the default f_A values for inhaled materials are applied [i.e. the product of f_r for the absorption type and the f_A value for ingested soluble forms of sodium (1)].

‡Default Type M is recommended for use in the absence of specific information on which the exposure material can be assigned to an absorption type (e.g. if the form is unknown, or if the form is known but there is no information available on the absorption of that form from the respiratory tract. For guidance on the use of specific information, see Section 1.1).

§Activity transferred from systemic compartments into segments of the alimentary tract is assumed to be subject to reabsorption to blood. The default absorption fraction f_A for the secreted activity is the highest value for any form of the radionuclide ($f_A = 1$).

4.2.2. Ingestion

(46) Virtually all sodium is absorbed from the gastrointestinal tract of man (Wiseman, 1964). While some sodium ions are absorbed from the saliva and across the gastric mucosa, sodium absorption occurs predominantly in the small intestine by passive cotransport with chloride ions or glucose, amino acids or bile acids, and by active transport by the sodium pump. Less than 0.5% of intestinal sodium is lost in the faeces each day. The mucosa of the large

intestine, like that of the small intestine, has a high capability for active absorption of sodium (ICRP, 2006).

(47) f_1 was taken to be 1 in *Publications 30* and *68* (ICRP, 1980, 1994a). The same value of $f_A = 1$ is adopted here for sodium intake at the workplace.

4.2.3. Systemic distribution, retention and excretion of sodium

4.2.3.1. Biokinetic data

(48) The adult human body typically contains about 1 g sodium (Na) per kg body weight (ICRP, 1975; Mole, 1984; Zhu et al., 2010). The body's sodium is freely exchangeable with the extracellular fluids except for a portion of sodium in bone representing roughly 10% of total-body sodium in an adult human (Mole, 1984). The turnover rate of the body's exchangeable sodium is inversely related to the level of sodium in diet. Blood, bone, and soft tissues contain roughly 10%, 40%, and 50%, respectively, of the sodium content of the adult human body (ICRP, 1975; Zhu et al., 2010).

(49) Richmond (1980) studied the biokinetics of ^{22}Na over time periods up to about 9 months after its oral administration to mice, rats, and human subjects; intraperitoneal (ip) administration to mice and rats; and intravenous administration to monkeys and dogs. Average total-body retention expressed as a percentage of administered activity (corrected for physical decay of ^{22}Na) in three human subjects was described as a sum of three exponential terms:

$$R(t) = 48.8e^{-0.0815t} + 51.0\exp^{-0.513t} + 0.267\exp^{-0.0015t} \qquad \text{(Eq. 4.1)}$$

where t is in days. Total-body retention in dogs and monkeys resembled that in human subjects. Activity was removed from the body at a moderately higher rate in rats and a much higher rate in mice than in human subjects. Tissue distribution studies on rats indicated that muscle, bone, skin, gastrointestinal (GI) tract, and blood plasma contained the preponderance of the retained activity 1-20 d after intraperitoneal administration. Blood plasma contained ~10% and bone contained 17-31% of total-body activity during this period.

(50) Vennart (1963) reported a long-term component of sodium retention in the human body of about 1100 d, representing about 0.3% of the administered amount. At 6-11 months after oral administration of ^{22}Na to 12 patients, median total-body retention represented ~0.35% of the administered amount (Smilay et al., 1961). In other human studies, Veall et al. (1955) estimated ^{22}Na retention of 1% after 75 d, and Miller et al. (1957) estimated ^{22}Na retention of 0.1% at 1 y.

(51) Following intravenous administration of ^{22}Na to four healthy adult human subjects (three females and one male), the serum concentration declined to half the initial value in 12-14 d (Threefoot et al., 1949). Based on average urinary losses, about half the administered amount was removed from the body in 29 d.

(52) Bergstrom (1955) studied the sodium loss from bone in rats due to various procedures resulting in acute acidosis or sodium depletion. Only about 29% of bone sodium could be mobilised.

(53) Forbes and McCoord (1969) studied the behaviour of sodium in bone is rats for periods up to 650 d post intraperitoneal injection of ^{22}Na. Most of the activity taken up by bone was removed with a half-time of a few days, but about 5% of the deposited activity exhibited slow removal with an estimated half-time of ~700 d. The investigators concluded that the tenaciously retained activity had become an integral part of the bone crystal structure.

836 *4.2.3.2. Biokinetic model for systemic sodium*

837 (54) The structure of the biokinetic model for systemic Na used in this publication is shown
838 in Fig. 4.1. Transfer coefficients are listed in Table 4.3.

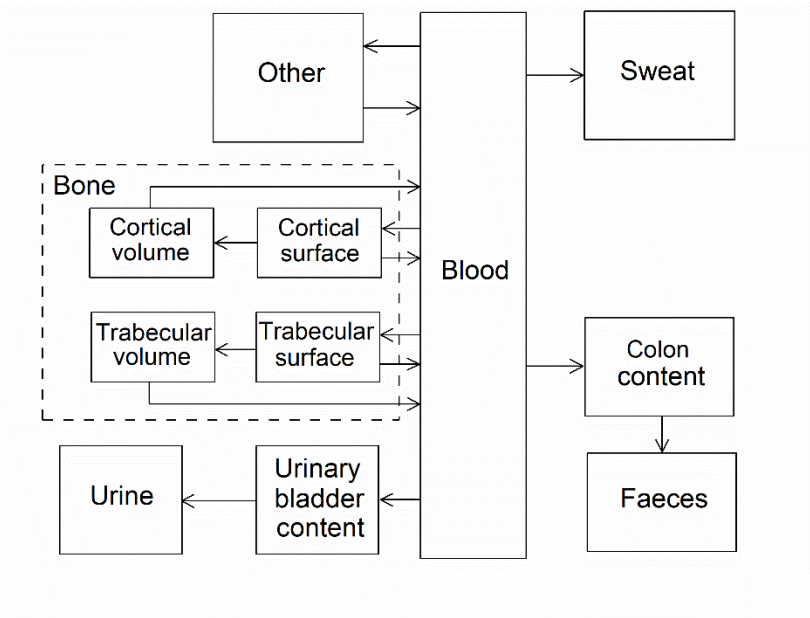

839
840 Fig. 4.1. Structure of the biokinetic model for systemic sodium.

841 Table 4.3. Transfer coefficients in the biokinetic model for systemic sodium.

From	To	Transfer coefficient (d^{-1})
Blood	Urinary bladder content	0.4418
Blood	Right colon content	0.0047
Blood	Excreta (sweat)	0.0235
Blood	Other	95
Blood	Trabecular bone surface	1.0
Blood	Cortical bone surface	4.0
Other	Blood	25
Trabecular bone surface	Blood	2.0
Trabecular bone surface	Trabecular bone volume	0.00055
Cortical bone surface	Blood	2.0
Cortical bone surface	Cortical bone volume	0.00055
Trabecular bone volume	Blood	0.002
Cortical bone volume	Blood	0.002

842 (55) The transfer coefficients were selected for reasonable consistency between model
843 predictions and the following data sets or assumptions. Excretion in urine, faeces, and sweat
844 represent 94%, 1%, and 5%, respectively, of total excretion. Total-body retention is described
845 by Eq. 4.1 over the observation period in the study by Richmond (1980), with long-term
846 retention (third term in Eq. 4.1) representing retention of a portion of sodium depositing in bone.
847 Non-exchangeable Na represents ~10% of total-body Na during chronic intake at a constant
848 rate. The short-term distribution of ^{22}Na is consistent with data of Richmond (1980) for rats.
849 The total-body concentration in adults is ~1 g kg^{-1} based on chronic intake of 4.4 g Na d^{-1}
850 [reference intake value given in *Publication 23* (ICRP, 1975)]. The long-term distribution of
851 stable Na in the body is consistent with autopsy study of Zhu et al. (2010).

4.3. Individual monitoring

4.3.1. ^{22}Na

(56) Measurements of ^{22}Na may be performed by in vivo whole-body measurement technique and by gamma measurement in urine.

Table 4.4. Monitoring techniques for ^{22}Na.

Isotope	Monitoring Technique	Method of Measurement	Typical Detection Limit
^{22}Na	Urine Bioassay	γ-ray spectrometry[a]	1.2 Bq L^{-1}
^{22}Na	Whole-body monitoring	γ-ray spectrometry[ab]	37 Bq

[a] Measurement system comprised of Germanium Detectors
[b] Counting time of 20 minutes

4.3.2. ^{24}Na

(57) Measurements of ^{24}Na may be performed by in vivo whole-body measurement technique and by gamma measurement in urine.

Table 4.5. Monitoring techniques for ^{24}Na.

Isotope	Monitoring Technique	Method of Measurement	Typical Detection Limit
^{24}Na	Urine Bioassay	γ-ray spectrometry[a]	1 Bq L^{-1}
^{24}Na	Whole-body monitoring	γ-ray spectrometry[ab]	25Bq

[a] Measurement system comprised of Germanium Detectors
[b] Counting time of 20 minutes

4.4. Dosimetric data for sodium

Table 4.6. Committed effective dose coefficients (Sv Bq^{-1}) for the inhalation or ingestion of ^{22}Na and ^{24}Na compounds.

Inhaled particulate materials (5 µm AMAD aerosols)	Effective dose coefficients (Sv Bq^{-1})	
	^{22}Na	^{24}Na
Type F, — NB: Type F should not be assumed without evidence	2.4E-09	3.0E-10
Type M, default	5.3E-09	4.9E-10
Type S	2.2E-08	5.2E-10
Ingested materials		
All forms	3.5E-09	4.8E-10

AMAD, activity median aerodynamic diameter

Table 4.7. Dose per activity content of ^{22}Na in total body and in daily excretion of urine (Sv Bq^{-1}); 5µm activity median aerodynamic diameter aerosols inhaled by a reference worker at light work.

	Type F		Type M		Type S	
Time after intake (d)	Total body	Urine	Total body	Urine	Total body	Urine
1	3.6E-09	7.4E-08	8.5E-09	9.5E-07	3.6E-08	8.2E-05
2	4.0E-09	6.5E-08	1.4E-08	6.8E-07	6.6E-08	5.7E-05
3	4.3E-09	6.9E-08	2.2E-08	7.2E-07	1.4E-07	6.0E-05
4	4.6E-09	7.4E-08	3.0E-08	7.6E-07	2.5E-07	6.4E-05
5	4.9E-09	7.9E-08	3.4E-08	8.1E-07	3.2E-07	6.8E-05
6	5.2E-09	8.4E-08	3.6E-08	8.6E-07	3.5E-07	7.2E-05
7	5.5E-09	9.0E-08	3.8E-08	9.2E-07	3.6E-07	7.6E-05
8	5.9E-09	9.6E-08	4.0E-08	9.8E-07	3.7E-07	8.1E-05
9	6.3E-09	1.0E-07	4.2E-08	1.0E-06	3.7E-07	8.7E-05
10	6.7E-09	1.1E-07	4.4E-08	1.1E-06	3.8E-07	9.2E-05
15	9.2E-09	1.5E-07	5.4E-08	1.5E-06	4.0E-07	1.3E-04
30	2.4E-08	4.0E-07	9.0E-08	3.6E-06	4.3E-07	3.1E-04
45	6.1E-08	1.0E-06	1.3E-07	8.1E-06	4.6E-07	7.3E-04
60	1.5E-07	2.7E-06	1.6E-07	1.6E-05	4.8E-07	1.5E-03
90	6.5E-07	1.9E-05	2.1E-07	3.5E-05	5.2E-07	3.6E-03
180	1.9E-06	8.6E-04	4.2E-07	8.3E-05	6.6E-07	5.8E-03
365	3.1E-06	1.6E-03	1.5E-06	3.1E-04	9.9E-07	9.2E-03

Table 4.8. Dose per activity content of ^{24}Na in total body and in daily excretion of urine (Sv Bq^{-1}); 5µm activity median aerodynamic diameter aerosols inhaled by a reference worker at light work.

	Type F		Type M		Type S	
Time after intake (d)	Total body	Urine	Total body	Urine	Total body	Urine
1	1.4E-09	2.8E-08	2.4E-09	2.7E-07	2.6E-09	5.9E-06
2	4.5E-09	7.4E-08	1.2E-08	5.8E-07	1.4E-08	1.2E-05
3	1.5E-08	2.4E-07	5.8E-08	1.9E-06	9.3E-08	4.0E-05
4	4.8E-08	7.8E-07	2.3E-07	6.0E-06	4.9E-07	1.3E-04
5	1.6E-07	2.5E-06	8.1E-07	2.0E-05	1.9E-06	4.1E-04
6	5.0E-07	8.2E-06	2.7E-06	6.3E-05	6.4E-06	1.3E-03
7	1.6E-06	2.6E-05	8.5E-06	2.0E-04	2.0E-05	4.3E-03
8	5.3E-06	8.6E-05	2.7E-05	6.6E-04	6.3E-05	1.4E-02
9	1.7E-05	2.8E-04	8.6E-05	2.1E-03	1.9E-04	4.5E-02
10	5.5E-05	9.0E-04	2.7E-04	6.9E-03	6.0E-04	1.5E-01
15	2.0E-02	3.2E-01	8.8E-02	2.4E+00	1.6E-01	N/A
30	N/A	N/A	N/A	N/A	N/A	
45						
60						
90						
180						
365						

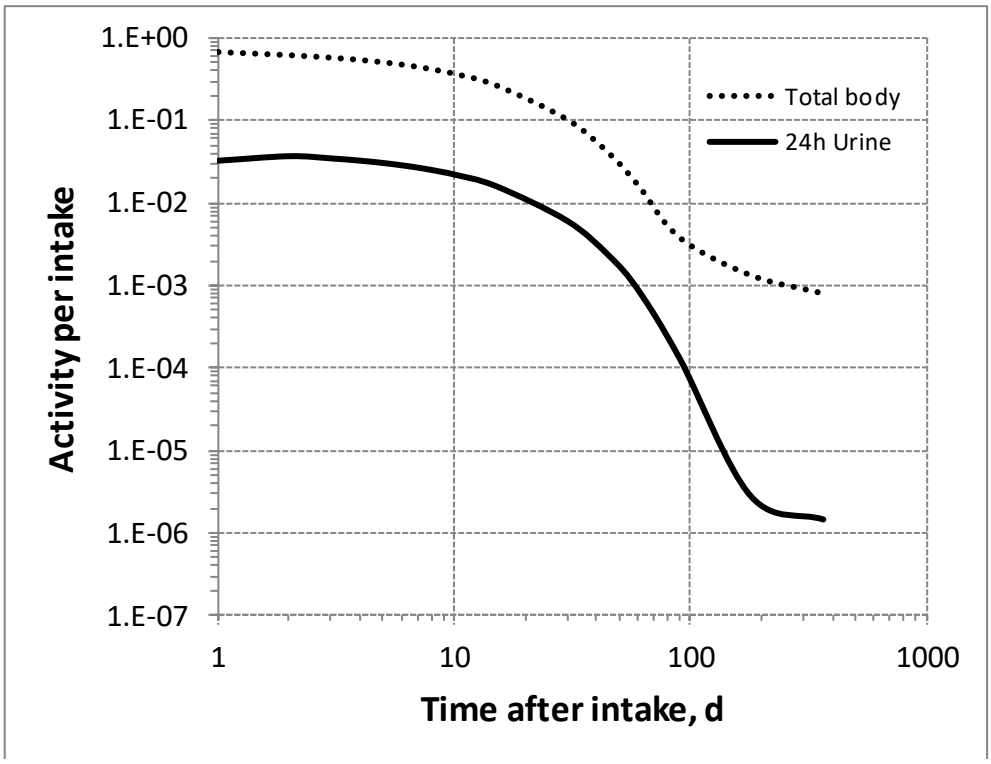

873

874 Fig. 4.2. Daily excretion of ^{22}Na following inhalation of 1 Bq Type F.

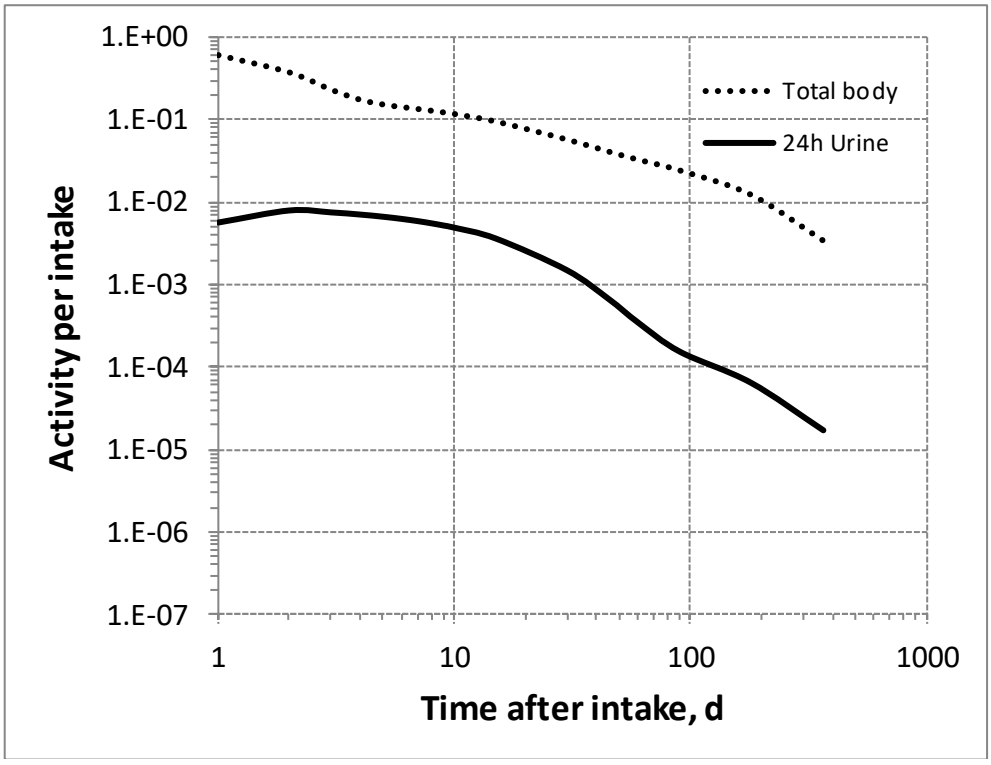

875

876 Fig. 4.3. Daily excretion of ^{22}Na following inhalation of 1 Bq Type M.

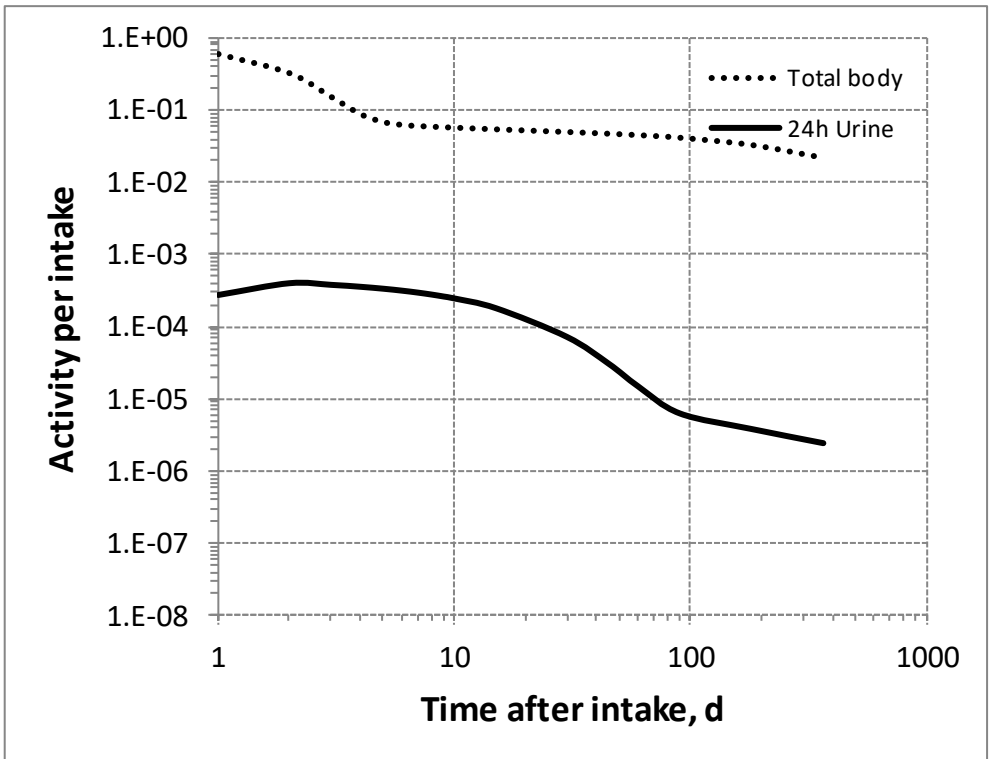

877

878 Fig. 4.4. Daily excretion of ^{22}Na following inhalation of 1 Bq Type S.

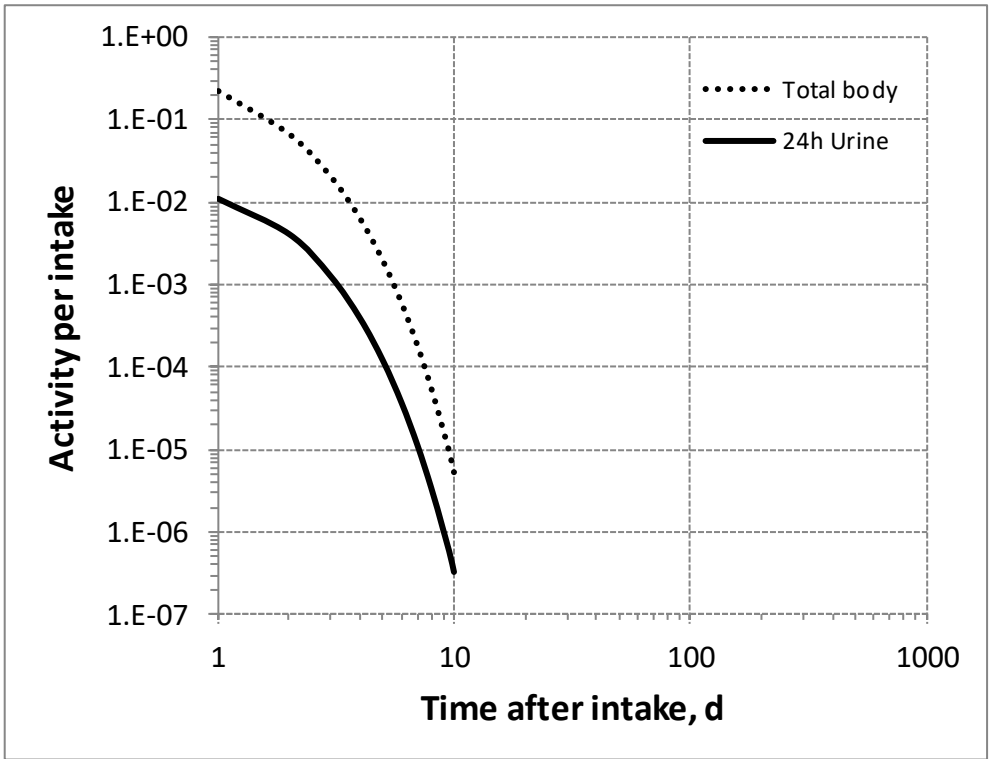

879

880 Fig. 4.5. Daily excretion of ^{24}Na following inhalation of 1 Bq Type F.

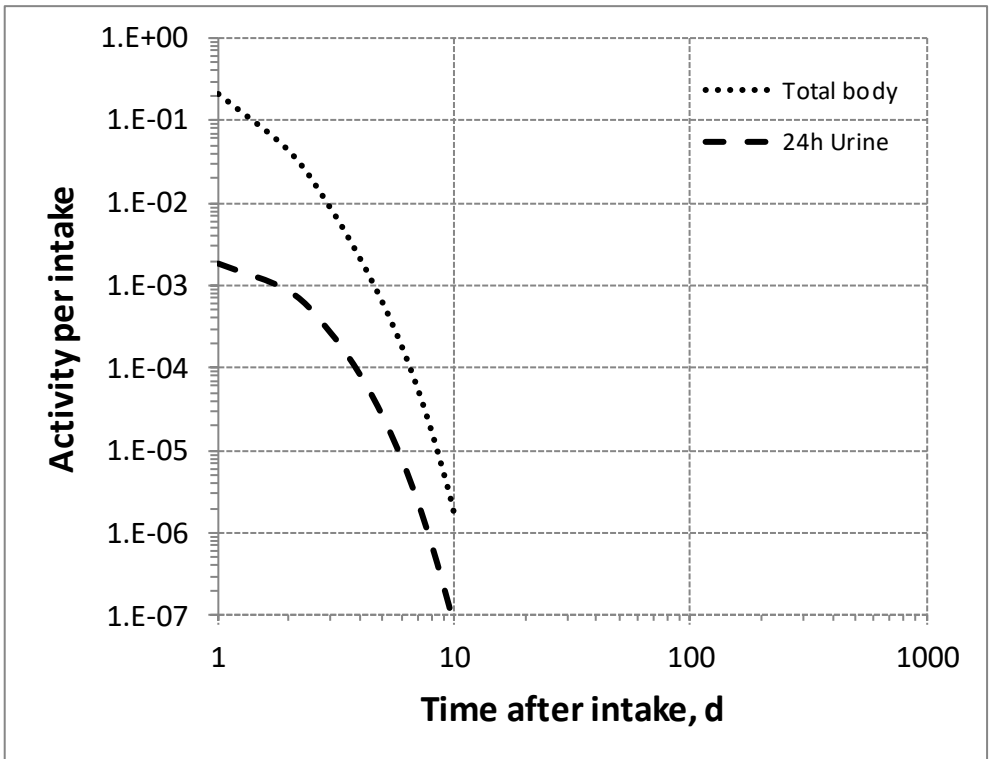

881

882 Fig. 4.6. Daily excretion of ^{24}Na following inhalation of 1 Bq Type M.

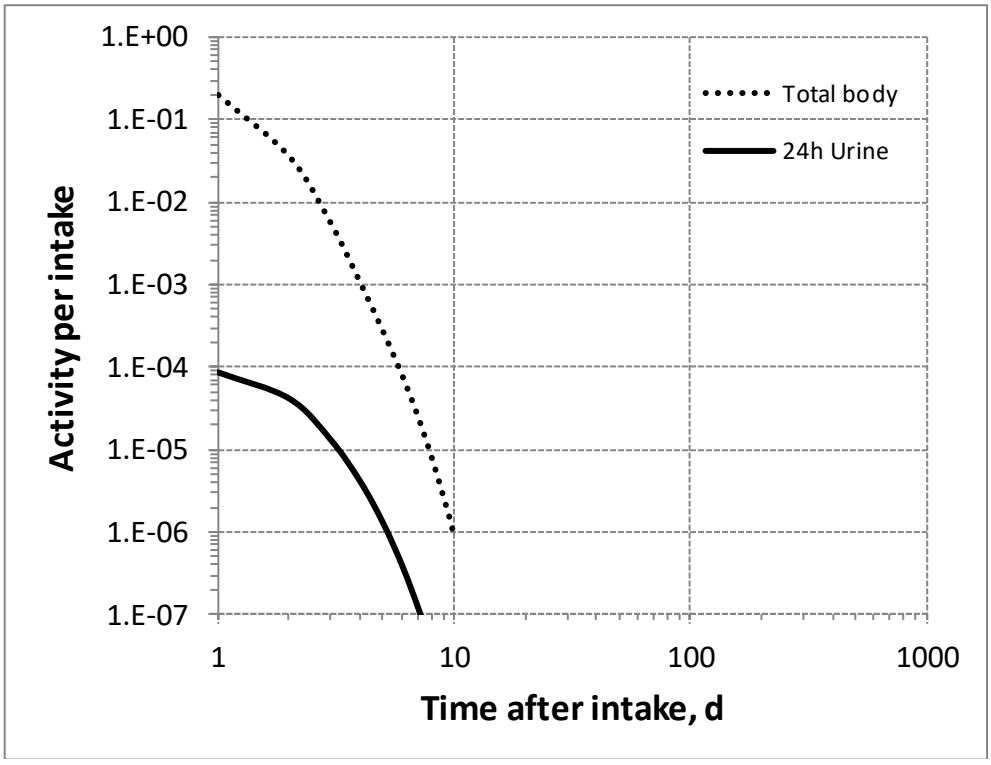

883

884 Fig. 4.7. Daily excretion of ^{24}Na following inhalation of 1 Bq Type S.

885

5. MAGNESIUM (Z = 12)

5.1. Isotopes

Table 5.1. Isotopes of magnesium addressed in this publication.

Isotope	Physical half-life	Decay mode
^{28}Mg*	20.915 h	B-

B- beta-minus decay

*Dose coefficients and bioassay data for this radionuclide are given in the printed copy of this publication.

5.2. Routes of Intake

5.2.1. Inhalation

(58) For magnesium, default parameter values were adopted on absorption to blood from the respiratory tract (ICRP, 2015). Absorption parameter values and types, and associated f_A values for particulate forms of magnesium are given in Table 5.2.

Table 5.2. Absorption parameter values for inhaled and ingested magnesium.

	Absorption parameter values*			
Inhaled particulate materials	f_r	s_r (d^{-1})	s_s (d^{-1})	Absorption from the alimentary tract, f_A
Default parameter values†				
Absorption type				
F	1	30	–	0.5
M‡	0.2	3	0.005	0.1
S	0.01	3	1×10^{-4}	0.005
Ingested materials§				
Magnesium oxide				0.2
All other forms, unspecified forms				0.5

*It is assumed that the bound state can be neglected for magnesium (i.e. $f_b = 0$). The values of s_r for Type F, M and S forms of magnesium (30, 3 and 3 d^{-1} respectively) are the general default values.

†For inhaled material deposited in the respiratory tract and subsequently cleared by particle transport to the alimentary tract, the default f_A values for inhaled materials are applied [i.e. the product of f_r for the absorption type and the f_A value for ingested soluble forms of magnesium (0.5)].

‡Default Type M is recommended for use in the absence of specific information on which the exposure material can be assigned to an absorption type (e.g. if the form is unknown, or if the form is known but there is no information available on the absorption of that form from the respiratory tract). For guidance on the use of specific information, see Section 1.1.

§Activity transferred from systemic compartments into segments of the alimentary tract is assumed to be subject to reabsorption to blood. The default absorption fraction f_A for the secreted activity is the highest value for any form of the radionuclide ($f_A = 0.5$).

5.2.2. Ingestion

(59) The fractional intestinal absorption of magnesium is generally considered to be in the order of 40-50%, with figures reported from 10 to 70% (Schwartz et al., 1978; ICRP, 1981; EFSA, 2015b). It appears to decrease with increasing magnesium intake (Roth and Werner, 1979; Sabatier et al., 2003). Magnesium, when present in high concentration, forms an insoluble salt at neutral pH with phytate (Cheryan, 1980). Dietary fibre may bind a variety of elements, including magnesium, and render them unavailable for absorption (Campbell et al., 1976;

Reinhold et al., 1976; Knudsen et al., 1996). High intakes of zinc from supplements decrease magnesium absorption (Spencer et al., 1994).

(60) The bioavailability of magnesium from mineral water was observed to be 46% in a group of adult women [increased to 52% when water was consumed with a meal (Sabatier et al., 2003)] and 59% in a group of adult men (Verhas et al., 2002). Magnesium in the aspartate, citrate, lactate, and chloride forms is absorbed more completely by humans than magnesium oxide and magnesium sulphate (Morris et al., 1987; Lindberg et al., 1990; Mühlbauer et al., 1991; Firoz and Graber, 2001; Ranade and Somberg, 2001; Walker et al., 2003). Specifically, the fractional absorption of magnesium oxide appears 2 to 4 times less than that of soluble forms. Still, in rats, Coudray et al. (2005) and Bertinato et al. (2014) observed neither significant differences among the bioavailability of MgO and various soluble organic and inorganic magnesium salts nor negative influence of phytate in diet. The total amount of magnesium in diet therefore seems to be the main factor influencing gastrointestinal absorption.

(61) In *Publications 30* and *68* (ICRP, 1981, 1994a), f_1 was taken to be 0.5 for all compounds of magnesium. The same value of $f_A = 0.5$ is used here for all chemical forms of magnesium, except the oxide for which a lower $f_A = 0.2$ is used.

5.2.3. Systemic distribution, retention and excretion of magnesium

5.2.3.1. Biokinetic data

(62) Magnesium (Mg) is an essential element needed for a variety of physiological functions, mainly related to enzyme activity. The adult human body typically contains about 24 g of magnesium. Only a small portion of the total-body content is carried in blood. The normal concentration in plasma is 0.75-1.0 mmol Mg L^{-1}. The concentration in red blood cells (RBC) is about three times that in plasma. Bone contains about 60% of the total-body content, and the remainder excluding blood is nearly equally divided between muscle and other soft tissues. Part of bone magnesium exchanges extremely slowly with plasma magnesium. Magnesium residing on bone surfaces is readily released to blood when plasma concentrations decline but remains bound to bone surface at adequate plasma concentrations (Elin, 1987; Vormann, 2003).

(63) Aikawa et al. (1960) investigated the behaviour of intravenously administered ^{28}Mg ($T_{1/2}$ = 20.9 h) in nine normal human subjects (7 males and 2 females) in the age range 17-54 y. About 20% was removed in urine over 24 h. Faecal excretion was negligible. Exchangeable magnesium was estimated to represent less than 16% of total-body magnesium. Activity exchanged slowly with stable magnesium in bone, muscle, and RBC.

(64) Avioli and Berman (1966) studied magnesium kinetics in 15 normal adult humans, ages 23-34 y, following intravenous administration of ^{28}Mg. Studies of individual subjects were terminated at 2-6 d post injection. Mean urinary and faecal excretion accounted for about 17% and 2.6%, respectively, of the administered amount (after adjustment for radioactive decay) in five subjects followed for 6 d. Exchangeable magnesium was estimated to represent about 15% of total-body magnesium. The rapidly exchanging pool was judged to represent extracellular fluid. The data indicated a larger pool of ^{28}Mg that exchanged stable magnesium with a biological half-life of ~42 d.

(65) Watson et al. (1979) studied magnesium kinetics in the whole body, plasma, and RBC in five healthy adult male humans following intravenous administration of ^{28}Mg. Exchangeable magnesium was estimated to represent less than one-fourth of total-body magnesium after 5 d. Total-body retention over the relatively short observation period was described as a sum of two exponential terms, with ~4.5% removed with a biological half-time of a few hours and the remainder with a half-time of ~30 d.

(66) Sabatier et al. (2003) developed a compartmental model of magnesium metabolism based on results of a stable isotope study involving oral administration of ^{26}Mg and intravenous administration of ^{25}Mg to six healthy adult men in the age range 26-41 y. Isotopic concentrations were determined in blood, urine, and faeces collected over 12 d. The use of stable isotopes enabled longer observation of exchange of magnesium tracers with the body's magnesium stores and identification of a larger exchangeable pool than estimated in an earlier study by Avioli and Berman (1966) involving the relatively short-lived radionuclide ^{28}Mg. The exchangeable pool was interpreted as representing 25% of total-body magnesium and consisting of two extra-plasma pools that exchange magnesium with plasma and contain 80% and 20% of exchangeable magnesium. The model also described exchange of systemic magnesium with the gastrointestinal (GI) tract resulting from secretion of magnesium into the GI content and reabsorption to blood. Excretion of magnesium was depicted as transfer from plasma to urine and faecal loss of unabsorbed magnesium. The model did not address non-exchangeable magnesium.

(67) At 1 d after intravenous administration of ^{28}Mg to dogs, the heart showed the highest activity, followed by kidney, liver, and pancreas, among eight examined soft tissues (Brandt et al., 1958). The activity concentration in bone varied greatly from one bone to another and generally was lower than that in heart, kidneys, liver, and pancreas.

(68) Lazzara et al. (1963) performed a detailed examination of the time-dependent behaviour of ^{28}Mg in dogs over the first 68 h after intravenous administration. There were considerable differences in the rate of exchange of ^{28}Mg with stable magnesium in different tissues. The activity concentration in the kidneys rose rapidly, peaked at about 4 h, and then gradually declined. The left ventricle, liver, and pancreas initially showed similar ^{28}Mg uptake curves, but peak concentrations occurred at different times for the three organs. There was a continual rise in activity in the cerebellum throughout the observation period. Bone and teeth showed highly variable activity concentrations from one location to another, and neither reached a peak average concentration over the 68-h observation period. The biological half-time for the total body was about 11 d.

5.2.3.2. Biokinetic model for systemic magnesium

(69) The structure of the biokinetic model for systemic magnesium used in this publication is shown in Fig. 5.1. Transfer coefficients are listed in Table 2.1.

(70) The model is an extension of the model of Sabatier et al. (2003) described above. The median transfer coefficients derived by Sabatier and coworkers were used as a starting point. Their extra-plasma compartment with relatively slow return to blood is assumed here to represent exchangeable sodium in bone. Long-term retention bone compartments were added, and a third soft-tissue compartment was added to represent slowly exchangeable magnesium and to approximate the total-body stable magnesium content of adult humans. Model predictions are reasonably consistent with the bone and soft tissue magnesium contents in humans (about 55-60% in bone), central urinary and faecal excretion rates reported in the literature, and buildup of the magnesium ratio RBC:Plasma as observed by Watson et al. (1979) in normal male subjects.

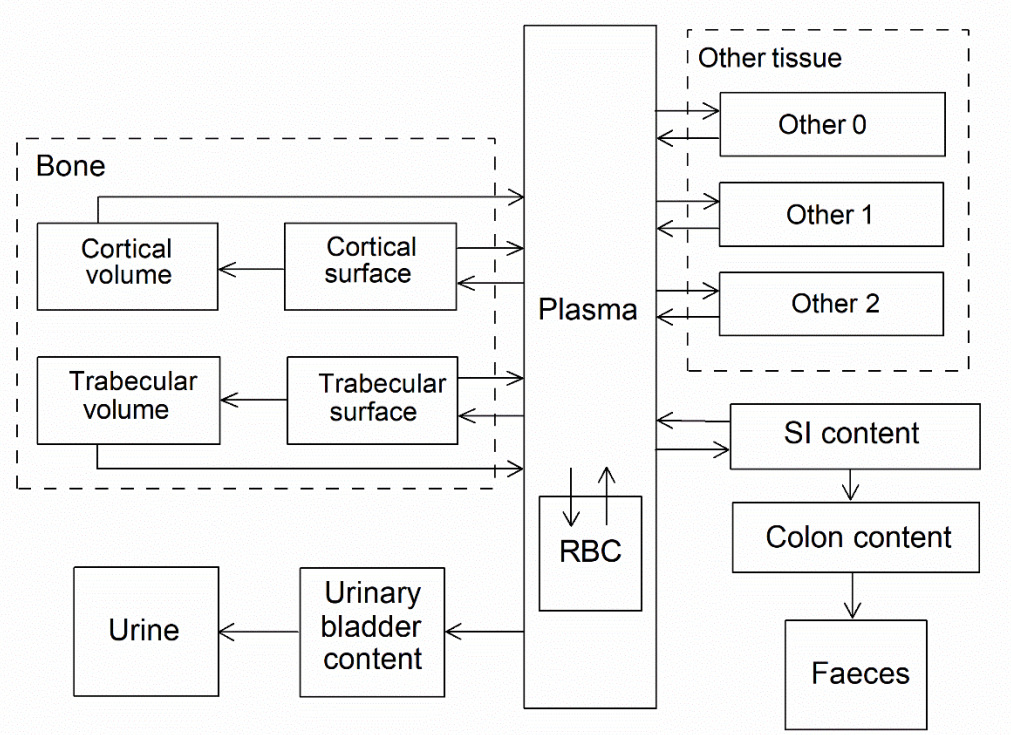

Fig. 5.1. Structure of the biokinetic model for systemic magnesium.

Table 5.3. Transfer coefficients in the biokinetic model for systemic magnesium.

	To	Transfer coefficient (d^{-1})
Plasma	RBC	0.05
Plasma	Urinary bladder content	1
Plasma	Small intestine content	0.2
Plasma	Trabecular bone surface	4
Plasma	Cortical bone surface	4
Plasma	Other 0	70
Plasma	Other 1	19.75
Plasma	Other 2	1
RBC	Plasma	0.03
Trabecular bone surface	Plasma	0.18
Trabecular bone surface	Trabecular bone volume	0.02
Cortical bone surface	Plasma	0.18
Cortical bone surface	Cortical bone volume	0.02
Other 0	Plasma	60
Other 1	Plasma	3
Other 2	Plasma	0.023
Trabecular bone volume	Plasma	0.023
Cortical bone volume	Plasma	0.023

5.2.3.3. Treatment of progeny

(71) The only progeny of magnesium addressed in this publication is ^{28}Al produced by decay of ^{28}Mg. The model for aluminium as a progeny of magnesium is an expansion of the characteristic model for aluminium with added compartments and associated transfer coefficients needed to solve the linked biokinetic models for magnesium and aluminium (see Annex B). For ^{28}Al produced in a compartment not contained in the characteristic model for aluminium, ^{28}Al is assumed to transfer to the central blood compartment of that model at the rate 1000 d^{-1} if produced in a blood compartment and 0.5 d^{-1} if produced in a tissue compartment, and to follow the characteristic model for aluminium thereafter.

5.3. Individual monitoring

(72) Information of detection limit for routine individual measurement is not available.

5.4. Dosimetric data for magnesium

Table 5.4. Committed effective dose coefficients (Sv Bq^{-1}) for the inhalation or ingestion of ^{28}Mg compounds.

Inhaled particulate materials (5 µm AMAD aerosols)	Effective dose coefficients (Sv Bq^{-1})
	^{28}Mg
Type F	6.0E-10
Type M, default	9.1E-10
Type S	9.6E-10
Ingested materials	
Magnesium oxide	1.1E-09
All other forms, unspecified forms	1.0E-09

AMAD, activity median aerodynamic diameter

6. ALUMINIUM (Z = 13)

6.1. Isotopes

Table 6.1. Isotopes of aluminium addressed in this publication.

Isotope	Physical half-life	Decay mode
^{26}Al*	7.17×10^5 y	EC, B+

EC, electron-capture decay; B+, beta-plus decay
*Dose coefficients and bioassay data for this radionuclide are given in the printed copy of this publication.

6.2. Routes of Intake

6.2.1. Inhalation

6.2.1.1. Absorption types and parameter values

(73) *Publication 30* (ICRP, 1981) assigned oxides, hydroxides, carbides, halides and nitrates of aluminium as well as metallic aluminium to inhalation class W and all other commonly occurring compounds of the element to inhalation class D, on the basis of animal data. Since then, a large amount of information on the behaviour of inhaled aluminium in human subjects has been collected, mostly from workers exposed to aluminium metal and oxide.

(74) Absorption parameter values and types, and associated f_A values for particulate forms of aluminium are given in Table 6.6.

(75) Reference biokinetic models were used here (i.e. by the Task Group) for the analysis of the data and the determination of absorption parameter values for aluminium particles. Lung retention data were interpreted using the revised HRTM (ICRP, 2015) and the respiratory tract model for rat described in Supporting Guidance 3 (ICRP, 2002b). Aluminium in lung tissue and blood was taken into account in the comparison with experimental data by using the systemic model for aluminium described in Section 6.2.3.

a. Aluminium oxide [Al_2O_3]

(76) Mussi et al. (1984) measured aluminium in urine and plasma of seven workers exposed for 6 months to aluminium dust or to aluminium welding fumes. Aluminium was determined from samples of blood and urine. The levels of aluminium in plasma were mostly within the range of values found in non-occupationally exposed subjects. The urinary aluminium levels were much higher than in non-occupationally exposed subjects and increased from the beginning (mean 46 µg L^{-1}) to the end (mean 93 µg L^{-1}) of the workshift. Two weeks after the termination of exposure, the urinary aluminium levels had decreased to a mean of 9 µg L^{-1}. The exposure at the workplace was also determined from personal air samples (mean 3.7 mg m^{-3}). Analysis here of the data suggested assignment to Type S of inhaled aluminium in both dust and fumes.

(77) Sjögren et al. (1985) investigated the relation between exposure to welding fumes, assumed to consist mainly of aluminium oxide, and aluminium urinary excretion over a week. Three male volunteers previously unexposed to aluminium, 3 male welders exposed to aluminium-containing welding fumes for short periods (1-24 months) and 3 male welders exposed to aluminium-containing welding fumes for long periods (18-20 y) were subject to air and urine monitoring. The mass median aerodynamic diameter (MMAD) was about 0.4 µm in the metal inert-gas (MIG) welding of aluminium and somewhat smaller in tungsten inert-gas (TIG) welding. The volunteers performed very light physical work during exposure and their

pulmonary ventilation was estimated to be about 20 L min^{-1}. The exposure varied between 0.3 and 10.2 mg m^{-3}. The urinary excretion of aluminium for the volunteers was 0.1-0.3 % of the total inhaled mass within the next 2 d after exposure. Analysis here of the data gave $f_r = 0.03$, $s_s < 10^{-4}$ d^{-1} for a volunteer (BS); $f_r = 0.02$, $s_r = 3$ d^{-1}, $s_s = 2 \times 10^{-4}$ d^{-1} for a welder (JH) exposed for a month; $f_r = 0.02$, $s_s = 10^{-4}$ d^{-1} for a welder (BJ) exposed for 19 y; and assignment to Type S for the three individuals.

(78) Sjögren at al. (1998) conducted similar investigations in 25 welders by personal air sampling during a workshift, urine sampling at the end of the workshift and after a period of 16-37 d without exposure. The urinary concentration of aluminium was dependent on the level of current exposure and on the duration of exposure. The observed relations between air concentrations of aluminium and urinary excretion were consistent with $f_r = 0.05$ when s_r and s_s were fixed at default values for Type S, suggesting aluminium welding fumes could be assigned to Type S.

(79) Elinder et al. (1991) assessed the concentrations of aluminium in blood, urine and bone biopsies of two welders exposed to fumes from MIG welding for 20 y. Air concentrations were measured during 1 week at an average of 3-9 mg Al m^{-3}. The level of aluminium in urine dropped by 14-63% over 5 y after the end of exposure (from 370-560 µg d^{-1} during exposure to 170-400 µg d^{-1} afterwards). The level of aluminium in the skeleton was 18-29 µg per g dry weight. Analysis here gave f_r = 0.02-0.04 and s_s = 1-8 × 10^{-5} d^{-1}. This is consistent with assignment to Type S.

(80) Pierre et al. (1995) investigated the variations of atmospheric concentration of aluminium and fluorine compounds at workplaces and of the corresponding urinary excretion of the two elements in 16 male workers over a working week. Detailed air and urine data are provided for 6 individuals (Table 6.2). Five of them were potentially exposed to aluminium oxide as well as to other aluminium compounds. In the analysis of the air samples, the collected particles yielded a soluble fraction of aluminium obtained by dissolution in water and an insoluble fraction of aluminium obtained by dissolution in hydrofluoric and nitric acids. The relative soluble and insoluble fractions indicate exposure to less soluble compounds for workers A1 and A2 than for workers B1, B2, C1 and C2. Analysis here of the urine and exposure data gave the absorption parameter values in Table 6.3 and assignment to the type indicated.

Table 6.2. Aluminium exposure and bioassay data for 6 workers.

Worker ID	Exposure to Al compounds	Duration of exposure (years)	Worked days in the week	8 h time weighted average Al concentration (mg m^{-3})		Number of urine samples	Mean urinary Al (µg d^{-1})
				soluble	insoluble		
A1	AlF_3 dust	0.17	5	0.29	4.79	37	36
A2	AlF_3 and Al_2O_3	14		0.03	0.33	33	20
B1	$NaAlF_4$, Na_2AlF_5, $Na_2Al_2F_8$, Al_2O_3, AlF_3 and Na_3AlF_6	9	3	0.22	0.35	28	70
B2		13		0.25	0.53	20	86
C1		9	4	0.56	0.76	36	98
C2		10		0.31	0.10	27	118

Table 6.3. Aluminium absorption parameter values for 6 workers.

Worker ID	f_r	s_r (d^{-1})	s_s (d^{-1})	Absorption type
A1	0.01	0.5	0	S
A2	0.01	2	3×10^{-5}	S
B1	0.08	4	1×10^{-4}	S
B2	0.1	4	9×10^{-5}	S (close to M)
C1	0.1	2	7×10^{-5}	S
C2	0.4	2	2×10^{-5}	M

(81) Pierre et al. (1998) studied the individual exposure, plasma and urine levels of aluminium for 335 workers from 7 aluminium industry plants. Detailed air and urine data are provided for 6 individuals monitored over a week (Table 6.4). One of them (Worker 2) was exposed to aluminium oxide. The authors estimated the solubility of the oxide to be low. Analysis here of the urine and exposure data gave the absorption parameter values in Table 6.5 and assignment to the type indicated (i.e. Type S for exposure to aluminium oxide). However, the lack of information on the duration of former exposure made bioassay interpretation difficult for the most insoluble compounds, so s_r and s_s were fixed to default values for Type S and only the value for f_r was derived from the individual bioassay and air sampling data.

Table 6.4. Aluminium exposure and bioassay data for 6 workers.

Worker ID	Exposure to Al compounds	Worked days in the week	8 h time weighted average Al concentration (mg m^{-3})		Number of urine samples	Mean plasma Al in the exposure group (µg L^{-1})	Mean urinary Al in the exposure group (µg per g creatinine)
			soluble	insoluble			
1	bauxite in mine	5	<0.005	1.45	35	7.1	33.3
2	Al_2O_3	4	0.001-0.008	0.98-9.88	24	6.9-12.8	15.8-27.8
3	AlF_3	5	0.03-0.11	0.33-4.78	26	12.3	13.4
4	Al and F^- in potroom	4	0.28	0.30	20	21.9	31.4
5	Al and F^- in potroom	3	0.19	0.39	18	14.9	20.32
6	Al flake powder	5	0.003	0.88	30	21.6	55.9

Table 6.5. Aluminium absorption parameter values for 6 workers.

Worker ID	f_r	s_r (d^{-1})	s_s (d^{-1})	Absorption type
1	0.02	3 (fixed)	1×10^{-4} (fixed)	S
2	0.02	3 (fixed)	1×10^{-4} (fixed)	S
3	0.02	3 (fixed)	1×10^{-4} (fixed)	S
4	0.2	4	5×10^{-4}	M
5	0.1	4	3×10^{-4}	S (close to M)
6	0.04	1	4×10^{-4}	S (close to M)

(82) McAughey et al. (1998) and Priest et al. (1998, 2004) reported the results of a study where two male human volunteers inhaled ^{26}Al-labelled aluminium oxide particles of MMAD 1.2 µm. The intakes were estimated, from whole-body gamma spectrometry and early faecal samples, as 6 and 16 Bq respectively. Urinary excretion was monitored for a thousand days: about 0.02% initial lung deposit (ILD) was cleared each day during the first month but the amount of aluminium in urine decreased with a half time of about 90 d. Overall, the fraction that was transferred to blood was estimated to be 1.9% ILD. Simultaneous analysis here of the urine data from both workers gave $f_r = 0.004$, $s_s = 2 \times 10^{-4}$ d^{-1} and assignment to Type S.

(83) Riihimäki et al. (2008) assessed the airborne and internal aluminium exposure of 12 aluminium welders and fitters in a shipyard and 5 manufacturers of aluminium sulphate. The welders were exposed to aluminium oxide fumes made of ultrafine (diameter < 0.1 µm) particles and agglomerates. Personal air samples were collected during two consecutive workdays. Urine and blood samples were collected over 48 h, after a summer vacation, and 1-2 y later. Aluminium in samples was measured by electrothermal atomic absorption

spectrometry. Analysis by the authors of the data for a welder (worker C) suggested $f_r = 0.012$. This is consistent with assignment to Type S.

(84) Kiesswetter et al. (2007) studied the exposure and neurobehavioural data of 20 male aluminium welders in the train and truck construction industry. Three investigations were conducted over 4 years to measure total dust in air as well as aluminium in urine and plasma. The comparison of the levels of exposure with the urine bioassay data would be compatible with Type S behaviour of inhaled aluminium.

(85) Kiesswetter et al. (2009) conducted a similar study for 92 male aluminium welders in the automobile industry, compared with 50 non-exposed construction workers of the same industry. Three investigations were performed over 4 years and indicated mean values for total dust in air of 0.5-0.8 mg m^{-3}, aluminium in pre-shift urine 23-43 µg per g creatinine, aluminium in post-shift urine 21-43 µg per g creatinine, aluminium in plasma 5-9 µg L^{-1}. In a control group, the mean aluminium in pre-shift urine was 9-10 µg per g creatinine and the mean aluminium in pre-shift plasma was 2-5 µg L^{-1}. The comparison of the levels of exposure with the urine bioassay data would be compatible with Type S behaviour of inhaled aluminium.

(86) Klosterkötter (1960) investigated the elimination of aluminium oxide for 3 months after short-term inhalation by 40 female white rats. The animals were exposed to high concentrations (33 g Al_2O_3 m^{-3}) 5 h per d for 4 d. The particle sizes were 5-40 nm, tending to agglomerate in aggregates measuring several microns. The initial alveolar deposit (IAD) was estimated as the retention 24 h after the termination of the last inhalation. The lung burden then decreased to 87% IAD after 1 month, 72% after 2 months and 69% after 3 months. About 0.4% (respectively 1%) IAD was translocated to mediastinal lymph nodes after 1 month (respectively 3 months). This indicates Type S behaviour.

(87) Christie et al. (1963) investigated the lung burden of aluminium oxide in rats and hamsters exposed by inhalation to 'aluminium powder' (20% aluminium, 80% aluminium oxide with particle sizes 0.05-7 µm) or to alumina fume produced by arcing two aluminium electrodes (particles with diameters from 0.02-0.2 µm). The powder and the fume were administered separately, hourly and every 2 h respectively throughout an 8-h day. The rats were exposed to powder or fume for 9-13 months and the resulting lung burden was assessed after sacrifice at 10, 13, 16 and 20 months. The hamsters were exposed to dust for 4-19 months and then sacrificed for assessment of the lung burden. In rats, 1-6% of the lung deposit at the end of chronic exposure to powder was still in lungs 6-7 months latter, which would indicate Type F or M behaviour. Analysis here gave $s_s = 0.009$-0.01 d^{-1}, which is consistent with assignment to Type M. Following exposure to the fume, 34–74 % of the lung deposit was still there 6-7 months after the end of exposure, suggesting Type S behaviour. Analysis here gave $s_s = 1 \times 10^{-5}$ - 7×10^{-4} d^{-1}, which is consistent with assignment to Type S. In hamsters, the level of aluminium in lungs was stable over 4-19 months of inhalation of the powder, suggesting F or M behaviour. During chronic inhalation of the fume, the lung burden increased by a factor of 4-5 from 4 to 19 months, suggesting Type S behaviour.

(88) Röllin et al. (1991) studied the tissue distribution of aluminium in rabbits chronically exposed to inhalation of aluminium oxide at 0.56 mg Al m^{-3} for 5 months. The ratio of aluminium content in the organs of the exposed animals to that in the organs of the controls, was 67 times higher in lung than in bone and even more so than in other soft tissues. As noted by the authors, the high concentration of aluminium in lung tissue confirms the very slow rate of uptake of aluminium oxide.

Table 6.6. Absorption parameter values for inhaled and ingested aluminium.

Inhaled particulate materials	Absorption parameter values*

		f_r	s_r (d^{-1})	s_s (d^{-1})	Absorption from the alimentary tract, f_A
Default parameter values[†,‡]					
Absorption type	Assigned forms				
F	-	1	30	-	0.003
M	aluminium metal	0.2	3	0.005	0.0006
S[§]	aluminium oxide, fluoride, bauxite ore, chlorhydrate, sulphate, all unspecified forms	0.01	3	0.0001	3×10^{-5}
Ingested material[¶]					
Soluble forms					0.003
Insoluble forms (oxide, hydroxide, sulphate, metal), all unspecified forms					1×10^{-4}

[*]It is assumed that the bound state can be neglected for aluminium (i.e. $f_b = 0.0$). The values of s_r for Type F, M and S forms of aluminium (30, 3 and 3 d^{-1} respectively) are the general default values.
[†]Materials (e.g. oxide) are generally listed here where there is sufficient information to assign to a default absorption type, but not to give specific parameter values (see text).
[‡]For inhaled material deposited in the respiratory tract and subsequent cleared by particle transport to the alimentary tract, the default f_A values for inhaled materials are applied [i.e. the product of f_r for the absorption type and the f_A value for ingested soluble forms of aluminium (0.003)].
[§]Default Type S is recommended for use in the absence of specific information (i.e. if the form is unknown, or if the form is known but there is no information available on the absorption of that form from the respiratory tract). For guidance on the use of specific information, see Section 1.1.
[¶]Activity transferred from systemic compartments into segments of the alimentary tract is assumed to be subject to reabsorption to blood. The default absorption fraction f_A for the secreted activity is the highest value for any form of the radionuclide ($f_A = 0.003$).

b. Aluminium metal

(89) Several studies provided data on exposure to aluminium metal, as flake powder, dust from metal cutting and milling or collected from a potroom (building housing the electrolysis cells). However, aluminium oxidises in air and exposure to aluminium metal is therefore likely to include a significant but unknown fraction of aluminium oxide that may influence the analysis of absorption.

(90) McLaughlin et al. (1962) conducted the autopsy of a man having worked for 13.5 y in the ball-mill room of an aluminium powder factory and measured the aluminium content of body tissues. This was 340-430 µg Al per g of wet lung and 5-90 µg Al per g wet weight of brain, liver and bone. Air sampling was performed at the workplace that gave average dust concentrations of 0.94-1.75 mg m^{-3} containing 60-71% aluminium and flakes of diameter up to 35 µm. The comparison of the long-term body retention with the measured exposure at the workplace and the relative concentrations of aluminium in lung and in systemic tissues indicate Type M or Type S behaviour.

(91) As explained above, Mussi et al. (1984) monitored aluminium in urine and plasma, and airborne aluminium at the workplace, of seven workers exposed for 6 months to aluminium dust from polishing and shape cutting or to aluminium welding fumes. Analysis here of the data suggested assignment to Type S of inhaled aluminium in both dust and fumes.

(92) Ljunggren et al. (1991) investigated the blood and urine concentrations of aluminium in 13 workers exposed to aluminium flake powder, before and after 4-5 weeks of vacation, and

among 10 other workers, before and after retirement. The powder consisted of flakes of aluminium metal plus some aluminium oxide, of diameter 5-200 µm and thickness 0.05-1 µm. Urinary concentration of aluminium was 80-90 times higher in currently exposed workers than in occupationally non-exposed persons. After vacations, a median decrease of 36% was observed. After retirement, aluminium in urine decreased with half-lives from less than 1 to 8 y depending on the number of years since retirement. The observed variations in urinary aluminium would be compatible with Type M or Type S behaviour.

(93) As explained above, Pierre et al. (1998) studied the individual exposure and plasma and urine levels of aluminium for 335 workers from 7 aluminium industry plants. Detailed air and urine data are provided for 6 individuals monitored over a week (Table 6.4). The dust sampled close to the electrolysis tanks was 30-50% soluble in water, and this type of exposure corresponded to relatively high aluminium excretion. However, the highest urinary concentrations were encountered in the case of exposure to aluminium powder whose aqueous solubility was very low in the experimental conditions employed. Analysis here of the urine and exposure data gave the absorption parameter values of Table 6.5 and assignment to Type M or S for exposure to aluminium metal.

(94) Röllin et al. (2001) investigated the aluminium uptake and excretion of 115 newly employed potroom workers during the construction of an aluminium smelter and up to 1 y into full production. Air, blood and urine samples were collected over 3 y. Analysis here of the results gave $f_r = 0.04$ and $s_s = 0.003$ d^{-1}. This is consistent with assignment to Type M.

(95) As explained above, Riihimäki et al. (2008) assessed the airborne and internal aluminium exposure of 12 aluminium welders and fitters in a shipyard and 5 manufacturers of aluminium sulphate. The fitters were exposed to grinding and polishing dusts containing larger particles of metallic aluminium and its oxide. Analysis here of the data for a fitter (Worker A) suggested $f_r = 0.1$ and $s_s = 1 \times 10^{-4}$ d^{-1}. This is consistent with assignment to Type S.

c. Aluminium fluoride (AlF_3)

(96) As explained above, Pierre et al. (1995) investigated the variations of atmospheric concentration of aluminium and fluorine compounds at workplaces and of the corresponding urinary excretion of the two elements in 16 male workers over a working week. Detailed air and urine data are provided for 6 individuals (Table 6.2). Analysis here of the urine and exposure data for Worker A1 gave assignment to Type S for AlF_3 dust (Table 6.3).

(97) As already mentioned, Pierre et al. (1998) studied the individual exposure and plasma and urine levels of aluminium for 335 workers from 7 aluminium industry plants. Detailed air and urine data are provided for 6 individuals monitored over a week (Table 6.4). The authors estimated the solubility of aluminium fluoride compounds to be low. Analysis here of the urine and exposure data of worker 3 gave assignment to Type S for aluminium fluoride (Table 6.5).

d. Bauxite ore [mainly $Al(OH)_3$]

(98) Pierre et al. (1998) estimated the solubility of aluminium hydroxide to be low. Analysis here of the urine and exposure data of worker 1 gave assignment to Type S for bauxite ore (Table 6.5).

(99) As explained above, Riihimäki et al. (2008) assessed the airborne and internal aluminium exposure of 12 aluminium welders and fitters in a shipyard and 5 manufacturers of aluminium sulphate ($Al_2(SO_4)_3$). The manufacturers were exposed to water insoluble bauxite ore and to water soluble aluminium sulphate, as dusts of particles with diameters from 1 to 10

μm. For the aluminium sulphate plant workers, a mean rapidly absorbed fraction $f_r = 0.067$ was estimated by the authors, consistent with assignment to Type S.

e. Aluminium chlorhydrate [$Al_2(OH)_5Cl(H_2O)_x$]

(100) Aluminium chlorhydrate (ACH) is a common ingredient in antiperspirant deodorants. Steinhagen et al. (1978) studied the distribution and effects of aluminium in the body of rats and guinea pigs exposed by inhalation to ACH of MMAD 1.2-1.6 μm for 6 months at levels 0.25-25 mg m^{-3}. Blood, heart, lung, liver, kidney, spleen and brain tissues were analysed but aluminium could be detected only in lungs and peribronchial lymph nodes. The absence of detectable aluminium in systemic tissues, even after 6 months of exposure at the highest level suggests poor absorption from the lung. Stone et al. (1979) conducted a similar study for 2 y. Again, no aluminium in excess of the control value was detected in systemic tissues, except for the adrenals of rats exposed to medium and high levels of ACH. The long-term accumulation of aluminium in lung and peribronchial lymph nodes, despite mucociliary clearance, and the lack of increased aluminium concentration in systemic organs except adrenals points toward absorption Type S.

f. Unspecified compounds

(101) Teraoka (1981) reported the concentrations of 24 elements, including aluminium, in internal organs from 12 healthy males and 7 metal workers in Japan, immediately after postmortem examination. On average, aluminium concentration was about 15 times higher in lungs than in other soft tissues at the time of death, and 50 times higher in hilar lymph nodes than in systemic soft tissues. This distribution would point toward inhalation of insoluble aluminium compounds.

(102) Gitelman (1995) reported the means and confidence intervals for aluminium inhalation exposures and urinary excretion among 279 workers from reduction, extrusion, powder, paste, forge, cable, aluminium and rolling mills from 15 plants representative of the US aluminium industry, divided into two groups based on the median exposure to aluminium. The low-exposure group was exposed to a geometric mean of 7 μg Al m^{-3} and excreted on average 9.4 μg Al per g creatinine. The high-exposure group was exposed to a geometric mean of 550 μg Al m^{-3} and excreted on average 15.1 μg Al per g creatinine. A control group was exposed to a geometric mean of 3 μg Al m^{-3} and excreted on average 6.3 μg Al per g creatinine. All those workers had been employed for a minimum of 2 years and a median duration of 9 years. Under standard assumptions for exposure, those data would be consistent with Type S absorption of inhaled aluminium.

6.2.1.2. Rapid dissolution rate for aluminium

(103) No reliable estimates have been made of the rapid dissolution rate of aluminium in particulate form. The general default value of 30 d^{-1} is therefore applied to all Type F forms of aluminium.

6.2.1.3. Extent of binding of aluminium to the respiratory tract

(104) No evidence was found for binding of aluminium to the respiratory tract. It is therefore assumed that the bound state can be neglected for aluminium (i.e. $f_b = 0.0$).

6.2.2. Ingestion

6.2.2.1. Human studies

(105) Hohl et al. (1994) measured ^{26}Al by mass spectrometry in blood and urine of two volunteers over 23 days after ingestion of the chloride ($AlCl_3$), which indicated fractional absorption in the range of 0.1%. Two young male adults ingested ^{26}Al in tap water after overnight fasting. Gastrointestinal uptake determined from the measurement of blood and was on average 0.22% of the ingested dose (Priest et al., 1998). Steinhausen et al. (2004) studied the biokinetics of aluminium in 6 healthy volunteers and 2 patients with chronic renal failure. Fractional intestinal absorption in the range of 0.1% of aluminium ingested as the chloride was derived from measurement of blood and urine samples.

(106) Weberg and Berstad (1986) measured the increase of aluminium concentration in serum and urine of ten healthy subjects after ingestion of aluminium hydroxide antacids and estimated fractional absorption of 0.004% based on 72 hour excretion. This increased to 0.03 and 0.2% when the antacids were ingested with orange juice and citric acid respectively. Haram et al. (1987) compared the absorption of aluminium from sucralfate (a sucrose aluminium sulphate and aluminium hydroxide complex) and an aluminium hydroxide-containing antacid. The measurement of daily urinary excretion before and after drug administration indicated similar absorption of about 0.005% ingested aluminium. Priest et al. (1996) assessed the fractional absorption of ingested aluminium to be 0.5% from citrate and 0.01% from hydroxide in two volunteers, from the measurement of ^{26}Al content in blood (over 24h), urine and faeces (over 6 days) of two volunteers. The administration of aluminium hydroxide together with citrate increased absorption to 0.14%. Mashitsuka and Inoue (1998) compared the aluminium intake and urinary excretion of 4 volunteers ingesting an aluminium hydroxide gel with those of 9 volunteers ingesting only ordinary food. They derived fractional aluminium absorption from aluminium hydroxide of 0.003%.

6.2.2.2. Animal studies

(107) Yokel and McNamara (1988) evaluated the uptake of aluminium in different chemical forms (Table 6.7) by comparing plasma concentration over time after oral and intravenous administration to 10 rabbits. Partial nephrectomy did not significantly affect aluminium absorption in ten other animals, except for an increase to 4.6% for aluminium citrate. By monitoring urinary excretion after gastric gavage, Froment et al. (1989) estimated absorption in rats for several of these aluminium compounds (Table 6.7). Wilhelm et al. (1992) estimated a 0.02% fractional absorption of aluminium lactate in rats by comparison of aluminium in blood after intravenous and intragastric administration. Administrating lower doses of ^{26}Al to 9 rats by gavage and following blood and urine aluminium content, Schönholzer et al. (1997) estimated fractional intestinal absorption for hydroxide, citrate and matotate and the influence of sodium citrate addition (Table 6.7). The fractional absorption of aluminium from the food additive acidic sodium aluminium phosphate (SALP) was estimated at about 0.1% in rats (Yokel and Florence, 2006). EFSA (2011) evaluated a more recent study from the industry on the oral bioavailability of various aluminium compounds, including several common food additives (Table 6.7). The carcass ^{26}Al content was measured 7 days after intravenous and oral administration to groups of 6 rats. However the level of ^{26}Al after ingestion of aluminium metal and SALP was below the limit of detection. When comparing the bioavailability of orally gavaged aluminium citrate, nitrate, chloride, sulphate and hydroxide in rats for 7 or 14 days, Poirier et al. (2011) noted little differences in blood and tissue concentrations, except for significantly higher aluminium content in rats gavaged with aluminium citrate. Despite a continued aluminium intake, blood and tissue contents decreased between 7 and 14 days.

Table 6.7. Gastrointestinal absorption of aluminium in various chemical forms given by gavage to rabbits (Yokel and McNamara, 1988) and rats (Froment et al., 1989; Wilhelm et al., 1992; Schönholzer et al., 1997; Yokel and Florence, 2006; EFSA, 2011).

Aluminium chemical form	Fractional absorption (%)					
Study	Yokel and McNamara 1988	Froment et al. 1989a	Schönholzer et al. 1992	Wilhelm et al. 1992	Yokel and Florence, 2006	EFSA 2011
acidic SALP	-	-	-	-	0.1	< 0.024
Allura Red AC aluminium lake	-	-	-	-	-	0.093
basic SALP	-	-	-	-	-	< 0.015
borate	0.27	-	-	-	-	-
chloride	0.57	0.037	-	-	-	0.054
citrate	2.18	1.49	0.7	-	-	0.079
citrate + sodium citrate	-	-	5	-	-	-
glycinate	0.39	-	-	-	-	-
hydroxide	0.45	0.015	0.1	-	-	0.025
lactate	0.63	0.037	-	0.02	-	-
maltotate	-	-	0.1	-	-	-
metal	-	-	-	-	-	< 0.015
nitrate	1.16	-	-	-	-	0.045
oxide	-	-	-	-	-	0.018
powdered pot electrolyte	-	-	-	-	-	0.042
sodium aluminium silicate	-	-	-	-	-	0.12
sucralfate	0.60	0.015	-	-	-	-
sulphate	-	-	-	-	-	0.21

(108) An absorption value of 0.01 was recommended in *Publications 30* and *68* (ICRP, 1981, 1994a) for all compounds of aluminium. The new available data allow more precise estimate for gastrointestinal absorption of aluminium in different forms. In this publication, a f_A value of 0.003 is adopted for soluble forms of aluminium, including aluminium chloride. A lower value of 1×10^{-4} is adopted for insoluble forms, including aluminium metal, oxide, hydroxide and sulphate.

6.2.3. Systemic distribution, retention and excretion of aluminium

6.2.3.1. Biokinetic data

(109) Aluminium (Al) is the most abundant metal in the earth's crust. It is not an essential element but is of interest to nutritionists because of its interactions with nutrients such as phosphorus, calcium, magnesium, iron, and vitamin D. It is of interest to toxicologists because of the potential adverse heath effects of aluminium-containing products (Greger, 1993).

(110) The preponderance of absorbed aluminium binds to the circulating iron-transport protein transferrin, which has receptors in many tissues. As much as 15-20% of aluminium entering blood forms small-molecule complexes that presumably are readily excreted (DeVoto and Yokel, 1994). Urinary losses accounts for more than 90% of endogenous excretion of aluminium. Biliary secretion accounted for ≤2% of total excretion of aluminium in human subjects, dogs, rabbits, and rats (Yokel and McNamara, 2001). Post-mortem measurements of

aluminium in 17 tissues of up to 68 adult male subjects indicate a central total-body content of ~0.2 g, with lungs, bone, and soft tissues containing about 13%, 31%, and 55%, respectively, of the total-body content (Zhu et al., 2010). These values are reasonably consistent with conclusions of Skalsky and Carchman (1983), who use published autopsy data to estimate ~0.3 g aluminium in the adult human body, with lungs, bone, and soft tissues containing about 12%, 40%, and 47%, respectively.

(111) The gastrointestinal absorption and systemic biokinetics of aluminium have been difficult to characterise due to difficulties in identifying a suitable tracer (Greger, 1993; Priest, 2004). Except for the long-lived isotope ^{26}Al ($T_{1/2} = 7.2 \times 10^5$ y), radioisotopes of aluminium have half-lives less than 10 min. Application of ^{26}Al in biokinetic studies has been limited by its scarcity and high cost. Until the early 1990s, studies of aluminium biokinetics in human subjects were limited to administration of the stable isotope ^{27}Al. Human studies of ^{26}Al biokinetics initiated in 1991 provided improved information on the bioavailability, blood clearance, excretion pattern, long-term retention, and variable kinetics of aluminium in the human body (Priest, 1997).

(112) Priest et al. (1995) investigated the systemic kinetics of ^{26}Al administered intravenously as citrate to a healthy adult male volunteer. Activity disappeared rapidly from blood. Less than 1% of the injected amount remained in blood after 2 d. Cumulative urinary and faecal excretion accounted for 83% and 1.8%, respectively, of the administered amount after 13 d. Total-body retention of the retained ~15% declined to ~4% by 1178 d. A long-term biological half-time of 7 y was estimated.

(113) Talbot et al. (1995) studied the biokinetics of ^{26}Al in six healthy adult males over 5-6 d after intravenous administration as citrate. The activity concentration in blood was in the range 3.3-13% of injected ^{26}Al L^{-1} blood at 1 h and 0.093-0.73 % L^{-1} at 1 d. Mean cumulative urinary ^{26}Al represented 59% (range, 46-74%) of injected activity at 1 d and 72% (62-83%) at 5 d. Faecal excretion accounted for about 1% of injected ^{26}Al over the first 5 d. Mean total-body retention at 5 d represented 27% (16-36%) of administered activity.

(114) In biokinetic studies on laboratory animals, the behaviour of aluminium has been found to vary with age, administered form, and route of administration, and to some extent with animal species. Important systemic repositories of aluminium identified in animal studies include bone, liver, and kidneys (Berlyne et al., 1972; Zafar et al., 1997; Wu et al., 2012). The brain shows a low uptake rate but a relatively long retention time of aluminium (Yokel, 2002).

6.2.3.2. Biokinetic model for systemic aluminium

(115) The structure of the biokinetic model for systemic aluminium applied in this publication is shown in Fig. 6.1. Transfer coefficients are listed inTable 6.8. Parameter values are set primarily for consistency of model predictions and two primary data sets: blood clearance, urinary and faecal excretion rates, and total-body retention of intravenously administered ^{26}Al in human subjects (Priest et al., 1995; Talbot et al., 1995), and the distribution of aluminium in adult male humans as indicated by autopsy data (Skalsky and Carchman, 1983; Zhu et al., 2010).

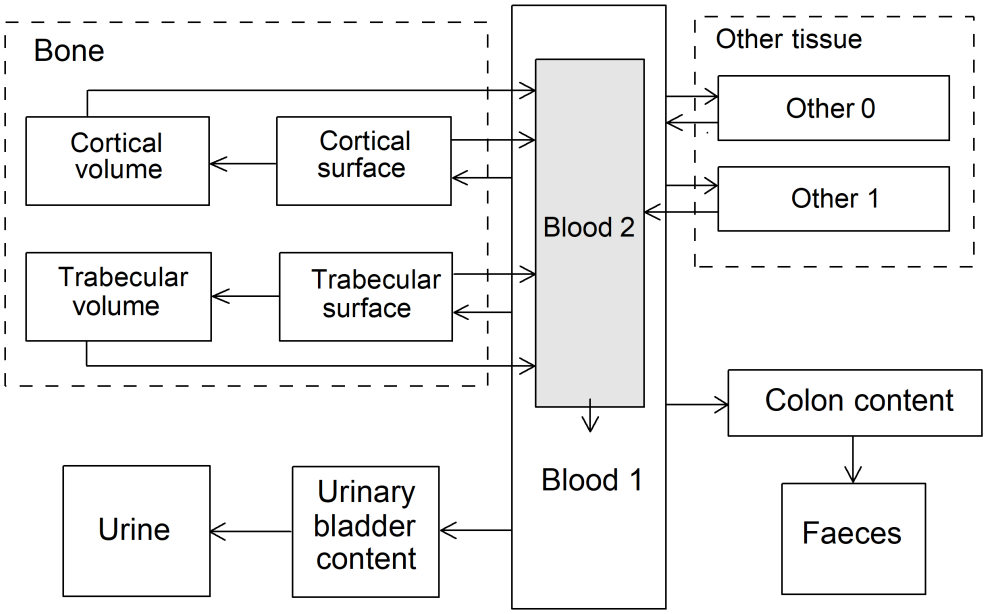

Fig. 6.1. Structure of the biokinetic model for systemic aluminium.

Table 6.8 Transfer coefficients in the biokinetic model for systemic aluminium.

From	To	Transfer coefficients (d^{-1})
Blood 1	Urinary bladder content	9.98
Blood 1	Right colon content	0.166
Blood 1	Trabecular bone surface	0.0832
Blood 1	Cortical bone surface	0.0832
Blood 1	Other 0	5.74
Blood 1	Other 1	0.582
Blood 2	Blood 1	0.035
Other 0	Blood 1	0.5
Other 1	Blood 2	0.0005
Trabecular bone surface	Blood 2	0.000493
Trabecular bone surface	Trabecular bone volume	0.000247
Trabecular bone volume	Blood 2	0.000493
Cortical bone surface	Blood 2	0.0000821
Cortical bone surface	Cortical bone volume	0.0000411
Cortical bone volume	Blood 2	0.0000821

6.3. Individual monitoring

(116) Information of detection limit for routine individual measurement is not available.

6.4. Dosimetric data for aluminium

Table 6.9. Committed effective dose coefficients (Sv Bq^{-1}) for the inhalation or ingestion of ^{26}Al compounds

Inhaled particulate materials	Effective dose coefficients (Sv Bq^{-1})

(5 µm AMAD aerosols)	^{26}Al
Type F, — NB: Type F should not be assumed without evidence	1.2E-08
Type M, aluminium metal	1.1E-08
Type S, Aluminium oxide, fluoride, bauxite ore, chlorhydrate, sulphate, all unspecified forms	2.0E-07
Ingested materials	
Soluble forms	1.3E-09
Insoluble forms (oxide, hydroxide, sulphate, metal), all unspecified forms	1.2E-09

AMAD, activity median aerodynamic diameter

7. SILICON (Z=14)

7.1. Isotopes

Table 7.1. Isotopes of silicon addressed in this publication.

Isotope	Physical half-life	Decay mode
^{31}Si	157.3 min	B-
^{32}Si*	132 y	B-

B-, beta-minus decay

*Dose coefficients and bioassay data for this radionuclide are given in the printed copy of this publication. Data for other radionuclides listed in this table are given in the online electronic files on the ICRP website.

7.2. Routes of Intake

7.2.1. Inhalation

(117) For silicon, default parameter values were adopted on absorption to blood from the respiratory tract (ICRP, 2015). Absorption parameter values and types, and associated f_A values for particulate forms of silicon are given in Table 7.2.

Table 7.2. Absorption parameter values for inhaled and ingested silicon.

	Absorption parameter values*			
Inhaled particulate materials	f_r	s_r (d^{-1})	s_s (d^{-1})	Absorption from the alimentary tract, f_A
Default parameter values†				
Absorption type				
F	1	30	–	0.5
M‡	0.2	3	0.005	0.1
S	0.01	3	1×10^{-4}	0.005
Ingested materials§				
Silicon dioxide and silicates				0.01
Orthosilicic acid				0.5

*It is assumed that the bound state can be neglected for silicon (i.e. $f_b = 0$). The values of s_r for Type F, M and S forms of silicon (30, 3 and 3 d^{-1} respectively) are the general default values.

†For inhaled material deposited in the respiratory tract and subsequently cleared by particle transport to the alimentary tract, the default f_A values for inhaled materials are applied [i.e. the product of f_r for the absorption type and the f_A value for ingested soluble forms of silicon (0.5)].

‡Default Type M is recommended for use in the absence of specific information on which the exposure material can be assigned to an absorption type (e.g. if the form is unknown, or if the form is known but there is no information available on the absorption of that form from the respiratory tract). For guidance on the use of specific information, see Section 1.1.

§Activity transferred from systemic compartments into segments of the alimentary tract is assumed to be subject to reabsorption to blood. The default absorption fraction f_A for the secreted activity is the highest value for any form of the radionuclide ($f_A = 0.5$).

7.2.2. Ingestion

(118) Silicon occurs naturally in food as silicon dioxide and silicates. Orthosilicic acid, formed by hydration of the oxide, is the major silicon species present in drinking water and other liquids and a natural biological form of silicon (EFSA, 2009). All forms of silica are considered to be poorly soluble particles which absorption is not well documented (ATSDR,

2017). Early balance studies in animals and limited human data indicate low absorption of silicon dioxide and silicates in diet: less than 5% from magnesium trisilicate, < 2% from talc and < 0.5% from silica (EFSA, 2018a,b). However, orthosilicic acid is readily absorbed (20-75%) from the gastro-intestinal tract in humans (Popplewell et al., 1998; Sripanyakorn et al., 2004, 2009; EFSA, 2009; Van Paemel et al., 2010).

(119) In *Publications 30* and *68* (ICRP, 1981, 1994a), f_1 was taken to be 0.01 for all compounds of silicon. In this publication a value of $f_A = 0.01$ is used for silicon dioxide and silicates, and a larger $f_A = 0.5$ is adopted for orthosilicic acid.

7.2.3. Systemic distribution, retention and excretion of silicon

7.2.3.1. Biokinetic data

(120) Silicon is the second most abundant element in the earth's crust, following oxygen. It is a member of Group VIA of the periodic table and a chemical and biological analogue of the heavier Group VIA element germanium (Mehard and Volcani, 1975). Silicon is rarely found in its elemental form but is usually combined with oxygen to form silica (SiO_2) or silicates (Jugdaohsingh, 2007). Silicon is present in all tissues of the human body. Excretion of systemic silicon is predominantly in urine. There is evidence of a beneficial role of silicon in bone formation (Jugdaohsingh, 2007).

(121) Absorption and urinary excretion of ingested ^{32}Si ($T_{1/2}$ =132 y) were measured over the first 2 d in a healthy male subject, age 59 y (Popplewell et al., 1998). Urinary ^{32}Si accounted for about 34% of the administered amount over 0-12 h, 1% over 12-24 h, and 0.5% over 24-48 h.

(122) Sauer et al. (1959) measured the concentration of ^{31}Si in liver, kidneys, muscle, brain, and blood of guinea pigs over the first 8 h after oral administration of $^{31}SiO_2$. At all measurement times the highest concentration was found in kidney, but the liver contained roughly twice as much and the skeletal muscle 20-50 times as much total activity as the kidneys.

(123) Adler et al. (1986) examined the biokinetics of ^{31}Si in rats after intracardiac injection of $^{31}Si(OH)_4$. Activity in blood was nearly equally distributed between plasma and erythrocytes. Activity in plasma was associated almost entirely with protein-free filtrate. From 1-4 h after injection the concentration in plasma decreased with a half-time of ~1 h. The highest tissue concentration at 1-2 h was found in kidney. At 3 h nearly equal concentrations were seen in kidney and liver. Initially, ~85% of total-body activity was found in skin, muscle, and bone. An increasing concentration ratio of bone to plasma was observed over the first few hours.

(124) Berlyne et al. (1986) studied the distribution of ^{31}Si in rats 30 min after its injection as ^{31}S-labelled silicic acid. Activity concentrations were measured in 10 tissues. The highest concentration was found in kidney, followed by skin and testis (each 0.35, normalised to 1.0 for kidney), bone (0.30), and liver (0.25). The skeletal muscle, skin, bone, liver, and kidneys contained about 15%, 11%, 3.4%, 1.6%, and 1.5%, respectively, of the administered amount.

(125) Mehard and Volcani (1975) compared the behaviours of ^{31}Si ($T_{1/2}$ = 157 min) and ^{68}Ge (271 d) in rats following intravenous (IV) or intraperitoneal (IP) administration of $^{31}Si(OH)_4$ and $^{68}Ge(OH)_4$. Following IV or IP injection, accumulation of ^{31}Si and ^{68}Ge in tissues increased for about 15-40 min, declined rapidly for about 30 min, and then declined more gradually. The distribution of ^{31}Si differed somewhat for IV and IP injection. The peak concentration of ^{31}Si in kidney was about 3 times that in liver following IV injection and about 5 times that in liver following IP injection. An apparent difference in kinetics of ^{68}Ge and ^{31}Si was more rapid depletion of ^{68}Ge. The concentration of ^{31}Si in the liver was moderately higher than that of ^{68}Ge over the first two hours after intravenous injection.

7.2.3.2. Biokinetic model for systemic silicon

(126) The structure of the biokinetic model for systemic silicon used in this publication is shown in Fig. 7.1. Transfer coefficients are listed in Table 7.3.

(127) The model is a modification of the systemic model for germanium, a chemical and biological analogue of silicon (see Section 18.2.3). Based on results of a detailed comparative study of the behaviour of ^{68}Ge and ^{31}Si in rats at the total body, tissue, and subcellular levels (Mehard and Volcani, 1975), it is assumed that the systemic kinetics of germanium and silicon are qualitatively similar but differ quantitively due to slower urinary loss of germanium associated with moderately higher deposition of silicon in systemic tissues. The deposition fractions in tissues assigned to germanium are adjusted to depict a lower flow rate of silicon from blood to the urinary bladder contents and higher flow rates of silicon to tissues, while keeping the total outflow rate of silicon from blood the same as assumed for germanium. The decrease in flow rate from blood to the urinary bladder content was set to approximate comparative observed concentrations of ^{68}Ge and ^{31}Si in rats over the first 2 h after their intravenous injection (Mehard and Volcani, 1975). The increases in germanium flow rates to tissues applied to silicon were proportional to the flow rates of germanium from blood to individual systemic tissues (kidney, liver, bone, and other tissue).

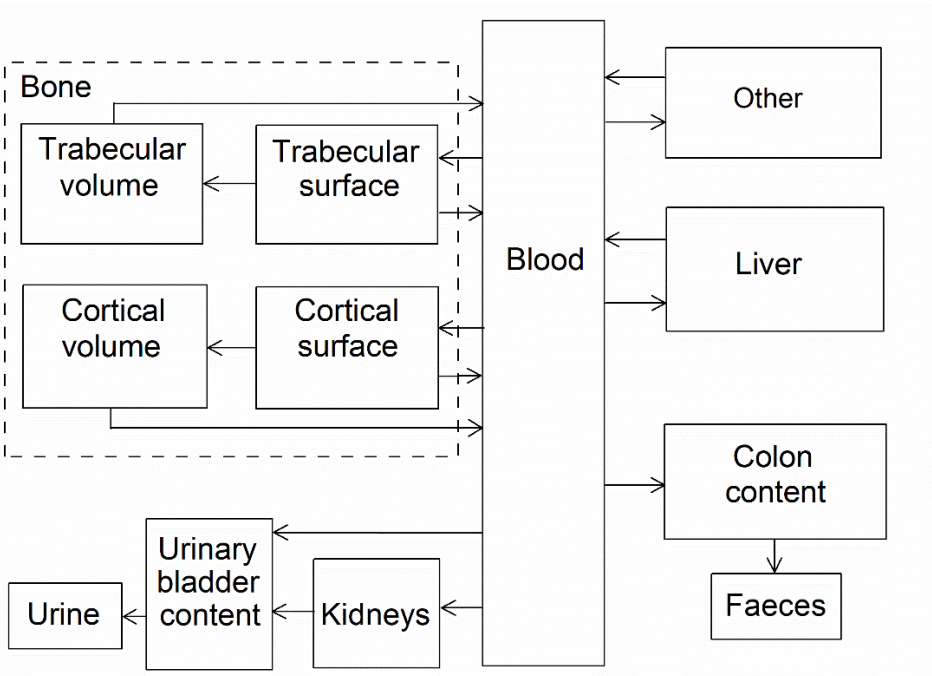

Fig. 7.1. Structure of the biokinetic model for systemic silicon.

Table 7.3. Transfer coefficients (d-1) in the biokinetic model for systemic silicon.

From	To	Transfer coefficient (d^{-1})
Blood	Other	1.204
Blood	Kidneys	0.2706
Blood	Liver	0.5412
Blood	Urinary bladder content	7.7
Blood	Right colon content	0.01353
Blood	Trabecular bone surface	0.1353
Blood	Cortical bone surface	0.1353

Other	Blood	0.3
Kidneys	Urinary bladder content	1.2
Liver	Blood	0.9
Trabecular bone surface	Blood	0.3
Cortical bone surface	Blood	0.3
Trabecular bone surface	Trabecular bone volume	0.0015
Cortical bone surface	Cortical bone volume	0.0015
Trabecular bone volume	Blood	0.000493
Cortical bone volume	Blood	0.0000821

7.2.3.3. Treatment of progeny

(128) The only progeny of silicon addressed in this publication is ^{32}P as a progeny of ^{32}Si. The characteristic model for phosphorus (ICRP, 2016) was expanded for application to ^{32}P as a progeny of ^{32}Si with added compartments and associated transfer coefficients needed to solve the linked biokinetic models for silicon and phosphorus (see Annex B). If produced in a compartment not contained in the characteristic model for phosphorus, ^{32}P is assumed to transfer to the central blood compartment of the phosphorous model at the rate 0.3466 d^{-1} and to follow that model thereafter.

7.3. Individual monitoring

(129) Information of detection limit for routine individual measurement is not available.

7.4. Dosimetric data for silicon

Table 7.4 Committed effective dose coefficients (Sv Bq^{-1}) for the inhalation or ingestion of ^{32}Si compounds.

Inhaled particulate materials (5 µm AMAD aerosols)	Effective dose coefficients (Sv Bq^{-1}) ^{32}Si
Type F, — NB: Type F should not be assumed without evidence	1.2E-10
Type M, default	6.4E-09
Type S	1.7E-07
Ingested materials	
Silicon dioxide and silicates	3.8E-11
Orthosilicic acid	1.1E-10

AMAD, activity median aerodynamic diameter

8. CHLORINE (Z=17)

8.1. Isotopes

Table 8.1. Isotopes of chlorine addressed in this publication.

Isotope	Physical half-life	Decay mode
^{34m}Cl	32.00 min	EC, B+, IT
^{36}Cl*	3.01E+5 y	B-, EC, B+
^{38}Cl	37.24 min	B-
^{39}Cl	55.6 min	B-

EC, electron-capture decay; B+, beta-plus decay; B-, beta-minus decay
*Dose coefficients and bioassay data for this radionuclide are given in the printed copy of this publication.
Data for other radionuclides listed in this table are given in the online electronic files on the ICRP website.

8.2. Routes of Intake

8.2.1. Inhalation

(130) For chlorine, default parameter values were adopted for the absorption to blood from the respiratory tract (ICRP, 2015). For chlorine, and the other halogens, intakes could be in both particulate and gas and vapour forms, and it is therefore assumed that inhaled chlorine is 50% particulate and 50% gas/vapour in the absence of information (ICRP, 2002b). Absorption parameter values and types, and associated f_A values for gas and vapour forms of chlorine are given in Table 8.2 and for particulate forms in Table 8.3. By analogy with the halogen iodine, considered in detail in *Publication 137* (ICRP, 2017), default Type F is recommended for particulate forms in the absence of specific information on which the exposure material can be assigned to an absorption type.

Table 8.2. Deposition and absorption for gas and vapour compounds of chlorine.

	Percentage deposited (%)*						Absorption†	
Chemical form/origin	Total	ET_1	ET_2	BB	bb	AI	Type	Absorption from the alimentary tract, f_A‡
Unspecified	100	0	20	10	20	50	F	1.0

ET_1, anterior nasal passage; ET_2, posterior nasal passage, pharynx and larynx; BB, bronchial; bb, bronchiolar; AI, alveolar-interstitial.
*Percentage deposited refers to how much of the material in the inhaled air remains in the body after exhalation. Almost all inhaled gas molecules contact airway surfaces, but usually return to the air unless they dissolve in, or react with, the surface lining. The default distribution between regions is assumed: 20% ET_2, 10% BB, 20% bb, and 50% AI.
†It is assumed that the bound state can be neglected for chlorine (i.e. $f_b = 0$).
‡For inhaled material deposited in the respiratory tract and subsequently cleared by particle transport to the alimentary tract, the default f_A values for inhaled materials are applied [i.e. the product of f_r for the absorption type(or specific value where given) and the f_A value for ingested soluble forms of chlorine (1)].

Table 8.3. Absorption parameter values for inhaled and ingested chlorine.

	Absorption parameter values*			
Inhaled particulate materials	f_r	s_r (d^{-1})	s_s (d^{-1})	Absorption from the alimentary tract, f_A
Default parameter values†				
Absorption type				
F‡	1	30	–	1
M	0.2	3	0.005	0.2

S	0.01	3	1×10^{-4}	0.01
Ingested materials[§]				
All forms	–	–	–	1

[*]It is assumed that the bound state can be neglected for chlorine (i.e. $f_b = 0$). The values of s_r for Type F, M and S forms of chlorine (30, 3 and 3 d^{-1} respectively) are the general default values.
[†]For inhaled material deposited in the respiratory tract and subsequently cleared by particle transport to the alimentary tract, the default f_A values for inhaled materials are applied [i.e. the product of f_r for the absorption type and the f_A value for ingested soluble forms of chlorine (1)].
[‡]Default Type F is recommended for use in the absence of specific information on which the exposure material can be assigned to an absorption type (e.g. if the form is unknown, or if the form is known but there is no information available on the absorption of that form from the respiratory tract). For guidance on the use of specific information, see Section 1.1.
[§]Activity transferred from systemic compartments into segments of the alimentary tract is assumed to be subject to reabsorption to blood. The default absorption fraction f_A for the secreted activity is the highest value for any form of the radionuclide ($f_A = 1$).

8.2.2. Ingestion

(131) Chlorine (Cl_2) dissolves in water and is converted into chloride (Cl^-) and hypochlorite anion (ClO^-) or hypochlorous acid (HOCl). Small quantities of chlorite (ClO_2^-), chlorate (ClO_3^-) and perchlorate (ClO_4^-) are also formed (Nakagawara et al., 1998). Mainly following the electrochemical gradient created by sodium transport, chloride is passively absorbed in the proximal small intestine and actively transported in the ileum. It is almost completely absorbed from the gut (Burrill et al., 1945; Wiseman, 1964). Perchlorate has been shown, in both human and animal studies, to be readily absorbed after oral exposure with rapid and near complete absorption through the digestive system (ATSDR, 2008). Based on short-term urinary excretion in rats, at least 20-40% of orally administered radiolabelled chlorine as hypochlorous acid, chlorate, ClO_2 or chlorite is absorbed (Abdel-Rahman et al., 1982, 1983). In non-fasted rats, the absorption of hypochlorite anion is delayed, presumably due to reaction of chlorine with biomolecules in food (Fukayama et al., 1986). Additional studies in rat, dog and swine showed 40-90% gastrointestinal absorption of chlorate salts. Data obtained after chlorate poisoning demonstrated that chlorate is also biologically available in human after ingestion (EFSA, 2015c).

(132) In *Publications 30* and *68* (ICRP, 1980, 1994a), f_1 was taken to be 1 for all compounds of chlorine. In this publication, a $f_A = 1$ is used for all chemical forms of chlorine.

8.2.3. Systemic distribution, retention and excretion of chlorine

8.2.3.1. Biokinetic data

(133) Inorganic chloride is the dominant form of chlorine in the human body. Ingested chloride is rapidly and nearly completely absorbed to blood and largely cleared from blood within a few minutes (Ray et al., 1952). It is distributed mainly in extracellular fluids. The biological half-time for the total body is typically on the order of 8-15 d (Ray et al., 1952), but the half-time can be reduced considerably by elevated intake of chloride or increased considerably by a salt-deficient diet.

(134) The systemic kinetics of chloride closely resembles that of bromide (Reid et al., 1956; Pavelka, 2004). Absorbed bromide clears rapidly from blood and replaces part of the extracellular chloride, with the molar sum of chloride and bromide remaining constant at about

110 mmol L^{-1} (Pavelka, 2004). The biological half-time of bromide in the human body typically is on the order of 12 d (Söremark, 1960b).

8.2.3.2. Biokinetics of systemic chlorine

(135) The systemic behaviour of chlorine is assumed to be the same as that of bromine. The relevant physiological forms of chlorine and bromine are assumed to be chloride and bromide, respectively. The common biokinetic model for chloride and bromide is based on the assumptions of rapid removal from blood ($T_{1/2}$ = 5 min), a uniform distribution in tissues, removal of 50% of absorbed chloride or bromide from the body in 12 d, and a urinary to faecal excretion ratio of 100:1. These conditions are approximated, using a first-order recycling model, with the transfer coefficients listed in Table 8.4.

Table 8.4. Transfer coefficients in the biokinetic model for systemic bromine.

From	To	Transfer coefficient (d^{-1})
Blood	Other	200
Blood	Urinary bladder content	0.83
Blood	Right colon content	0.0083
Other	Blood	15

8.2.3.3. Treatment of progeny

(136) Progeny of chlorine addressed in this publication are radioisotopes of chlorine and argon. The model for chlorine as a parent is assigned to chlorine as a progeny of chlorine. Argon produced in a tissue (i.e. in Other) is assumed to transfer to blood with a halftime of 15 min and from blood to the environment (via exhalation) at the rate 1000 d^{-1}.

8.3. Individual monitoring

8.3.1. ^{36}Cl

(137) Measurements of ^{36}Cl in urine may be used to determine intakes of the radionuclide. The main technique used for urine analysis is liquid scintillation.

Table 8.5. Monitoring techniques for ^{36}Cl.

Isotope	Monitoring Technique	Method of Measurement	Typical Detection Limit
^{36}Cl	Urine Bioassay	liquid scintillation	47 Bq L^{-1}

8.4. Dosimetric data for chlorine

Table 8.6. Committed effective dose coefficients (Sv Bq^{-1}) for the inhalation or ingestion of ^{36}Cl compounds.

	Effective dose coefficients (Sv Bq^{-1})
Inhaled gases or vapours	^{36}Cl
Unspecified	1.0E-09

Inhaled particulate materials (5 μm AMAD aerosols)	
Type F, default	7.0E-10
Type M	2.7E-09
Type S	5.2E-08
Ingested materials	
All forms	9.9E-10

AMAD, activity median aerodynamic diameter

Table 8.7 Dose per activity content of ^{36}Cl in daily excretion of urine (Sv Bq^{-1}); 5μm activity median aerodynamic diameter aerosols inhaled by a reference worker at light work.

Time after intake (d)	Gases or vapours	Type F	Type M	Type S
	Urine	Urine	Urine	Urine
1	1.9E-08	2.5E-08	5.7E-07	2.3E-04
2	1.9E-08	2.0E-08	3.7E-07	1.4E-04
3	2.1E-08	2.0E-08	3.7E-07	1.4E-04
4	2.2E-08	2.2E-08	3.9E-07	1.5E-04
5	2.3E-08	2.3E-08	4.1E-07	1.6E-04
6	2.4E-08	2.4E-08	4.3E-07	1.7E-04
7	2.6E-08	2.6E-08	4.6E-07	1.8E-04
8	2.7E-08	2.7E-08	4.9E-07	1.9E-04
9	2.9E-08	2.9E-08	5.1E-07	2.0E-04
10	3.1E-08	3.0E-08	5.4E-07	2.1E-04
15	4.1E-08	4.1E-08	7.1E-07	2.8E-04
30	9.9E-08	9.8E-08	1.6E-06	6.4E-04
45	2.4E-07	2.3E-07	3.3E-06	1.4E-03
60	5.7E-07	5.6E-07	6.2E-06	2.7E-03
90	3.3E-06	3.2E-06	1.4E-05	6.7E-03
180	6.2E-04	6.1E-04	3.5E-05	1.1E-02
365	N/A	N/A	1.2E-04	1.6E-02

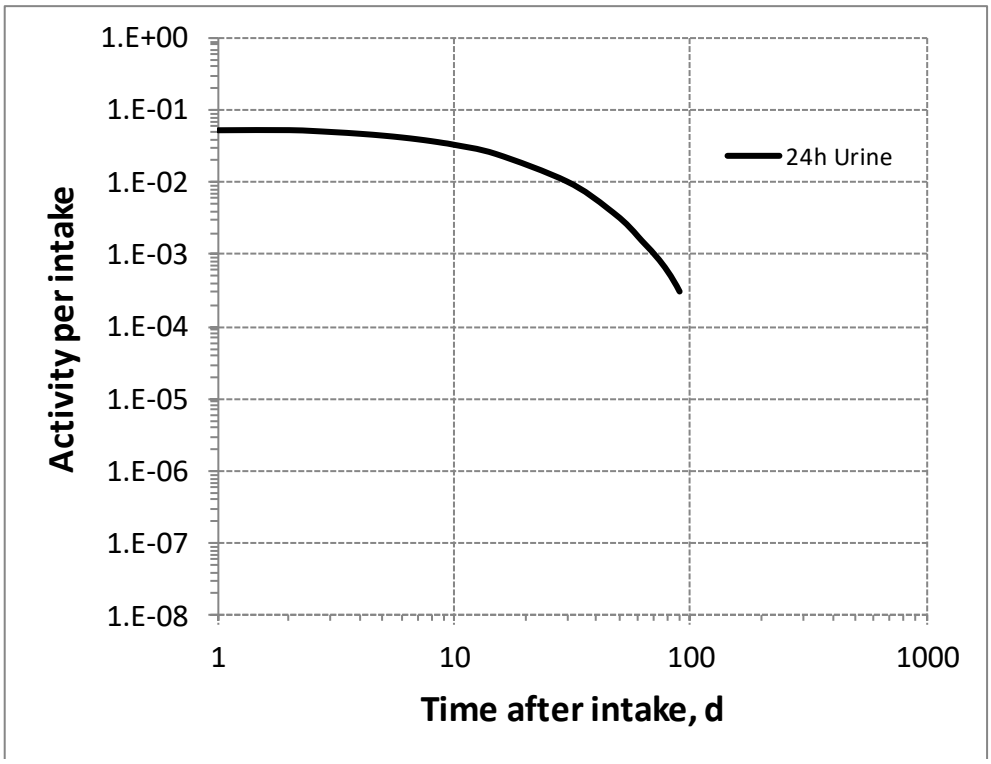

1611

1612 Fig. 8.1. Daily excretion of ^{36}Cl following inhalation of 1 Bq unspecified gases or vapours.

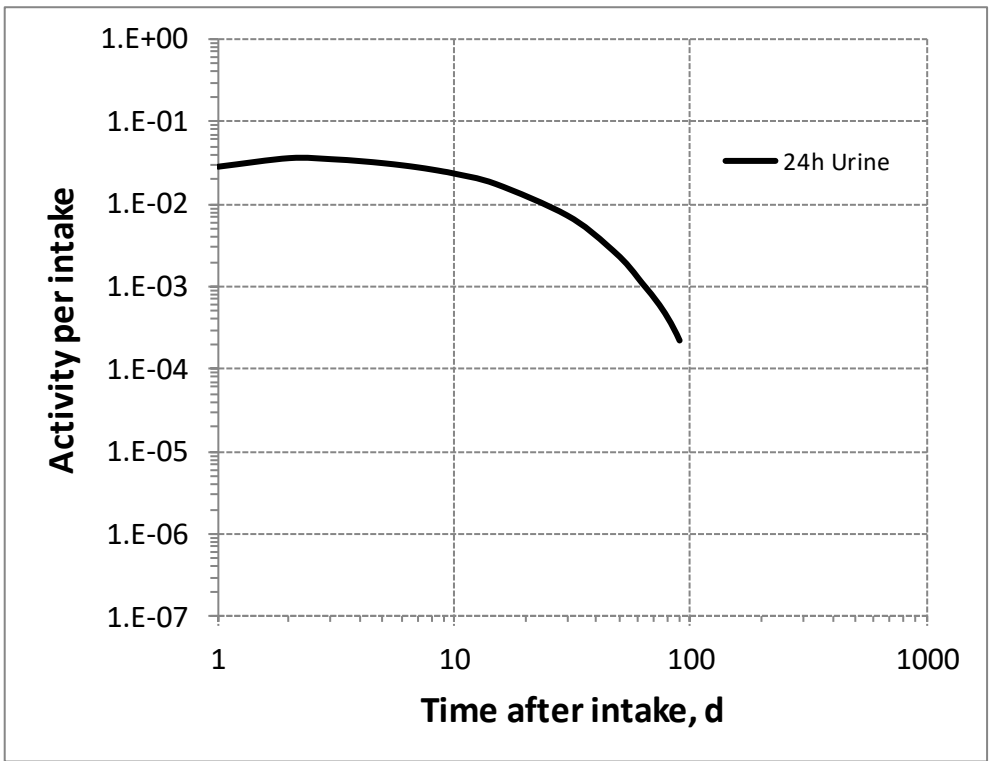

1613

1614 Fig. 8.2. Daily excretion of ^{36}Cl following inhalation of 1 Bq Type F.

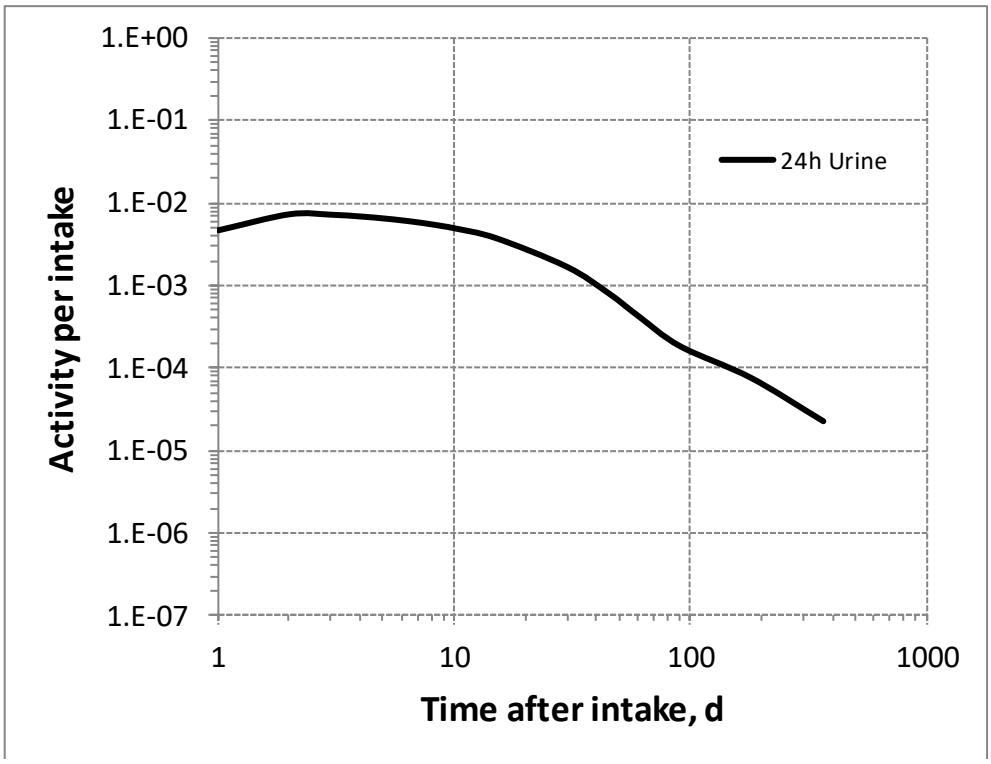

Fig. 8.3. Daily excretion of ^{36}Cl following inhalation of 1 Bq Type M.

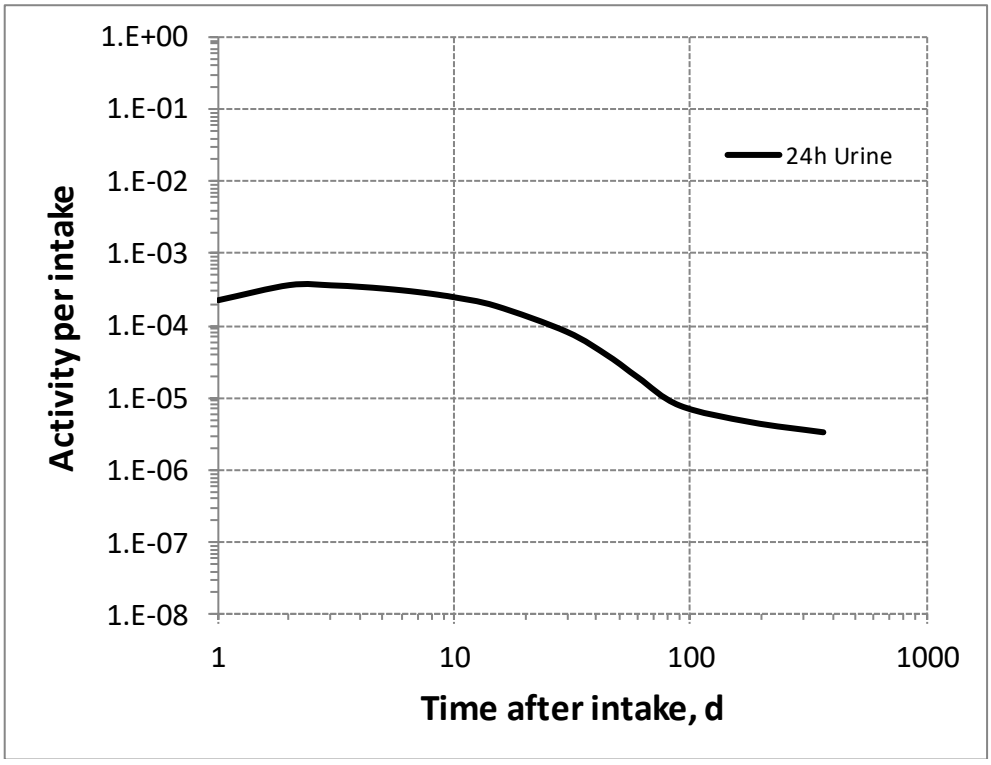

Fig. 8.4. Daily excretion of ^{36}Cl following inhalation of 1 Bq Type S.

9. POTASSIUM (Z = 19)

9.1. Isotopes

Table 9.1. Isotopes of potassium addressed in this publication.

Isotope	Physical half-life	Decay mode
^{40}K*	1.251E+9 y	B-, EC, B+
^{42}K	12.360 h	B-
^{43}K	22.3 h	B-
^{44}K	22.13 m	B-
^{45}K	17.3 m	B-

EC, electron-capture decay; B+, beta-plus decay; B-, beta-minus decay.
*Dose coefficients and bioassay data for this radionuclide are given in the printed copy of this publication.
Data for other radionuclides listed in this table are given in the online electronic files on the ICRP website.

9.2. Routes of Intake

9.2.1. Inhalation

(138) For potassium, default parameter values were adopted on absorption to blood from the respiratory tract (ICRP, 2015). Absorption parameter values and types, and associated f_A values for particulate forms of potassium are given in Table 9.2.

Table 9.2. Absorption parameter values for inhaled and ingested potassium.

	Absorption parameter values*			Absorption from the alimentary tract, f_A
Inhaled particulate materials	f_r	s_r (d^{-1})	s_s (d^{-1})	
Default parameter values†				
Absorption type				
F	1	30	–	1
M‡	0.2	3	0.005	0.2
S	0.01	3	1×10^{-4}	0.01
Ingested materials§				
All forms				1

*It is assumed that the bound state can be neglected for potassium (i.e. $f_b = 0$). The values of s_r for Type F, M and S forms of potassium (30, 3 and 3 d^{-1} respectively) are the general default values.
†For inhaled material deposited in the respiratory tract and subsequently cleared by particle transport to the alimentary tract, the default f_A values for inhaled materials are applied [i.e. the product of f_r for the absorption type and the f_A value for ingested soluble forms of potassium (1)].
‡Default Type M is recommended for use in the absence of specific information on which the exposure material can be assigned to an absorption type (e.g. if the form is unknown, or if the form is known but there is no information available on the absorption of that form from the respiratory tract). For guidance on the use of specific information, see Section 1.1.
§Activity transferred from systemic compartments into segments of the alimentary tract is assumed to be subject to reabsorption to blood. The default absorption fraction f_A for the secreted activity is the highest value for any form of the radionuclide ($f_A = 1$).

9.2.2. Ingestion

(139) Absorption of potassium mainly takes place by passive diffusion from the small intestine contents. Potassium salts are very soluble and about 90% of dietary potassium is

absorbed; while actual absorption is even slightly higher because of reabsorption of endogenous secretions into the lumen of the digestive tract (ICRP, 1975; Leggett and Williams, 1986; Demigné et al., 2004).

(140) Absorption of potassium from the gastrointestinal tract being nearly complete, f_1 has been taken to be 1 in *Publications 30* and *68*(ICRP, 1980, 1994a). In this publication, $f_A = 1$ is also used for all forms of potassium.

9.2.3. Systemic distribution, retention and excretion of potassium

9.2.3.1. Biokinetic data

(141) Potassium (K) is an essential element with multiple functions in the human body including regulation of fluid balance and control of electrical activity of the heart, skeletal muscle, and nerves. The K content of the adult human body is on average about 1.6-2.0 kg^{-1} body weight but varies with the fraction of body weight represented by skeletal muscle, which has a high concentration of K. Measurements of K concentrations in postmortem tissues and in plasma and red blood cells of living subjects indicate the following approximate distribution of K in an adult male human: skeletal muscle, 65% of the total-body content, skeleton 9%, red blood cells 8%, liver 3%, brain 3%, kidneys 0.6%, blood plasma, 0.4%, remainder 11% [based on Leggett and Williams (1986) and Zhu et al. (2010)]. About 80-90% of losses from the body are in urine, with the remainder removed mainly in faeces and sweat.

(142) About 98% of the body's K resides intracellularly, and 2% is distributed in extracellular fluids (ECF). The ECF concentration is strictly maintained in a range of about 137-215 mg L^{-1}. The kidneys are primarily responsible for homeostatic control of the body's K content through adjustment of urinary losses to accommodate variation in K intake. Adjustments in renal K excretion occur over several hours, and changes in extracellular K are buffered during that time by movement of K between skeletal muscle and blood plasma (Langham-New and Lambert, 2012; Palmer, 2015; Hinderling, 2016; Udensi and Tchounwou, 2017).

(143) Potassium is the principal intracellular cation in most tissues and is critical to maintenance of membrane potential of cells. An electrochemical gradient across the cell membrane resulting from a high intracellular concentration of K and low intracellular concentration of sodium (Na) relative to concentrations in the ECF is required to sustain intracellular tonicity, transmission of nerve impulses, contraction of muscles including heart, and maintenance of normal kidney function. The gradient is maintained predominantly by the activity of the membrane-bound transporter Na^+-K^+-ATPase, also called the Na-K pump. A single cycle of the pump moves two K ions into the cell and extrudes three Na ions (Palmer, 2015; Hinderling, 2016; Udensi and Tchounwou, 2017).

(144) The biokinetics of K has been studied extensively in human subjects and laboratory animals, and many kinetic analyses and system models for K have been published (Love and Burch, 1953; Ginsburg and Wilde, 1954; Black et al., 1955; Ginsburg, 1962; Downey and Bashour, 1975; Sterns et al., 1979; Leggett and Williams, 1986; Hinderling, 2016). Intravenously injected K is rapidly removed from blood plasma and distributed to tissues and to a lesser extent to excretion pathways (Corsa et al., 1950; Black et al., 1955; Burch et al., 1955). Following intravenous administration of radio-potassium to human subjects, about 2% remains in plasma at 20 min and 1% or less remains at 2 h (Corsa et al., 1950; Black et al., 1955). The rate of transfer from plasma to a tissue depends on the percentage of cardiac output received by the tissue and the tissue's extraction fraction (i.e. the fraction of K extracted by the tissue from plasma during passage from the tissue's arterial input to its venous output). For

example, a K extraction fraction of 0.9 has been estimated for kidneys, heart tissue, and lung tissue; 0.8 for intestines, 0.6 for liver, and 0.01-0.02 for brain (Leggett and Williams, 1986). The kidneys, which have a high extraction fraction and receive nearly one-fifth of cardiac output, accumulate as much as 20% of intravenously injected K within a few minutes after intravenous administration (Black et al., 1955; Emery et al., 1955). Tissues with a low blood perfusion rate such as fat or resting skeletal muscle, or a low extraction fraction such as brain, accumulate K relatively slowly. Tissues such as kidneys with a high rate of uptake but a relatively low content of K return much of the accumulated K to blood over a relatively short period (Black et al., 1955). Over a period of about 15 min to several hours the systemic distribution of K shifts away from tissues with relatively high blood flow and extraction to tissues with relatively low blood flow and/or extraction but high K content. By several hours after intravenous injection of radio-potassium, skeletal muscle typically contains most of the retained activity. Over the first 2-3 d after intravenous injection the red blood cells gradually accumulate several percent of the injected amount (Corsa et al., 1950). A biological half-time of ~30 d has been estimated for total-body K in adult humans, based on reference values for daily intake and total-body content and treatment of the body's K as a well-mixed pool (ICRP, 1979a).

9.2.3.2. Biokinetic model for systemic potassium

(145) A relatively detailed biokinetic model for systemic K was proposed by Leggett and Williams (1986). The model was built around a blood flow model depicting the distribution of cardiac output to 12 tissue compartments. Additional compartments were added to address transfer of K between plasma and red blood cells and between systemic pools and gastrointestinal content. Three excretion pathways were addressed: urinary loss via the kidneys, faecal loss via the intestines, and loss in sweat via skin. Movement of K was depicted as a system of first-order processes. The transfer rate from plasma into a tissue T was estimated as the product of the plasma flow rate to that tissue (that is, the fraction of cardiac output received by the tissue, times 1766 plasma volumes per day as a reference value for cardiac output, and a tissue-specific extraction fraction, E_T. The transfer rate from tissue T to plasma was estimated from the relative contents of K in plasma and T at equilibrium. The equilibrium distribution of K was based mainly on autopsy data and typical concentrations of K in plasma and red blood cells. Transfer rates between plasma and red blood cells and between systemic compartments and gastrointestinal contents were based on empirical data. Model predictions of the blood clearance, uptake and loss by systemic tissues, total-body retention, and path-specific excretion rates of K were shown to be consistent with observations for human subjects.

(146) The biokinetic model for systemic K used in this publication is a simplification of the model of Leggett and Williams (1986). The structure of the simplified model (Fig. 9.1) is more consistent with the structures of other systemic models applied in this publication series. That is, the model depicts a central blood compartment (plasma) in exchange with a set of peripheral tissue compartments representing relatively important systemic repositories. The transfer coefficients of the simplified model (Table 9.3) were set for reasonable consistency with the original model regarding retention in the total body and in individual tissues depicted explicitly in both models.

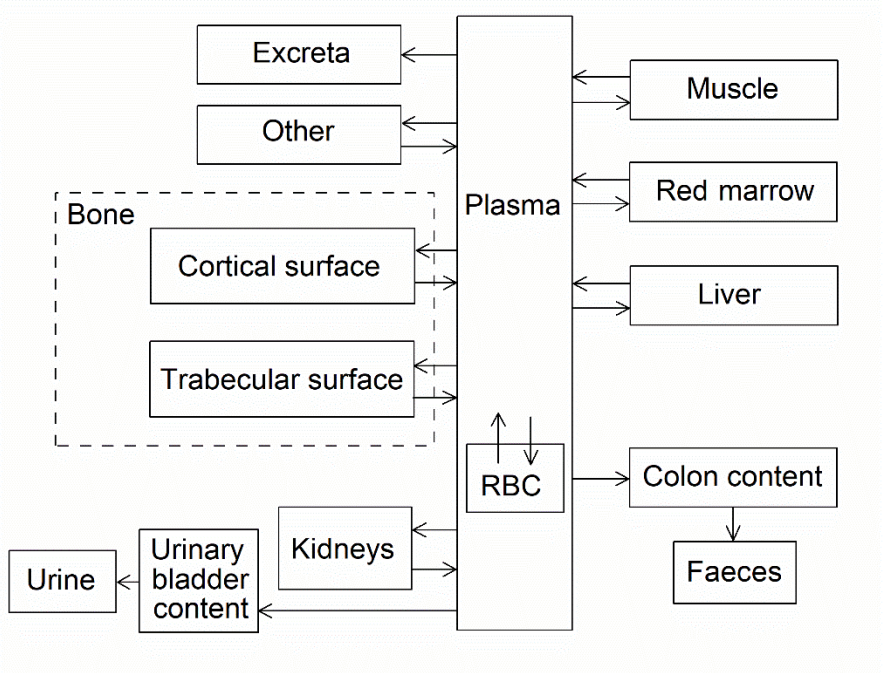

Fig. 9.1. Structure of the biokinetic model for systemic potassium.

Table 9.3. Transfer coefficients in the biokinetic model for systemic potassium.

From	To	Transfer coefficient (d^{-1})
Plasma	RBC	6
Plasma	Kidneys	257
Plasma	Liver	230
Plasma	Muscle	255
Plasma	Trabecular bone surface	16.8
Plasma	Cortical bone surface	11.2
Plasma	Red marrow	28
Plasma	Other	470
Plasma	Urinary bladder content	5.5
Plasma	Right colon content	0.83
Plasma	Excreta	0.2
RBC	Plasma	0.38
Kidneys	Plasma	214
Liver	Plasma	24.5
Muscle	Plasma	1.345
Trabecular bone surface	Plasma	2.67
Cortical bone surface	Plasma	2.67
Red marrow	Plasma	2.67
Other	Plasma	12

9.2.3.3. Treatment of progeny

(147) The only progeny of a potassium parent addressed in this publication is ^{45}Ca produced by decay of ^{45}K. For application to ^{45}Ca produced in systemic compartments the characteristic model for calcium (ICRP, 2016) was expanded to address explicitly each of the tissues and individual compartments addressed explicitly in the model for potassium. The following transfer coefficients from added tissue compartments to the central blood compartment of the

calcium model were assigned: red blood cells, 1000 d^{-1} (default value); kidneys, 0.1733 d^{-1}; liver, 0.1733 d^{-1}; muscle, 0.1733 d^{-1}; red marrow, 0.1733 d^{-1}; other, 2.9 d^{-1}. The following transfer coefficients from blood to tissues were also added to the calcium model: kidneys, 0.00766 d^{-1}; liver, 0.0445 d^{-1}, muscle, 0.716 d^{-1}; red marrow, 0.0289 d^{-1}. The transfer coefficient from blood to the intermediate-term soft-tissue compartments of the calcium model was reduced from 1.5 d^{-1} to 0.703 d^{-1} to leave the total outflow rate of calcium from blood at 15 d^{-1}.

9.3. Individual monitoring

9.3.1. ^{40}K

(148) Measurements of ^{40}K may be performed by *in vivo* whole-body measurement technique.

Table 9.4. Monitoring techniques for ^{40}K.

Isotope	Monitoring Technique	Method of Measurement	Typical Detection Limit
^{40}K	Urine Bioassay	γ-ray spectrometry[a]	32 Bq L^{-1}
^{40}K	Whole-body measurement	γ-ray spectrometry[ab]	360 Bq

[a] Measurement system comprised of Germanium Detectors
[b] Counting time of 20 minutes

9.4. Dosimetric data for potassium

Table 9.5. Committed effective dose coefficients (Sv Bq-1) for the inhalation or ingestion of ^{40}K compounds.

Inhaled particulate materials (5 µm AMAD aerosols)	Effective dose coefficients (Sv Bq^{-1})
	^{40}K
Type F, — NB: Type F should not be assumed without evidence	2.2E-09
Type M, default	5.8E-09
Type S	1.3E-07
Ingested materials	
All forms	3.2E-09

AMAD, activity median aerodynamic diameter

Table 9.6. Dose per activity content of ^{40}K in total body and in daily excretion of urine (Sv Bq^{-1}); 5µm activity median aerodynamic diameter aerosols inhaled by a reference worker at light work.

	Type F		Type M		Type S	
Time after intake (d)	Total body	Urine	Total body	Urine	Total body	Urine
1	3.2E-09	1.4E-07	9.2E-09	2.0E-06	2.1E-07	9.4E-04
2	3.4E-09	1.6E-07	1.5E-08	2.0E-06	3.9E-07	9.1E-04
3	3.5E-09	1.7E-07	2.3E-08	2.2E-06	8.3E-07	9.8E-04
4	3.6E-09	1.8E-07	2.9E-08	2.2E-06	1.4E-06	1.0E-03
5	3.6E-09	1.8E-07	3.2E-08	2.3E-06	1.8E-06	1.0E-03

6	3.7E-09	1.9E-07	3.4E-08	2.3E-06	2.0E-06	1.1E-03
7	3.8E-09	1.9E-07	3.5E-08	2.4E-06	2.1E-06	1.1E-03
8	3.9E-09	2.0E-07	3.5E-08	2.5E-06	2.1E-06	1.1E-03
9	4.0E-09	2.0E-07	3.6E-08	2.5E-06	2.1E-06	1.1E-03
10	4.1E-09	2.1E-07	3.7E-08	2.6E-06	2.2E-06	1.2E-03
15	4.6E-09	2.3E-07	4.0E-08	2.8E-06	2.2E-06	1.3E-03
30	6.5E-09	3.3E-07	5.2E-08	3.9E-06	2.4E-06	1.8E-03
45	9.2E-09	4.7E-07	6.6E-08	5.3E-06	2.5E-06	2.5E-03
60	1.3E-08	6.6E-07	8.2E-08	7.1E-06	2.6E-06	3.4E-03
90	2.6E-08	1.3E-06	1.2E-07	1.2E-05	2.8E-06	6.0E-03
180	2.1E-07	1.1E-05	3.1E-07	4.8E-05	3.4E-06	2.1E-02
365	1.5E-05	7.8E-04	1.1E-06	2.4E-04	4.5E-06	4.4E-02

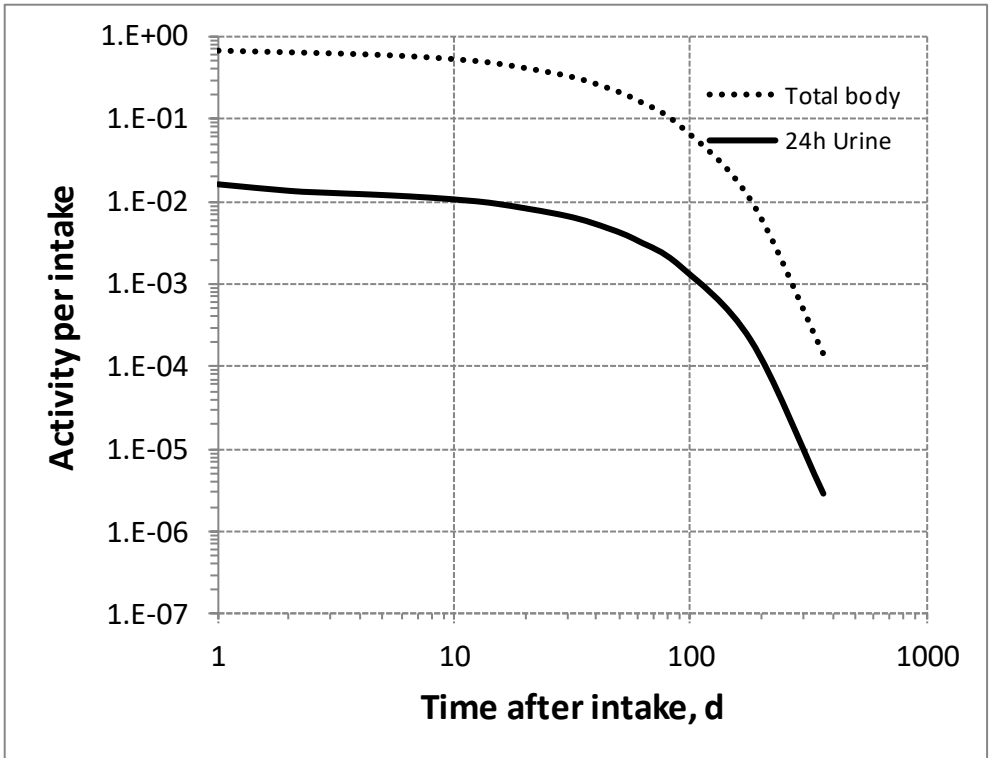

Fig. 9.2. Daily excretion of ^{40}K following inhalation of 1 Bq Type F.

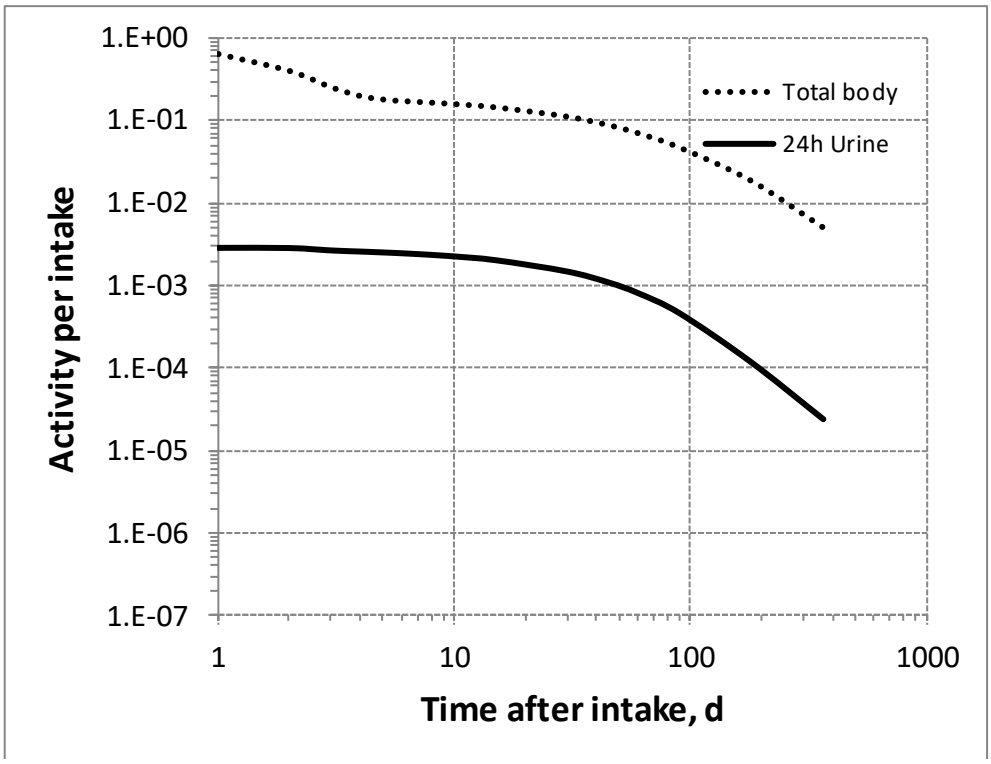

Fig. 9.3. Daily excretion of ^{40}K following inhalation of 1 Bq Type M.

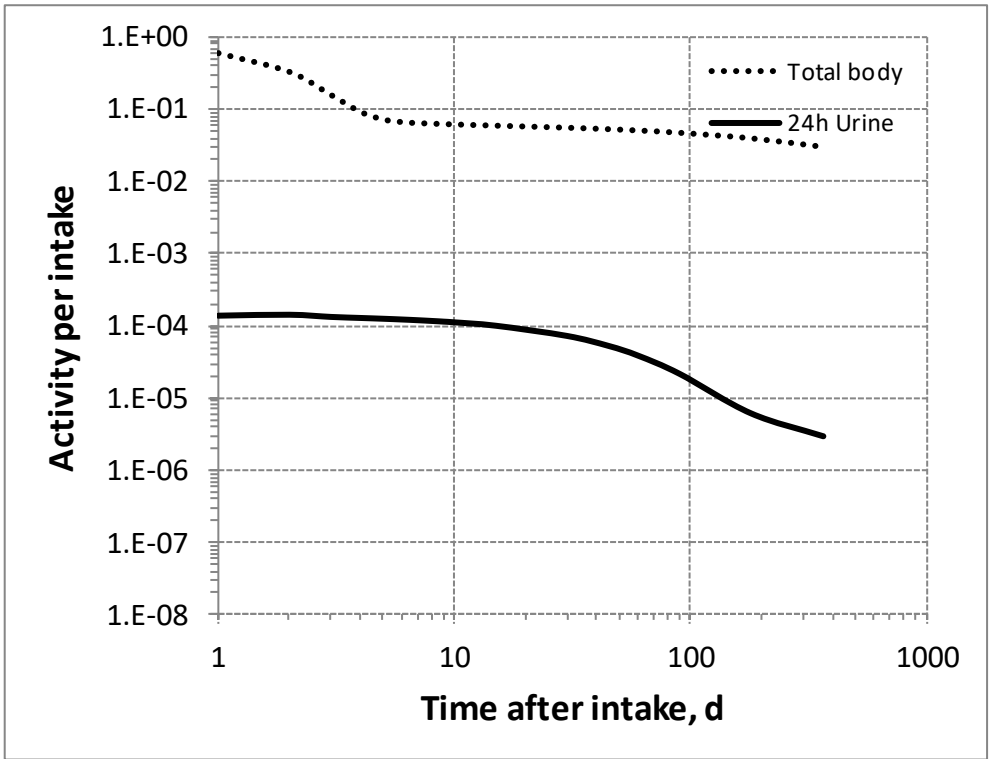

Fig. 9.4. Daily excretion of ^{40}K following inhalation of 1 Bq Type S.

10. SCANDIUM (Z=21)

10.1. Isotopes

Table 10.1. Isotopes of scandium addressed in this publication.

Isotope	Physical half-life	Decay mode
^{43}Sc	3.891 h	EC, B+
^{44}Sc*	3.97 h	EC, B+
^{44m}Sc	58.61 h	IT, EC
^{46}Sc	83.79 d	B-
^{47}Sc	3.3492 d	B-
^{48}Sc	43.67 h	B-
^{49}Sc	57.2 m	B-

EC, electron-capture decay; B+, beta-plus decay; B-, beta-minus decay; IT, isomeric transition decay.
[a]Dose coefficients and bioassay data for this radionuclide are given in the printed copy of this publication.
Data for other radionuclides listed in this table are given in the online electronic files on the ICRP website.

10.2. Routes of Intake

10.2.1. Inhalation

(149) For scandium, default parameter values were adopted on absorption to blood from the respiratory tract (ICRP, 2015). Absorption parameter values and types, and associated f_A values for particulate forms of scandium are given in Table 10.2.

Table 10.2. Absorption parameter values for inhaled and ingested scandium.

	Absorption parameter values*			
Inhaled particulate materials	f_r	s_r (d^{-1})	s_s (d^{-1})	Absorption from the alimentary tract, f_A
Default parameter values†				
Absorption type				
F	1	30	–	0.001
M‡	0.2	3	0.005	2×10^{-4}
S	0.01	3	1×10^{-4}	1×10^{-5}
Ingested materials§				
All forms				0.001

*It is assumed that the bound state can be neglected for scandium (i.e. $f_b = 0$). The values of s_r for Type F, M and S forms of scandium (30, 3 and 3 d^{-1} respectively) are the general default values.
†For inhaled material deposited in the respiratory tract and subsequently cleared by particle transport to the alimentary tract, the default f_A values for inhaled materials are applied [i.e. the product of f_r for the absorption type and the f_A value for ingested soluble forms of scandium (0.001)].
‡Default Type M is recommended for use in the absence of specific information on which the exposure material can be assigned to an absorption type (e.g. if the form is unknown, or if the form is known but there is no information available on the absorption of that form from the respiratory tract). For guidance on the use of specific information, see Section 1.1.
§Activity transferred from systemic compartments into segments of the alimentary tract is assumed to be subject to reabsorption to blood. The default absorption fraction f_A for the secreted activity is the highest value for any form of the radionuclide ($f_A = 0.001$).

10.2.2. Ingestion

(150) There appears to be little absorption of scandium when administered as ^{46}Sc tagged sand (Miller et al., 1972) or as scandium chloride (Miller and Byrne, 1970). 96% of ^{47}Sc is recovered in faeces after intragastric administration to rats. Farrar et al. (1987) assessed intestinal absorption of about 0.1% of ^{46}Sc after oral administration to rats. In *Publications 30* and *68* (ICRP, 1981, 1994a), f_1 was taken to be 10^{-4} for scandium by analogy with yttrium. Based on the work of Farrar et al. (1987), a higher value of $f_A = 10^{-3}$ is adopted here for all chemical forms of scandium.

10.2.3. Systemic distribution, retention and excretion of scandium

10.2.3.1. Biokinetic data

(151) Rosoff et al. (1965) studied the systemic behaviour of ^{46}Sc in 12 hospital patients following its intravenous administration as the weakly chelated ^{46}Sc nitrilotriacetate (NTA). Activity cleared slowly from blood, apparently due in part to formation of Sc-globulin complexes that were only slowly removed from blood plasma the reticuloendothelial system. About one fourth of the administered amount remained in plasma at 1 d and one tenth at 2 d. Postmortem measurements on three subjects who died 5-7 months later showed relatively high activity concentrations in the spleen, liver, and bone. Roughly 10% of the administered amount was excreted during the first 2-3 week, and the remaining body burden was lost much more slowly. Excretion during the first 2-3 week was primarily in faeces. In a study of biliary excretion of activity by one of the patients, biliary ^{46}Sc approximated its faecal excretion. Biological half-times based on whole-body counting of two subjects from 2-3 week to ~1.5 y post injection were 1300 and 1557 d.

(152) Rosoff et al. (1963) measured the distribution and excretion of ^{46}Sc after intravenous administration of different chemical forms of this radionuclide or physiologically related elements to mice. Weakly bound forms of ^{46}Sc such as ^{46}Sc citrate showed relatively high uptake by liver, spleen, and bone. Strongly chelated forms showed high excretion rates and relatively little accumulation in tissues.

(153) At 4 d after intravenous administration of ^{46}Sc citrate to rats, the liver and bone contained on average 21% and 16%, respectively, of the administered activity (Durbin, 1959). About 31% of the administered amount had been excreted by that time, mainly in faeces.

(154) Following intravenous administration of a mixture of ^{47}Ca and its progeny ^{47}Sc to rats, ^{47}Sc accumulated mainly in liver, spleen, kidneys, and bone (Taylor, 1966). The ^{47}Sc activity in liver and spleen decreased with effective half-times of 3.1 d and 3.8 d, respectively. Buildup in liver and spleen over time indicated that activity was moving to these organs after production at other sites. Nearly all the ^{47}Sc produced in the body by decay of ^{47}Ca arose in bone due to the high uptake and retention of ^{47}Ca by bone. A few percent of ^{47}Sc produced in bone escaped from bone at early times, but little if any escaped at later times.

(155) Basse-Cathalinat et al. (1968) used bone scintigraphy to study the behaviour of ^{47}Sc produced in bone following intravenous administration of ^{47}Ca to rats, rabbits, and human subjects. The clearest images were obtained for rats and rabbits due to the relatively low activity administered to human subjects. At 2 d post administration, elevated levels of ^{47}Sc were found in liver and spleen, presumably representing mainly the ^{47}Sc present at near equilibrium with ^{47}Ca in the injected solution. During days 4-8 the concentration of ^{47}Sc in the liver declined while the concentration of ^{47}Sc in the skeleton rose sharply.

(156) Zalikin et al. (1969) studied the behaviour of ^{46}Sc in rats following intravenous, intratracheal, or oral administration. Following intravenous injection, the systemic distribution of activity depended on the pH of the injected solution. As the pH was increased from 3.0 to

10, deposition in the liver and spleen increased sharply while deposition in the skeleton and kidneys decreased considerably.

(157) The distribution of ^{47}Sc was observed in tumor-bearing mice from 1 h to 3 d after intravenously administration (Hara and Freed, 1973). Highest concentrations in healthy tissues at 3 d were found, in decreasing order, in bone, liver, spleen, and kidney. Autoradiographic examination of bones from a rabbit intravenously injected with ^{47}Sc indicated that skeletal activity was associated mainly with bone marrow. Relatively fast clearance of activity was observed for blood, brain, heart, lung, stomach, intestines, pancreas, kidney, and muscle. Liver, spleen, and bone retained scandium over an extended period.

(158) Redistribution of ^{47}Sc produced in the body following intravenous administration of ^{47}Ca to mice accounted for a large portion of ^{47}Sc in soft tissues and blood (Freed et al., 1975). Most ^{47}Sc produced in vivo arose from decay of ^{47}Ca in bone, particularly after the first day. Scandium-47 escaped to some extent from sites of production in bone in the early hours after administration of ^{47}Ca, but no preferential loss of ^{47}Sc from bone was observed thereafter. Loss of ^{47}Sc from bone over days 1-11 was slower than that of ^{47}Ca. After 11 d the rate of loss of ^{47}Sc from bone approached that of the parent, suggesting removal of both the parent and the progeny by bone resorption.

(159) At 2 h after intravenous administration of ^{47}Sc chloride to mice, the highest concentration ratio tissue:blood was found in liver (1.2), followed by spleen (1.1), lung (0.84), gallbladder (0.36), heart (0.26), kidney (0.24), and bone (0.24) (Lachine et al., 1976). Relatively low concentrations were found in brain (0.02), muscle (0.03), and urinary bladder with contents (0.03).

10.2.3.2. Biokinetic model for systemic scandium

(160) The structure of the systemic model for scandium (Fig. 10.1) is a modification of the generic model structure for bone-surface-seeking radionuclides. Scandium is treated as a bone-surface seeker based on analogy with its chemical analogue yttrium. The spleen is added to the generic model structure as this organ appears to be an important repository for scandium in laboratory animals. The generic structure is also modified regarding routes of transfer to and from bone marrow compartments, based on indications from animal studies of relatively high transfer from plasma to marrow.

(161) Transfer coefficients are listed in Table 10.3. The transfer coefficients describing outflow from bone tissue compartments are default values for bone-surface seekers. The remaining transfer coefficients were set as far as feasible for consistency with the biokinetic database for scandium summarised earlier. For example, parameter values were set for reasonable consistency with the blood kinetics and urinary and faecal excretion rates observed in human subjects (Rosoff et al., 1965; Taylor, 1966) and the time-dependent distribution of scandium in laboratory animals over the early months after acute intake. Where data for scandium were lacking, parameter values were based on analogy with yttrium.

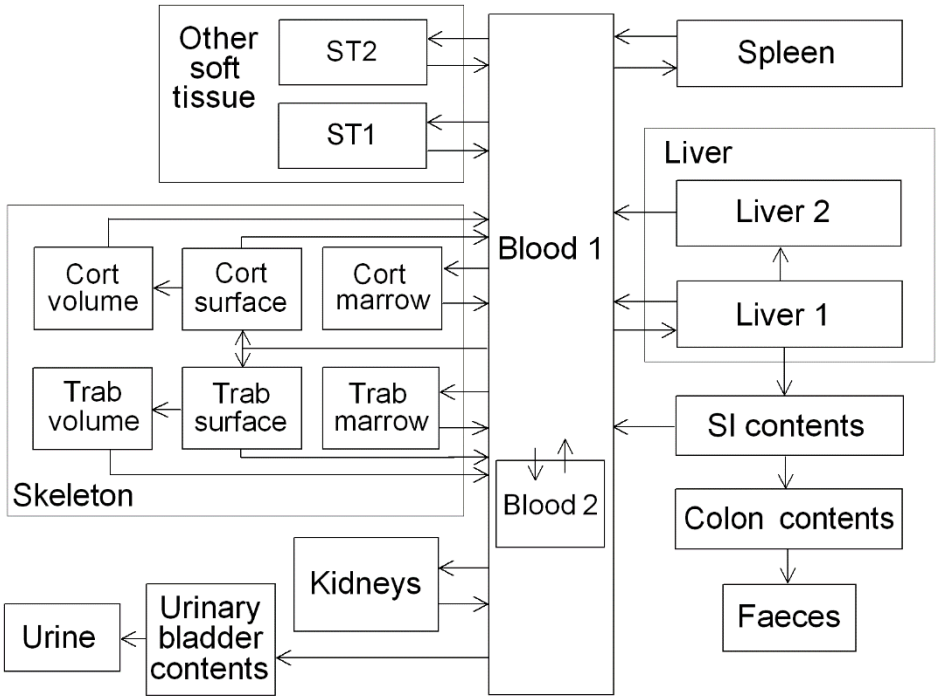

Fig. 10.1. Structure of the biokinetic model for systemic scandium. Trab = trabecular, Cort = cortical. ST1 and ST2 are soft tissue compartments with relatively short and relatively long removal half-times, respectively.

1883 Table 10.3. Transfer coefficients in the biokinetic model for systemic scandium.

From	To	Transfer coefficient (d^{-1})
Blood 1	Blood 2	0.45
Blood 1	Urinary bladder content	0.054
Blood 1	Liver 1	0.60
Blood 1	Kidneys	0.09
Blood 1	Spleen	0.06
Blood 1	Trabecular marrow	0.15
Blood 1	Cortical marrow	0.15
Blood 1	Trabecular bone surface	0.15
Blood 1	Cortical bone surface	0.15
Blood 1	ST1	0.60
Blood 1	ST2	0.546
Blood 2	Blood 1	0.462
Liver 1	Small intestine content	0.0578
Liver 1	Liver 2	0.0578
Liver 1	Blood 1	0.116
Liver 2	Blood 1	0.00693
Kidneys	Blood 1	0.0347
Spleen	Blood 1	0.0019
Trabecular marrow	Blood 1	0.00693
Cortical marrow	Blood 1	0.00693
ST1	Blood 1	0.231
ST2	Blood 1	0.00693
Trabecular bone surface	Blood 1	0.000493
Trabecular bone surface	Trabecular bone volume	0.000247
Trabecular bone volume	Blood 1	0.000493
Cortical bone surface	Blood 1	0.0000821
Cortical bone surface	Cortical bone volume	0.0000411
Cortical bone volume	Blood 1	0.0000821

1884 *10.2.3.3. Treatment of progeny*

1885 (162) The only scandium chain addressed in this publication is the two-member chain
1886 consisting of ^{44m}Sc and its progeny ^{44}Sc. The biokinetics of the progeny is assumed to be the
1887 same as that of the parent from its time of production in a systemic compartment.

1888 ## 10.3. Individual monitoring

1889 (163) Information of detection limit for routine individual measurement is not available.
1890

10.4. Dosimetric data for scandium

Table 10.4 Committed effective dose coefficients (Sv Bq^{-1}) for the inhalation or ingestion of ^{44}Sc compounds.

Inhaled particulate materials (5 µm AMAD aerosols)	Effective dose coefficients (Sv Bq^{-1})
	^{44}Sc
Type F, — NB: Type F should not be assumed without evidence	1.1E-10
Type M, default	1.5E-10
Type S	1.5E-10
Ingested materials	
All forms	2.3E-10

AMAD, activity median aerodynamic diameter

11. TITANIUM (Z = 22)

11.1. Isotopes

Table 11.1. Isotopes of titanium addressed in this publication.

Isotope	Physical half-life	Decay mode
^{44}Ti*	60.0 y	EC
^{45}Ti	184.8 m	EC, B+

EC, electron-capture decay; B+, beta-plus decay

*Dose coefficients and bioassay data for this radionuclide are given in the printed copy of this publication. Data for other radionuclides listed in this table are given in the online electronic files on the ICRP website.

11.2. Routes of Intake

11.2.1. Inhalation

(164) For titanium, default parameter values were adopted on absorption to blood from the respiratory tract (ICRP, 2015). Absorption parameter values and types, and associated f_A values for particulate forms of titanium are given in Table 11.2.

Table 11.2. Absorption parameter values for inhaled and ingested titanium.

	Absorption parameter values*			Absorption from the
Inhaled particulate materials	f_r	s_r (d^{-1})	s_s (d^{-1})	alimentary tract, f_A
Default parameter values†				
Absorption type				
F	1	30	–	0.001
M‡	0.2	3	0.005	2×10^{-4}
S	0.01	3	1×10^{-4}	1×10^{-5}
Ingested materials§				
All forms				0.001

*It is assumed that the bound state can be neglected for titanium (i.e. $f_b = 0$). The values of s_r for Type F, M and S forms of titanium (30, 3 and 3 d^{-1} respectively) are the general default values.

†For inhaled material deposited in the respiratory tract and subsequently cleared by particle transport to the alimentary tract, the default f_A values for inhaled materials are applied [i.e. the product of f_r for the absorption type and the f_A value for ingested soluble forms of titanium (0.001)].

‡Default Type M is recommended for use in the absence of specific information on which the exposure material can be assigned to an absorption type (e.g. if the form is unknown, or if the form is known but there is no information available on the absorption of that form from the respiratory tract). For guidance on the use of specific information, see Section 1.1.

§Activity transferred from systemic compartments into segments of the alimentary tract is assumed to be subject to reabsorption to blood. The default absorption fraction f_A for the secreted activity is the highest value for any form of the radionuclide ($f_A = 0.001$).

11.2.2. Ingestion

(165) Titanium compounds are poorly absorbed from the gastro-intestinal tract (UNEP, 1982). Human studies of ingestion of titanium dioxide micro- and nano-particles by volunteers (West and Wyzan, 1963; Böckmann et al., 2000; Jones et al., 2015; Pele et al., 2015) were reviewed by EFSA (2016) who estimated fractional absorption to be in the range 0.02 – 0.1%. When ^{44}Ti tetrachloride was given orally to sheep, the comparison of tissues content with that observed after intravenous injection indicated an absorption less than 0.5%.

(166) In *Publications 30* and *68* (ICRP, 1981, 1994a), a fractional absorption of 0.01 was retained for titanium. In this publication, based on recent human studies with titanium dioxide, f_A is taken to be 10^{-3} for all chemical forms of titanium at the workplace.

11.2.3. Systemic distribution, retention and excretion of titanium

11.2.3.1. Biokinetic data

(167) Titanium is a member of Group IVB of the periodic table, where it sits above the chemically similar element zirconium (Zr). The high reactivity of these elements at high temperatures can result in the formation of extremely stable compounds. Durable materials made from Ti and Zr are widely used in industry and medicine.

(168) The biokinetics of systemic titanium (Ti) has been studied in laboratory animals and to a lesser extent in human subjects, primarily in investigations of the fate of Ti ions or compounds released into the body from Ti-based implants (Merritt et al., 1992; Merritt and Brown, 1995; Golasik et al., 2016a,b); and tissue accumulation and potential adverse effects of internally deposited TiO_2 nanoparticles, which are used in many consumer products including paints, dyes, inks, plastics, paper, cosmetics, and food additives (Fabian et al., 2008; Shi et al., 2013; Geraets et al., 2014; Schinohara et al., 2014; Elgrabli et al., 2015; Kreyling et al., 2017a,b,c). Titanium-45 has been investigated for use in radiopharmceuticals due to the tendency of various Ti compounds to form colloids in the body with resulting accumulate in the liver and spleen, suggesting potential applications of ^{45}Ti in imaging the body's reticuloendothelial (RE) system (Ishiwata et al., 1991).

(169) Development of a biokinetic model for systemic Ti from the reported data is complicated by an apparent dependence of the systemic behaviour of Ti on the form and mass of administered Ti and the mode of administration. Such differences in experimental conditions may result in variable accumulation of Ti by the RE system.

(170) Thomas and Archuleta (1980) studied the distribution and retention of ^{44}Ti in mice following its intraperitoneal (IP) or intravenous (IV) administration as a chloride. The results indicated that titanium is relatively insoluble in body fluids. The initial systemic distribution depended strongly on the exposure mode but did not vary noticeably over time after either IP or IV administration. Liver, spleen, kidneys, and gastrointestinal tract contained about 25%, 3.3%, 1.7%, and 3.6%, respectively, of the total-body content after intravenous injection and 8.4%, 2.1%, 2.0%, and 15%, respectively, after intraperitoneal injection. Differences in the distributions following IP and IV administration appeared to result largely from adherence of injected material to visceral organs near the injection site and elevated uptake by the RE system in the case of IV injection. A mean biological half-time of 642 d was estimated for the total body.

(171) Merritt et al. (1992, 1995) examined the behaviour of Ti in hamsters following repeated intraperitoneal or intramuscular injections of Ti salts over a few weeks. Transport from the site of injection was slow. One week after the end of six weekly injections of 100 µg of Ti tetrachloride, the following tissues showed Ti concentrations noticeably higher than found in control animals: spleen, 40.5 µg g^{-1} (above the control level); liver, 6.9 µg g^{-1}; bone matrix, 3.3 µg g^{-1}; bone mineral, 0.9 µg g^{-1}; kidney, 2.1 µg g^{-1}.

(172) Sarmiento-Gonzalez et al. (2009) determined Ti concentration in tissues of rats 18 months after implant of Ti wires in the femur, 1 week after intraperitoneal injection of soluble Ti as citrate, or 1 week after intraperitoneal injection of TiO_2 microparticles. The Ti concentrations in kidneys, spleen, lungs, and heart normalised to a concentration of 1.0 in the

liver were, respectively, 2.7, 8.1, 7.4, and 2.1 for rats with implants; 6.5, 6.7, 1.8, and 0.74 for rats injected with Ti citrate; and 2.1, 2.1, 15, and 2.5 for rats injected with Ti dioxide.

(173) Golasik et al. (2016a,b) studied the Ti distribution in selected tissues of rats following administration in ionic form, either as a single IV injection or daily oral administration for 30 d. During the first 24 h after IV injection or after the end of oral administration, the highest tissue concentration was found in the kidneys, followed by liver. Over this period the liver contained a greater portion of the administered Ti than the kidneys due to the larger mass of the liver. In the early hours after IV injection the biological half-time was about 3.3 h for the kidneys and 1.9 h for the liver. Much slower removal from these tissues was seen from 3 h to 24 h after the end of oral administration.

(174) Miller et al. (1976) determined the distribution of ^{44}Ti in lambs after oral or intravenous (IV) administration of $^{44}TiCl_4$. At 2 d after oral administration the mean activity concentration in systemic tissues, normalised to 1.0 for liver, decreased in the order liver (1.0) > kidneys (0.74) > pancreas (0.49) > spleen (0.28) > lung, heart, adrenals (<0.15). At 2 d after IV administration the blood, skeleton, kidneys, liver, and remaining tissue contained about 18.4%, 24.8%, 2.1%, 1.3%, and 48.8%, respectively, of the administered activity; cumulative urinary excretion accounted for about 3%; and faecal excretion plus gastrointestinal (GI) tract contents accounted for about 1.6%. This distribution broadly resembles that predicted by the systemic model for Zr adopted in *Publication 34* (2016): blood, 38%; bone, 22.8%; kidneys, 0.4%; liver, 1.8%; other tissue, 33%, urine, 3%; faeces, 1%. Noticeable differences are that the Zr model predicts slower removal from blood, balanced by slower accumulation in 'other tissue' and lower accumulation in the kidneys.

(175) Zhu et al. (2010) measured concentrations of 60 elements including Ti and Zr in 17 tissues obtained from autopsies of 68 Chinese men from four areas of China. All 68 subjects were considered healthy until the time of sudden accidental death. Concentrations of the elements were also measured in blood of living subjects from each of the four areas. The concentration of an element in a tissue or blood was reported as a median and range of measured values. The results for Ti and Zr indicate considerable differences in their long-term distributions in the adult human body. For example, the median concentration of Zr in rib (the only bone addressed) was considerably greater than that in soft tissues other than liver, while the median concentration of Ti in rib (983 μg kg^{-1}) was lower than the median concentration in 8 soft tissues (e.g., liver, 3220 μg kg^{-1}; muscle, 2060 μg kg^{-1}; kidney, 1770 μg kg^{-1}). A relatively low median concentration (201 μg kg^{-1}) was determined for spleen. Blood, liver, kidneys, bone, and all other tissues combined contained about 0.4%, 6%, 0.6%, 11%, and 82%, respectively, of total-body Ti in these subjects based on median concentrations in tissues.

(176) The systemic behaviour of Ti administered as TiO_2 nanoparticles has been studied extensively in laboratory animals and to a lesser extent in human subjects (Fabian et al., 2008; Patri et al., 2009; Xie et al., 2011; Shi et al., 2013; Baisch et al., 2014; Geraets et al., 2014; Elgrabli et al., 2015; Bello and Warheit, 2017; Kreyling et al., 2017a,b,c). Following IV injection, Ti generally accumulates mainly in the liver (roughly half the administered amount during the first week), spleen (roughly 2% the first week) and lungs (a few tenths of 1% the first week) and was largely removed from the body after 8 week. Kreyling and coworkers (2017a,b,c) investigated the biokinetics of Ti in rats following IV, oral, and intratracheal (IT) administration of TiO_2 nanoparticles. The systemic behaviour of Ti following IT administration differed from that seen after IV injection (Kreyling et al., 2017a), particularly regarding the distribution of systemic Ti over time. The highest concentrations following IT administration were found in kidneys, liver, and spleen, while the largest fraction of absorbed activity was found in remaining soft tissues, followed by skeleton. The systemic behaviour of Ti at 1-7 d after administration along the gastrointestinal (GI) route was closer to that seen after IT than

after IV administration. About 0.6% of the oral intake was absorbed to blood and about 0.05% remained in systemic tissues after 7 d, with rounded relative concentrations of 1 in liver, 1 in lungs, 3 in kidneys, 4 in brain, 5 in spleen, 6 in uterus, and 11 in the skeleton.

11.2.3.2. Biokinetic model for systemic titanium

(177) Development of a biokinetic model for systemic Ti is complicated by considerable inconsistencies in reported data. These inconsistencies may arise in large part due to variable uptake of Ti by the RE system under different experimental conditions. The Ti model used in this publication is based on results of studies that do not appear to reflect elevated uptake by the RE system (e.g. Miller et al., 1976; Zhu et al., 2010; Golasik et al., 2016a,b), as such studies may be most appropriate for assessing the fate of radio-titanium in the body. The initial distribution of Ti is based mainly on results of the study of Miller et al. (1976), which suggest that the initial distribution of systemic Ti is similar but not identical to that of Zr as depicted in the biokinetic model for systemic Zr in *Publication 134* (2016). The long-term kinetics of Ti is based on relative concentrations of Ti in tissues as determined in the autopsy study of Zhu et al. (2010). Transfer coefficients describing removal of Ti from bone volume are generic values based on reference rates of cortical and trabecular bone turnover (ICRP, 2002a).

(178) The structure of the systemic model for Ti is shown in Fig. 11.1. Transfer coefficients are listed in Table 11.3.

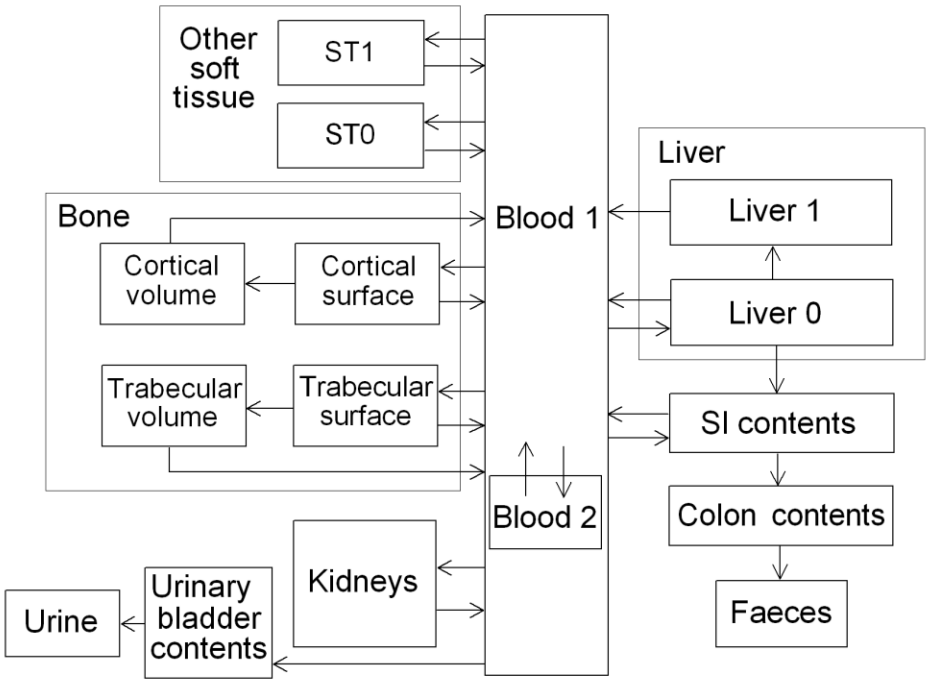

Fig. 11.1. Structure of the biokinetic model for systemic titanium.

Table 11.3. Transfer coefficients in the biokinetic model for systemic titanium.

From	To	Transfer coefficient (d^{-1})
Blood 1	Blood 2	2.0
Blood 1	Liver 0	0.05
Blood 1	Kidneys	0.075

Blood 1	ST0	1.0
Blood 1	ST1	1.0
Blood 1	Urinary bladder content	0.1
Blood 1	SI contents	0.025
Blood 1	Trabecular surface	0.375
Blood 1	Cortical surface	0.375
Blood 2	Blood 1	1.6
Liver 0	SI contents	0.116
Liver 0	Blood 1	0.116
Liver 0	Liver 1	0.462
Liver 1	Blood 1	0.00105
Kidneys	Blood 1	0.021
ST0	Blood 1	0.462
ST1	Blood 1	0.002
Trabecular surface	Blood 1	0.02
Trabecular surface	Trabecular volume	0.000247
Trabecular volume	Blood 1	0.000493
Cortical surface	Blood 1	0.02
Cortical surface	Cortical volume	0.0000411
Cortical volume	Blood 1	0.0000821

11.2.3.3. Treatment of progeny

(179) The only progeny of titanium addressed in this publication is ^{44}Sc, produced by decay of ^{44}Ti. The characteristic model for scandium is applied to ^{44}Sc as progeny of ^{44}Ti, with added compartments and associated transfer coefficients needed to solve the linked biokinetic models of titanium and scandium. The following transfer rates from compartments appearing in the titanium model to scandium's central blood compartment are added to the characteristic model for scandium: 1000 d^{-1} if ^{44}Si is produced in a blood compartment not identified in the scandium model, and at the rate 0.231 d^{-1} if ^{44}Si is produced in a compartment in titanium's Other not identified in the scandium model.

11.3. Individual monitoring

(180) Information of detection limit for routine individual measurement is not available.

11.4. Dosimetric data for titanium

Table 11.4. Committed effective dose coefficients (Sv Bq^{-1}) for the inhalation or ingestion of ^{44}Ti compounds.

Inhaled particulate materials (5 µm AMAD aerosols)	Effective dose coefficients (Sv Bq^{-1})
	^{44}Ti
Type F, — NB: Type F should not be assumed without evidence	2.4E-07
Type M, default	6.5E-08
Type S	2.1E-07

Ingested materials	
All forms	2.2E-09

AMAD, activity median aerodynamic diameter

12. VANADIUM (Z=23)

12.1. Isotopes

Table 12.1. Isotopes of vanadium addressed in this publication.

Isotope	Physical half-life	Decay mode
^{47}V	32.6 min	EC, B+
^{48}V*	15.9735 d	EC, B+
^{49}V	330 d	EC
^{50}V	1.50E+17 y	EC, B-

EC, electron-capture decay; B+, beta-plus decay; B-, beta-minus decay; IT, isomeric transition decay.
*Dose coefficients and bioassay data for this radionuclide are given in the printed copy of this publication.
Data for other radionuclides listed in this table are given in the online electronic files on the ICRP website.

12.2. Routes of Intake

12.2.1. Inhalation

(181) For vanadium, default parameter values were adopted on absorption to blood from the respiratory tract (ICRP, 2015). Absorption parameter values and types, and associated f_A values for particulate forms of vanadium are given in Table 12.2.

Table 12.2. Absorption parameter values for inhaled and ingested vanadium.

	Absorption parameter values*			Absorption from the alimentary tract, f_A
Inhaled particulate materials	f_r	s_r (d^{-1})	s_s (d^{-1})	
Default parameter values†				
Absorption type				
F	1	30	–	0.2
M‡	0.2	3	0.005	0.04
S	0.01	3	1×10^{-4}	2×10^{-3}
Ingested materials§				
Sodium metavanadate				0.2
All other chemical forms				0.01

*It is assumed that the bound state can be neglected for vanadium (i.e. $f_b = 0$). The values of s_r for Type F, M and S forms of vanadium (30, 3 and 3 d^{-1} respectively) are the general default values.
†For inhaled material deposited in the respiratory tract and subsequently cleared by particle transport to the alimentary tract, the default f_A values for inhaled materials are applied [i.e. the product of f_r for the absorption type and the f_A value for ingested soluble forms of vanadium (0.2)].
‡Default Type M is recommended for use in the absence of specific information on which the exposure material can be assigned to an absorption type (e.g. if the form is unknown, or if the form is known but there is no information available on the absorption of that form from the respiratory tract). For guidance on the use of specific information, see Section 1.1.
§Activity transferred from systemic compartments into segments of the alimentary tract is assumed to be subject to reabsorption to blood. The default absorption fraction f_A for the secreted activity is the highest value for any form of the radionuclide ($f_A = 0.2$).

12.2.2. Ingestion

(182) A comparison of the low concentrations of vanadium normally present in urine with the estimated daily intake and faecal levels of the element indicates that less than 5% of dietary vanadium is absorbed from the gastrointestinal tract (ICRP, 1975; Byrne and Kosta, 1978;

WHO, 1996). In vitro digestion of soil, dust and concentrate fines from a vanadium titanomagnetite mining region showed higher bioaccessibility of vanadium (V) than vanadium (IV) (Yu and Yang, 2019).

(183) Measurement of urinary excretion after administration of vanadium (IV) as ammonium vanadyl tartrate to 6 human patients (Dimond et al., 1963) and as diammonium oxytartratovanadate to 5 healthy volunteers (Curran et al., 1959) suggested a fractional absorption in a range about 0.1 - 1%. Conversely, Proescher et al. (1917) (as cited by WHO, 1988) observed 12.4% excretion of in urine from vanadium (V) as sodium metavanadate orally given to a man. Animal experiments confirm the low fractional absorption of vanadium (IV): 0.5 – 1% of vanadyl sulphate in rats (UNEP, 1988) and rabbits (Curran and Costello, 1956), 2.6% of vanadium oxydichloride in rats (Sollenberger, 1981). However, by comparing vanadium concentration in blood after oral and intravenous administration of vanadyl sulphate to rats, Azay et al. (2001) estimated a higher fractional absorption of 16%. On the other hand, vanadium (V) orally given to rats as sodium metavanadate appears to be absorbed to a relatively large extent of 16.5 – 40% (Bogden et al., 1982; Wiegmann et al., 1982; Adachi et al., 2000). Still, only 2.6% of the slightly soluble vanadium (V) pentoxide was absorbed by rats after oral administration (Conklin et al., 1982). Hill (1980) found that ascorbic acid reduced vanadium absorption in rats.

(184) In *Publications 30* and *68* (ICRP, 1981, 1994a), f_1 was taken to be 0.01 for all compounds of vanadium. In this publication, the same value of $f_A = 0.01$ is retained for all chemical forms of vanadium, except sodium metavanadate for which a higher value of $f_A = 0.2$ is adopted.

12.2.3. Systemic distribution, retention and excretion of vanadium

12.2.3.1. Biokinetic data

(185) The behaviour of vanadium (V) in the human body has been observed in workers exposed to airborne vanadium and in controlled inhalation or ingestion studies (Curran et al., 1959; Barceloux and Barceloux, 1999). These studies address mainly the respiratory behaviour and gastrointestinal absorption of vanadium and provide little specific information on its systemic behaviour.

(186) Information on the systemic kinetics of vanadium are available from studies of the fate of radioactive or stable vanadium administered after administration to rodents (Strain et al., 1964; Thomassen and Leicester, 1964; Sabbioni et al., 1978, 1981; Roshchin et al., 1980; Sharma et al., 1980, 1987; Hansen et al., 1982; Ando et al., 1989; Ando and Ando, 1990; Merritt and Brown, 1995; Amano et al., 1996; Setyawati et al., 1998; Barceloux and Barceloux, 1999; Hirunuma et al., 1999; Alimonti et al., 2000). Following injection or absorption of vanadium into blood, relatively high concentrations are observed in the kidneys, bone, and liver, with bone becoming the dominant systemic repository at times remote from uptake to blood. The main route of excretion of absorbed vanadium is through the kidneys. Normally no more than 10% of absorbed vanadium is excreted in faeces (Barceloux and Barceloux, 1999). Half or more of the amount reaching blood typically is excreted within the first 3-4 days (Durbin, 1959; Barceloux and Barceloux, 1999; Hirunuma et al., 1999).

(187) Comparative biokinetic studies of the Group VB elements vanadium, niobium, and tantalum (Durbin, 1959; Ando et al., 1989; Ando and Ando, 1990) indicate that these three elements share some biokinetic properties including primary sites of deposition in the body. However, vanadium is less firmly fixed in tissues and more readily absorbed to blood from intramuscular injection sites and shows distinctive systemic kinetics including more rapid

excretion than the other Group VB elements. In the study described by Durbin (1959), <10% of absorbed vanadium was retained after 2 months, compared with at least threefold higher retention of niobium or tantalum.

(188) The reader is referred to a paper by Leggett and O'Connell (2018) for a more detailed discussion of biokinetic data for systemic vanadium.

12.2.3.2. Biokinetic model for systemic vanadium

(189) A biokinetic model for systemic vanadium proposed by Leggett and O'Connell (2018) is adopted here. The model structure is shown in Fig. 12.1. Transfer coefficients are listed in Table 12.3.

(190) The transfer coefficients for vanadium listed in Table 12.3 were based to a large extent on comparative biokinetics of vanadium and niobium (Leggett and O'Connell, 2018). The transfer coefficients for niobium (ICRP, 2016) were modified for closer agreement with the distinctive systemic behaviour of vanadium indicated by data for rodents. Compared with the model for niobium, the parameter values for vanadium were set to predict faster outflow from blood, a higher rate of urinary excretion, a higher rate of removal from the total body, greater uptake by the kidneys, and faster loss from bone and liver indicated by studies on rats. The reader is referred to Leggett and O'Connell (2018) for more details on selection of transfer coefficients for vanadium.

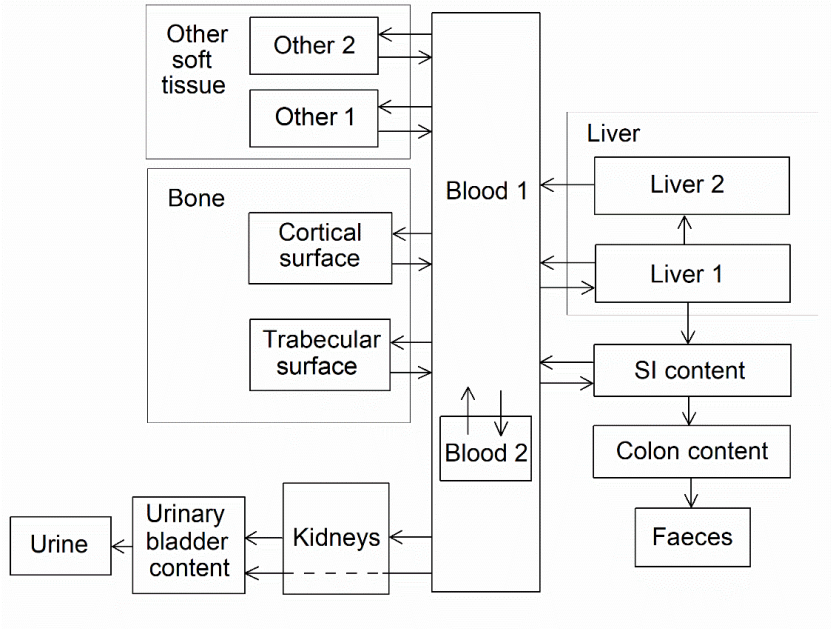

Fig. 12.1. Structure of the biokinetic model for systemic vanadium.

Table 12.3. Transfer coefficients in the biokinetic model for systemic vanadium.

From	To	Transfer coefficient (d^{-1})
Blood 1	Blood 2	2.8
Blood 1	Liver 1	0.24
Blood 1	Kidneys	0.4
Blood 1	Other 1	2.44
Blood 1	Other 2	0.24
Blood 1	Urinary bladder content	1.52
Blood 1	SI content	0.12
Blood 1	Trabecular surface	0.12

Blood 1	Cortical surface	0.12
Blood 2	Blood 1	0.5
Liver 1	SI contents	0.09
Liver 1	Blood 1	0.375
Liver 1	Liver 2	0.035
Liver 2	Blood 1	0.01
Kidneys	Urinary bladder content	1.8
Other 1	Blood 1	0.14
Other 2	Blood 1	0.01
Trabecular surface	Blood 1	0.01
Cortical surface	Blood 1	0.01

12.3. Individual monitoring

(191) Information of detection limit for routine individual measurement is not available.

12.4. Dosimetric data for vanadium

Table 12.4 Committed effective dose coefficients (Sv Bq^{-1}) for the inhalation or ingestion of ^{48}V compounds.

Inhaled particulate materials (5 µm AMAD aerosols)	Effective dose coefficients (Sv Bq^{-1})
	^{48}V
Type F, — NB: Type F should not be assumed without evidence	1.2E-09
Type M, default	1.6E-09
Type S	1.7E-09
Ingested materials	
Sodium metavanadate	1.4E-09
All other chemical forms	1.1E-09

AMAD, activity median aerodynamic diameter

13. CHROMIUM (Z=24)

13.1. Isotopes

Table 13.1. Isotopes of chromium addressed in this publication.

Isotope	Physical half-life	Decay mode
^{48}Cr	21.56 h	EC, B+
^{49}Cr	42.3 min	EC, B+
^{51}Cr*	27.7025 d	EC

EC, electron-capture decay; B+, beta-plus decay.
*Dose coefficients and bioassay data for this radionuclide are given in the printed copy of this publication.
Data for other radionuclides listed in this table are given in the online electronic files on the ICRP website.

13.2. Routes of Intake

13.2.1. Inhalation

(192) For chromium, default parameter values were adopted on absorption to blood from the respiratory tract (ICRP, 2015). Absorption parameter values and types, and associated f_A values for particulate forms of chromium are given in Table 13.2.

Table 13.2. Absorption parameter values for inhaled and ingested chromium.

	Absorption parameter values*			Absorption from the alimentary tract, f_A
Inhaled particulate materials	f_r	s_r (d^{-1})	s_s (d^{-1})	
Default parameter values†				
Absorption type				
F	1	30	–	0.01
M‡	0.2	3	0.005	0.002
S	0.01	3	1×10^{-4}	1×10^{-4}
Ingested materials§				
Trivalent state Cr(III)				0.01

*It is assumed that the bound state can be neglected for chromium (i.e. $f_b = 0$). The values of s_r for Type F, M and S forms of chromium (30, 3 and 3 d^{-1} respectively) are the general default values.
†For inhaled material deposited in the respiratory tract and subsequently cleared by particle transport to the alimentary tract, the default f_A values for inhaled materials are applied [i.e. the product of f_r for the absorption type and the f_A value for ingested soluble forms of chromium (0.05)].
‡Default Type M is recommended for use in the absence of specific information on which the exposure material can be assigned to an absorption type (e.g. if the form is unknown, or if the form is known but there is no information available on the absorption of that form from the respiratory tract). For guidance on the use of specific information, see Section 1.1.
§Activity transferred from systemic compartments into segments of the alimentary tract is assumed to be subject to reabsorption to blood. The default absorption fraction f_A for the secreted activity is the highest value for any form of the radionuclide ($f_A = 0.01$).

13.2.2. Ingestion

(193) The US Agency for Toxic Substances and Disease Registry (ATSDR, 2012b) and the European Food Safety Authority (EFSA, 2014) reviewed chromium absorption, which is poor from the gastrointestinal tract. In humans and rats, 0.4 to 2.8% of chromium in the trivalent state was reported to be absorbed following oral administration. The rate of uptake depends on the water solubility of the chemical compounds. Chromium appears to be better absorbed from

the soil than from chromate salts. Ingested hexavalent chromium is absorbed to a slightly greater extent than trivalent chromium in both rats and humans, with fractional absorption in the range 1-7%. The reduction of Cr(VI) to Cr(III) by gastric juices, or by mixture with orange juice or ascorbic acid appears to decrease its intestinal absorption.

(194) In *Publications 30* and *68* (ICRP, 1980, 1994a), f_1 was taken to be 0.01 for chromium in the trivalent state and 0.1 for chromium in the hexavalent state. In this publication, f_A values of 0.01 and 0.05 are retained respectively for Cr(III) and Cr(VI).

13.2.3. Systemic distribution, retention and excretion of chromium

13.2.3.1. Biokinetic data

(195) Chromium (Cr) exists in several oxidation states. The trivalent state [Cr(III)] is the most stable and the dominant naturally occurring form. Chromium in other oxidation states tends to be converted to the trivalent oxide in the environment and in biological systems.

(196) The hexavalent form [Cr(VI)] is the second most stable oxidation state of Cr. It behaves differently from Cr(III) in the body and is categorised as a chemical toxin and carcinogen. The different behaviours and effects of Cr(VI) and Cr(III) in the body are associated with the ability of Cr(VI) compounds to cross cell membranes, while Cr(III) is blocked by the membrane (Christensen et al., 1993; O'Flaherty, 1996).

(197) Chromium(III) is an essential nutrient in humans and several non-human species (Hambidge and Baum, 1972; Christensen et al., 1993; Mertz, 1993; Anderson, 1997). Dietary intake of Cr typically is on the order of 75 μg d^{-1} (Pechova and Pavlata, 2007). Postmortem measurements of Cr concentrations in 17 tissues of up to 68 adult male subjects (Zhu et al., 2010) indicate a central total-body content of about 4 g Cr. Based on median chromium concentrations in tissues and reference tissues masses, about 55% of total-body chromium is contained in muscle and fat, 25% in bone, 4% in the liver, and 0.5% in the kidneys.

(198) Doisy et al. (1971) studied the blood kinetics and excretion of intravenously administered ^{51}Cr(III) in seven normal subjects. The earliest measurements of activity in blood were at 10 min. Blood clearance was slow after 1 h, with the blood content gradually dropping to ~40% of the early content (average content at 10 min and 1 h) by 3 d post injection and ~25% by 7 d. Excretion of ^{51}Cr was primarily in urine. Less than 1% of the injected amount appeared in faeces over the first 5 d.

(199) Sargent et al. (1979) measured the retention of intravenously administered ^{51}Cr(III) in five normal adult male humans. Total-body activity was measured externally for 8 months, and activity in blood was measured for 40-80 d post injection. Data fitting indicated three components of retention with mean half-times of 0.56 d (35%), 12.7 d (27%), and 192 d (38%). Blood clearance, apparently excluding a rapid phase of removal immediately after injection, was described in terms of four components of retention with mean half-times of 13 min, 6.3 h, 1.9 d, and 8.3 d.

(200) Lim et al. (1983) studied the behaviour of intravenously administered ^{51}Cr(III) in three normal subjects using external scanning and measurement of activity in plasma. Highest activity concentrations were seen in the liver, spleen, and bone. The data were used to develop a biokinetic model for systemic Cr consisting of physiological compartments including two plasma pools representing Cr bound to plasma transferrin (BB) and Cr in unbound form (BF), and tissue compartments representing liver (2 compartments), adipose plus muscle tissue, spleen (2 compartments), bone, and remaining tissues (2 compartments). A complex set of paths of movement between the two plasma compartments and eight tissue compartments was depicted. In view of similarities in the derived kinetics for some tissue compartments, a simpler

functional model was developed by grouping tissue compartments with similar kinetics. The functional model consisted of the two plasma compartments BB and BF included in the physiological model, with exchange of Cr between BB and BF; three tissue compartments representing fast (hours), medium (days), and slow (months) exchange between tissues and BB; loss from BF in urine; and loss from BB via all other excretion pathways combined. Derived transfer components were tabulated for the functional model for individual subjects.

(201) Chromium has been used to measure the volume and lifetime of red blood cells (RBC) in patients and normal subjects, based on tenacious retention of ^{51}Cr(III) in RBC after passage of intravenously administered ^{51}Cr(VI) across RBC membranes and reduction of ^{51}Cr(VI) to ^{51}Cr(III) within the RBC. Following administration of ^{51}Cr(VI) to normal subjects, the label disappeared from blood with a biological half-time of about 30 d (Korst, 1968).

(202) Hopkins (1965) examined the systemic kinetics of intravenously injected ^{51}Cr(III) in rats from 15 min to 4 d after administration. The kinetics varied little if any with dosage level, previous diet, or sex. Initial accumulation in most tissues decreased substantially over the 4-day period, but the kidneys and spleen continued to concentrate ^{51}Cr. Growing rats retained greater amounts than mature animals in bones, while mature animals showed higher retention than younger animals in the kidneys, spleen, and testes. Activity was excreted predominantly in urine.

(203) Mertz et al. (1965) studied the long-term behaviour of ^{51}Cr in rats. Total-body retention was not affected by dietary history or amounts injected. Retention R(t) through time t =72 d could be closely approximated by a sum of three exponential terms:

$$R(t) = 0.43e^{-0.693t/0.5} + 0.32e^{-0.693t/5.9} + 0.25e^{-0.693t/83.4}.$$

(204) Onkelinx (1977) studied the systemic behaviour of Cr(III) following intravenous administration of $^{51}CrCl_3$ to female Wistar rats of different ages (35, 60, and 120 d). Observations included measurements of activity in urine, faeces, and blood over the first few days in all groups, and in tissues of a group of 60-day-old rats at intervals ranging from 1 h to 11 d post injection. In all age groups, urinary excretion accounted for roughly 90% of urinary plus faecal excretion during days 0-3 post injection. In all age groups, plasma clearance from 0-265 h post injection could be described as a sum of three exponential terms. As an average for the 120-day-old rats, about 45% of the initial blood content cleared with a half-time of 2 h, 36% with a half-time of 16 h, and 14% with a half-time of 45 h. In the 60-day-old group, the average activity concentration over the first 24 h normalised to 1.0 for liver decreased in the order: bone epiphyses (8.8) > kidney (3.1) > bone diaphysis (2.5) > lungs (1.2) > liver (1.0) > spleen (0.85) > pancreas (0.36). The average activity concentration over days 2-11 normalised to 1.0 for liver decreased in the order: bone epiphyses (10.5) > bone diaphysis (3.6) > kidney (2.9) > spleen (1.9) > liver (1.0) > lungs (0.5) > pancreas (0.27). In the 60-day-old group the activity concentration in erythrocytes remained much lower than that in plasma. The derived data were used to develop a first-order compartmental biokinetic model consisting of a central pool presumably representing extracellular fluids, two hypothetical tissue pools representing rapid and slow exchange with the central pool, and removal from the system due to outflow from the central pool to urine, faeces, and a body sink. Removal to urine represented 51-64% of loss from the system in individual rats, removal to faeces represented 5-8%, and removal to the body sink represented 31-41%.

(205) The biokinetics of Cr(VI) has been studied mainly in rodents (Sayato et al., 1980; Weber, 1983; O'Flaherty, 1996; O'Flaherty et al., 2001; Kirman et al., 2012). Considerable reduction of ingested Cr(VI) to Cr(III) occurs in the alimentary tract, starting in the oral cavity and continuing in the stomach and intestines. Low oral intakes of Cr(VI) may be completely reduced to Cr(III) in the alimentary tract (Kerger et al., 1997). Chromium(VI) that reaches the

systemic circulation appears to be reduced to Cr(III) in red blood cells and tissues over a relatively short but imprecisely known time period.

(206) Weber (1983) studied the respiratory and systemic behaviour of Cr(VI) over a 40-d period following intratracheal administration of ^{51}Cr-labelled chromate to rats. Activity in the lungs declined to about one-third of the deposited amount over the first 2-3 d and was retained mainly in alveolar cells. Considerable absorption of Cr(VI) to blood was indicated, for example, by a relatively high uptake of activity by RBC. Much of the absorbed activity was removed from blood with a half-time of 3-4 d. Biological half-times of ^{51}Cr in tissues ranged from 14 to 50 d. The initial concentrations in kidneys, RBC, and testes showed little decline for 10-15 d but substantial decline by 25-40 d post administration.

(207) The biokinetic model for systemic Cr adopted in *Publication 30* was based mainly on results of studies by Hopkins (1965) and Mertz et al. (1965) of Cr(III) behaviour in rats (summarised above). The model did not address the kinetics of Cr(IV) on the basis that ingested or inhaled Cr(VI) will have been largely reduced to Cr(III) before reaching the systemic circulation. It was assumed that Cr leaves blood with a half-time of 0.5 d, with 30% entering excretion pathways, 5% depositing in bone, and 65% distributing uniformly in other tissues. A removal half-time of 1000 d was assigned to Cr depositing in bone. The 65% entering other tissues was divided into two retention components representing 40% and 25% of activity leaving blood and having removal half-times of 6 and 80 d, respectively. Chromium isotopes with half-life less than 15 d were assumed to be uniformly distributed on bone surfaces, and all others were assumed to be distributed in bone volume.

(208) Hiller and Leggett (2020) reviewed information on the biokinetics of Cr(III) and Cr(VI) in human subjects and laboratory animals and proposed systemic models for both forms. Parameter values for Cr(III) were based mainly on results of biokinetic and autopsy studies involving human subjects, particularly data of Sargent et al. (1979), Lim et al. (1983), and Zhu et al. (2010). Data for laboratory animals were used to fill gaps in the data for human subjects. Parameter values for Cr(VI) were based on data on the behaviour of Cr(VI) for rodents, except that the fate of Cr(IV) that enters RBC was based on data for human subjects. Chromium(VI) reaching blood was assumed to be reduced to Cr(III) in the RBC and tissues. Reduction of Cr(VI) to Cr(III) was not depicted explicitly but was represented as transfer of absorbed Cr(VI) to RBC, Kidneys 2, Liver 2, and remaining tissues, which gradually release chromium to blood as Cr(III). The model for Cr(III) was applied to Cr(III) that reached blood.

13.2.3.2. Biokinetic model for systemic chromium

(209) The biokinetic model for systemic Cr(III) proposed by Hiller and Leggett (2020) is adopted here for application to radioisotopes of chromium, as Cr(III) is expected to be the dominant form in the workplace under most conditions and the dominant systemic form after intake of Cr(VI).

(210) The structure of the systemic model for Cr(III) is shown in Fig. 13.1. Transfer coefficients for Cr(III) are listed in Table 13.3.

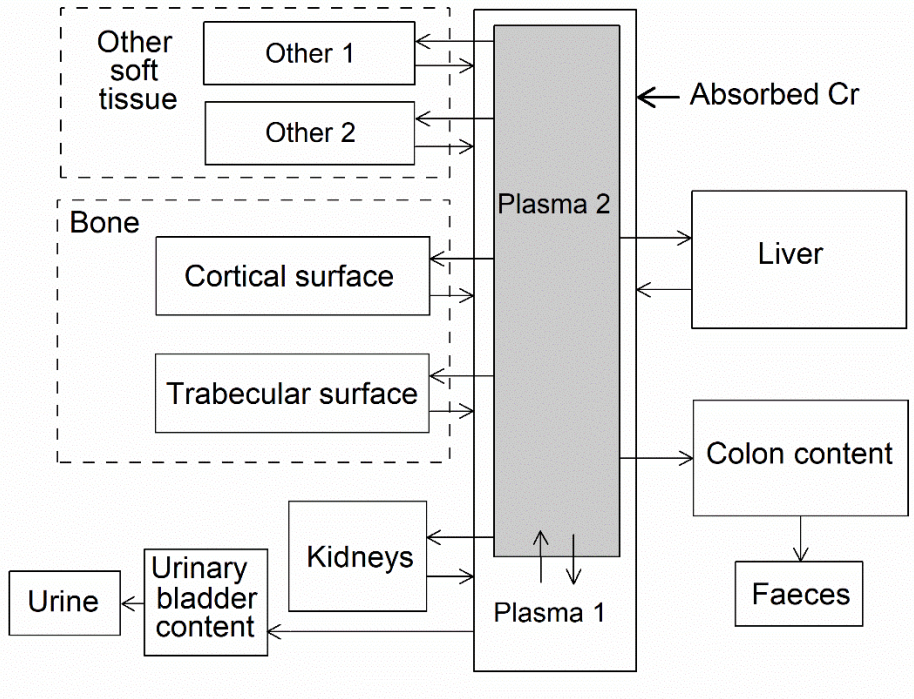

Fig. 13.1. Structure of the biokinetic model for systemic chromium.

Table 13.3. Transfer coefficients in the biokinetic model for systemic chromium

From	To	Transfer coefficient (d^{-1})
Plasma 1	Plasma 2	220
Plasma 1	Urinary bladder content	4.8
Plasma 2	Plasma 1	10
Plasma 2	Right colon content	0.1
Plasma 2	Other 1	0.7
Plasma 2	Other 2	0.027
Plasma 2	Kidneys	0.015
Plasma 2	Liver	0.15
Plasma 2	Trabecular bone surface	0.01
Plasma 2	Corical bone surface	0.01
Other 1	Plasma 1	0.25
Other 2	Plasma 1	0.00005
Liver	Plasma 1	0.01
Kidneys	Plasma 1	0.007
Trabecular bone surface	Plasma 1	0.000493
Corical bone surface	Plasma 1	0.0000821

13.2.3.3. Treatment of progeny

(211) Progeny of chromium addressed in this publication are radioisotopes of vanadium. The model for vanadium as a progeny of chromium is an expanded version of the characteristic model for vanadium with added compartments and associated transfer coefficients needed to solve the linked biokinetic models for chains headed by chromium. If vanadium is produced in a blood compartment of the chromium model not contained in the characteristic model for vanadium, it is assumed to transfer to its central blood compartment at the rate 1000 d^{-1} and to follow its characteristic model thereafter. If produced in a tissue compartment not contained in

the characteristic model for vanadium, vanadium is assumed to transfer to its central blood compartment at the rate 0.14 d^{-1} and to follow its characteristic model thereafter.

13.3. Individual monitoring

13.3.1. ^{51}Cr

(212) Measurements of ^{51}C may be performed by *in vivo* whole-body measurement technique and by gamma measurement in urine.

Table 13.4. Monitoring techniques for ^{51}Cr.

Isotope	Monitoring Technique	Method of Measurement	Typical Detection Limit
^{51}Cr	Urine Bioassay	γ-ray spectrometry[a]	9.1 Bq L^{-1}
^{51}Cr	Whole-body measurement	γ-ray spectrometry[a]	310 Bq

[a] Measurement system comprised of Germanium Detectors
[b] Counting time of 20 minutes

13.4. Dosimetric data for chromium

Table 13.5. Committed effective dose coefficients (Sv Bq^{-1}) for the inhalation or ingestion of ^{51}Cr compounds.

Inhaled particulate materials (5 µm AMAD aerosols)	Effective dose coefficients (Sv Bq^{-1})
	^{51}Cr
Type F, — NB: Type F should not be assumed without evidence	2.8E-11
Type M, default	2.4E-11
Type S	2.8E-11
Ingested materials	
Trivalent state	1.3E-11

AMAD, activity median aerodynamic diameter

Table 13.6. Dose per activity content of ^{51}Cr in total body and in daily excretion of urine (Sv Bq^{-1}); 5µm activity median aerodynamic diameter aerosols inhaled by a reference worker at light work.

	Type F		Type M		Type S	
Time after intake (d)	Total body	Urine	Total body	Urine	Total body	Urine
1	4.7E-11	1.1E-09	4.1E-11	1.3E-08	4.7E-11	3.0E-07
2	7.8E-11	2.1E-09	7.7E-11	1.9E-08	9.0E-11	4.6E-07
3	1.3E-10	4.0E-09	1.7E-10	3.6E-08	2.0E-10	8.8E-07
4	1.8E-10	5.8E-09	3.1E-10	5.3E-08	3.6E-10	1.3E-06
5	2.1E-10	7.2E-09	4.2E-10	6.4E-08	4.9E-10	1.6E-06
6	2.3E-10	8.4E-09	4.8E-10	7.3E-08	5.5E-10	1.8E-06
7	2.5E-10	9.5E-09	5.1E-10	8.1E-08	5.8E-10	2.1E-06
8	2.6E-10	1.1E-08	5.3E-10	8.9E-08	6.1E-10	2.3E-06

9	2.8E-10	1.2E-08	5.6E-10	9.7E-08	6.3E-10	2.5E-06
10	2.9E-10	1.4E-08	5.8E-10	1.1E-07	6.5E-10	2.8E-06
15	3.8E-10	2.4E-08	7.0E-10	1.6E-07	7.7E-10	4.5E-06
30	7.0E-10	1.0E-07	1.1E-09	4.0E-07	1.2E-09	1.3E-05
45	1.1E-09	2.9E-07	1.8E-09	7.2E-07	1.8E-09	2.4E-05
60	1.8E-09	5.6E-07	2.8E-09	1.2E-06	2.6E-09	3.9E-05
90	4.2E-09	1.6E-06	6.8E-09	2.9E-06	5.9E-09	8.8E-05
180	5.4E-08	2.7E-05	9.5E-08	4.3E-05	6.6E-08	9.7E-04
365	8.0E-06	8.9E-03	1.8E-05	1.1E-02	8.9E-06	1.3E-01

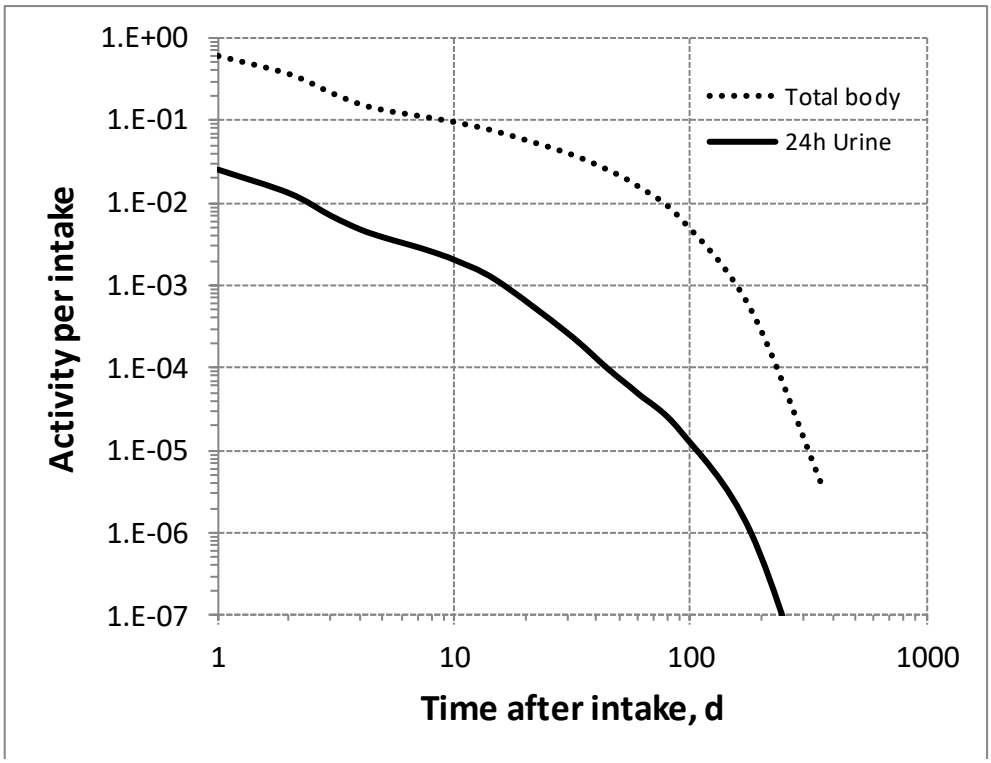

Fig. 13.2. Daily excretion of ^{51}Cr following inhalation of 1 Bq Type F.

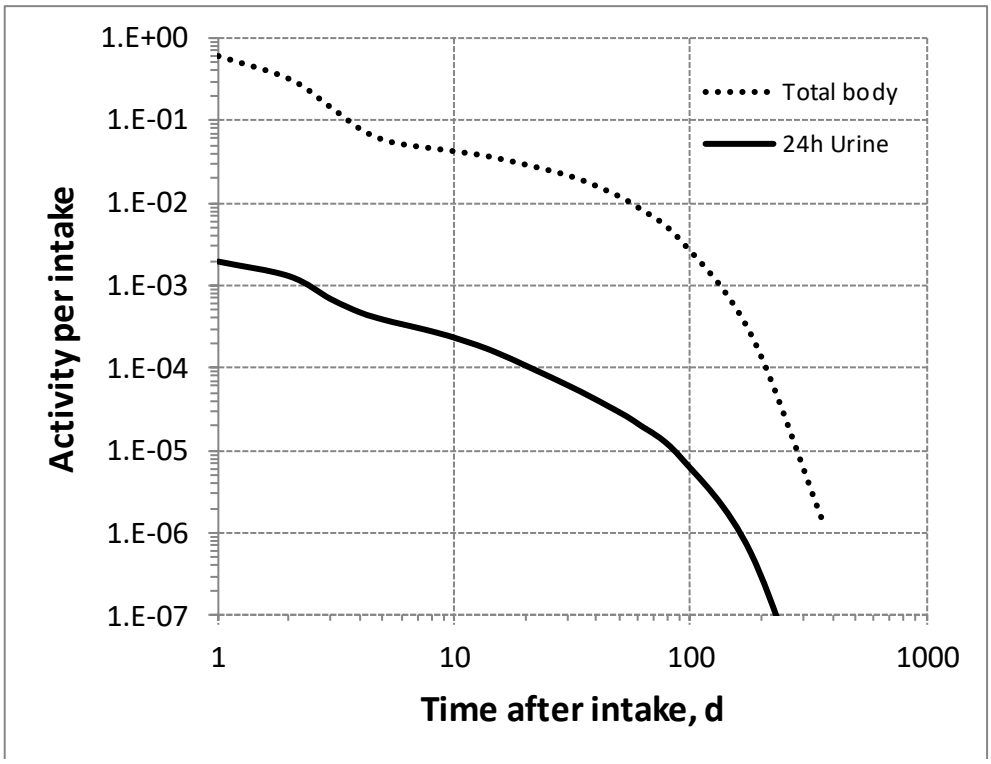

Fig. 13.3. Daily excretion of ^{51}Cr following inhalation of 1 Bq Type M.

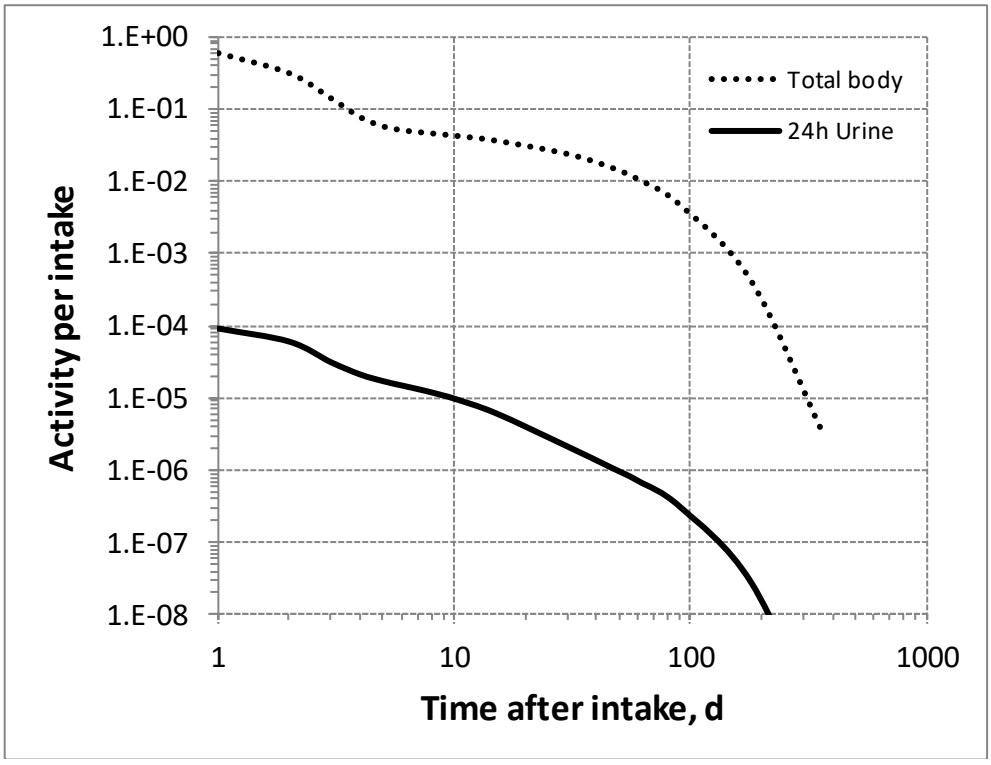

Fig. 13.4. Daily excretion of ^{51}Cr following inhalation of 1 Bq Type S.

14. MANGANESE (Z=25)

14.1. Isotopes

Table 14.1. Isotopes of manganese addressed in this publication.

Isotope	Physical half-life	Decay mode
^{51}Mn	46.2 min	EC, B+
^{52m}Mn	21.1 min	EC, B+, IT
^{52}Mn	5.591 d	EC, B+
^{53}Mn	3.7E+6 y	EC
^{54}Mn*	312.12 d	EC, B+, B-
^{56}Mn	2.5789 h	B-

EC, electron-capture decay; B+, beta-plus decay; B-, beta-minus decay; IT, isomeric transition decay.
*Dose coefficients and bioassay data for this radionuclide are given in the printed copy of this publication.
Data for other radionuclides listed in this table are given in the online electronic files on the ICRP website.

14.2. Routes of Intake

14.2.1. Inhalation

(213) For manganese, default parameter values were adopted on absorption to blood from the respiratory tract (ICRP, 2015). Absorption parameter values and types, and associated f_A values for particulate forms of manganese are given in Table 14.2.

Table 14.2. Absorption parameter values for inhaled and ingested manganese.

	Absorption parameter values*			Absorption from the
Inhaled particulate materials	f_r	s_r (d^{-1})	s_s (d^{-1})	alimentary tract, f_A
Default parameter values†				
Absorption type				
F	1	30	–	0.05
M‡	0.2	3	0.005	0.01
S	0.01	3	1×10^{-4}	5×10^{-4}
Ingested materials§				
All forms				0.05

*It is assumed that the bound state can be neglected for manganese (i.e. $f_b = 0$). The values of s_r for Type F, M and S forms of manganese (30, 3 and 3 d^{-1} respectively) are the general default values.
†For inhaled material deposited in the respiratory tract and subsequently cleared by particle transport to the alimentary tract, the default f_A values for inhaled materials are applied [i.e. the product of f_r for the absorption type and the f_A value for ingested soluble forms of manganese (0.05)].
‡Default Type M is recommended for use in the absence of specific information on which the exposure material can be assigned to an absorption type (e.g. if the form is unknown, or if the form is known but there is no information available on the absorption of that form from the respiratory tract). For guidance on the use of specific information, see Section 1.1.
§Activity transferred from systemic compartments into segments of the alimentary tract is assumed to be subject to reabsorption to blood. The default absorption fraction f_A for the secreted activity is the highest value for any form of the radionuclide ($f_A = 0.05$).

14.2.2. Ingestion

(214) The fractional absorption of manganese averages around 3-5% in adults (ATSDR, 2012c) and stays below 10% (EFSA, 2013). It is under homeostatic control and negatively

correlated with total dietary manganese and iron intakes. High intakes of calcium, phosphorus, ascorbate and phytates have been reported to impair manganese absorption. Manganese appears to be more absorbed in the gastrointestinal tract of women than men. The absorption is also higher from water than from food (Ruoff, 1995) and from manganese chloride than from manganese oxide (Roels et al., 1997; Zheng et al., 2000).

(215) For all compounds of manganese, f_1 had been taken to be 0.1 in *Publications 30* and *68* (ICRP, 1979a, 1994a). In this publication, the value of $f_A = 0.05$ is applied to all chemical forms of manganese.

14.2.3. Systemic distribution, retention and excretion of manganese

14.2.3.1. Biokinetic data

(216) Manganese is an essential element required for metabolism of amino acids, proteins, carbohydrates, and lipids. Excessive intake of manganese can result in adverse health effects including progressive neurodegenerative damage with an associated motor dysfunction syndrome similar to that seen in Parkinson's disease. Most cases of manganese intoxication have been linked to occupational exposure to airborne manganese.

(217) Dietary intake of manganese typically is about 2-6 mg d^{-1} for adult humans. The adult human body contains about 10-15 mg of manganese. The body's manganese is maintained at a nearly constant level by homeostatic controls involving regulation of gastrointestinal uptake and intestinal secretions. High dietary manganese enhances metabolism of manganese in the liver and increases secretion of systemic manganese into the gastrointestinal contents (Andersen et al., 1999; Dorman et al., 2001). Inhaled manganese initially bypasses the homeostatic control processes in the liver and becomes largely bound to transferrin. In persons chronically exposed to elevated mass concentrations of manganese in air, atypically high masses of manganese can accumulate in the brain and other tissues due to delivery by transferrin receptors.

(218) Results of a large autopsy study of element concentrations in tissues of adult male humans indicate that highest median concentrations of manganese, normalised to the concentration in liver, decrease in the order liver (1.0) > pancreas, kidney (~0.65) > gastrointestinal tissues (0.35-0.55) (Zhu et al., 2010). Lowest concentrations (0.02-0.05) were found in blood, fat, and skin. Based on median concentrations in tissues and reference tissue masses, about 34% of the body burden was contained in muscle, 24% in bone, 16% in liver, and 2% in kidneys.

(219) Isotopic studies on laboratory animals show that absorbed or intravenously injected manganese leaves blood rapidly and initially concentrates largely in organs rich in mitochondria such as the liver, pancreas, and kidneys (Kato, 1963; Dastur et al., 1971; Chauncey et al., 1977; Dorman et al., 2006). Over time, other organs including brain, bone, and muscle contain increasingly greater portions of the retained activity (Furchner et al., 1966; Dastur et al., 1969, 1971).

(220) Excretion of systemic manganese is predominantly in faeces and appears to arise mainly from biliary secretion, although substantial amounts are also removed to the gastrointestinal tract in pancreatic juices and other intestinal fluids (Maynard and Fink, 1956; Mahoney and Small, 1968; Dorman et al., 2001). In hospital patients, faecal excretion of activity was about 40 times greater than urinary excretion over the first six days following intravenous injection of ^{52}Mn in water (Maynard and Fink, 1956). Mahoney and Small (1968) found virtually no ^{54}Mn in urine following its intravenous injection as chloride into healthy subjects. Davidsson et al. (1989) found that faecal excretion accounted for virtually all biological removal of absorbed activity following ingestion of ^{54}Mn by healthy subjects.

(221) Most of the manganese in blood is contained in red blood cells (1990). The concentration of manganese in blood plasma typically is about 0.6-0.7 μg L^{-1} (Versieck and Cornelis, 1980; Baruthio et al., 1988; Versieck et al., 1988). Reported concentrations in whole blood of healthy adult subjects are typically on the order of 8-12 μg L^{-1} (Pleban and Pearson, 1979; Milne et al., 1990; Kristiansen et al., 1997).

(222) Mena et al. (1967) observed total-body retention of intravenously injected ^{54}Mn in 8 healthy adult humans (4 of each sex, age range 20-30 y), in 14 current manganese miners in good health (ages 23-60 y), and 10 former manganese miners with chronic manganese poisoning (ages 18-56 y). Total-body removal half-times were 35.5 +/- 8.4 d (mean +/- standard deviation) in the control group, 12.5 +/- 2.3 d in the healthy miners, and 26.5 +/- 4.8 d in the subjects with manganese poisoning.

(223) Mahoney and Small (1968) measured retention of intravenously injected ^{54}Mn in six subjects including both sexes (age range 25-45 y) and studied factors affecting the rate of biological removal of the tracer from the body. About 30% of the injected amount was removed with a half-time of 4 d and 70% with a half-time of 39 d. Low manganese intake increased the size of the slow component to 84% and the retention half-time to 90 d but had no effect on the half-time of the fast component. Administration of a large mass of stable manganese two months after the start of the study substantially increased the rate of elimination of ^{54}Mn.

(224) Davidsson et al. (1989) measured retention and excretion of ^{54}Mn in 14 healthy adults after its ingestion in infant formula. The mean biological half-time of absorbed activity over the period 10-30 d post ingestion was 16.4 d with a range of 6-32 d. Following intravenous administration of ^{54}Mn to two subjects, the turnover rate during days 10-30 corresponded to biological half-times of 74 and 24 d, compared with 27 and 8 d, respectively, in the same subjects following oral administration.

(225) Finley and coworkers (1994, 1999) studied the effects of gender and other factors on absorption and retention of manganese in healthy adult human subjects. Retention data for absorbed manganese for days 10-20 indicated mean whole-body biological half-times of about 15 d for men and 12 d for women. Data for days 19 to 70 indicated mean half-times of about 48 d for men and 34 d for women.

14.2.3.2. Biokinetic model for systemic manganese

(226) The biokinetic model for systemic manganese adopted for use in this publication was proposed by Leggett (2011). The model structure is shown in Fig. 14.1. Transfer coefficients are listed in Table 14.3. The reader is referred to the paper by Leggett (2011) for descriptions of the bases for parameter values and comparisons of model predictions with observations of retention of manganese tracers in human subjects.

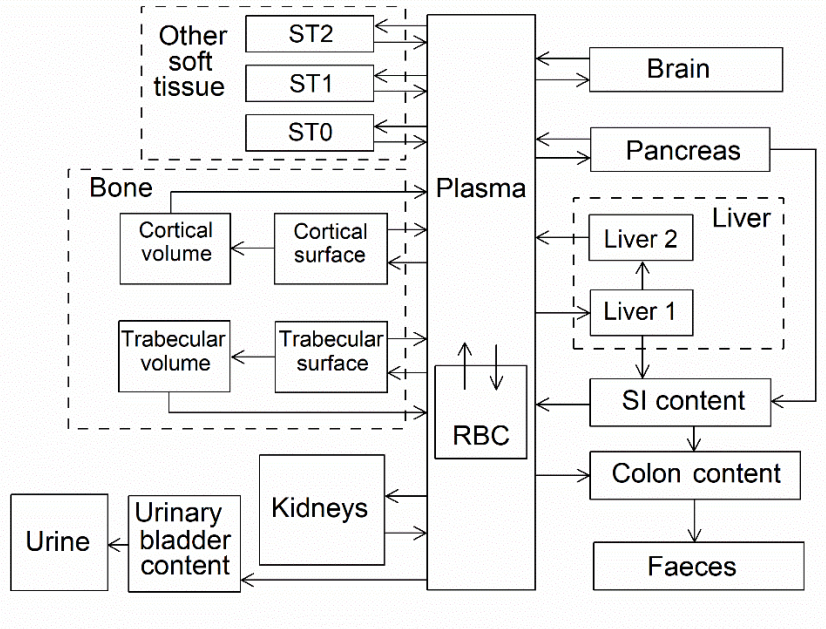

Fig. 14.1. Structure of the biokinetic model for systemic manganese.

Table 14.3. Transfer coefficients in the biokinetic model for systemic manganese.

From	To	Transfer coefficient (d^{-1})
Plasma	Liver 1	300
Plasma	Kidneys	50
Plasma	Pancreas	50
Plasma	Urinary bladder contents	2
Plasma	Right colon contents	10
Plasma	ST0	391.8
Plasma	ST1	150
Plasma	ST2	40
Plasma	Cortical bone surface	2.5
Plasma	Trabecular bone surface	2.5
Plasma	Brain	1.0
Plasma	RBC	0.2
Liver 1	Small intestine contents	0.139
Liver 1	Liver 2	0.555
Liver 2	Plasma	0.347
Kidneys	Plasma	0.347
Pancreas	Plasma	0.347
Pancreas	Small intestine contents	0.347
ST0	Plasma	33.3
ST1	Plasma	0.347
ST2	Plasma	0.0173
Cortical bone surface	Plasma	0.01716
Cortical bone surface	Cortical bone volume	0.0001733
Trabecular bone surface	Plasma	0.01716
Trabecular bone surface	Trabecular bone volume	0.0001733
Cortical bone volume	Plasma	0.0000821
Trabecular bone volume	Plasma	0.000493
Brain	Plasma	0.00462
RBC	Plasma	0.00833

14.2.3.3. Treatment of progeny

(227) Progeny of manganese addressed in this publication are radioisotopes of manganese and chromium. The model for manganese as a parent is applied to manganese produced by decay of another manganese isotope. The model for chromium as progeny of manganese is an expansion of the characteristic model for chromium with added compartments and associated transfer coefficients needed to solve the linked biokinetic models for manganese and chromium (see Annex B). If produced in a compartment not explicitly named in the model for chromium, chromium is assumed to transfer at the following rate: 1000 d^{-1} if produced in a blood compartment; at the rate of bone turnover if produced in a bone volume compartment; and at the rate 0.25 d^{-1} if produced in any other compartment.

14.3. Individual monitoring

14.3.1. ^{54}Mn

(228) Measurements of ^{54}Mn may be performed by *in vivo* whole-body measurement technique and by gamma measurement in urine.

Table 14.4. Monitoring techniques for ^{54}Mn.

Isotope	Monitoring Technique	Method of Measurement	Typical Detection Limit
^{54}Mn	Urine Bioassay	γ-ray spectrometry[a]	1.2 Bq L^{-1}
^{54}Mn	Whole-body measurement	γ-ray spectrometry[ab]	22 Bq

[a] Measurement system comprised of Germanium Detectors
[b] Counting time of 20 minutes

14.4. Dosimetric data for manganese

Table 14.5. Committed effective dose coefficients (Sv Bq^{-1}) for the inhalation or ingestion of ^{54}Mn compounds.

Inhaled particulate materials (5 µm AMAD aerosols)	Effective dose coefficients (Sv Bq^{-1})
	^{54}Mn
Type F, — NB: Type F should not be assumed without evidence	1.1E-09
Type M, default	1.3E-09
Type S	2.8E-09
Ingested materials	
All forms	5.0E-10

AMAD, activity median aerodynamic diameter

2489 Table 14.6 Dose per activity content of ^{54}Mn in total body and in daily excretion of urine (Sv Bq^{-1});
2490 5µm activity median aerodynamic diameter aerosols inhaled by a reference worker at light work.

	Type F		Type M		Type S	
Time after intake (d)	Total body	Urine	Total body	Urine	Total body	Urine
1	1.7E-09	1.3E-06	2.0E-09	1.6E-05	4.6E-09	7.2E-04
2	2.6E-09	5.9E-06	3.8E-09	6.1E-05	8.5E-09	2.8E-03
3	3.9E-09	7.2E-06	7.9E-09	7.9E-05	1.8E-08	3.6E-03
4	5.0E-09	7.6E-06	1.4E-08	8.2E-05	3.3E-08	3.8E-03
5	5.6E-09	8.0E-06	1.8E-08	8.5E-05	4.3E-08	3.9E-03
6	5.9E-09	8.5E-06	1.9E-08	8.8E-05	4.7E-08	4.1E-03
7	6.2E-09	9.0E-06	2.0E-08	9.2E-05	4.9E-08	4.3E-03
8	6.5E-09	9.5E-06	2.1E-08	9.7E-05	5.0E-08	4.6E-03
9	6.7E-09	1.0E-05	2.1E-08	1.0E-04	5.1E-08	4.8E-03
10	7.0E-09	1.1E-05	2.1E-08	1.1E-04	5.1E-08	5.1E-03
15	8.3E-09	1.5E-05	2.3E-08	1.3E-04	5.4E-08	6.5E-03
30	1.3E-08	3.2E-05	2.8E-08	2.1E-04	5.8E-08	1.2E-02
45	1.7E-08	5.6E-05	3.2E-08	2.9E-04	6.2E-08	1.7E-02
60	2.1E-08	8.4E-05	3.7E-08	3.5E-04	6.6E-08	2.1E-02
90	3.2E-08	1.4E-04	4.7E-08	4.6E-04	7.5E-08	2.6E-02
180	9.7E-08	4.6E-04	1.0E-07	9.3E-04	1.1E-07	4.2E-02
365	8.2E-07	4.6E-03	4.6E-07	4.2E-03	2.1E-07	9.1E-02

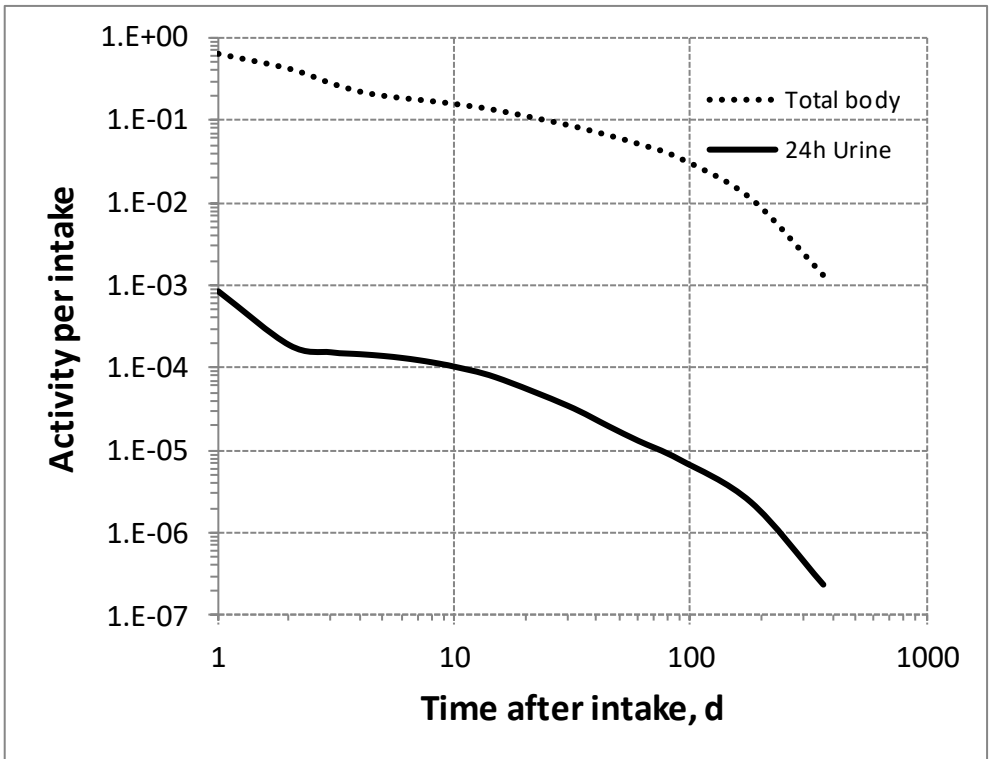

2491
2492 Fig. 14.2. Daily excretion of ^{54}Mn following inhalation of 1 Bq Type F.

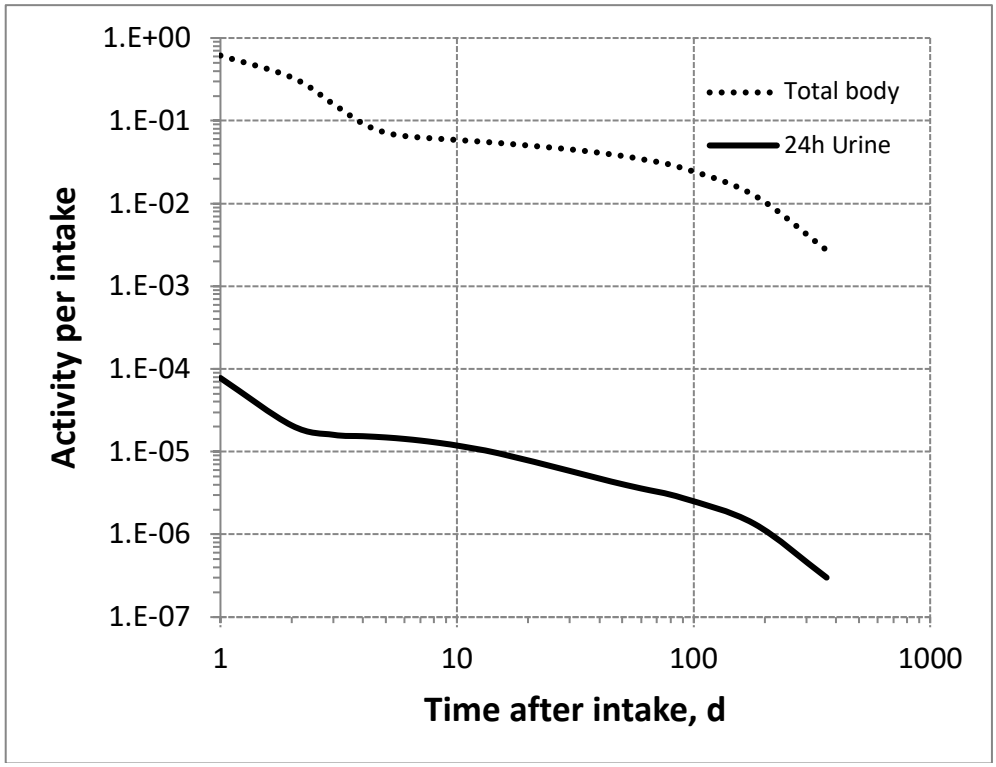

Fig. 14.3. Daily excretion of ^{54}Mn following inhalation of 1 Bq Type M.

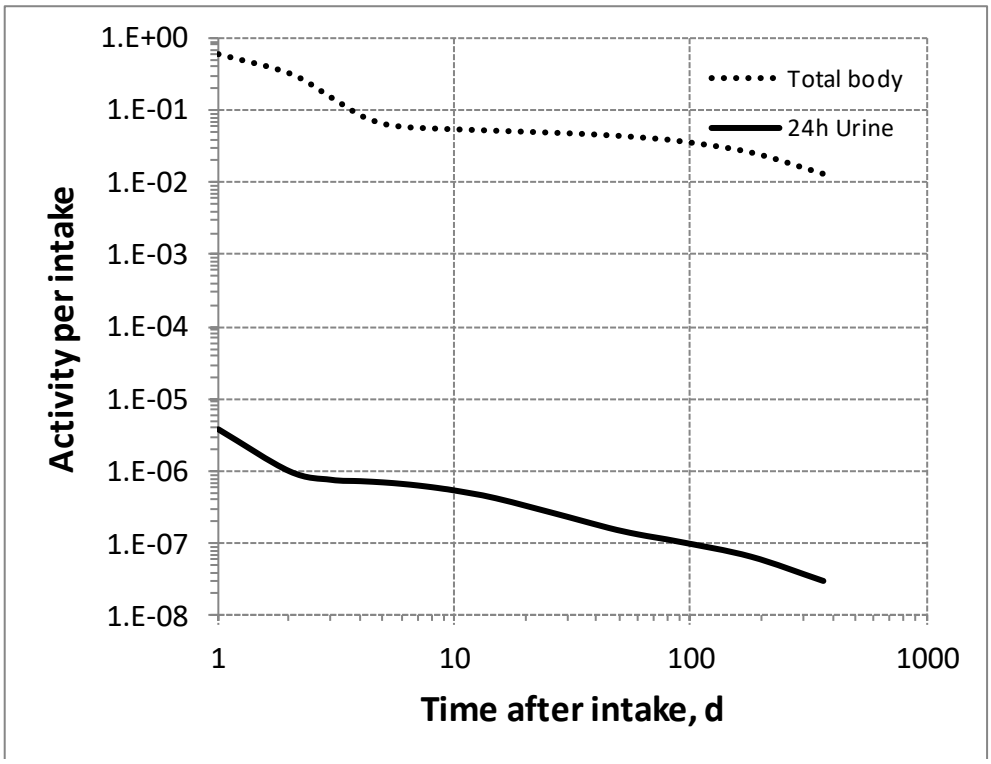

Fig. 14.4. Daily excretion of ^{54}Mn following inhalation of 1 Bq Type S.

15. NICKEL (Z=28)

15.1. Isotopes

Table 15.1. Isotopes of nickel addressed in this publication.

Isotope	Physical half-life	Decay mode
^{56}Ni	6.1 d	EC, B+
^{57}Ni	35.6 h	EC, B+
^{59}Ni*	7.6 10^4 y	EC, B+
^{63}Ni*	100.6 y	B-
^{65}Ni	2.5 h	B-
^{66}Ni	54.6 h	B-

EC, electron-capture decay; B+, beta-plus decay; B-, beta-minus decay.
*Dose coefficients and bioassay data for this radionuclide are given in the printed copy of this publication.
Data for other radionuclides listed in this table are given in the online electronic files on the ICRP website.

15.2. Routes of Intake

15.2.1. Inhalation

(229) Little information was found on the behaviour of inhaled nickel in man: NRC (1975) reports post-mortem measurements of nickel concentrations averaging 0.1, 0.6 and 70 μg g^{-1} lung (dry weight), respectively, in groups of normal subjects, ore miners, and 'victims of nickel carbonyl poisoning' who had also been chronically exposed to dust with a high nickel content. However, although they show some accumulation following occupational exposure, the deposits were not related to specific exposures, and the retention time in the lung cannot be estimated. Inhalation of nickel radioisotopes is not generally of major concern, but because of the recognised chemical toxicity of nickel, numerous studies have been conducted on its behaviour following deposition in the respiratory tract (see e.g. NRC, 1975; Sivulka, 2005; Goodman et al., 2011). Information is available from experimental studies of nickel compounds including carbonyl, chloride, sulphate, sulphides, and oxide: mostly in rats, with a few studies in dogs or monkeys.

(230) Absorption parameter values and types, and associated f_A values for gas and vapour forms of nickel are given in Table 15.2 and for particulate forms in Table 15.3. Exposures to gas or vapour forms of nickel are relatively unusual compared to exposures to particulate forms, and it is therefore recommended in this series of documents that particulate form should be assumed in the absence of information (ICRP, 2002b).

(231) Reference biokinetic models were used here (i.e. by the Task Group) for the analysis of the data and the determination of absorption parameter values. The systemic model for nickel described in Section 15.2.3 was used for all studies. Data from studies in monkeys were interpreted using human particle transport rates from the revised HRTM (ICRP, 2015), and the gastro-intestinal tract model from *Publication 30* (ICRP, 1979a): respiratory tract deposition fractions were determined from measured bioassay data. The rodent studies were interpreted using the respiratory tract model described in ICRP Supporting Guidance 3 (ICRP, 2002b), and a simplified (three-compartment) version of the *Publication 30* gastro-intestinal tract model. Unless stated otherwise, in analyses carried out here, the fraction absorbed in the alimentary tract, f_A, was taken to be 0.05 (ICRP, 1993, 1994a). Generally, respiratory tract parameter values were sensitive to the choice of value of f_A for soluble, but not for insoluble, forms.

(232) In all the analyses carried out here it was assumed that the bound state could be neglected (or was included in the dissolution phases) [i.e. $f_b = 0$ (see below)]. In a number of the studies on relatively soluble forms (chloride, sulphate, sulphide), the authors of the reports represented lung retention of most of the estimated initial lung deposit (ILD) by a single exponential function with associated biological half-time, T_b, of the order of 1 d. As this is short, absorption dominates lung clearance and the rapid dissolution rate, s_r, approximates to $\ln(2)/T_b$ (i.e. approximately 1 d^{-1}). However, some absorption would have taken place between deposition of material in the lungs and the first measurement (possibly leading to underestimation of s_r), and there would have been a contribution from mucociliary clearance from the conducting airways (possibly leading to overestimation of s_r). An estimate of s_r based on T_b is therefore only approximate, but considerable effort, and assumptions relating to factors such as the initial deposition, would be required to improve on it, and in most cases was not justified.

15.2.1.1. Gases and vapours

a. Nickel carbonyl [$Ni(CO)_4$]

(233) Tedeschi and Sunderman (1957) measured nickel excreted in urine and faeces during two consecutive 3-d periods following inhalation of nickel carbonyl [$Ni(CO)_4$] vapour by dogs. They estimated that most of the inhaled nickel had deposited in the respiratory tract, and that most of the deposited nickel was excreted rapidly in urine. There was high urinary excretion during the first 3-d period, but not during the second. In complementary balance studies they concluded that about 90% of nickel ingested in diet was excreted in faeces and 10% in urine. They commented that since nickel carbonyl is highly reactive in the presence of oxygen there was a possibility that it might decompose to produce colloidal nickel on the pulmonary epithelium.

(234) Sunderman and Selin (1968) followed the biokinetics of ^{63}Ni for 4 d after inhalation of $^{63}Ni(CO)_4$ by rats. In complementary experiments they followed the biokinetics of ^{63}Ni after intravenous (IV) injection of $^{63}Ni(CO)_4$ and ^{63}Ni-chloride ($^{63}NiCl_2$). By 4 d after IV injection of $^{63}Ni(CO)_4$, 31% of the injected activity (IA) was excreted in urine and 38% in breath – mostly during the first day, and approximately 0.5% was excreted in faeces each day. By 4 d after IV injection of ^{63}Ni chloride, 90% IA was excreted in urine – mostly during the first day; approximately 1% was excreted in faeces each day. After inhalation of $^{63}Ni(CO)_4$, similar amounts were excreted in urine and faeces: approximately 13% of the estimated amount inhaled in 1 d and 25% by 4 d. At 1 d approximately 25% of the estimated amount inhaled was retained in the body, mainly distributed in soft tissues. The authors noted that contamination of the pelt with $^{63}Ni(CO)_4$ resulted in rats ingesting an indeterminate amount of ^{63}Ni by preening, and also made it impractical to measure excretion in exhaled breath. Following inhalation there was greater excretion in faeces and retention in the respiratory and alimentary tracts than following IV injection, probably because of retention in the former of inhaled nickel, and in the latter ingested nickel (from preening).

(235) Oskarsson and Tjälve (1979) studied, by autoradiography, the distribution of ^{63}Ni at times up to 1 d after inhalation of $^{63}Ni(CO)_4$ by mice. In complementary experiments they studied the distribution of ^{63}Ni and ^{14}C after IV injection of ^{63}Ni-carbonyl and inhalation and IV injection of $Ni(^{14}CO)_4$. After inhalation of $^{63}Ni(CO)_4$, the highest concentrations of ^{63}Ni were found in the respiratory tract, but high levels were also reported in a variety of other tissues, notably brain and spinal cord. A broadly similar distribution was seen after IV injection of $^{63}Ni(CO)_4$. After IV injection or inhalation of $Ni(^{14}CO)_4$, the highest concentrations of ^{14}C were

in blood, indicating that decomposition of $Ni(CO)_4$, followed by formation of ^{14}CO-haemoglobin, took place.

(236) The experimental data indicate that following inhalation of nickel carbonyl, a large fraction is deposited in the respiratory tract, and most of the deposit is rapidly absorbed into blood. However, there is insufficient information to determine specific parameter values. The general defaults for gases and vapours are therefore adopted here: 100% total deposition in the respiratory tract (regional deposition 20% ET_2, 10% BB, 20% bb, and 50% AI), with Type F absorption. It seems possible that the systemic behaviour of nickel absorbed following inhalation of the carbonyl may differ from the model assumed for nickel in this document: in particular, some may be lost in breath, but this would probably lead to reduction in effective dose per intake.

15.2.1.2. Particulate aerosols

a. Nickel chloride ($NiCl_2$)

(237) Clary (1975) measured the tissue distribution of ^{63}Ni at 6 h, 1 and 3 d after intratracheal instillation of a large mass (1 mg) of ^{63}Ni-labelled $^{63}NiCl_2$ into rats. There was rapid absorption and excretion of the ^{63}Ni. The author noted that by 3 d, 90% of the instilled Ni had been excreted, mainly in the urine (75%), but no other excretion data were reported. At 6 h, the concentration was higher in the kidneys than the lungs, but subsequently clearance from lung was slower than from other tissues. The results are consistent with assignment to Type F. No analysis was conducted here, because the studies below were considered to provide more reliable biokinetic information, being of longer duration and involving much lower masses.

(238) English et al. (1981) followed the biokinetics of ^{63}Ni after intratracheal instillation of a low mass (6 µg) of ^{63}Ni-labelled $^{63}NiCl_2$ (or ^{63}NiO, see below) into rats. Tissue distributions were measured at times between 0.5 h and 90 d. There was rapid clearance from the lung to other tissues, and to excretion, mainly in urine. Analysis here gave $f_r = 0.98$; $s_r = 33\ d^{-1}$ ($T_b = 0.021$ d); $s_s = 0.07\ d^{-1}$ ($T_b = 10$ d), and assignment to Type F.

(239) Carvalho and Ziemer (1982) followed the biokinetics of ^{63}Ni after intratracheal instillation of a low mass (1 µg) of $^{63}NiCl_2$ into rats. Tissue distributions were measured at times between 35 min and 21 d. The authors fit lung retention with a three-component exponential function with approximately 60%, 37%, and 4% ILD retained with T_b approximately 0.03, 1, and 3 d, respectively. Although lung clearance was rapid, the highest concentration of ^{63}Ni was found in the lungs at all times. Approximately 75% ILD was excreted at 1 d, and >99% at 21 d, mostly in urine. Analysis here gave $f_r = 0.81$; $s_r = 24\ d^{-1}$ ($T_b = 0.03$ d); $s_s = 0.24\ d^{-1}$ ($T_b = 3$ d), and assignment to Type F.

(240) Graham et al. (1971) measured nickel concentrations in lung and spleen at times up to 4 d after inhalation of (stable) $NiCl_2$ by mice. Concentrations of nickel in lung, but not in spleen, were significantly higher than in controls at all times. Lung retention at 4 d was <30% ILD. Analysis here, assuming a single phase of dissolution ($f_r = 1.0$), gave a reasonable fit to the data with $s_r = 0.36\ d^{-1}$ ($T_b = 2$ d). A better fit was obtained with $f_r = 0.1$; s_r poorly defined but of order of $10\ d^{-1}$ ($T_b = 0.1$ d); and $s_s = 0.3\ d^{-1}$ ($T_b = 2$ d). The values of s_r and s_s are similar to those obtained from the results of the instillation experiments above (English et al., 1981; Carvalho and Ziemer, 1982), but that of f_r is much lower. It is possible that the faster uptake after instillation is an artefact of that method of administration, but it could be due to other reasons.

(241) Although specific parameter values for nickel chloride based on in-vivo data are available, they are not adopted here, because of the wide range in values of f_r, and because

inhalation exposure to it is unlikely. Instead, nickel chloride is assigned to Type F. However, with the data on nickel sulphate the results contribute to the selection of the default rapid dissolution rate for nickel, and the basis for bound state parameter values for nickel (see below).

b. Nickel sulphate ($NiSO_4.6H_2O$)

(242) Benson et al. (1993, 1995) followed the biokinetics of ^{63}Ni after inhalation of ^{63}Ni-labelled $NiSO_4.6H_2O$ by cynomolgus monkeys. The aim, as with parallel experiments on nickel subsulphide and oxide inhaled by monkeys (see below), was to aid in the extrapolation to man of the results of more comprehensive toxico-kinetic studies in rodents. Tissue distributions were measured within 1 h of exposure and at times up to 30 d. Nickel cleared rapidly from the lungs and body: by 30 d, approximately 1% of the Initial Body Burden (IBB: sum of ^{63}Ni in all tissues and excreta) remained in the body, measurable only in lung and kidney. The authors represented lung retention by a two-component exponential function with approximately 96% and 4% IBB retained with T_b 0.2 and 10 d, respectively. They noted the possibility that the slower phase might be due to binding of nickel to tissue. However, it was found that a large fraction of the ^{63}Ni retained in the lungs could be removed by lavage at all times, indicating that it was not bound to lung structures. Analysis here, assuming a single phase of dissolution ($f_r = 1.0$), gave a reasonable fit to the data with $s_r = 0.29$ d^{-1} ($T_b = 2.4$ d). A much better fit was obtained with $f_r = 0.94$; $s_r = 2.7$ d^{-1} ($T_b = 0.3$ d); and $s_s = 0.13$ d^{-1} ($T_b = 5$ d). The values of s_r and s_s are similar to those obtained from the results of the parallel study of ^{63}Ni-labelled Ni_3S_2 inhaled by monkeys (see below), although f_r was lower (0.14) for Ni_3S_2. Simultaneous analysis of both, with s_r and s_s optimised as shared parameters, gave for $NiSO_4$: $f_r = 0.95$; $s_r = 2.6$ d^{-1}; ($T_b = 0.3$ d); and $s_s = 0.11$ d^{-1} ($T_b = 6$ d). These values are similar to those obtained by the authors to describe overall lung retention, and give assignment to Type F.

(243) Benson et al. (1991) measured the tissue distribution of ^{63}Ni in rats at times up to 64 d after inhalation of ^{63}Ni-labelled $NiSO_4.6H_2O$. It was reported that clearance of ^{63}Ni from the body was rapid, with less than 1% IBB remaining in the rats at 10 to 13 d. In general, respiratory tract tissues, especially lung, had the highest Ni concentrations. However, by 20 d less than 0.1% IBB remained in the lungs: a single component exponential fit gave T_b approximately 1 d. Few details are given, insufficient to estimate parameter values, although the information indicates that f_r and s_r are approximately 1.0, and 1 d^{-1}, respectively, with assignment to Type F.

(244) Benson et al. (1992, 1995b,c) investigated the effects on lung clearance of repeated inhalation exposure of rats and mice to $NiSO_4.6H_2O$ (and to NiO – see below). Animals were exposed (whole body) for 6 months to $NiSO_4.6H_2O$ at concentrations of 0, 0.12 and 0.5 mg m^{-3} (rats) or 0, 0.25 and 1 mg m^{-3} (mice). At 2 or 6 months from the start of exposure, subgroups (A and C) inhaled $^{63}NiSO_4.6H_2O$, and ^{63}Ni tissue distributions were measured at times up to 32 d. Repeated inhalation of $NiSO_4.6H_2O$ did not result in accumulation of nickel in lungs of either rats or mice and did not impair the clearance of inhaled $^{63}NiSO_4.6H_2O$. The authors represented lung retention by a two-component exponential function. In rats, >99% ILD was retained with T_b 2.0 – 2.9 d; with no measurable clearance of the remaining <0.5% ILD. In mice, 78 – 96% ILD was retained with T_b approximately 1.5 d: the rest with T_b approximately 5 d. A large fraction of the ^{63}Ni retained in the lungs could be removed by lavage at all times, indicating that it was not bound to lung structures. The information indicates that f_r and s_r are approximately 0.9, and 0.5 d^{-1}, respectively, broadly similar to that in monkeys (see above) with assignment to Type F.

(245) Medinsky et al. (1987) followed the biokinetics of ^{63}Ni in rats at times up to 4 d after intratracheal instillation of ^{63}Ni-labelled $NiSO_4.6H_2O$, at three mass levels of stable nickel: 17,

190, or 1800 nmoles nickel. There was rapid clearance from lungs to blood. At the lowest mass, approximately 50% ILD remained in the lungs. Lung retention from 1 – 4 d was represented by a single exponential function with T_b 1.5 d. At higher masses lung clearance was faster, the slower-clearing phase was smaller, and with a shorter T_b. The authors considered that this suggested that potential binding sites for nickel in lung tissue or carrier-mediated clearance mechanisms for nickel were becoming saturated, resulting in more rapid clearance at higher masses due to diffusion of nickel ions.

(246) Hirano et al. (1994) measured the lung retention of nickel in rats at times up to 14 d after intratracheal instillation, and 7 d after inhalation, of (stable) $NiSO_4$. Lung retention as a fraction of ILD was represented by a single exponential function with T_b = 1.3 d in both experiments. By the end of the experiments, nickel concentrations in the lungs had returned to control levels: however, a small slowly clearing component as seen in some studies using ^{63}Ni tracer would not have been detectable against the background.

(247) The dissolution parameter values derived above for the study in monkeys are broadly supported by the results of the rodent studies outlined. Although specific parameter values for nickel sulphate based on in-vivo data are available, they are not adopted here, because they are close to those for Type F, and inhalation exposure to it is unlikely. Instead, nickel sulphate is assigned to Type F. However, with the data on nickel chloride the results contribute to the selection of the default rapid dissolution rate for nickel, and the basis for bound state parameter values for nickel (see below).

c. Ni monosulphide (NiS)

(248) Tanaka et al. (1988) measured tissue distributions of nickel in rats at times up to 76 h after inhalation of (stable) amorphous nickel monosulphide, NiS(A). Nickel cleared rapidly from the lung with T_b estimated by the authors at 20 h (0.83 d). Analysis here (assuming f_r = 1.0) gave a good fit to both lung and kidney data with s_r = 0.74 d^{-1} (T_b = 0.94 d), in agreement with the authors' estimate of lung retention and assignment to Type F.

(249) Kuehn and Sunderman (1982) measured in-vitro dissolution rates in water, rat serum, and renal cytosol over 3 d for 17 nickel compounds. Results are only given here for those compounds for which in-vivo studies are included. Results were expressed as dissolution half-times: in the case of amorphous NiS between 19 and 34 d, longer than observed by Tanaka et al. (1988) *in vivo*.

(250) Although specific parameter values for nickel monosulphide based on in-vivo data are available, they are not adopted here, because they are close to those for Type F, and inhalation exposure to it is unlikely. Instead, nickel monosulphide is assigned to Type F.

d. Nickel subsulphide (Ni_3S_2)

(251) Benson et al. (1993, 1995) followed the biokinetics of ^{63}Ni after inhalation of ^{63}Ni-labelled Ni_3S_2 by cynomolgus monkeys. The aim, as with parallel experiments with nickel sulphate (see above) and oxide (see below) inhaled by monkeys, was to aid in the extrapolation to man of the results of more comprehensive toxico-kinetic studies in rodents. Tissue distributions were measured within 1 h of exposure and at times up to 16 d. Nickel cleared rapidly from the lungs, but not as rapidly as for Ni sulphate (see above), and there was less distribution to other tissues: by 16 d, approximately 10% IBB remained in the body, mostly in lung. The authors represented lung retention (as a fraction of IBB) by a single exponential function with T_b approximately 4 d. It was found that a large fraction of the ^{63}Ni retained in the lungs could be removed by lavage at all times, indicating that it was not bound to lung structures.

Analysis here, assuming a single phase of dissolution (f_r = 1.0), gave a reasonable fit to the data with s_r = 0.13 d^{-1} (T_b = 6 d): this is similar to the value obtained by the authors to describe overall lung retention. A much better fit was obtained with f_r = 0.14; s_r = 6 d^{-1} (T_b = 0.11 d); and s_s = 0.11 d^{-1} (T_b = 6 d). The values of s_r and s_s are similar to those obtained from the results of the parallel study of ^{63}Ni-labelled $NiSO_4$ inhaled by monkeys (see above), although f_r was higher (0.94) for $NiSO_4$. Simultaneous analysis of both, with s_r and s_s optimised as shared parameters, gave for Ni_3S_2: f_r = 0.11; s_r = 2.6 d^{-1}; (T_b = 0.3 d); and s_s = 0.11 d^{-1} (T_b = 6 d), and assignment to Type F.

(252) Benson et al. (1994) followed the biokinetics of ^{63}Ni for 64 d after inhalation of ^{63}Ni-labelled nickel subsulphide ($^{63}Ni_3S_2$) by rats. There was rapid lung clearance and distribution to extra-respiratory tract tissues and urine. The authors represented lung retention (as a fraction of IBB) by a single exponential function with T_b = 4.6 d, similar to the result above for monkeys. This indicates that f_r and s_r are approximately 1.0, and 0.15 d^{-1}, respectively, with assignment to Type F.

(253) Benson et al. (1995) measured lung content of nickel in rats at times between 1 and 22 d after the start of a programme of repeated (6 h d^{-1}) inhalation exposure of rats to (stable) Ni_3S_2. Nickel concentrations in lung increased rapidly over the first 7 d of exposure and less rapidly, if at all, thereafter. From the rate of accumulation of nickel, the authors calculated the lung retention T_b in the range 3.5 – 8 d, consistent with the value of approximately 5 d reported for similar rats after acute inhalation of $^{63}Ni_3S_2$ (Benson et al., 1994). The lack of further accumulation beyond 7 d also confirms the absence of a significant slow phase (i.e. f_r = 1.0).

(254) Valentine and Fisher (1984) followed the biokinetics of ^{63}Ni for 32 d after intratracheal administration of ^{63}Ni-labelled Ni_3S_2 to mice. The authors represented lung retention (after the initial rapid clearance) by a two-component exponential function, with approximately 38% and 42% ILD retained with T_b of approximately 1.2 and 12 d, respectively.

(255) Kuehn and Sunderman (1982) measured in-vitro dissolution rates over 3 d for 17 nickel compounds in water, rat serum, and renal cytosol. Results were expressed as dissolution half-times: in the case of Ni_3S_2, ranging between 21 d and >11 y, longer than observed in the in-vivo studies above.

(256) The dissolution parameter values derived above for the study in monkeys are broadly supported by the results of the rodent studies outlined. Although specific parameter values for nickel subsulphide based on in-vivo data are available, they are not adopted here, because inhalation exposure to it is unlikely. Instead, nickel subsulphide is assigned to Type F.

e. Nickel hydroxide [$Ni(OH)_2$ (nanoparticles)]

(257) Gillespie et al. (2010) and Kang et al. (2011a,b) investigated the pulmonary toxicity of (stable) nickel hydroxide nanoparticles (nano-NH, 5-nm primary particles produced by arc discharge between nickel electrodes) inhaled (whole-body) by mice, and made limited measurements of lung deposition and clearance. Gillespie et al. (2010) measured the nickel lung content at 24 or 48 h after a 4-h inhalation exposure: or 1 d after repeated exposures for 1 week, 3 or 5 months. The authors estimated that after the single exposure approximately 50% ILD cleared within 24 h, most likely via the mucociliary escalator, and a further 10 – 20% ILD by 48 h. They estimated T_b to be of the order of 1 d, due mainly to dissolution. This was supported by the results of in-vitro dissolution tests in which approximately 90% dissolved in 24 h. However, following repeated exposures, lung nickel content increased with exposure duration, indicating greater lung retention.

(258) Kang et al. (2011b) compared the nickel lung content in mice at 0.5 and 24 h after a 4-h inhalation exposure to (stable) nano-NH or to $NiSO_4.6H_2O$ nanoparticles (count median

diameter 40 nm, produced by nebulising a dilute solution and drying the droplets). For both materials retention at 24 h was approximately 55% of that at 0.5 h, suggesting similar dissolution rates in the lungs, even though nano-NH dissolved much more slowly in water than $NiSO_4.6H_2O$. The results suggest T_b to be of the order of 1 d, which is consistent with the estimates above from more detailed studies of $NiSO_4.6H_2O$.

(259) Kang et al. (2011a) measured the tissue distribution of nickel 24 h after inhalation of (stable) nano-NH for either 1 week or 5 months. The average mass of nickel in the lungs of the 5-month group was several times that in the 1-week group, showing that accumulation continued. No significant difference was found from control animals in nickel content of any other tissue measured: liver, heart, spleen, and whole blood. Overall the results indicate Type F or M behaviour, but there is insufficient information to distinguish between the two.

f. Nickel metal

(260) Serita et al. (1999) followed lung retention in rats of (stable) nickel for up to 84 d after 5-h whole-body inhalation exposure to (stable) ultrafine metallic nickel (Uf-Ni) at three concentrations: 0.15; 1.14; 2.54 mg m^{-3}. The T_b for nickel in lung was similar in the three groups, between 28 and 39 d. The authors observed that this was shorter than for NiO, perhaps because of higher solubility in physiological media. The results indicate Type M or S behaviour.

(261) Oller et al. (2008) exposed rats (whole body; 6 h d^{-1}, 5 d $week^{-1}$) for up to 24 months to (stable) metallic nickel particles (0, 0.1, 0.4 and 1.0 mg m^{-3}). Nickel levels in lung measured at 3, 6, 12 and 24 months indicated that steady state levels were reached by 12 months. Nickel levels in blood measured at 3 and 6 months also suggested that steady state levels were reached by 12 months. The results, notably detectable nickel in blood, indicate Type M behaviour.

(262) Kuehn and Sunderman (1982) measured in-vitro dissolution rates over 3 d for 17 nickel compounds in water, rat serum, and renal cytosol. Results were expressed as dissolution half-times: in the case of Ni metal, ranging between 8.4 y and >11 y, indicating Type S behaviour.

(263) The lung retention half-times measured by Serita et al. (1999) suggest Type M or S behaviour. The study by Oller et al. (2008) is the only one available in full with measurements related to systemic uptake. The detectable levels of nickel suggest Type M behaviour, and nickel metal is assigned to Type M.

g. Nickel oxide (NiO)

(264) Benson et al. (1993, 1995) followed the biokinetics of ^{63}Ni after inhalation by cynomolgus monkeys of ^{63}Ni-labelled NiO [NiO(G), 'green' oxide calcined at 1200 °C for 1 h]. The aim, as with parallel experiments with nickel sulphate and subsulphide inhaled by monkeys (see above), was to aid in the extrapolation to man of the results of more comprehensive toxico-kinetic studies in rodents. Tissue distributions were measured within 1 h of exposure and at times up to 200 d. After rapid clearance from the upper respiratory tract, clearance from the lung was very slow with the lung T_b estimated at >200 d. Nickel was detected in the trachea and tracheal bifurcation after the first measurement: analysis here showed that particles in transit from the alveolar region could account for it. Little ^{63}Ni dissolved in the lungs and deposited in tissues outside the respiratory tract. Analysis here was limited by the small amounts absorbed. With s_r fixed at the general default value for Type M and S materials of 3 d^{-1}, analysis here gave $f_r = 0.002$; and s_s approximately 5×10^{-6} d^{-1}, but not well defined, with an upper limit of approximately 4×10^{-5} d^{-1}. These values give assignment to Type S: and are lower than the default values for Type S.

(265) Benson et al. (1992, 1995a,b) investigated the effects on lung clearance of repeated inhalation exposure of rats and mice to NiO [NiO(G), 'green' oxide calcined at 1200 °C], (and to $NiSO_4.6H_2O$ – see above). Animals were exposed (whole body) for 6 months to NiO at concentrations of 0, 0.62 and 2.5 mg m^{-3} (rats) or 0, 1.25 and 5 mg m^{-3} (mice). At 2 or 6 months from the start of exposure, subgroups inhaled ^{63}NiO, and ^{63}Ni tissue distributions were measured at times up to 200 d. Repeated inhalation of NiO resulted in accumulation of nickel in lungs of both rats and mice, and impaired the clearance of ^{63}NiO inhaled subsequently. The authors represented lung retention by two-component exponential functions. In rats sham-exposed (0 mg NiO m^{-3}) for 2 months, 92% ILD was retained with T_b 33 d, with negligible clearance of the remaining 8% ILD. In mice sham-exposed for 2 months, 80% and 20% ILD were retained with T_b 10 d and 77 d, respectively. After ^{63}NiO exposure, no ^{63}Ni was detected in the blood, liver, kidneys, or carcass of any rat, nor in blood, liver, or kidneys of any mice. All the results are consistent with assignment to Type S.

(266) Benson et al. (1994) followed the biokinetics of ^{63}Ni for 180 d after inhalation of ^{63}Ni-labelled NiO [NiO(G), 'green' oxide calcined at 1200 °C] by rats. The authors represented lung retention (as a fraction of IBB) by a single exponential function with T_b = 120 d. Little ^{63}Ni dissolved in the lungs: none was detected in tissues outside the respiratory tract. Excretion was only detectable in faeces, and most occurred in the first few days. The results give assignment to Type S.

(267) Wehner and Craig (1972) followed the tissue distribution of nickel in Syrian golden hamsters for 155 d after 2-d (7 h d^{-1}) inhalation of (stable) nickel oxide. This deposition and clearance study complemented 3-week and 3-month inhalation toxicity studies. Nickel cleared slowly from the lungs, as expected for an insoluble material: after 45 d, approximately 50% ILD remained. No significant quantities of nickel were found in the liver, kidney or carcass at any time after exposure, indicating that absorption was negligible, and Type S behaviour.

(268) Hochrainer et al. (1980) followed lung retention of nickel in rats for 100 d after inhalation of (stable) nickel oxide. The authors represented lung retention by a two-component exponential function with 21% and 79% ILD retained with T_b 0.82 d and 36.5 d, which they attributed to bronchial and alveolar clearance, respectively. No measurements of nickel were reported in excreta or other tissues, but lung retention appears typical of insoluble particles, indicating Type S behaviour.

(269) English et al. (1981) followed the biokinetics of ^{63}Ni after intratracheal instillation into rats of ^{63}Ni-labelled ^{63}NiO, prepared by heating the hydroxide at 250 °C – conversion was incomplete (or to $^{63}NiCl_2$, see above). Tissue distributions were measured at times between 0.5 h and 90 d. There was slow transfer from the lung to other tissues, and high retention in lung and associated lymph nodes. Analysis here (with s_r fixed at the general default value for Type M and S materials of 3 d^{-1}) gave f_r = 0.6; s_s = 0.005 d^{-1}; and assignment to Type M.

(270) Tanaka et al. (1985) measured tissue distributions of nickel in rats at 12 and 20 months after 140 h (7 h d^{-1} for 1 mo) inhalation of (stable) green nickel oxide, NiO(G) with AMAD 1.2 µm; and at 0 and 12 mo after a similar exposure with AMAD 4.0 µm. The authors represented lung retention by a single exponential function, with T_b = 350 d and 640 d for the 1.2 µm and 4 µm aerosols, respectively. These are high values for insoluble particles in rats, suggesting some impairment of clearance. Some increase in nickel concentrations at the later times was observed in liver and spleen, but not in kidney, indicating Type M or S behaviour.

(271) Kuehn and Sunderman (1982) measured in-vitro dissolution rates over 3 d for 17 nickel compounds in water, rat serum, and renal cytosol. Results were expressed as dissolution half-times: in the case of NiO >11 y in all three media, indicating Type S behaviour.

(272) In most studies no nickel (stable or ^{63}Ni) tracer was detected in systemic tissues following deposition in the lungs. Analysis is limited by the small amounts absorbed, and in

most cases would only give upper limits on parameter values. Greater dissolution in others suggests that its in-vivo behaviour varies with the method of particle preparation. Nickel oxide is therefore assigned to Type S.

15.2.1.3. Rapid dissolution rate for nickel

(273) Nickel sulphate ($NiSO_4.6H_2O$) is the most extensively studied form of nickel that is soluble in biological fluids. Analysis of the results of the study in which it was inhaled by cynomolgus monkeys gave: $f_r = 0.95$; $s_r = 2.6$ d^{-1}; ($T_b = 0.3$ d); and $s_s = 0.11$ d^{-1} ($T_b = 6$ d). Analysis here, assuming a single phase of dissolution ($f_r = 1.0$), gave a reasonable fit to the data with $s_r = 0.3$ d^{-1} ($T_b = 2$ d). Studies in which $NiSO_4.6H_2O$ was administered to rats and mice by inhalation or intratracheal instillation gave similar results. The two studies in which nickel chloride was administered to rats by intratracheal instillation gave higher values of s_r, approximately 30 d^{-1}. However, the one study in which nickel chloride was administered by inhalation (to mice) did not support such rapid overall dissolution. Based mainly on the results of the study of nickel sulphate inhaled by monkeys, a value for s_r of 3 d^{-1}, is applied here to all Type F forms of nickel.

15.2.1.4. Extent of binding of nickel to the respiratory tract

(274) The possibility of nickel binding to lung structures has been noted in several of the reports describing the studies above with soluble forms. For example, following inhalation of ^{63}Ni-labelled $NiSO_4.6H_2O$ by cynomolgus monkeys, Benson et al. (1995) represented lung retention by a two-component exponential function with approximately 96% and 4% IBB retained with T_b of approximately 0.2 and 10 d, respectively. They noted the possibility that the slower phase might be due to binding of nickel to tissue for several days. However, it was found that a large fraction of the ^{63}Ni retained in the lungs could be removed by lavage at all times, indicating that it was not all bound to lung structures. Medinsky et al. (1987) observed that after intratracheal instillation of ^{63}Ni-labelled $NiSO_4.6H_2O$, lung clearance was faster at higher masses, and that this suggested that potential binding sites for nickel in lung tissue or carrier-mediated clearance mechanisms for nickel were becoming saturated, resulting in more rapid clearance at higher masses due to diffusion of nickel ions. However, for the most soluble forms (e.g. chloride or sulphate) the possible bound fraction and associated T_b are both small, and it is therefore assumed here that for nickel the bound state can be neglected (i.e. $f_b = 0.0$).

Table 15.2. Deposition and absorption for gas and vapour compounds of nickel.

	Percentage deposited (%)*						Absorption†	
Chemical form/origin	Total	ET_1	ET_2	BB	bb	AI	Type	f_A‡
Nickel carbonyl	100	0	20	10	20	50	F	0.05

ET_1, anterior nasal passage; ET_2, posterior nasal passage, pharynx and larynx; BB, bronchial; bb, bronchiolar; AI, alveolar-interstitial.

*Percentage deposited refers to how much of the material in the inhaled air remains in the body after exhalation. Almost all inhaled gas molecules contact airway surfaces, but usually return to the air unless they dissolve in, or react with, the surface lining. The default distribution between regions is assumed: 20% ET_2, 10% BB, 20% bb, and 50% AI.

†It is assumed that the bound state can be neglected for nickel (i.e. $f_b = 0$).

‡For inhaled material deposited in the respiratory tract and subsequently cleared by particle transport to the alimentary tract, the default f_A values for inhaled materials are applied [i.e. the product of f_r for the absorption type (or specific value where given) and the f_A value for ingested soluble forms of nickel (0.05)].

Table 15.3. Absorption parameter values for inhaled and ingested nickel.

Inhaled particulate materials		Absorption parameter values* f_r	s_r (d^{-1})	s_s (d^{-1})	Absorption from the alimentary tract, f_A
Default parameter values†,‡					
Absorption type	Assigned forms				
F	Nickel chloride, sulphate, monosulphide, subsulphide	1	3	–	0.05
M§	Nickel metal	0.2	3	0.005	0.01
S	Nickel oxide	0.01	3	1×10^{-4}	5×10^{-4}
Ingested materials¶					
Nickel in soluble forms (including chloride, sulphate and sulphide) and in unspecified forms					0.05
Nickel metal					0.01
Nickel oxide					5×10^{-4}

*It is assumed that for nickel the bound state can be neglected (i.e. $f_b = 0.0$). The value of s_r for Type F forms of nickel (3 d^{-1}) is element-specific. The values for Types M and S (3 d^{-1}) are the general default values.

†Materials (e.g. nickel chloride) are generally listed here where there is sufficient information to assign to a default absorption type, but not to give specific parameter values (see text).

‡For inhaled material deposited in the respiratory tract and subsequently cleared by particle transport to the alimentary tract, the default f_A values for inhaled materials are applied [i.e. the product of f_r for the absorption type (or specific value where given) and the f_A value for ingested soluble forms of nickel (0.05)].

§Default Type M is recommended for use in the absence of specific information on which the exposure material can be assigned to an absorption type (e.g. if the form is unknown, or if the form is known but there is no information available on the absorption of that form from the respiratory tract). For guidance on the use of specific information, see Section 1.1.

¶Activity transferred from systemic compartments into segments of the alimentary tract is assumed to be subject to reabsorption to blood. The default absorption fraction f_A for the secreted activity is the highest value for any form of the radionuclide ($f_A = 0.05$).

15.2.2. Ingestion

(275) Nickel absorption studies were reviewed in *Publications 30* and *67* (ICRP, 1981, 1993), by the International Agency for Research on Cancer (1990), by the United Nations International Programme on Chemical Safety (US IPCS, 1991), by the Nickel Producers Environmental Research Association (NiPERA, 1996), by Toxicology Excellence for Risk Assessment for the Metal Finishing Association of Southern California, the United States Environmental Protection Agency and Health Canada (TERA, 1999), by the United States Agency for Toxic Substances and Disease Registry (ATDSR, 2005a), and by the Danish Environmental Protection Agency (2008).

(276) Ingested nickel is transported through the membrane of the intestinal epithelium into the interstitial areas proximal to capillaries although the specific mechanism is not exactly known. Specific transport processes may control the manner by which nickel is absorbed from the lumen and transported into the interstitial space. The absorption and secretion of nickel by the jejunum of rats occurs by transmembrane diffusion (Foulkes and McMullen, 1986). Refvik and Andreassen (1995) investigated the surface binding and uptake of Ni^{2+} in human kidney epithelial cells and found that calcium ionophore potentiated nickel uptake into cells suggesting that nickel may be transported via Ca^{2+} channels. The third mechanism of nickel uptake is the

phagocytosis of particulate nickel or nickel compounds (Heck and Costa, 1982; Kuehn et al., 1982).

15.2.2.1. Controlled human ingestion studies

(277) Information on nickel absorption in the alimentary tract is available from several controlled studies of adult human volunteers ingesting nickel in food or drinking water, with or without fasting. Menne et al. (1978) studied nickel excretion in urine for 3 d after oral administration of 5.6 mg as the sulphate to 6 female and 7 male volunteers, aged 29-64 y, with psoriasis or leg ulcers. Analysis here gave a mean absorbed fraction of 0.02 with a range from 0.003 to 0.05. Christensen et al. (1979) measured nickel concentration in the serum of 3 male and 9 female healthy volunteers aged 20-35 y, 2 h after ingestion of 5.6 mg as the sulphate in lactose. Analysis here indicated mean fractional absorption of 0.05 with a range from 0.004 to 0.2. Christensen and Lagesson (1981) performed another similar study with 6 female and 2 male healthy volunteers aged 21-32 y and monitored nickel in whole blood for 4 h post ingestion and in 24 h urine. The peak level of nickel in blood occurred 2.5 h after ingestion and the maximum urinary excretion occurred in the first 8 h after ingestion. Analysis here gave a mean fractional absorption of 0.07 with a range from 0.007 to 0.2.

(278) Solomons et al. (1982) investigated the influence of diet on nickel absorption. Healthy adult subjects were orally given 5 mg of nickel as sulphate hexahydrate in water following overnight fasting. Plasma nickel concentration was monitored for 4 h post ingestion in five subjects and up to 24 h post ingestion in one subject. Analysis here gave a mean fractional absorption of 0.2 with a range from 0.1 to 0.3. When nickel was given with a typical Guatemalan meal, the observed fractional absorption was only 0.02. No absorption of nickel given with a North American breakfast was observed. Food constituents, possibly phosphate, phytate, fibers, and similar metal-ion-binding components, may bind nickel and make it much less available for absorption than nickel dissolved in water and ingested on an empty stomach. Nickel absorption also appeared to be significantly reduced after ingestion of cow milk, coffee, tea, orange juice, ascorbic acid but less so after ingestion of Coca Cola or phytic acid. Disodium EDTA depressed plasma nickel below the level observed in fasting controls. Sunderman et al. (1989) monitored nickel concentration in serum, urine and faeces of 10 healthy volunteer subjects (6 men, 4 women, ages 22-55 y) for 1 d before and 4 d after ingestion of 12-50 µg of nickel per kg body weight. The subjects had fasted for 12 h prior to nickel ingestion and intake was followed by an additional 3-h fasting period. Nickel was given as the sulphate either with drinking water or with a standard North American breakfast. The authors estimated absorbed fractions of approximately 0.01 for nickel in food and about 0.3 for nickel in drinking water.

(279) Hindsen et al. (1994) measured nickel concentration in blood and urine of 52 female patients with five different types of eczema, 3 h and 24 h respectively after ingestion of 1 mg of nickel as the sulphate in lactose. The subjects were fasting for at least 8 h before and 1 h after nickel ingestion. Analysis here gave fractional absorption around 0.09, with a range from 0.07 to 0.13 for the 5 groups of patients with the same type of eczema. Repeated oral administration of nickel sulphate might decrease intestinal absorption (Santucci et al., 1994). Patriarca et al. (1997) measured nickel concentrations in blood, urine and faeces of four healthy adult human subjects up to 5 d after ingestion of 10 µg of ^{62}Ni as the metal diluted in water per kg body weight. The subjects fasted overnight before and 2.5 h after the isotope ingestion. The mean observed absorption fraction was 0.3 of ingested nickel, with a range up to 0.4. Nielsen et al. (1999) have reported values of fractional gastrointestinal absorption for 8 healthy adult male volunteers of 0.3 when administered in water after 4-h fasting, 0.09 after 1.5-h fasting, 0.04 when administered at the same time of food, 0.1 when administered after 12-h fasting and 0.5

h before meal, 0.2 when administered after 12-h fasting and 1 h before meal, and 0.03 when Ni is mixed with meal. In 40 adult women with vesicular hand eczema having ingested nickel in water after 12-h fasting and 4 h before meal, Nielsen et al. (1999) observed absorption of a fraction of about 0.1 of intake.

15.2.2.2. Accidental and environmental human exposure studies

(280) Complementary information is brought by studies of environmental balance and accidental exposure. But this is assumed to be less reliable for estimate of absorption fraction since intake is more difficult to assess with precision. Tipton et al. (1966) monitored trace elements in diet, urine and faeces of two, male and female, human subjects of ages 34 and 35. The comparison of intake and urine excretion averaged over a month indicated fractional absorption in the order of 0.5. Similarly, an American hospital reported values of intake and excretion for two patients corresponding to fractional absorptions of 0.5 and 0.6 (Veterans Administration Hospital and Hines IL, 1976).

(281) Nomoto and Sunderman (1970), McNeely et al. (1972) and Horak and Sunderman (1973) reported values of nickel concentration measured in the serum, urine and faeces of healthy adult inhabitants of Hartford, Connecticut (USA). The ratio of daily urine excretion measured in 50 subjects to daily faecal excretion measured in 10 subjects corresponded to a fractional absorption of about 0.01. Nodiya (1972) reported the daily ingestion intake, urinary and faecal excretion of 10 male volunteers aged 17 years. The results indicated fractional absorption in a range from 0.09 to 0.12 with a mean of 0.1. *Publication 23* (ICRP, 1975) reported values for nickel balance. The ratio between intake in food and fluids and the loss in urine, sweat and hair indicates a fractional absorption about 0.08.

(282) Sunderman et al. (1988) followed the consequences of the accidental ingestion of a solution of nickel sulphate and nickel chloride by 32 workers in an electroplating plant. Nickel concentrations in serum and urine were measured for 5 d after exposure. The oral intake was estimated to range from 0.5 to 2.5 g for 20 symptomatic workers. Analysis here of the serum and urine measurement data for a subgroup of 10 heavily exposed workers admitted to hospital indicated fractional absorption of a few percent of the nickel intake. For a group of 11 other workers followed as outpatients, the estimated fractional absorption would be about 10 times lower.

15.2.2.3. Animal studies

(283) The gastrointestinal absorption of dietary nickel was also studied in a few animal experiments involving rats, calves and dogs. These studies provide information on absorption of specific chemical forms of nickel and for neonates. Phatak and Patwardhan (1952) investigated over 4 d the retention and excretion of nickel in rats fed with 25-100 mg of nickel per 100 mg of basal diet. Measurement results of nickel in food, urine and faeces indicated fractional absorption in the order of 0.2 for nickel carbonate (24 animals) and 0.1 for nickel soap (12 animals) or finely divided nickel metal (12 animals). Tedeschi and Sunderman (1957) studied nickel balance in dogs. The ratio of nickel excreted in urine to that ingested in food indicated fractional absorption in the order of 0.06. O'Dell et al (1971) fed 12 male calves with a basal diet supplemented with 0 to 1.4 g d^{-1} of nickel as the carbonate. The comparison of urine and faecal excretion indicated absorption of 0.02 to 0.05 of ingested nickel. Elakhovskaya (1972) orally administered nickel as the chloride in drinking water to rats (0.005, 0.5, or 5 mg L^{-1}) and measured urinary and faecal excretion. The distribution between excretion pathways was consistent with fractional absorption about 0.04 (range 0.02 – 0.06). Ho and Furst (1973)

studied nickel urinary excretion after either intraperitoneal injection or oral intubation of a nickel chloride solution to rats. They estimated that 3-6% of the ingested quantity reached the bloodstream.

(284) A study in rats suggested gastrointestinal absorption fractions for soluble forms of nickel: 0.3 for the nitrate [$Ni(NO_3)_2$]; 0.1 for the sulphate ($NiSO_4$) and chloride ($NiCl_2$); 0.02 for the monosulphide (NiS). This study has also suggested gastrointestinal absorption of 0.005 for nickel subsulphide (Ni_3S_2) and 0.0009 for nickel metal. For gastrointestinal absorption of nickel oxide, produced at 1030 °C [NiO(G)] or at 550 °C [NiO(B)], the suggested values were 0.0001 for NiO(G) and 0.0004 for NiO(B) (Ishimatsu et al., 1995). More recent data obtained on rats fed with nickel citrate, oxalate or chloride show gastrointestinal absorption ranging from 0.03 to 0.05 (Paquet et al., 1998).

(285) In *Publications 30* and *67* (ICRP, 1981, 1993) an absorption fraction of 0.05 was recommended for all ingested nickel compounds. For risk characterisation purpose, the Danish environmental protection agency retained absorption fractions for nickel metal of 0.003 for fasting individuals and 0.0005 for non-fasting individuals, an absorption fraction of 0.3 for nickel sulphate, chloride, carbonate and nitrate ingested by fasting individuals, and an absorption fraction of 0.05 for all other scenarios of ingestion exposure.

(286) As indicated in Table 15.3, a value of $f_A = 0.05$ is adopted here for nickel ingested in soluble form (carbonate, citrate, oxalate, nitrate, chloride) or in unspecified form. Values of $f_A = 0.01$ for nickel metal and $f_A = 5 \times 10^{-4}$ for nickel oxide are also retained here.

15.2.3. Systemic distribution, retention and excretion of nickel

15.2.3.1. Biokinetic data

(287) The following summary of biokinetic data for nickel is taken from a review by Melo and Leggett (2017). The reader is referred to that paper for a more detailed discussion of the database and a more extensive bibliography.

(288) The nickel content of the adult human body and individual tissues has been estimated from postmortem measurements. Estimates of total-body nickel in adult humans range from about 0.5 mg (Sunderman, 2004) to more than 20 mg (Zhu et al., 2010).

(289) Urinary excretion is the primary route of elimination of systemic nickel (Sunderman et al., 1989; Patriarca et al., 1997). Estimates of endogenous faecal excretion of nickel vary from a few percent to 20% or more of the amount reaching blood. Nickel is also removed from the body in sweat, hair, saliva, and other typically minor excretion pathways (Sunderman, 1993).

(290) The average concentration of nickel in serum is 0.2 μg L^{-1} or lower. The average concentration in urine is in the range 1-3 μg L^{-1}, depending on food and fluid intake and environmental factors (Templeton et al., 1994).

(291) Sunderman et al. (1989) studied the biokinetics of nickel in healthy adult human subjects following acute ingestion of elevated quantities of stable nickel in water (Experiment 1) or food (Experiment 2). The concentrations of nickel in serum, urine, and faeces were determined from 2 d before to 4 d after administration of 12 (n=4), 18 (n=4), or 50 (n=1) μg Ni kg^{-1}. Normal daily intake of nickel by these subjects was on the order of 1-4 μg kg^{-1}. In Experiment 1, the subjects fasted for 12 h before and 3 h after drinking $NiSO_4$ dissolved in water. In Experiment 2, the subjects fasted for 12 h before ingesting a standard American breakfast containing $NiSO_4$. Mean absorption of nickel was about 27% of the amount ingested in water and 0.7% of the amount ingested in food. The estimated mean removal half-time of absorbed nickel from the body was 28 h. On average urinary excretion accounted for over 90% of absorbed nickel over the observation period. The estimated mean renal clearance of nickel

was 8.3 ml min^{-1} in Experiment 1 and 5.8 ml min^{-1} in Experiment 2. The results of Experiment 1 are more useful than those of Experiment 2 for purposes of modeling the systemic behaviour of nickel due to the relatively small amount of administered nickel reaching blood in Experiment 2.

(292) Patriarca et al. (1997) studied the behaviour of ingested nickel in four healthy adult human subjects using the stable nickel isotope ^{62}Ni as a tracer. The subjects ingested 10 µg ^{62}N per kg body weight, compared with their normal daily intakes of total stable nickel of about 1-6 µg kg^{-1}. Concentrations of ^{62}Ni were measured in plasma, red blood cells (RBC), urine, and faeces up to 5 d after administration in water. The inter-individual variability of results was considerably lower than in the study by Sunderman et al. (1989), in which naturally abundant nickel isotopes were administered. The investigators attributed the comparatively low variability of their data to the ability to distinguish the tracer from other sources of nickel in the tissue and fluid samples, including nickel from normal diet and nickel contamination of samples. Plasma clearance curves were consistent with the serum clearance curve generated by the Sunderman model. However, mean urinary losses of the tracer accounted only for about two-thirds of the absorbed amount over five days in the subjects of Patriarca et al. (1997), compared with a central estimate of ~93% over 4 d in the study by Sunderman et al. (1989). The data of Patriarca et al. (1997) indicate that total-body retention at 5 d plus losses from the body by that time via pathways other than urine accounted for about one-third of absorbed ^{62}Ni. Endogenous faecal excretion of ^{62}Ni appeared to represent at most a few percent of absorbed ^{62}Ni.

(293) Nieboer et al. (1992) surveyed experimental and occupational data on the absorption, distribution, and excretion of nickel. They estimated a mean renal clearance of plasma nickel of 7.7 mL min^{-1} based on data for 26 male workers at two electrolytic refining operations. This is consistent with the estimate of 8.3 ml min^{-1} by Sunderman et al. (1989) based on a study involving ingestion of nickel in drinking water. Renal clearance of ~8 mL min^{-1} corresponds to clearance of 3.8 plasma volumes per day based on the reference plasma volume of 3000 mL for an adult male (ICRP, 2002a). Data collected by Nieboer and coworkers indicate that, at typical urine flow rates, roughly 30% of nickel filtered by the kidneys enters the urinary bladder content and the remainder returns to blood.

(294) Information on uptake and retention of nickel by specific organs and tissues of the body comes mainly from animal studies. At early times after administration the highest tissue concentration in laboratory animals usually is found in the kidneys. For example, at 24 h after oral administration of three soluble nickel compounds [$Ni(NO_3)_2$, $NiCl_2$ and $NiSO_4$] to male Wistar rats, the kidneys contained an estimated 80% of the nickel recovered in measured organs (Ishimatsu et al., 1995). Elevated concentrations at early times after administration also have been observed in lung, pituitary, skin, adrenals, and gonads (Parker and Sunderman, 1974; Jacobsen et al., 1978; Olsen and Jonsen, 1979).

(295) Smith and Hackley (1968) measured the distribution of activity in rats over the first 72 h after intravenous administration of carrier-free ^{63}Ni. The kidneys showed a much higher activity concentration than other tissues at all times. For example, the concentration ratio kidneys:liver was in the range 18-32 over the first 4 h, and the concentration ratio kidneys:femur was 27-59 during that time. The ^{63}Ni content of the kidneys was at least three times greater than that of the liver and at least as much as the skeleton throughout the 72-h observation period.

(296) At 1 d after intravenous administration of $^{63}NiCl_2$ to rabbits the activity concentration in kidneys was about 23, 18, and 29 times that in liver, bone, and muscle, respectively (Parker and Sunderman, 1974). At 1 d after intramuscular administration of $^{63}NiCl_2$ to rats the concentration of ^{63}Ni in kidneys was about 29 times that in liver and 86 times that in muscle (Sunderman et al., 1978).

(297) Several short-term studies (days) of the behaviour of nickel in laboratory animals indicate that nickel has a low affinity for bone, but some longer-term studies (weeks or longer) indicate that a portion of nickel entering bone is removed relatively slowly compared with removal from most soft tissues. For example, following intraperitoneal injection of $^{63}NiCl_2$ to adult mice, the activity concentration was greater in the kidney than in other investigated tissues at 1-5 d after injection but much lower than that of the skull, long bones, and incisors at 22 d (Jacobsen et al., 1978).

(298) Onkelinx et al. (1973) studied the early kinetics of systemic nickel ^{63}Ni in rats and rabbits following intravenous injection of $^{63}NiCl_2$. In rats, about 78% of injected activity was lost in urine and 15% in faeces over 3 d. In rabbits, about 78% of injected activity was removed in urine during the first 24 h, and biliary secretion during the first 5 h was about 9% of the administered activity.

15.2.3.2. Biokinetic model for systemic nickel

(299) The model for systemic nickel is taken from Melo and Leggett (2017). The structure of the model is shown in Fig. 15.1. Transfer coefficients are listed in Table 15.4.

(300) The model divides systemic nickel into compartments representing blood plasma, red blood cells (RBC), a rapid-turnover kidney compartment (Kidneys 1), a slow-turnover kidney compartment (Kidneys 2), a liver compartment with a moderate turnover rate (Liver 1), a liver compartment with slow turnover (Liver 2), four bone compartments (cortical and trabecular surface and volume), a compartment of other soft tissues with a moderate turnover rate (ST0), and a compartment of other soft tissues with a slow turnover rate (ST1). Removal of systemic nickel from the body is assumed to occur via urine, faeces, and a third excretion pathway representing total losses in sweat, saliva, hair, and nails.

(301) The reader is referred to the paper by Melo and Leggett (2017) for a detailed description of the basis of the parameter values listed in Table 15.4. Briefly, parameter values were set mainly for consistency with the following data sets:

- Blood kinetics and excretion rates of nickel observed in the controlled human studies of Sunderman et al. (1989) and Patriarca et al. (1997), with preference given to results of the Ni tracer study of Patriarca et al. where data from the two studies were inconsistent.
- Renal clearance (plasma volumes per day) of 3.8 d^{-1}, based on data of Nieboer et al. (1992) for occupationally exposed subjects, and data of Sunderman et al. (1989) for human subjects administered nickel in drinking water.
- Relative rates of nickel excretion via urine, faeces, and combined minor excretion routes, as indicated by collective findings for human subjects and laboratory animals.
- A typical systemic distribution of nickel in the early hours, days, and weeks after uptake to blood, as inferred from collected animal studies.
- The long-term distribution of nickel in the body as indicated by postmortem measurements of nickel in human tissues.
- Reference trabecular and cortical bone turnover rates for adult humans (ICRP, 2002a) as estimators of the long-term rates of removal of nickel from these two types of bone.

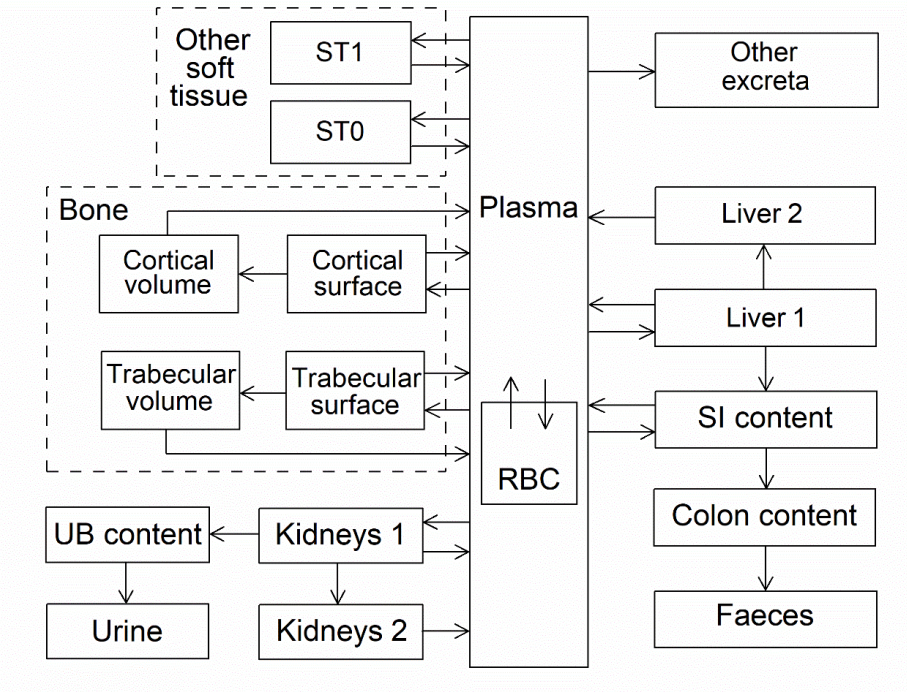

Fig. 15.1. Structure of the proposed model for systemic nickel. UB = urinary bladder, RBC = red blood cells, SI = small intestine.

Table 15.4. Transfer coefficients in the biokinetic model for systemic nickel.

From	To	Transfer coefficient (d^{-1})
Plasma	Kidneys 1	12. 7
Plasma	Small intestine content	0.18
Plasma	Liver 1	0.45
Plasma	Cortical bone surface	0.675
Plasma	Trabecular bone surface	0.675
Plasma	Other 1	7.2
Plasma	Other 2	1.2
Plasma	Red blood cells (RBC)	0.075
Plasma	Excreta	0.34
Red blood cells (RBC)	Plasma	0.231
Kidneys 1	Plasma	35
Kidneys 1	Urinary bladder content	15
Kidneys 1	Kidneys 2	0.0013
Kidneys 2	Plasma	0.00173
Liver 1	Plasma	1.9
Liver 1	Liver 2	0.29
Liver 1	Small intestine content	1.46
Liver 2	Plasma	0.00173
Other 1	Plasma	1.9
Other 2	Plasma	0.00173
Cortical bone surface	Plasma	1.9
Cortical bone surface	Cortical bone volume	0.0192
Trabecular bone surface	Plasma	1.9
Trabecular bone surface	Trabecular bone volume	0.019
Cortical bone volume	Plasma	0.0000821
Trabecular bone volume	Plasma	0.000493

15.2.3.3. Treatment of progeny

(302) Progeny of nickel addressed in this publication are ^{56}Co ($T_{1/2}$ = 77.2 d), ^{57}Co (272 d), and ^{66}Cu (5.12 min). Copper-66 produced in a systemic compartment is assumed to decay at its site of production. The model for cobalt as a progeny of nickel is an expansion of the characteristic model for cobalt with added compartments and associated transfer coefficients needed to solve the linked biokinetic models for nickel and cobalt (see Annex B). If produced in a compartment not explicitly identified in its characteristic model, cobalt is assumed to transfer to its central blood compartment at 1000 d^{-1} if produced in a blood compartment and at 0.099 d^{-1} if produced in a tissue compartment, and to follow its characteristic model thereafter.

15.3. Individual monitoring

15.3.1. ^{59}Ni

(303) Measurements of ^{59}Ni may be performed by Liquid Scintillation Counting in urine.

Table 15.5. Monitoring techniques for ^{59}Ni.

Isotope	Monitoring Technique	Method of Measurement	Typical Detection Limit
^{59}Ni	Urine Bioassay	Liquid Scintillation Counting	20 Bq L^{-1}

15.3.2. ^{63}Ni

(304) Measurements of ^{63}Ni may be performed by Liquid Scintillation Counting in urine.

Table 15.6. Monitoring techniques for ^{63}Ni.

Isotope	Monitoring Technique	Method of Measurement	Typical Detection Limit
^{63}Ni	Urine Bioassay	Liquid Scintillation Counting	1 Bq L^{-1}

15.4. Dosimetric data for nickel

Table 15.7. Committed effective dose coefficients (Sv Bq^{-1}) for the inhalation or ingestion of ^{59}Ni and ^{63}Ni compounds.

	Effective dose coefficients (Sv Bq^{-1})	
Inhaled gases or vapours	^{59}Ni	^{63}Ni
Nickel carbonyl	1.6E-10	4.7E-10
Inhaled particulate materials (5 µm AMAD aerosols)		
Type F, Nickel chloride, sulphate, monosulphide, subsulphide	2.6E-11	7.1E-11
Type M, Nickel metal	4.0E-11	1.5E-10
Type S, Nickel oxide	7.6E-10	1.7E-09
Ingested materials		
Nickel in soluble forms (including chloride, sulphate, sulphides) and in unspecified forms	1.1E-11	3.0E-11
Nickel metal	2.8E-12	6.0E-12
Nickel oxide	6.7E-13	3.0E-13

AMAD, activity median aerodynamic diameter

Table 15.8 Dose per activity content of ^{59}Ni in daily excretion of urine (Sv Bq^{-1}); 5µm activity median aerodynamic diameter aerosols inhaled by a reference worker at light work.

Time after intake (d)	Nickel carbonyl Urine	Type F Urine	Type M Urine	Type S Urine
1	6.4E-10	6.7E-10	5.2E-09	1.9E-06
2	1.4E-09	1.3E-09	1.0E-08	3.8E-06
3	2.9E-09	2.8E-09	2.0E-08	7.7E-06
4	5.7E-09	5.5E-09	3.7E-08	1.5E-05
5	1.1E-08	1.1E-08	6.3E-08	2.7E-05
6	2.1E-08	2.1E-08	9.9E-08	4.5E-05
7	3.9E-08	3.8E-08	1.4E-07	7.0E-05
8	7.0E-08	6.8E-08	1.8E-07	9.7E-05
9	1.2E-07	1.1E-07	2.1E-07	1.2E-04
10	1.8E-07	1.8E-07	2.3E-07	1.4E-04
15	5.5E-07	5.5E-07	2.8E-07	1.9E-04
30	9.1E-07	9.2E-07	3.2E-07	2.0E-04
45	9.4E-07	9.5E-07	3.5E-07	2.1E-04
60	9.6E-07	9.7E-07	3.9E-07	2.1E-04
90	1.0E-06	1.0E-06	4.6E-07	2.2E-04
180	1.1E-06	1.1E-06	7.7E-07	2.6E-04
365	1.5E-06	1.5E-06	1.8E-06	3.2E-04

Table 15.9. Dose per activity content of ^{63}Ni in daily excretion of urine (Sv Bq^{-1}); 5μm activity median aerodynamic diameter aerosols inhaled by a reference worker at light work.

Time after intake (d)	Nickel carbonyl Urine	Type F Urine	Type M Urine	Type S Urine
1	1.8E-09	1.8E-09	1.9E-08	4.3E-06
2	3.9E-09	3.7E-09	3.6E-08	8.4E-06
3	8.2E-09	7.6E-09	7.2E-08	1.7E-05
4	1.6E-08	1.5E-08	1.3E-07	3.2E-05
5	3.2E-08	3.0E-08	2.3E-07	5.9E-05
6	6.1E-08	5.7E-08	3.6E-07	1.0E-04
7	1.1E-07	1.1E-07	5.1E-07	1.5E-04
8	2.0E-07	1.9E-07	6.5E-07	2.2E-04
9	3.3E-07	3.1E-07	7.7E-07	2.7E-04
10	5.1E-07	4.9E-07	8.5E-07	3.2E-04
15	1.6E-06	1.5E-06	1.0E-06	4.1E-04
30	2.6E-06	2.5E-06	1.2E-06	4.5E-04
45	2.7E-06	2.6E-06	1.3E-06	4.6E-04
60	2.8E-06	2.7E-06	1.4E-06	4.7E-04
90	2.9E-06	2.8E-06	1.7E-06	5.0E-04
180	3.3E-06	3.2E-06	2.8E-06	5.7E-04
365	4.2E-06	4.1E-06	6.7E-06	7.1E-04

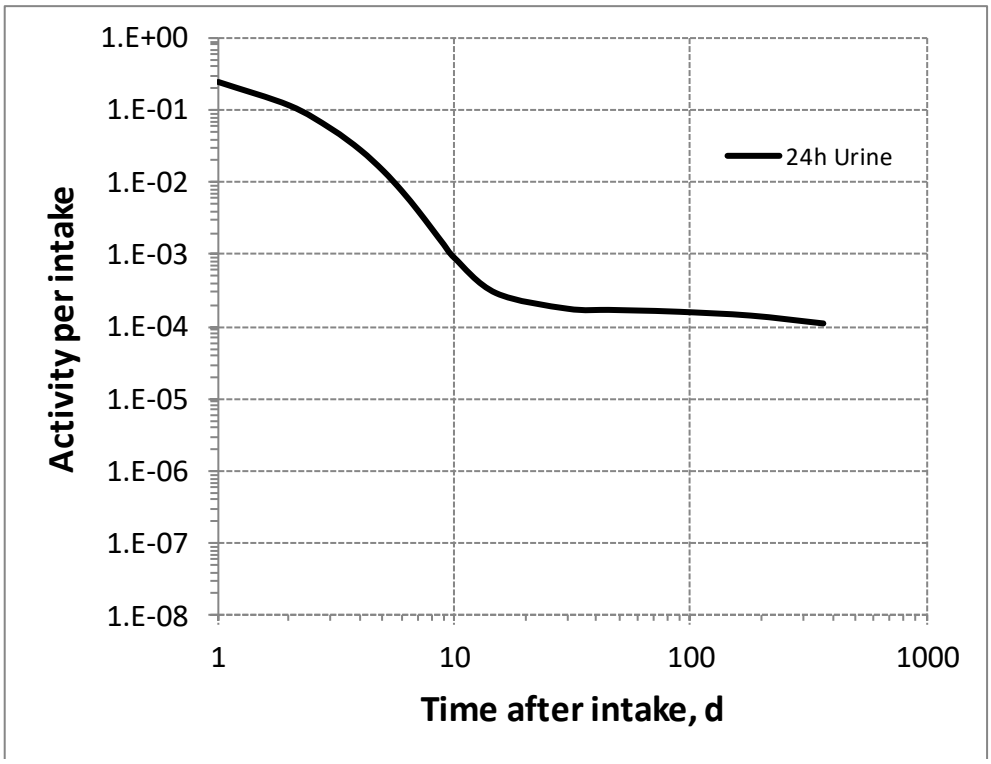

Fig. 15.2. Daily excretion of ^{59}Ni following inhalation of 1 Bq nickel carbonyl.

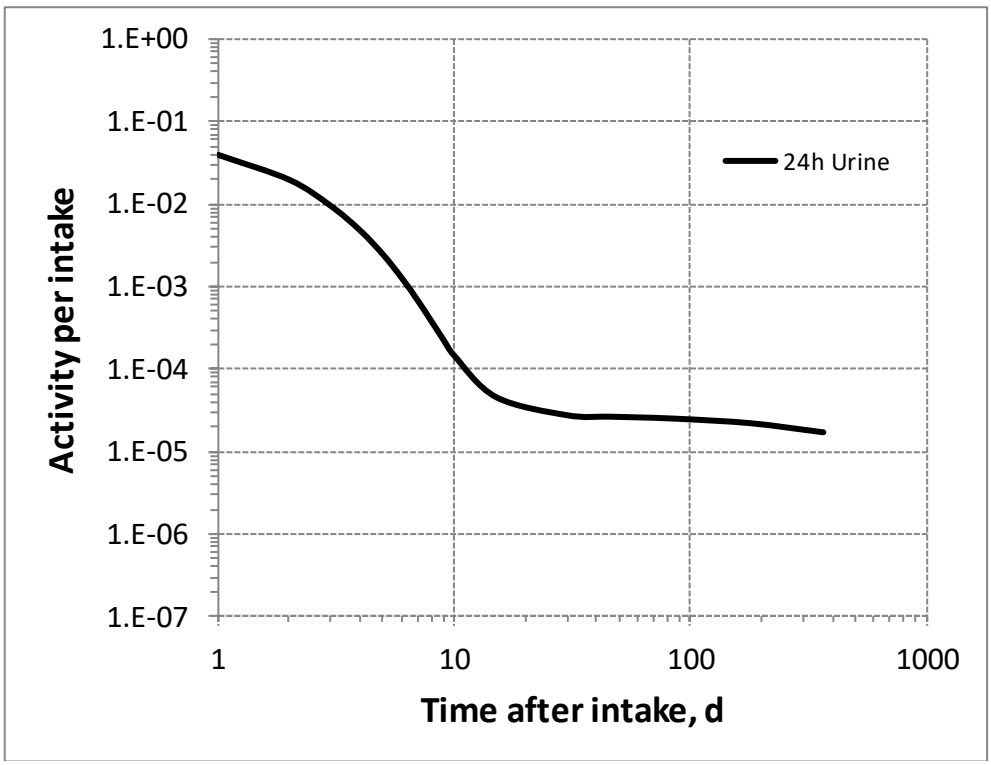

Fig. 15.3. Daily excretion of ^{59}Ni following inhalation of 1 Bq Type F.

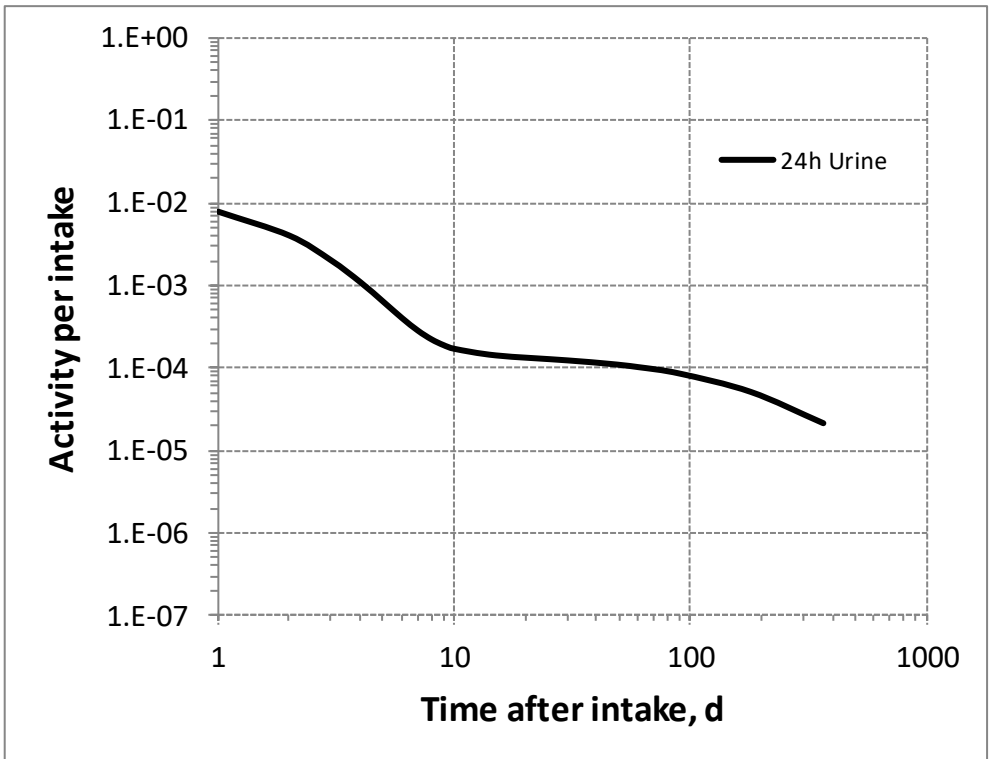

Fig. 15.4. Daily excretion of ^{59}Ni following inhalation of 1 Bq Type M.

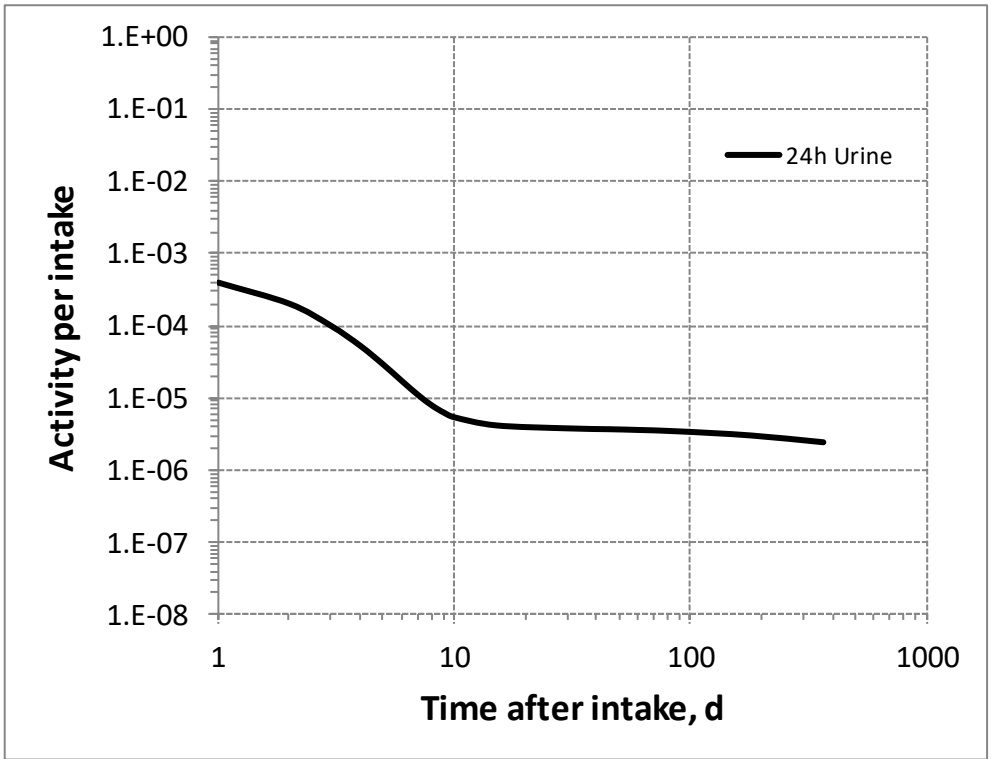

Fig. 15.5. Daily excretion of ^{59}Ni following inhalation of 1 Bq Type S.

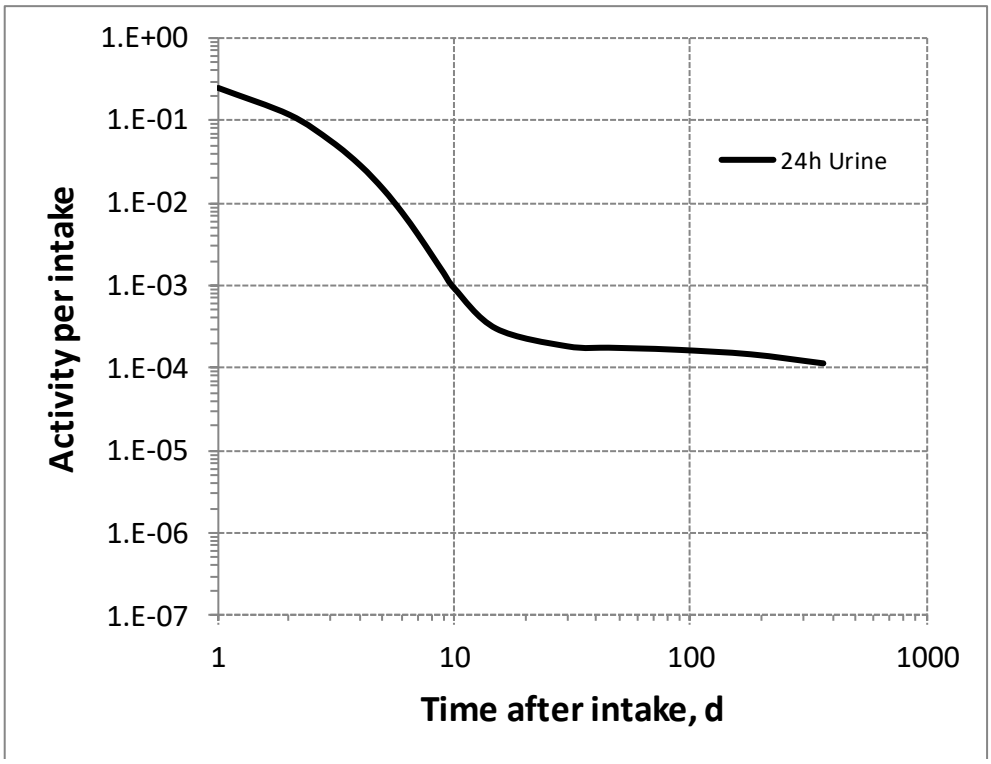

Fig. 15.6. Daily excretion of ^{63}Ni following inhalation of 1 Bq nickel carbonyl.

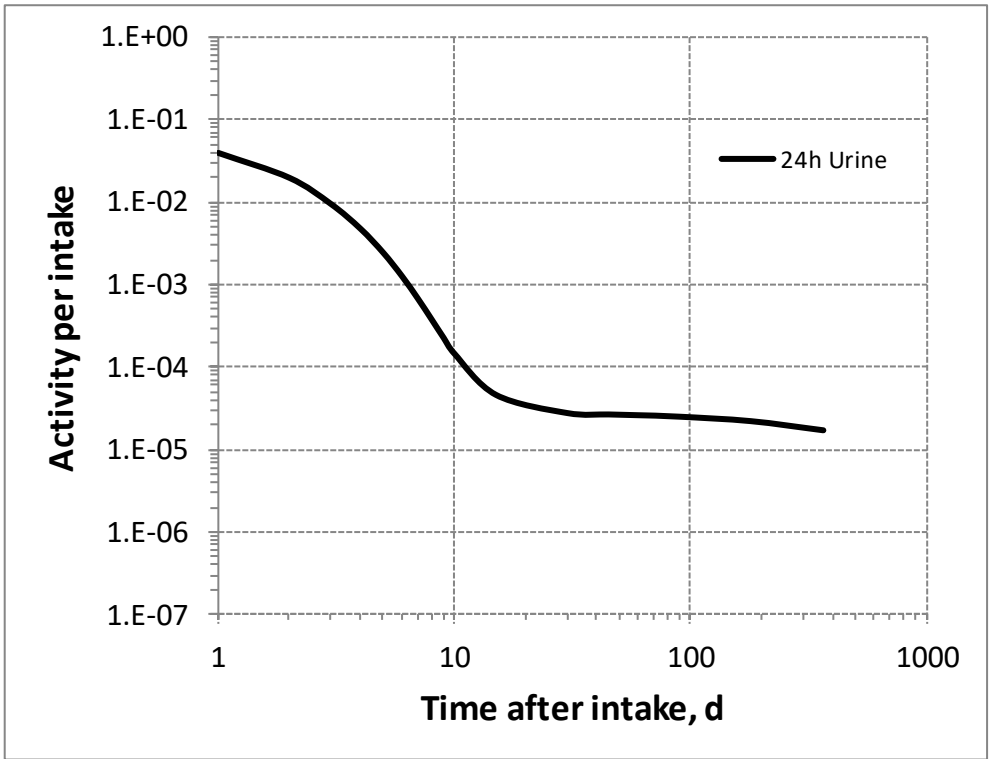

Fig. 15.7. Daily excretion of ^{63}Ni following inhalation of 1 Bq Type F.

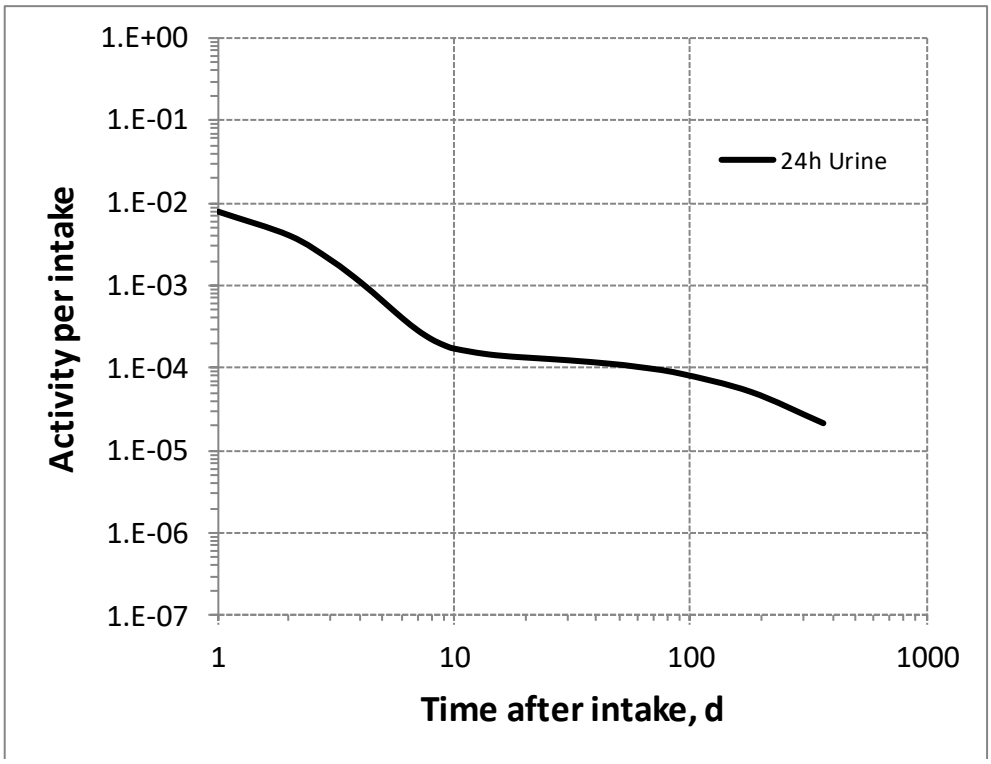

Fig. 15.8. Daily excretion of ^{63}Ni following inhalation of 1 Bq Type M.

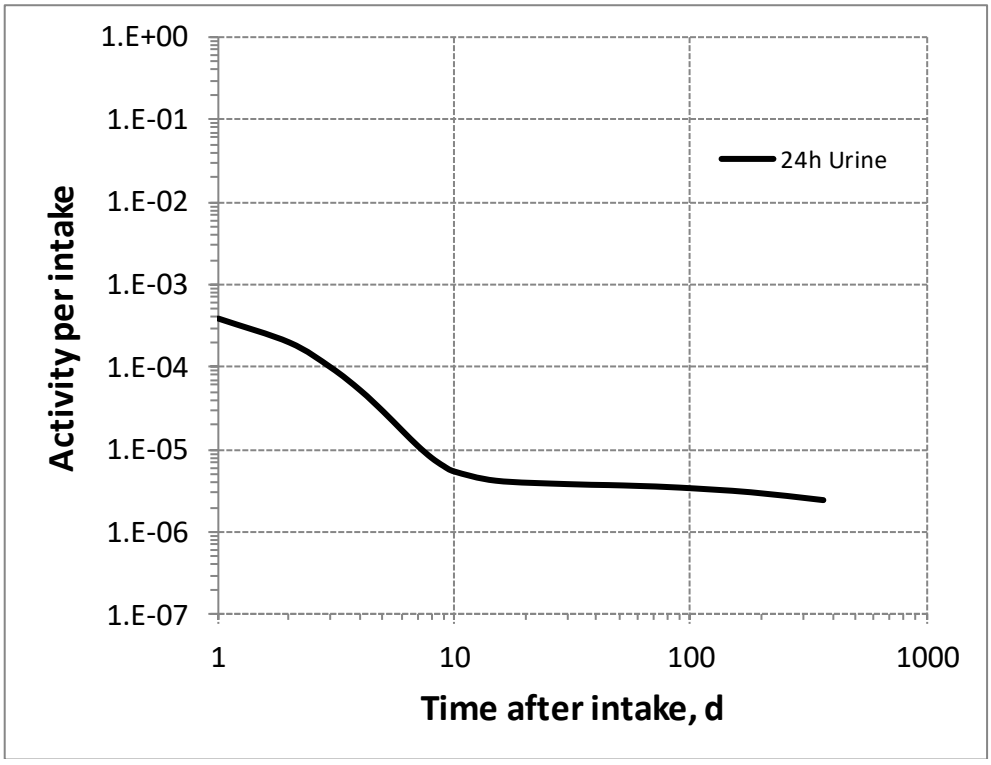

Fig. 15.9. Daily excretion of ^{63}Ni following inhalation of 1 Bq Type S.

16. COPPER (Z=29)

16.1. Isotopes

Table 16.1. Isotopes of copper addressed in this publication.

Isotope	Physical half-life	Decay mode
^{60}Cu	23.7 min	EC, B+
^{61}Cu	3.333 h	EC, B+
^{64}Cu*	12.700 h	EC, B+, B-
^{67}Cu	61.83 h	EC, B-

EC, electron-capture decay; B+, beta-plus decay; B-, beta-minus decay.
*Dose coefficients and bioassay data for this radionuclide are given in the printed copy of this publication.
Data for other radionuclides listed in this table are given in the online electronic files on the ICRP website.

16.2. Routes of Intake

16.2.1. Inhalation

(305) For copper, default parameter values were adopted on absorption to blood from the respiratory tract (ICRP, 2015). Absorption parameter values and types, and associated f_A values for particulate forms of copper are given in Table 16.2.

Table 16.2. Absorption parameter values for inhaled and ingested copper.

	Absorption parameter values*			
Inhaled particulate materials	f_r	s_r (d^{-1})	s_s (d^{-1})	Absorption from the alimentary tract, f_A
Default parameter values†				
Absorption type				
F	1	30	–	0.5
M‡	0.2	3	0.005	0.1
S	0.01	3	1×10^{-4}	0.005
Ingested materials§				
All forms				0.5

*It is assumed that the bound state can be neglected for copper (i.e. $f_b = 0$). The values of s_r for Type F, M and S forms of copper (30, 3 and 3 d^{-1} respectively) are the general default values.
†For inhaled material deposited in the respiratory tract and subsequently cleared by particle transport to the alimentary tract, the default f_A values for inhaled materials are applied [i.e. the product of f_r for the absorption type and the f_A value for ingested soluble forms of copper (0.5)].
‡Default Type M is recommended for use in the absence of specific information on which the exposure material can be assigned to an absorption type (e.g. if the form is unknown, or if the form is known but there is no information available on the absorption of that form from the respiratory tract). For guidance on the use of specific information, see Section 1.1.
§Activity transferred from systemic compartments into segments of the alimentary tract is assumed to be subject to reabsorption to blood. The default absorption fraction f_A for the secreted activity is the highest value for any form of the radionuclide ($f_A = 0.5$).

16.2.2. Ingestion

(306) A number of human studies have examined the uptake of copper from the human gastrointestinal tract. They were reviewed in *Publication 30* (ICRP, 1980), and more recently by WHO (2011b), the ATSDR (2004) and the EFSA (2015a). Copper is absorbed from the

stomach and the small intestine. The average fractional absorption ranges from 12% to 60%, with possible underestimate of the true absorption in many balance studies that did not consider endogenous losses in faecal excretion. The absorption of copper appears to be inversely related to the amount of copper, zinc, iron and cadmium in the gut.

(307) In *Publications 30* and *68* (ICRP, 1981, 1994a), f_1 was taken to be 0.5 for all compounds of copper. In this publication, the same value of $f_A = 0.5$ is recommended for all chemical forms of copper ingested by adults.

16.2.3. Systemic distribution, retention and excretion of copper

16.2.3.1. Biokinetic data

(308) Copper (Cu) is a functional component of several essential enzymes in the human body. It is necessary for normal iron metabolism and formation of red blood cells. Many enzymatic reactions that are essential for functioning of the brain and nervous system are catalyzed by copper.

(309) Studies of copper metabolism in human subjects began after the discovery in the late 1920s that copper was required for hemoglobin formation in rats (Hart et al., 1928; Tompsett, 1934, 1935; Chou and Adolph, 1935; Leverton and Binkley, 1944). Biokinetic studies involving administration of radioisotopes of copper to laboratory animals or human subjects began in the 1940s (Turnland, 1998). The half-lives of the longest-lived radioisotopes of copper (^{64}Cu, 12.7 h, and ^{67}Cu, 61.8 h) have limited their uses to relatively short-term studies.

(310) Dietary intake of copper by an adult human typically is about 1-3 mg d^{-1}. About 30-70% of ingested copper is absorbed to blood. Absorption of copper is inversely related to the level of copper intake. Absorbed copper becomes bound to two plasma proteins, albumin and transcuprein. Much of the bound copper is rapidly deposited in the liver, the key organ regarding copper metabolism and homeostasis. Most of the copper entering liver is incorporated into the enzyme ceruloplasmin, which is released to blood and transferred to tissues (Cartwright and Wintrobe, 1964; Linder and Hazegh-Azam, 1996; Cromwell, 1997; Turnland, 1998; Angelova et al., 2011; Osredkar and Sustar, 2011).

(311) The total mass of copper in the adult male human body is about 70-80 mg (Cartwright and Wintrobe, 1964; Zhu et al., 2010). Measurements of copper concentrations in postmortem tissues and in blood of living subjects indicate the following approximate distribution of copper in an adult male: blood 5%, skeletal muscle 48%, liver 18%, bone 8%, and other tissue 21% (Zhu et al., 2010).

(312) Copper has two stable isotopes, ^{63}Cu and ^{65}Cu, with natural abundances of 69.2% and 30.8%, respectively. Scott and Turnland (1994) investigated the biokinetics of copper in healthy young adult male humans over a 90-day period in which the less abundant isotope ^{65}Cu was administered at different times. The subjects received adequate dietary copper (1.7 mg d^{-1}) for 24 d, low dietary copper (0.79 mg d^{-1}) for 42 d, and high dietary copper (7.5 mg d^{-1}) for 24 d. A solution containing ^{65}Cu was injected intravenously on days 7, 49, and 73, and ^{65}Cu was added to diet on days 13, 31-32, 55-56, and 79. The time-dependent concentrations of ^{65}Cu were determined in blood components. Observed changes in the ^{65}Cu concentrations were interpreted in view of previously established characteristics of copper in the human body such as the typical mass, distribution, and faecal and urinary excretion rates of copper in adult humans and the roles of the liver in copper metabolism and storage. The data indicated that plasma contained about 4% of total-body copper, with ceruloplasmin containing 56-68% of plasma copper. The dietary copper level was judged to influence the flow rate from liver to plasma and from plasma to tissues other than liver. The investigators developed a biokinetic model depicting the

observed behaviour of ^{65}Cu in blood plasma and the inferred time-dependent systemic distribution and excretion of ^{65}Cu. First-order transfer rates between compartments (or delay times, for two of the nine depicted transfers) were developed separately for each subject as fits to subject-specific data. Separate transfer coefficients were developed for oral intake and injection.

(313) Relative losses of copper along different excretion pathways were studied in dogs (Cartwright and Wintrobe, 1964). The results indicated that about 80% of excretion of systemic copper is due to biliary secretion into the small intestine, 16% is excreted after endogenous secretion directly across the intestinal wall, and 4% is excreted in urine.

(314) Following administration of ^{64}Cu as cupric acetate to rats, maximal activity concentrations were reached quickly in the liver, kidney, and gastrointestinal tract (Owen, 1965). Other tissues showed a progressive accumulation of ^{64}Cu after the disappearance of most of the non-ceruloplasmin ^{64}Cu from plasma and emergence of plasma ceruloplasmin ^{64}Cu, suggesting that ceruloplasmin may be the source of copper for tissues. The disappearance of ^{64}Cu from plasma tended to parallel that from the liver after 2 d.

(315) Dunn et al. (1991) developed a compartmental model of copper biokinetics in rats based on measurements of intravenously administered ^{64}Cu in plasma, tissues, and excreta over the first 3 d post injection. They interpreted the data in the context of a 16-compartment model that included 2 plasma compartments representing ceruloplasmin copper (Cp) and all other copper in plasma (NCp), 2 liver compartments, 2 compartments representing skin plus muscle (S-M), 2 compartments representing intestinal tissue, 2 compartments representing remaining tissue, and 6 compartments representing excretion pathways and excreta. Movement between compartments was described by first-order transfers. Skin and muscle were treated as a single tissue because the data indicated virtually identical kinetics in these two tissues. The direct observations together with the results of the compartmental analysis indicated the following behaviour of ^{64}Cu. The injected activity entered the NCp fraction of plasma, cleared rapidly into the liver and S-M, and was initially removed at a high rate from liver in bile. The plasma content levelled out within the first hour, remained constant for about 10 h, and then began to decline gradually. This was attributed to a decreasing content of activity in NCp, offset by an increasing content in Cp. By 1 h post injection about 32% of the administered amount (after correction for physical decay) had accumulated in the liver. Activity was lost from the liver at a relatively high rate for a few hours and more slowly thereafter. Activity in S-M accounted for about 25% of the administered amount at 2 h, decreased slightly to about 10 h post administration, and then plateaued or slightly increased over the rest of the observation period, indicating a relatively long component of copper retention. About 25% of the administered amount was excreted in faeces in the first 24 h and about 45% by 72 h, apparently representing mainly biliary secretion of the tracer.

16.2.3.2. Biokinetic model for systemic copper

(316) The biokinetic model for systemic copper used in this publication is a modification of the model of Scott and Turnland (1994). The model structure applied by those investigators was modified to depict the faecal and urinary excretion pathways applied in this publication series.

(317) The modified model structure is shown in Fig. 16.1. Transfer coefficients are listed in Table 16.3.

(318) The mean transfer rates developed by Scott and Turnland (1994) for intravenous administration of ^{65}Cu during the period of adequate intake of copper were used as a starting point. Two delays depicted in the model of Scott and Turnland were replaced with first-order transfer coefficients. The transfer rate from liver 2 to plasma 2 derived by Scott and Turnland

was increased moderately for consistency with the long-term distribution of copper as indicated by autopsy data (Zhu et al., 2010). The transfer rate from Other tissue to Plasma 1 was decreased to reflect longer retention in soft tissues indicated by data of Dunn et al. (1991) and for consistency with autopsy data.

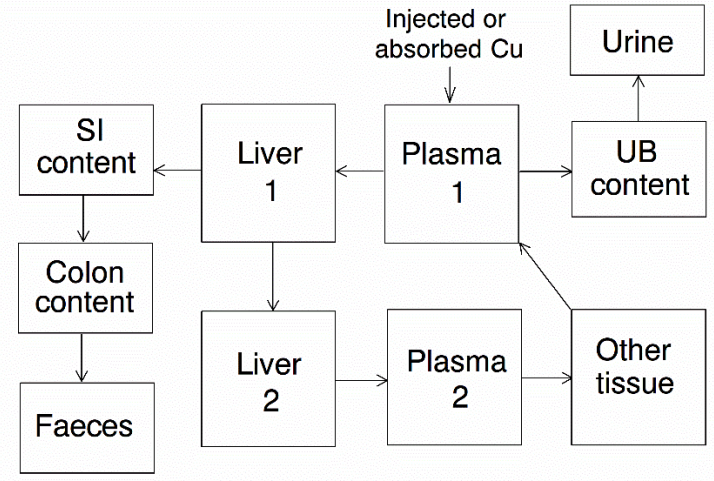

Fig. 16.1. Structure of the biokinetic model for systemic copper.

Table 16.3. Transfer coefficients in the biokinetic model for systemic copper.

From	To	Transfer coefficient (d^{-1})
Plasma 1	Liver 1	25
Plasma 1	Urinary bladder content	0.00014
Liver 1	Small intestine content	19
Liver 1	Liver 2	200
Liver 2	Plasma 2	1.3
Plasma 2	Other	15
Other	Plasma 1	0.3

16.3. Individual monitoring

16.3.1. ^{64}Cu

(319) Measurements of ^{64}Cu may be performed by *in vivo* whole-body measurement technique and by gamma measurement in urine.

Table 16.4. Monitoring techniques for ^{64}Cu.

Isotope	Monitoring Technique	Method of Measurement	Typical Detection Limit
^{64}Cu	Urine Bioassay	γ-ray spectrometry[a]	6.2 Bq L^{-1}
^{64}Cu	Whole-body measurement	γ-ray spectrometry[ab]	6400 Bq

[a] Measurement system comprised of Germanium Detectors
[b] Counting time of 20 minutes

16.4. Dosimetric data for copper

Table 16.5. Committed effective dose coefficients (Sv Bq^{-1}) for the inhalation or ingestion of ^{64}Cu compounds.

Inhaled particulate materials (5 µm AMAD aerosols)	Effective dose coefficients (Sv Bq^{-1})
	^{64}Cu
Type F, — NB: Type F should not be assumed without evidence	4.2E-11
Type M, default	6.7E-11
Type S	6.9E-11
Ingested materials	
All forms	5.4E-11

AMAD, activity median aerodynamic diameter

Table 16.6. Dose per activity content of ^{64}Cu in total body and in daily excretion of urine (Sv Bq^{-1}); 5µm activity median aerodynamic diameter aerosols inhaled by a reference worker at light work.

	Type F		Type M		Type S	
Time after intake (d)	Total body	Urine	Total body	Urine	Total body	Urine
1	2.4E-10	6.3E-05	4.0E-10	6.0E-04	4.2E-10	1.2E-02
2	1.1E-09	8.9E-04	2.5E-09	7.2E-03	2.9E-09	1.5E-01
3	4.7E-09	3.7E-03	1.7E-08	3.3E-02	2.3E-08	6.8E-01
4	1.8E-08	1.4E-02	8.7E-08	1.2E-01	1.5E-07	N/A
5	7.0E-08	5.1E-02	3.7E-07	4.5E-01	7.1E-07	
6	2.6E-07	1.9E-01	1.4E-06	N/A	2.9E-06	
7	9.9E-07	N/A	5.4E-06		1.1E-05	
8	3.7E-06		2.0E-05		4.1E-05	
9	1.4E-05		7.6E-05		1.5E-04	
10	5.2E-05		2.9E-04		5.8E-04	
15	3.8E-02		2.1E-01		4.2E-01	
30	N/A		N/A		N/A	
45						
60						
90						
180						
365						

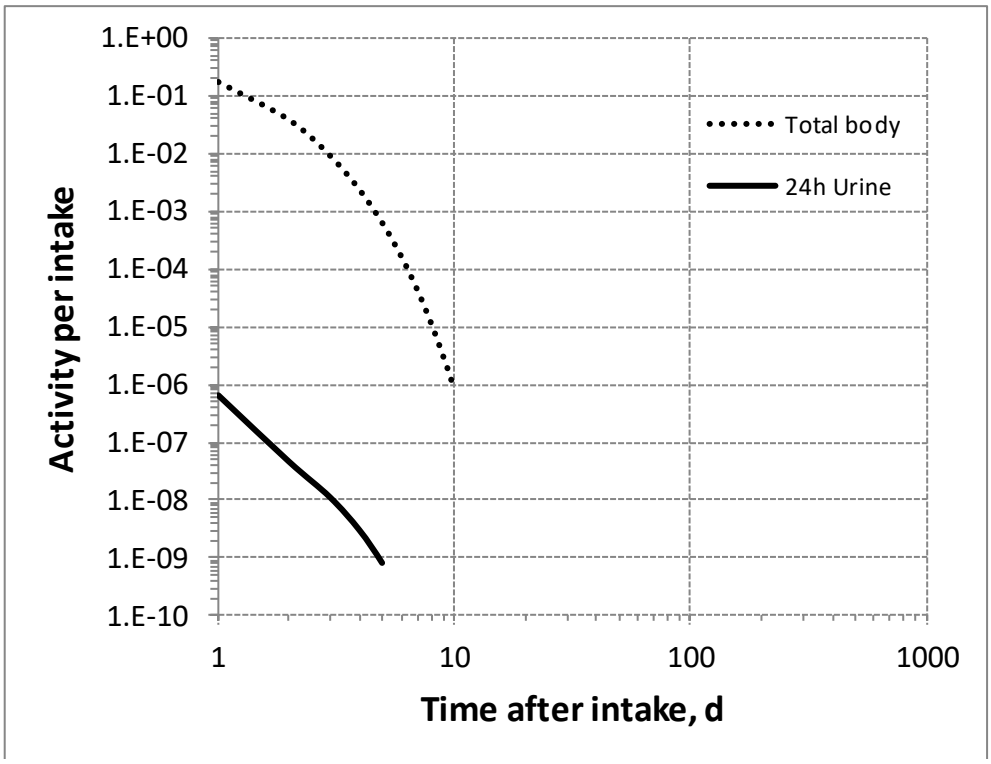

Fig. 16.2. Daily excretion of ^{64}Cu following inhalation of 1 Bq Type F.

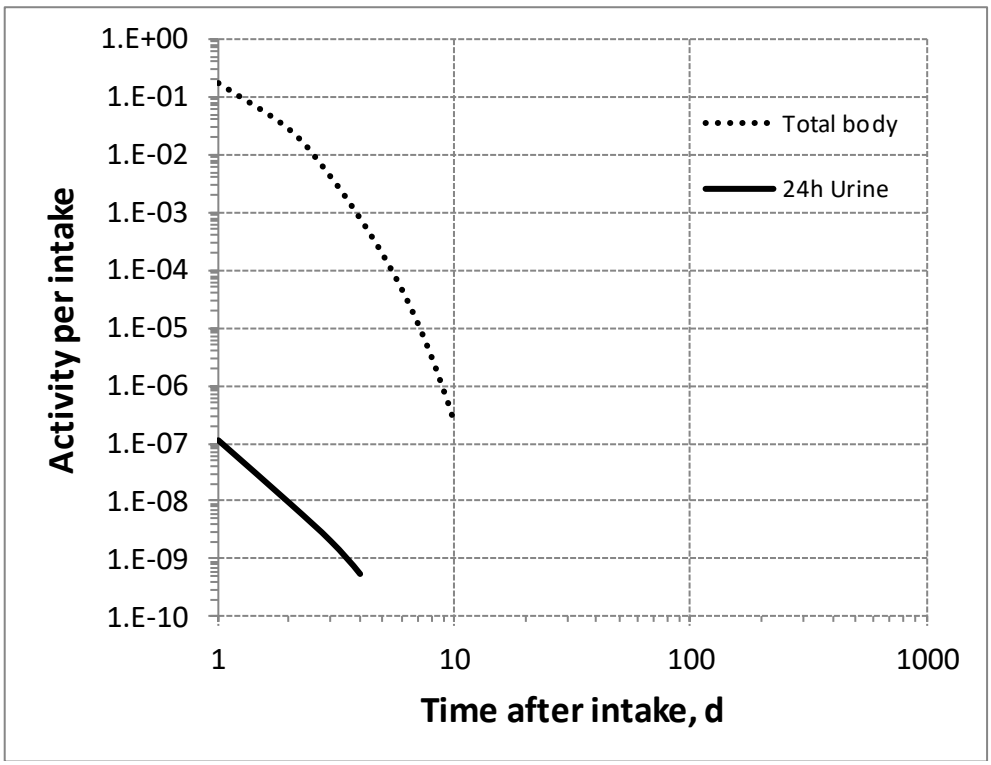

Fig. 16.3. Daily excretion of ^{64}Cu following inhalation of 1 Bq Type M.

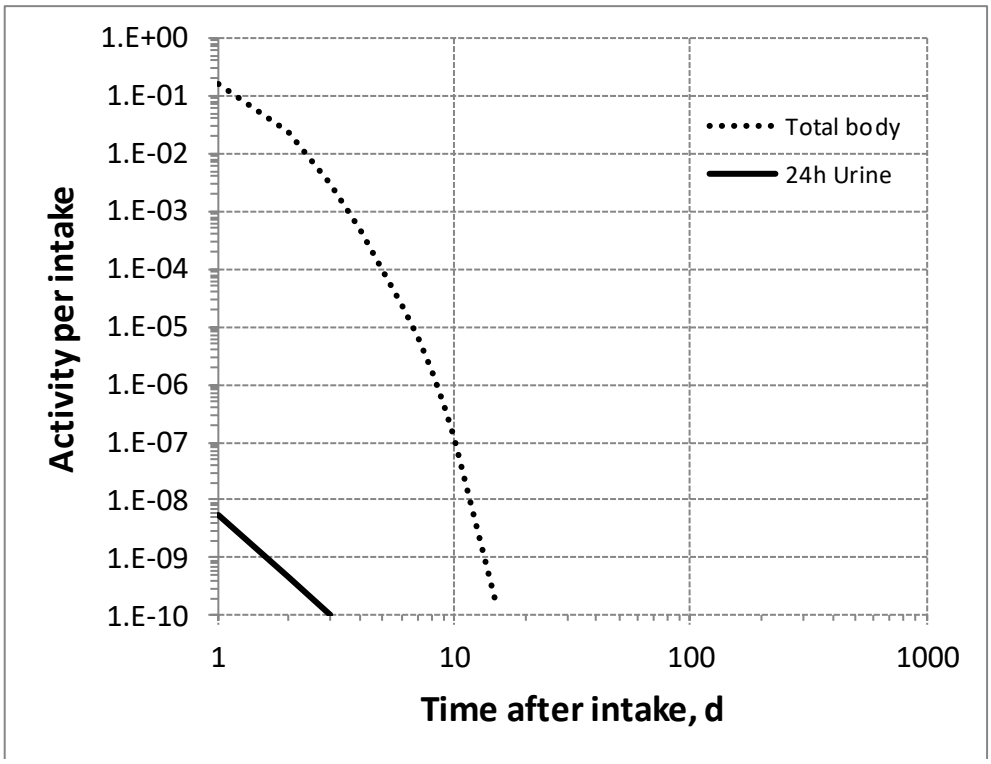

Fig. 16.4. Daily excretion of ^{64}Cu following inhalation of 1 Bq Type S.

17. GALLIUM (Z=31)

17.1. Isotopes

Table 17.1. Isotopes of gallium addressed in this publication.

Isotope	Physical half-life	Decay mode
^{65}Ga	15.2 min	EC, B+
^{66}Ga	9.49 h	EC, B+
^{67}Ga*	3.2612 d	EC
^{68}Ga	67.71 min	EC, B+
^{70}Ga	21.14 min	B-, EC
^{72}Ga	14.10 h	B-
^{73}Ga	4.86 h	B-

EC, electron-capture decay; B+, beta-plus decay; B-, beta-minus decay.
*Dose coefficients and bioassay data for this radionuclide are given in the printed copy of this publication.
Data for other radionuclides listed in this table are given in the online electronic files on the ICRP website.

17.2. Routes of Intake

17.2.1. Inhalation

(320) For gallium, default parameter values were adopted on absorption to blood from the respiratory tract (ICRP, 2015). Absorption parameter values and types, and associated f_A values for particulate forms of gallium are given in Table 17.2.

17.2.2. Ingestion

(321) The work of Dudley and Levine (1949) showed that little or no gallium administered as the chloride is absorbed from the gastrointestinal tract of the rat. Valberg et al. (1981) confirmed in mice that gallium is poorly absorbed, less than 0.5% of intake, after a single oral administration. Rubow et al. (1991) observed the inadvertent ingestion of ^{67}Ga by a 9-month-old child breast-fed by her mother who underwent gallium scan after Hodgkin's lymphoma. All ingested activity appeared to be localised in the intestines of the child, with no apparent absorption from the gastrointestinal tract.

(322) In *Publications 30* and *68* (ICRP, 1981, 1994a), f_1 was taken to be 10^{-3} for all compounds of the element. In this publication, the same value $f_A = 10^{-3}$ is applied to all chemical forms of gallium.

Table 17.2. Absorption parameter values for inhaled and ingested gallium.

Inhaled particulate materials	Absorption parameter values* f_r	s_r (d^{-1})	s_s (d^{-1})	Absorption from the alimentary tract, f_A
Default parameter values†				
Absorption type				
F	1	30	–	0.001
M‡	0.2	3	0.005	2×10^{-4}
S	0.01	3	1×10^{-4}	1×10^{-5}
Ingested materials§				
All forms				0.001

[*]It is assumed that the bound state can be neglected for gallium (i.e. $f_b = 0$). The values of s_r for Type F, M and S forms of gallium (30, 3 and 3 d^{-1} respectively) are the general default values.
[†]For inhaled material deposited in the respiratory tract and subsequently cleared by particle transport to the alimentary tract, the default f_A values for inhaled materials are applied [i.e. the product of f_r for the absorption type and the f_A value for ingested soluble forms of gallium (0.001)].
[‡]Default Type M is recommended for use in the absence of specific information on which the exposure material can be assigned to an absorption type (e.g. if the form is unknown, or if the form is known but there is no information available on the absorption of that form from the respiratory tract). For guidance on the use of specific information, see Section 1.1.
[§]Activity transferred from systemic compartments into segments of the alimentary tract is assumed to be subject to reabsorption to blood. The default absorption fraction f_A for the secreted activity is the highest value for any form of the radionuclide ($f_A = 0.001$).

17.2.3. Systemic distribution, retention and excretion of gallium

17.2.3.1. Biokinetic data

(323) The biokinetics of systemic gallium (Ga) has been investigated in several human studies, usually in conjunction with medical applications of ^{67}Ga ($T_{1/2} = 3.26$ d) or stable gallium. Gallium-67 has been investigated as a prospective agent for diagnosis and treatment of neoplasms involving bone and has been used extensively to determine the location of tumors, inflammations, and infections (Nelson et al., 1972). Stable gallium has been found to have beneficial effects in the treatment of conditions associated with accelerated bone resorption (Bockman et al., 1986).

(324) Results of *in vivo* studies using ^{67}Ga indicate that nearly all gallium in blood is present in plasma, where it is largely bound to the iron-transport protein transferrin (Bernstein, 1998). In addition to its tendency to accumulate in tumors and at sites of inflammation and infection, gallium has a strong affinity for certain healthy tissues including growing and remodelling bone (Bernstein, 1998). In growing bone gallium is concentrated in the metaphysis, particularly the cartilaginous growth plate. It accumulates to some extent on the endosteal and periosteal surfaces of diaphyseal bone (Bockman et al., 1986). Elevated concentrations of gallium are also commonly observed in the liver, spleen, and kidneys (Bernstein, 1998).

(325) Blood clearance of gallium can be described reasonably well in terms of two phases of disappearance with half-times of on the order of 0.25 d and 7 d (Kriegel, 1984). About one-third of the amount deposited in tissues is removed from the body over a relatively short period, mainly in urine, and the remainder is removed relatively slowly in urine and faeces (Kriegel, 1984). In the biokinetic model for gallium adopted in *Publication 30* (1981), short- and long-term retention of gallium in each modelled tissue (bone surface, liver, spleen, and 'other') was characterised by half-times of 1 d and 50 d, applicable to 30% and 70%, respectively, of the amount entering the tissue.

(326) Priest et al. (1995) studied the biokinetics of ^{67}Ga over a 21-d period following its intravenous administration to a healthy adult male volunteer. After correction for radioactive decay, retention R(t) in blood at t days post injection ($t \geq 0.2$), expressed as a percentage of the injected amount, was described by the power function $R(t)=10.5t^{-0.75}$. Urinary and faecal excretion over the first 13 d, corrected for decay, represented about 27% and 10%, respectively, of the injected amount.

(327) Nelson et al. (1972) measured activity concentrations in postmortem samples of 23 patients administered ^{67}Ga intravenously at various times before death. Highest mean concentrations expressed as % kg^{-1} were found in spleen (4.1), kidney cortex (3.8), adrenals (3.8), bone marrow (3.6), liver (2.8), kidney (2.7), and bone (2.6). Some organs including the kidneys showed a rapid decrease in activity from high early values but a later slow decrease of

retained activity. Considerable variation in tissue concentrations from patient to patient was observed, with most tissues having at least a 10-fold variation.

(328) Zhu et al. (2010) measured concentrations of gallium in 17 tissues obtained from autopsies of up to 68 Chinese men from four areas of China. All subjects were considered healthy until the time of sudden accidental death. Based on median gallium concentrations in tissue and reference tissue masses, the preponderance of total-body Ga was contained in fat (31%), bone (25%), and muscle (23%).

17.2.3.2. Biokinetic model for systemic gallium

(329) The structure of the biokinetic model for systemic gallium is shown in Fig. 17.1. Transfer coefficients are listed in Table 17.3.

(330) Transfer coefficients were based on data summarised above on the behaviour of human subjects and set for consistency with postmortem measurements on patients receiving ^{67}Ga injections (Nelson et al., 1972; MIRD, 1973) and total body retention, blood clearance, and urinary and faecal excretion rates (Priest et al., 1995). Derivation of transfer coefficients focused on data for relatively early times after administration, as radioisotopes of gallium addressed in this publication have relatively short half-lives, from 15.2 min to 3.26 d.

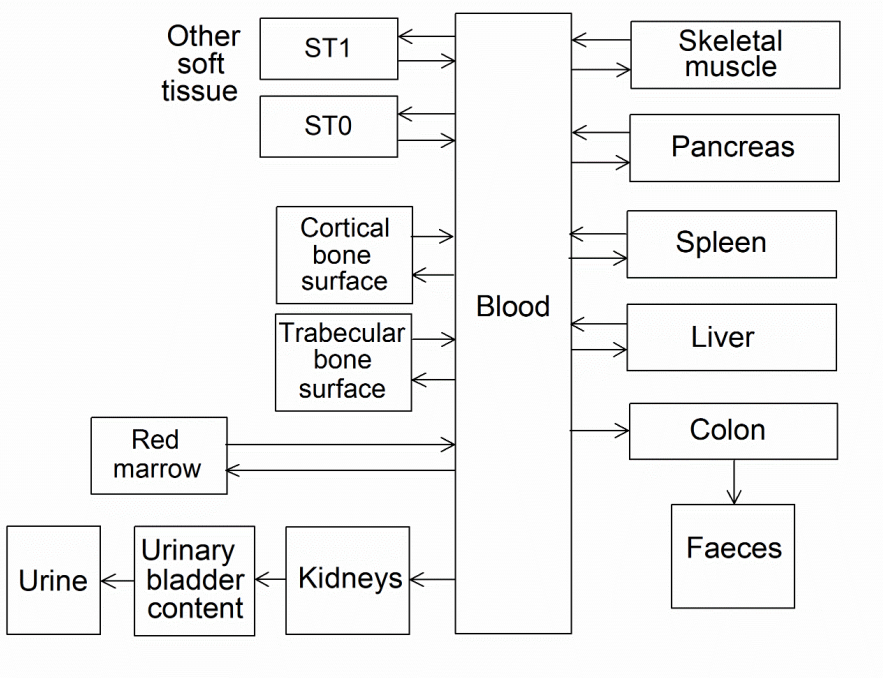

Fig. 17.1. Structure of the biokinetic model for systemic gallium.

Table 17.3. Transfer coefficients in the biokinetic model for systemic gallium.

From	To	Transfer coefficients (d^{-1})
Blood	Right colon content	0.15
Blood	Liver	0.3
Blood	Kidneys	0.4
Blood	Spleen	0.05
Blood	Trabecular bone surface	0.5
Blood	Cortical bone surface	0.5
Blood	Red marrow	0.25

Blood	Muscle	0.2
Blood	Pancreas	0.005
Blood	ST0	2.145
Blood	ST1	0.5
Liver	Blood	0.139
Kidneys	Urinary bladder content	1.39
Spleen	Blood	0.139
Trabecular bone surface	Blood	0.347
Cortical bone surface	Blood	0.347
Red marrow	Blood	0.347
Muscle	Blood	0.139
Pancreas	Blood	0.139
ST0	Blood	1.39
ST1	Blood	0.0019

17.2.3.3. Treatment of progeny

(331) The only progeny of gallium addressed in this publication is ^{65}Zn, produced by decay of ^{65}Ga. The model for systemic zinc as a progeny of gallium is an expansion of the characteristic model for zinc with added compartments and associated transfer coefficients needed to solve the linked biokinetic models for gallium and zinc (see Annex B). Compartments representing the spleen and red marrow were added to the model for zinc to address all tissues considered explicitly in the model for gallium. The following transfer coefficients were added to the characteristic model for zinc: blood to spleen, 3.0 d^{-1}; blood to red marrow, 3.0 d^{-1}; spleen to blood, 2.5 d^{-1}; red marrow to blood, 2.5 d^{-1}; other to blood, 10 d^{-1}.

17.3. Individual monitoring

17.3.1. ^{67}Ga

(332) Measurements of ^{67}Ga may be performed by *in vivo* whole-body measurement technique and by gamma measurement in urine.

Table 17.4. Monitoring techniques for ^{67}Ga.

Isotope	Monitoring Technique	Method of Measurement	Typical Detection Limit
^{67}Ga	Urine Bioassay	γ-ray spectrometry[a]	5.6 Bq L^{-1}
^{67}Ga	Whole-body measurement	γ-ray spectrometry[a]	140 Bq

[a] Measurement system comprised of Germanium Detectors
[b] Counting time of 20 minutes

17.4. Dosimetric data for gallium

Table 17.5. Committed effective dose coefficients (Sv Bq^{-1}) for the inhalation or ingestion of ^{67}Ga compounds.

Inhaled particulate materials (5 µm AMAD aerosols)	Effective dose coefficients (Sv Bq^{-1})
	^{67}Ga

Type F, — NB: Type F should not be assumed without evidence	5.5E-11
Type M, default	9.6E-11
Type S	1.1E-10
Ingested materials	
All forms	5.4E-11

AMAD, activity median aerodynamic diameter

Table 17.6. Dose per activity content of ^{67}Ga in total body and in daily excretion of urine (Sv Bq^{-1}); 5μm activity median aerodynamic diameter aerosols inhaled by a reference worker at light work.

	Type F		Type M		Type S	
Time after intake (d)	Total body	Urine	Total body	Urine	Total body	Urine
1	1.1E-10	6.7E-09	1.9E-10	1.8E-07	2.1E-10	3.9E-06
2	2.1E-10	7.5E-09	4.4E-10	1.5E-07	4.9E-10	3.4E-06
3	4.2E-10	1.3E-08	1.2E-09	2.7E-07	1.3E-09	6.1E-06
4	6.8E-10	2.3E-08	2.6E-09	4.5E-07	2.9E-09	1.0E-05
5	9.4E-10	3.6E-08	4.2E-09	6.9E-07	4.7E-09	1.6E-05
6	1.2E-09	5.3E-08	5.7E-09	9.9E-07	6.4E-09	2.3E-05
7	1.6E-09	7.5E-08	7.3E-09	1.4E-06	8.1E-09	3.3E-05
8	2.0E-09	1.0E-07	9.2E-09	1.9E-06	1.0E-08	4.5E-05
9	2.5E-09	1.4E-07	1.2E-08	2.5E-06	1.3E-08	6.1E-05
10	3.2E-09	1.9E-07	1.5E-08	3.3E-06	1.6E-08	8.1E-05
15	1.0E-08	8.5E-07	4.4E-08	1.3E-05	4.8E-08	3.3E-04
30	2.9E-07	5.8E-05	1.2E-06	5.1E-04	1.2E-06	1.5E-02
45	7.5E-06	3.3E-03	3.0E-05	1.6E-02	3.0E-05	5.3E-01
60	1.9E-04	1.5E-01	7.8E-04	4.7E-01	7.6E-04	N/A
90	1.2E-01	N/A	5.1E-01	N/A	4.7E-01	
180	N/A		N/A		N/A	
365						

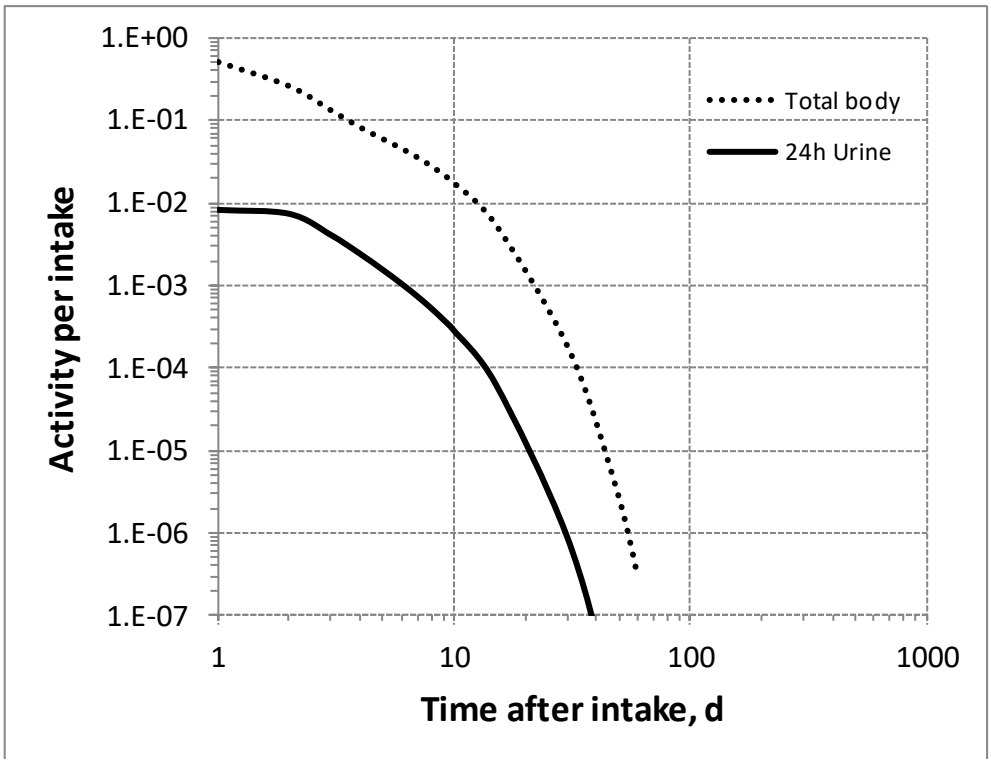

Fig. 17.2. Daily excretion of ^{67}Ga following inhalation of 1 Bq Type F.

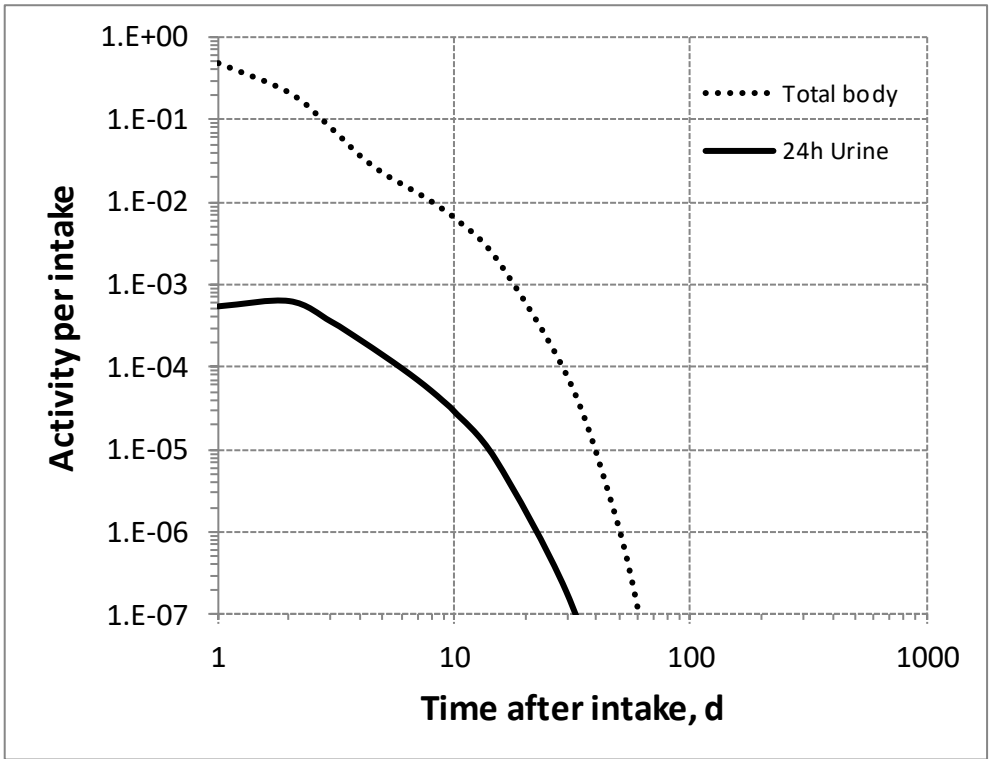

Fig. 17.3. Daily excretion of ^{67}Ga following inhalation of 1 Bq Type M.

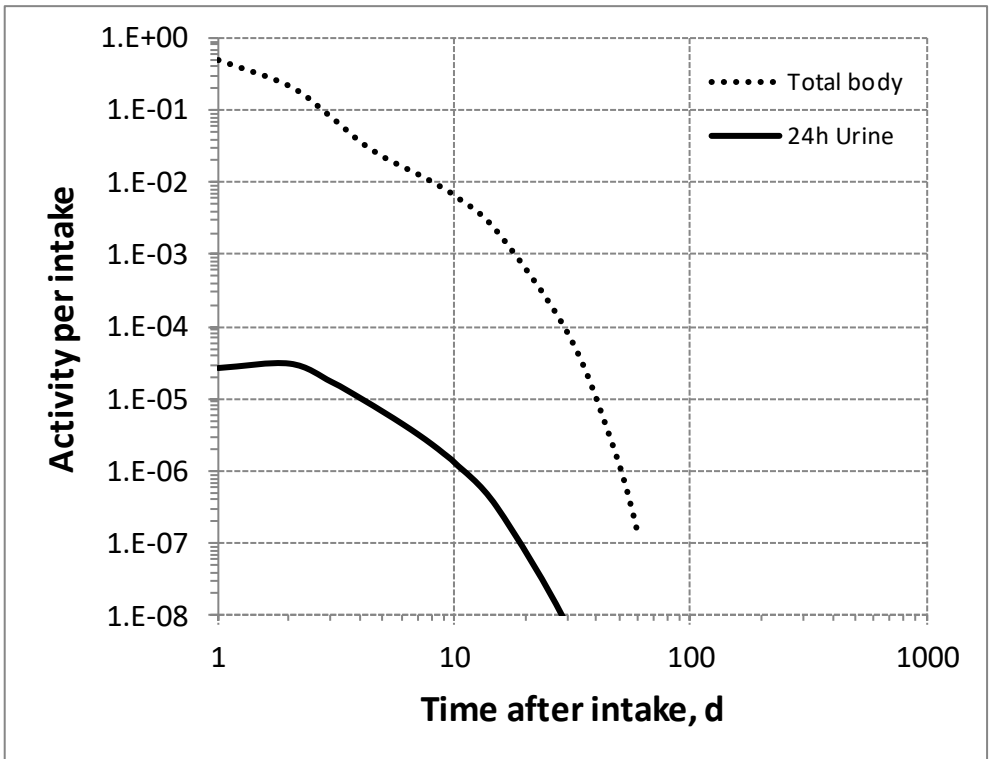

Fig. 17.4. Daily excretion of ^{67}Ga following inhalation of 1 Bq Type S.

18. GERMANIUM (Z=32)

18.1. Isotopes

Table 18.1. Isotopes of germanium addressed in this publication.

Isotope	Physical half-life	Decay mode
^{66}Ge	2.26 h	EC, B+
^{67}Ge	18.9 min	EC, B+
^{68}Ge*	270.95 d	EC
^{69}Ge	39.05 h	EC, B+
^{71}Ge	11.43 d	EC
^{75}Ge	82.78 min	B-
^{77}Ge	11.30 h	B-
^{78}Ge	88 min	B-

EC, electron-capture decay; B+, beta-plus decay; B-, beta-minus decay.
*Dose coefficients and bioassay data for this radionuclide are given in the printed copy of this publication.
Data for other radionuclides listed in this table are given in the online electronic files on the ICRP website.

18.2. Routes of Intake

18.2.1. Inhalation

(333) For germanium, default parameter values were adopted on absorption to blood from the respiratory tract (ICRP, 2015). Absorption parameter values and types, and associated f_A values for particulate forms of germanium are given in Table 18.2.

18.2.2. Ingestion

(334) Data on the germanium content of urine suggest that dietary forms of the element are well absorbed from the gastrointestinal tract of man (Schroeder and Balassa, 1967): of a calculated daily intake of 1.5 mg in the diet, 1.4 mg appears in the urine and 0.1 mg in the faeces. In experiments on rats, germanium, orally administered in the form of GeO_2, was almost completely absorbed from the gastrointestinal tract (Rosenfeld, 1954). Pharmacokinetics studies with an oral dose of 100 mg kg^{-1} of ^{14}C labelled carboxyethyl-germanium sesquioxide (^{132}Ge) indicated 30% intestinal absorption. Human patients treated with 25 to 75 mg kg^{-1} of ^{132}Ge also had an absorption rate of 30% (Miyao et al., 1980). Tao and Bolger (1997) reviewed 31 published human cases of prolonged intake of germanium leading to renal failure. Although intestinal absorption was not explicitly quantified, high levels of germanium were found in many body tissues and in urine of these patients.

(335) In *Publications 30* and *68* (ICRP, 1981, 1994a), f_1 was taken as 1 for all compounds of germanium. In this publication, the value $f_A = 1$ is used for all chemical forms of germanium.

Table 18.2. Absorption parameter values for inhaled and ingested germanium.

Inhaled particulate materials	Absorption parameter values* f_r	s_r (d^{-1})	s_s (d^{-1})	Absorption from the alimentary tract, f_A
Default parameter values†				
Absorption type				
F	1	30	–	1
M‡	0.2	3	0.005	0.2
S	0.01	3	1×10^{-4}	0.01

Ingested materials[§]	
All forms	1

[*]It is assumed that the bound state can be neglected for germanium (i.e. $f_b = 0$). The values of s_r for Type F, M and S forms of germanium (30, 3 and 3 d^{-1} respectively) are the general default values.
[†]For inhaled material deposited in the respiratory tract and subsequently cleared by particle transport to the alimentary tract, the default f_A values for inhaled materials are applied [i.e. the product of f_r for the absorption type and the f_A value for ingested soluble forms of germanium (1)].
[‡]Default Type M is recommended for use in the absence of specific information on which the exposure material can be assigned to an absorption type (e.g. if the form is unknown, or if the form is known but there is no information available on the absorption of that form from the respiratory tract). For guidance on the use of specific information, see Section 1.1.
[§]Activity transferred from systemic compartments into segments of the alimentary tract is assumed to be subject to reabsorption to blood. The default absorption fraction f_A for the secreted activity is the highest value for any form of the radionuclide ($f_A = 1$).

18.2.3. Systemic distribution, retention and excretion of germanium

18.2.3.1. Biokinetic data

(336) Nagata et al. (1985) reported post-mortem measurements of germanium in a long-term user of a germanium preparation (Subject A) who died of renal failure, and a non-user (Subject B) who died of liver cirrhosis. Highest tissue concentrations in Subject A were seen in spleen and bone (vertebra), with 12 other tissues showing more than 5-fold lower concentrations. The highest concentration in Subject B was seen in bone, with 13 other tissues showing more than 30-fold lower concentrations.

(337) Zhu et al. (2010) measured concentrations of germanium in 17 tissues obtained from autopsies of up to 68 Chinese men from four areas of China and in blood of 10 volunteers from the same areas. Highest median concentrations were found in rib (89 μg kg^{-1}) followed by blood, liver, and spleen (~45 μg kg^{-1} each); lung (33 μg kg^{-1}); kidney (19 μg kg^{-1}); and thyroid (18 μg kg^{-1}). Concentrations in the range 4-13 μg kg^{-1} were found in gastrointestinal tract tissues, skeletal muscle, heart, testes, thymus, fat, and skin. Based on median tissue concentrations and reference masses of tissues, bone contained about 50% of total-body germanium, blood 15%, liver 4.5%, kidney 0.4%, and other tissue 30%. The estimated total-body content based on median tissue concentrations was 1.4 mg, which is roughly the same as typical daily intake of germanium in food (Schauss, 1991; Scansetti, 1992). As germanium in food appears to be nearly completely absorbed from the gut (Rosenfeld, 1954; Scansetti, 1992), this suggests low systemic retention of germanium.

(338) During the early hours after parenteral administration of germanium compounds to rats or mice (Rosenfeld, 1954; Durbin, 1959; Mehard and Volcani, 1975; Shinogi et al., 1989), the concentration of germanium in the kidneys was much greater than in other tissues. Germanium was rapidly excreted in urine. At 4 d after intravenous administration of ^{71}Ge as $NaHGeO_3$ to rats, cumulative excretion accounted for about 98.5% of the administered amount, and the bone, liver, and kidney contents accounted for about 0.4%, 0.5%, and 1.1%, respectively (Durbin, 1959). At 3 h after intraperitoneal administration of Na_2GeO_3 to rats, the concentration of Ge in the kidneys was 2-20 times that in 14 other examined tissues and fluids (Rosenfeld, 1954). Germanium did not appear to be stored by any tissue after multiple weekly doses (Rosenfeld, 1954).

(339) Velikyan et al. (2013) investigated the organ distribution of ^{68}Ge in rats through day 7 following intravenous administration of $^{68}GeCl_4$. Activity was distributed somewhat uniformly among tissues beyond a few hours. Excretion was rapid and primarily in urine. About 90% of

the injected activity was eliminated in urine with half-time < 1 h. A second, slower phase of retention was observed, with ~1.8% of the activity remaining in the animals after 1 week. Velikyan and coworkers estimated absorbed doses to tissues for adult male and female humans based on the observed residence times in rat tissues. Highest dose estimates for females, expressed as μSv MBq^{-1}, were obtained for kidney (185), adrenals (83), liver (38), colon wall (~20), red marrow (13), osteogenic cells (11), and spleen (11). Lowest dose estimates were obtained for lungs (3.2), heart wall (2.6), muscle (2.0), pancreas (1.9), and brain (1.2). Dose estimates for 10 other tissues were in the range 7-10 μSv MBq^{-1}.

(340) Shinogi et al. (1989) studied uptake and retention of stable germanium in mice after a single peroral administration of GeO_2 solution. Germanium concentrations in blood, stomach, small intestine, and 8 systemic soft tissues were measured from 1-24 h after administration. The maximum concentration in blood and systemic tissues was reached within 1 h. The kidneys showed the highest concentration from 1-24 h. The highest biological half-time was seen in brain (6.3 h). The half-time in blood was 1.2 h and in soft tissues other than brain was in the range 2.4-4.4 h. The area under the time-concentration curve, expressed as μg h g^{-1}, decreased in the order: kidney (51), liver (23), pancreas (13), blood and spleen (11), lung (10), heart (7), testis (6), brain (1.5). At 24 h germanium was detectable only in kidney, liver, spleen, and brain.

(341) Germanium is a member of Group VIA of the period table, located just below silicon. In trace amounts, germanium mimics uptake and accumulation of silicon in laboratory animals. Mehard and Volcani (1975) compared the behaviours of ^{31}Si ($T_{1/2}$ = 157 min) and ^{68}Ge ($T_{1/2}$ = 271 d) in rats following intravenous (IV) or intraperitoneal (IP) administration of $^{31}Si(OH)_4$ and $^{68}Ge(OH)_4$. The IV and IP injection studies yielded broadly similar results, but accumulation of ^{68}Ge was somewhat higher in liver, kidney, bladder, and blood after IP injection than after IV injection. Accumulation of ^{31}Si and ^{68}Ge in tissues increased for about 15-40 min, declined rapidly for ~30 min, and then declined more gradually. Faster depletion of ^{68}Ge than ^{31}Si was indicated. By 2 h after IV injection the concentration of ^{68}Ge in liver was about 65% higher than that of ^{31}Si. Concentrations of ^{68}Ge were measured in blood and 11 tissues at five times from 0.1-20 d after IV injection. Highest concentrations (normalised to 1.0 for kidney at each time) were seen in kidney (1.0), liver (0.29), and blood (0.19) at 0.1 d; kidney (1.0), spleen (0.31, and liver (0.28) at 4 d; and spleen (2.0), kidney (1.0), and urinary bladder (0.15) at 20 d.

18.2.3.2. Biokinetic model for systemic germanium

(342) The structure of the biokinetic model for systemic germanium used in this publication is shown in Fig. 18.1. Transfer coefficients are listed in Table 18.3.

(343) The model for systemic germanium describes the following systemic behaviour of germanium indicated by the biokinetic data summarised above together with findings for its chemical and biological analogue silicon (see the Section 7.2.3.2 on silicon in this publication). The preponderance of germanium injected into blood (roughly 90%) is removed in urine over the first day. The rest is distributed throughout the body, with the kidneys showing the highest concentration of any tissue over the first day and the highest time-integrated concentration over the first week. After 1 week about 2% of the absorbed amount is retained in the total body. The long-term distribution of germanium is consistent with autopsy data of Zhu et al. (2010). Model predictions are also reasonably consistent with the central total-body content of germanium estimated by Zhu et al. (2010), assuming dietary intake of germanium of 1.0-1.5 mg d^{-1} (Schauss, 1991; Scansetti, 1992) and complete absorption from the gut.

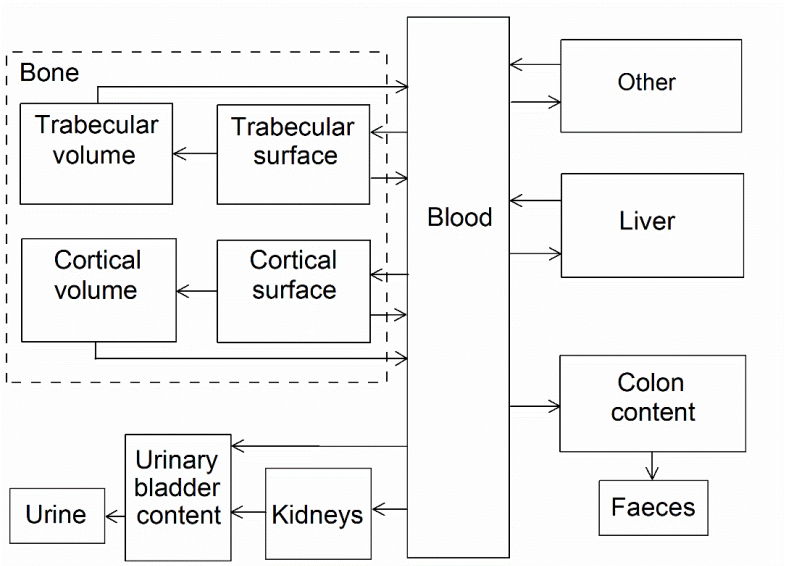

Fig. 18.1. Structure of the biokinetic model for systemic germanium.

Table 18.3. Transfer coefficients in the biokinetic model for systemic germanium.

From	To	Transfer coefficient (d^{-1})
Blood	Other	0.89
Blood	Kidneys	0.2
Blood	Liver	0.4
Blood	Urinary bladder content	8.3
Blood	Right colon content	0.01
Blood	Trabecular bone surface	0.1
Blood	Cortical bone surface	0.1
Other	Blood	0.3
Kidneys	Urinary bladder content	1.2
Liver	Blood	0.9
Trabecular bone surface	Blood	0.3
Cortical bone surface	Blood	0.3
Trabecular bone surface	Trabecular bone volume	0.0015
Cortical bone surface	Cortical bone volume	0.0015
Trabecular bone volume	Blood	0.000493
Cortical bone volume	Blood	0.0000821

18.2.3.3. Treatment of progeny

(344) Progeny of germanium addressed in this publication are radioisotopes of gallium and arsenic. The models for gallium and arsenic as germanium progeny are expansions of the characteristic models for these elements with added compartments and associated transfer coefficients needed to solve the linked biokinetic models for chains headed by germanium (see Annex B). If produced in a compartment not explicitly named in the progeny's model, the progeny is assumed to transfer to the central blood compartment of its characteristic biokinetic model and to follow that model thereafter. The assigned transfer rate to the central blood compartment is the rate of bone turnover for the indicated bone type if the progeny is produced

in a bone volume compartment and at the following element-specific rate if produced in any other ambiguous compartment: gallium, 1.39 d^{-1}; arsenic, 0.6 d^{-1}.

18.3. Individual monitoring

18.3.1. ^{68}Ge

(345) Measurements of ^{68}Ge in urine may be used to determine intakes of the radionuclide.

Table 18.4. Monitoring techniques for ^{68}Ge.

Isotope	Monitoring Technique	Method of Measurement	Typical Detection Limit
^{68}Ge	Urine Bioassay	γ-ray spectrometry[a]	1.2 Bq L^{-1}
^{68}Ge	Whole-body measurement	γ-ray spectrometry[ab]	34 Bq

[a] Measurement system comprised of Germanium Detectors
[b] Counting time of 20 minutes

18.4. Dosimetric data for germanium

Table 18.5. Committed effective dose coefficients (Sv Bq^{-1}) for the inhalation or ingestion of ^{68}Ge compounds.

Inhaled particulate materials (5 µm AMAD aerosols)	Effective dose coefficients (Sv Bq^{-1})
	^{68}Ge
Type F, — NB: Type F should not be assumed without evidence	4.6E-09
Type M, default	7.6E-09
Type S	1.7E-08
Ingested materials	
All forms	6.7E-09

AMAD, activity median aerodynamic diameter

Table 18.6 Dose per activity content of ^{68}Ge in total body and in daily excretion of urine (Sv Bq^{-1}); 5µm activity median aerodynamic diameter aerosols inhaled by a reference worker at light work.

	Type F		Type M		Type S	
Time after intake (d)	Total body	Urine	Total body	Urine	Total body	Urine
1	1.4E-09	4.6E-10	1.2E-08	6.4E-08	2.8E-08	3.4E-06
2	3.2E-09	3.1E-09	2.4E-08	2.9E-07	5.3E-08	1.4E-05
3	5.0E-09	9.9E-09	5.1E-08	1.0E-06	1.1E-07	5.3E-05
4	7.0E-09	1.9E-08	8.9E-08	2.0E-06	2.0E-07	1.1E-04
5	9.4E-09	2.8E-08	1.2E-07	2.9E-06	2.7E-07	1.6E-04
6	1.2E-08	3.9E-08	1.3E-07	3.9E-06	2.9E-07	2.1E-04
7	1.6E-08	5.3E-08	1.4E-07	5.0E-06	3.0E-07	2.7E-04
8	2.1E-08	7.0E-08	1.4E-07	6.2E-06	3.1E-07	3.5E-04
9	2.8E-08	9.3E-08	1.5E-07	7.6E-06	3.2E-07	4.4E-04

10	3.6E-08	1.2E-07	1.5E-07	9.2E-06	3.2E-07	5.4E-04
15	1.3E-07	4.6E-07	1.7E-07	1.9E-05	3.4E-07	1.3E-03
30	2.3E-06	2.6E-05	2.0E-07	3.6E-05	3.7E-07	3.0E-03
45	3.4E-06	1.3E-03	2.3E-07	4.2E-05	3.9E-07	3.3E-03
60	3.6E-06	1.1E-02	2.6E-07	4.9E-05	4.2E-07	3.5E-03
90	3.9E-06	1.4E-02	3.5E-07	6.5E-05	4.8E-07	4.1E-03
180	5.1E-06	1.8E-02	8.0E-07	1.5E-04	7.1E-07	6.1E-03
365	8.5E-06	3.1E-02	4.2E-06	8.0E-04	1.5E-06	1.3E-02

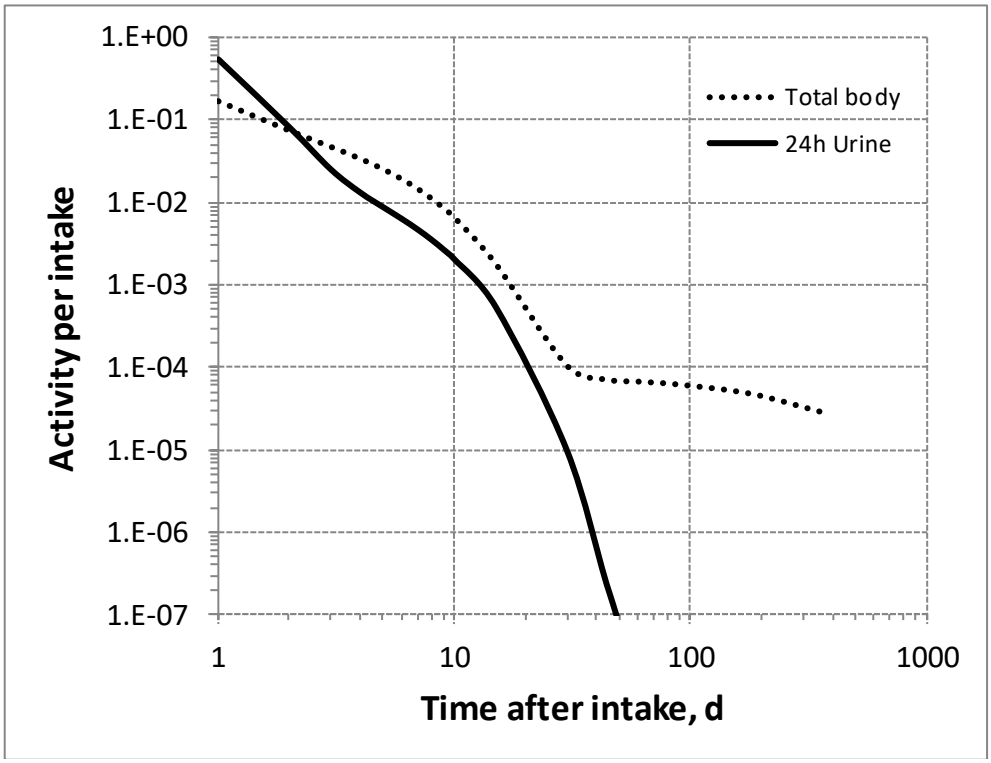

Fig. 18.2. Daily excretion of ^{68}Ge following inhalation of 1 Bq Type F.

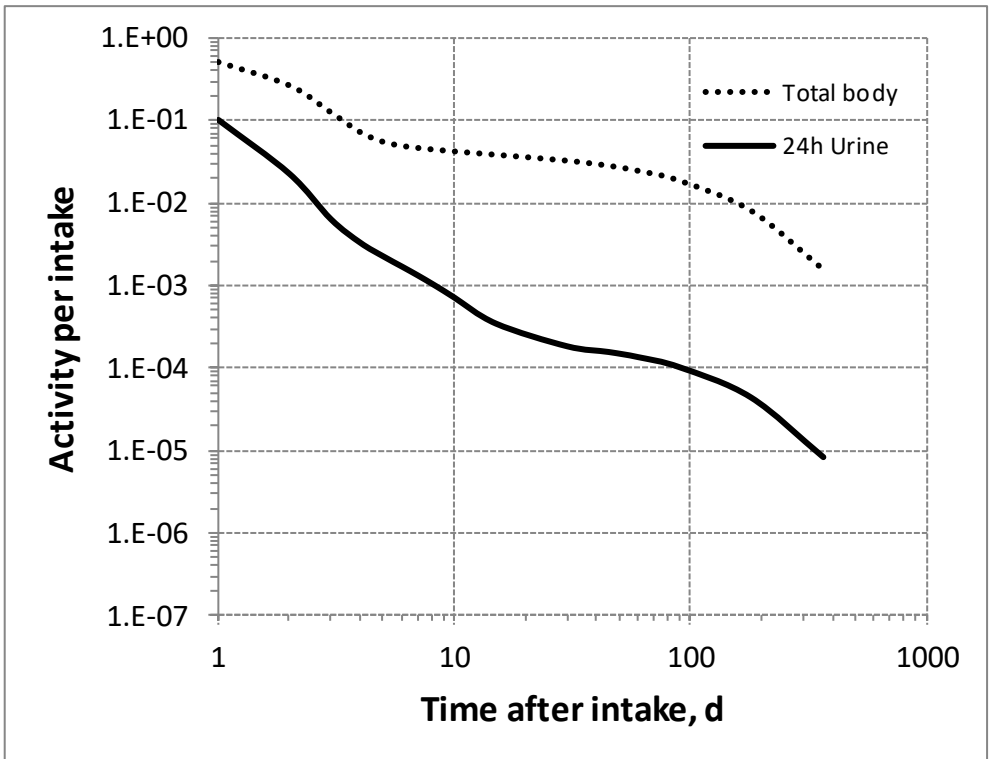

Fig. 18.3. Daily excretion of ^{68}Ge following inhalation of 1 Bq Type M.

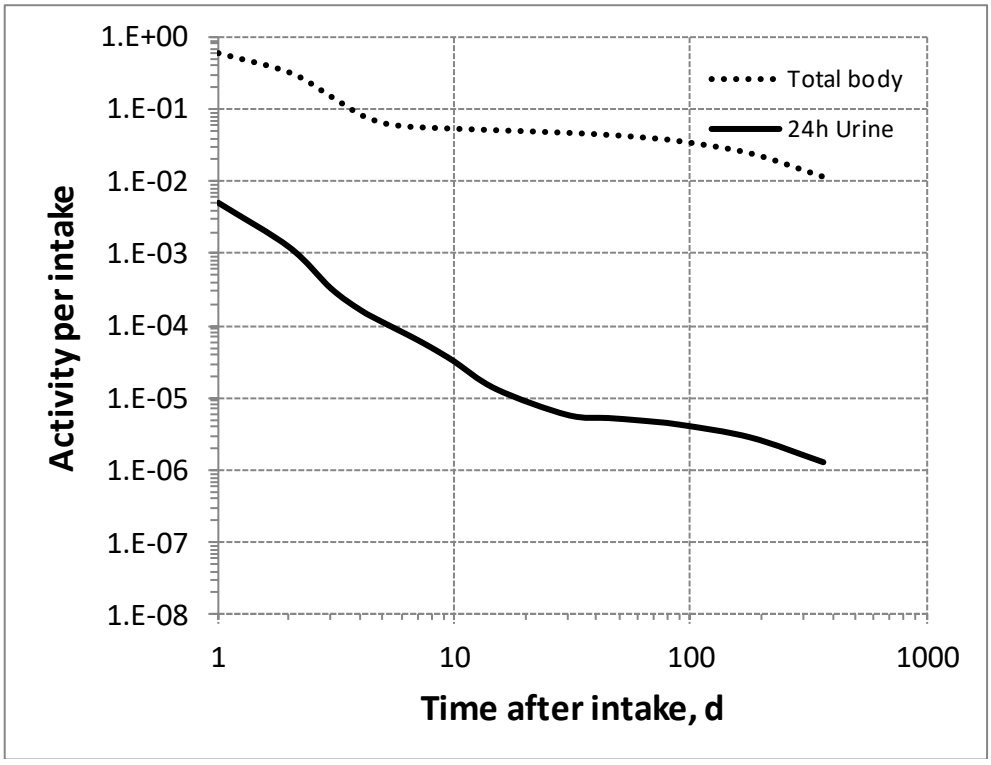

Fig. 18.4. Daily excretion of ^{68}Ge following inhalation of 1 Bq Type S.

19. ARSENIC (Z=33)

19.1. Isotopes

Table 19.1. Isotopes of arsenic addressed in this publication.

Isotopes	Physical half-life	Decay mode
^{69}As	15.23 min	EC, B+
^{70}As	52.6 min	EC, B+
^{71}As	65.28 h	EC, B+
^{72}As	26.0 h	EC, B+
^{73}As	80.30 d	EC
^{74}As	17.77 d	EC, B+, B-
^{76}As*	1.0778 d	B-
^{77}As	38.83 h	B-
^{78}As	90.7 min	B-

EC, electron-capture decay; B+, beta-plus decay; B-, beta-minus decay.
*Dose coefficients and bioassay data for this radionuclide are given in the printed copy of this publication.
Data for other radionuclides listed in this table are given in the online electronic files on the ICRP website.

19.2. Routes of Intake

19.2.1. Inhalation

(346) For arsenic, default parameter values were adopted on absorption to blood from the respiratory tract (ICRP, 2015). Absorption parameter values and types, and associated f_A values for particulate forms of arsenic are given in Table 19.2.

19.2.2. Ingestion

a. Human studies

(347) Bettley and O'Shea (1975) measured arsenic in blood, urine and faeces of four patients with carcinoma given a test dose of water-soluble arsenic trichloride and in three control subjects. The administered arsenic appeared to be almost completely absorbed from the gut. Mappes (1977) observed the urinary excretion of about 70% of arsenic ingested as the trioxide As_2O_3 dissolved in water. In contrast, the absorption of the insoluble arsenic triselenide (As_2Se_3) was not detected. Similarly, in hamsters, the fractional absorption of insoluble arsenic compounds (arsenic trisulfide, lead arsenate) was reduced to 20–30% (Marafante and Vahter, 1987).

(348) Crecelius (1977) studied the speciation of arsenic in urine after ingestion of arsenic-rich wine, drinking water and crab meat: about 80% of arsenic (mostly arsenite As^{3+}) from wine was excreted in urine within 61 hours, 50% of arsenate (As^{5+}) from well-water was excreted in urine over 70 hours and most of organic arsenic from crab was excreted within 1-2 days. Tam et al. (1982) determined that 58% of ^{74}As ingested by six adult volunteers as arsenic acid was excreted in urine over 5 days. The cumulated urinary excretion of arsenic for 14 days after repeated oral administration of up to 1 mg sodium metaarsenite $NaAsO_2$ amounted to 60% of the ingested quantity (Buchet et al., 1981b). Kumana et al. (2002) evaluated a mean systemic bioavailability of 87% of arsenic trioxide given to nine patients with leukemia by comparing the arsenic blood content over 2 days after ingestion of a 10 mg oral solution with that measured after intra-venous infusion. Zheng et al. (2002) studied the balance over a week of arsenic in

diet and excretion of six healthy adult volunteers drinking water with high concentrations of arsenic and fluoride. They evaluated a fractional absorption of about 94% of arsenic intake, with no significant influence of the level of fluoride intake.

b. Arsenic in soils and animal studies

(349) Stanek et al. (2010) compared the bioavailability of arsenic in diet and in soil in 13 human volunteers. A 7-day mass-balance study of arsenic in diet, urine and faeces indicated a mean absorption of 91% of arsenic in food and beverages. In 5-day balance study after ingestion of 0.63 g of arsenic-contaminated soil, the soil-arsenic fractional absorption was estimated on average as 49%.

(350) The US Environmental Protection Agency (EPA, 2012) reviewed the data on relative bioavailability of arsenic in soils: 103 values were estimated from relevant studies involving bioassay in juvenile swines, monkeys and mice having ingested soils contaminated by arsenic from various activities including mining, smelting, agriculture and chemical processes. The estimated systemic absorption of arsenic in soil ranged from 4 to 78% (7-57% 5^{th}-95^{th} percentile range) of that of water soluble sodium arsenate, with a mean of 31% (median 28%).

(351) In *Publications 30* and *68* (ICRP, 1981, 1994a) an f_1 of 0.5 was recommended for all compounds of arsenic. In this publication, a f_A value of 1 is adopted for water soluble arsenic compounds. A f_A value of 0.3 is adopted for insoluble arsenic compounds and arsenic is soils.

Table 19.2. Absorption parameter values for inhaled and ingested arsenic.

	Absorption parameter values*			Absorption from the alimentary tract, f_A
Inhaled particulate materials	f_r	s_r (d^{-1})	s_s (d^{-1})	
Default parameter values†				
Absorption type				
F	1	30	–	1
M‡	0.2	3	0.005	0.2
S	0.01	3	1×10^{-4}	0.01
Ingested materials§				
Water soluble compounds				1
Water insoluble compounds and arsenic in soil				0.3

*It is assumed that the bound state can be neglected for arsenic (i.e. $f_b = 0$). The values of s_r for Type F, M and S forms of arsenic (30, 3 and 3 d^{-1} respectively) are the general default values.

†For inhaled material deposited in the respiratory tract and subsequently cleared by particle transport to the alimentary tract, the default f_A values for inhaled materials are applied [i.e. the product of f_r for the absorption type and the f_A value for ingested soluble forms of arsenic (1)].

‡Default Type M is recommended for use in the absence of specific information on which the exposure material can be assigned to an absorption type (e.g. if the form is unknown, or if the form is known but there is no information available on the absorption of that form from the respiratory tract). For guidance on the use of specific information, see Section 1.1.

§Activity transferred from systemic compartments into segments of the alimentary tract is assumed to be subject to reabsorption to blood. The default absorption fraction f_A for the secreted activity is the highest value for any form of the radionuclide ($f_A = 1$).

19.2.3. Systemic distribution, retention and excretion of arsenic

19.2.3.1. Biokinetic data

(352) Arsenic (As) is ubiquitous in nature. It exists primarily in the trivalent state in the earth's crust but is largely oxidised to pentavalent arsenic in soil and water (Mochizuki, 2019).

(353) The neurotoxicity of arsenic has long been recognised, and there is epidemiological evidence that it is a carcinogen (WHO, 2000; ATSDR, 2007; Mochizuki, 2019). Inorganic trivalent (arsenite) and pentavalent (arsenate) compounds are the most hazardous forms, with the trivalent state having much more potent toxic properties than the pentavalent form (Hughes, 2002). The toxicokinetics of these two forms has been investigated in human subjects, dogs, rabbits, mice, rats, hamsters, guinea pigs, farm animals, and a variety of non-human primates. Several biokinetic models for inorganic arsenic have been proposed (e.g. Menzel et al., 1994; Mann et al., 1996; Yu, 1999; El-Masri and Kenyon, 2008; Ling and Liao, 2009; Adeyemi et al., 2010).

(354) Absorbed or injected inorganic As(III) and As(V) initially have noticeably different systemic kinetics (Vahter and Norin, 1980; Lindgren et al., 1982). A substantial portion of absorbed As(V) is reduced to As(III) in the body (Vahter and Marafante, 1985; Vahter, 2002), resulting in more similar distributions of the initially different forms over time.

(355) Lindgren et al. (1982) examined the systemic distribution of intravenously injected ^{74}As as As(III) or As(V) in mice using whole-body autoradiography, external counting, and measurement of activity in dissected tissues. Total-body retention over the first 3 d was greater for As(III) than As(V). Comparison of autoradiograms at 1 h indicated higher uptake of As(III) in oral mucosa, stomach wall, and liver, and lower uptake in bone compared with As(V). The relatively high skeletal accumulation of As(V) was attributed to substitution of arsenate ions for the physiologically similar phosphate ions in bone crystal. Comparisons at 24 h indicated similar distributions of activity administered in the different forms except for higher skeletal uptake of activity administered as As(V).

(356) Trivalent arsenic is oxidised in the body to arsenites that are methylated in the liver and to lesser extent in other tissues, to form methylarsonic acid (MMA) and dimethylarsinic acid (DMA), which are excreted in urine at a relatively high rate. Buchet et al. (1981a) compared rates of urinary excretion of arsenic and its metabolites following a single oral intake of sodium arsenite (As_i), MMA, or DMA by healthy adult men, ages 27-42 y. Total urinary arsenic over 4 d represented 46, 78, and 75% of arsenic ingested as As_i, MMA, and DMA, respectively. The time post exposure at which 50% of the 4-d excretion was reached was < 4 h for intake of MMA, 11 h for DMA, and 28 h for As_i.

(357) Activity concentrations were measured in post-mortem tissues of an adult female cancer patient who was administered ^{76}As intravenously 20 h before death (Ducoff et al., 1948). The highest concentration was found in the liver, followed by the kidneys. Normalised to a concentration of 1.0 in liver, the concentrations decreased in the order: kidneys (0.64) > spleen, heart, marrow, lymph nodes, stomach, pancreas, muscle, small intestine, and lung (0.23-0.35) > adrenals, ovary, thyroid, and skin (0.14-0.18) > brain and femoral cortical bone (0.05).

(358) Mealey et al. (1959) summarised observations of the systemic behaviour of ^{74}As in >100 patients administered ^{74}As(III) intravenously for brain tumor localisation. In four patients followed up to 10 d, blood clearance C(t) of ^{74}As expressed as % dosage L^{-1} blood at t hours ($t \geq 0.25$), was described by a sum of three exponential terms:

$$C(t) = 7.0\exp^{-1.54t} + 0.07e^{-0.025t} + 0.015e^{-0.003t}.$$

The activity concentration in red blood cells increased over time and was about 3 times the plasma concentration by 10 h post injection. Renal clearance of ^{74}As was estimated as 3.54 L plasma h^{-1}. Cumulative urinary activity was in the range 18-30% of the administered amount at

1 h post injection, 36-56% at 4 h, and 57-90% at 9 d. In a patient followed for 18 d, urinary activity accounted for ~97% of the injected amount. Only small amounts were recovered in faeces (e.g. 0.21% of the administered amount in one case during the first week, and 1.3% in a second case over 17 d). The concentration of ^{74}As in tissues was determined for 11 patients who died at times ranging from 1 h to 71 d after injection. In all cases the highest concentrations were found in the liver and kidneys. These two tissues contained roughly 20% and 10%, respectively, at 1 h after injection. The sequential data for the 11 cases indicated that roughly 90% or more of the activity retained in the kidneys at 1 h was removed with a half-time of about 8 h, and the remainder declined with a half-time of 2-3 d. The indicated time-dependent behaviour of ^{74}As in the liver also suggested two components of retention, with half-times of roughly 1 d for 90% or more of the retained activity and 2 weeks for the remainder.

(359) Pomroy et al. (1980) studied the biokinetics of ^{74}As in six healthy adult male subjects (ages 28-60 y) following its oral administration as arsenic acid [As(V)]. Total-body retention was measured externally for periods up to 103 d, and losses in urine and faeces were measured up to 7 d. The pooled measurements of total-body retention were fit by a sum of three exponential terms indicating biological half-times of 2.1 d (65.9%), 9.5 d (30.4%), and 38.4 d (3.7%). Cumulative urinary and faecal excretion of ^{74}As over the first 7 d represented on average 62% and 6%, respectively, of the administered amount. The portions of faecal losses representing unabsorbed and endogenously secreted activity could not be determined. The excretion patterns are qualitatively consistent with findings of Mealey et al. (1959) for intravenously injected ^{74}As(III) in that most of the amount entering blood was largely excreted in urine over the next few days. However, the initial urinary excretion rate was higher in the subjects of Mealey et al.: 36-56% at 4 h, compared with 18-27% at 1 d observed by Pomroy et al. (1980).

(360) Zhu et al. (2010) reported medians and ranges of arsenic concentration in 17 tissues collected at autopsy from up to 68 adult males from 4 regions of China, and in blood of 16 living subjects from the same regions. The highest median concentration was found in rib (102 μg kg^{-1} wet weight), followed by thyroid (53) and liver (41). Concentrations in blood and the remaining 14 tissues were in the range 19-38 μg kg^{-1}. Based on the observed median concentrations of arsenic in tissues and reference masses of tissues, about 38% of total-body arsenic was contained in bone, 29% in muscle, 11% in fat, 5% in blood, 4% in skin, 3% in liver, and 10% in remaining tissues.

(361) In biokinetic studies of inorganic arsenic in laboratory animals, the liver and kidneys usually show high concentrations of arsenic soon after administration of either As(III) or As(V) (Ducoff et al., 1948; Marafante et al., 1981; Lindgren et al., 1982). This is consistent with findings for human subjects (Ducoff et al., 1948; Mealey et al., 1959).

19.2.3.2. Biokinetic model for systemic arsenic

(362) The structure of the biokinetic model for systemic arsenic applied in this publication is shown in Fig. 19.1. Transfer coefficients are listed in Table 19.3.

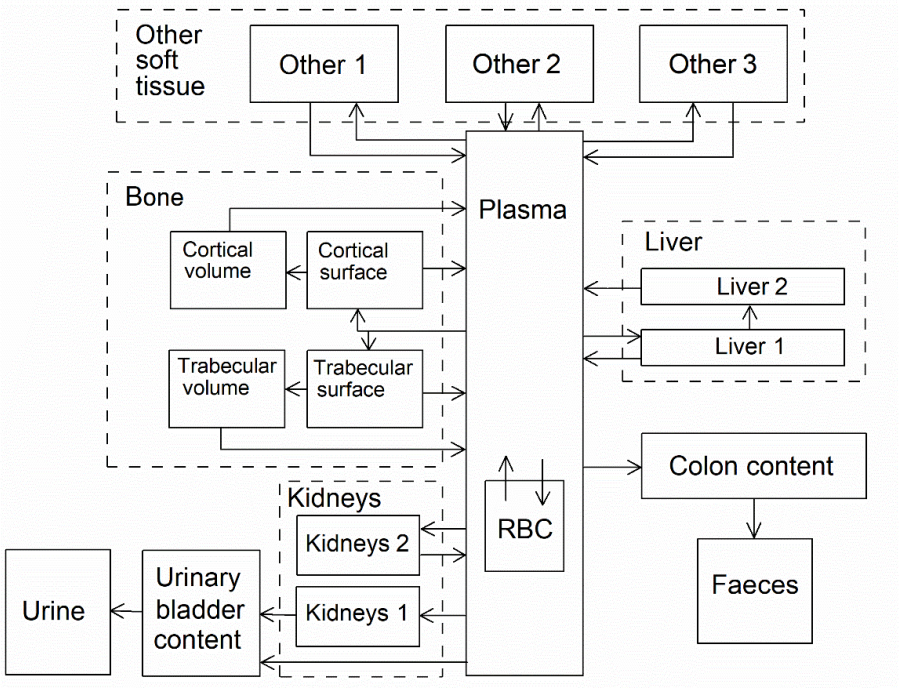

Fig. 19.1. Structure of the biokinetic model for systemic arsenic.

(363) The model is assumed to apply to both As(III) and As(V). Where differences in the kinetics of these two forms are indicated by data from human or animal studies, preference was given to data for As(V). The model was designed for consistency of predictions with the central whole-body retention data determined in human subjects in the study by Pomroy et al. (1980) and reasonable consistency with the early systemic behaviour of inorganic arsenic in human subjects and laboratory animals. Reasonable consistency with the long-term systemic distribution of arsenic in adult humans indicated by autopsy data (Zhu et al., 2010) was required. The model predicts high accumulation of arsenic in the kidneys and liver soon after uptake to blood but removal of the preponderance of accumulated arsenic from both organs over the next few days. Predicted long-term cumulative urinary and faecal losses represent about 95 and 5% of total excretion of arsenic.

19.2.3.3. Treatment of progeny

(364) Progeny of arsenic addressed in this publication are radioisotopes of germanium. The model for germanium produced in systemic compartments by decay of arsenic is an expanded version of the characteristic model for germanium with added compartments and associated transfer coefficients needed to solve the linked biokinetic models for arsenic and germanium. Germanium produced in compartments of the model for arsenic that are not addressed in the characteristic model for germanium is assumed to transfer to the central blood compartment of the germanium model at the rate 1000 d^{-1} and to follow the characteristic model for germanium thereafter.

Table 19.3. Transfer coefficients in the biokinetic model for systemic arsenic.

From	To	Transfer coefficients (d^{-1})
Blood	RBC	2.0
Blood	Other 1	20
Blood	Other 2	1.52

Blood	Other 3	0.28
Blood	Liver 1	2.4
Blood	Kidneys 1	2.52
Blood	Kidneys 2	0.28
Blood	Cortical bone surface	1.0
Blood	Trabecular bone surface	1.0
Blood	Urinary bladder content	8.4
Blood	Right colon content	0.6
RBC	Blood	0.3
Other 1	Blood	0.6
Other 2	Blood	0.08
Other 3	Blood	0.018
Liver 1	Blood	0.95
Liver 1	Liver 2	0.05
Liver 2	Blood	0.07
Kidneys 1	Urinary bladder content	5.0
Kidneys 2	Blood	0.7
Cortical bone surface	Blood	0.6
Trabecular bone surface	Blood	0.6
Cortical bone surface	Cortical bone volume	0.003
Trabecular bone surface	Trabecular bone volume	0.006
Cortical bone volume	Blood	0.0000821
Trabecular bone volume	Blood	0.000493

19.3. Individual monitoring

(365) Information of detection limit for routine individual measurement is not available.

19.4. Dosimetric data for arsenic

Table 19.4. Committed effective dose coefficients (Sv Bq^{-1}) for the inhalation or ingestion of ^{76}As compounds.

Inhaled particulate materials (5 µm AMAD aerosols)	Effective dose coefficients (Sv Bq^{-1})
	^{76}As
Type F, — NB: Type F should not be assumed without evidence	2.9E-10
Type M, default	5.2E-10
Type S	5.6E-10
Ingested materials	
Water insoluble compounds and arsenic in soil	5.7E-10
Water soluble compounds	4.9E-10

AMAD, activity median aerodynamic diameter

20. SELENIUM (Z=34)

20.1. Isotopes

Table 20.1. Isotopes of selenium addressed in this publication.

Isotopes	Physical half-life	Decay mode
^{70}Se	41.1 min	EC, B+
^{72}Se	8.4 d	EC
^{73}Se	7.15 h	EC, B+
^{73m}Se	39.8 min	IT, EC, B+
^{75}Se*	119.779 d	EC
^{79}Se*	2.95E+5 y	B-
^{81}Se	18.45 min	B-
^{81m}Se	57.28 min	ITB-
^{83}Se	22.3 min	B-

EC, electron-capture decay; B+, beta-plus decay; B-, beta-minus decay; IT, isomeric transition decay.
*Dose coefficients and bioassay data for this radionuclide are given in the printed copy of this publication.
Data for other radionuclides listed in this table are given in the online electronic files on the ICRP website.

20.2. Routes of Intake

20.2.1. Inhalation

(366) No information was found on the behaviour of inhaled selenium in man. Information on absorption of selenium from the respiratory tract is available from experimental studies of forms of selenium including selenious acid (H_2SeO_3) and elemental selenium, which were conducted mainly to investigate the potential health hazard of selenium emitted during fossil fuel combustion. Absorption parameter values and types, and associated f_A values for particulate forms of selenium are given in Table 20.2.

20.2.1.1. Particulate Materials

a. Selenious acid (H_2SeO_3)

(367) Medinsky et al. (1981) followed the biokinetics of ^{75}Se for 72 d after inhalation of ^{75}Se-labelled selenious acid by rats. The aerosol was heated to 150 °C, to form mainly selenium dioxide (SeO_2), but this subsequently rehydrated to selenious acid soon after contact with moist air (Burkstaller et al., 1977; Heisler Weissman and Cuddihy, 1979). Complementary experiments were conducted in which the biokinetics of ^{75}Se were followed for 4 d after administration of ^{75}Se-selenious acid to rats by intravenous injection, nasal instillation, gavage, and cutaneous application (Medinsky et al., 1981). The authors estimated that approximately 94% of the initial alveolar deposit (IAD) was absorbed by the time of the first measurement of tissue distribution, at 4 h. Medinsky et al. (1981) applied simulation modelling to the results, and represented the absorption of selenium from the respiratory tract by an absorption function (fractional dissolution rate):

$$S(t) = 99\ e^{-50t} + 20\ e^{-10t} + 0.08\ d^{-1}$$

at time t (d) after intake.

(368) This can be approximated using the HRTM with $f_r = 0.99$, $s_r = 26\ d^{-1}$ and $s_s = 0.08\ d^{-1}$, consistent with assignment to Type F.

(369) Weissman et al. (1983) followed the biokinetics of ^{75}Se for 256 d after inhalation of ^{75}Se-labelled selenious acid (heat-treated at 150 °C) by beagle dogs. Complementary experiments were conducted in which the biokinetics of ^{75}Se were followed for 4 d after administration of ^{75}Se-selenious acid to dogs by nasal instillation, intravenous injection, gavage, and in food. The authors estimated that approximately 97% of the initial lung deposit (ILD) was absorbed by the time of the first measurement of tissue distribution, at 2 h, giving assignment to Type F. Assuming absorption at a constant rate, this gives a value of s_r approximately 40 d^{-1}. The remaining lung content decreased with a biological half-time, T_b, of approximately 30 d: however, this was similar to the retention half-time in blood and other soft tissues, and so some (if not all) of it could have been systemic activity rather than retention of the ILD. The authors estimated that following nasal instillation approximately 75% of the initial deposit was absorbed by 4 d.

(370) Burkstaller et al. (1977) measured the in-vitro dissolution of ^{75}Se-labelled selenious acid (heat-treated at 150 °C), as used in the rat and dog inhalation experiments summarised above. Similar results were obtained with four different solvents: 95 – 97% dissolved within 0.85 days; the rest at 0.1 – 0.4% of the original activity per day.

(371) Parallel studies in rats and dogs were carried out with ^{75}Se-labelled elemental selenium (see below). It was observed that both forms were rapidly absorbed from the respiratory tract, but selenious acid was absorbed somewhat faster. The distribution of ^{75}Se following absorption to blood was similar in both cases.

(372) Although specific parameter values for selenious acid based on in-vivo data are available, they are not adopted here, because the data are used as the basis for the default rapid dissolution rate for selenium. Hence specific parameter values for selenious acid would be the same as default Type F selenium parameter values. Instead, selenious acid is assigned to Type F.

b. Sodium selenate and selenite

(373) Rhoads and Sanders (1985) followed the biokinetics of ^{75}Se for 14 days after intratracheal instillation of sodium selenate and selenite into rats. Results were very similar for the two compounds. Lung retention was fit by a two-component exponential function: 8% and 92% with T_b 30 min and 1.9 d, respectively. The rapid lung clearance was mainly by absorption to blood, and also consistent with assignment to Type F.

c. Elemental selenium

(374) Medinsky et al. (1981) followed the biokinetics of ^{75}Se for 72 d after inhalation of ^{75}Se-labelled elemental selenium particles by rats. Complementary experiments were conducted in which the biokinetics of ^{75}Se were followed for 4 d after administration of ^{75}Se-selenious acid to rats by intravenous injection, nasal instillation, gavage, and cutaneous application (Medinskyet al., 1981). The authors estimated that approximately 57% IAD was absorbed by the time of the first measurement of tissue distribution, at 4 h. Medinsky et al. (1981) applied simulation modelling to the results, in which they represented the absorption of selenium from the respiratory tract by an absorption function (fractional dissolution rate):

$$S(t) = 15\ e^{-50t} + 20\ e^{-10t} + 0.08\ d^{-1}$$

at time t (d) after intake.

(375) This can be approximated using the HRTM with $f_r = 0.92$, $s_r = 18$ d^{-1} and $s_s = 0.08$ d^{-1}, consistent with assignment to Type F.

(376) Weissman et al. (1983) followed the biokinetics of ^{75}Se for 256 d after inhalation of ^{75}Se-labelled elemental selenium by beagle dogs. Complementary experiments were conducted in which the biokinetics of ^{75}Se were followed for 4 d after administration of ^{75}Se-metal to dogs by nasal instillation, gavage, and in food. The authors estimated that approximately 80% ILD was absorbed by the time of the first measurement of tissue distribution, at 2 h, indicating assignment to Type F. Assuming absorption at a constant rate, this gives a value of s_r approximately 20 d^{-1}. The remaining lung content decreased with a half-time of approximately 30 d: this was similar to the T_b in blood and other soft tissues, and so some (if not all) of it could have been systemic activity rather than retention of the ILD. The authors estimated that following nasal instillation approximately 50% of the initial deposit was absorbed by 4 d.

(377) Although specific parameter values for elemental selenium based on in-vivo data are available, they are not adopted here, because the specific values would be similar to those for default Type F. Instead, elemental selenium is assigned to Type F.

Table 20.2. Absorption parameter values for inhaled and ingested selenium.

		Absorption parameter values*			Absorption from the alimentary tract,
Inhaled particulate materials		f_r	s_r (d^{-1})	s_s (d^{-1})	f_A
Default parameter values†,‡					
Absorption type	Assigned forms				
F	Selenium dioxide, selenious acid, elemental selenium	1	30	–	0.8
M§	—	0.2	3	0.005	0.2
S	—	0.01	3	0.0001	0.008
Ingested materials¶					
Selenide and elemental selenium					0.05
All other forms					0.8

*It is assumed that for selenium the bound state can be neglected (i.e. $f_b = 0$). The values of s_r for Type F, M and S forms of selenium (30, 3 and 3 d^{-1}, respectively) are the general default values.

†Materials (e.g. selenium dioxide) are generally listed here where there is sufficient information to assign to a default absorption Type, but not to give specific parameter values (see text).

‡For inhaled material deposited in the respiratory tract and subsequently cleared by particle transport to the alimentary tract, the default f_A values for inhaled materials are applied [i.e. the product of f_r for the absorption type and the f_A value for ingested soluble forms of selenium (0.8)].

§Default Type M is recommended for use in the absence of specific information on which the exposure material can be assigned to an absorption type (e.g. if the form is unknown, or if the form is known but there is no information available on the absorption of that form from the respiratory tract). For guidance on the use of specific information, see Section 1.1.

¶Activity transferred from systemic compartments into segments of the alimentary tract is assumed to be subject to reabsorption to blood. The default absorption fraction f_A for the secreted activity is the reference f_A (= 0.8) for ingestion of the radionuclide.

d. Copper gallium diselenide (CGS) and Copper indium diselenide (CIS)

(378) As part of a toxicological study of novel compounds used in the photovoltaic and semiconductor industries, Morgan et al. (1997) measured tissue concentrations of copper, gallium and selenium up to 28 d after administration of CGS to rats by intratracheal instillation. There was no appreciable lung clearance or extrapulmonary accumulation of any of these elements, suggesting Type S behaviour. In a similar study with copper indium diselenide, Morgan et al. (1997) detected no change in lung concentrations of copper, indium or selenium.

The concentration of indium (but not that of copper or selenium) in extrapulmonary tissues increased, suggesting Type M behaviour.

20.2.1.2. Rapid dissolution rate for selenium

(379) Evidence from the experimental studies outlined above shows that absorption is rapid. Values of s_r estimated for selenious acid were approximately 30 – 40 d^{-1}: close to the general default value of 30 d^{-1}, which is applied here to all Type F forms of selenium.

20.2.1.3. Extent of binding of selenium to the respiratory tract

(380) Evidence from the experimental studies outlined above suggests that there is probably little binding of selenium. It is therefore assumed that for selenium the bound state can be neglected (i.e., $f_b = 0.0$).

20.2.2. Ingestion

(381) Selenium (Se) is an essential trace element. Several reviews of its behaviour in the body have been published (Muth et al., 1967; Frost and Lish, 1975; Underwood, 1977; Levander, 1987; Alexander et al., 1988; Magos and Berg, 1988; Dainty, 2001; ATSDR, 2003). Most of the available information about intestinal absorption refers to dietary selenium and was obtained from balance studies, stable isotope and radiotracer experiments, great part of them originally carried out in New Zealand where selenium intake is particularly low. Considerably less information is available for other organic and inorganic forms of selenium, especially for those most commonly found at the workplace. For selenomethionine, mean values above 0.95 have been reported by Griffiths et al (1976), Swanson et al. (1983) and Moser-Veillon et al. (1992), whereas Robinson et al. (1978) found an absorption of 0.75. Quite a wide range of values [0.4-0.9] have been reported for selenium administered as selenite (Thomson and Stewart, 1974; Janghorbani et al., 1982, 1984; Martin et al., 1989; Patterson et al., 1989; Moser-Veillon et al., 1992). The variations were sometimes observed between studies made by the same group, with the authors being unable to provide a clear interpretation of the findings. Thomson and Robinson (1986) found that absorption of selenium from selenates was superior to that from selenites (0.94±0.04 vs. 0.62±0.14). The absorption of elemental selenium appears to be much lower; a value of 0.03 having been reported by Robinson et al. (1985) after selenite had been reduced with ascorbic acid. The ATSDR (2003) notes that the estimated low intestinal absorption of elemental selenium is consistent with its relatively low toxicity.

(382) Results for Se absorption in animals are in the same range as the human data and show a similar effect of chemical form. Absorption values above 0.9 were observed in rats, mice and dogs for selenomethionine and selenites (Graham et al., 1971; Thomson and Stewart, 1973; Furchner et al., 1975), whereas monkeys showed, in comparison, lower values of absorption for selenites (Furchner et al., 1975). Lower values were also reported for elemental selenium and selenides (Luckey et al., 1975; Nishimura et al., 1991; Archimbaud et al., 1992).

(383) In vivo studies of rats (Whanger et al., 1976) showed that intestinal absorption occurred mainly in the duodenum and to a lesser extent, in the jejunum and ileum. Absorption of selenium from seleniomethionine was not significantly lower than from sodium selenate (Finley, 1998). On the other side, in vivo experiments with ligated rat intestines (Vendeland et al., 1992) and in vitro experiments with membrane vesicles from rat intestines (Vendeland et al., 1992, 1994) showed significant differences in the velocity and extent of intestinal absorption of selenium from selenocysteine, selenodiglutathione, sodium selenite or sodium selenate from different parts of the intestines.

(384) In *Publication 30* (ICRP, 1981), the recommended absorption values were 0.05 for elemental selenium and selenides and 0.8 for all other compounds. In *Publication 69* (ICRP, 1995a), a value of 0.8 was applied to dietary forms. The *Publication 30* values are used here; that is, $f_A = 0.05$ for selenides and elemental selenium, and 0.8 for all other compounds.

20.2.3. Systemic distribution, retention and excretion of selenium

20.2.3.1. Biokinetic data

(385) The biological behaviour of selenium has been investigated extensively in human subjects and laboratory animals, primarily in connection with studies of selenium nutrition and use of ^{75}Se as a diagnostic tool in nuclear medicine (Jereb et al., 1975; Hawkes et al., 2003; Burk, 2013). The systemic behaviour of selenium does not appear to depend strongly on the chemical form administered.

(386) Results of human studies (Lathrop et al., 1968, 1972; Falk and Lindhe, 1975; Jereb et al., 1975; Johnson, 1977; Toohey et al., 1979) indicate that total-body retention of ingested or intravenously injected selenium can be described as a sum of three exponential terms representing biological half-times in the range 0.5-7 d for the short-term component of retention, 20-70 d for the intermediate-term component, and 120-330 d for the long-term component (ICRP, 1995a). The following retention curve appears to be a reasonable central estimator of the percentage R(t) retained at time t (d) following intravenous administration of selenium to adult subjects:

$$R(t) = 13.2\ e^{-1.26t} + 44.6\ e^{-0.0151t} + 42.2\ e^{-0.00315\,t}, \qquad \text{(Eq. 20.1)}$$

where the three terms represent central biological half-times of 0.55 d, 46 d, and 220 d, respectively.

(387) Selenium is non-uniformly distributed in systemic tissues at all times after uptake to blood. In both human and animal studies the highest concentrations at early times after ingestion or injection typically are seen in the kidneys and liver, with spleen, pancreas, and testes also showing elevated concentrations compared with the average for the whole body (Wright and Bell, 1966; Lathrop et al., 1972; Furchner et al., 1975; ICRP, 1981, 1995a). In autopsy studies of human subjects these same tissues also generally show elevated concentrations of stable selenium compared with the average concentration in the body. Data from a modern study (Zhu et al., 2010) involving measurement of selenium concentrations in tissues of 68 cadavers and blood concentrations in 10 living subjects indicate the following distribution of stable selenium: blood, 6.3% (of total-body selenium); liver, 6.7%; kidneys, 3.2%; spleen, 0.6%; pancreas, 0.4%; bone, 11.9%; testes, 0.2%; remaining tissues, 70.7%.

(388) Lathrop et al. (1972) reviewed biokinetic data for selenium arising from investigations or applications of ^{75}Se-L-selenomethionine as a diagnostic agent. Following intravenous administration of a single dose, about 14% (range, 7.5-18.2%) of the injected amount was recovered in urine and faeces during the first 120 h, with urinary loss representing on average about 4.5 times faecal loss. Observations over two years or more after acute administration indicated that ~80% of the biological removal was in urine and ~15% was in faeces. Measurements of activity in expired breath at early times indicated that about 1% of the injected amount was lost by this route. No losses appeared to occur by sweat during the first 2-3 days. Measurements of activity in hair, nails, and skin of one subject indicated a total loss of ~4% by these routes during the first 280 days. Blood, liver, muscle, and skin contained about 15%, 20%, 34%, and 7%, respectively, at 1 d after administration. The systemic distribution changed

gradually over several months, with blood, liver, muscle, and skin containing about 8%, 3%, 56%, and 3%, respectively, at 300 d and 600 d after administration.

20.2.3.2. Biokinetic model for systemic selenium

(389) The systemic model applied here to selenium in the adult is a recycling model that consists of compartments representing blood, liver, kidneys, spleen, pancreas, trabecular bone surface, cortical bone surface, and gonads. Transfer coefficients are set for reasonable consistency with: total-body retention as described by Eq. 20.1; typical relative contents of selenium in the modelled compartments in the early days after acute input of selenium to blood, as judged from reported human and animal studies; and the distribution and total-body content of stable selenium in the body based on the study by Zhu et al. (2010).

(390) The model structure is shown in Fig. 20.1. The transfer coefficients are listed in Table 20.3.

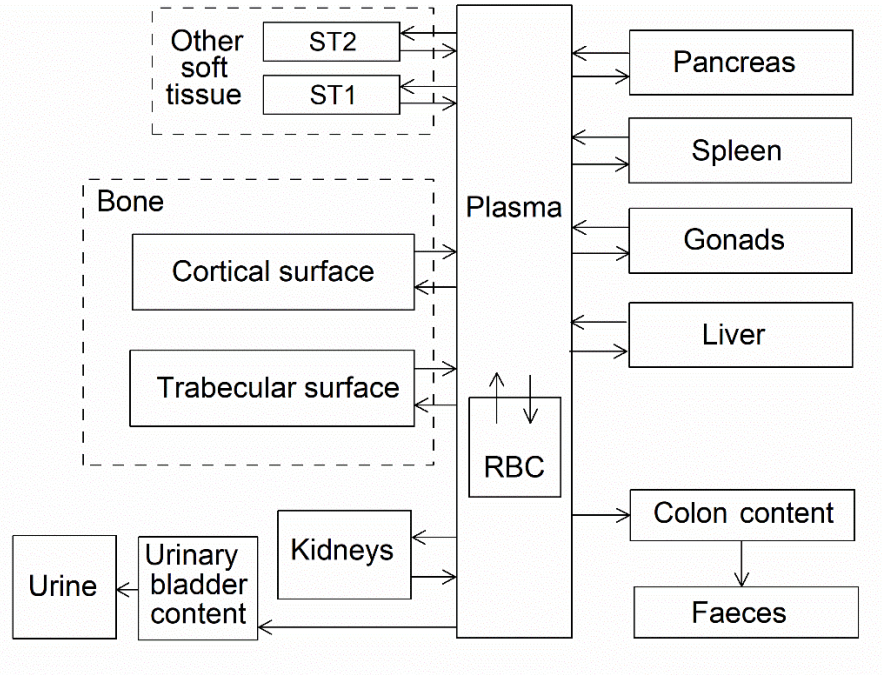

Fig. 20.1. Structure of the biokinetic model for systemic selenium.

20.2.3.3. Treatment of progeny

(391) Progeny of selenium addressed in this publication are isotopes of selenium, krypton, bromine, and arsenic. The model for selenium as a parent is applied to selenium as a progeny of selenium. Krypton produced in a tissue compartment is assumed to transfer to blood with a halftime of 15 min and to be removed from blood to the environment (exhaled) at the rate 1000 d^{-1}. For application to bromine as a progeny of selenium the characteristic model for bromine was expanded to include explicitly all tissues addressed in the selenium model. Deposition fractions for the tissues added to the bromine model were based on the mass fractions (of total body) of these tissues in the adult male. The assigned rates of transfer of bromine from blood to added tissues are as follows: liver, 5.4 d^{-1}; kidneys, 0.94 d^{-1}; pancreas, 0.42 d^{-1}; spleen, 0.45 d^{-1}; testes, 0.1 d^{-1}; ovaries, 0.033 d^{-1}. The transfer rate from blood to bromine's Other was reduced to 192.66 d^{-1} to leave the total outflow rate from blood unchanged. A removal halftime to blood of 15 d^{-1} was assigned to each of the added compartments. For an arsenic isotope produced in a compartment not contained in the characteristic model for arsenic, the isotope

was assumed to transfer to the central blood compartment of the characteristic model for arsenic at the rate 1000 d^{-1} if produced in a blood compartment and 0.6 d^{-1} if produced in a tissue compartment, and to follow the characteristic model for arsenic thereafter.

Table 20.3. Transfer coefficients (d^{-1}) in the biokinetic model for systemic selenium.

From	To	Transfer coefficient (d^{-1})
Plasma	Liver	1.2
Plasma	Kidneys	0.6
Plasma	Pancreas	0.08
Plasma	Spleen	0.11
Plasma	Testes	0.04
Plasma	Ovaries	0.013
Plasma	Other 1	5.2
Plasma	Other 2	0.5
Plasma	Urinary bladder content	1.0
Plasma	Right colon content	0.4
Plasma	Trabecular bone surface	0.2
Plasma	Cortical bone surface	0.2
Plasma	Red blood cells	0.5
Liver	Plasma	0.08
Kidneys	Plasma	0.08
Spleen	Plasma	0.08
Pancreas	Plasma	0.08
Testes	Plasma	0.08
Ovaries	Plasma	0.08
Other 1	Plasma	0.08
Other 2	Plasma	0.005
Red blood cells	Plasma	0.035
Trabecular bone surface	Plasma	0.015
Cortical bone surface	Plasma	0.015

20.3. Individual monitoring

20.3.1. ^{75}Se

(392) Measurements of ^{75}Se may be performed by *in vivo* whole-body measurement technique and by gamma measurement in urine.

Table 20.4. Monitoring techniques for ^{75}Se.

Isotope	Monitoring Technique	Method of Measurement	Typical Detection Limit
^{75}Se	Urine Bioassay	γ-ray spectrometry[a]	1.4 Bq L^{-1}
^{75}Se	Whole-body measurement	γ-ray spectrometry[a]	60 Bq

[a] Measurement system comprised of Germanium Detectors
[b] Counting time of 20 minutes

20.4. Dosimetric data for selenium

Table 20.5. Committed effective dose coefficients (Sv Bq^{-1}) for the inhalation or ingestion of ^{75}Se and ^{79}Se compounds.

Inhaled particulate materials (5 µm AMAD aerosols)	Effective dose coefficients (Sv Bq^{-1})	
	^{75}Se	^{79}Se
Type F, Selenium dioxide, selenious acid, elemental selenium	1.8E-09	1.4E-09
Type M, default	8.9E-10	9.7E-10
Type S	9.1E-10	7.4E-09
Ingested materials		
Selenide and elemental selenium	3.1E-10	1.2E-10
All other forms	2.5E-09	1.9E-09

AMAD, activity median aerodynamic diameter

Table 20.6. Dose per activity content of ^{75}Se in total body and in daily excretion of urine (Sv Bq^{-1}); 5µm activity median aerodynamic diameter aerosols inhaled by a reference worker at light work.

Time after intake (d)	Type F		Type M		Type S	
	Total body	Urine	Total body	Urine	Total body	Urine
1	3.0E-09	3.4E-08	1.5E-09	9.0E-08	1.5E-09	1.9E-06
2	3.4E-09	2.1E-07	2.4E-09	4.0E-07	2.8E-09	7.6E-06
3	3.7E-09	4.6E-07	4.1E-09	1.0E-06	5.9E-09	2.0E-05
4	3.8E-09	5.5E-07	5.5E-09	1.3E-06	1.0E-08	2.6E-05
5	3.9E-09	5.7E-07	6.2E-09	1.3E-06	1.3E-08	2.7E-05
6	3.9E-09	5.9E-07	6.5E-09	1.4E-06	1.5E-08	2.8E-05
7	4.0E-09	6.0E-07	6.6E-09	1.4E-06	1.5E-08	2.9E-05
8	4.1E-09	6.2E-07	6.7E-09	1.4E-06	1.6E-08	2.9E-05
9	4.1E-09	6.3E-07	6.8E-09	1.5E-06	1.6E-08	3.0E-05
10	4.2E-09	6.4E-07	6.9E-09	1.5E-06	1.6E-08	3.1E-05
15	4.5E-09	7.2E-07	7.4E-09	1.6E-06	1.7E-08	3.4E-05
30	5.6E-09	9.8E-07	9.0E-09	2.2E-06	2.0E-08	4.6E-05
45	6.8E-09	1.3E-06	1.1E-08	2.8E-06	2.2E-08	5.9E-05
60	8.2E-09	1.7E-06	1.3E-08	3.5E-06	2.5E-08	7.6E-05
90	1.2E-08	2.8E-06	1.8E-08	5.4E-06	3.2E-08	1.2E-04
180	3.1E-08	9.9E-06	4.5E-08	1.6E-05	6.4E-08	3.3E-04
365	1.8E-07	7.3E-05	2.7E-07	1.1E-04	2.5E-07	1.7E-03

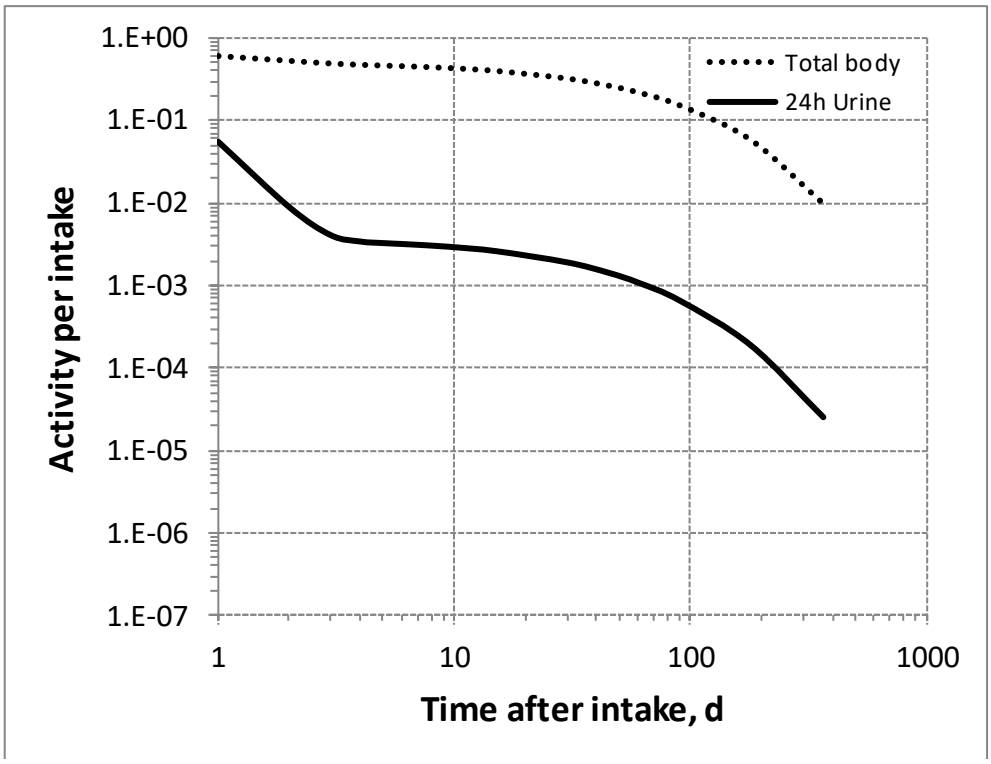

4046

4047 Fig. 20.2. Daily excretion of ^{75}Se following inhalation of 1 Bq Type F.

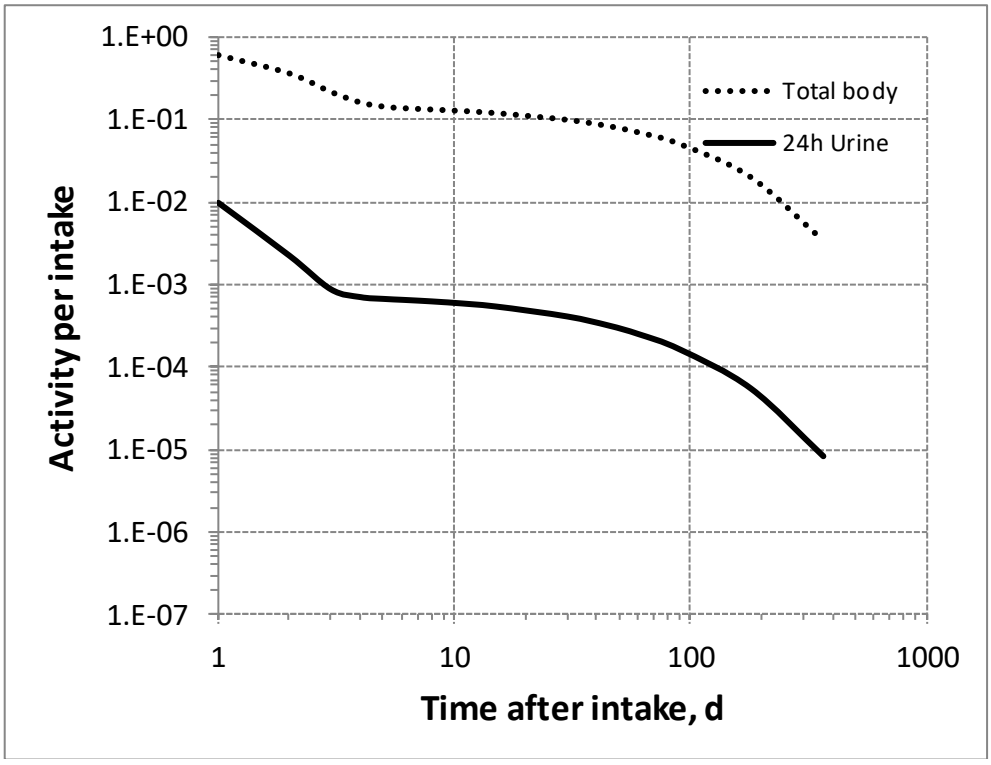

4048

4049 Fig. 20.3. Daily excretion of ^{75}Se following inhalation of 1 Bq Type M.

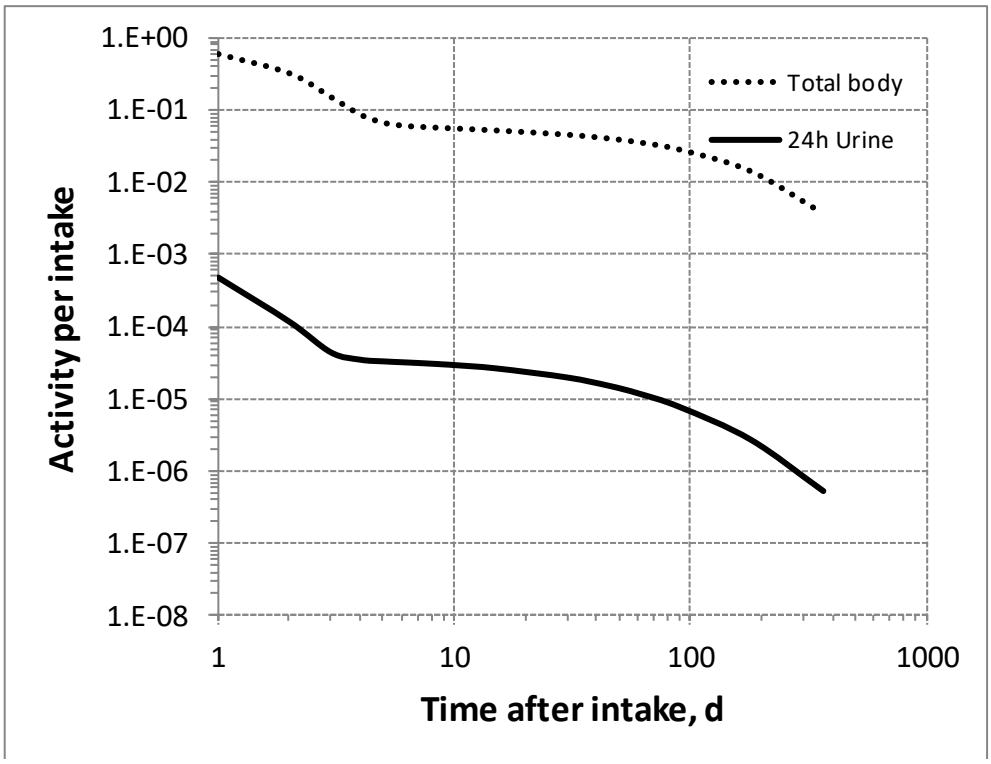

Fig. 20.4. Daily excretion of ^{75}Se following inhalation of 1 Bq Type S.

21. BROMINE (Z=35)

21.1. Isotopes

Table 21.1. Isotopes of bromine addressed in this publication.

Isotope	Physical half-life	Decay mode
^{74}Br	25.4 min	EC, B+
^{74m}Br	46 min	EC, B+
^{75}Br	96.7 min	EC, B+
^{76}Br*	16.2 h	EC, B+
^{77}Br	57.036 h	EC, B+
^{80}Br	17.68 min	B-, EC, B+
^{80m}Br	4.4205 h	IT
^{82}Br	35.30 h	B-
^{83}Br	2.40 h	B-
^{84}Br	31.80 min	B-

EC, electron-capture decay; B+, beta-plus decay; B-, beta-minus decay; IT, isomeric transition decay.
*Dose coefficients and bioassay data for this radionuclide are given in the printed copy of this publication.
Data for other radionuclides listed in this table are given in the online electronic files on the ICRP website.

21.2. Routes of Intake

21.2.1. Inhalation

(393) For bromine, default parameter values were adopted for the absorption to blood from the respiratory tract (ICRP, 2015). For bromine, and the other halogens, intakes could be in both particulate and gas and vapour forms, and it is therefore assumed that inhaled bromine is 50% particulate and 50% gas/vapour in the absence of information (ICRP, 2002b). Absorption parameter values and types, and associated f_A values for gas and vapour forms of bromine are given in Table 21.2 and for particulate forms in Table 21.3. By analogy with the halogen iodine, considered in detail in *Publication 137* (ICRP, 2017), default Type F is recommended for particulate forms in the absence of specific information on which the exposure material can be assigned to an absorption type.

Table 21.2. Deposition and absorption for gas and vapour compounds of bromine.

	Percentage deposited (%)*						Absorption†	
Chemical form/origin	Total	ET_1	ET_2	BB	bb	AI	Type	Absorption from the alimentary tract, f_A‡
Unspecified	100	0	20	10	20	50	F	1.0

ET_1, anterior nasal passage; ET_2, posterior nasal passage, pharynx and larynx; BB, bronchial; bb, bronchiolar; AI, alveolar-interstitial.
*Percentage deposited refers to how much of the material in the inhaled air remains in the body after exhalation. Almost all inhaled gas molecules contact airway surfaces, but usually return to the air unless they dissolve in, or react with, the surface lining. The default distribution between regions is assumed: 20% ET_2, 10% BB, 20% bb, and 50% AI.
†It is assumed that the bound state can be neglected for bromine (i.e. $f_b = 0$).
‡For inhaled material deposited in the respiratory tract and subsequently cleared by particle transport to the alimentary tract, the default f_A values for inhaled materials are applied [i.e. the product of f_r for the absorption type (or specific value where given) and the f_A value for ingested soluble forms of bromine (1)].

Table 21.3. Absorption parameter values for inhaled and ingested bromine.

Inhaled particulate materials	Absorption parameter values* f_r	s_r (d^{-1})	s_s (d^{-1})	Absorption from the alimentary tract, f_A
Default parameter values†				
Absorption type				
F‡	1	30	–	1
M	0.2	3	0.005	0.2
S	0.01	3	1×10^{-4}	0.01
Ingested materials§				
All forms				1

*It is assumed that the bound state can be neglected for bromine (i.e. $f_b = 0$). The values of s_r for Type F, M and S forms of bromine (30, 3 and 3 d^{-1} respectively) are the general default values.

†For inhaled material deposited in the respiratory tract and subsequently cleared by particle transport to the alimentary tract, the default f_A values for inhaled materials are applied [i.e. the product of f_r for the absorption type and the f_A value for ingested soluble forms of bromine (1)].

‡Default Type F is recommended for use in the absence of specific information on which the exposure material can be assigned to an absorption type (e.g. if the form is unknown, or if the form is known but there is no information available on the absorption of that form from the respiratory tract). For guidance on the use of specific information, see Section 1.1.

§Activity transferred from systemic compartments into segments of the alimentary tract is assumed to be subject to reabsorption to blood. The default absorption fraction f_A for the secreted activity is the highest value for any form of the radionuclide ($f_A = 1$).

21.2.2. Ingestion

(394) After ingestion, the bromide Br^- (Söremark, 1960a; Rauws, 1983; Food and Agriculture Organization of the United Nations, 1989) and bromate BrO_3^- (U.S. EPA, 2001) ions are rapidly and completely absorbed in the gastrointestinal tract. In *Publications 30* and *68* (ICRP, 1980, 1994a), f_1 was taken to be 1 for bromide. In this publication, a $f_A = 1$ is used for all chemical forms of bromine.

21.2.3. Systemic distribution, retention and excretion of bromine

21.2.3.1. Biokinetic data

(395) Inorganic bromide is the dominant form of bromine in the human body. The systemic kinetics of bromide closely resembles that of chloride (Reid et al., 1956; Pavelka, 2004). Ingested bromide is rapidly and nearly completely absorbed to blood and largely cleared from blood within a few minutes (Ray et al., 1952). It is distributed mainly in extracellular fluids where it replaces part of the extracellular chloride, with the molar sum of chloride and bromide remaining constant at about 110 mmol L^{-1} (Pavelka, 2004).

(396) The biological half-time of bromide in the human body is about 12 d (Söremark, 1960b), compared with an estimated half-time of 8-15 d for chloride (Ray et al., 1952). The biological half-time of bromide or chloride in the body can be reduced considerably by elevated intake of chloride and increased considerably by a salt-deficient diet.

21.2.3.2. Biokinetics of systemic bromine

(397) The systemic behaviour of bromine is assumed to be the same as that of chlorine. The relevant physiological forms of bromine and chlorine are assumed to be bromide and chloride,

respectively. The common biokinetic model for bromide and chloride is based on the assumptions of rapid removal from blood ($T_{1/2}$ = 5 min), a uniform distribution in tissues, removal of 50% of absorbed bromide or chloride from the body in 12 d, and a urinary to faecal excretion ratio of 100:1. These conditions are approximated, using a first-order recycling model, with the transfer coefficients listed in Table 21.4.

Table 21.4. Transfer coefficients in the biokinetic model for systemic bromine.

From	To	Transfer coefficient (d^{-1})
Blood	Other	200
Blood	Urinary bladder content	0.83
Blood	Right colon content	0.0083
Other	Blood	15

21.2.3.3. Treatment of progeny

(398) Progeny of bromine addressed in this publication are radioisotopes of bromine, krypton, and selenium. The model for bromine as a parent is assigned to bromine as a progeny. Krypton produced in tissues is assumed to transfer to blood with a halftime of 15 min and from blood to the environment (via exhalation) at the rate 1000 d^{-1}. Selenium produced in a tissue is assumed to transfer to blood at the rate 0.08 d^{-1} and then to follow the characteristic model for selenium.

21.3. Individual monitoring

(399) Information of detection limit for routine individual measurement is not available.

21.4. Dosimetric data for bromine

Table 21.5. Committed effective dose coefficients (Sv Bq^{-1}) for the inhalation or ingestion of ^{76}Br compounds.

	Effective dose coefficients (Sv Bq^{-1})
Inhaled gases or vapours	^{76}Br
Unspecified	3.9E-10
Inhaled particulate materials (5 μm AMAD aerosols)	
Type F, default	2.7E-10
Type M	4.6E-10
Type S	4.9E-10
Ingested materials	
All forms	4.5E-10

AMAD, activity median aerodynamic diameter

22. RUBIDIUM (Z=37)

22.1. Isotopes

Table 22.1. Isotopes of rubidium addressed in this publication.

Isotope	Physical half-life	Decay mode
^{78}Rb	17.66 min	EC, B+
^{79}Rb	22.9 min	EC, B^+
^{81}Rb	4.576 h	EC, B^+
^{81m}Rb	30.5 min	IT, B^+
^{82m}Rb	6.472 h	EC, B+
^{83}Rb*	86.2 d	EC
^{84}Rb*	32.77 d	EC, B+, B-
^{84m}Rb	20.26 m	IT
^{86}Rb*	18.642 d	B-, EC
^{87}Rb	4.923E10 y	B-
^{88}Rb	17.78 min	B-
^{89}Rb	15.15 min	B-

EC, electron-capture decay; B+, beta-plus decay; B-, beta-minus decay; IT, isomeric transition decay.
*Dose coefficients and bioassay data for this radionuclide are given in the printed copy of this publication.
Data for other radionuclides listed in this table are given in the online electronic files on the ICRP website.

22.2. Routes of Intake

22.2.1. Inhalation

(400) For rubidium, default parameter values were adopted on absorption to blood from the respiratory tract (ICRP, 2015). Absorption parameter values and types, and associated f_A values for particulate forms of rubidium are given in Table 22.2.

22.2.2. Ingestion

(401) In humans, ingested rubidium chloride is rapidly and almost completely absorbed from the gastrointestinal tract (Lloyd et al., 1973; Williams et al., 1987; Leggett and Williams, 1988). In rats, Usuda et al. (2014) observed comparable increase of serum concentration and urine excretion of rubidium 24 h after oral administration of either the acetate, bromide, carbonate, chloride or fluoride, with the highest increase from rubidium fluoride. In *Publications 30* and *68* (ICRP, 1980, 1994a), f_1 was taken as 1 for all compounds of rubidium. In the present publication, the same value $f_A = 1$ is used for all chemical forms of rubidium at the workplace.

Table 22.2. Absorption parameter values for inhaled and ingested rubidium.

	Absorption parameter values*			Absorption from the
Inhaled particulate materials	f_r	s_r (d^{-1})	s_s (d^{-1})	alimentary tract, f_A
Default parameter values†				
Absorption type				
F	1	30	–	1
M‡	0.2	3	0.005	0.2
S	0.01	3	1×10^{-4}	0.01

Ingested materials[§]	
All forms	1

[*]It is assumed that the bound state can be neglected for rubidium (i.e. $f_b = 0$). The values of s_r for Type F, M and S forms of rubidium (30, 3 and 3 d^{-1} respectively) are the general default values.
[†]For inhaled material deposited in the respiratory tract and subsequently cleared by particle transport to the alimentary tract, the default f_A values for inhaled materials are applied [i.e. the product of f_r for the absorption type and the f_A value for ingested soluble forms of rubidium (1)].
[‡]Default Type M is recommended for use in the absence of specific information on which the exposure material can be assigned to an absorption type (e.g. if the form is unknown, or if the form is known but there is no information available on the absorption of that form from the respiratory tract). For guidance on the use of specific information, see Section 1.1.
[§]Activity transferred from systemic compartments into segments of the alimentary tract is assumed to be subject to reabsorption to blood. The default absorption fraction f_A for the secreted activity is the highest value for any form of the radionuclide ($f_A = 1$).

22.2.3. Systemic distribution, retention and excretion of rubidium

22.2.3.1. Biokinetic data

(402) Rubidium (Rb) is an alkali metal and is a chemical and physiological analogue of the alkali metals potassium (K) and caesium (Cs) located, respectively, just above and below rubidium in Group IA of the periodic table. The physiological relationship of these three predominantly intracellular alkali metals has been investigated extensively. It is well established that Rb and Cs compete with K for both active and passive membrane transport across cell membranes. The rate of membrane transport generally decreases in the order K ≥ Rb > Cs, with the numerical relationship depending on the cell type and direction of transport. Typically, cell membranes show moderate discrimination between K and Rb and much greater discrimination between K and Cs (Relman, 1956; Sjodin, 1959; Kernan, 1969; Olsson et al., 1969; Sheehan and Renkin, 1972).

(403) Measurements of Rb and K concentrations in postmortem tissues and in plasma and red blood cells of living subjects indicate the following approximate distributions of these two elements in an adult male human, where values are % total-body Rb or K (shown as Rb/K): skeletal muscle 64/65, skeleton 9/9, red blood cells 6/8, liver 5/3, brain 2/3, kidneys 0.6/0.6, blood plasma 0.3/0.4, remainder 13/11 (based on Leggett and Williams, 1988; Zhu et al., 2010).

(404) The residence time of absorbed Rb in humans typically is moderately higher (~40-50%) and that of Cs is substantially higher (3-4 times) than the residence time of K (Leggett and Williams, 1986, 1988; Leggett et al., 2003).

(405) Burch et al. (1955) compared plasma clearance of simultaneously administered ^{86}Rb and ^{42}K in each of two human subjects, one a control subject and the other with congestive heart failure, over the first 2 h after intravenous injection. The clearance curves for ^{86}Rb and ^{42}K were identical in the subject with heart failure. Slightly slower clearance of ^{86}Rb than ^{42}K was observed in the control subject.

(406) Following oral administration of ^{83}Rb to four healthy adult male subjects, plasma contained an estimated 0.31% of the ingested activity at 1 d and 0.28% at 2 d (Lloyd et al., 1972, 1973). Following administration of ^{86}Rb to five adult male subjects, plasma contained 0.24-0.30% of injected ^{86}Rb (Mabille et al., 1961). Plasma concentrations of intravenously administered ^{86}Rb were measured by Burch et al. (1955) in an adult male subject over a 6-week period following injection. The plasma content remained near 0.3% of dosage from 3 to 14 d after injection, decreased to about 0.2% at three weeks, and fell to about 0.15% at four weeks.

(407) As is the case for K, over 90% of Rb in blood is contained in red blood cells by 1 d after absorption or injection. Lloyd et al. (1972, 1973) determined the ratio of the ^{83}Rb

concentration in red blood cells to that in plasma in several human subjects, some healthy and some with muscle disease, at one and two days after administration, and in one healthy male subject at 4-31 d. The ratio averaged 12 and 18 at one and two days, respectively, and 22-24 at 16-31 d. Five adult male subjects of Mabille et al. (1961) showed an average ^{86}Rb concentration ratio RBC:plasma of 24 (20-27) at 7- 14 d after injection.

(408) Ryan et al. (1985) determined the maximum uptake of ^{82}Rb in the left kidneys of two healthy subjects (after correction for rapid radioactive decay) to be 8.8% and 7.1%, respectively, of the intravenously injected amount, apparently occurring in the early minutes after administration. This suggests maximum accumulation of about 16% of administered Rb in the kidneys, which is of the same order as early uptake of radio-potassium by the kidneys (Black et al., 1955; Emery et al., 1955).

(409) Whole-body retention of radio-rubidium has been observed in a number of healthy adult humans subjects (Iinuma et al., 1967; Lloyd et al., 1973; Richmond, 1980). Retention can be described reasonably well by a single exponential term, although a small component of short-term retention has been observed in some subjects. The biological half-time based on a single-exponential fit typically is the range 1-2 months, with a central value of about 45 d.

(410) Love et al. (1954) compared the distributions of stable K and ^{86}Rb in 33 tissues or fluids following intravenous administration of ^{86}Rb to dogs. The distributions were compared in terms of a 'relative Rb concentration' for individual tissues or fluids, intended to reflect the relative levels of accumulation of circulating Rb and K in these pools. The relative Rb concentration for a tissue or fluid was defined as the average ratio A:B for days 1, 3, and 7 post injection, where A is the concentration ratio of ^{86}Rb to K in the tissue or fluid sample and B is the analogous ratio for simultaneously sampled blood plasma. The relative rubidium ratio was in the range 1.02-1.91 with mean 1.4 ± 0.23 (SD) for 29 of the 33 pools and less than 1.0 for the other 4 (urine, 0.66; femur, 0.56; brain, 0.55; cerebrospinal fluid, 0.55).

22.2.3.2. Biokinetic model for systemic rubidium

(411) A relatively detailed biokinetic model for systemic Rb (similar to the model for K described in the Section 9.2.3 on K in this publication) was proposed by Leggett and Williams (1988). The model was built around a blood flow model depicting the distribution of cardiac output to 12 tissue compartments. Additional compartments were added to address transfer of Rb between plasma and red blood cells and between systemic pools and gastrointestinal content. Three excretion pathways were addressed: urinary loss via the kidneys, faecal loss via the intestines, and loss in sweat via skin. Movement of Rb was depicted as a system of first-order processes. The transfer rate from plasma into a tissue T was estimated as the product of the plasma flow rate to that tissue (that is, the fraction of cardiac output received by the tissue, times 1766 plasma volumes per day as a reference value for cardiac output, and a tissue-specific extraction fraction, E_T). The transfer rate from tissue T to plasma was estimated from the relative contents of Rb in plasma and tissue T at equilibrium. The equilibrium distribution of Rb was based mainly on autopsy data and typical concentrations of Rb in plasma and red blood cells. Transfer rates between plasma and red blood cells and between systemic compartments and gastrointestinal contents were based on empirical data. Model predictions of the blood clearance, uptake and loss by systemic tissues, total-body retention, and path-specific excretion rates of Rb were shown to be consistent with observations for human subjects.

(412) The biokinetic model for systemic Rb used in this publication is a simplification of the model of Leggett and Williams (1986). The structure of the simplified model (Fig. 22.1) is more consistent with the structures of other systemic models applied in this publication series. That is, the model depicts a central blood compartment (plasma) in exchange with a set of peripheral

tissue compartments representing relatively important systemic repositories of Rb. The transfer coefficients of the simplified model (Table 22.3) were set for reasonable consistency with the original model regarding retention in the total body and in individual tissues depicted explicitly in both models.

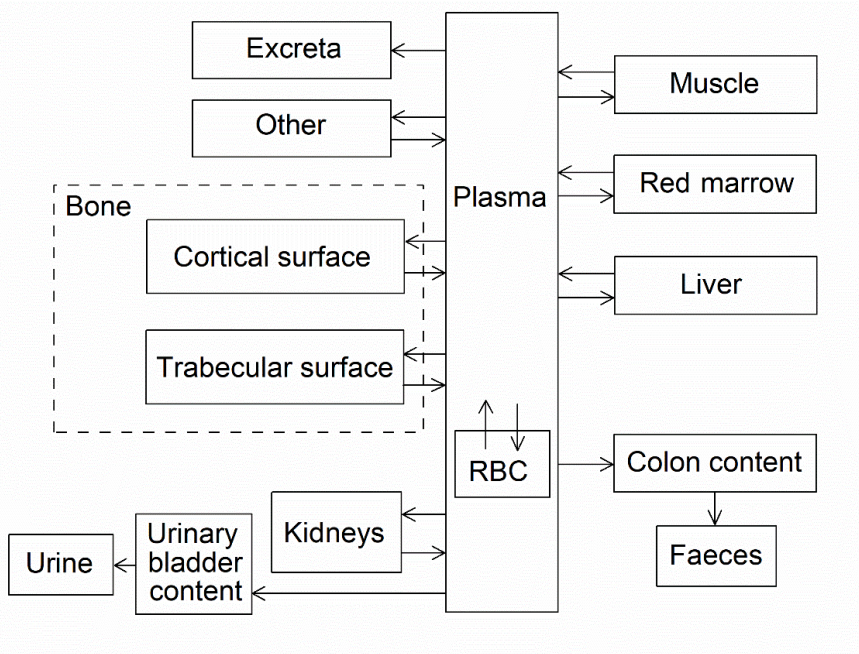

Fig. 22.1. Structure of the biokinetic model for systemic rubidium.

22.2.3.3. Treatment of progeny

(413) Progeny of rubidium addressed in this publication are radioisotopes of rubidium, krypton, and strontium. The model for rubidium as a parent is applied to rubidium as a progeny of rubidium. Krypton produced in a tissue compartment is assumed to transfer to blood with a halftime of 15 min and to be removed from blood to the environment (exhaled) at the rate 1000 d^{-1}. For application to strontium as a progeny of rubidium the characteristic model for strontium (ICRP, 2016) was modified to address explicitly each of the tissues addressed in the model for rubidium (see Annex B). The following transfer coefficients from compartments of the rubidium model to the central blood compartment of the strontium model were added to the characteristic model for strontium: red blood cells, 1000 d^{-1}; kidneys, 0.116 d^{-1}; liver, 0.116 d^{-1}; muscle, 0.116 d^{-1}; red marrow, 0.116 d^{-1}; rubidium's Other, 2.5 d^{-1}. The following transfer coefficients from blood were also added to the strontium model: kidneys, 0.00766 d^{-1}; liver, 0.0445 d^{-1}, muscle, 0.716 d^{-1}; red marrow, 0.0289 d^{-1}. The transfer coefficient from blood to the intermediate-term soft-tissue compartments of the strontium model was reduced from 1.5 d^{-1} to 0.703 d^{-1} to leave the total outflow rate of strontium from blood at 15 d^{-1}.

Table 22.3. Transfer coefficients in the biokinetic model for systemic rubidium.

From	To	Transfer coefficient (d^{-1})
Plasma	RBC	6
Plasma	Kidneys	240
Plasma	Liver	153
Plasma	Muscle	255
Plasma	Trabecular bone surface	8.4
Plasma	Cortical bone surface	5.6
Plasma	Red marrow	14

Plasma	Other	400
Plasma	Urinary bladder content	3.9
Plasma	Right colon content	1.2
Plasma	Excreta	0.1
RBC	Plasma	0.35
Kidneys	Plasma	120
Liver	Plasma	9.98
Muscle	Plasma	1.14
Trabecular bone surface	Plasma	1.68
Cortical bone surface	Plasma	1.68
Red marrow	Plasma	1.68
Other	Plasma	7.3

22.3. Individual monitoring

22.3.1. ^{83}Rb

(414) Measurements of ^{83}Rb may be performed by in vivo whole-body measurement technique and by gamma measurement in urine.

Table 22.4. Monitoring techniques for ^{83}Rb.

Isotope	Monitoring Technique	Method of Measurement	Typical Detection Limit
^{83}Rb	Urine Bioassay	γ-ray spectrometry[a]	2.1 Bq L^{-1}
^{83}Rb	Whole-body measurement	γ-ray spectrometry[ab]	55 Bq

[a] Measurement system comprised of Germanium Detectors
[b] Counting time of 20 minutes

22.3.2. ^{84}Rb

(415) Measurements of ^{84}Rb may be performed by *in vivo* whole-body measurement technique and by gamma measurement in urine.

Table 22.5. Monitoring techniques for ^{84}Rb.

Isotope	Monitoring Technique	Method of Measurement	Typical Detection Limit
^{84}Rb	Urine Bioassay	γ-ray spectrometry[a]	1.6 Bq L^{-1}
^{84}Rb	Whole-body monitoring	γ-ray spectrometry[ab]	33 Bq

[a] Measurement system comprised of Germanium Detectors
[b] Counting time of 20 minutes

22.3.3. ^{86}Rb

(416) Measurements of ^{86}Rb in urine may be used to determine intakes of the radionuclide.

Table 22.6. Monitoring techniques for ^{86}Rb.

Isotope	Monitoring Technique	Method of Measurement	Typical Detection Limit
^{86}Ru	Urine Bioassay	γ-ray spectrometry[a]	4 Bq L^{-1}

[a] Measurement system comprised of Germanium Detectors

22.4. Dosimetric data for rubidium

Table 22.7. Committed effective dose coefficients (Sv Bq^{-1}) for the inhalation or ingestion of ^{83}Rb, ^{84}Rb and ^{86}Rb compounds.

Inhaled particulate materials (5 µm AMAD aerosols)	Effective dose coefficients (Sv Bq^{-1})		
	^{83}Rb	^{84}Rb	^{86}Rb
Type F, — NB: Type F should not be assumed without evidence	1.1E-09	1.6E-09	1.2E-09
Type M, default	7.3E-10	1.3E-09	1.6E-09
Type S	8.1E-10	1.3E-09	1.8E-09
Ingested materials			
All forms	1.6E-09	2.4E-09	1.7E-09

AMAD, activity median aerodynamic diameter

Table 22.8. Dose per activity content of ^{83}Rb in total body and in daily excretion of urine (Sv Bq^{-1}); 5µm activity median aerodynamic diameter aerosols inhaled by a reference worker at light work.

Time after intake (d)	Type F		Type M		Type S	
	Total body	Urine	Total body	Urine	Total body	Urine
1	1.7E-09	1.1E-07	1.2E-09	4.0E-07	1.3E-09	9.2E-06
2	1.7E-09	1.4E-07	1.9E-09	4.2E-07	2.5E-09	9.3E-06
3	1.8E-09	1.5E-07	2.9E-09	4.6E-07	5.2E-09	1.0E-05
4	1.8E-09	1.5E-07	3.8E-09	4.7E-07	9.1E-09	1.1E-05
5	1.9E-09	1.6E-07	4.1E-09	4.9E-07	1.2E-08	1.1E-05
6	1.9E-09	1.6E-07	4.3E-09	5.0E-07	1.3E-08	1.1E-05
7	2.0E-09	1.7E-07	4.4E-09	5.1E-07	1.3E-08	1.1E-05
8	2.0E-09	1.7E-07	4.5E-09	5.2E-07	1.4E-08	1.2E-05
9	2.1E-09	1.8E-07	4.7E-09	5.3E-07	1.4E-08	1.2E-05
10	2.1E-09	1.8E-07	4.8E-09	5.4E-07	1.4E-08	1.2E-05
15	2.4E-09	2.0E-07	5.3E-09	6.1E-07	1.6E-08	1.4E-05
30	3.4E-09	2.9E-07	7.1E-09	8.4E-07	1.9E-08	1.9E-05
45	4.8E-09	4.1E-07	9.6E-09	1.2E-06	2.2E-08	2.6E-05
60	6.9E-09	5.9E-07	1.3E-08	1.6E-06	2.6E-08	3.7E-05
90	1.4E-08	1.2E-06	2.3E-08	3.0E-06	3.5E-08	7.0E-05
180	1.2E-07	9.9E-06	1.1E-07	1.8E-05	8.8E-08	4.0E-04
365	9.1E-06	7.8E-04	2.1E-06	4.4E-04	5.2E-07	5.1E-03

Table 22.9. Dose per activity content of ^{84}Rb in total body and in daily excretion of urine (Sv Bq^{-1}); 5µm activity median aerodynamic diameter aerosols inhaled by a reference worker at light work.

	Type F		Type M		Type S	
Time after intake (d)	Total body	Urine	Total body	Urine	Total body	Urine
1	2.4E-09	1.6E-07	2.1E-09	7.2E-07	2.2E-09	1.5E-05
2	2.6E-09	2.0E-07	3.4E-09	7.6E-07	4.1E-09	1.6E-05
3	2.7E-09	2.2E-07	5.4E-09	8.4E-07	8.9E-09	1.7E-05
4	2.8E-09	2.3E-07	7.0E-09	8.8E-07	1.6E-08	1.8E-05
5	2.9E-09	2.4E-07	7.8E-09	9.1E-07	2.1E-08	1.9E-05
6	3.0E-09	2.5E-07	8.2E-09	9.5E-07	2.3E-08	2.0E-05
7	3.1E-09	2.6E-07	8.6E-09	9.8E-07	2.4E-08	2.0E-05
8	3.2E-09	2.7E-07	8.9E-09	1.0E-06	2.5E-08	2.1E-05
9	3.3E-09	2.8E-07	9.2E-09	1.1E-06	2.6E-08	2.2E-05
10	3.4E-09	2.9E-07	9.5E-09	1.1E-06	2.7E-08	2.3E-05
15	4.1E-09	3.5E-07	1.1E-08	1.3E-06	3.1E-08	2.7E-05
30	7.2E-09	6.1E-07	1.9E-08	2.2E-06	4.5E-08	4.6E-05
45	1.2E-08	1.1E-06	3.0E-08	3.7E-06	6.5E-08	7.8E-05
60	2.2E-08	1.8E-06	4.9E-08	6.2E-06	9.3E-08	1.3E-04
90	6.5E-08	5.6E-06	1.3E-07	1.7E-05	1.9E-07	3.7E-04
180	1.8E-06	1.5E-04	2.1E-06	3.3E-04	1.5E-06	6.9E-03
365	1.6E-03	1.3E-01	4.4E-04	9.3E-02	1.0E-04	1.0E+00

Table 22.10. Dose per activity content of ^{86}Rb in daily excretion of urine (Sv Bq^{-1}); 5µm activity median aerodynamic diameter aerosols inhaled by a reference worker at light work.

Time after	Type F	Type M	Type S
intake (d)	Urine	Urine	Urine
1	1.2E-07	9.0E-07	2.1E-05
2	1.6E-07	9.7E-07	2.2E-05
3	1.7E-07	1.1E-06	2.5E-05
4	1.8E-07	1.2E-06	2.6E-05
5	1.9E-07	1.2E-06	2.8E-05
6	2.0E-07	1.3E-06	2.9E-05
7	2.2E-07	1.4E-06	3.1E-05
8	2.3E-07	1.4E-06	3.3E-05
9	2.4E-07	1.5E-06	3.4E-05
10	2.5E-07	1.6E-06	3.6E-05
15	3.3E-07	2.1E-06	4.7E-05
30	7.3E-07	4.4E-06	1.0E-04
45	1.6E-06	9.4E-06	2.2E-04
60	3.5E-06	2.0E-05	4.7E-04
90	1.7E-05	9.0E-05	2.1E-03
180	2.0E-03	7.4E-03	1.7E-01
365	N/A	N/A	N/A

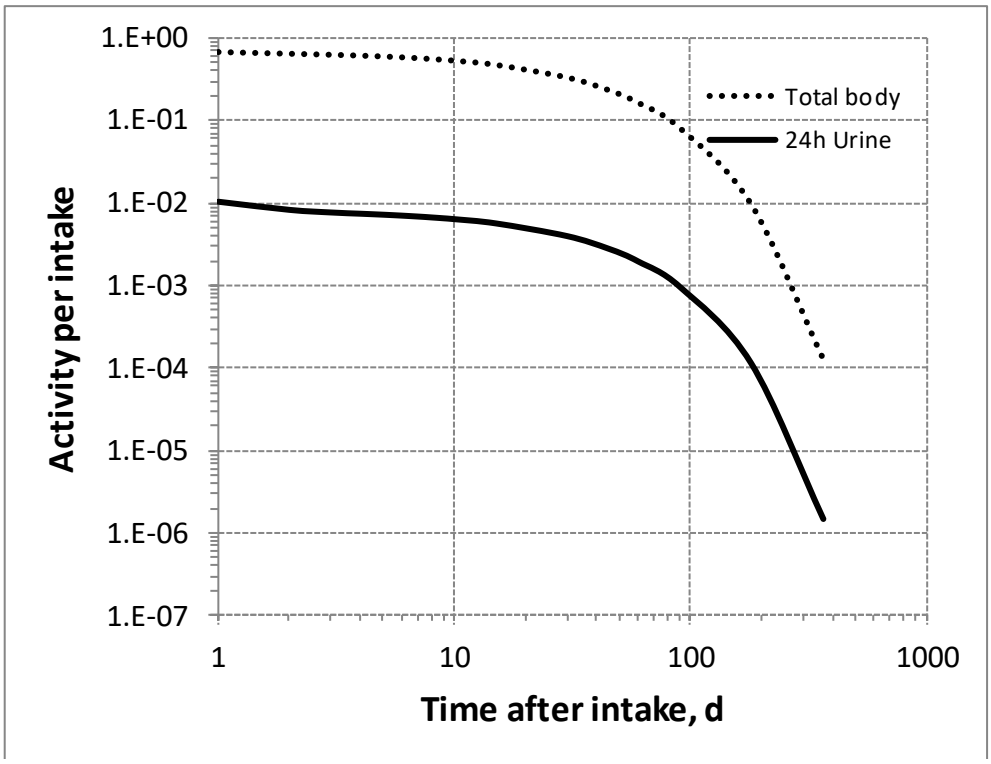

4298

4299 Fig. 22.2. Daily excretion of ^{83}Rb following inhalation of 1 Bq Type F.

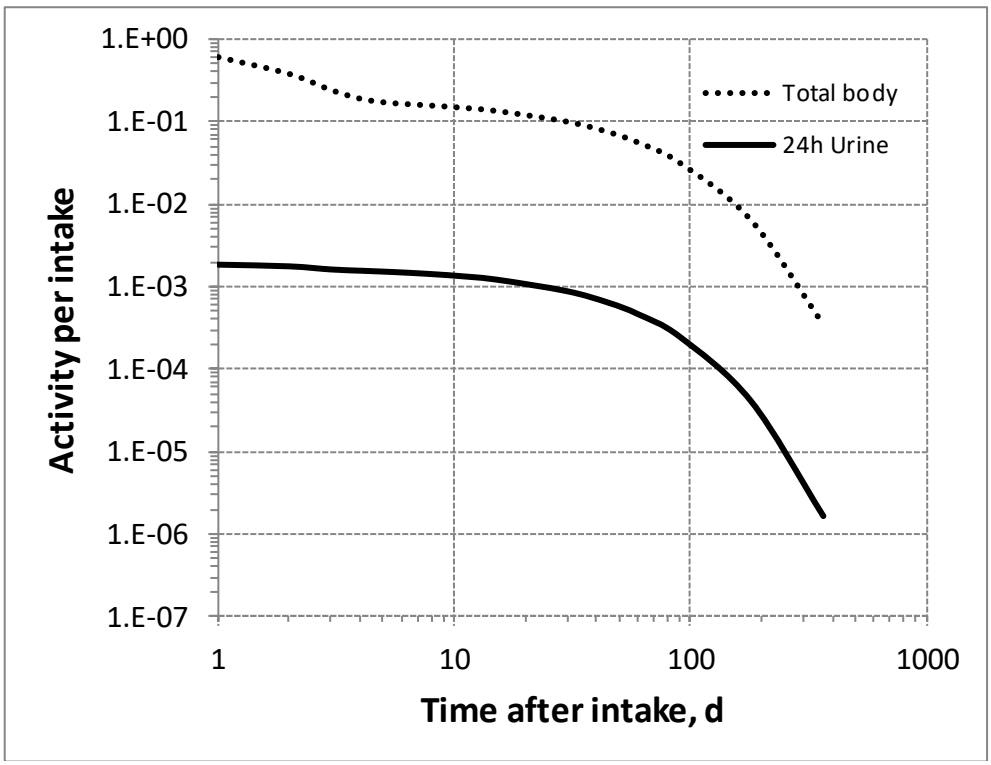

4300

4301 Fig. 22.3. Daily excretion of ^{83}Rb following inhalation of 1 Bq Type M.

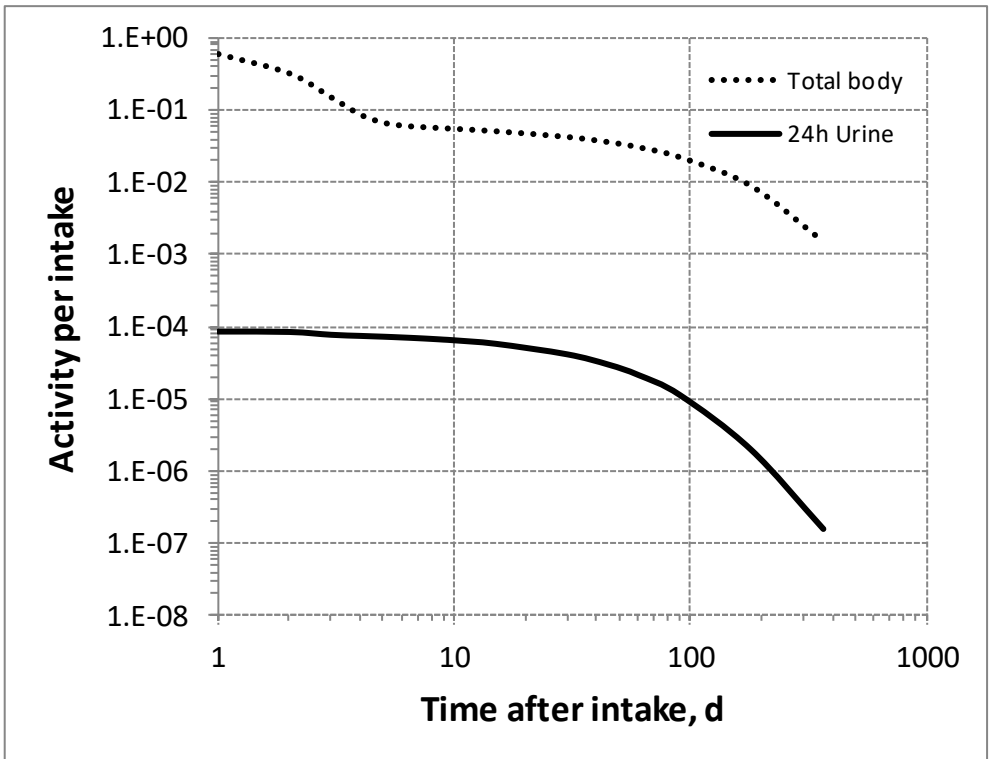

4302

4303 Fig. 22.4. Daily excretion of ^{83}Rb following inhalation of 1 Bq Type S.

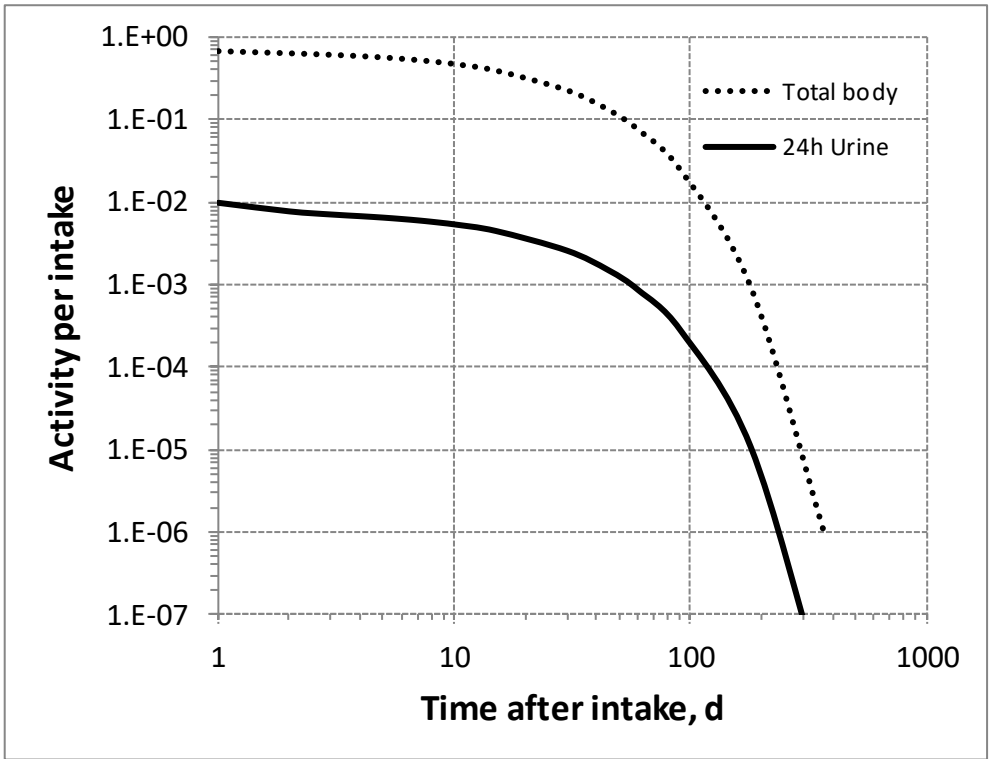

4304

4305 Fig. 22.5. Daily excretion of ^{84}Rb following inhalation of 1 Bq Type F.

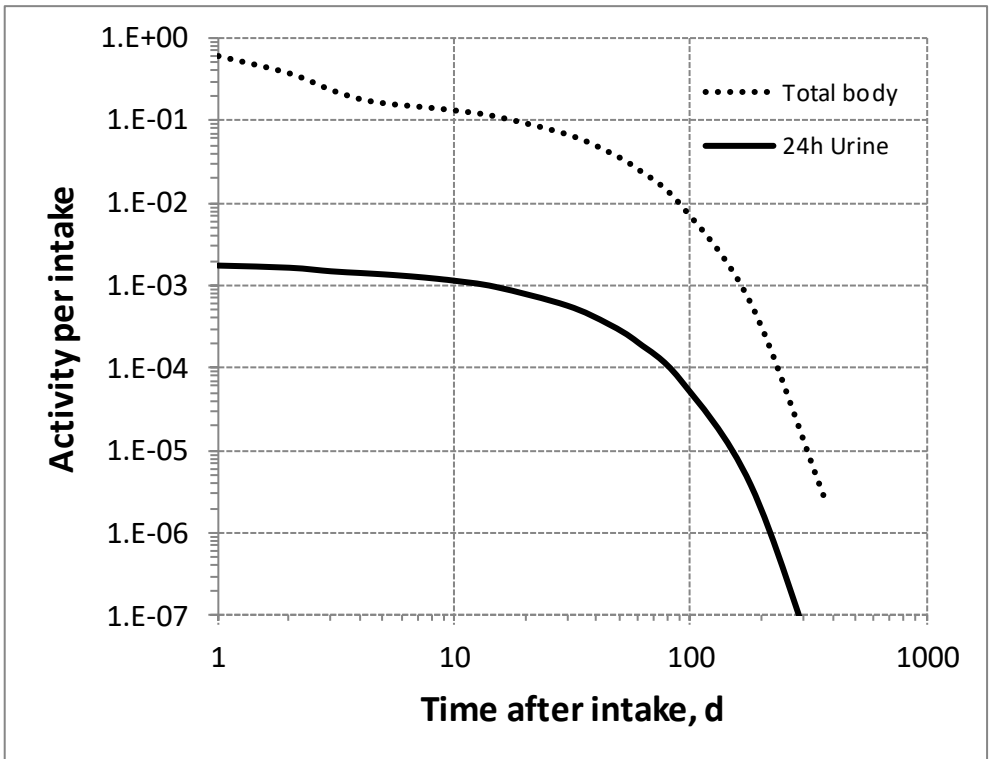

4306

4307 Fig. 22.6. Daily excretion of ^{84}Rb following inhalation of 1 Bq Type M.

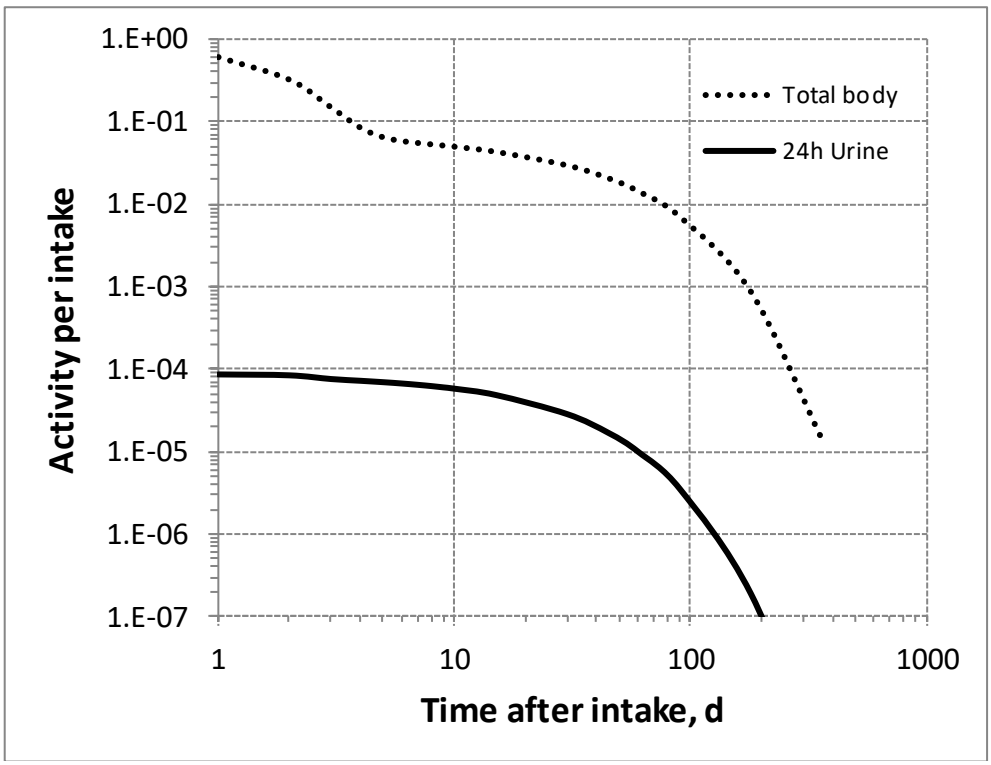

4308

4309 Fig. 22.7. Daily excretion of ^{84}Rb following inhalation of 1 Bq Type S.

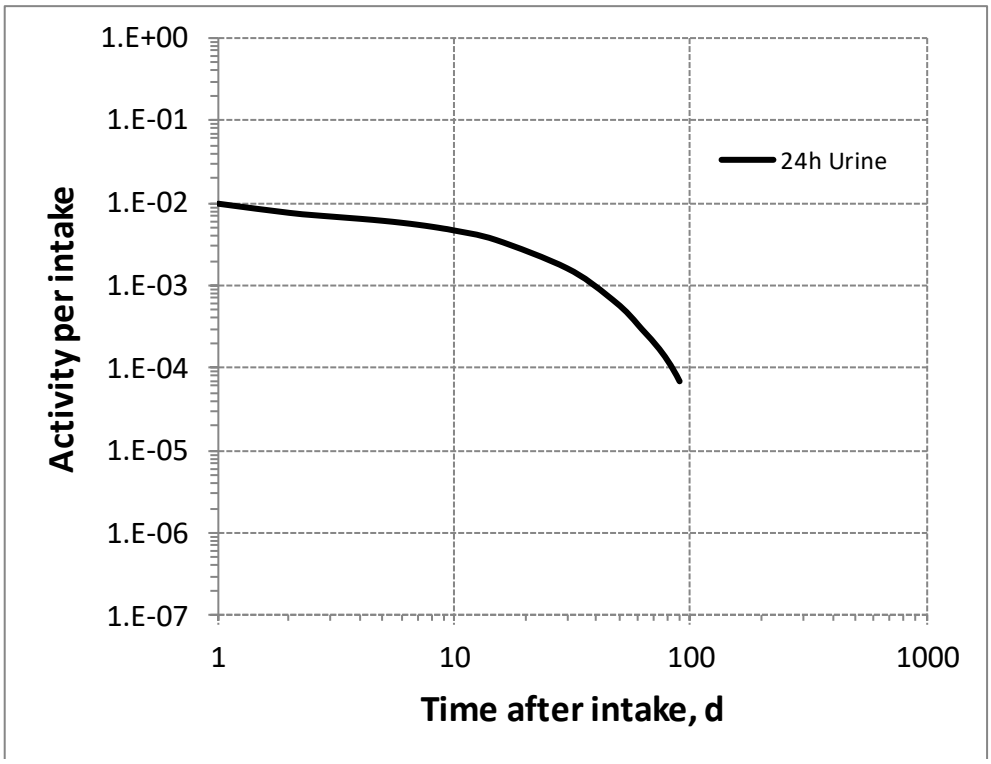

4310

4311 Fig. 22.8. Daily excretion of ^{86}Rb following inhalation of 1 Bq Type F.

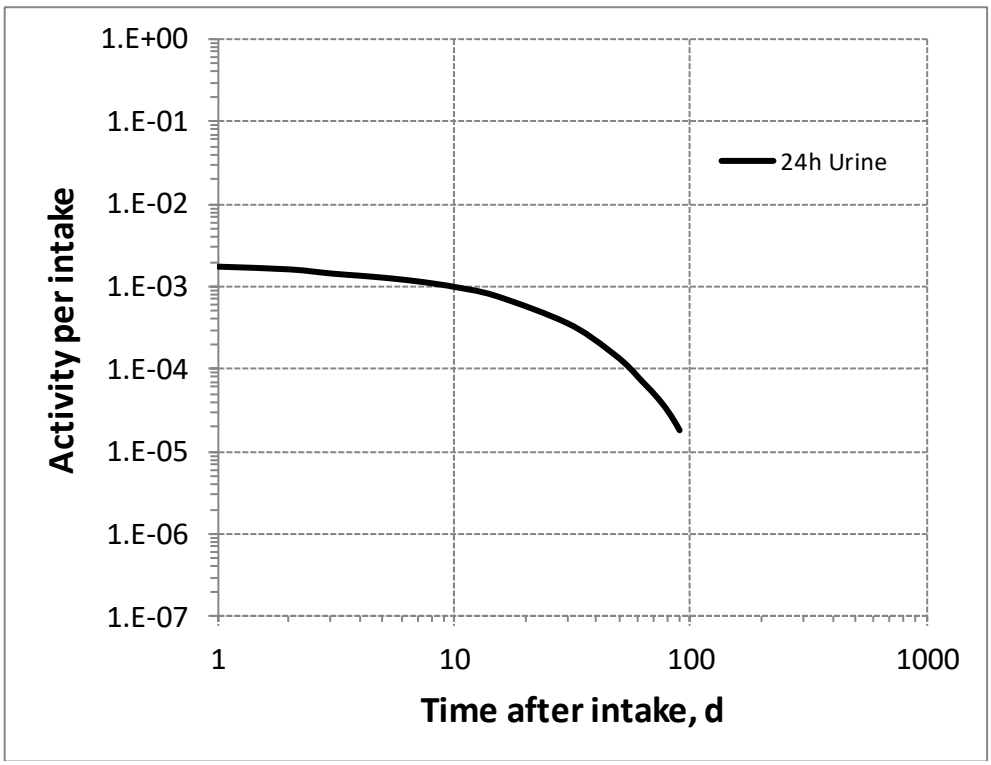

4312

4313 Fig. 22.9. Daily excretion of ^{86}Rb following inhalation of 1 Bq Type M.

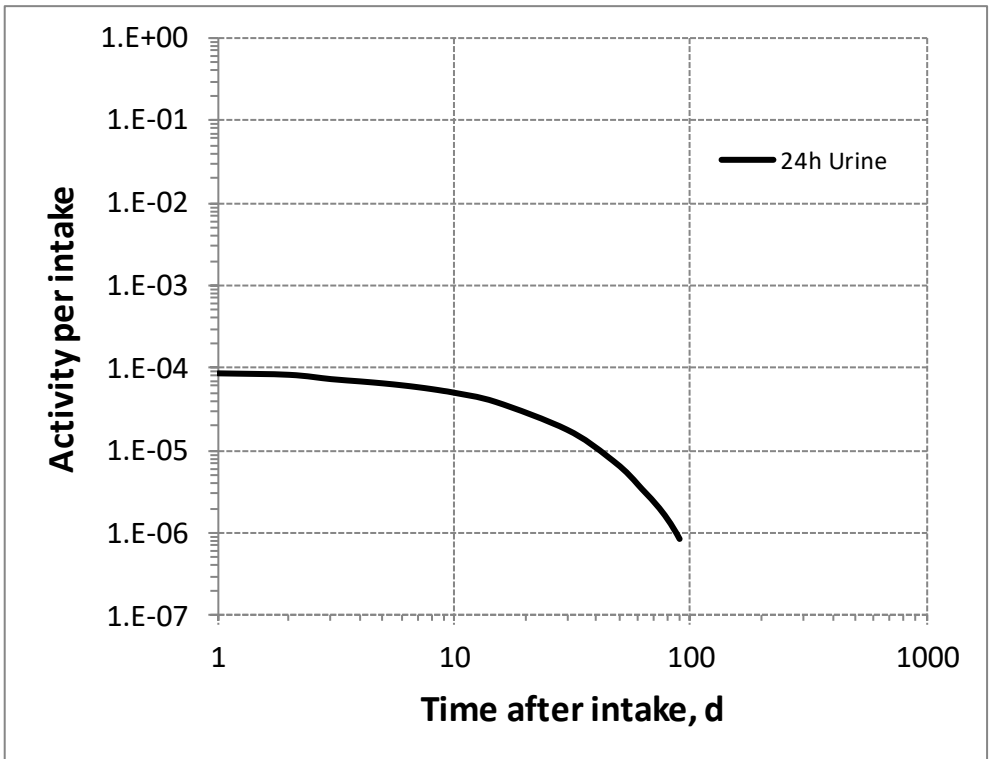

Fig. 22.10. Daily excretion of ^{86}Rb following inhalation of 1 Bq Type S.

23. RHODIUM (Z=45)

23.1. Isotopes

Table 23.1. Isotopes of rhodium addressed in this publication.

Isotope	Physical half-life	Decay mode
^{97}Rh	30.7 min	EC, B+
^{97m}Rh	46.2 min	EC, B+, IT
^{99}Rh	16.1 d	EC, B+
^{99m}Rh	4.7 h	EC, B+
^{100}Rh	20.8 h	EC, B+
^{101}Rh*	3.3 y	EC
^{101m}Rh	4.34 d	EC, IT
^{102}Rh	207 d	EC, B+, B-
^{102m}Rh	3.742 y	EC, B+, IT
^{103m}Rh	56.114 min	IT
^{105}Rh	35.36 h	B-
^{106m}Rh	131 min	B-
^{107}Rh	21.7 min	B-

EC, electron-capture decay; B+, beta-plus decay; B-, beta-minus decay; IT, isomeric transition decay.
*Dose coefficients and bioassay data for this radionuclide are given in the printed copy of this publication.
Data for other radionuclides listed in this table are given in the online electronic files on the ICRP website.

23.2. Routes of Intake

23.2.1. Inhalation

(417) For rhodium, default parameter values were adopted on absorption to blood from the respiratory tract (ICRP, 2015). Absorption parameter values and types, and associated f_A values for particulate forms of rhodium are given in Table 23.2.

23.2.2. Ingestion

(418) There appears to be no information concerning the uptake of rhodium from the gastrointestinal tract. With an in vitro assay, Colombo et al. (2008) have estimated the dissolution of rhodium to be about 66% from road dust, but less than 0.04% from hydroxide samples and 0.7% from an automobile catalyst powder. Chemically the element resembles ruthenium (Partington, 1954) and f_1 was therefore taken to be 0.05 for all its compounds in *Publications 30* and *68* (ICRP, 1980, 1994a). The value of f_A = 0.05 for ruthenium was confirmed in OIR Part 3 (ICRP, 2017). In this publication, the default assumption is f_A = 0.05 for all forms of rhodium at the workplace.

Table 23.2. Absorption parameter values for inhaled and ingested rhodium.

	Absorption parameter values*			Absorption from the
Inhaled particulate materials	f_r	s_r (d^{-1})	s_s (d^{-1})	alimentary tract, f_A
Default parameter values†				
Absorption type				
F	1	30	–	0.05
M‡	0.2	3	0.005	0.01

S	0.01	3	1×10^{-4}	5×10^{-4}
Ingested materials[§]				
All forms				0.05

[*]It is assumed that the bound state can be neglected for rhodium (i.e. $f_b = 0$). The values of s_r for Type F, M and S forms of rhodium (30, 3 and 3 d^{-1} respectively) are the general default values.
[†]For inhaled material deposited in the respiratory tract and subsequently cleared by particle transport to the alimentary tract, the default f_A values for inhaled materials are applied [i.e. the product of f_r for the absorption type and the f_A value for ingested soluble forms of rhodium (0.05)].
[‡]Default Type M is recommended for use in the absence of specific information on which the exposure material can be assigned to an absorption type (e.g. if the form is unknown, or if the form is known but there is no information available on the absorption of that form from the respiratory tract). For guidance on the use of specific information, see Section 1.1.
[§]Activity transferred from systemic compartments into segments of the alimentary tract is assumed to be subject to reabsorption to blood. The default absorption fraction f_A for the secreted activity is the highest value for any form of the radionuclide ($f_A = 0.05$).

23.2.3. Systemic distribution, retention and excretion of rhodium

23.2.3.1. Biokinetic data

(419) Durbin et al. (1957) summarised data on the behaviour of rhodium in rats during the first few days after administration of carrier-free ^{105}Rh by various routes. At 4 d after oral administration, activity was measurable only in the kidneys, which contained 0.04% of the administered amount. Excretion after intramuscular administration was mainly in urine during the first few hours. At 18 d after intramuscular injection about 46% had been eliminated in urine and 28% in faeces. Throughout the study the highest concentrations of activity were found in kidney, spleen, lymph glands, and skin. At 18 d after injection these tissues contained 1.1, 0.50, 0.35, and 0.33% of the injected amount, respectively. Distribution and excretion at these times resembled that observed for the chemically similar element ruthenium.

(420) Erck et al. (1976) studied the biokinetics of Rh in tumour-bearing mice after single therapeutic doses of Rh(II) acetate. The primary organ of deposition of rhodium was the liver. No measurable quantity was found in the brain. During the first 24 h about 5% of the administered rhodium was eliminated in urine.

23.2.3.2. Biokinetic model for systemic rhodium

(421) The biokinetic model for ruthenium described in *Publication 134* (2016) is applied in this publication to rhodium. The model structure is shown in Fig.23.1. Transfer coefficients are listed in Table 23.3.

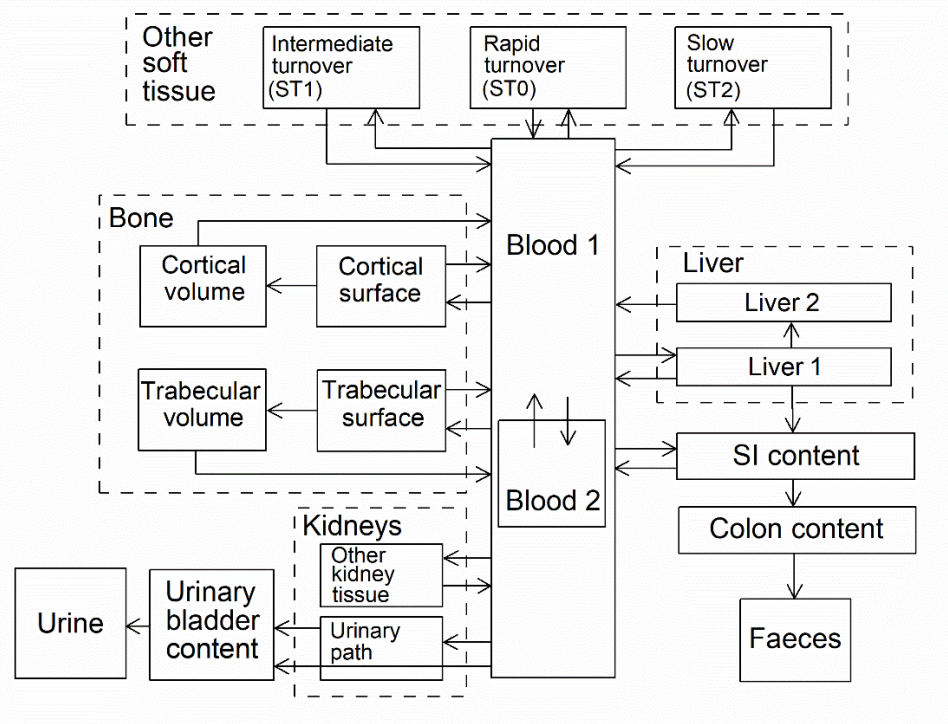

Fig. 23.1. Structure of the biokinetic model for systemic rhodium.

23.2.3.3. Treatment of progeny

(422) Progeny of rhodium addressed in this publication are isotopes of rhodium, ruthenium, and technetium. The common model for rhodium and ruthenium as parents applied in this publication series is applied to isotopes of these two elements as progeny of rhodium. The model for technetium as a progeny of ruthenium applied in Part 3 of this publication series (ICRP, 2017) is applied to technetium as a progeny of rhodium.

Table 23.3. Transfer coefficients in the biokinetic model for systemic rhodium.

From	To	Transfer coefficient (d^{-1})
Blood 1	Small intestine contents	3.0
Blood 1	Urinary bladder contents	17
Blood 1	Liver 1	12
Blood 1	Kidney urinary path	7.76
Blood 1	Other kidney tissue	0.24
Blood 1	Blood 2	27
Blood 1	ST0	15
Blood 1	ST1	5.0
Blood 1	ST2	5.0
Blood 1	Cortical bone surface	2.0
Blood 1	Trabecular bone surface	6.0
Blood 2	Blood 1	0.6931
Liver 1	Blood 1	0.09704
Liver 1	Small intestine contents	0.03466
Liver 1	Liver 2	0.006931
Liver 2	Blood 1	0.003798
Kidney urinary path	Urinary bladder contents	0.1386

Other kidney tissue	Blood 1	0.003798
ST0	Blood 1	0.09902
ST1	Blood 1	0.0231
ST2	Blood 1	0.0009495
Cortical bone surface	Blood 1	0.07922
Trabecular bone surface	Blood 1	0.07922
Cortical bone surface	Cortical bone volume	0.0198
Trabecular bone surface	Trabecular bone volume	0.0198
Cortical bone volume	Blood 1	0.0000821
Trabecular bone volume	Blood 1	0.000493

23.3. Individual monitoring

(423) Information of detection limit for routine individual measurement is not available.

23.4. Dosimetric data for rhodium

Table 23.4 Committed effective dose coefficients (Sv Bq^{-1}) for the inhalation or ingestion of ^{101}Rh compounds.

Inhaled particulate materials (5 µm AMAD aerosols)	Effective dose coefficients (Sv Bq^{-1})
	^{101}Rh
Type F, — NB: Type F should not be assumed without evidence	1.3E-09
Type M, default	1.0E-09
Type S	4.0E-09
Ingested materials	
All forms	3.8E-10

AMAD, activity median aerodynamic diameter

24. PALLADIUM (Z=46)

24.1. Isotopes

Table 24.1. Isotopes of palladium addressed in this publication.

Isotope	Physical half-life	Decay mode
^{98}Pd	17.7 min	EC, B+
^{99}Pd	21.4 min	EC, B+
^{100}Pd	3.63 d	EC
^{101}Pd	8.47 h	EC, B+
^{103}Pd*	16.991 d	EC
^{107}Pd*	6.5E+6 y	B-
^{109}Pd	13.7012 h	B-
^{111}Pd	23.4 min	B-
^{112}Pd	21.03 h	B-

EC, electron-capture decay; B+, beta-plus decay; B-, beta-minus decay.
*Dose coefficients and bioassay data for this radionuclide are given in the printed copy of this publication.
Data for other radionuclides listed in this table are given in the online electronic files on the ICRP website.

24.2. Routes of Intake

24.2.1. Inhalation

(424) For palladium, default parameter values were adopted on absorption to blood from the respiratory tract (ICRP, 2015). Absorption parameter values and types, and associated f_A values for particulate forms of palladium are given in Table 24.2.

24.2.2. Ingestion

(425) The fractional absorption of palladium, administered as the chloride, from the gastrointestinal tract of adult rats is less than 5×10^{-3} (Moore Jr. et al., 1974; Moore et al., 1975). Acute toxicity data from experiments on rats indicate that the fractional absorption of palladium administered as PdO or $PdSO_4$ is even smaller than that of the chloride (Holbrook et al., 1975).

(426) In *Publications 30* and *68* (ICRP, 1981, 1994a) f_1 was taken to be 5 x 10^{-3} for all compounds of the element. In this publication the value of $f_A = 5 \times 10^{-3}$ is also used for all ingested forms of palladium.

Table 24.2. Absorption parameter values for inhaled and ingested palladium.

Inhaled particulate materials	Absorption parameter values* f_r	s_r (d^{-1})	s_s (d^{-1})	Absorption from the alimentary tract, f_A
Default parameter values†				
Absorption type				
F	1	30	–	0.005
M‡	0.2	3	0.005	0.001
S	0.01	3	1×10^{-4}	5×10^{-5}
Ingested materials§				
All forms				0.005

[*]It is assumed that the bound state can be neglected for palladium (i.e. $f_b = 0$). The values of s_r for Type F, M and S forms of palladium (30, 3 and 3 d^{-1} respectively) are the general default values.
[†]For inhaled material deposited in the respiratory tract and subsequently cleared by particle transport to the alimentary tract, the default f_A values for inhaled materials are applied [i.e. the product of f_r for the absorption type and the f_A value for ingested soluble forms of palladium (0.005)].
[‡]Default Type M is recommended for use in the absence of specific information on which the exposure material can be assigned to an absorption type (e.g. if the form is unknown, or if the form is known but there is no information available on the absorption of that form from the respiratory tract). For guidance on the use of specific information, see Section 1.1.
[§]Activity transferred from systemic compartments into segments of the alimentary tract is assumed to be subject to reabsorption to blood. The default absorption fraction f_A for the secreted activity is the highest value for any form of the radionuclide ($f_A = 0.005$).

24.2.3. Systemic distribution, retention and excretion of palladium

24.2.3.1. Biokinetic data

(427) Palladium (Pd) is a member of the platinum group, which also contains ruthenium, rhodium, osmium, iridium, and platinum. These six metals are chemically similar and generally are found together in ores. There is little quantitative data on the behaviour of palladium in humans, but the biokinetics of palladium has been studied in several animal species.

(428) Meek et al. (1943) studied the biokinetics and toxic effects of palladium salts in rabbits. Over the first four days after intravenous injection about 40% of the administered palladium was recovered in urine. Only traces were found in faeces. Palladium accumulated to some extent in the kidneys, liver, lung, bone marrow, spleen, and muscle.

(429) Durbin et al. (1957) and Durbin (1959) described the results of tracer studies of platinum metals in rats including data for ^{103}Pd administered as $Na_2{}^{103}PdCl_4$. About 60% of intravenously injected ^{103}Pd was excreted in urine over the first 4 h, 71% after 1 d, and 76% after 7 d (after correction for radioactive decay). Faecal excretion accounted for about 4% of the administered amount after 1 d and 13% after 7 d. At 1 d the liver, kidneys, muscle, bone, and blood contained 8.6%, 8.4%, 1.3%, 1.0%, and 0.8%, respectively, of the administered amount. At 7 d the liver contained about 4%, the kidneys 5%, the bone 0.2-0.3%, and the spleen 0.2% of the administered amount. At 16 d the liver and kidneys still contained detectable activity.

(430) Moore et al. (1974, 1975) studied the retention, distribution, and excretion of ^{103}Pd in rats following different modes of administration of $^{103}PdCl_2$. At 1 d after oral intake, detectable activity was found only in the kidneys and liver, with the kidneys showing a much greater concentration than the liver. After intravenous injection, ^{103}Pd was lost mainly in urine during the first 1-2 d, mainly in faeces from 2 d to 2 weeks, and mainly in urine after 2 weeks. Male rats excreted about 30% of intravenously injected ^{103}Pd during the first day. At 1 d after intravenous injection, the highest concentrations were seen in the kidneys, followed by the spleen, liver, adrenal gland, lung, and bone. About 20% of the intravenously injected amount was retained in the body after 40 d, and about 10% was retained after 76 days (Moore Jr. et al., 1974; Moore et al., 1975). At 104 d after intravenous injection the highest concentrations of ^{103}Pd were found in the spleen, kidneys, liver, lung, and bone.

(431) Ando et al. (1989, 1994) determined the distribution of ^{103}Pd in rats at 3, 24, and 48 h after intravenous injection of $^{103}PdCl_2$. Cumulative urinary excretion at 3 h represented 6.4% of injected ^{192}Ir. At all three observation times the highest concentration was found in the kidneys: 20.2, 17.1, and 21.4% g^{-1} at 3, 24, and 48 h, respectively, followed by liver (14.1, 9.9, and 9.9%/g, respectively).

(432) Ducoulombier-Crépineau et al. (2007) examined the transfer of palladium to systemic tissues and milk following a single oral intake of $PdCl_2$ by lactating goats. Tissues were sampled 8 d after administration to determined palladium concentrations. The highest concentration was found in the kidneys. Little palladium was transferred to milk.

24.2.3.2. Systemic model for palladium

(433) The systemic model for palladium is patterned after the models for the chemically similar elements ruthenium and iridium described in *Publication 134* (2016). The same model structure is applied in this publication series to all six platinum metals. The parameter values developed for iridium are modified for application to palladium, based on two sets of comparative data for palladium and iridium: (1) data of Durbin and coworkers (Durbin, 1957, 1959) on the behaviour of both elements in rats, and (2) biokinetic data of Moore et al. (1974, 1975) for palladium in rats compared with biokinetic data of Furchner et al. (1971) for iridium in rats. The modifications of the parameter values in the iridium model are made to depict: faster disappearance of palladium than iridium from blood; a nearly two-fold higher rate of clearance of palladium from blood to urine; two-fold greater deposition of palladium in the kidneys; similar deposition of palladium and iridium in the liver; similar rates of secretion of palladium and iridium from blood to gastrointestinal contents; two-fold lower deposition of palladium in bone; nearly one-third lower deposition of palladium in other tissues; and two-fold faster removal of palladium from all systemic compartments.

(434) The structure of the biokinetic model for systemic palladium is shown in Fig. 24.1. Transfer coefficients for palladium are listed in Table 24.3.

24.2.3.3. Treatment of progeny

(435) Progeny of palladium addressed in this publication are isotopes of rhodium and silver. The characteristic model for rhodium used in this publication is applied to rhodium as a progeny of palladium. The model for silver as a progeny of osmium is an expansion of the characteristic model for silver with added compartments and associated transfer coefficients needed to solve the linked biokinetic models for chains headed by palladium (see Annex B). For a silver isotope produced in a compartment not contained in in the characteristic model for silver, the isotope is assumed to transfer to the central blood compartment of the model for silver at the rate 1000 d^{-1} if produced in a blood compartment and 8.0 d^{-1} if produced in a tissue compartment, and to follow the characteristic model for silver thereafter.

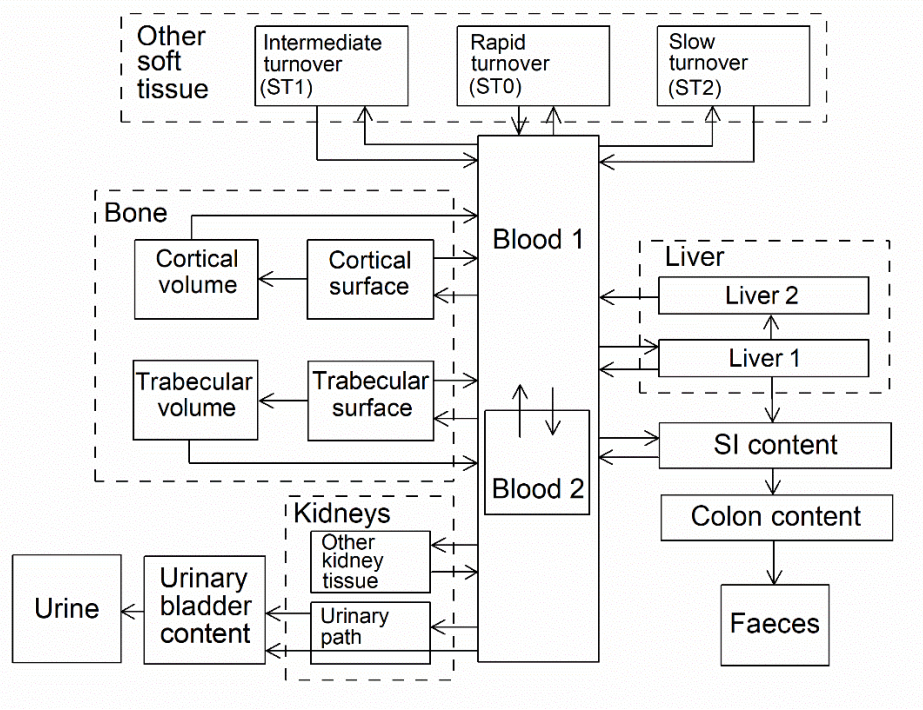

Fig. 24.1. Structure of the biokinetic model for systemic palladium.

Table 24.3. Transfer coefficients in the biokinetic model for systemic palladium.

From	To	Transfer coefficients (d^{-1})
Blood 1	Small intestine contents	4.0
Blood 1	Urinary bladder contents	20
Blood 1	Liver 1	12
Blood 1	Urinary path	8.0
Blood 1	Other kidney tissue	4.0
Blood 1	Blood 2	27
Blood 1	ST0	10
Blood 1	ST1	10
Blood 1	ST2	1.0
Blood 1	Cortical bone surface	1.0
Blood 1	Trabecular bone surface	3.0
Blood 2	Blood 1	2.773
Liver 1	Blood 1	0.04621
Liver 1	Small intestine contents	0.09242
Liver 1	Liver 2	0.1386
Liver 2	Blood 1	0.01386
Urinary path	Urinary bladder contents	0.2773
Other kidney tissue	Blood 1	0.01386
ST0	Blood 1	0.1386
ST1	Blood 1	0.01386
ST2	Blood 1	0.0019
Cortical bone surface	Blood 1	0.03697
Trabecular bone surface	Blood 1	0.03697

Cortical bone surface	Cortical bone volume	0.009242
Trabecular bone surface	Trabecular bone volume	0.009242
Cortical bone volume	Blood 1	0.0000821
Trabecular bone volume	Blood 1	0.000493

24.3. Individual monitoring

(436) Information of detection limit for routine individual measurement is not available.

24.4. Dosimetric data for palladium

Table 24.4. Committed effective dose coefficients (Sv Bq^{-1}) for the inhalation or ingestion of ^{103}Pd and ^{107}Pd compounds.

Inhaled particulate materials (5 μm AMAD aerosols)	Effective dose coefficients (Sv Bq^{-1})	
	^{103}Pd	^{107}Pd
Type F, — NB: Type F should not be assumed without evidence	4.5E-11	3.3E-11
Type M, default	1.2E-10	4.4E-11
Type S	1.5E-10	9.2E-10
Ingested materials		
All forms	2.5E-11	7.4E-13

AMAD, activity median aerodynamic diameter

25. SILVER (Z=47)

25.1. Isotopes

Table 25.1. Isotopes of silver addressed in this publication.

Isotope	Physical half-life	Decay mode
^{101}Ag	11.1 min	EC, B+
^{102}Ag	12.9 min	EC, B+
^{103}Ag	65.7 m	EC, B+
^{104}Ag	69.2 min	EC, B+
^{104m}Ag	33.5 min	EC, B+, IT
^{105}Ag	41.29 d	EC
^{106}Ag	23.96 min	EC, B+, B-
^{106m}Ag	8.28 d	EC
^{108m}Ag	418 y	EC, IT
^{110m}Ag*	249.76 d	B-, IT
^{111}Ag	7.45 d	B-
^{112}Ag	3.130 h	B-
^{113}Ag	5.37 h	B-
^{115}Ag	20.0 min	B-

EC, electron-capture decay; B+, beta-plus decay; B-, beta-minus decay.
*Dose coefficients and bioassay data for this radionuclide are given in the printed copy of this publication.
Data for other radionuclides listed in this table are given in the online electronic files on the ICRP website.

25.2. Routes of Intake

25.2.1. Inhalation

(437) A few studies give information on absorption of silver from the respiratory tract. Analysis of experimental data to derive absorption parameter values is more difficult than for most elements, because excretion of systemic silver is mainly faecal, and so faecal excretion does not enable particle transport from the respiratory tract to be easily distinguished from absorption.

(438) Absorption parameter values and Types, and associated f_A values for inhaled particulate forms of silver are given in Table 25. 2.

25.2.1.1. Particulate Materials

a. Elemental silver

(439) Hahn et al. (1952) followed the tissue distribution of ^{111}Ag for 15 d after instillation of a suspension of ^{111}Ag-labelled silver colloid (via a bronchoscope) into the lungs of dogs. Most of the ^{111}Ag was retained in the lung in which it was deposited, although higher concentrations were measured in some associated lymph nodes. There was very little translocation to liver or spleen, indicating that little absorption occurred, and therefore Type M or S behaviour.

(440) Phalen and Morrow (1973) followed the biokinetics of ^{110m}Ag for 225 d after inhalation (via endotracheal tube) of metallic silver fume by dogs. The particles were aggregates (AMAD approximately 0.5 μm) of primary particles with diameters approximately 0.05 μm. Much of the initial lung deposit (ILD) was cleared rapidly: the authors assessed that it was mainly by absorption to blood rather than by mucociliary clearance. Lung retention was represented by a three-component exponential function with rates of 0.4 d^{-1} (59%), 0.08 d^{-1}

(39%) and 0.017 d^{-1} (2%). Analysis carried out here (i.e. by the Task Group), assuming that the bound fraction $f_b = 0.0$ (see below), showed that the results could fit with dissolution parameter values of $f_r = 0.7$; $s_r = 0.3$ d^{-1}; and $s_s = 0.005$ d^{-1} (fixed at the default Type M value), giving assignment to Type M. Phalen and Morrow also measured dissolution rate constants *in vitro* of 0.1 µg cm^{-2} d^{-1} in distilled water and 10 µg cm^{-2} d^{-1} in an interstitial fluid simulant (at approximately 36 °C). They calculated that the latter would give 99% dissolution in approximately 2 d.

(441) Camner et al. (1973, 1977) produced ^{51}Cr-labelled Teflon particles coated with silver (and other elements) for lung clearance experiments. In-vitro tests (up to 30 d in saline and 12 d in rabbit serum) showed that most particles retained some silver coating. Thus the silver coating did not dissolve rapidly, indicating Type M behaviour.

(442) Takenaka et al. (2000) investigated the behaviour of non-radioactive ultrafine metallic silver particles deposited in the lungs (diameters of primary particles 0.02 µm). They observed that particles in aqueous suspension added to cultured mouse peritoneal macrophages were mainly associated with cells; the size and form of the agglomerated particles remained unchanged over 9 d; and the silver content of the medium was low, indicating Type M behaviour.

(443) Takenaka et al. (2000, 2001) also followed the biokinetics of silver for 7 d following intratracheal instillation into rats of an aqueous suspension of these particles: predominantly agglomerates > 0.1 µm diameter. There was little change in the silver content of the lungs between 1 and 7 d. The silver content of liver, and lung-associated lymph nodes, remained low: a few percent of lung content. In analyses carried out here, because there were few data, absorption parameter values were fit simultaneously to the results of this experiment, and the two other experiments on the biokinetics of silver deposited in rat lungs carried out by Takenaka et al. (2000, 2001): inhalation of metallic silver, and instillation of silver nitrate (see below). Values of f_r were varied independently, while values of s_r (and systemic rates) were 'shared' (i.e. they were varied, but assumed to be the same in the three studies). It was assumed that the bound fraction $f_b = 0.0$ (see below) and that $s_s = 0.005$ d^{-1} (fixed at the default Type M value). For instillation of metallic silver, analysis here gave $f_r = 0.3$ and $s_r = 0.4$ d^{-1}, and assignment to Type M.

(444) Takenaka et al. (2001) also followed the tissue distribution of silver for 7 d after inhalation of non-radioactive ultrafine metallic silver particles (diameters of primary particles 0.02 µm). In contrast to the behaviour after instillation of agglomerated particles, there was rapid clearance from lungs to the systemic circulation. At 1, 4 and 7 d, retention in lungs was approximately 38, 9 and 4% ILD. Liver content was approximately 9% ILD at 1 h, and 1% ILD at 7 d. Analysis here gave f_r approximately 1.0 and $s_r = 0.4$ d^{-1}, giving assignment to Type F.

(445) Overall, the results suggest that the behaviour of elemental silver particles may be either Type F or Type M, perhaps depending on the method of preparation and/or particle size.

b. Silver iodide (AgI)

(446) Following inhalation of ^{131}I-labelled silver iodide by mice and sheep (Bair, 1961; Willard and Bair, 1961), the ^{131}I was rapidly absorbed from the lungs: there was little difference between its absorption administered as silver iodide and as iodine vapour. The results indicate Type F behaviour, even though silver iodide was studied because it is relatively insoluble in water. Morrow et al. (1968) followed lung retention of ^{110}Ag for at least 7 d after inhalation of silver iodide by dogs and rats, but few details are given. Lung retention followed a two-component exponential function with rates of 0.14 d^{-1} (7%) and 0.011 d^{-1} (93%), giving predicted lung retention at 30 d and 180 d to be approximately 67% and 13% ILD. These results are consistent with assignment to Type M. Morrow et al. (1968) noted that during aerosolisation

some conversion to silver oxide probably occurs. Hence it is possible that the rapid absorption of ^{131}I observed by Willard and Bair (1961) resulted from decomposition of the silver iodide.

c. Silver nitrate ($AgNO_3$)

(447) Takenaka et al. (2001) followed the tissue distribution of silver for 7 d after intratracheal instillation of $AgNO_3$, for comparison with that after inhalation of ultrafine silver particles (see above). At 1, 4 and 7 d, lung retention was approximately 24%, 8% and 6% ILD, and liver content approximately 8%, 4% and 1% ILD. In analyses carried out here, because there were few data, absorption parameter values were fit simultaneously to the results of this experiment, and the two other experiments on the biokinetics of silver deposited in rat lungs carried out by Takenaka et al. (2000, 2001): inhalation and instillation of metallic silver (see above). It was assumed that the bound fraction $f_b = 0.0$ (see below) and $s_s = 0.005$ d^{-1} (fixed at the default Type M value). For instillation of silver nitrate, analysis here gave $f_r = 0.95$ and $s_r = 0.4$ d^{-1}, giving assignment to Type F.

25.2.1.2. Unknown forms

(448) In one case of accidental human inhalation of ^{110m}Ag associated with particles of unknown composition, lung clearance for the silver was apparently completed within a few days, which is consistent with Type F behaviour (Newton and Holmes, 1966).

(449) Poulheim (1984) made in-vivo external measurements of ^{60}Co, ^{58}Co/^{54}Mn, and ^{110m}Ag on several workers following inhalation of activated corrosion products. Most of the activity was located in the thoracic area. Measurements of ^{110m}Ag were made in four workers for up to 71 d. Assuming that the retention function given describes retention in the lungs and that the bound fraction $f_b = 0.0$ (see below), analysis carried out here showed that the results could be fit well with dissolution parameter values of $f_r = 0.9$; $s_r = 0.1$ d^{-1}; and $s_s = 0.005$ d^{-1} (fixed at the default Type M value). This result gives assignment of the ^{110m}Ag present to Type F, but very close to the boundary with Type M.

25.2.1.3. Rapid dissolution rate for silver

(450) Analysis carried out here, assuming that the bound fraction $f_b = 0.0$ (see below), gave values of $s_r = 0.3$ or 0.4 d^{-1}; for elemental silver inhaled by dogs and rats, and for silver nitrate instilled into the lungs of rats. Based on these results, a rounded value of 1 d^{-1} is applied here to all Type F forms of silver. Because it is lower than the general default value of 3 d^{-1} for Type M and S materials, it is also applied here to Type M and S forms of silver.

25.2.1.4. Extent of binding of silver to the respiratory tract

(451) There is some experimental information on silver iodide suggesting that silver seems to form stable complexes with ligands of the lungs (Morrow et al., 1968). Phalen and Morrow (1973) observed that the rate associated with the rapid phase of lung clearance was much lower than the dissolution rate in interstitial fluid simulant, and that this might be due to retention of dissolved silver in lung tissues. Takanaka et al. (2001) noted that absorption of silver from the lungs was slower following instillation of the nitrate than following inhalation of ultrafine silver particles, and that this might be due to binding of silver ions to proteins. However, the information is insufficient to estimate the extent of any bound state, and it is largely taken into account by the low value of s_r (1 d^{-1}) used. It is therefore assumed that for silver the bound state can be neglected (i.e., $f_b = 0$).

Table 25.2. Absorption parameter values for inhaled and ingested silver.

Inhaled particulate materials		Absorption parameter values* f_r	s_r (d^{-1})	s_s (d^{-1})	Absorption from the alimentary tract, f_A
Default parameter values†,‡					
Absorption type	Assigned forms				
F	Silver nitrate	1	1	–	0.05
M§	Silver iodide	0.2	1	0.005	0.01
S	—	0.01	1	$1x10^{-4}$	$5x10^{-4}$
Ingested materials¶					
All chemical forms					0.05

*It is assumed that for silver the bound state can be neglected (i.e. $f_b = 0$). The values of s_r for Type F, M and S forms of silver (1 d^{-1}) are element-specific.

†Materials (e.g. silver nitrate) are listed here where there is sufficient information to assign to a default absorption type, but not to give specific parameter values (see text).

‡For inhaled material deposited in the respiratory tract and subsequent cleared by particle transport to the alimentary tract, the default f_A values for inhaled materials are applied [i.e. the (rounded) product of f_r for the absorption type and the f_A value for ingested soluble forms of silver (0.05)].

§Default Type M is recommended for use in the absence of specific information on which the exposure material can be assigned to an absorption type (e.g. if the form is unknown, or if the form is known but there is no information available on the absorption of that form from the respiratory tract). For guidance on the use of specific information, see Section 1.1.

¶Activity transferred from systemic compartments into segments of the alimentary tract is assumed to be subject to reabsorption to blood. The default absorption fraction f_A for the secreted activity is the reference f_A (=0.05) for ingestion of the radionuclide.

25.2.2. Ingestion

(452) There are no human and very few animal data on Ag absorption. Furchner et al. (1968) reported a comparative study of the whole-body retention of Ag after intravenous and oral administration of $^{110m}AgNO_3$ in mice, rats, dogs and monkeys, which indicated that absorption was less than 0.1 in each species. Harrison (1979) investigated the oral absorption of ^{110}Ag-labelled sulfadiazine silver (AgSU) in rats. He showed that oral ingestion resulted in substantial silver deposition, particularly in liver and lungs but the data provided were not sufficient to derive a fractional absorption factor.

(453) In *Publication 30* (ICRP, 1980), an absorption fraction of 0.05 was recommended for all chemical forms of Ag. This value was adopted in *Publication 67* (ICRP, 1993) for dietary intakes. Since no new data on the gastrointestinal absorption seem to be available, this value is adopted here as a default value for all chemical forms ($f_A = 0.05$).

25.2.3. Systemic distribution, retention and excretion of silver

25.2.3.1. Summary of the database

a. Human studies

(454) Silver is located in Group 11 (IB) of the periodic table, between copper and gold. It exhibits chemical properties intermediate to those two metals.

(455) Silver has been used for therapeutic purposes since at least the 17th century. Several adverse health effects can result from continued or high acute exposure to silver, the most common being a permanent blue-gray discoloration of the skin (argyria) or eyes (argyrosis).

Other potential effects include liver and kidney damage, changes in blood cells, and irritation of the eyes, skin, respiratory tract, and intestinal tract. The reader is referred to a review by Drake and Hazelwood (2005) of exposure-related health effects of silver including a discussion of metabolic properties of silver associated with its adverse effects and case studies of effects of elevated exposure to different forms of silver. Findings on such studies are of limited value for modelling the normal biokinetics of silver in view of the variability of the human data and an apparent mass effect on silver biokinetics as demonstrated in rats (Scott and Hamilton, 1950).

(456) Polachek et al. (1960) studied the metabolic pathways of radiosilver (a mixture of ^{105}Ag, ^{106}Ag, ^{110m}Ag, and ^{111}Ag) in a patient with malignant carcinoid. The radiosilver was injected intravenously after incubation in the patient's blood. Activity was initially associated mainly with red blood cells (perhaps an artifact of the method of administration) and the globulin fraction of plasma. After one day the concentration in whole blood was similar to that in plasma. Activity was removed from blood largely by the liver. External measurements over the liver indicated a single component of retention with a biological half-time of about 48 d. Measurements over the sacrum, chest, and heart indicated two components of retention with half-times of 3.8 d and 48 d; the short-term component represented 30-50% of the initial activity over these regions. The urinary to faecal excretion ratio over the first three weeks was ~0.05. At postmortem, activity was found mainly in the liver and skin, with the liver showing a twofold higher concentration than skin.

(457) Newton and Holmes (1966) studied the behaviour of ^{110m}Ag following its accidental inhalation by a worker. Lung clearance of activity appeared to be completed within a few days. Distribution studies based on external counting were continued for five months post exposure. A marked localisation of activity in the liver showed a biological half-time of about 52 d.

(458) Zhu et al. (2010) measured concentrations of silver in 17 tissues obtained from autopsies of 68 Chinese men living in four areas of China with different dietary patterns and considered healthy until the time of sudden accidental death. The investigators also measured concentrations of silver in blood of 10 volunteers from each of the four areas. Highest median concentrations (μg kg^{-1}) were found in liver (52.2), rib (2.54), kidney (2.44), adrenals (0.50), and blood (0.43). The following distribution of silver in the body is estimated from median concentrations and reference weights of blood and tissues in Chinese adult males: liver, 64.5%; bone, 17.8%; blood, 1.7%; kidney, 0.62%; remaining tissues and fluids, 15.4%.

b. Animal studies

(459) Hanson et al. (2001) investigated the behaviour of ^{110m}Ag administered intraperitoneally as the nitrate to virgin and lactating female rats, in an effort to determine whether the behaviour of silver resembles that of copper. They found that the transport and distribution of silver resemble those of copper in some aspects, particularly with regard to high accumulation in the liver and lactating mammary gland and the fact that silver attaches to some extent to the copper-carrying protein ceruloplasmin in plasma and milk. However, silver was mainly carried in plasma by a different macroglobulin from that involved in copper transport and, overall, was distributed somewhat differently from copper in tissues.

(460) Klaassen (1979) investigated the behaviour of silver in rats, rabbits, and dogs after intravenous administration of various masses of silver nitrate. Distribution studies on rats indicated that liver was the dominant repository at early times. Biliary secretion was found to be an important route of elimination of silver in all three species, but the secretion rate varied markedly with species. For example, the secretion rate over the first two hours was an order of magnitude lower in rabbits than in rats and two orders of magnitude lower in dogs than in rats.

By 4 d after administration of 0.1 mg silver kg^{-1} to rats, about 70% of the injected silver was eliminated in faeces and less than 1% was eliminated in urine.

(461) Following intramuscular administration of radiosilver to rats, most of the absorbed activity was apparently secreted into the gastrointestinal tract in bile during the first day (Scott and Hamilton, 1950). At 1 d and 4 d the primary systemic repositories were blood (4.1% and 0.85%, respectively, of the absorbed activity), liver (2.8% and 1.3%), bone (4.2% and 0.66%), muscle (2.2% and 2.3%), and skin (1.9% and 0.61%).

(462) Furchner et al. (1968) administered ^{110m}Ag nitrate to mice, rats, monkeys, and dogs orally, intravenously, and intraperitoneally. Total-body retention and urinary and faecal excretion rates were determined in all species for the intravenous and oral routes, and in mice and rats for intraperitoneal injection. The time-dependent distribution of activity was determined in rats injected intraperitoneally. The urinary to faecal excretion ratio was generally less than 0.1 over the first two weeks. Total-body retention of activity, expressed as the integral of the retention curve, generally increased in the order mice < rats < monkeys < dogs. For monkeys injected intravenously, about 84.4% was retained with a biological half-time of 1.8 d, 14% with a half-time of 7.0 d, and 1.2% with a half-time of 73 d. For dogs injected intravenously, about 7.1% was retained with a half-time of 2.4 d, 78.2%% with a half-time of 11 d, and 2.1% with a half-time of 39 d. In rats, the pattern of removal from all tissues over the first three weeks resembled that in the total body except for a relatively slow loss from the brain and spleen.

(463) The biokinetics of silver was studied in dogs exposed by inhalation or tracheal intubation to ^{110m}Ag-tagged metallic silver (Phalen and Morrow, 1973). The lung deposit showed biological clearance half-times of about 2, 8, and 40 d corresponding to about 59, 39, and 2%, respectively, of the deposited amount. Absorbed activity deposited primarily in the liver, which contained on average about 40% of the recovered systemic activity at 111 and 225 d post exposure. The liver showed two phases of retention with biological half-times of 9 d (97%) and 40 d (3%). At most 1% of the excreted activity was in urine. It appeared that the bulk of excreted ^{110m}Ag represented absorbed activity that deposited in the liver and was excreted in faeces following biliary secretion.

(464) Beresford et al. (1994) studied the accumulation of ^{110m}Ag in female lambs following acute administration as the nitrate directly into the rumen. Activity concentrations were determined in blood, muscle, liver, lung, kidney, spleen, brain, and bone through 369 d post exposure. Throughout the study the liver accounted for more than 90% of the total ^{110m}Ag found in the sampled tissues. A biological half-time of 79 d was estimated for liver, compared with 39 d for muscle and 29 d for kidney.

25.2.3.2. Biokinetic model for systemic silver

(465) The structure of the model adopted for systemic silver is shown in Fig. 25.1. Transfer coefficients are listed in Table 25.3.

(466) The model was designed to approximate the following features of silver kinetics:

- The plasma clearance curve determined for a human subject by Polachek et al. (1960). For modelling purposes it was assumed that the silver concentration in total blood is the same as the observed time-dependent concentration in plasma.
- A biological half-time of ~50 d for the total body, as indicated by data of Polachek et al. (1960) and Newton and Holmes (1966) for human subjects.
- A urinary to faecal excretion ratio of 0.05. This is consistent with findings of Polachek et al. (1960) for a human subject. A ratio of this order is also indicated by animal studies.
- The distribution of chronically ingested stable silver as indicated by autopsy data together with blood data for living subjects (Zhu et al., 2010).

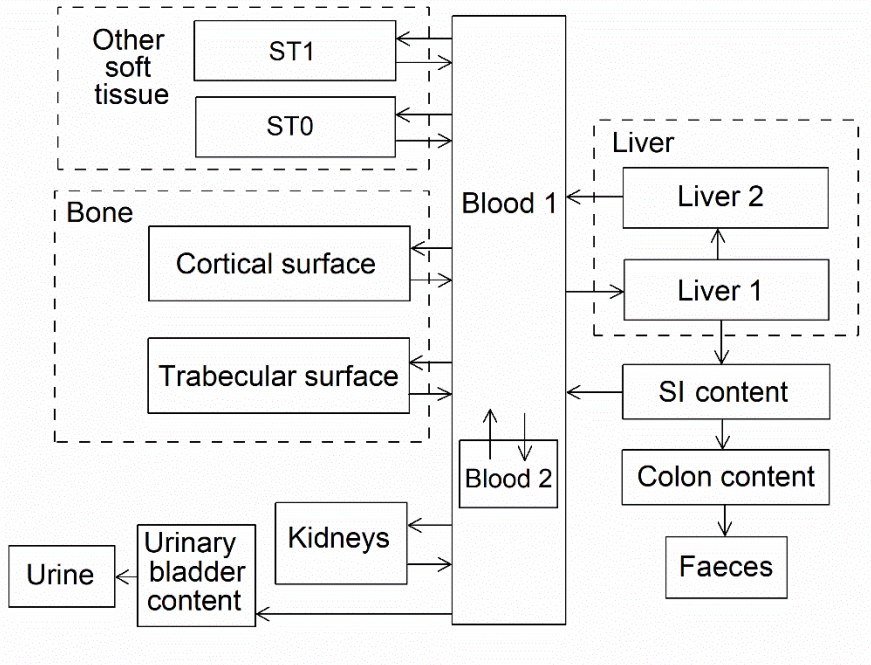

Fig. 25.1. Structure of the biokinetic model for systemic silver.

Table 25.3. Transfer coefficients in the biokinetic model for systemic silver.

From	To	Transfer coefficient (d^{-1})
Blood 1	Blood 2	0.72
Blood 1	Kidneys	1.2
Blood 1	Liver 1	30
Blood 1	Trabecular bone surface	1.2
Blood 1	Cortical bone surface	1.2
Blood 1	Other 0	12.8
Blood 1	Other 1	12.8
Blood 1	Urinary bladder content	0.13
Blood 2	Blood 1	0.231
Kidneys	Blood 1	0.8
Liver 1	Small intestine content	1.0
Liver 1	Liver 2	9.0
Liver 2	Blood 1	0.2
Other 0	Blood 1	8.0
Other 1	Blood 1	0.4
Trabecular bone surface	Blood 1	0.07
Cortical bone surface	Blood 1	0.07

25.2.3.3. Treatment of progeny

(467) Progeny of silver addressed in this publication are isotopes of silver, rhodium, palladium, indium, and cadmium. The model for silver as a parent is applied to silver produced by decay of another isotope of silver. The models for rhodium, palladium, indium, and cadmium as progeny of silver are the characteristic models for these elements with added compartments

and associated transfer coefficients needed to solve the linked biokinetic models for chains headed by silver. Muscle and pancreas were added to the explicitly identified tissues in the characteristic model for indium. The following rates of transfer of indium between blood compartments in the characteristic model for indium and the added tissues were assigned: transferrin to pancreas, 0.001 d^{-1}; transferrin to muscle, 0.2 d^{-1}; pancreas to plasma, 2.37 d^{-1}; muscle to plasma, 2.37 d^{-1}. Rhodium, palladium, indium, or cadmium produced in a compartment of the model for a preceding chain that is not a compartment in the model for that progeny (an ambiguous compartment) is assumed to transfer to the central blood compartment of the progeny's model and to follow that model thereafter. The following transfer rates are assigned to progeny produced in ambiguous compartments: 1000 d^{-1} if produced in a blood compartment; at the rate of bone turnover for the indicated bone type if produced in a bone volume compartment; and at the following element-specific rates if produced in any other compartment: rhodium, 0.09902 d^{-1}; palladium, 0.1386 d^{-1}; indium, 2.37 d^{-1}; cadmium, 0.5 d^{-1}.

25.3. Individual monitoring

25.3.1. ^{110m}Ag

(468) Measurements of ^{110m}Ag may be performed by *in vivo* whole-body measurement technique and by gamma measurement in urine.

Table 25.4. Monitoring techniques for ^{110m}Ag.

Isotope	Monitoring Technique	Method of Measurement	Typical Detection Limit
^{110m}Ag	Urine Bioassay	γ-ray spectrometry[a]	1.8 Bq L^{-1}
^{110m}Ag	Whole-body measurement	γ-ray spectrometry[ab]	20 Bq

[a] Measurement system comprised of Germanium Detectors
[b] Counting time of 20 minutes

25.4. Dosimetric data for silver

Table 25.5. Committed effective dose coefficients (Sv Bq^{-1}) for the inhalation or ingestion of ^{110m}Ag compounds.

Inhaled particulate materials (5 µm AMAD aerosols)	Effective dose coefficients (Sv Bq^{-1})
	^{110m}Ag
Type F, silver nitrate	3.3E-09
Type M, silver iodide	5.0E-09
Type S	9.3E-09
Ingested materials	
All forms	2.3E-09

AMAD, activity median aerodynamic diameter

Table 25.6. Dose per activity content of ^{110m}Ag in total body and in daily excretion of urine (Sv Bq^{-1}); 5µm activity median aerodynamic diameter aerosols inhaled by a reference worker at light work.

	Type F		Type M		Type S	
Time after intake (d)	Total body	Urine	Total body	Urine	Total body	Urine
1	5.3E-09	1.5E-05	8.1E-09	1.2E-04	1.5E-08	4.3E-03
2	9.4E-09	3.0E-05	1.5E-08	2.2E-04	2.8E-08	8.2E-03
3	1.8E-08	4.4E-05	3.2E-08	3.1E-04	6.1E-08	1.2E-02
4	2.8E-08	5.2E-05	5.5E-08	3.6E-04	1.1E-07	1.4E-02
5	3.4E-08	5.6E-05	7.0E-08	3.9E-04	1.4E-07	1.5E-02
6	3.6E-08	5.9E-05	7.7E-08	4.0E-04	1.6E-07	1.6E-02
7	3.7E-08	6.1E-05	7.9E-08	4.1E-04	1.6E-07	1.6E-02
8	3.8E-08	6.3E-05	8.1E-08	4.2E-04	1.7E-07	1.7E-02
9	3.9E-08	6.5E-05	8.2E-08	4.2E-04	1.7E-07	1.7E-02
10	3.9E-08	6.7E-05	8.3E-08	4.3E-04	1.7E-07	1.7E-02
15	4.3E-08	7.4E-05	8.8E-08	4.5E-04	1.8E-07	1.8E-02
30	5.4E-08	9.6E-05	1.0E-07	5.1E-04	2.0E-07	2.2E-02
45	6.9E-08	1.2E-04	1.2E-07	5.7E-04	2.1E-07	2.5E-02
60	8.7E-08	1.6E-04	1.3E-07	6.3E-04	2.3E-07	2.9E-02
90	1.4E-07	2.5E-04	1.7E-07	8.0E-04	2.6E-07	3.7E-02
180	5.8E-07	1.0E-03	3.9E-07	1.7E-03	3.9E-07	6.9E-02
365	1.1E-05	1.9E-02	2.1E-06	8.7E-03	8.7E-07	1.8E-01

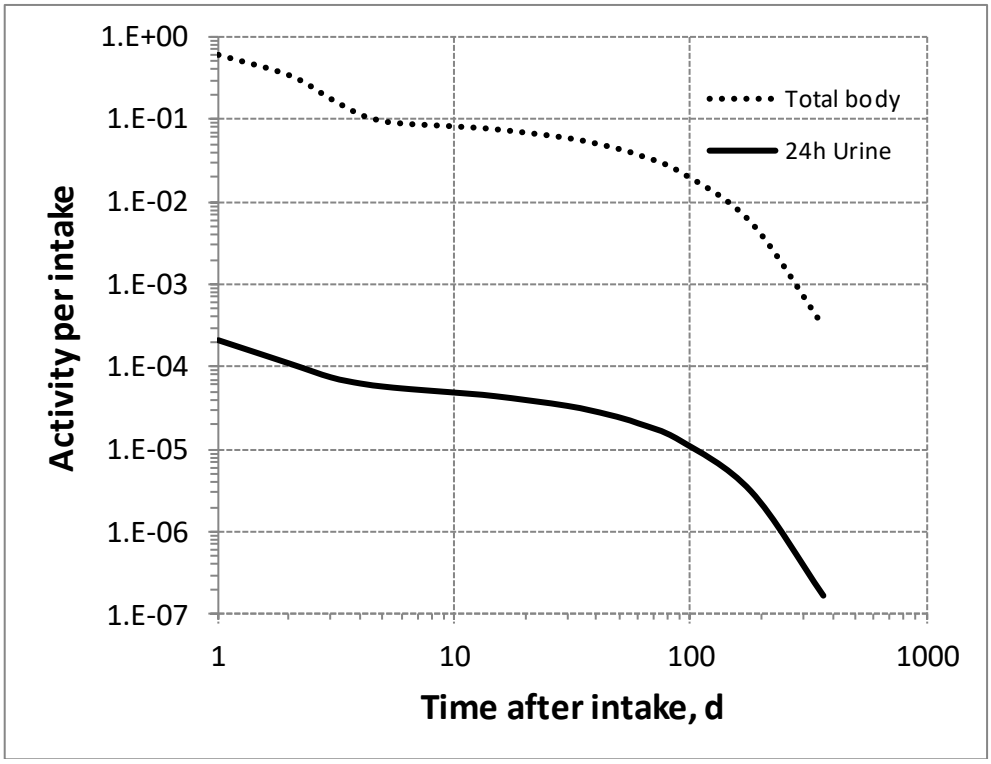

Fig. 25.2. Daily excretion of ^{110m}Ag following inhalation of 1 Bq Type F.

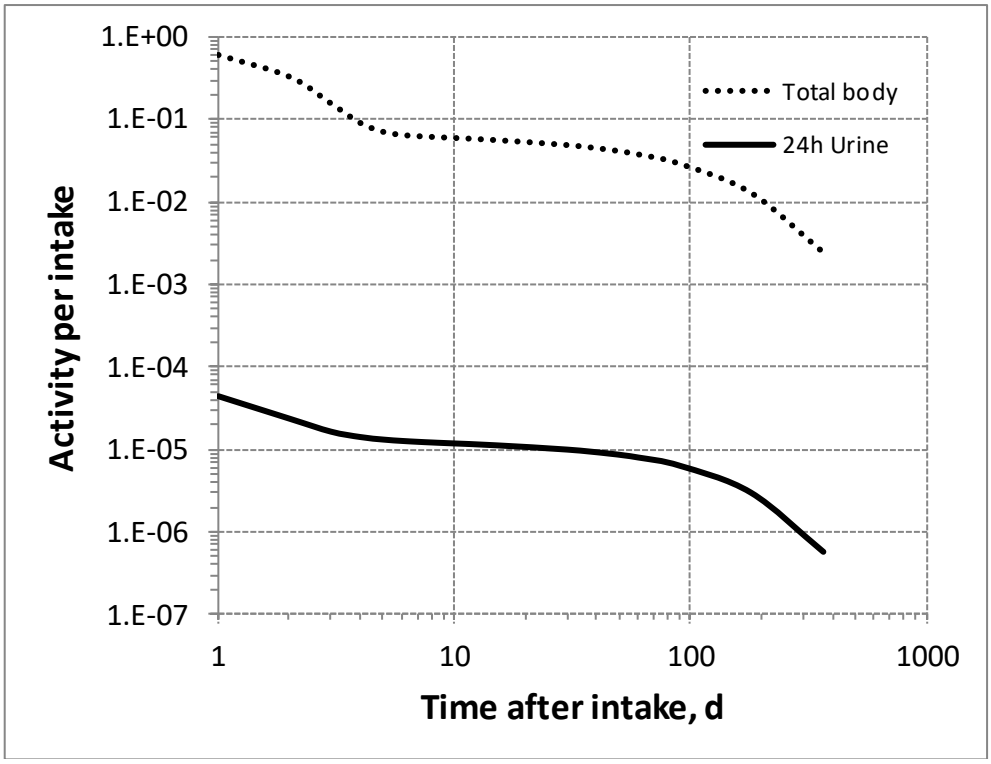

Fig. 25.3. Daily excretion of ^{110m}Ag following inhalation of 1 Bq Type M.

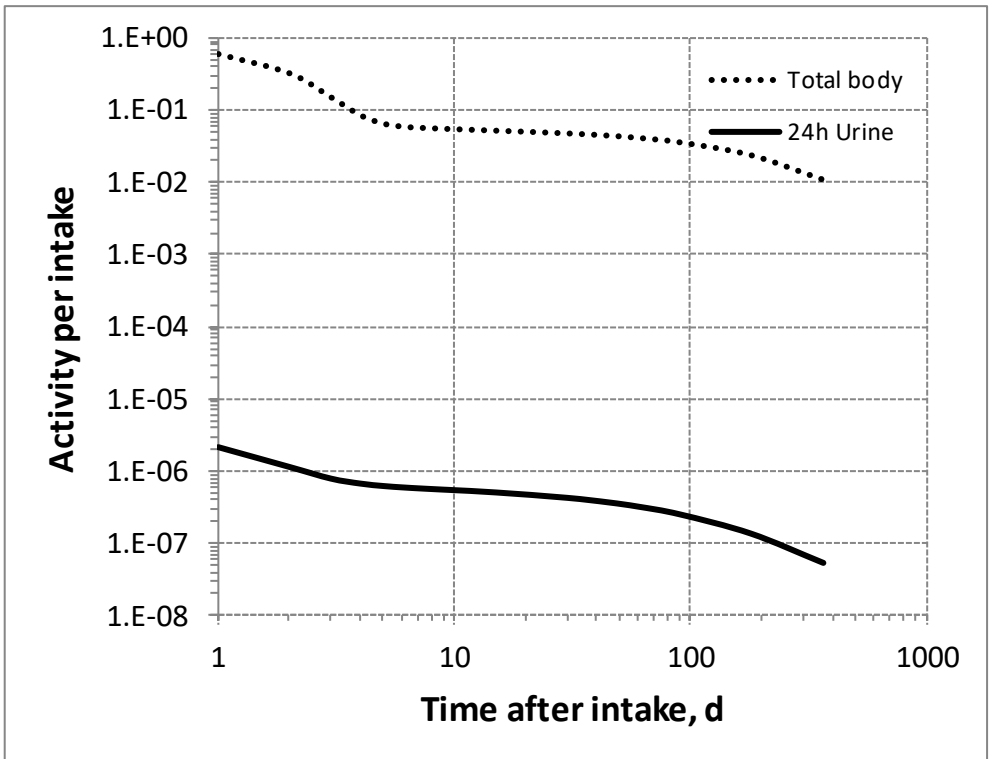

Fig. 25.4. Daily excretion of ^{110m}Ag following inhalation of 1 Bq Type S.

26. CADMIUM (Z=48)

26.1. Isotopes

Table 26.1. Isotopes of cadmium addressed in this publication.

Isotope	Physical half-life	Decay mode
^{104}Cd	57.7 min	EC
^{105}Cd	55.5 min	EC, B+
^{107}Cd	6.50 h	EC, B+
^{109}Cd*	461.4 d	EC
^{111m}Cd	48.50 min	IT
^{113}Cd	7.7E+15 y	B-
^{113m}Cd	14.1 y	B-, IT
^{115}Cd	53.46 h	B-
^{115m}Cd	44.6 d	B-
^{117}Cd	2.49 h	B-
^{117m}Cd	3.36 h	B-
^{118}Cd	50.3 min	B-

EC, electron-capture decay; β^+, beta-plus decay; β^-, beta-minus decay; IT, isomeric transition decay.
*Dose coefficients and bioassay data for this radionuclide are given in the printed copy of this publication.
Data for other radionuclides listed in this table are given in the online electronic files on the ICRP website.

26.2. Routes of Intake

26.2.1. Inhalation

26.2.1.1. Absorption types and parameter values

(469) The ICRP Task Group on Lung Dynamics (TGLD, 1966) assigned oxides and hydroxides of cadmium to inhalation class Y, sulphides, halides and nitrates to inhalation class W and all other compounds of the element to inhalation class D. This classification was adopted by ICRP in *Publication* 30 (ICRP, 1980), although it was noted that in dogs exposed to near lethal doses of cadmium chloride by inhalation a long term component of lung retention was observed (Harrison et al., 1947). Because of its recognised hazards, the inhalation toxicology of cadmium has been studied extensively (ATSDR, 2012a). Information is available on the behaviour of inhaled cadmium particles from animal studies and limited empirical human data.

(470) Absorption parameter values and types, and associated f_A values for particulate forms of cadmium are given in Table 26.2.

(471) Reference biokinetic models were used here (i.e. by the Task Group) for the analysis of the data and the determination of absorption parameter values for cadmium particles. Lung retention data were interpreted using the revised HRTM (ICRP, 2015) and the respiratory tract model for rat described in Supporting Guidance 3 (ICRP, 2002b). Cadmium in lung tissue and blood was taken into account in the comparison with experimental data by using the systemic model for cadmium described in Section 26.2.3 and the simple rat systemic model described by Moore et al. (1973). Substantial lung retention of cadmium has been observed following deposition of soluble forms in the lungs (see Section 26.2.1.2) that might be explained either by a bound state or by the formation of particles. It was decided here to assume no bound state ($f_b = 0$) of cadmium in the respiratory tract, as discussed in Section 26.2.1.4.

Table 26.2. Absorption parameter values for inhaled and ingested cadmium.

Inhaled particulate materials		Absorption parameter values* f_r	s_r (d^{-1})	s_s (d^{-1})	Absorption from the alimentary tract, f_A
Default parameter values†,‡					
Absorption type	Assigned forms				
F	-	1	30	–	0.05
M§	Oxide, chloride, sulphide, carbonate, telluride, all unspecified forms	0.2	3	0.005	0.01
S	-	0.01	3	1×10^{-4}	0.0005
Ingested materials¶					
All compounds					0.05

*It is assumed that the bound state can be neglected for cadmium (i.e. $f_b = 0$). The values of s_r for Type F, M and S forms of cadmium (30, 3 and 3 d^{-1} respectively) are the general default values.

†Materials (e.g. oxide) are generally listed here where there is sufficient information to assign to a default absorption type, but not to give specific parameter values (see text).

‡For inhaled material deposited in the respiratory tract and subsequently cleared by particle transport to the alimentary tract, the default f_A values for inhaled materials are applied [i.e. the product of f_r for the absorption type (or specific value where given) and the f_A value for ingested soluble forms of cadmium (0.05)].

§Default Type M is recommended for use in the absence of specific information on which the exposure material can be assigned to an absorption type (e.g. if the form is unknown, or if the form is known but there is no information available on the absorption of that form from the respiratory tract). For guidance on the use of specific information, see Section 1.1.

¶Activity transferred from systemic compartments into segments of the alimentary tract is assumed to be subject to reabsorption to blood. The default absorption fraction f_A for the secreted activity is the highest value for any form of the radionuclide ($f_A = 0.05$).

26.2.1.2. Particulate aerosols

a. Cadmium chloride ($CdCl_2$)

(472) In an early study, Harrison et al. (1947) determined the distribution over 15 weeks of stable cadmium in the tissues of dogs exposed to $CdCl_2$ aerosols by inhalation. The Cd concentration in lungs decreased rapidly during the first few days but residual pulmonary Cd was still observed 15 weeks after exposure. A significant proportion of inhaled Cd was found in kidneys and liver. Therapy with 2,3 dimercaptopropanol did not appear to influence its biokinetics. Analysis here of the data gave $f_r = 0.3$; $s_r = 0.7$ d^{-1} and $s_s < 0.005$ d^{-1}. This is consistent with Type M behaviour.

(473) Moore et al. (1973) studied the whole-body retention of ^{115m}Cd in rats after administration of $^{115m}CdCl_2$ by either ingestion, inhalation, intraperitoneal or intravenous (IV) injection. After initial clearance of 7.3% of IV injected activity through faecal excretion during the first 24 h, the biological half-life (T_b) of systemic Cd was 252 d. Comparison here of the whole body retention data after inhalation and IV injection suggested $f_r \approx 0.2$; $s_s \approx 0.01$ d^{-1} and assignment to Type M.

(474) Henderson et al. (1979) measured ^{115m}Cd in lungs, GI tract, liver, kidney and skull of hamsters for 3 weeks after inhalation of $CdCl_2$ aerosols with mass median aerodynamic diameter (MMAD) 1.7 µm at two levels of exposure. Two h after exposure, an upward trend of the amount of Cd^{2+} transferred to the liver with increasing amounts of $CdCl_2$ deposited in the lung was observed. Approximately one-third initial lung deposit (ILD) had left the lungs by 24

h. At 3 weeks, lung burdens were about 40% ILD. Lavages of excised lung failed to remove a significant amount of Cd^{2+}: about 3.5% of the material present in lung was removed at any time. Analysis here of the data gave $f_r = 0.3$; $s_r = 30$ d^{-1}; $s_s < 0.005$ d^{-1} and assignment to Type M.

(475) Oberdörster et al. (1979) observed the clearance and translocation of stable cadmium from rat lungs for 100 d after inhalation of CdO and $CdCl_2$ aerosols with respective MMAD 0.46 and 0.38 µm. Inhaled $CdCl_2$ particles did not exhibit the initial clearance of CdO, with only 2% removed from lungs between day 0 and day 1; although the liver and kidney exhibited significant increases in Cd on day 1, attributed to Cd absorbed through the alimentary tract. After that, the lung clearance was mono-exponential with the same T_b of 67 d as for the less soluble CdO. The authors therefore noted that the dissolution rate of Cd compounds apparently did not play a major role in the long term clearance of inhaled Cd from the lung. The Cd burden in liver and kidney was 5-7 times higher than in the CdO experiment. Analysis here of the $CdCl_2$ data gave $f_r = 0.28$; $s_r = 2$ d^{-1}; $s_s = 0.0055$ d^{-1} and assignment to Type M.

(476) Oberdörster et al. (1980) studied the lung deposition and clearance over 100 d of ^{115m}Cd in rats exposed to $CdCl_2$ aerosols by nose-only inhalation or by intratracheal instillation. The results showed a bi-exponential pattern with about half of the deposited Cd cleared with short half-lives of 1.1 d (inhalation) and 0.7 d (instillation) and the rest cleared with long half-lives of 61 d (inhalation) and 66 d (instillation). After day 2 post-instillation, less than 2% Cd could be lavaged out of the lungs. Maxima of 54% and 13% of instilled Cd eventually reached liver and kidney respectively. Analysis here of the instillation data gave $f_r = 0.55$; $s_r = 1$ d^{-1}; $s_s = 0.006$ d^{-1} and assignment to Type M.

(477) Glaser et al. (1986) determined the retention of stable cadmium in lungs, liver and kidney of rats after a month of chronic inhalation of cadmium chloride, cadmium oxide and cadmium sulphide aerosols, and two months after the end of exposure. At the end of the inhalation period, lung cytosolic Cd was not preferentially bound to metallothionein but this changed 2 months later, when 70-86% of the cytosolic Cd was measured to be bound to metallothionein. Analysis here of the $CdCl_2$ data indicated absorption of about 30% of deposited Cd and assignment to Type M.

(478) Oberdörster et al. (1987) determined the pulmonary retention of Cd in two female Macaca fascicularis monkeys up to 650 d after inhalation of $^{109}CdCl_2$ via endotracheal tubes, by in vivo lung and renal measurement. Lung retention showed T_b of 736 and 964 d while the kidney content steadily increased. A third monkey inhaled ^{115m}CdO and was followed for 240 d. ^{115m}Cd lung retention showed a half-life of 637 d while ^{115m}Cd in the kidney showed a steady state level after about day 50. Autoradiographic measurements in the interstitium of the lung showed that interstitial macrophages carried the highest amount of label, whereas alveolar epithelial cells showed less activity. Analysis here of the ^{109}Cd data suggested $f_r = 0.7$; s_r about 100 d^{-1} and $s_s < 0.0001$ d^{-1}, which would be consistent with Type M behaviour.

b. Cadmium carbonate ($CdCO_3$)

(479) Rusch et al. (1986) studied the distribution and excretion of cadmium in rats over a month after inhalation of cadmium carbonate ($CdCO_3$) and two insoluble Cd pigments (see below). Cd blood levels indicated that Cd was absorbed to a greater degree from $CdCO_3$ than from the pigments. The levels of Cd in the liver and kidney were much higher following exposure to the carbonate than following exposure to the pigments. Analysis here of the $CdCO_3$ data gave $f_r = 0.2$; $s_r = 10$ d^{-1}; $s_s = 0.007$ d^{-1} and assignment to Type M.

c. Cadmium telluride (CdTe)

(480) Morgan et al. (1997) measured the absorption and distribution of Cd over 4 weeks after intratracheal instillation of cadmium telluride (CdTe) by rats. Cd and Te levels decreased significantly in the lungs after exposure and concomitant increases in Cd levels were detected in spleen, kidney, femur and liver. Analysis here of the Cd data gave $f_r = 0.4$; $s_r = 2$ d^{-1}; $s_s = 0.02$ d^{-1} and assignment to Type M.

d. Cadmium oxide (CdO)

(481) Barret et al. (1947) generated cadmium oxide fumes with an electric arc striking metallic cadmium and groups of mice, rats, guinea pigs, rabbits, dogs and monkeys were exposed to the fume for 10-30 min. A lung fractional retention of 5-20% inhaled Cd was estimated at the time of death, from 1 h to 44 d post exposure. For animals exposed to similar concentrations of fume, the authors noted no significant difference in the Cd content of the lungs related to time after inhalation or to animal species. Although no temporal pattern was evident, appreciable amounts of cadmium were found in liver and kidney, with concentrations comparable to that of the lung for monkeys, indicating significant absorption.

(482) Boisset et al. (1978) measured the stable cadmium content of lungs, liver and kidney in unexposed control rats and for 3 months after repeated exposures to CdO particles. 12% of inhaled Cd was deposited in lungs and cleared with $T_b = 56$ d while a slight but statistically significant accumulation was seen in kidney and liver. The authors considered that 60% of the lung-deposited Cd was absorbed. The difference in lung and systemic Cd content between exposed rats and controls was assessed here to be consistent with $f_r = 0.2$; $s_r = 3$ d^{-1}; $s_s = 0.008$ d^{-1}; indicating assignment to Type M.

(483) As explained above, Oberdörster et al. (1979) observed the clearance of Cd from rat lungs for 100 d after inhalation of CdO and $CdCl_2$. After an initial phase of rapid clearance, CdO lung retention beyond day 8 could be described by a mono-exponential curve with $T_b = 67$ d. About 10% of the lung Cd appeared in liver and kidney. Analysis here of the CdO data gave $f_r = 0.1$; $s_r = 1$ d^{-1}; $s_s = 0.0055$ d^{-1} and assignment to Type M.

(484) Hadley et al. (1980) studied the pulmonary absorption of Cd in rats for two weeks after intratracheal instillation of micrometric particles of ^{109}CdO. The half-life of ^{109}Cd in lungs was about 4 h, at which time nearly 40% of the ^{109}Cd body burden was in the liver. Less than 10% of the instilled ^{109}Cd was excreted in either urine or faeces during two weeks. Analysis here gave $f_r = 0.7$; $s_r = 3.5$ d^{-1}; $s_s = 0.027$ d^{-1} indicating borderline Type F – Type M behaviour.

(485) Rhoads and Sanders (1985) studied the lung clearance and translocation of the oxides of eight elements, including Cd, over two weeks after deposition in rat lung. After intratracheal instillation, 50% ILD of cadmium was cleared in 8 h. The Cd liver concentration peaked at about 60% initial alveolar deposit (IAD) by 7 d and decreased slowly thereafter. The activity in the kidney was about 8% IAD and increasing at the end of the study. Only 10% of the instilled activity had been excreted at 2 weeks, largely in faeces. Analysis here of the CdO data gave $f_r = 0.75$; $s_r = 5$ d^{-1}; $s_s = 0.005$ d^{-1} and assignment to Type M.

(486) As mentioned above, Glaser et al. (1986) determined the distribution of Cd after a month of chronic inhalation of $CdCl_2$, CdO and CdS and at two months after the end of exposure. The results indicate rapid absorption of CdO in the order of 50%, about twice that of the chloride and sulphide, and are consistent with assignment to Type M.

e. Cadmium sulphide (CdS)

(487) Analysis here of the cadmium sulphide data from Glaser et al. (1986) indicated absorption of about 30% of deposited Cd and assignment to Type M.

f. Insoluble pigments

(488) As mentioned above, Rusch et al. (1986) studied the distribution and excretion of Cd in rats over a month after inhalation of $CdCO_3$ and two highly insoluble cadmium pigments (finely divided red and yellow powders of Cd, Se, S and Zn in hexagonal form produced by high temperature calcination). Cd blood levels indicated that Cd from $CdCO_3$ was absorbed to a greater degree than Cd from the pigments. The major route of Cd elimination was through faeces with 80% being cleared within 24 h, whereas much lower amounts were eliminated in the faeces of the $CdCO_3$-exposed rats. Analysis here of the data for the insoluble Cd pigments gave $f_r = 0.001 – 0.002$ and $s_s < 5 \times 10^{-4}$ d^{-1}, consistent with Type S behaviour.

g. Unspecified forms

(489) Edvardsson (1971) followed by whole-body measurements during two months the elimination of ^{115}Cd and ^{115m}Cd by workers who had been contaminated while repacking an irradiated sample. A urine sample was taken 3 d after the incident from the most contaminated person. In the two most contaminated persons, ^{115m}Cd was eliminated with two components of T_b 1.8 and 34 d, and 0.8 and 12 d respectively. The low urinary excretion measured was considered here to rule out absorption type F.

(490) Nordberg et al. (1985) reviewed the studies comparing the increased body burden of cadmium among smokers and estimates of the total inhaled amount of Cd from the cigarette smoke: Friberg et al. (1974) calculated long-term body retentions of 27 to 54% from data of Lewis et al. (1972) and suggested that absorption would be higher than this retention. Elinder et al (1976) used autopsy data from Swedish smokers to estimate respiratory absorption to be about 45%. The 10 times ratio between concentrations of Cd in the blood of Swedish smokers and non-smokers determined by Elinder et al. (1983) would indicate almost complete absorption of Cd inhaled from cigarettes.

26.2.1.3. Rapid dissolution rate for cadmium

(491) Although data are available to estimate the rapid dissolution rate of cadmium in particulate form, the values obtained here are not different enough from general default values to justify adopting element specific values.

26.2.1.4. Extent of binding of cadmium to the respiratory tract

(492) There is substantial retention of Cd in the lungs following deposition of soluble forms such as chloride. In the study by Oberdörster et al. (1979), water soluble $CdCl_2$ was retained in rat lung with a similar retention half-life of about two months as the insoluble CdO. This was interpreted by Oberdörster (1988) as the consequence of the chemical binding of dissolved Cd to lung tissues. This interpretation is supported by the observation of the small fractions (a few percent) of Cd removed by lavage of lung tissues (Henderson et al., 1979; Oberdörster et al., 1980).

(493) An alternative explanation of the relatively long Cd retention following deposition of soluble forms is the formation of particles, such as colloids or aggregates, within lung fluids.

These would be subject to particle transport and the retention T_b of about two months is indeed very similar to that expected for insoluble particles in rat lung over the same period. Moreover, Oberdörster et al. (1987) observed much longer retention half-lives, around 2 years, of Cd in monkey lung then in rat lung after inhalation of either $CdCl_2$ or CdO than could be explained by the different particle transport rates in the two species. Finally, lung autoradiography showed that interstitial macrophages carried the highest Cd amount, whereas alveolar epithelial cells showed less activity. This would also be more consistent with Cd in phagocyted particles than in the bound state.

(494) In view of these observations it was assumed here that unabsorbed cadmium was predominantly cleared by particle transport, and that cadmium was retained in the lungs in particulate form, rather than in the bound state. Adequate fits to data were obtained here on that assumption. It is therefore assumed that the bound state can be neglected for cadmium (i.e. f_b = 0.0).

(495) Note that no evidence was found for binding of cadmium in the conducting airways (extrathoracic, bronchial and bronchiolar regions). Hence if a bound state had been assumed here, it would have been applied only in the alveolar-interstitial region (AI) and thoracic lymph nodes (LN_{TH}). The source regions in AI and LN_{TH} are the same for particulate and bound activity, and therefore the equivalent lung doses are the same whether the retained activity is assumed to be particulate or bound. There would be some difference in the route of clearance and hence doses to other organs.

26.2.2. Ingestion

(496) The United States Agency for Toxic Substances and Disease Registry (ATSDR, 2012a) reviewed studies of cadmium absorption, estimated from 1 to 11% from the retention of cadmium in the bodies of humans following ingestion of radioactive cadmium. From dietary balance studies, the average normal gastrointestinal absorption of ingested cadmium in humans ranged from 3 to 7% (WHO, 2011a; ATSDR, 2012a). The Joint Food and Agriculture Organization /World Health Organization of the United Nations Expert Committee on Food Additives (JEFCA, 2001) considered the overall point estimate of 5% for bioavailability to be appropriate. The bioavailability of cadmium can be affected markedly by nutritional factors. Low iron status, as determined from serum ferritin levels, increases the uptake of cadmium from the gastrointestinal tract in the range from 5 to 10%.

(497) Most estimates of cadmium absorption in animals are somewhat lower than the values found from human studies. In rats, cadmium sulphide and cadmium sulphoselenide appear to be absorbed much less than cadmium chloride. The presence of divalent and trivalent cations, such as calcium, chromium, magnesium and zinc, may also decrease cadmium uptake. On the opposite, diets low in iron or calcium increase cadmium absorption.

(498) Ingestion of isotopes of cadmium by workers was considered in *Publications 30* and *68* (ICRP, 1980, 1994a). The f_1 value adopted for ingestion of inorganic forms of cadmium was 0.05 on the basis of animal studies. In this publication, the f_A value of 0.05 is recommended for all situations where specific information is not available.

26.2.3. Systemic distribution, retention and excretion of cadmium

26.2.3.1. Biokinetic data

(499) The biokinetics of cadmium (Cd) has been studied frequently in human subjects and laboratory animals due to its importance as an industrial and environmental toxicant. Absorbed

cadmium is distributed throughout the body, with highest concentrations in the liver and kidneys (Zhu et al., 2010; ATSDR, 2012a;). In a worker exposed to cadmium dust, highest concentrations were found in the liver, kidneys, pancreas, and vertebrae (Friberg, 1984). In workers dying from cadmium inhalation, the concentration of cadmium in lung tissue was lower than in liver or kidney (ATSDR, 2012a).

(500) Cadmium is in Group IIB of the periodic table, below the chemically similar element zinc (Zn). Cadmium is commonly found in zinc ores. Cadmium and zinc have the same valence (2+) in their stable form, but zinc is more stable in its divalent state and unlike cadmium does not undergo redox changes. In contrast to zinc, cadmium is not homeostatically controlled by the body and appears to have no essential physiological role. However, cadmium bears some physiological resemblance to zinc. In the mammalian body, cadmium and zinc bind preferentially to the same proteins and compete for uptake by many of the same cells and binding to the same intracellular sites. Cadmium can replace zinc in several biological processes. The toxic effects of cadmium appear to result in part from interactions with zinc at the stage of zinc biological function (Cotzias et al., 1961; Brzoska and Moniuszko-Jakoniuk, 2001).

(501) Systemic cadmium enters the urinary bladder and intestines much more slowly than zinc and hence has a much longer residence time than zinc in the body. A biological half-time on the order of 25 y has been estimated for cadmium (ICRP, 1980; Thorne et al., 1986).

(502) Zhu et al. (2010) measured concentrations of cadmium in 17 tissues obtained from autopsies of up to 68 Chinese men from four areas of China. All subjects were considered healthy until the time of sudden accidental death. Based on median cadmium concentrations in tissues and reference tissue masses, about 30% of total-body cadmium was contained in the kidneys, 24% in liver, 12% in muscle, 11% in bone, 9% in lung, and 14% in other tissues and fluids.

(503) The distribution of cadmium in laboratory animals resembles that found in humans, with highest concentrations in the liver and kidneys. Similar concentrations are found in liver and kidneys at early times, but during prolonged exposure the concentration in the kidneys exceeds that in the liver except for very high exposure (ATSDR, 2012a).

(504) The kidney is the primary target organ for chronic exposure to cadmium. Long-term exposure to cadmium may result in various levels of kidney damage from minor tubular dysfunction to severe kidney impairment. Absorbed cadmium is transported to the liver, where it stimulates synthesis of metallothionein. Cadmium bound to metallothionein is subsequently transported to the kidneys. A portion of the cadmium filtered by the kidneys and a portion of cadmium stored in kidney tissue is excreted in urine. Over time urinary cadmium becomes closely related to the kidney content (Friberg, 1984).

(505) Jarup et al. (1983) estimated the biological half-time of cadmium in blood based on measurements over 10-13 y of blood cadmium in five persons with previous occupational exposure to cadmium. The collected data were fit by a bi-exponential function. The estimated half-times ranged from 75-128 d for the short-term component and 7.4-16 y for the long-term component.

26.2.3.2. Biokinetic model for systemic cadmium

(506) The structure of the biokinetic model for systemic cadmium applied in this publication is shown in Fig. 26.1. Transfer coefficients are listed in Table 26.3.

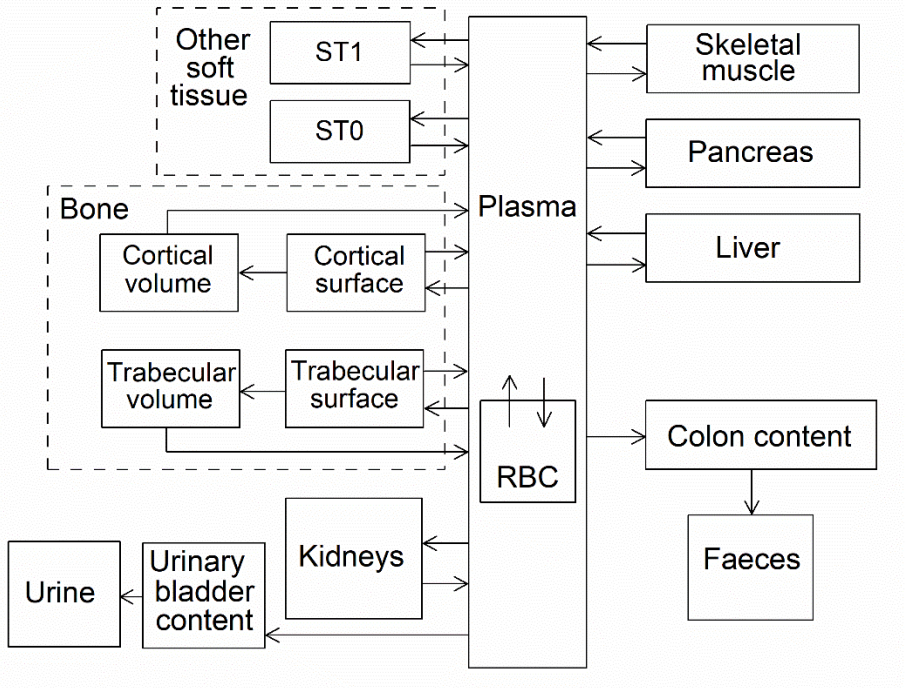

Fig. 26.1. Structure of the biokinetic model for systemic cadmium.

(507) This model is a modification of the model for zinc applied in Part 2 of this publication series (ICRP, 2016). The models for cadmium and zinc differ in the following ways: the total outflow rate from plasma is three times greater for cadmium than for zinc; uptake by red blood cells is lower for cadmium than zinc; the net excretion rate is much lower for cadmium than for zinc; and rates of return from peripheral systemic compartments to the central compartment (plasma) are much lower for cadmium than for zinc. Also, some structural simplifications of the model for zinc are made for application to cadmium in view of the more limited biokinetic data for cadmium. The number of compartments of Other tissue is reduced from three to two, and fewer excretion pathways are depicted.

(508) The transfer coefficients in the cadmium model were designed to reproduce the following information or assumptions: the initial systemic distribution of cadmium as indicated by studies on laboratory animals; a retention half-time of ~25 y in the total body; the long-term distribution of stable cadmium in the body as indicated by a recently published study of element contents in tissues of adult males (Zhu et al., 2010); and typical steady-state contents of stable cadmium in total body, blood, and urine of adult humans. Comparison of model predictions with the observed steady-state contents of stable cadmium in tissues was based on a reference gastrointestinal absorption fraction of 0.05 and a reference dietary intake of 15 μg Cd per day (ATSDR, 2012a).

26.2.3.3. Treatment of progeny

(509) Progeny of cadmium addressed in this publication are radioisotopes of cadmium, tin, indium, and silver. The model for cadmium as a parent is applied to cadmium as a progeny of cadmium. The models for tin, indium, and silver as cadmium progeny are expansions of the characteristic models for these elements with added compartments and associated transfer coefficients needed to solve the linked biokinetic models for chains headed by cadmium (see Annex B). The following transfer rates to the central blood compartment in the model for tin, indium, or silver are assigned to these progeny when produced in a compartment of a model for

a preceding chain member that is not contained in the model for tin, indium, or silver: 1000 d^{-1} if produced in a blood compartment; at the rate of bone turnover if produced in a bone volume compartment; and at the following element-specific rates if produced in any other compartment: tin, 0.139 d^{-1}; indium, 2.37 d^{-1}; silver, 0.4 d^{-1}. Other transfers added to the characteristic models for progeny are as follows: for tin, blood to muscle = 0.297 d^{-1}, blood to pancreas = 0.0012 d^{-1}, blood to red marrow = 0.012 d^{-1}; for indium, blood to muscle = 0.2 d^{-1}, blood to pancreas = 0.001 d^{-1}; for silver, blood to muscle = 5.8 d^{-1}, blood to pancreas =0.028 d^{-1}.

Table 26.3. Transfer coefficients in the biokinetic model for systemic cadmium.

From	To	Transfer coefficients (d^{-1})
Plasma	Liver	180
Plasma	Kidneys	12
Plasma	Pancreas	9.00
Plasma	Muscle	6.0
Plasma	RBC	0.1
Plasma	ST0	120
Plasma	ST1	94.5
Plasma	Urinary bladder content	1.5
Plasma	Right colon content	1.5
Plasma	Trabecular bone surface	0.45
Plasma	Cortical bone surface	0.9
Liver	Plasma	0.018
Kidneys	Plasma	0.0008
Pancreas	Plasma	0.018
Muscle	Plasma	0.0011
RBC	Plasma	0.00833
ST0	Plasma	0.5
ST1	Plasma	0.017
Trabecular bone surface	Plasma	0.0002
Cortical bone surface	Plasma	0.0002
Trabecular bone surface	Trabecular bone volume	0.00001
Cortical bone surface	Trabecular bone volume	0.00001
Trabecular bone volume	Plasma	0.000493
Cortical bone volume	Plasma	0.0000821

26.3. Individual monitoring

26.3.1. ^{109}Cd

(510) Measurements of ^{109}Cd in urine may be used to determine intakes of the radionuclide.

Table 26.4. Monitoring techniques for ^{109}Cd.

Isotope	Monitoring Technique	Method of Measurement	Typical Detection Limit
^{109}Cd	Urine Bioassay	γ-ray spectrometry[a]	19 Bq L^{-1}
^{109}Cd	Whole-body measurement	γ-ray spectrometry[ab]	110 Bq

[a] Measurement system comprised of Germanium Detectors
[b] Counting time of 20 minutes

26.4. Dosimetric data for cadmium

Table 26.5. Committed effective dose coefficients (Sv Bq^{-1}) for the inhalation or ingestion of ^{109}Cd compounds.

Inhaled particulate materials (5 µm AMAD aerosols)	Effective dose coefficients (Sv Bq^{-1})
	^{109}Cd
Type F, — NB: Type F should not be assumed without evidence	4.7E-09
Type M, oxide, chloride, sulphide, carbonate, telluride, all unspecified forms	1.9E-09
Type S	2.8E-09
Ingested materials	
All forms	1.0E-09

AMAD, activity median aerodynamic diameter

Table 26.6. Dose per activity content of ^{109}Cd in total body and in daily excretion of urine (Sv Bq^{-1}); 5µm activity median aerodynamic diameter aerosols inhaled by a reference worker at light work.

	Type F		Type M		Type S	
Time after intake (d)	Total body	Urine	Total body	Urine	Total body	Urine
1	7.3E-09	5.3E-06	3.1E-09	2.3E-05	4.6E-09	6.8E-04
2	1.1E-08	3.5E-05	5.7E-09	1.2E-04	8.5E-09	3.5E-03
3	1.5E-08	6.3E-05	1.2E-08	2.2E-04	1.8E-08	6.9E-03
4	1.8E-08	8.5E-05	2.0E-08	2.9E-04	3.3E-08	9.2E-03
5	1.9E-08	1.1E-04	2.5E-08	3.5E-04	4.3E-08	1.1E-02
6	2.0E-08	1.3E-04	2.7E-08	4.1E-04	4.7E-08	1.3E-02
7	2.0E-08	1.5E-04	2.8E-08	4.6E-04	4.9E-08	1.5E-02
8	2.0E-08	1.7E-04	2.8E-08	5.0E-04	5.0E-08	1.7E-02
9	2.0E-08	1.9E-04	2.9E-08	5.4E-04	5.0E-08	1.9E-02
10	2.0E-08	2.1E-04	2.9E-08	5.7E-04	5.1E-08	2.0E-02
15	2.0E-08	2.4E-04	3.0E-08	6.3E-04	5.3E-08	2.3E-02
30	2.1E-08	2.6E-04	3.1E-08	6.4E-04	5.7E-08	2.3E-02
45	2.1E-08	2.7E-04	3.2E-08	6.4E-04	6.0E-08	2.3E-02
60	2.2E-08	2.8E-04	3.4E-08	6.4E-04	6.3E-08	2.3E-02
90	2.3E-08	3.1E-04	3.6E-08	6.5E-04	6.9E-08	2.3E-02
180	2.6E-08	3.9E-04	4.4E-08	7.3E-04	9.2E-08	2.4E-02
365	3.6E-08	6.1E-04	6.1E-08	1.0E-03	1.5E-07	2.8E-02

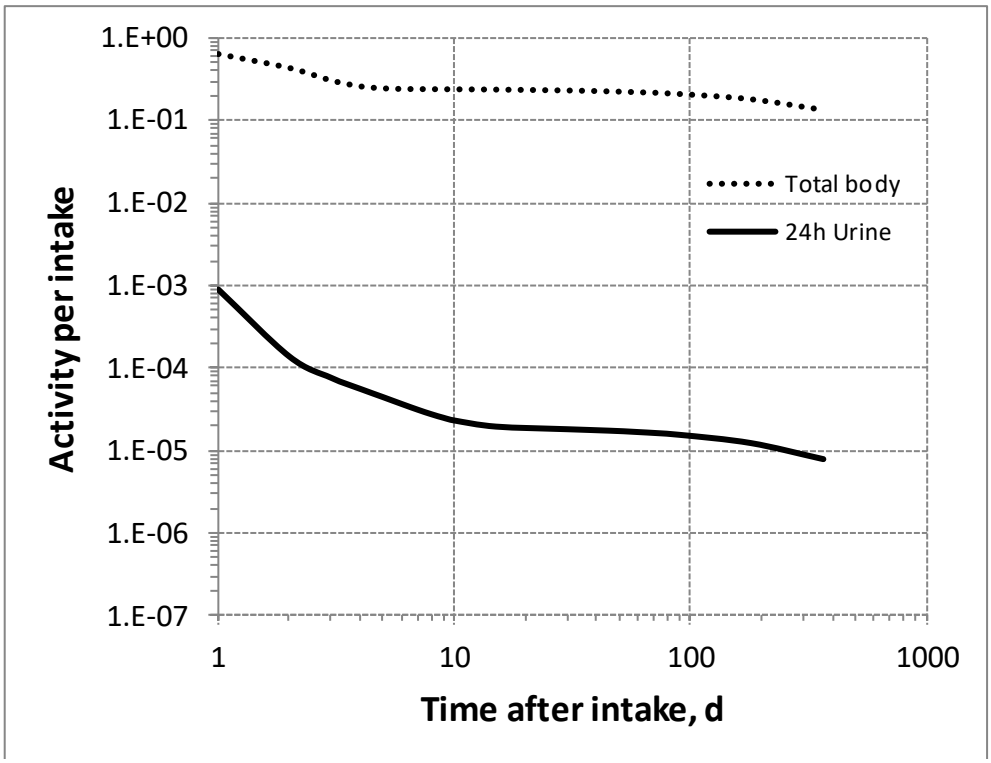

Fig. 26.2. Daily excretion of ^{109}Cd following inhalation of 1 Bq Type F.

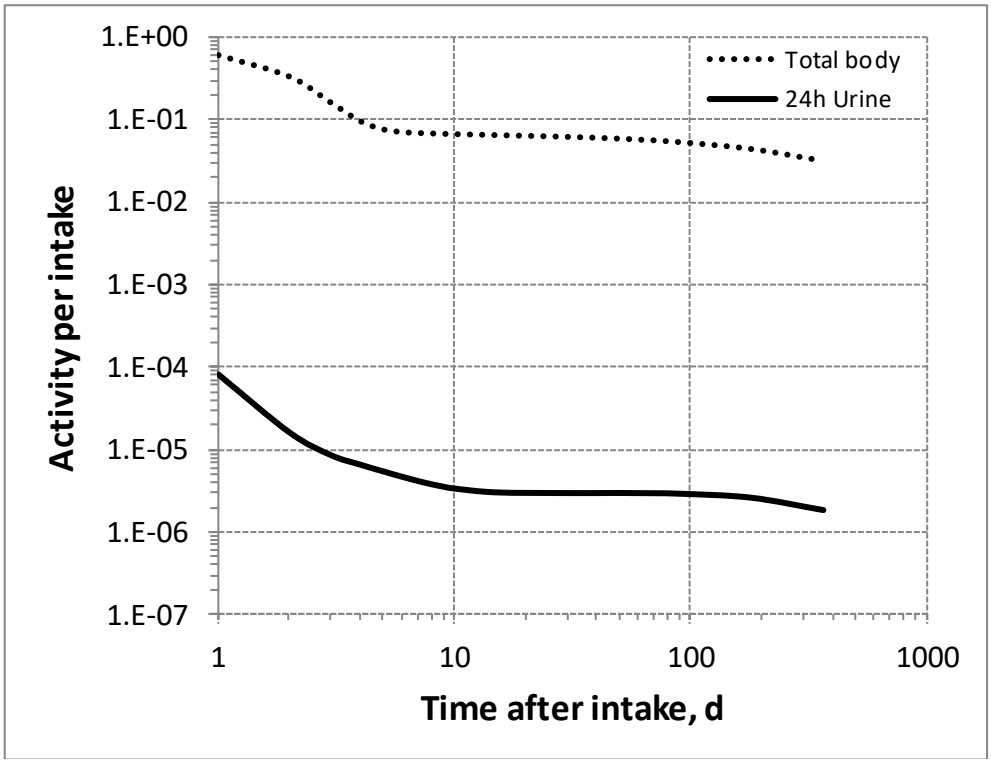

Fig. 26.3. Daily excretion of ^{109}Cd following inhalation of 1 Bq Type M.

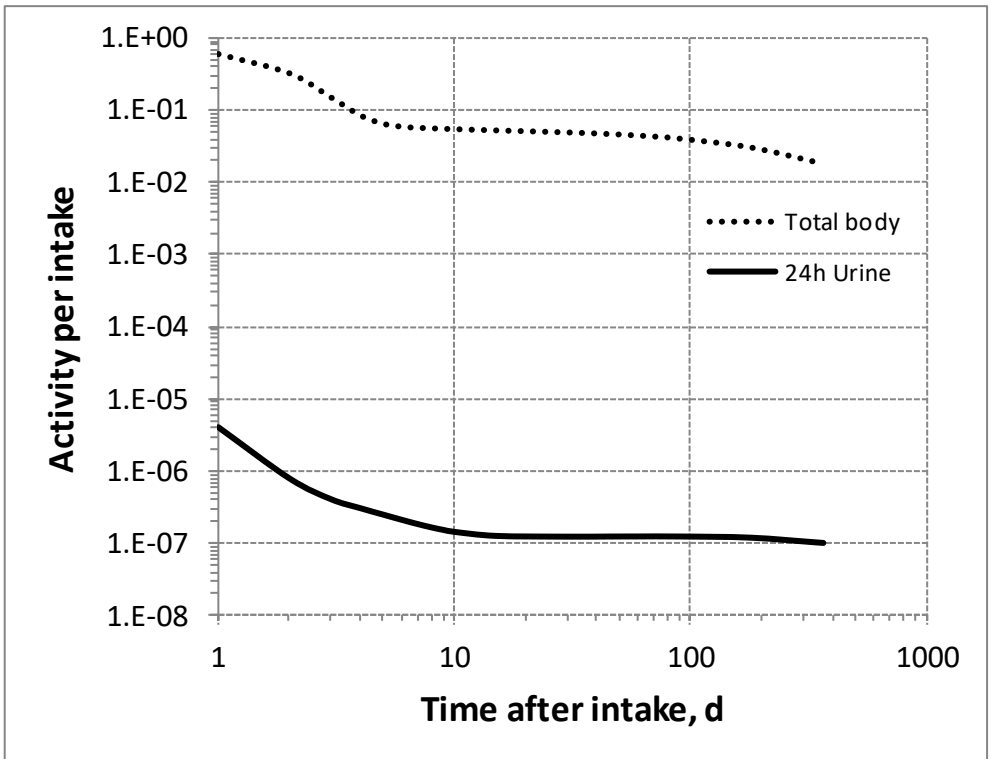

Fig. 26.4. Daily excretion of ^{109}Cd following inhalation of 1 Bq Type S.

27. INDIUM (Z=49)

27.1. Isotopes

Table 27.1. Isotopes of indium addressed in this publication.

Isotope	Physical half-life	Decay mode
^{107}In	32.4 min	EC, B+
^{108m}In	39.6 min	EC, B+
^{108}In	58.0 min	EC, B+
^{109}In	4.2 h	EC, B+
^{110m}In	69.1 min	EC, B+
^{110}In	4.9 h	EC, B+
^{111}In*	2.8047 d	EC
^{112m}In	20.56 min	IT
^{112}In	14.97 min	EC, B+, B-
^{113m}In	1.6579 h	IT
^{114m}In	49.51 d	IT, EC
^{115m}In	4.486 h	IT, B-
^{115}In	4.41E+14 y	B-
^{116m}In	54.41 min	B-
^{117m}In	116.2 min	B-, IT
^{117}In	43.2 min	B-
^{119m}In	18.0 min	B-, IT

EC, electron-capture decay; B+, beta-plus decay; B-, beta-minus decay; IT, isomeric transition decay.
*Dose coefficients and bioassay data for this radionuclide are given in the printed copy of this publication.
Data for other radionuclides listed in this table are given in the online electronic files on the ICRP website.

27.2. Routes of Intake

27.2.1. Inhalation

(511) For indium, default parameter values were adopted on absorption to blood from the respiratory tract (ICRP, 2015). Absorption parameter values and types, and associated f_A values for particulate forms of indium are given in Table 27.2.

27.2.2. Ingestion

(512) Experiments on rats (Smith et al., 1960) indicated a fractional absorption from the gastrointestinal tract of no more than about 2%, likely about 0.5%, of indium trichloride diluted with water. Valberg et al. (1981) confirmed in mice that indium chloride is poorly absorbed, less than 0.5%, after a single oral administration. Toxicity studies (Castronovo and Wagner, 1971) have shown that the toxicity of orally administered indium is much less than the toxicity of indium administered intravenously. In nuclear medicine, Coates et al. (1973) detected no ^{113m}In activity in blood samples of patients having ingested 500 μCi of the radionuclide as chloride in food, indicating very low absorption if any. Kabe et al. (1996) observed a large in vitro solubility of indium phosphide (InP) powder in synthetic gastric fluid. In adult male rats, 0.7% of a single InP oral dose was absorbed and retained in tissues or excreted in urine after 24 h (Zheng et al., 1994). Van Hulle et al. (2005) studied the biokinetics of indium arsenide (InAs)

after subcutaneous and oral administration: in vitro, only 1.3% of an InAs suspension dissolved after 48 h in simulated gastric fluid and no dissolution was observed in simulated intestinal fluid. In vivo, gastrointestinal absorption in rats was less than 1%. Asakura et al. (2008) observed no toxicity of indium metal administered orally to rats with a single dosage of 2 g kg^{-1} or a repeated oral dose of 1 g kg^{-1} daily for 28 d. Andersen et al. (2017) studied the in vitro dissolution of indium-tin oxide (ITO) powder in simulated gastric environment and observed the release of less than 0.1% indium from the ITO powder over 4 h. After 60 d of mouse gavage with metal salts of bismuth, indium and ruthenium, Laval et al. (2018) observed similar ratios of In^{3+} and Bi^{3+} concentration in serum to the orally given amount.

(513) f_1 was taken to be 0.02 for all compounds of indium in *Publications 30* and *68* (ICRP, 1980, 1994a). In view of the current database, a lower value of $f_A = 0.005$ is adopted in this publication for all forms of indium, acknowledging it could be even lower for insoluble compounds like indium-tin oxide.

Table 27.2. Absorption parameter values for inhaled and ingested indium.

	Absorption parameter values*			Absorption from the
Inhaled particulate materials	f_r	s_r (d^{-1})	s_s (d^{-1})	alimentary tract, f_A
Default parameter values†				
Absorption type				
F	1	30	–	0.005
M‡	0.2	3	0.005	0.001
S	0.01	3	1×10^{-4}	5×10^{-5}
Ingested materials§				
All forms				0.005

*It is assumed that the bound state can be neglected for indium (i.e. $f_b = 0$). The values of s_r for Type F, M and S forms of indium (30, 3 and 3 d^{-1} respectively) are the general default values.

†For inhaled material deposited in the respiratory tract and subsequently cleared by particle transport to the alimentary tract, the default f_A values for inhaled materials are applied [i.e. the product of f_r for the absorption type and the f_A value for ingested soluble forms of indium (0.005)].

‡Default Type M is recommended for use in the absence of specific information on which the exposure material can be assigned to an absorption type (e.g. if the form is unknown, or if the form is known but there is no information available on the absorption of that form from the respiratory tract). For guidance on the use of specific information, see Section 1.1.

§Activity transferred from systemic compartments into segments of the alimentary tract is assumed to be subject to reabsorption to blood. The default absorption fraction f_A for the secreted activity is the highest value for any form of the radionuclide ($f_A = 0.005$).

27.2.3. Systemic distribution, retention and excretion of indium

27.2.3.1. Biokinetic data

(514) Most biokinetic studies of indium in human subjects and laboratory animals have involved the administration of InCl, InAs, or In(III), all of which form strong complexes with the iron-transport protein transferrin. This results in some similarities in sites of deposition of indium and iron. Due to chemical differences between indium and iron, however, transferrin-bound indium follows only a portion of the iron distribution pathway and, overall, distributes differently from iron. The biokinetics of indium oxide, another common form of indium, is not well established but appears to differ from that of InCl, InAs, or In(III).

(515) In a study of 15 patients used as a relatively healthy control group, transferrin-bound ^{111}In cleared from plasma with a half-time of about 10.5 h (Simonsen et al., 2009). This is consistent with data of Goodwin et al. (1971) involving 8 patients, which indicates a half-time

of ~10 h. Uptake of indium by red blood cells has been observed in studies on dogs (McIntyre et al., 1974) and rats (Jönsson, 1991).

(516) Largely qualitative results of human studies of the systemic behaviour of indium indicate substantial uptake by liver and bone marrow (McNeil et al., 1974; Sayle et al., 1982; Datz and Taylor, 1985). McNiel et al. (1974) found that neither the retention nor the distribution of indium in the liver changed between 1 and 2 d post injection. In studies on rats, mice, and hamsters, 11-14 % of the injected indium accumulated in the liver (Castronovo Jr and Wagner Jr, 1973; McIntyre et al., 1974; Jönsson, 1991; Yamauchi et al., 1992) and was gradually removed in faeces. About 10-12% of injected indium was retained in bone marrow (Smith et al., 1960; Beamish and Brown, 1974; McIntyre et al., 1974; Jeffcoat et al., 1978; Jönsson, 1991). Some indium is removed from the body in urine, but faecal excretion appears to be the dominant excretion pathway.

(517) There are some indications from human studies of elevated deposition of indium in bone and spleen. However, it is generally difficult to differentiate between uptake by bone and bone marrow in the external images, and uptake data for the spleen are sparse and not definitive.

(518) Indium is removed slowly from the human body. Simonsen et al. (2009) estimated that only 1.8 ± 1.3% of indium entering blood was excreted over the first 4 d.

(519) The reader is referred to Andersson et al. (2017) for a more detailed review of information on the systemic behaviour of indium in human subjects and laboratory animals.

27.2.3.2. Biokinetic model for systemic indium

(520) A biokinetic model for systemic indium developed by Andersson et al. (2017) is used in this publication, together with the default transfer rates of the ICRP's Human Alimentary Tract Model and the default emptying rate of the urinary bladder content (12 d^{-1}). The reader is referred to Andersson et al. (2017) for a discussion of the bases for individual parameter values.

(521) The model structure is shown in Fig. 27.1. Transfer coefficients are listed in Table 27.3.

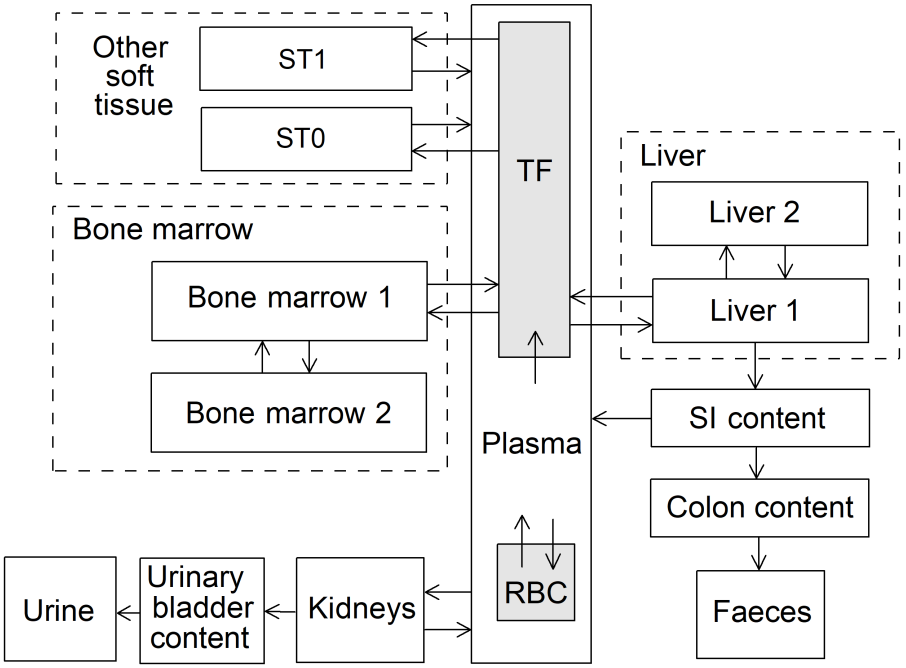

Fig. 27.1. The structure of the biokinetic model for systemic indium (from Andersson et al., 2017). TF = transferrin, RBC = red blood cells, SI = small intestine.

5208 Table 27.3. Transfer coefficients in the biokinetic model for systemic indium.

From	To	Transfer coefficient (d^{-1})
Plasma	Transferrin	83
Plasma	RBC	0.415
RBC	Plasma	0.0554
Transferrin	Bone marrow 1	0.316
Transferrin	Liver 1	0.253
Transferrin	ST1	0.427
Transferrin	ST2	0.586
Bone marrow 1	Transferrin	1.10
Bone marrow 1	Bone marrow 2	0.475
Bone marrow 2	Bone marrow 1	0.00831
Liver 1	Transferrin	0.475
Liver 1	Small intestine contents	0.110
Liver 1	Liver 2	0.554
Liver 2	Liver 1	0.00831
ST1	Plasma	2.37
ST2	Plasma	0.00475
Plasma	Kidneys	1.66
Kidneys	Plasma	0.0166
Kidneys	Urinary bladder content	0.0268

5209 *27.2.3.3. Treatment of progeny*

5210 (522) Progeny of indium addressed in this publication are radioisotopes of indium, tin, and
5211 cadmium. The model for indium as a parent is applied to indium produced by decay of another
5212 indium isotope. The models for tin and cadmium as progeny of indium are expansions of the
5213 characteristic models for these elements with added compartments and associated transfer
5214 coefficients needed to solve the linked biokinetic models for chains headed by indium (see
5215 Annex B). If produced in a compartment not explicitly named in the progeny's model (an
5216 ambiguous compartment), the progeny is assumed to transfer at a specified rate to the central
5217 blood compartment of its characteristic biokinetic model and to follow that model thereafter.
5218 The following transfer rates to the central blood compartment are assigned to tin or cadmium
5219 produced in an ambiguous compartment: 1000 d^{-1} if produced in a blood compartment; and at
5220 the following element-specific rates if produced in any other ambiguous compartment: tin, 1.39
5221 d^{-1}; cadmium, 0.5 d^{-1}. Other transfers added to the characteristic model for cadmium are blood
5222 to red marrow = 3.7 d^{-1}, red marrow to blood = 0.017 d^{-1}.

5223 ## 27.3. Individual monitoring

5224 ### 27.3.1. ^{111}In

5225 (523) Measurements of ^{111}In in urine may be used to determine intakes of the radionuclide.

5226 Table 27.4. Monitoring techniques for ^{111}In.

Isotope	Monitoring Technique	Method of Measurement	Typical Detection Limit
^{111}In	Urine Bioassay	γ-ray spectrometry[a]	1 Bq L^{-1}
^{111}In	Whole-body measurement	γ-ray spectrometry[ab]	25 Bq

5227 [a] Measurement system comprised of Germanium Detectors
5228 [b] Counting time of 20 minutes

27.4. Dosimetric data for indium

Table 27.5. Committed effective dose coefficients (Sv Bq^{-1}) for the inhalation or ingestion of ^{111}In compounds.

Inhaled particulate materials (5 µm AMAD aerosols)	Effective dose coefficients (Sv Bq^{-1})
	^{111}In
Type F, — NB: Type F should not be assumed without evidence	1.3E-10
Type M, default	1.4E-10
Type S	1.5E-10
Ingested materials	
All forms	1.5E-10

AMAD, activity median aerodynamic diameter

Table 27.6. Dose per activity content of ^{111}In in total body and in daily excretion of urine (Sv Bq^{-1}); 5µm activity median aerodynamic diameter aerosols inhaled by a reference worker at light work.

	Type F		Type M		Type S	
Time after intake (d)	Total body	Urine	Total body	Urine	Total body	Urine
1	2.5E-10	1.8E-06	3.0E-10	3.0E-05	3.1E-10	6.4E-04
2	4.9E-10	1.6E-06	7.0E-10	2.2E-05	7.4E-10	4.7E-04
3	9.2E-10	1.9E-06	1.9E-09	2.6E-05	2.0E-09	5.4E-04
4	1.4E-09	2.4E-06	4.2E-09	3.2E-05	4.7E-09	6.8E-04
5	2.0E-09	3.0E-06	6.9E-09	4.0E-05	7.8E-09	8.6E-04
6	2.6E-09	4.0E-06	9.6E-09	5.2E-05	1.1E-08	1.1E-03
7	3.3E-09	5.2E-06	1.3E-08	6.7E-05	1.4E-08	1.5E-03
8	4.3E-09	6.9E-06	1.6E-08	8.7E-05	1.9E-08	1.9E-03
9	5.5E-09	9.1E-06	2.1E-08	1.1E-04	2.4E-08	2.5E-03
10	7.0E-09	1.2E-05	2.7E-08	1.5E-04	3.2E-08	3.3E-03
15	2.4E-08	5.0E-05	9.7E-08	5.7E-04	1.1E-07	1.3E-02
30	1.0E-06	3.4E-03	4.1E-06	3.1E-02	4.8E-06	7.7E-01
45	4.1E-05	2.2E-01	1.7E-04	N/A	2.0E-04	N/A
60	1.7E-03	N/A	7.0E-03		8.4E-03	
90	N/A		N/A		N/A	
180						
365						

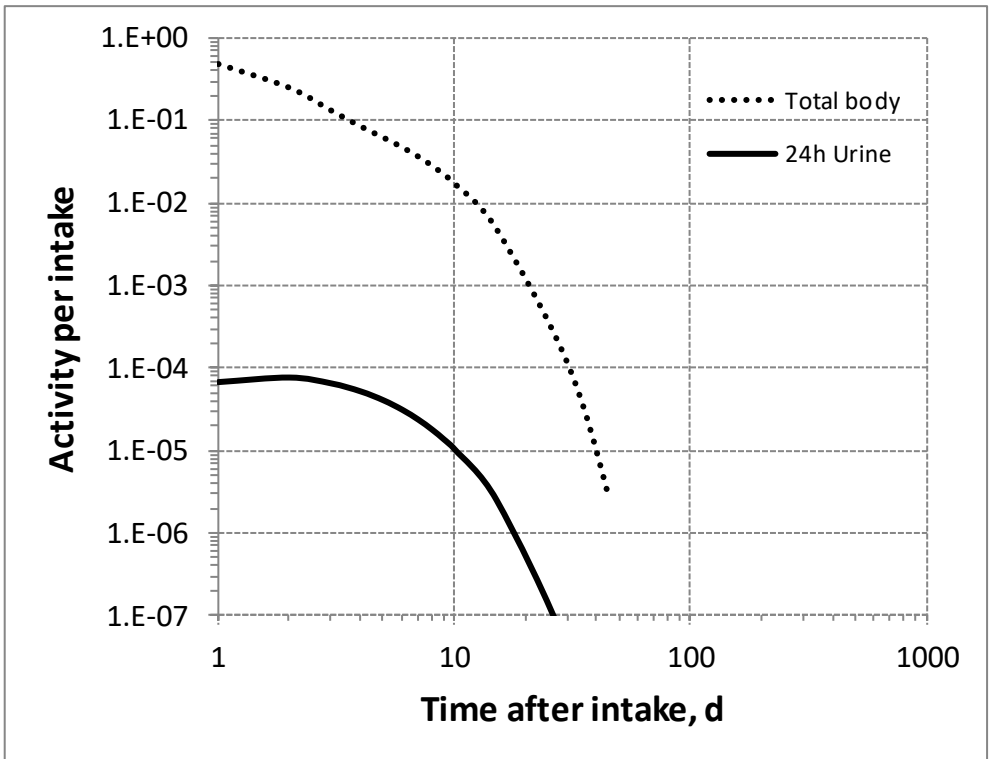

5235

5236 Fig. 27.2. Daily excretion of ^{111}In following inhalation of 1 Bq Type F.

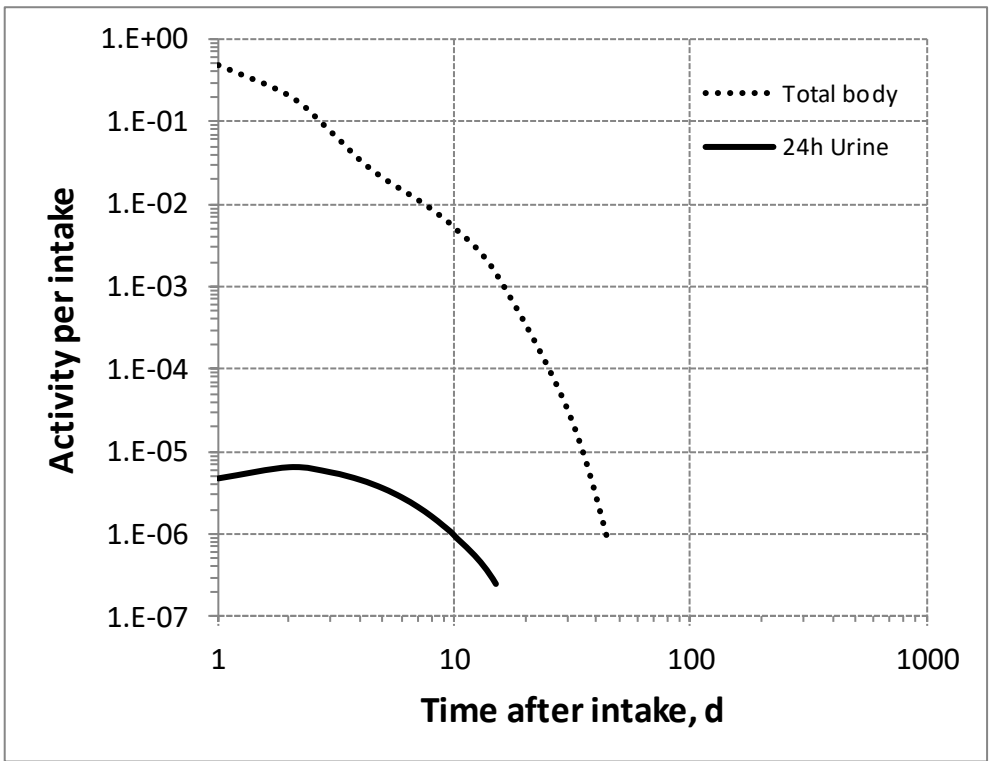

5237

5238 Fig. 27.3. Daily excretion of ^{111}In following inhalation of 1 Bq Type M.

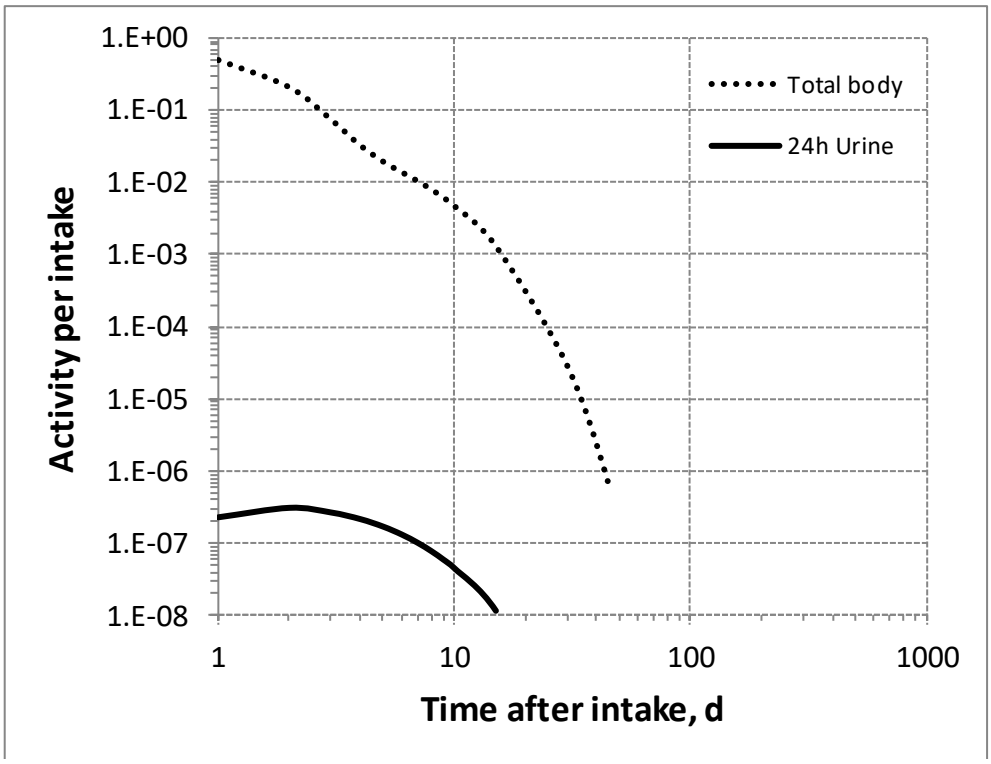

Fig. 27.4. Daily excretion of ^{111}In following inhalation of 1 Bq Type S.

28. TIN (Z=50)

28.1. Isotopes

Table 28.1. Isotopes of tin addressed in this publication.

Isotope	Physical half-life	Decay mode
^{108}Sn	10.30 min	EC, B+
^{109}Sn	18.0 min	EC, B+
^{110}Sn	4.11 h	EC
^{111}Sn	35.3 min	EC, B+
^{113m}Sn	21.4 min	IT, EC
^{113}Sn*	115.09 d	EC
^{117m}Sn	13.76 d	IT
^{119m}Sn	293.1 d	IT
^{121m}Sn	43.9 y	IT, B-
^{121}Sn	27.03 h	B-
^{123m}Sn	40.06 m	B-
^{123}Sn	129.2 d	B-
^{125}Sn	9.64 d	B-
^{126}Sn	2.30E+5 y	B-
^{127}Sn	2.10 h	B-
^{128}Sn	59.07 m	B-

EC, electron-capture decay; B+, beta-plus decay; B-, beta-minus decay; IT, isomeric transition decay.
*Dose coefficients and bioassay data for this radionuclide are given in the printed copy of this publication.
Data for other radionuclides listed in this table are given in the online electronic files on the ICRP website.

28.2. Routes of Intake

28.2.1. Inhalation

(524) For tin, default parameter values were adopted on absorption to blood from the respiratory tract (ICRP, 2015). Absorption parameter values and types, and associated f_A values for particulate forms of tin are given in Table 28.2.

28.2.2. Ingestion

(525) The fractional absorption of dietary or inorganic tin from the gastrointestinal tract is generally small (Barnes and Stoner, 1959; ICRP, 1975; Furchner and Drake, 1976; Underwood, 1977; ATSDR, 2005b). In the case of stannous chloride the fractional gastrointestinal absorption in mice, rats, rabbits, monkeys and dogs was always less than 0.1 and was typically about 0.02 (Kutzner and Brod, 1971; Furchner and Drake, 1976; Fritsch et al., 1977). The absorption of the citrate, fluoride or pyrophosphate was similar, with Sn(IV) inorganic compounds being less absorbed than those of Sn(II) (Benoy et al., 1971; Hiles, 1974).

(526) In *Publications 30* and *68* (ICRP, 1981, 1994a), f_1 was taken as 0.02 for all compounds of tin. In this publication, the value of $f_A = 0.02$ is also adopted for all chemical forms of tin ingested at the workplace.

Table 28.2. Absorption parameter values for inhaled and ingested tin.

Inhaled particulate materials	Absorption parameter values* f_r	s_r (d^{-1})	s_s (d^{-1})	Absorption from the alimentary tract, f_A
Default parameter values†				
Absorption type				
F	1	30	–	0.02
M‡	0.2	3	0.005	0.004
S	0.01	3	1×10^{-4}	2×10^{-4}
Ingested materials§				
All forms				0.02

*It is assumed that the bound state can be neglected for tin (i.e. $f_b = 0$). The values of s_r for Type F, M and S forms of tin (30, 3 and 3 d^{-1} respectively) are the general default values.

†For inhaled material deposited in the respiratory tract and subsequently cleared by particle transport to the alimentary tract, the default f_A values for inhaled materials are applied [i.e. the product of f_r for the absorption type and the f_A value for ingested soluble forms of tin (0.02)].

‡Default Type M is recommended for use in the absence of specific information on which the exposure material can be assigned to an absorption type (e.g. if the form is unknown, or if the form is known but there is no information available on the absorption of that form from the respiratory tract). For guidance on the use of specific information, see Section 1.1.

§Activity transferred from systemic compartments into segments of the alimentary tract is assumed to be subject to reabsorption to blood. The default absorption fraction f_A for the secreted activity is the highest value for any form of the radionuclide ($f_A = 0.02$).

28.2.3. Systemic distribution, retention and excretion of tin

28.2.3.1. Biokinetic data

(527) Environmental tin exists in one of two series of compounds, the stannous compounds formed by bivalent tin and the stannic compounds formed by tetravalent tin. Bivalent tin can exist in ionic form. Stannic compounds are covalent, and the ionic form of tetravalent tin does not exist. Common inorganic compounds of tin include stannous chloride ($SnCl_2$), stannous oxide (SnO), stannous fluoride (SnF_2), stannic chloride ($SnCl_4$), and stannic oxide (SnO_2). Stannic tin can form a volatile hydride (SnH_4) and toxicologically important organometallic compounds (Cima, 2011).

(528) Several investigators have reported tin concentrations in tissues collected at autopsy from non-occupationally exposed subjects. Hamilton et al. (1973) found highest concentrations in lymph nodes (1.5 mg kg^{-1} wet weight) and bone (1.1), followed by lungs (0.8), liver (0.4), and kidneys (0.2); relatively low concentrations were found in muscle (0.07) and brain (0.06). Garcia et al. (2001) determined the following mean tissue concentrations in 78 subjects: 0.47 (mg kg^{-1} wet weight) in bone, 0.27 in brain, 0.25 in kidney, 0.24 in lung, and 0.16 in liver. Tissues from 11–13 adult males had mean concentrations of 2.1 mg kg^{-1} dry weight in testes, 1.1 in liver, 0.83 in kidney cortex, 0.75 in heart, 0.45 in lung, and 0.61 in rib (Chiba et al., 1991).

(529) Zhu et al. (2010) reported median values and ranges of tin concentrations in 17 tissues collected at autopsy from up to 68 adult males. The measured concentrations generally were lower than earlier reported values for tin. The highest median concentrations were found in lung (0.031 mg kg^{-1} wet weight), liver (0.022), rib (0.013), and kidneys (0.012). Concentrations in stomach, small intestine, large intestine, heart, adrenals, testes, spleen, skin, fat, skeletal muscle, thyroid, pancreas, and thymus were in the range 0.005-0.009 mg kg^{-1}. The investigators estimated a central total-body content of 0.51 mg. Based on the observed median concentrations

of tin in tissues and reference masses of tissues, about half of total-body tin was contained in skeletal muscle plus fat and 22% was contained in bone, assuming rib is representative of bone.

(530) Hiles (1974) studied the biokinetics of inorganic tin in rats following oral or intravenous administration of ^{113}Sn(II) or ^{113}Sn(IV). About 2.85% and 0.64% of ^{113}Sn administered orally as Sn(II) and Sn(IV), respectively, was absorbed to blood. At 48 d after oral intake, the skeleton, liver, and kidneys contained about 1.0, 0.08, and 0.09%, respectively, of ^{113}Sn administered as Sn(II), and 0.24, 0.02, and 0.02%, respectively, of ^{113}Sn administered as Sn(IV), indicating similar systemic distributions of the absorbed activity for the two forms. At 48 h after intravenous administration, cumulative urinary excretion accounted for about 35% of activity administered as Sn(II) and 40% administered as Sn(IV). Cumulative faecal excretion at 48 h represented about 12% of activity administered as Sn(II) and 3% of activity administered as Sn(IV). This result, together with observations on bile-duct cannulated rats, indicated that the biliary pathway was a more important mode of excretion for Sn(II) than for Sn(IV). At 48 h after intravenous injection, the bone, liver, and kidneys contained about 35, 2.0, and 5.9%, respectively, of ^{113}Sn administered as Sn(II), and 46, 0.2, and 5.3%, respectively, of ^{113}Sn administered as Sn(IV). The difference in accumulation of activity by the liver following administration of Sn(II) and Sn(IV) suggests that these forms were not reduced to a common form over the observation period. In an experiment involving oral administration of ^{113}Sn(II) and ^{113}Sn(IV) for 6 days a week for 4 weeks, only the bone contained a higher activity concentration at 28 d than at 1 d. Over a 40-d period following the end of the 28-d feeding period, activity was lost from bone with an estimated biological half-time of 34-40 d. For comparison, Hamilton (1948) estimated a biological half-time of ^{113}Sn in bone of 3-4 months based on results of a study involving a single intravenous administration of ^{113}Sn(IV) to rats.

(531) Furchner and Drake (1976) compared the behaviour of ^{113}Sn in mice, Sprague-Dawley (S. D.) rats, African white-tailed rats (Mystromys), monkeys, and dogs following oral, intraperitoneal (IP), or intravenous (IV) administration as ^{113}Sn(II) chloride. The IP injection study involved only mice and rats. Mean total excretion over the first 3 d after IV injection was about 25% for mice, 38% for Mystromys, 45% for S. D. rats, 39% for monkeys, and 69% for dogs. Excretion over the first 3 d was primarily in urine (e.g., 84% of total excretion in monkeys and 91% in dogs). Total-body retention following IV injection was measured for periods of 291 d for rats, 319 d for Mystromys, 325 d for dogs, 338 d for mice, and 469 d for monkeys. Retention in each species could be described as a sum of four exponential terms. Retention was broadly similar across species and showed no relation to body size. As an average over the five studied species, the biological half-times of the four phases of retention for IV injection were about 0.5 d (50%), 4.3 d (13%), 28 d (9%), and 510 d (28%). The mean long-term half-time was about 760 d for mice, 580 d for Mystromys, 420 d for S. D. rats, 370 d for monkeys, and 430 d for dogs. The time-dependent distribution of systemic activity was measured in S. D. rats at 10 times from 1-141 d post IP injection. Bone contained 69% of total-body activity at 1 d, 71-76% at 6-113 d, and 65% at 141 d; muscle contained 12-20% at 1-141 d; liver contained 2.4-5.9% at 1-141 d; and kidneys contained 3.5% at 1 d, gradually decreasing to ~1% at 85-141 d.

28.2.3.2. Biokinetic model for systemic tin

(532) The structure of the biokinetic model for systemic tin applied in this publication is shown in Fig. 28.1. Transfer coefficients are listed in Table 28.3.

(533) Parameter values were set for reasonable consistency with total-body retention of tin observed in monkeys over the early months after acute input to blood, and with the early systemic distribution of tin observed in rats (Furchner and Drake, 1976). Parameter values

determining the long-term distribution of tin are set for reasonable consistency with the central systemic distribution of tin indicated by results of an autopsy study by Zhu et al. (2010).

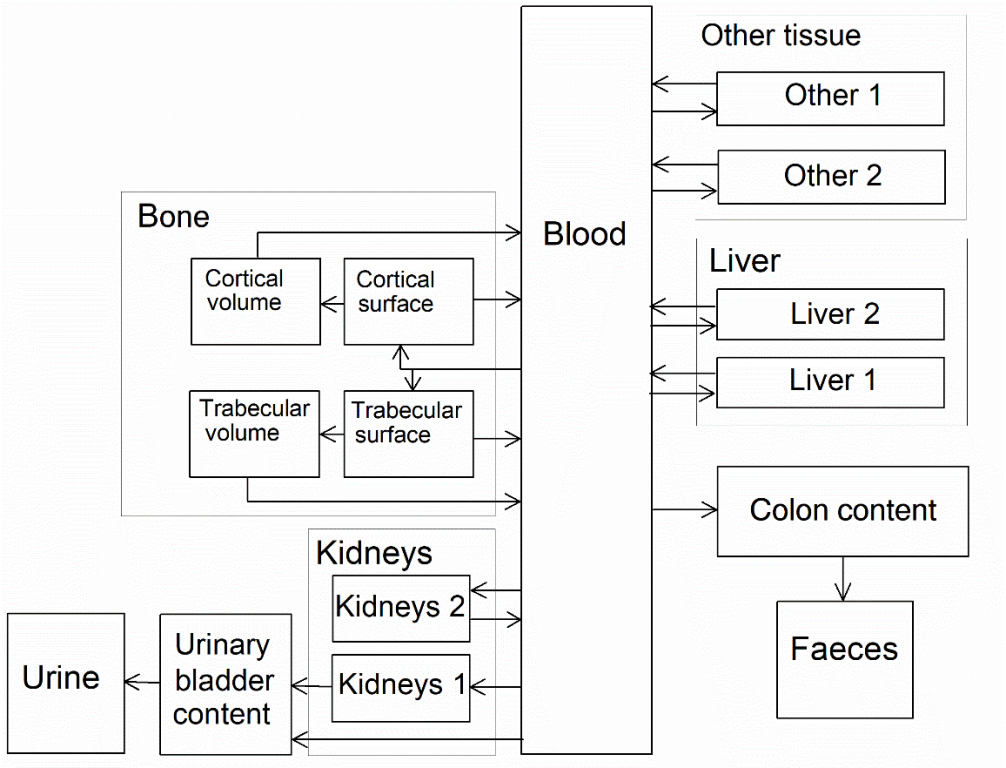

Fig. 28.1. Structure of the biokinetic model for systemic tin.

28.2.3.3. Treatment of progeny

(534) Progeny of tin addressed in this publication are isotopes of tin, indium, cadmium, tellurium, and antimony. The model for tin as a parent is applied to tin produced by decay of another isotope of tin. The models for indium, cadmium, tellurium, and antimony as progeny of tin are expansions of their characteristic models with added compartments and associated transfer coefficients needed to solve the linked biokinetic models of chains headed by tin. Muscle and pancreas were added to the explicitly identified tissues in the characteristic model for indium. The following rates of transfer of indium between blood compartments in the characteristic model for indium and the added tissues were assigned: transferrin to pancreas, 0.001 d^{-1}; transferrin to muscle, 0.2 d^{-1}; pancreas to plasma, 2.37 d^{-1}; muscle to plasma, 2.37 d^{-1}. Indium, cadmium, tellurium, or antimony produced in a compartment of the model for a preceding chain that is not a compartment in the model for that progeny (an ambiguous compartment) is assumed to transfer to the central blood compartment of the progeny's model and to follow that model thereafter.The following transfer coefficients are assigned to progeny produced in ambiguous compartments: 1000 d^{-1} if produced in a blood compartment; at the rate of bone turnover for the indicated bone type if produced in a bone volume compartment; and at the following element-specific rates if produced in any other compartment: indium, 2.37 d^{-1}; cadmium, 0.5 d^{-1}; tellurium, 0.0693 d^{-1}; antimony, 1.39 d^{-1}.

Table 28.3. Transfer coefficients in the biokinetic model for systemic tin.

From	To	Transfer coefficients (d^{-1})
Blood	Urinary bladder content	1.8

Blood	Right colon content	0.2
Blood	Trabecular bone surface	0.6
Blood	Cortical bone surface	0.6
Blood	Other 1	0.6
Blood	Other 2	1.0
Blood	Liver 1	0.075
Blood	Liver 2	0.025
Blood	Kidneys 1	0.05
Blood	Kidneys 2	0.05
Trabecular bone surface	Blood	0.035
Cortical bone surface	Blood	0.035
Trabecular bone surface	Trabecular bone volume	0.035
Cortical bone surface	Cortical bone volume	0.035
Trabecular bone volume	Blood	0.0035
Cortical bone volume	Blood	0.0035
Liver 1	Blood	0.0116
Liver 2	Blood	0.00077
Kidneys 1	Urinary bladder content	0.139
Kidneys 2	Blood	0.0116
Other 1	Blood	0.139
Other 2	Blood	0.0035

28.3. Individual monitoring

28.3.1. ^{113}Sn

(535) Measurements of ^{113}Sn in urine may be used to determine intakes of the radionuclide.

Table 28.4. Monitoring techniques for ^{113}Sn

Isotope	Monitoring Technique	Method of Measurement	Typical Detection Limit
^{113}Sn	Urine Bioassay	γ-ray spectrometry[a]	1.4 Bq L^{-1}
^{113}Sn	Whole-body measurement	γ-ray spectrometry[ab]	45 Bq

[a] Measurement system comprised of Germanium Detectors
[b] Counting time of 20 minutes

28.4. Dosimetric data for tin

Table 28.5 Committed effective dose coefficients (Sv Bq^{-1}) for the inhalation or ingestion of ^{113}Sn compounds.

Inhaled particulate materials (5 µm AMAD aerosols)	Effective dose coefficients (Sv Bq^{-1})
	^{113}Sn
Type F, — NB: Type F should not be assumed without evidence	8.7E-10
Type M, default	1.1E-09
Type S	1.9E-09

Ingested materials	
All forms	2.4E-10

AMAD, activity median aerodynamic diameter

Table 28.6 Dose per activity content of ^{113}Sn in total body and in daily excretion of urine (Sv Bq^{-1}); 5μm activity median aerodynamic diameter aerosols inhaled by a reference worker at light work.

	Type F		Type M		Type S	
Time after intake (d)	Total body	Urine	Total body	Urine	Total body	Urine
1	1.6E-09	1.2E-08	1.9E-09	1.8E-07	3.1E-09	6.2E-06
2	2.6E-09	9.1E-08	3.5E-09	8.9E-07	5.7E-09	3.1E-05
3	4.4E-09	3.0E-07	7.6E-09	3.3E-06	1.2E-08	1.2E-04
4	6.0E-09	4.4E-07	1.4E-08	4.3E-06	2.2E-08	1.7E-04
5	6.8E-09	5.0E-07	1.8E-08	4.7E-06	3.0E-08	1.9E-04
6	7.1E-09	5.5E-07	2.0E-08	5.0E-06	3.3E-08	2.0E-04
7	7.3E-09	6.0E-07	2.1E-08	5.3E-06	3.4E-08	2.2E-04
8	7.5E-09	6.6E-07	2.1E-08	5.5E-06	3.5E-08	2.3E-04
9	7.6E-09	7.1E-07	2.2E-08	5.8E-06	3.5E-08	2.5E-04
10	7.7E-09	7.7E-07	2.2E-08	6.1E-06	3.6E-08	2.6E-04
15	8.4E-09	1.1E-06	2.4E-08	7.4E-06	3.8E-08	3.3E-04
30	1.0E-08	2.6E-06	2.8E-08	1.1E-05	4.4E-08	5.3E-04
45	1.2E-08	4.4E-06	3.3E-08	1.4E-05	4.9E-08	6.7E-04
60	1.3E-08	6.1E-06	3.8E-08	1.7E-05	5.6E-08	7.8E-04
90	1.7E-08	9.0E-06	5.1E-08	2.3E-05	7.1E-08	9.9E-04
180	3.4E-08	2.0E-05	1.2E-07	5.7E-05	1.4E-07	1.9E-03
365	1.5E-07	8.8E-05	5.9E-07	3.1E-04	5.7E-07	6.5E-03

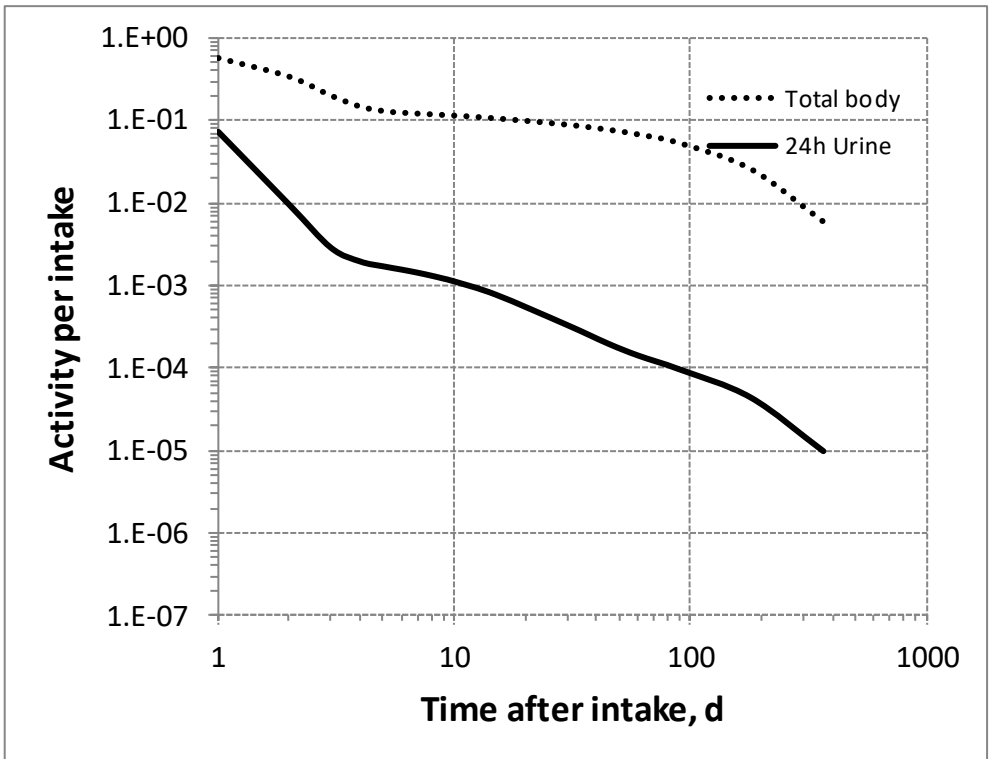

Fig. 28.2. Daily excretion of ^{113}Sn following inhalation of 1 Bq Type F.

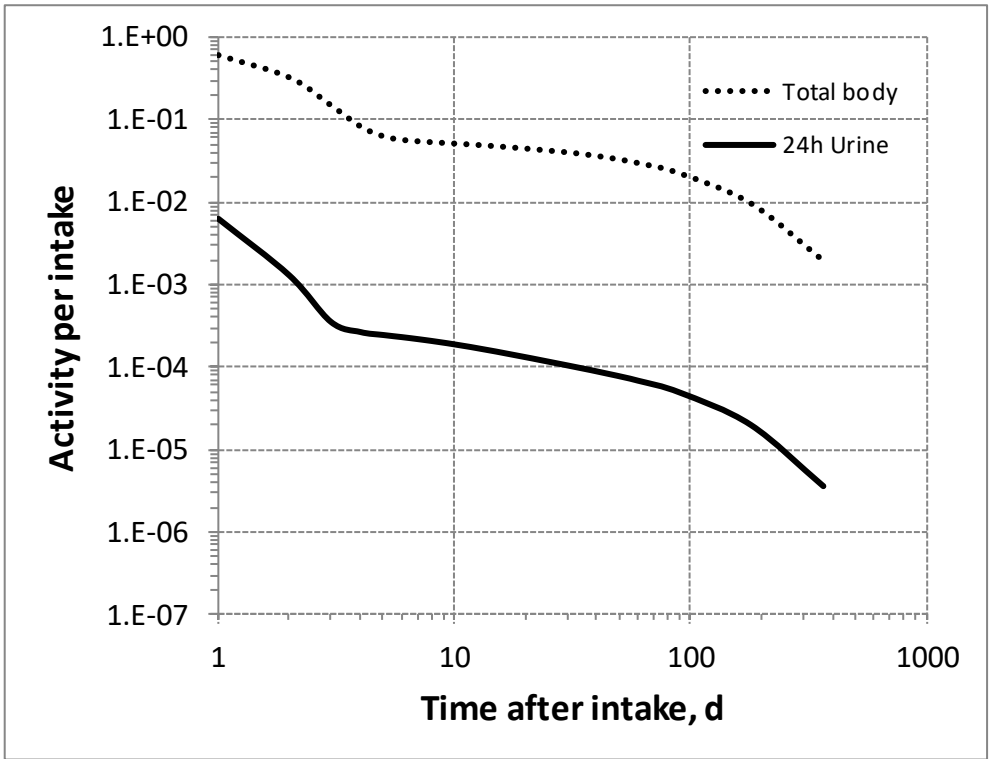

Fig. 28.3. Daily excretion of ^{113}Sn following inhalation of 1 Bq Type M.

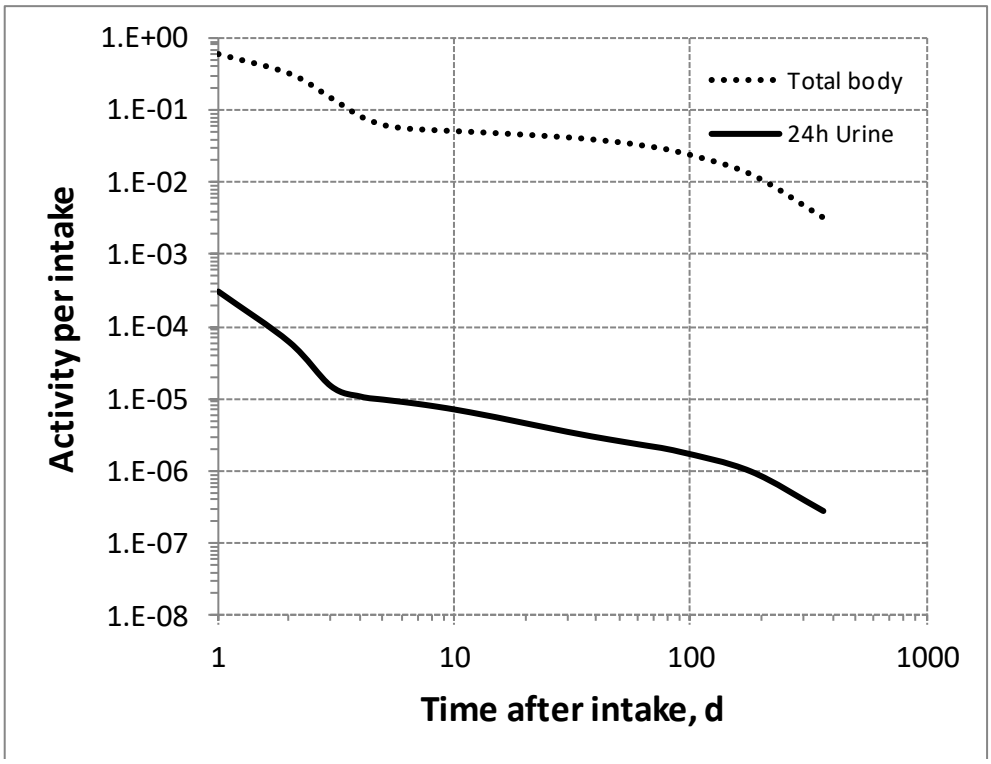

Fig. 28.4. Daily excretion of ^{113}Sn following inhalation of 1 Bq Type S.

29. HAFNIUM (Z=72)

29.1. Isotopes

Table 29.1. Isotopes of hafnium addressed in this publication.

Isotope	Physical half-life	Decay mode
^{170}Hf	16.01 h	EC
^{172}Hf	1.87 y	EC
^{173}Hf	23.6 h	EC, B+
^{174}Hf	2.0E+15 y	A
^{175}Hf	70 d	EC
^{177m}Hf	51.4 min	IT
^{178m}Hf	31 y	IT
^{179m}Hf	25.05 d	IT
^{180m}Hf	5.5 h	IT, B-
^{181}Hf	42.39 d	B-
^{182}Hf*	9E+6 y	B-
^{182m}Hf	61.5 m	B-, IT
^{183}Hf	1.067 h	B-
^{184}Hf	4.12 h	B-

EC, electron-capture decay; B+, beta-plus decay; B-, beta-minus decay; IT, isomeric transition decay; A, alpha decay.
*Dose coefficients and bioassay data for this radionuclide are given in the printed copy of this publication. Data for other radionuclides listed in this table are given in the online electronic files on the ICRP website.

29.2. Routes of Intake

29.2.1. Inhalation

(536) For hafnium, default parameter values were adopted on absorption to blood from the respiratory tract (ICRP, 2015). Absorption parameter values and types, and associated f_A values for particulate forms of hafnium are given in Table 29.2.

29.2.2. Ingestion

(537) There do not appear to be any relevant data available on the absorption of compounds of hafnium from the gastrointestinal tract. In *Publications 30* and *68* (ICRP, 1981, 1994a), by analogy with the chemically similar and more extensively studied element zirconium, f_1 was taken to be 0.002 for all compounds of hafnium. The same value of $f_A = 0.002$ is used in this publication.

Table 29.2. Absorption parameter values for inhaled and ingested hafnium.

	Absorption parameter values*			Absorption from the alimentary tract, f_A
Inhaled particulate materials	f_r	s_r (d^{-1})	s_s (d^{-1})	
Default parameter values†				
Absorption type				
F	1	30	–	0.002
M‡	0.2	3	0.005	4×10^{-4}
S	0.01	3	1×10^{-4}	2×10^{-5}

Ingested materials[§]	
All forms	0.002

[*]It is assumed that the bound state can be neglected for hafnium (i.e. $f_b = 0$). The values of s_r for Type F, M and S forms of hafnium (30, 3 and 3 d^{-1} respectively) are the general default values.
[†]For inhaled material deposited in the respiratory tract and subsequently cleared by particle transport to the alimentary tract, the default f_A values for inhaled materials are applied [i.e. the product of f_r for the absorption type and the f_A value for ingested soluble forms of hafnium (0.002)].
[‡]Default Type M is recommended for use in the absence of specific information on which the exposure material can be assigned to an absorption type (e.g. if the form is unknown, or if the form is known but there is no information available on the absorption of that form from the respiratory tract). For guidance on the use of specific information, see Section 1.1.
[§]Activity transferred from systemic compartments into segments of the alimentary tract is assumed to be subject to reabsorption to blood. The default absorption fraction f_A for the secreted activity is the highest value for any form of the radionuclide ($f_A = 0.002$).

29.2.3. Systemic distribution, retention and excretion of hafnium

29.2.3.1. Summary of biokinetic data

(538) The chemical and physical properties of the Group IVB element Hf are virtually identical to those of the lighter IVB element Zr, making these elements difficult to separate in the laboratory. Hf and Zr are found together in nature and are sometimes referred to as geochemical twins because the mass ratio Zr/Hf typically shows little variation in rocks and soil. The limited fractionation of Hf and Zr in geological material is attributed to their identical valence state in geological circumstances together with their nearly identical ionic radii (Bau and Dulski, 1995; Breiter and Škoda, 2017).

(539) Comparisons of the behaviours of Hf and Zr in laboratory animals also indicate closely similar biological behaviours of these elements. For example, virtually identical total-body retention curves over 140 d were derived in biokinetic studies of parenterally administered ^{95}Zr (Richmond et al., 1960) and ^{181}Hf (Taylor et al., 1985) in rats. Comparisons of the systemic behaviours of Hf and Zr isotopes in rats indicate similar soft-tissue distributions over the first two days after intravenous injection (Ando and Ando, 1986). Electron microprobe studies of intracellular localisation of Zr and Hf in nodular lymphatic cells after administration of low doses of soluble salts indicated that both elements were localised in the lysosomes of macrophages, where they were both associated with phosphorus (Berry and Galle, 1992). Identical effects of cartilaginous dysplasia could be induced in mice by Hf or Zr but not by several other tested metals (Shelley, 1973).

(540) Taylor et al. (1983, 1985) investigated the systemic behaviour of ^{181}Hf or $^{175+181}$Hf in rats, Chinese hamsters, and marmosets for times up to 6 months post administration by various routes. Total-body retention curves over 150 d was closely similar for the three animal species following parenteral administration of Hf as a citrate complex. Relatively detailed studies of the time-dependent systemic distribution of activity were conducted for hamsters and rats. The skeleton was the main systemic repository for Hf, containing ~29% of intravenously administered Hf in rats at 14 d post injection and ~43% at 21 d post subcutaneous administration to hamsters. In rats, the liver content peaked at 6.5% at 7 d and declined to 1.2% at 168 d. In hamsters the liver content peaked at 5% at 1 d and declined to 2.1% at 168 d. Limited tissue measurements on marmosets suggested a higher liver content than observed in rats and hamsters.

(541) Ando and Ando (1986) investigated the biokinetics of ^{181}Hf and ^{95}Zr in tumour-bearing rats following intravenous injection of ^{181}Hf chloride, ^{95}Zr oxalate, and ^{95}Zr nitrate. The activity concentrations were determined at 3, 24, and 48 h after injection for blood, muscle, liver, spleen,

kidney, pancreas, heart, lung, adrenal, thymus, and tumour. Bone and brain were also addressed in the ^{181}Hf study but not in the ^{95}Zr study. The kinetics of Hf closely followed that of Zr in most tissues. The liver and spleen accumulated a larger portion of Hf than Zr, which was attributed by the investigations to formation of some colloidal Hf in the injected solution and its removal from blood by phagocytic cells of liver and spleen. Bone was the dominant repository of ^{181}Hf at 24 and 48 h.

(542) At 4 d after IV administration of ^{181}Hf as citrate to rats, the median concentration ratios liver:femur and kidney:femur were ~0.5 (MacDonald and Bahner, 1953). At 14 d after IV administration of $^{175+181}$Hf as citrate, the total body, liver, and skeleton contained ~71%, 4.1%, and 29%, respectively, of the administered amount (Taylor et al., 1983). At 4 d after IV administration of ^{181}Hf mandelate to rats, the median concentration ratios liver:femur and kidney:femur were ~6 and 1.4, respectively (MacDonald and Bahner, 1953). At 16 d after IV administration of ^{181}Hf mandelate to rats, the total body, liver, and bone contained ~93%, 45%, and 13%, respectively, of the administered activity corrected for radioactive decay (Kittle et al., 1951).

29.2.3.2. Biokinetic model for systemic hafnium

(543) In view of the close physical and chemical similarities of Zr and Hf, their apparently similar biological behaviour as indicated by available comparative studies, and difficulties in developing a biokinetic model for systemic Hf based on Hf-specific information, the systemic model for Zr applied in *Publication 134* (ICRP, 2016) is assigned to Hf.

(544) The structure of the biokinetic model for systemic hafnium is shown in Fig. 29.1. The transfer coefficients are listed in Table 29.3.

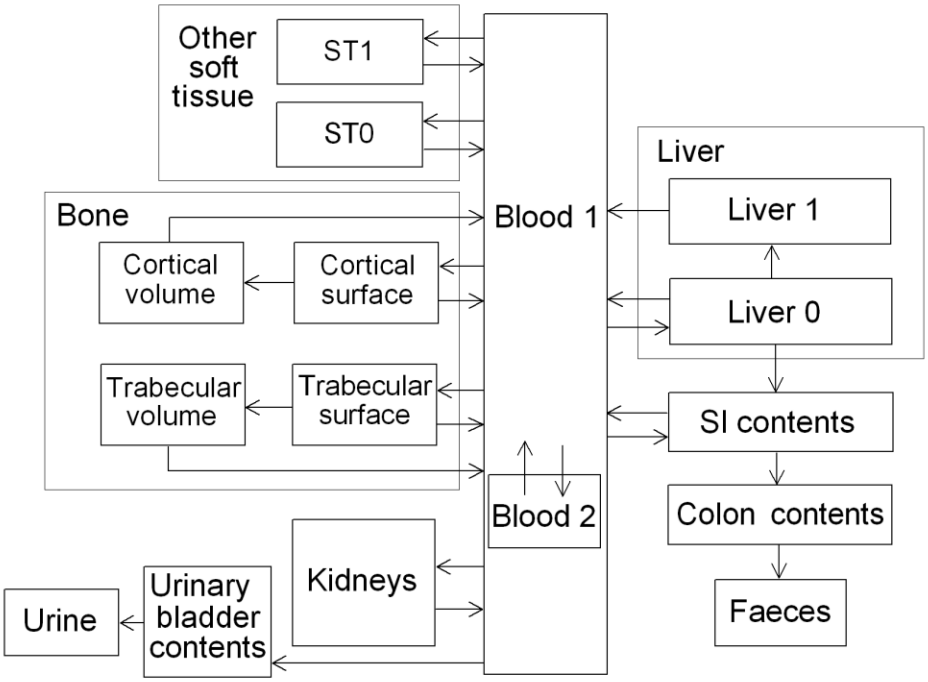

Fig. 29.1. Structure of the biokinetic model for systemic hafnium.

Table 29.3. Parameter values in the biokinetic model for systemic Hf.

From:	To:	Transfer coefficient (d^{-1})
Blood 1	Blood 2	2.0

Blood 1	Liver 0	0.075
Blood 1	Kidneys	0.0125
Blood 1	ST0	2.0
Blood 1	ST1	0.0375
Blood 1	Urinary bladder content	0.1
Blood 1	SI contents	0.025
Blood 1	Trabecular surface	0.375
Blood 1	Cortical surface	0.375
Blood 2	Blood 1	0.462
Liver 0	SI contents	0.116
Liver 0	Blood 1	0.116
Liver 0	Liver 1	0.462
Liver 1	Blood 1	0.01
Kidneys	Blood 1	0.01
ST0	Blood 1	0.462
ST1	Blood 1	0.02
Trabecular surface	Blood 1	0.000493
Trabecular surface	Trabecular volume	0.000247
Trabecular volume	Blood 1	0.000493
Cortical surface	Blood 1	0.0000821
Cortical surface	Cortical volume	0.0000411
Cortical volume	Blood 1	0.0000821

29.2.3.3. Treatment of progeny

(545) Progeny of hafnium addressed in this publication are radioisotopes of hafnium, tantalum, and lutetium. The model for hafnium as a parent is applied to hafnium produced by decay of another hafnium isotope. The models for tantalum and lutetium as progeny of hafnium are expansions of the characteristic models for these elements with added compartments and associated transfer coefficients needed to solve the linked biokinetic models for chains headed by hafnium (see Annex B). For lutetium as a progeny of hafnium, the issue arises that the progeny is produced in some compartments not contained in the characteristic model for lutetium. If produced in a blood compartment not contained in the model for lutetium, the progeny is assumed to transfer to the central blood compartment of its characteristic biokinetic model at the rate 1000 d^{-1} and to follow that model thereafter. If produced in a tissue compartment not in the lutetium model, the progeny is assumed to transfer to the central blood compartment of the characteristic model for lutetium at the rate 1.39 d^{-1} and to follow that model thereafter.

29.3. Individual monitoring

(546) Information of detection limit for routine individual measurement is not available.

29.4. Dosimetric data for hafnium

Table 29.4 Committed effective dose coefficients (Sv Bq^{-1}) for the inhalation or ingestion of ^{182}Hf compounds.

Inhaled particulate materials (5 μm AMAD aerosols)	Effective dose coefficients (Sv Bq^{-1})
	^{182}Hf

Type F, — NB: Type F should not be assumed without evidence	3.2E-07
Type M, default	7.5E-08
Type S	1.2E-07
Ingested materials	
All forms	3.0E-09

5500 AMAD, activity median aerodynamic diameter
5501

30. TANTALUM (Z=73)

30.1. Isotopes

Table 30.1. Isotopes of tantalum addressed in this publication.

Isotope	Physical half-life	Decay mode
^{172}Ta	36.8 min	EC, B+
^{173}Ta	3.14 h	EC, B+
^{174}Ta	1.14 h	EC, B+
^{175}Ta	10.5 h	EC, B+
^{176}Ta	8.09 h	EC, B+
^{177}Ta	56.56 h	EC
^{178m}Ta	2.36 h	EC
^{179}Ta	1.82 y	EC
^{180}Ta	8.152 h	EC, B-
^{182}Ta*	114.43 d	B-
^{182m}Ta	15.84 min	IT
^{183}Ta	5.1 d	B-
^{184}Ta	8.7 h	B-
^{185}Ta	49.4 min	B-
^{186}Ta	10.5 min	B-

EC, electron-capture decay; B+, beta-plus decay; B-, beta-minus decay; IT, isomeric transition decay.
*Dose coefficients and bioassay data for this radionuclide are given in the printed copy of this publication.
Data for other radionuclides listed in this table are given in the online electronic files on the ICRP website.

30.2. Routes of Intake

30.2.1. Inhalation

(547) For tantalum, default parameter values were adopted on absorption to blood from the respiratory tract (ICRP, 2015). Absorption parameter values and types, and associated f_A values for particulate forms of tantalum are given in Table 30.2.

30.2.2. Ingestion

(548) Data from experiments on rats (Fleshman et al., 1971) suggest that the fractional absorption of tantalum, administered as potassium tantalate, from the gastrointestinal tract of the rat is about 10^{-3}. Other studies on rats (Doull and Dubois, 1949; Cochran et al., 1950) indicate that the fractional absorption of tantalum, administered as the oxide, is also small. When ^{182}Ta was given orally as tantalate to dogs, all but 1% appeared in the faeces (Rydzynski and Pakulska, 2012).

(549) In *Publications 30* and *68* (ICRP, 1981, 1994a), f_1 was taken as 10^{-3} for all compounds of tantalum. In this publication, the value of fractional absorption $f_A = 10^{-3}$ is also used as the default for all forms of tantalum at the workplace.

Table 30.2. Absorption parameter values for inhaled and ingested tantalum.

Inhaled particulate materials	Absorption parameter values*	Absorption from the alimentary tract, f_A

	f_r	s_r (d^{-1})	s_s (d^{-1})	
Default parameter values†				
Absorption type				
F	1	30	–	0.001
M‡	0.2	3	0.005	2×10^{-4}
S	0.01	3	1×10^{-4}	1×10^{-5}
Ingested materials§				
All forms				0.001

*It is assumed that the bound state can be neglected for tantalum (i.e. $f_b = 0$). The values of s_r for Type F, M and S forms of tantalum (30, 3 and 3 d^{-1} respectively) are the general default values.

†For inhaled material deposited in the respiratory tract and subsequently cleared by particle transport to the alimentary tract, the default f_A values for inhaled materials are applied [i.e. the product of f_r for the absorption type and the f_A value for ingested soluble forms of tantalum (0.001)].

‡Default Type M is recommended for use in the absence of specific information on which the exposure material can be assigned to an absorption type (e.g. if the form is unknown, or if the form is known but there is no information available on the absorption of that form from the respiratory tract). For guidance on the use of specific information, see Section 1.1.

§Activity transferred from systemic compartments into segments of the alimentary tract is assumed to be subject to reabsorption to blood. The default absorption fraction f_A for the secreted activity is the highest value for any form of the radionuclide ($f_A = 0.001$).

30.2.3. Systemic distribution, retention and excretion of tantalum

30.2.3.1. Summary of selected studies

(550) The chemical and physical properties of the Group VB element tantalum (Ta) closely resemble those of the lighter Group VB element niobium (Nb). Tantalum and niobium are found together in nature and are sometimes referred to as geochemical twins because of their similar mass ratios in different geological material from the bulk silicate Earth as well as extraterrestrial sources (Münker et al., 2003). The limited fractionation of Ta and Nb in geological material is attributed to their identical valence state in geological circumstances together with their nearly identical ionic radii.

(551) Information on the biokinetics of systemic Ta comes mainly from limited studies on rats (Durbin, 1959; Fleshman et al., 1971; Ando et al., 1989; Ando and Ando, 1990). Comparative data for Ta and Nb provided in these studies suggest that these geochemical twins also behave similarly in biological systems.

(552) Ando et al. (1989, 1990) studied the distribution and excretion of radioisotopes of 54 elements, including Ta and Nb both as oxalate, following intravenous administration of individual elements to tumour-bearing rats. Activity concentrations were measured in blood, bone, ten different soft tissues, and an implanted sarcoma. The behaviour of Ta closely followed that of Nb at all studied sites.

(553) In rats administered ^{95}Nb and $^{182}Ta_2O_5$ in citrate solution via intramuscular injection, both radionuclides showed elevated concentrations in liver, kidney, and bone (Durbin, 1959). At 4 d post injection, cumulative excretion of activity accounted for 48.6% of administered ^{182}Ta and 39.4% of administered ^{95}Nb. At that time, activity in bone, liver, and kidneys represented roughly 23%. 14%, and 10%, respectively of retained ^{182}Ta and 27%, 14%, and 5%, respectively, of retained ^{95}Nb.

(554) Fleshman et al. (1971) investigated the biokinetics of ^{182}Ta in rats over 106 d after its oral administration as potassium tantalite to rats. Bone was the dominant long-term repository,

followed by pelt. At 106 d, bone, liver, and kidneys contained about 46%, 3.4%, and 1.2% respectively, of the total-body content.

30.2.3.2. Biokinetic model for systemic tantalum

(555) In view of the close physical and chemical similarities of Ta and Nb, their apparently similar biological behaviour as indicated by available comparative studies, and difficulties in developing a biokinetic model for systemic Ta based on Ta-specific information, the systemic model for Nb applied in *Publication 134* (ICRP, 2016) is assigned to Ta.

(556) The structure of the systemic model for Ta is shown in Fig. 30.1. Transfer coefficients are listed in Table 30.3.

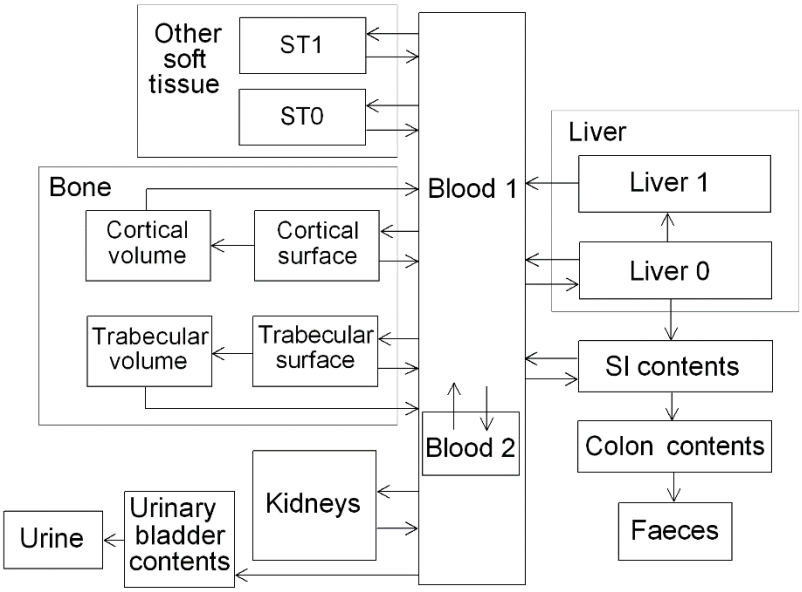

Fig. 30.1. Structure of the biokinetic model for systemic tantalum.

30.2.3.3. Treatment of progeny

(557) Progeny of tantalum addressed in this publication are isotopes of tantalum, hafnium, lutetium, and tungsten. The characteristic models for tantalum and hafnium are applied to these elements as progeny of tantalum. The models for lutetium and tungsten as progeny of tantalum are the characteristic models for these elements with added transfer coefficients needed to solve the linked biokinetic models for chains headed by tantalum. Lutetium or tungsten produced in an ambiguous compartment (i.e. a compartment of the model for a preceding chain that is not a compartment in the model for the progeny) is assumed to transfer to the central blood compartment of the progeny's model and to follow that model thereafter. The following transfer rates are assigned to lutetium or tungsten produced in ambiguous compartments: 1000 d^{-1} if produced in a blood compartment; at the rate of bone turnover for the indicated bone type if produced in a bone volume compartment; and at the following element-specific rates if produced in any other compartment: lutetium, 1.39 d^{-1}; tungsten, 8.32 d^{-1}.

Table 30.3. Parameter values in the biokinetic model for systemic tantalum.

From	To	Transfer coefficient (d^{-1})
Blood 1	Blood 2	3.2
Blood 1	Liver 0	0.24

Blood 1	Kidneys	0.04
Blood 1	ST0	3.2
Blood 1	ST1	0.12
Blood 1	Urinary bladder contents	0.88
Blood 1	SI contents	0.08
Blood 1	Trabecular surface	0.12
Blood 1	Cortical surface	0.12
Blood 2	Blood 1	1.39
Liver 0	SI contents	0.0578
Liver 0	Blood 1	0.0578
Liver 0	Liver 1	0.231
Liver 1	Blood 1	0.005
Kidneys	Blood 1	0.005
ST0	Blood 1	1.39
ST1	Blood 1	0.01
Trabecular surface	Blood 1	0.000493
Trabecular surface	Trabecular volume	0.000247
Trabecular volume	Blood 1	0.000493
Cortical surface	Blood 1	0.0000821
Cortical surface	Cortical volume	0.0000411
Cortical volume	Blood 1	0.0000821

30.3. Individual monitoring

(558) Information of detection limit for routine individual measurement is not available.

30.4. Dosimetric data for tantalum

Table 30.4. Committed effective dose coefficients (Sv Bq^{-1}) for the inhalation or ingestion of ^{182}Ta compounds.

Inhaled particulate materials (5 µm AMAD aerosols)	Effective dose coefficients (Sv Bq^{-1})
	^{182}Ta
Type F, — NB: Type F should not be assumed without evidence	2.2E-09
Type M, default	2.8E-09
Type S	4.4E-09
Ingested materials	
All forms	5.0E-10

AMAD, activity median aerodynamic diameter

31. TUNGSTEN (Z=74)

31.1. Isotopes

Table 31.1. Isotopes of tungsten addressed in this publication.

Isotope	Physical half-life	Decay mode
^{177}W	132 min	EC, B+
^{178}W	21.6 d	EC
^{179}W	37.05 min	EC
^{181}W*	121.2 d	EC
^{185}W	75.1 d	B-
^{187}W	23.72 h	B-
^{188}W	69.78 d	B-
^{190}W	30.0 min	B-

EC, electron-capture decay; B+, beta-plus decay; B-, beta-minus decay.
*Dose coefficients and bioassay data for this radionuclide are given in the printed copy of this publication.
Data for other radionuclides listed in this table are given in the online electronic files on the ICRP website.

31.2. Routes of Intake

31.2.1. Inhalation

(559) For tungsten, default parameter values were adopted on absorption to blood from the respiratory tract (ICRP, 2015). Absorption parameter values and types, and associated f_A values for particulate forms of tungsten are given in Table 31.2.

31.2.2. Ingestion

(560) In a controlled balance study involving four adult human volunteers during 5 days, the comparison of the amount of tungsten in daily diet, urine and faeces suggests that about half of the ingested tungsten in absorbed to blood (Wester, 1974). Animal ingestion studies were reviewed by Leggett (1997) and the ATSDR (ATSDR, 2005c). The fractional absorption of tungsten from sodium tungstate or tungsten oxide orally administered to rats, dogs, pigs and sheep was in a range from 25 to 92%.

(561) Absorption decreased markedly when the animals were fed on a diet high in roughage (Bell and Sneed, 1970). This suggests that tungsten absorption may be inhibited by adsorption of the element to food particles, especially those high in cellulose. This may explain why in experiments on goats the fractional gastrointestinal absorption of tungsten, administered as tungstate, has been reported as about 5% (Ekman et al., 1977). A lower absorption about 1% was also observed when tungsten was administered to rats as tungstic acid (Ballou, 1960). Experiments in which peccaries ingested debris from a nuclear explosion gave a fractional absorption of between 10 and 20% for tungsten (Chertok and Lake, 1971c,d).

(562) In *Publications 30* and *68* (ICRP, 1981, 1994a), f_1 was taken as 0.01 for tungstic acid and 0.3 for all other compounds of the element. In this publication, the value of $f_A = 0.01$ is applied to tungstic acid and $f_A = 0.5$ is adopted for all other compounds, taking into account the recent animal studies and the limited human data.

Table 31.2. Absorption parameter values for inhaled and ingested tungsten.

Inhaled particulate materials	Absorption parameter values* f_r	s_r (d^{-1})	s_s (d^{-1})	Absorption from the alimentary tract, f_A
Default parameter values†				
Absorption type				
F	1	30	–	0.5
M‡	0.2	3	0.005	0.1
S	0.01	3	1×10^{-4}	0.005
Ingested materials§				
Tungstic acid				0.01
All other forms				0.5

*It is assumed that the bound state can be neglected for tungsten (i.e. $f_b = 0$). The values of s_r for Type F, M and S forms of tungsten (30, 3 and 3 d^{-1} respectively) are the general default values.

†For inhaled material deposited in the respiratory tract and subsequently cleared by particle transport to the alimentary tract, the default f_A values for inhaled materials are applied [i.e. the product of f_r for the absorption type and the f_A value for ingested soluble forms of tungsten (0.5)].

‡Default Type M is recommended for use in the absence of specific information on which the exposure material can be assigned to an absorption type (e.g. if the form is unknown, or if the form is known but there is no information available on the absorption of that form from the respiratory tract). For guidance on the use of specific information, see Section 1.1.

§Activity transferred from systemic compartments into segments of the alimentary tract is assumed to be subject to reabsorption to blood. The default absorption fraction f_A for the secreted activity is the highest value for any form of the radionuclide ($f_A = 0.5$).

31.2.3. Systemic distribution, retention and excretion of tungsten

31.2.3.1. Biokinetic data

(563) Direct information on the behaviour of absorbed tungsten (W) in humans consists largely of measurements of the concentration of tungsten in blood, tissues, and excreta of chronically exposed human subjects (Wester, 1973, 1974; Brune et al., 1980; Nicolaou et al., 1987; Zhu et al., 2010). The time dependent distribution and excretion of systemic tungsten following short-term intake has been studied in a variety of laboratory animals including: dogs receiving radio-tungsten by inhalation or injection (Aamodt, 1973, 1975); swine exposed to radionuclides produced by a nuclear explosion (Chertok and Lake, 1971a,b,c); rodents administered radio-tungsten by different routes (Scott, 1952; Wase, 1956; Ballou, 1960; Fleshman et al., 1966; Kaye, 1968; Ando et al., 1989); and various farm animals (sheep, pigs, cows, goats) receiving radio-tungsten by injection or ingestion (Bell and Sneed, 1970; Mullen et al., 1976; Ekman et al., 1977). Relatively detailed data are available for rats, but the rat is not a preferred model for tungsten behaviour in the human body because of the rat's unusually low requirements for the essential element molybdenum (Higgins et al., 1956), a chemical and physiological analogue of tungsten. While the initial systemic distribution of tungsten appears to be reasonably similar in rats and larger animals, rats appear to excrete tungsten at a higher rate than most of the other studied animals.

(564) Data for laboratory animals indicate an initially rapid clearance of tungsten from blood but retention of a few tenths of a percent of the absorbed or injected amount in blood over a period of days (Durbin et al., 1957; Durbin, 1959; Ballou, 1960; Chertok and Lake, 1971a,b,c; Aamodt, 1973; Mullen et al., 1976; Ekman et al., 1977; Ando et al., 1989; Mason et al., 1989). Following intravenous administration of ^{181}W as sodium tungstate to beagles, about 70% of the injected activity was removed from blood with a biological half-time of 35 min, 25% with a

half time of 70 min, and most of the remainder with a half time of 5 h (Aamodt, 1973). In goats administered $Na_2{}^{181}WO_4$ intravenously, about 84% of activity was removed from plasma with a half time of 2 h, 15% with a half time of 9 h, and 0.7% was removed with a half time of 63 h (Ekman et al., 1977). Following intravenous injection of ^{185}W as tungstate into a sheep, about 25% of injected activity remained in blood after 0.5 h and about 10% remained after 2 h (Mason et al., 1989). Tissue analysis of young Yorkshire pigs exposed to radioactive fallout from a detonation (Chertok and Lake, 1971a,b,c) suggest that blood may have contained 10% or more of total body radio-tungsten after 3 d.

(565) Reported data on the relative concentrations of tungsten in plasma and red blood cells (RBC) are variable, perhaps reflecting species differences in the affinity of tungsten for red blood cells. In beagles receiving ^{181}W as sodium tungstate by intravenous injection, the ratio of the concentration of ^{181}W in plasma to that in RBC averaged about 3 during the first 24 h (Aamodt, 1973). In goats administered $Na_2{}^{181}WO_4$ intravenously, steady-state conditions between plasma and RBC were reached at about 6 h after injection, at which time the RBC contained 10% of ^{181}W in blood (Ekman et al., 1977). Higher RBC-to-plasma activity ratios for radio-tungsten have been determined in rodents than in larger animals (Wase, 1956; Kaye, 1968).

(566) Useful data on early exchange of tungsten between blood and tissues were found only for rats (Scott, 1952; Ando et al., 1989). Mathematical analysis of the data suggest that a sizable portion, on the order of one-third, of the amount leaving blood returns to blood within a few hours.

(567) Potentially important systemic repositories for tungsten include the liver, kidneys, spleen, and bone. Data for laboratory animals indicate that a few percent of absorbed tungsten deposits in bone, at least a few tenths of the deposited amount is retained for an extended period, and accumulation of tungsten is greater in growing than in mature bone (Fleshman et al., 1966; Kaye, 1968; Aamodt, 1975; Mullen et al., 1976; Ando et al., 1989). Similarities in the behaviour of tungstate, molybdate, and phosphate in biological systems have been observed, and it seems likely that uptake and retention of tungsten by bone are due to substitution of tungstate for phosphate (Fleshman et al., 1966).

(568) The systemic biokinetics of tungsten bears some resemblance to that of the chemically similar essential element molybdenum. Tungsten has been used experimentally as a physiological analogue of molybdenum, as it is the best known biological antagonist of molybdenum and the only element capable of producing experimental deficiency of molybdenum, resulting from prevention of incorporation of molybdenum into certain enzymes (Cardin and Mason, 1976). Membrane transport may not distinguish between tungsten and molybdenum, although differences in the biokinetics of these elements may result from the fact that molybdenum compounds are more easily reduced in biological systems (Callis and Wentworth, 1977). An apparent difference in the systemic kinetics of these two elements is that the liver appears to accumulate considerably more molybdenum than tungsten (Leggett, 1997).

31.2.3.2. Biokinetic model for systemic tungsten

(569) A biokinetic model for systemic tungsten developed by Leggett (1997) is adopted here. The model structure is shown in Fig. 31.1. The transfer coefficients are listed in Table 31.3.

(570) The model structure is a modest variation of the systemic model for uranium in the adult used in *Publication 69* (ICRP, 1995a) for adult members of the public and in *Publications 68* and *137* (ICRP, 1994a, 2017) for workers. This is not based on known or suspected physiological similarities of tungsten and uranium, as the biological interactions of tungsten as well as its chemistry appear to differ markedly from those of uranium. Rather, the rationale for

using the uranium model structure as a starting place is essentially that tungsten and uranium appear to have similar repositories, modes of excretion, and sites of long-term retention (bone volume); and deposition and retention of both elements in bone appear to be related to one of the major components of bone crystal, calcium or phosphorus (Leggett, 1997). The primary change made for application of the model structure to tungsten is the addition of a compartment representing the spleen.

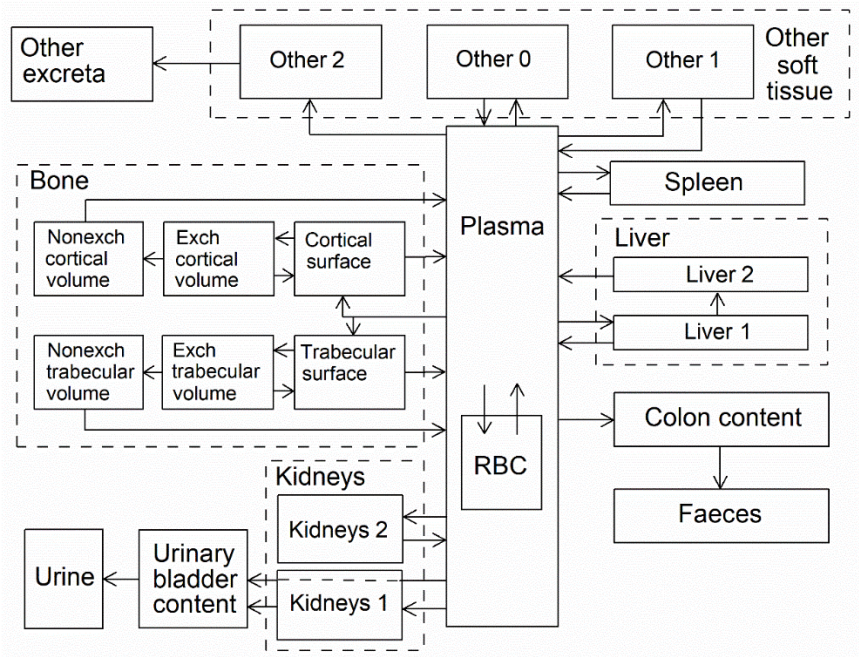

Fig. 31.1. Structure of the biokinetic model for systemic tungsten.

31.2.3.3. Treatment of progeny

(571) Progeny of tungsten addressed in this publication are isotopes of tantalum and rhenium. The characteristic models for tantalum and rhenium are applied to these elements as members of chains headed by tungsten with added transfer coefficients needed to solve the linked biokinetic models for chains headed by tungsten. Tantalum or rhenium produced in an ambiguous compartment (i.e. a compartment of the model for a preceding chain that is not a compartment in the model for the progeny) is assumed to transfer to the central blood compartment of the progeny's characteristic model and to follow that model thereafter. The following transfer rates are assigned to tantalum or rhenium produced in ambiguous compartments: 1000 d^{-1} if produced in a blood compartment; at the reference rate of bone turnover for the indicated bone type if produced in a bone volume compartment; and at the following element-specific rates if produced in any other compartment: tantalum, 1.39 d^{-1}; rhenium, 0.462 d^{-1}.

Table 31.3. Transfer coefficients in the biokinetic model for systemic tungsten.

From	To	Transfer coefficients (d^{-1})
Blood	Other 0	4.99
Blood	RBC	0.0582
Blood	Urinary bladder content	8.74
Blood	Kidneys1	0.524
Blood	Kidneys2	0.0582

Blood	Right colon content	0.582
Blood	Spleen	0.00582
Blood	Liver 1	0.466
Blood	Other 1	0.262
Blood	Other 2	0.0233
Blood	Trabecular bone surface	0.518
Blood	Cortical bone surface	0.414
Other 0	Blood	8.32
RBC	Blood	0.347
Kidneys 1	Urinary bladder content	1.39
Kidneys 2	Blood	0.0019
Liver 1	Blood	0.312
Liver 1	Liver_2	0.0347
Other 1	Blood	0.0693
Other 2	Excreta	0.0019
Spleen	Blood	0.0019
Trabecular bone surface	Blood	0.578
Trabecular bone surface	Trabecular bone volume 1	0.116
Cortical bone surface	Blood	0.578
Cortical bone surface	Cortical bone volume 1	0.116
Liver 2	Blood	0.0019
Trabecular bone volume 2	Blood	0.000493
Cortical bone volume 2	Blood	0.0000821
Trabecular bone volume 1	Trabecular bone surface	0.00277
Trabecular bone volume 1	Trabecular bone volume 2	0.00416
Cortical bone volume 1	Cortical bone surface	0.00277
Cortical bone volume 1	Cortical bone volume 2	0.00416

31.3. Individual monitoring

(572) Information of detection limit for routine individual measurement is not available.

31.4. Dosimetric data for tungsten

Table 31.4. Committed effective dose coefficients (Sv Bq^{-1}) for the inhalation or ingestion of ^{181}W compounds.

Inhaled particulate materials (5 µm AMAD aerosols)	Effective dose coefficients (Sv Bq^{-1})
	^{181}W
Type F, — NB: Type F should not be assumed without evidence	2.4E-11
Type M, default	1.0E-10
Type S	1.8E-10
Ingested materials	
Tungstic acid	2.4E-11

All other forms	3.2E-11

AMAD, activity median aerodynamic diameter

32. RHENIUM (Z=75)

32.1. Isotopes

Table 32.1. Isotopes of rhenium addressed in this publication.

Isotope	Physical half-life	Decay mode
^{178}Re	13.2 min	EC, B+
^{179}Re	19.5 min	EC, B+
^{181}Re	19.9 h	EC, B+
^{182}Re	64.0 h	EC
^{182m}Re	12.7 h	EC, B+
^{183}Re	70.0 d	EC
^{184}Re	38.0 d	EC, B+
^{184m}Re	169 d	IT, EC
^{186}Re*	3.7183 d	B-, EC
^{186m}Re	2.00E+5 y	IT
^{187}Re	4.12E+10 y	B-
^{188}Re*	17.0040 h	B-
^{188m}Re	18.59 min	IT
^{189}Re	24.3 h	B-
^{190m}Re	3.2 h	B-

EC, electron-capture decay; B+, beta-plus decay; B-, beta-minus decay; IT, isomeric transition decay.
*Dose coefficients and bioassay data for this radionuclide are given in the printed copy of this publication.
Data for other radionuclides listed in this table are given in the online electronic files on the ICRP website.

32.2. Routes of Intake

32.2.1. Inhalation

(573) For rhenium, default parameter values were adopted on absorption to blood from the respiratory tract (ICRP, 2015). Absorption parameter values and types, and associated f_A values for particulate forms of rhenium are given in Table 32.2.

32.2.2. Ingestion

(574) In *Publication 30* (ICRP, 1980), since there appeared to be no information available concerning the uptake of rhenium from the gastrointestinal tract, a fractional absorption value of 0.8 was recommended for all chemical forms of rhenium based on the chemical analogy with technetium (Durbin et al., 1957; Durbin, 1959; Zuckier et al., 2004). This value was also adopted in *Publication 68* (ICRP, 1994a). In OIR Part 2 (ICRP, 2016), a f_A value of 0.9 is used for all chemical forms of technetium in the workplace.

(575) The same value $f_A = 0.9$ is therefore adopted here for all chemical forms of rhenium.

Table 32.2. Absorption parameter values for inhaled and ingested rhenium.

	Absorption parameter values*			Absorption from the
Inhaled particulate materials	f_r	s_r (d^{-1})	s_s (d^{-1})	alimentary tract, f_A
Default parameter values†				
Absorption type				
F	1	30	–	0.9

M‡	0.2	3	0.005	0.18
S	0.01	3	1×10^{-4}	0.009

Ingested materials§	
All forms	0.9

*It is assumed that the bound state can be neglected for rhenium (i.e. $f_b = 0$). The values of s_r for Type F, M and S forms of rhenium (30, 3 and 3 d^{-1} respectively) are the general default values.

†For inhaled material deposited in the respiratory tract and subsequently cleared by particle transport to the alimentary tract, the default f_A values for inhaled materials are applied [i.e. the product of f_r for the absorption type and the f_A value for ingested soluble forms of rhenium (0.9)].

‡Default Type M is recommended for use in the absence of specific information on which the exposure material can be assigned to an absorption type (e.g. if the form is unknown, or if the form is known but there is no information available on the absorption of that form from the respiratory tract). For guidance on the use of specific information, see Section 1.1.

§Activity transferred from systemic compartments into segments of the alimentary tract is assumed to be subject to reabsorption to blood. The default absorption fraction f_A for the secreted activity is the highest value for any form of the radionuclide ($f_A = 0.9$).

32.2.3. Systemic distribution, retention and excretion of rhenium

32.2.3.1. Biokinetic data

(576) Rhenium (Re) is a member of Group VIIA of the period table. It exhibits biokinetic properties close to those of the lighter Group VIIA element technetium, presumably due to the similar ionic radii as well as the similar chemical properties of rhenium and technetium (Deutsch et al., 1986; Dadachova et al., 2002; Zuckier et al., 2004). Rhenium and technetium have similar coordination chemistry, often resulting in isostructural rhenium and technetium complexes. These two elements presumably become covalently bound with oxide ions to form the structurally similar anions perrhenate (ReO_4^-) and pertechnetate (TcO_4^-) in the body. These anions have medical applications as physiological analogues of iodide (Dadachova et al., 2002).

32.2.3.2. Biokinetic model for systemic rhenium

(577) The systemic biokinetic model applied in this publication series to technetium is also applied to rhenium. The model structure is shown in Fig. 32.1. Transfer coefficients are listed in Table 32.3.

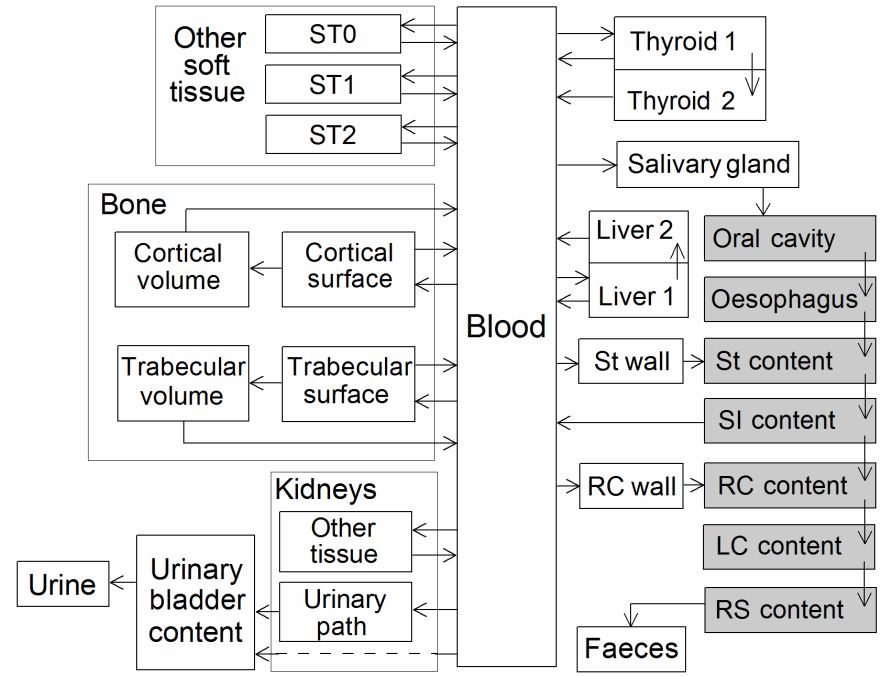

Fig. 32.1. Structure of the biokinetic model for systemic rhenium.

32.2.3.3. Treatment of progeny

(578) Progeny of rhenium isotopes addressed in this publication are radioisotopes of tungsten, tantalum, rhenium, and osmium. The model for rhenium as a parent is applied to rhenium produced by decay of another rhenium isotope. The models for tungsten, tantalum, and osmium as rhenium progeny are their characteristic models with added compartments and associated transfer coefficients needed to solve the linked biokinetic models for chains headed by rhenium (see Annex B). If produced in an ambiguous compartment (i.e. a compartment contained in the model for a preceding chain member but not contained in the progeny's characteristic model), the progeny is assumed to transfer at a specified rate to the central blood compartment of its characteristic biokinetic model and to follow that model thereafter. The following transfer rates to the central blood compartment are assigned to tungsten, tantalum, or osmium produced in an ambiguous compartment: 1000 d^{-1} if produced in a blood compartment; and at the following element-specific rates if produced in any other ambiguous compartment: tungsten, 8.32 d^{-1}; tantalum, 1.39 d^{-1}; osmium, 0.09902 d^{-1}

Table 32.3. Transfer coefficients in the biokinetic model for systemic rhenium.

From	To	Transfer coefficient (d^{-1})
Blood	Thyroid 1	7.0
Blood	ST0	71.88
Blood	ST1	3.0
Blood	ST2	0.18
Blood	Urinary bladder content	1.7
Blood	Salivary glands	2.6
Blood	Stomach wall	4.3
Blood	Kidneys 1	0.7
Blood	Kidneys 2	0.04
Blood	Liver 1	4.5

Blood	Right colon wall	3.4
Blood	Trabecular bone surface	0.35
Blood	Cortical bone surface	0.35
Thyroid 1	Blood	100
Thyroid 1	Thyroid 2	1.0
Thyroid 2	Blood	1.0
ST0	Blood	50
ST1	Blood	0.462
ST2	Blood	0.0347
Salivary glands	Oral cavity	50
Stomach wall	Stomach content	50
Kidneys 1	Urinary bladder content	8.32
Kidneys 2	Blood	0.0347
Liver 1	Blood	8.234
Liver 1	Liver 2	0.0832
Liver 2	Blood	0.0347
Right colon wall	Right colon content	1.39
Trabecular bone surface	Blood	0.457
Trabecular bone surface	Trabecular bone volume	0.00462
Cortical bone surface	Blood	0.457
Cortical bone surface	Cortical bone volume	0.00462
Trabecular bone volume	Blood	0.000493
Cortical bone volume	Blood	0.0000821

32.3. Individual monitoring

32.3.1. ^{186}Re

(579) Measurements of ^{186}Re may be performed by in vivo whole-body measurement technique and by gamma measurement in urine.

Table 32.4. Monitoring techniques for ^{186}Re

Isotope	Monitoring Technique	Method of Measurement	Typical Detection Limit
^{186}Re	Urine Bioassay	γ-ray spectrometry[a]	8 Bq L^{-1}
^{186}Re	Whole-body measurement	γ-ray spectrometry[ab]	265 Bq

[a] Measurement system comprised of Germanium Detectors
[b] Counting time of 20 minutes

32.3.2. ^{188}Re

(580) Measurements of ^{188}Re may be performed by in vivo whole-body measurement technique and by gamma measurement in urine. Measurements of in urine may be used to determine intakes of the radionuclide.

Table 32.5. Monitoring techniques for ^{188}Re.

Isotope	Monitoring Technique	Method of Measurement	Typical Detection Limit
^{188}Re	Urine Bioassay	γ-ray spectrometry[a]	5 Bq L^{-1}
^{188}Re	Whole-body measurement	γ-ray spectrometry[ab]	190 Bq

[a] Measurement system comprised of Germanium Detectors
[b] Counting time of 20 minutes

32.4. Dosimetric data for rhenium

Table 32.6. Committed effective dose coefficients (Sv Bq^{-1}) for the inhalation or ingestion of ^{186}Re and ^{188}Re compounds.

Inhaled particulate materials (5 µm AMAD aerosols)	Effective dose coefficients (Sv Bq^{-1})	
	^{186}Re	^{188}Re
Type F, — NB: Type F should not be assumed without evidence	3.9E-10	3.7E-10
Type M, default	3.7E-10	3.2E-10
Type S	3.6E-10	3.0E-10
Ingested materials		
All forms	5.5E-10	6.2E-10

AMAD, activity median aerodynamic diameter

Table 32.7 Dose per activity content of ^{186}Re in total body and in daily excretion of urine (Sv Bq^{-1}); 5µm activity median aerodynamic diameter aerosols inhaled by a reference worker at light work.

	Type F		Type M		Type S	
Time after intake (d)	Total body	Urine	Total body	Urine	Total body	Urine
1	8.3E-10	4.2E-09	7.3E-10	2.2E-08	7.0E-10	4.4E-07
2	1.4E-09	1.3E-08	1.5E-09	4.8E-08	1.6E-09	9.0E-07
3	2.4E-09	3.5E-08	3.6E-09	1.4E-07	4.0E-09	2.7E-06
4	4.1E-09	6.7E-08	7.0E-09	2.8E-07	8.7E-09	5.4E-06
5	6.8E-09	1.1E-07	1.1E-08	4.6E-07	1.4E-08	8.9E-06
6	1.1E-08	1.7E-07	1.6E-08	7.2E-07	1.8E-08	1.4E-05
7	1.6E-08	2.8E-07	2.1E-08	1.1E-06	2.3E-08	2.2E-05
8	2.4E-08	4.3E-07	2.8E-08	1.7E-06	2.8E-08	3.4E-05
9	3.6E-08	6.8E-07	3.5E-08	2.6E-06	3.4E-08	5.2E-05
10	5.1E-08	1.1E-06	4.5E-08	4.0E-06	4.2E-08	8.0E-05
15	2.5E-07	8.7E-06	1.3E-07	2.5E-05	1.1E-07	5.5E-04
30	8.9E-06	7.5E-04	2.6E-06	1.0E-03	1.9E-06	2.6E-02
45	2.3E-04	2.1E-02	4.7E-05	2.0E-02	3.2E-05	5.3E-01
60	6.0E-03	5.8E-01	8.7E-04	3.9E-01	5.4E-04	N/A
90	3.5E+00	N/A	2.9E-01	N/A	1.5E-01	
180	N/A		N/A		N/A	
365						

Table 32.8. Dose per activity content of ^{188}Re in total body and in daily excretion of urine (Sv Bq^{-1}); 5µm activity median aerodynamic diameter aerosols inhaled by a reference worker at light work.

	Type F		Type M		Type S	
Time after intake (d)	Total body	Urine	Total body	Urine	Total body	Urine
1	1.8E-09	8.8E-09	1.4E-09	4.3E-08	1.3E-09	8.2E-07
2	6.3E-09	5.8E-08	6.5E-09	2.0E-07	6.4E-09	3.7E-06
3	2.4E-08	3.6E-07	3.3E-08	1.3E-06	3.7E-08	2.5E-05
4	9.3E-08	1.5E-06	1.5E-07	5.8E-06	1.7E-07	1.1E-04
5	3.4E-07	5.5E-06	5.1E-07	2.1E-05	6.0E-07	3.9E-04
6	1.2E-06	1.9E-05	1.6E-06	7.3E-05	1.8E-06	1.4E-03
7	4.0E-06	6.7E-05	4.7E-06	2.5E-04	4.9E-06	4.7E-03
8	1.3E-05	2.3E-04	1.3E-05	8.4E-04	1.3E-05	1.6E-02
9	4.2E-05	8.1E-04	3.8E-05	2.8E-03	3.6E-05	5.5E-02
10	1.3E-04	2.8E-03	1.1E-04	9.4E-03	9.6E-05	1.8E-01
15	3.5E-02	1.2E+00	1.6E-02	3.1E+00	1.3E-02	N/A
30	N/A	N/A	N/A	N/A	N/A	
45						
60						
90						
180						
365						

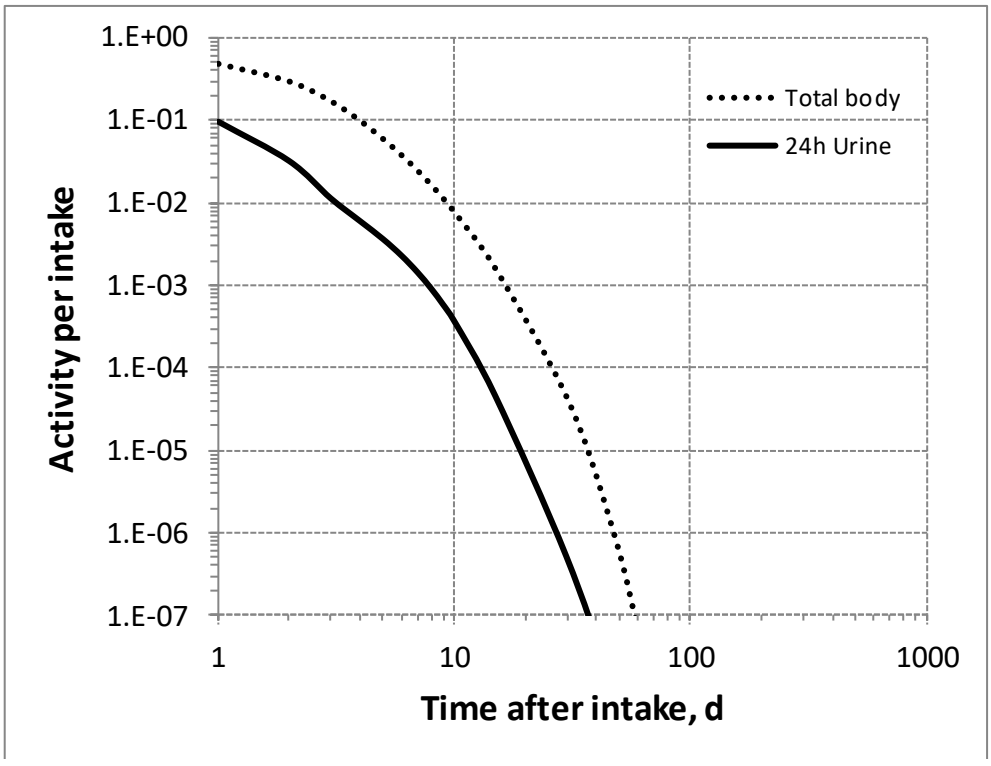

Fig. 32.2. Daily excretion of ^{186}Re following inhalation of 1 Bq Type F.

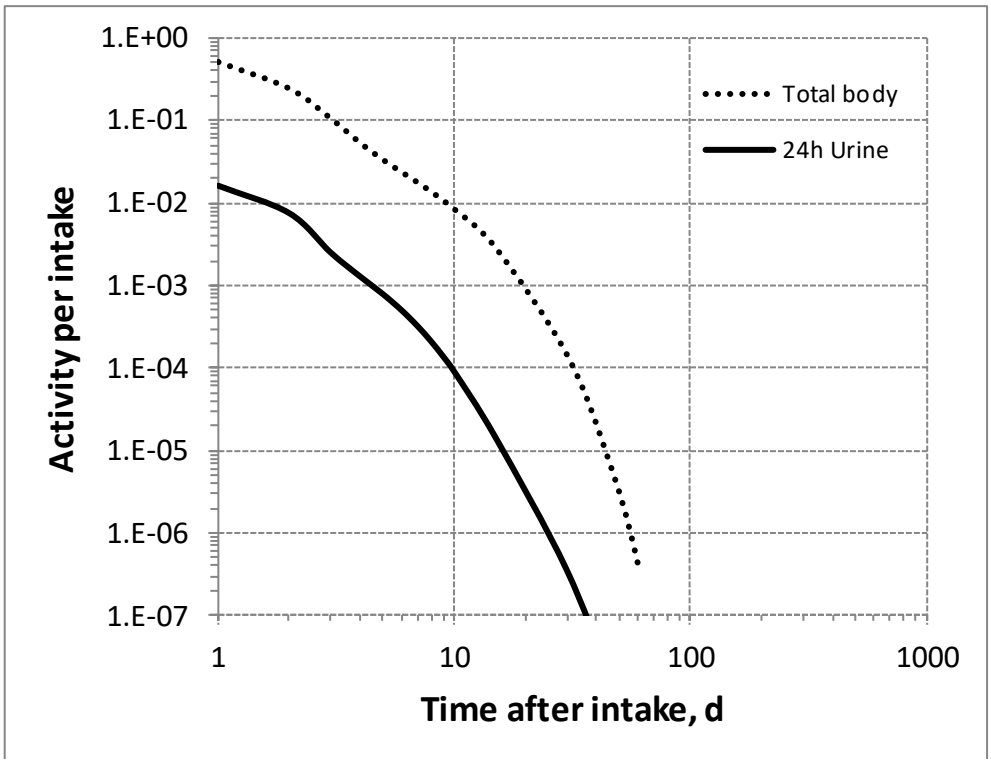

Fig. 32.3. Daily excretion of ^{186}Re following inhalation of 1 Bq Type M.

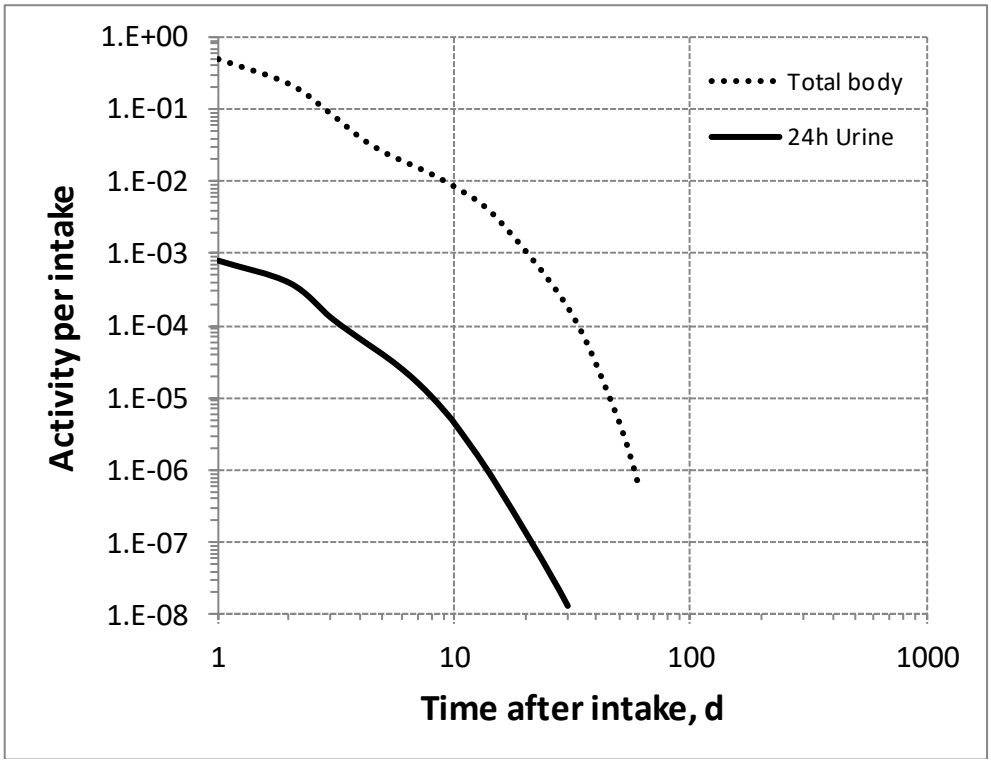

Fig. 32.4. Daily excretion of ^{186}Re following inhalation of 1 Bq Type S.

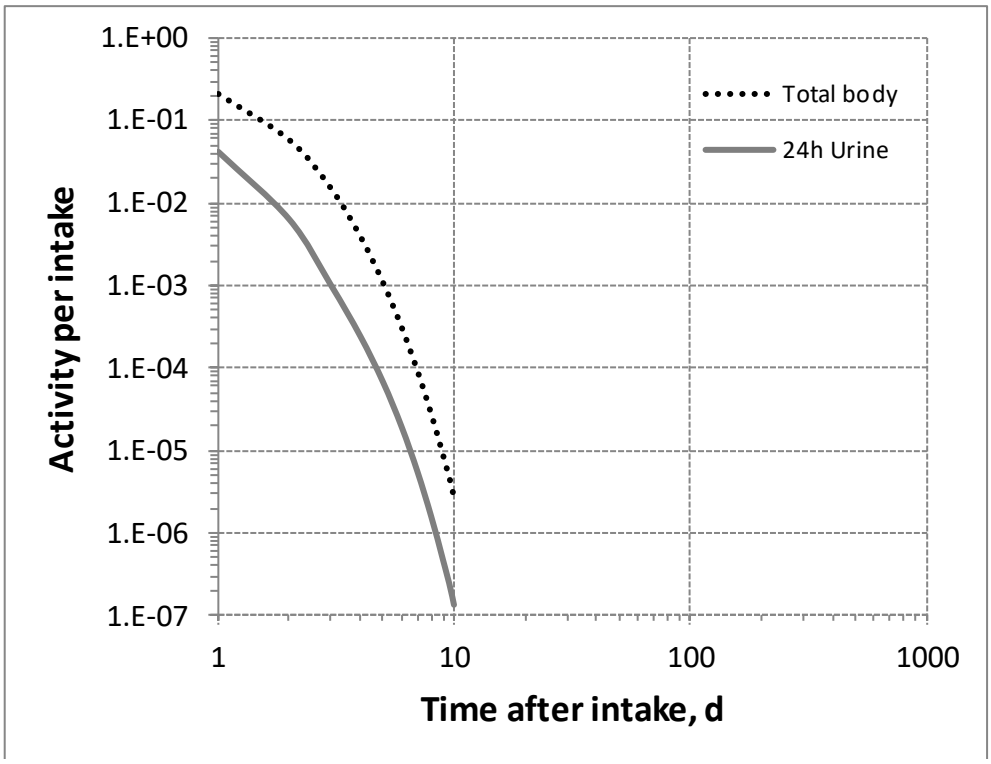

Fig. 32.5. Daily excretion of ^{188}Re following inhalation of 1 Bq Type F.

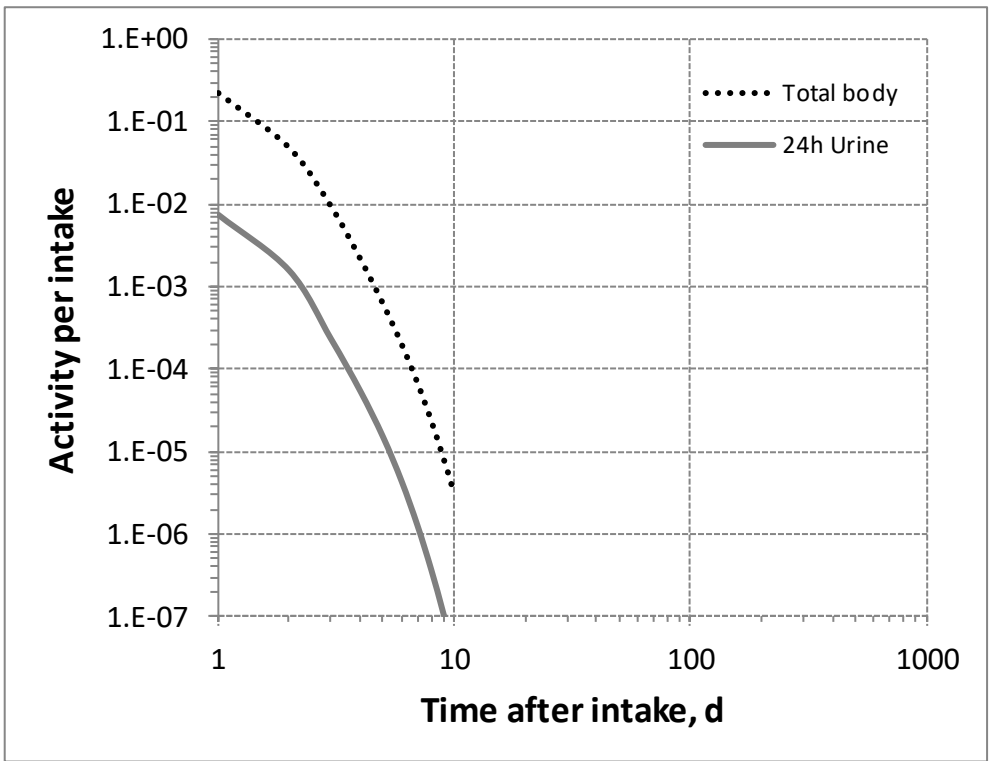

Fig. 32.6. Daily excretion of ^{188}Re following inhalation of 1 Bq Type M.

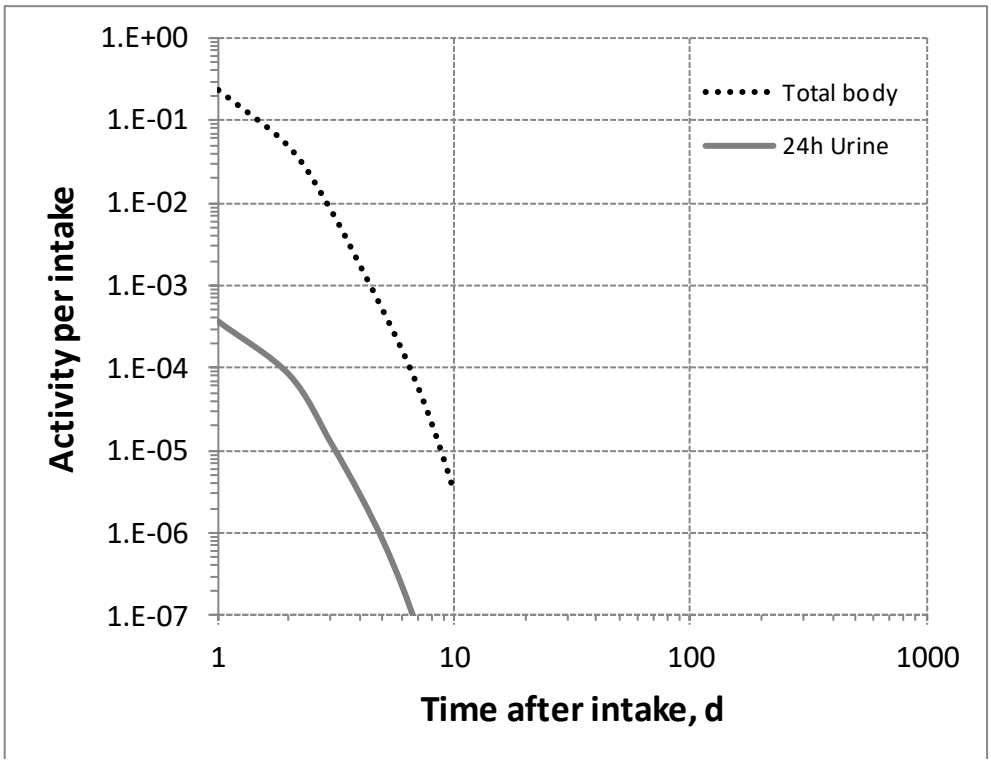

Fig. 32.7. Daily excretion of ^{188}Re following inhalation of 1 Bq Type S.

33. OSMIUM (Z=76)

33.1. Isotopes

Table 33.1. Isotopes of osmium addressed in this publication.

Isotope	Physical half-life	Decay mode
^{180}Os	21.5 min	EC, B+
^{181}Os	105 min	EC, B+
^{182}Os	22.10 h	EC
^{183}Os	13.0 h	EC, B+
^{183m}Os	9.9 h	EC, B+, IT
^{185}Os	93.6 d	EC
^{186}Os	2.0E+15 y	A
^{189m}Os	5.8 h	IT
^{191}Os	15.4 d	B-
^{191m}Os	13.10 h	IT
^{193}Os	30.11 h	B-
^{194}Os*	6.0 y	B-
^{196}Os	34.9 min	B-

EC, electron-capture decay; B+, beta-plus decay; B-, beta-minus decay; IT, isomeric transition decay; A, alpha decay.
*Dose coefficients and bioassay data for this radionuclide are given in the printed copy of this publication.
Data for other radionuclides listed in this table are given in the online electronic files on the ICRP website.

33.2. Routes of Intake

33.2.1. Inhalation

(581) For osmium, default parameter values were adopted on absorption to blood from the respiratory tract (ICRP, 2015). Absorption parameter values and types, and associated f_A values for particulate forms of osmium are given in Table 33.2.

33.2.2. Ingestion

(582) In *Publication 30* (ICRP, 1980), since there appeared to be no information available concerning the uptake of osmium from the gastrointestinal tract, a fractional absorption value of 0.01 was recommended for all chemical forms of osmium based on the chemical analogy with iridium. This value was also adopted in *Publication 68* (ICRP, 1994a). In OIR Part 3 (ICRP, 2017), the value of $f_A = 0.01$ was confirmed for all chemical forms of iridium.

(583) Rodushkin et al. (2011) investigated osmium retention in 22 bank voles trapped in north eastern Sweden and observed whole-body concentrations of up to about 7 pg g^{-1}, with highest concentration in kidney tissue, correlated with proximity of a steelwork and with lichen osmium concentration, about 10^4 times higher than in voles, at the location of animal sampling. Still, the available data are not sufficient to quantify the gastrointestinal absorption of osmium.

(584) The same value of $f_A = 0.01$ as in *Publications 30* and *68* is therefore adopted here for all chemical forms of osmium.

Table 33.2. Absorption parameter values for inhaled and ingested osmium.

Inhaled particulate materials	Absorption parameter values* f_r	s_r (d^{-1})	s_s (d^{-1})	Absorption from the alimentary tract, f_A
Default parameter values†				
Absorption type				
F	1	30	–	0.01
M‡	0.2	3	0.005	0.002
S	0.01	3	1×10^{-4}	1×10^{-4}
Ingested materials§				
All forms				0.01

*It is assumed that the bound state can be neglected for osmium (i.e. $f_b = 0$). The values of s_r for Type F, M and S forms of osmium (30, 3 and 3 d^{-1} respectively) are the general default values.

†For inhaled material deposited in the respiratory tract and subsequently cleared by particle transport to the alimentary tract, the default f_A values for inhaled materials are applied [i.e. the product of f_r for the absorption type and the f_A value for ingested soluble forms of osmium (0.01)].

‡Default Type M is recommended for use in the absence of specific information on which the exposure material can be assigned to an absorption type (e.g. if the form is unknown, or if the form is known but there is no information available on the absorption of that form from the respiratory tract). For guidance on the use of specific information, see Section 1.1.

§Activity transferred from systemic compartments into segments of the alimentary tract is assumed to be subject to reabsorption to blood. The default absorption fraction f_A for the secreted activity is the highest value for any form of the radionuclide ($f_A = 0.01$).

33.2.3. Systemic distribution, retention and excretion of osmium

33.2.3.1. Biokinetic data

(585) Osmium (Os) is a member of the platinum group, which comprises six chemically similar elements generally found together in ores: platinum, iridium, ruthenium, rhodium, palladium, and osmium. Biokinetic studies on rodents indicate broadly similar systemic behaviour across the platinum group following administration of relatively soluble forms (Durbin et al., 1957; Durbin, 1959; Mooreet al., 1975a,b,c; Weininger et al., 1990; Jamre et al., 2011).

(586) Highest concentrations of systemic osmium in rodents typically are seen in kidney and liver (Durbin et al., 1957; Durbin, 1959; Weininger et al., 1990; Jamre et al., 2011). Excretion is primarily in urine. The relative contents of systemic distribution of osmium at 1 d after intravenous injection closely resembled that of platinum (Durbin et al., 1957; Durbin, 1959).

(587) Weininger et al. (1990) investigated the influence of the pH of the injection solution on the systemic behaviour of the ^{191}Os impurity in ^{191}Os/^{191m}Ir generator eluates. Groups of mice were intravenously injected with ^{191}Os in one of four pH adjustment agents: phosphate, NaOH, lysine, or succinate. Retention was followed for 26 d in three of the groups but only 11 d in the group receiving ^{191}Os in the lysine buffer because of the fast body clearance in this case. Total-body retention curves for the NaOH (pH 4.5) and phosphate (pH 5.1) groups were similar to one another and to the retention pattern observed over a similar time period by Moore et al. (1975a,b,c) for systemic platinum in rats. Retention in the NaOH and phosphate groups was about twice that in the succinate group (pH 4.5) and >3 times that in the lysine group (pH 8.7) throughout common observation periods. The systemic distributions of ^{191}Os at 23 d were similar for the NaOH and succinate groups, with roughly 35% of total-body activity contained in bone, 25% in muscle, 20% in liver, and 2.5% in kidneys. For the phosphate group, nearly half the activity retained at 23 d was found in blood, 9% in bone, 8% in muscle, 12% in liver,

2% in kidneys, and 14% in spleen. In the lysine group, about 9% of the retained activity was in bone, 30% in muscle, 19% in liver, 13% in kidneys, and 24% in stomach and gut. These results indicate that the systemic kinetics of ^{191}Os depended on characteristics of the injection solution but not necessarily on pH alone, as different retention curves were seen for two agents with the same pH.

33.2.3.2. Biokinetics model for systemic osmium

(588) The systemic behaviour of osmium is assumed to be the same as that of the more frequently studied element platinum, in view of similarities in available comparative systemic data for these elements. The structure of the common biokinetic model for systemic platinum is shown in Fig. 33.1. The common set of transfer coefficients is listed in Table 33.3.

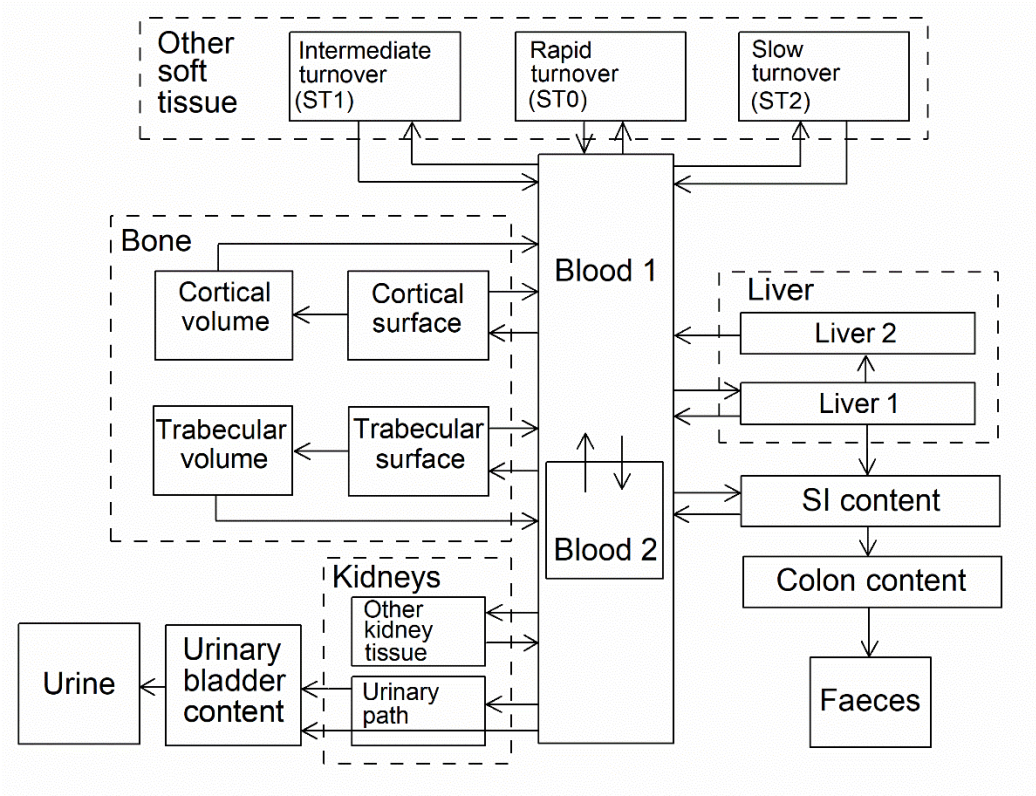

Fig. 33.1. Structure of the biokinetic model for systemic osmium.

33.2.3.3. Treatment of progeny

(589) Progeny of osmium addressed in this publication are isotopes of osmium, rhenium, tungsten, and iridium. The characteristic models for osmium and iridium are applied without change to these elements as progeny of osmium. The models for rhenium and tungsten as progeny of osmium are expansions of the characteristic models for these elements used in this publication, with added compartments and associated transfer coefficients needed to solve the linked biokinetic models for chains headed by osmium (see Annex B). If produced in an ambiguous compartment (i.e. a compartment not explicitly named in the model for rhenium or tungsten), the progeny is assumed to transfer at a specified rate to the central blood compartment of its characteristic biokinetic model and to follow that model thereafter. The following transfer rates to the central blood compartment are assigned to rhenium or tungsten produced in an

ambiguous compartment: 1000 d^{-1} if produced in a blood compartment; at the rate of bone turnover if produced in a bone volume compartment; and at the following element-specific rates if produced in any other ambiguous compartment: rhenium, 0.462 d^{-1}; tungsten, 8.32 d^{-1}.

Table 33.3. Transfer coefficients in the biokinetic model for systemic osmium.

From	To	Transfer coefficients (d^{-1})
Blood 1	Small intestine contents	3.0
Blood 1	Urinary bladder contents	23
Blood 1	Liver 1	12
Blood 1	Urinary path	10.67
Blood 1	Other kidney tissue	0.33
Blood 1	Blood 2	27
Blood 1	ST0	15
Blood 1	ST1	2.5
Blood 1	ST2	2.5
Blood 1	Cortical bone surface	1.0
Blood 1	Trabecular bone surface	3.0
Blood 2	Blood 1	0.6931
Liver 1	Blood 1	0.09704
Liver 1	Small intestine contents	0.03466
Liver 1	Liver 2	0.006931
Liver 2	Blood 1	0.003798
Urinary path	Urinary bladder contents	0.1386
Other kidney tissue	Blood 1	0.003798
ST0	Blood 1	0.09902
ST1	Blood 1	0.0231
ST2	Blood 1	0.0009495
Cortical bone surface	Blood 1	0.07922
Trabecular bone surface	Blood 1	0.07922
Cortical bone surface	Cortical bone volume	0.0198
Trabecular bone surface	Trabecular bone volume	0.0198
Cortical bone volume	Blood 1	0.0000821
Trabecular bone volume	Blood 1	0.000493

33.3. Individual monitoring

(590) Information of detection limit for routine individual measurement is not available.

33.4. Dosimetric data for osmium

Table 12.6. Committed effective dose coefficients (Sv Bq^{-1}) for the inhalation or ingestion of ^{194}Os compounds.

Inhaled particulate materials (5 µm AMAD aerosols)	Effective dose coefficients (Sv Bq^{-1})
	^{194}Os
Type F, — NB: Type F should not be assumed without evidence	4.1E-09
Type M, default	8.7E-09

Type S	6.7E-08
Ingested materials	
All forms	4.6E-10

AMAD, activity median aerodynamic diameter

34. PLATINUM (Z=78)

34.1. Isotopes

Table 34.1. Isotopes of platinum addressed in this publication.

Isotope	Physical half-life	Decay mode
^{184}Pt	17.3 min	EC, B+, A
^{186}Pt	2.08 h	EC, A
^{187}Pt	2.35 h	EC, B+
^{188}Pt	10.2 d	EC, A
^{189}Pt	10.87 h	EC, B+
^{190}Pt	6.50E+11 y	A
^{191}Pt	2.802 d	EC
^{193}Pt*	50 y	EC
^{193m}Pt	4.33 d	IT
^{195m}Pt	4.02 d	IT
^{197}Pt	19.8915 h	B-
^{197m}Pt	95.41 min	ITB-
^{199}Pt	30.80 min	B-
^{200}Pt	12.5 h	B-
^{202}Pt	44 h	B-

EC, electron-capture decay; B+, beta-plus decay; B-, beta-minus decay; IT, isomeric transition decay; A, alpha decay.
*Dose coefficients and bioassay data for this radionuclide are given in the printed copy of this publication. Data for other radionuclides listed in this table are given in the online electronic files on the ICRP website.

34.2. Routes of Intake

34.2.1. Inhalation

(591) For platinum, default parameter values were adopted on absorption to blood from the respiratory tract (ICRP, 2015). Absorption parameter values and types, and associated f_A values for particulate forms of platinum are given in Table 34.2.

34.2.2. Ingestion

34.2.2.1. Animal studies of soluble platinum

(592) In *Publication 30* (ICRP, 1981), a fractional absorption value of 0.01 was recommended for all chemical forms of platinum based on the animal studies by Moore et al. (1975) and Holbrook et al. (1975). This value was also adopted in *Publication 68* (ICRP, 1994a).

(593) Lown et al. (1980) analysed the systemic distribution of platinum after intragastric administration of the sulphate to adult male mice and found their results to be consistent with those of Moore at al. (1975). Hirunuma et al. (1997) and Yanaga et al. (1996) studied the uptake, retention and excretion of several elements including platinum, considered to be in anionic form. The multitracer experiment involved oral administration to 12 adult rats and monitoring of organ retention, urine and faecal excretion for 6 days after administration. 98% of the platinum dose was excreted into faeces and 1.4% of the dose into urine, the remainder being found in the

kidneys, liver, intestine and skeletal muscle. These results indicate gastrointestinal absorption around 0.02.

34.2.2.2. Experimental studies of platinum in vehicle exhaust catalysts

(594) Automobile exhaust catalytic converters emit fine platinum bearing particles. Platinum is initially in the metallic and oxide forms. After dispersion in road dust, water, sediments or vegetation, it may interact with environmental ligands, be transformed into more soluble species and eventually enter the food chain. To simulate the behaviour of exhaust particles, Artelt et al. (1998, 1999) investigated the bioavailability of metallic platinum attached to aluminium oxide particles of diameters less than 5 µm diameter. Platinum showed a solubility of 10% in a physiological sodium chloride solution. Oral administration to eight rats resulted in gastrointestinal absorption of about 0.1% of platinum intake as estimated from monitoring of urine and faeces over 8 days after administration. In an in vitro dissolution study, Colombo et al. (2008) have estimated the bioavailability of platinum to be 16% from road dust, but only 0.01% from $Pt(OH)_2$ hydroxide samples and 0.1% from an automobile catalyst powder. No strong influence of pH on dissolution was observed. In another study of dissolution of automobile catalysts in simulated human gastrointestinal tract medium, Turner and Price (2008) observed a relatively small bioavailability of platinum in the order of a few percents. The availability of platinum appeared to be controlled by the rate of dissolution of metallic particles in the stomach and by the kinetics of the formation and dissolution of inorganic comounds of the metal (chlorides or hydroxychlorides), and their organic complexes.

(595) Consistent with the above findings, in the study by Holbrook et al. (1975), not involving vehicle exhaust, the organ retention of platinum was at least an order of magnitude lower after ingestion of platinum dioxide than after ingestion of the chloride or sulphate.

34.2.2.3. Monitoring of population exposure

(596) The level of incorporated platinum in human populations due to dental alloys, environmental or occupational exposure was investigated in bioassay studies providing qualitative indication on platinum absorption: Begerow et al. (1999) measured higher levels of platinum in urine of 27 dental technicians than in urine of 17 road construction workers and 17 school-leavers, indicating occupational internal exposure from treatment of dental alloys. Enhanced urinary platinum concentrations (above 20 ng g^{-1}) and long term excretions were observed for persons having dental gold alloys (Begerow et al., 1999). Relatively high platinum concentrations were found in the urine of occupationally exposed persons (Ensslin et al., 1997; Nygren and Lundgren, 1997) and of school children residing in areas with high traffic density (Caroli et al., 2001). Becker et al. (2003) studied the levels of environmental pollutants in the urine of the German population and found a clear influence of the number of dental inlays, crowns and bridge elements on the mean levels of platinum in urine.

(597) The same value of f_A = 0.01 is adopted here for soluble forms of platinum as in *Publications 30* and *68*. For metallic, oxide and hydroxide platinum compounds a lower f_A = 0.001 is adopted.

Table 34.2. Absorption parameter values for inhaled and ingested platinum.

Inhaled particulate materials	Absorption parameter values* f_r	s_r (d^{-1})	s_s (d^{-1})	Absorption from the alimentary tract, f_A
Default parameter values†				
Absorption type				

F	1	30	–	0.01
M‡	0.2	3	0.005	0.002
S	0.01	3	1×10^{-4}	1×10^{-4}
Ingested materials§				
Soluble forms				0.01
Metal, oxide and hydroxide				0.001

*It is assumed that the bound state can be neglected for platinum (i.e. $f_b = 0$). The values of s_r for Type F, M and S forms of platinum (30, 3 and 3 d^{-1} respectively) are the general default values.

†For inhaled material deposited in the respiratory tract and subsequently cleared by particle transport to the alimentary tract, the default f_A values for inhaled materials are applied [i.e. the product of f_r for the absorption type and the f_A value for ingested soluble forms of platinum (0.01)].

‡Default Type M is recommended for use in the absence of specific information on which the exposure material can be assigned to an absorption type (e.g. if the form is unknown, or if the form is known but there is no information available on the absorption of that form from the respiratory tract). For guidance on the use of specific information, see Section 1.1.

§Activity transferred from systemic compartments into segments of the alimentary tract is assumed to be subject to reabsorption to blood. The default absorption fraction f_A for the secreted activity is the highest value for any form of the radionuclide ($f_A = 0.01$).

34.2.3. Systemic distribution, retention and excretion of platinum

34.2.3.1. Biokinetic data

(598) The platinum group comprises six chemically similar elements generally found together in ores: platinum, iridium, ruthenium, rhodium, palladium, and osmium. Biokinetic studies on rodents indicate broadly similar biokinetics across the platinum group (Durbin et al., 1957; Durbin, 1959; Moore et al., 1975a; Weininger et al., 1990; Jamre et al., 2011).

(599) The systemic behaviour of platinum has been studied in laboratory animals, mainly rats, and to some extent in human subjects (Durbin et al., 1957; Durbin, 1959; Lange et al., 1973; Smith and Taylor, 1974; Moore et al, 1975a,b,c; Yoakum et al., 1975; Litterst et al., 1976; Hirunuma et al., 1997). Platinum shows a high rate of urinary excretion in the early days after administration. Some but not all studies also indicate a relatively high rate of faecal excretion. Following intravenous administration of platinum isotopes as the chloride to rats, highest concentrations generally were found in the kidneys, followed by the liver (Durbin et al., 1957; Moore et al., 1975a,b,c). At 1 month the rats contained roughly 10-15% of the intravenously injected activity.

(600) The biokinetics of platinum has been studied in human subjects following administration of the antitumor agent cis-diamminedichloroplatinum (II) (DDP) (Lange et al., 1973; Smith and Taylor, 1974). The systemic behaviour of the platinum label resembled that of other forms of platinum administered to laboratory animals. Following intravenous administration of ^{195m}Pt-labelled DDP to two cancer patients, approximately 35% of the injected activity was excreted in urine during the first 3.5 d (Smith and Taylor, 1974). At most a few percent of the activity was excreted in faeces during that time. Based on external measurements, the liver accumulated about 10% of the injected activity during the first day. The estimated biological half-times of the label in the liver and total body during days 1-7 were 8 d and 10 d, respectively. The study period was too short to determine any longer-term components of retention.

34.2.3.2. Biokinetic model for systemic platinum

(601) The structure of the biokinetic model for systemic platinum used in this publication is shown in Fig. 34.1. Transfer coefficients are listed in Table 34.3. The same model was applied earlier in this publication series to platinum as a progeny of other platinum metals. The model is a modification of the characteristic biokinetic model for ruthenium described in Part 2 of this publication series. The ruthenium model was modified for application to platinum by shifting a portion of the deposition in bone and soft tissue compartments to the urinary bladder contents and kidneys. The modifications are described in Section 8.2.3.3 of *Publication 137* (2017).

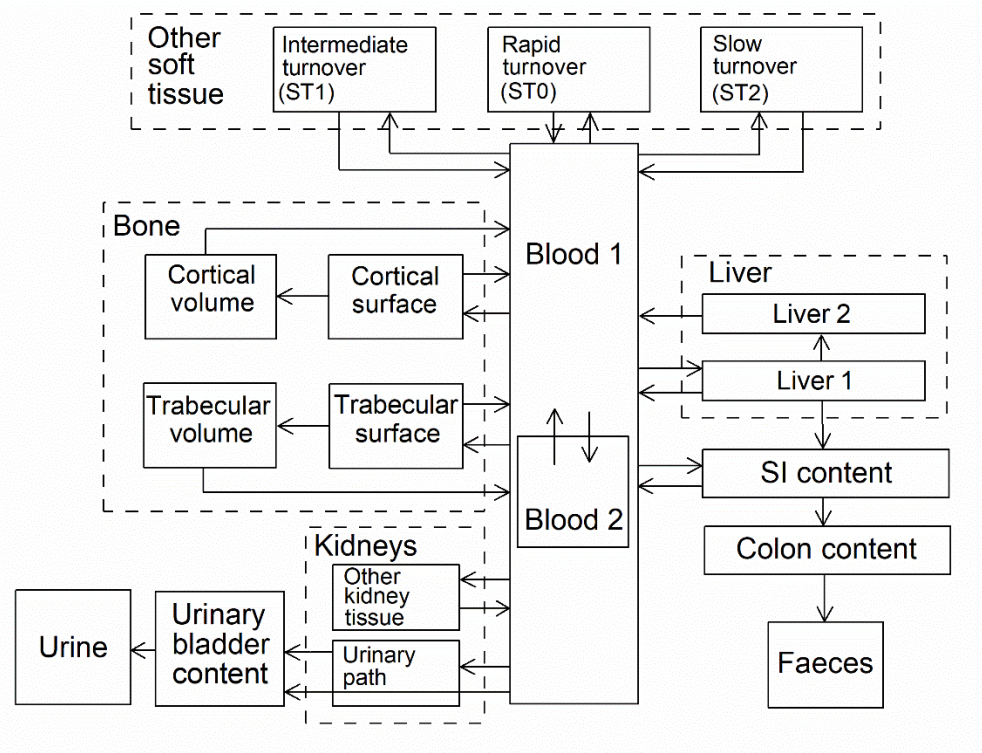

Fig. 34.1. Structure of the biokinetic model for systemic platinum.

34.2.3.3. Treatment of progeny

(602) Progeny of platinum addressed in this publication are isotopes of platinum, rhenium, osmium, iridium, and gold. The characteristic models for platinum, osmium, and iridium used in this publication are applied to these elements as progeny of platinum. The models for rhenium and gold as progeny of platinum are expansions of the characteristic models for these elements with added compartments and associated transfer coefficients needed to solve the linked biokinetic models for chains headed by platinum (see Annex B). The following transfer rates to the central blood compartment are assigned to rhenium or gold produced in an ambiguous compartment (i.e. a compartment of a preceding chain member that is not a compartment in the characteristic model for the progeny: 1000 d^{-1} if produced in a blood compartment; at the rate of bone turnover if produced in a bone volume compartment; and at the following element-specific rates if produced in any other ambiguous compartment: rhenium, 0.462 d^{-1}; gold, 0.0693 d^{-1}).

6057 Table 34.3. Transfer coefficients in the biokinetic model for systemic platinum.

From	To	Transfer coefficients (d^{-1})
Blood 1	Small intestine contents	3.0
Blood 1	Urinary bladder contents	23
Blood 1	Liver 1	12
Blood 1	Urinary path	10.67
Blood 1	Other kidney tissue	0.33
Blood 1	Blood 2	27
Blood 1	ST0	15
Blood 1	ST1	2.5
Blood 1	ST2	2.5
Blood 1	Cortical bone surface	1.0
Blood 1	Trabecular bone surface	3.0
Blood 2	Blood 1	0.6931
Liver 1	Blood 1	0.09704
Liver 1	Small intestine contents	0.03466
Liver 1	Liver 2	0.006931
Liver 2	Blood 1	0.003798
Urinary path	Urinary bladder contents	0.1386
Other kidney tissue	Blood 1	0.003798
ST0	Blood 1	0.09902
ST1	Blood 1	0.0231
ST2	Blood 1	0.0009495
Cortical bone surface	Blood 1	0.07922
Trabecular bone surface	Blood 1	0.07922
Cortical bone surface	Cortical bone volume	0.0198
Trabecular bone surface	Trabecular bone volume	0.0198
Cortical bone volume	Blood 1	0.0000821
Trabecular bone volume	Blood 1	0.000493

6058 ## 34.3. Individual monitoring

6059 (603) Information of detection limit for routine individual measurement is not available.
6060

6061 ## 34.4. Dosimetric data for platinum

6062 Table 34.4. Committed effective dose coefficients (Sv Bq^{-1}) for the inhalation or ingestion of ^{193}Pt
6063 compounds.

Inhaled particulate materials (5 µm AMAD aerosols)	Effective dose coefficients (Sv Bq^{-1})
	^{193}Pt
Type F, — NB: Type F should not be assumed without evidence	4.2E-11
Type M, default	5.3E-11
Type S	9.5E-10

Ingested materials	
Soluble forms	3.5E-12
Metal, oxide and hydroxide	1.8E-12

AMAD, activity median aerodynamic diameter

35. GOLD (Z=79)

35.1. Isotopes

Table 35.1. Isotopes of gold addressed in this publication.

Isotope	Physical half-life	Decay mode
^{186}Au	10.7 min	EC, B+
^{190}Au	42.8 min	EC, B+
^{191}Au	3.18 h	EC, B+
^{192}Au	4.94 h	EC, B+
^{193}Au	17.65 h	EC
^{194}Au	38.02 h	EC, B+
^{195}Au*	186.098 d	EC
^{196}Au	6.183 d	EC, B-
^{196m}Au	9.6 h	IT
^{198}Au	2.69517 d	B-
^{198m}Au	2.27 d	IT
^{199}Au	3.139 d	B-
^{200}Au	48.4 m	B-
^{200m}Au	18.7 h	B-IT
^{201}Au	26 m	B-

EC, electron-capture decay; B+, beta-plus decay; B-, beta-minus decay; IT, isomeric transition decay.
*Dose coefficients and bioassay data for this radionuclide are given in the printed copy of this publication.
Data for other radionuclides listed in this table are given in the online electronic files on the ICRP website.

35.2. Routes of Intake

35.2.1. Inhalation

(604) The ICRP Task Group on Lung Dynamics (TGLD, 1966) assigned oxides and hydroxides of gold to inhalation class Y, halides and nitrates to inhalation class W and all other compounds of the element to inhalation class D. In the absence of any relevant experimental data this classification was adopted by ICRP in *Publication 30* (ICRP, 1980).

(605) No information was found on the behaviour of inhaled gold in human subjects following accidental intake. The only in vivo experimental information found on the behaviour of gold following deposition of any soluble form in the respiratory tract was at a single time point in one experiment. Therefore, no estimates could be made of element-specific rapid dissolution rate or bound state parameter values.

(606) However, radioisotopes of gold have been used extensively to label relatively insoluble particles for experimental studies of particle deposition in and transport from the respiratory tract. The particle matrices include elemental gold, iron oxide, and Teflon (see below). Elemental gold has recently been used to investigate the behaviour of nanoparticles (particles with at least one dimension < 100 nm) after deposition in the lungs. Following deposition of relatively insoluble radiolabelled particles in the lungs, two distinct clearance phases are usually observed: a fast phase, completed in about a day, and a much slower phase. On the assumption that these represent, respectively, the mucociliary clearance of particles deposited in the conducting tracheo-bronchial airways, and clearance of particles deposited in the alveolar region, measurements of lung retention for at least a few days after inhalation were used to

assess regional deposition. Gold-198, a readily available beta-gamma emitter with a half-life of 2.7 d, was often used for regional deposition, and short-term clearance, studies. While such use of the labelled particles showed them to be relatively insoluble for the purposes of the experiment, the short half-life means that measurements were of insufficient duration to distinguish between Type M and Type S behaviour, and no attempt to do so was made here.

(607) A few experiments using ^{195}Au, half-life 183 d, were of much longer duration and do provide information to assign the materials used to Type S.

(608) Absorption parameter values and types, and associated f_A values for particulate forms of gold are given in Table 35.2.

35.2.1.1. Particulate materials

a. Ionic gold

(609) Kreyling et al. (2014) measured the tissue distribution and excretion of ^{198}Au in rats 24 h after intratracheal instillation of ^{198}Au-labelled soluble gold ions. About 28% of the initial lung deposit remained in the lungs. If lung retention followed a single exponential function, this result would give a biological half-time, T_b of about 0.5 d, indicating a rate of absorption to blood of about 1 d^{-1}.

(610) Bachler et al. (2015) measured the translocation across the epithelial tissue boundary of ionic gold, for comparison with that of gold nanoparticles (see below). The gold was deposited from an aerosol onto the surface of a monolayer of alveolar epithelial cells in vitro. Translocation in 24 hours was about 75%, similar to that of the smallest particles (2 nm diameter) and much higher than that of the larger particles studied.

b. Elemental gold

(611) Berg (1951) investigated the distribution of ^{198}Au in dogs 3 d after injection of ^{198}Au-labelled colloidal gold particles into the pleural cavity. Activity found outside the lungs was predominantly in liver and spleen and therefore may have transferred mainly in particulate form rather than in solution.

(612) Bryant et al. (1953) and Berg et al. (1954) measured the uptake of ^{198}Au-labelled colloidal gold (3 to 4 nm diameter) into the hilar lymph nodes of dogs for up to about 30 d after instillation into the bronchial lumen, or injection into the submucosa of a bronchus. The uptake in other organs, including spleen and liver was very low, indicating that little ^{198}Au entered the bloodstream.

(613) Meneely et al. (1953) studied the tissue distribution of ^{198}Au in dogs at times up to 15 d after intratracheal instillation of ^{198}Au-labelled colloidal gold (approximately 0.05 μm diameter). They concluded that the low level of activity in liver and spleen was evidence for a low rate of transfer of the colloid to blood.

(614) Welsh and Welsh (1963) investigated uptake by cervical lymph nodes for 8 d following instillation of radiolabelled gold into the human larynx.

(615) Gongora et al. (1973, 1974) followed lung retention of ^{198}Au for up to about 30 d after inhalation of ^{198}Au-labelled gold particles (0.03 μm) by 20 healthy volunteers. Lung retention was fit by a two-component exponential function: the slow phase T_b ranged from 26 to 1000 d.

(616) Takahashi et al. (1989) followed the lung retention and distribution of gold for 3 d after intratracheal instillation of stable colloidal gold particles (count median diameter, CMD, 10 nm) into rats.

(617) Patrick and Stirling (1992, 1994) administered ^{195}Au-labelled colloidal gold particles (CMD, 10 – 20 nm) to rats by microinjection into subpleural alveoli, to confine the initial deposition to alveolar tissue. They followed retention and distribution of ^{195}Au for 462 d. Lung retention was well described by a two-component exponential function, with approximately 22% of the initial lung deposit (ILD) clearing with T_b = 14 d, and the rest with a mean T_b = 583 d. Patrick and Stirling (1997a) carried out complementary experiments in which the biokinetics of ^{195}Au in rats was followed for 7 d after instillation of a suspension of the particles into the stomach, and for 21 d after intravenous injection of ^{195}Au-labelled gold chloride. Using the results, and measurements of excretion at times between 28 and 462 d, they assessed the rate of dissolution of the gold particles in the lungs to be between 5×10^{-5} and 4×10^{-4} d^{-1}, giving assignment to Type S.

(618) Patrick and Stirling (1997b) followed the lung retention and distribution of ^{195}Au for 7 d after intratracheal instillation of ^{195}Au-labelled colloidal gold particles (CMD, 10 – 20 nm) into rats.

(619) Takenaka et al. (2006) studied the distribution of ultrafine (5–8 nm diameter) stable gold particles for 7 days after inhalation by rats. Lung tissues and lavaged cells were examined by electron microscopy, and gold concentrations in lung, lavage fluid and blood measured. Only a little particle translocation to the systemic circulation took place.

(620) Smith et al. (2007, 2008) followed lung retention of ^{198}Au-labelled gold particles for up to about 10 d after inhalation by volunteers as an aerosol bolus at the end of each breath, to minimise alveolar deposition. The aim of the study was to investigate the effect of particle diameter on clearance from the bronchial tree. The volunteers also inhaled ^{111}In-labelled polystyrene (PSL) particles with the same aerodynamic diameter, d_{ae}, (5 µm and 8 µm in the two studies) but larger physical diameter, because of PSL's much lower density than that of gold. Some subjects provided 24-hour urine samples, which were used to confirm that there was no significant leaching of the radiolabels from the particles.

(621) Semmler-Behnke et al. (2008) measured the tissue distribution of ^{198}Au in rats 24 hours after intratracheal instillation of an aqueous suspension of ^{198}Au-labelled 18 nm or 1.4 nm diameter gold nanoparticles (NP). For the 18 nm NP, 99.8% of the retained ^{198}Au was in the lungs, but for the 1.4 nm NP, 91.5% was in the lungs, and the rest widely distributed through the body. Complementary experiments were conducted in which the NP were administered by instillation into the oesophagus or by intravenous (IV) injection. There was minimal absorption from the alimentary tract. The distributions were different after IV injection: notably the amounts retained in liver were 94% for the 18 nm NP and 48% for the 1.4 nm NP.

(622) Balasubramanian et al. (2013) measured the tissue distribution of (stable) gold in rats 2 days after inhalation (whole body, 6 hours per day, 5 days per week for three weeks) of agglomerates (about 45 nm diameter) of primary gold NP with diameter 7 nm or 20 nm. Faeces and urine were collected at times during the exposure period. The authors assessed that the ratio of gold detected in the blood and secondary target organs to that in the lungs was 1.4% and 0.2% respectively, after inhalation of agglomerates of 7 nm and 20 nm gold NP. There were also differences in tissue distributions between the two primary particle sizes.

(623) Schleh et al. (2013) measured the tissue distribution of ^{195}Au in mice immediately after inhalation of ^{195}Au-labelled 20 nm diameter gold nanoparticles (NP). The aerosol was inhaled via an intratracheal cannula, by mice that were anaesthetised and artificially ventilated. The authors assessed that 1.2 ± 0.5% (mean ± SEM) of the initial lung deposit translocated across the air-blood barrier.

(624) Kreyling et al. (2014) measured the tissue distribution of ^{198}Au in rats 1, 3 and 24 h after intratracheal instillation of ^{198}Au-labelled monodisperse NP: negatively charged 1.4, 2.8, 5, 18, 80 and 200 nm diameter NP; and positively charged 2.8 nm diameter NP. For the

negatively charged NP, assessed translocation across the air-blood barrier was about 7% for 1.4 nm NP [similar to that observed by Semmler-Behnke et al. (2008)]; about 2% for 2.8 nm NP, and less than 1% for the larger particles. Kreyling et al. (2014) concluded that translocation was inversely proportional to the gold NP core diameter between 1.4 nm and 80 nm NP. However, for the 200 nm particles it was higher than predicted by this relationship, and similar to that of the 5 nm NP. Translocation of the positively charged 2.8 nm NP was significantly lower than that of the negatively charged 2.8 nm NP. Tissue distributions of translocated ^{198}Au did not vary significantly with core diameter, but urinary excretion increased with decreasing size.

(625) Han et al. (2015) measured the tissue distribution of stable gold in rats at 1, 3 and 28 days after inhalation (6 hours per day for 5 days) of 13 nm or 105 nm gold NP. Transfer of the smaller particles from the lungs to other organs was significantly higher than that of the larger particles, but tissue concentrations were low: < 1% of that in the lungs.

(626) Bachler et al. (2015) measured the translocation across the epithelial tissue boundary of gold nanoparticles (2, 7, 18, 46, or 80 nm diameter) deposited (from an aerosol) onto the surface of a monolayer of alveolar epithelial cells in vitro. Translocation in 24 hours was much higher for the 2 nm particles (about 60%) and 7 nm (about 10%) than for the larger particles (about 2%). The translocation fraction for ionic gold (see above) was 75%.

(627) Miller et al. (2017) measured (stable) gold in the blood and urine of volunteers during the first 24 hours and at 3 months after inhalation of 4 nm (primary particle size) gold NP. Gold was detectable in the bloodstream in some subjects within 15 min of the 2 h exposure and in the majority (12/14) at 24 h. Gold was still detectable in blood and urine after 3 months. In a second volunteer study, the effect of particle size on translocation from lungs to blood was investigated at times up to 28 d. Concentrations of gold in blood and urine were much lower after inhalation of 34 nm NP than after inhalation of 4 nm NP. To address tissue accumulation over a wider range of particle sizes, mice were repeatedly intratracheally instilled for five weeks with 2, 5, 10, 30, or 200 nm gold particles, and euthanised for analysis 18 h after the last instillation. Gold was detectable in the blood following exposure to each size. However, the incidence of detectable gold, and the concentration of gold, in the blood was far greater following exposure to the smaller particles. Miller et al. (2017) also investigated accumulation of translocated gold NP in sites of vascular accumulation, following inhalation by volunteers, and instillation into mice.

(628) Kreyling et al. (2018) followed the biokinetics of ^{195}Au in rats for 28 d after inhalation (via an intratracheal tube) of 20 nm diameter ^{195}Au-labelled gold NP (The study also investigated the effect of age on pulmonary deposition of gold NP.). Lung retention fit by a single exponential function gave T_b = 28 d, but it was recognised that this short time for relatively insoluble particles was likely to be due to the short duration of measurements. It was assessed that about 2% of the 'initial deposited pulmonary lung dose (IPLD)' had been absorbed into blood by 1 day and was predominantly in soft tissue. This increased to about 4% at 28 d, mainly excreted in urine.

(629) There is evidence from several studies that translocation of gold NP from lungs to blood occurs and increases with decreasing particle size. Specific parameter values could in principle be calculated for 1.4 nm gold NP based on the study by Semmler-Behnke et al. (2008), but it is a single *in vivo* study and inhalation exposure to such particles is unlikely. Furthermore, the highest measured fraction translocated was only about 8%, for 1.4 nm gold NP, and at most sizes about 1% or less.

c. Iron oxide (Fe_2O_3)

(630) Monodisperse ^{198}Au-labelled iron oxide (Fe_2O_3) particles have been used extensively to assess regional deposition in the human respiratory tract.

(631) Lippmann and Albert (1969) studied the effect of particle size (d_{ae}) on regional deposition of ^{198}Au-labelled Fe_2O_3 particles inhaled by volunteers. External measurements were made of activity in head, lung and abdomen for at least 1 d.

(632) Stahlhofen et al. (1980) assessed regional deposition of monodisperse ^{198}Au-labelled Fe_2O_3 particles between 1 and 10 μm diameter. They followed lung retention for up to 10 d after inhalation by three healthy volunteers. The slow phase of lung retention had a mean T_b = 60 d (range 50 – 70 d). Stahlhofen et al. (1981) noted that this was shorter than for ^{198}Au-labelled Teflon particles (see below), possibly because of loss of label from the Fe_2O_3.

(633) Stahlhofen et al. (1986a,b, 1990) administered monodisperse ^{198}Au-labelled Fe_2O_3 particles to healthy volunteers as a small 'bolus' (i.e. confined to a small volume within the tidal air, to assess particle clearance from specific sites within the lungs). They followed lung retention for a few days after inhalation: long enough to determine the fractions cleared in the fast and slow phases.

(634) Stahlhofen et al. (1986b) refer to previously conducted in vitro dissolution tests in which: 'No disintegration of the Fe_2O_3 particles of ^{198}Au from particles suspended in body liquids could be found and the leakage of ^{198}Au from particles suspended in body liquid has been found to remain below 1%.'

d. Polystyrene

(635) Velasquez and Morrow (1984) measured mucociliary clearance rates in guinea pigs using monodisperse 7.9 μm MMAD (Mass Median Aerodynamic Diameter) polystyrene particles labelled with ^{198}Au and fluorescent dyes. The particles were inhaled via a cannula inserted in the trachea. Their distribution in the lungs was measured at times up to 60 h. The leakage of ^{198}Au from the particles in vitro was assessed to be 0.04 d^{-1}.

e. Fused aluminosilicate particles

(636) Fused aluminosilicate particles (FAP) or 'fused clay' particles have been used extensively as relatively insoluble particles in inhalation studies, both of biokinetics and of radiation effects. A natural clay mineral is labelled by ion exchange, and the labelled clay particles heated to approximately 1100 ˚C, to form aluminosilicate glass microspheres in which the label is incorporated. Stahlhofen et al. (1987) followed lung retention of ^{198}Au in six volunteers for up to 7 d after inhalation of ^{198}Au-labelled FAP.

f. Carnauba wax

(637) Bianco et al. (1980) followed lung retention of ^{198}Au for 15 d after inhalation of monodisperse carnauba wax particles containing ^{198}Au-labelled gold colloid. Lung retention was fit by two-component exponential functions with T_b averaging 11 hours and 13 d.

(638) Calamosca and Pagano (1991) followed the biokinetics of ^{198}Au for 23 d after inhalation of ^{198}Au-labelled carnauba wax particles by rats. The tissue distribution was reported only for respiratory tract and alimentary tract organs, but it was noted that lung clearance was slow, and activity in urine was only in some cases slightly positive, reflecting a low dissolution rate in the lungs. An in vitro test confirmed the low solubility, at least over 1 d.

g. Teflon

(639) Stahlhofen et al. (1981) followed lung retention of ^{198}Au in 5 volunteers for up to about 15 days after inhalation of ^{195}Au-labelled Teflon particles. The slow phase of lung retention had a mean (± SD) T_b of 128 (± 32) d.

(640) Philipson et al. (1996) followed lung retention of ^{195}Au in 10 volunteers for about 3 years after inhalation of ^{195}Au-labelled Teflon particles. The average lung retention T_b estimated from measurements from about 250 to 900 d was of the order of 1000 d. The leakage of ^{195}Au from the particles in vitro in water was less than 0.2% per year. No activity could be measured in the urine. The results indicate Type S behaviour.

35.2.1.2. Rapid dissolution rate for gold

(641) Only one in vivo experimental study was found on the behaviour of gold following deposition of any soluble form in the respiratory tract (see Ionic gold above), and measurements were made only at a single time point. Although the results suggest that absorption was relatively slow or incomplete, because of their limited scope, the general default value of 30 d^{-1} is applied to all Type F forms of gold.

Table 35.2. Absorption parameter values for inhaled and ingested gold.

Inhaled particulate materials		Absorption parameter values* f_r	s_r (d^{-1})	s_s (d^{-1})	Absorption from the alimentary tract, f_A
Default parameter values†,‡					
Absorption type	Assigned forms				
F	–	1	30	–	0.1
M§	–	0.2	3	0.005	0.02
S	Elemental gold, gold-labelled Teflon	0.01	3	$1x10^{-4}$	0.001
Ingested materials¶					
All forms					0.1

*It is assumed that the bound state can be neglected for gold (i.e. f_b=0). The values of s_r for Type F, M, and S forms of gold (30, 3, and 3 d^{-1}, respectively) are the general default values.

†Materials (e.g. elemental gold) are listed here where there is sufficient information to assign to a default absorption type, but not to give specific parameter values (see text).

‡For inhaled material deposited in the respiratory tract and subsequently cleared by particle transport to the alimentary tract, the default f_A values for inhaled materials are applied [i.e. the product of f_r for the absorption type and the f_A value for ingested soluble forms of gold (0.1)].

§Default Type M is recommended for use in the absence of specific information on which the exposure material can be assigned to an absorption type; for example, if the form is unknown, or if the form is known but there is no information available on the absorption of that form from the respiratory tract.

¶Activity transferred from systemic compartments into segments of the alimentary tract is assumed to be subject to reabsorption to blood. The default absorption fraction f_A for the secreted activity is the highest value for any form of the radionuclide (f_A = 0.1).

35.2.1.3. Extent of binding of gold to the respiratory tract

(642) No information was found that enabled bound state parameter values for gold to be estimated. It is therefore assumed that the bound state can be neglected for gold (i.e. f_b=0.0).

35.2.2. Ingestion

(643) In *Publication 30* (ICRP, 1980) a fractional absorption value of 0.1 was recommended for all chemical forms of gold at the workplace based on studies by Kleinsorge (1967), Chertok and Lake (1971c) and Silva et al. (1973) showing gastrointestinal absorption varying from 0.03 to 0.13. The value of 0.1 was also adopted in *Publication 68* (ICRP, 1994a).

(644) The gastrointestinal absorption of gold from the orally administered antiarthritis pharmaceutical Auranofin was estimated in the order of 20% (Tepperman et al., 1984) to 25% (Gottlieb, 1983).

(645) Russel et al. (1996) reported a case of gold-flake-containing liquor ingestion. A high level of gold in serum and urine was measured 3 months after the end of a one year of consumption, with daily urine excretion roughly similar to the estimated daily intake rate. This suggests a high gastrointestinal absorption of ingested gold.

(646) Begerow et al. (1999) measured higher levels of gold in urine of 27 dental technicians than in urine of 17 road construction workers and 17 school-leavers, indicating occupational internal exposure from treatment of dental alloys. Drasch et al. (2000) measured the level of gold in saliva, blood, urine and faeces of 81 volunteers and observed a positive correlation of gold concentration in all analysed bioassay with the number of teeth with gold restorations. The relative levels of gold measured in blood, urine and faeces are consistent with a gastrointestinal absorption in the order of 0.2. Becker et al. (2003) studied the levels of environmental pollutants in the urine of the German population and found a clear influence of the number of dental inlays, crowns and bridge elements on the mean levels of gold in urine.

(647) Schleh et al. (2012) investigated the gastrointestinal absorption of gold nanoparticles with sizes ranging from 1.4 to 200 nm administered by gavage to non-fasted rats. After 24h, 0.01 to 0.4% of gold was absorbed. Smallest and negatively charged particles were more absorbed.

(648) Although the reported studies indicate significant variations of absorption, the same value of f_A = 0.1 is adopted here for all chemical forms of gold at the workplace as in *Publications 30* and *68*.

35.2.3. Systemic distribution, retention and excretion of gold

35.2.3.1. Biokinetic data

(649) The biokinetics of gold has been investigated in human subjects and laboratory animals in studies related to its medical applications, particularly the use of stable gold for treating rheumatoid arthritis and short-lived radioactive gold as an imaging agent (Block et al., 1942, 1944; Freyberg et al., 1942; Jeffrey et al., 1958; Lawrence, 1961; Rubin et al., 1967; McQueen and Dykes, 1969; Mascarenhas et al., 1972; Sugawa-Katayama et al., 1975; Jellum et al., 1980; Gottlieb, 1983; Massarella and Pearlman, 1987; Andersson et al., 1988; Bacso et al., 1988; Brihaye and Guillaume, 1990); Other studies have addressed the biological behaviour of gold as a radioactive contaminant in the workplace or environment (Durbin, 1959; Fleshman et al., 1966; Chertok and Lake, 1971a,b,c; Silva et al., 1973).

(650) Development of a representative biokinetic model for systemic gold in adult humans is complicated by the apparent dependence of reported data on the mode of administration, chemical form, administered mass, and other study conditions. For gold administered in low mass and relatively soluble form, it appears that much of the absorbed or injected amount is excreted in the first week or two, but a nontrivial portion may be retained for several weeks or months. Excretion is primarily in urine. Most of the retained amount is found in the kidneys, liver, and blood. Most of the gold found in blood is bound to plasma proteins.

35.2.3.2. Biokinetic model for systemic gold

(651) The structure of the biokinetic model for systemic gold used in this publication is shown in Fig. 35.1. Transfer coefficients are listed in Table 35.3.

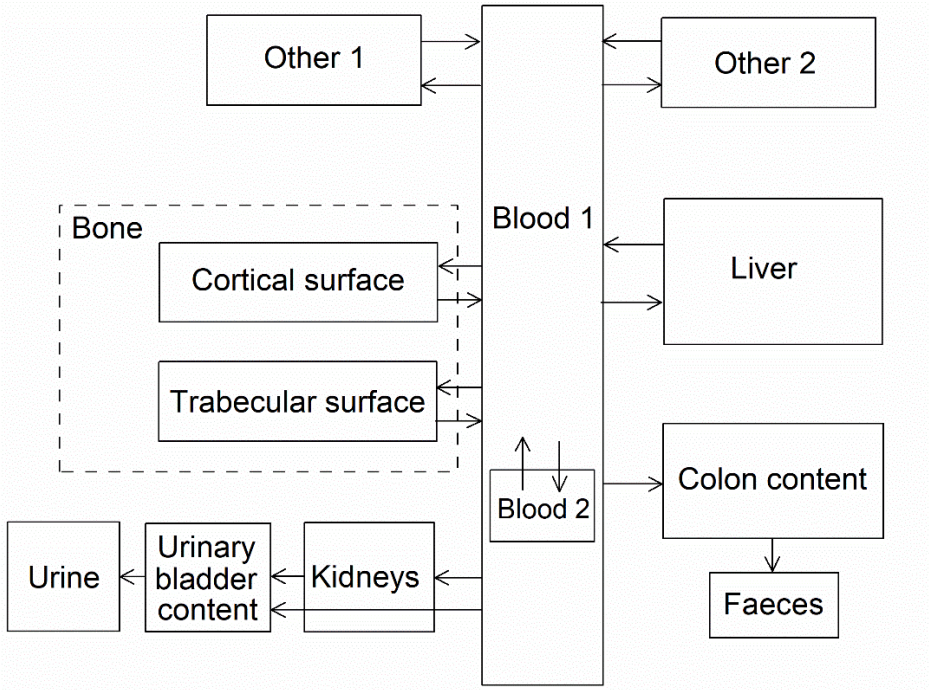

Fig. 35.1. Structure of the biokinetic model for systemic gold.

35.2.3.3. Treatment of progeny

(652) Progeny of gold addressed in this publication are radioisotopes of gold, rhenium, osmium, iridium, and platinum. The model for gold as a parent is applied to gold as a progeny of gold. The models for rhenium, osmium, iridium, and platinum as progeny of gold are expansions of the characteristic models for these elements with added compartments and associated transfer coefficients needed to solve the linked biokinetic models for chains headed by gold (see Annex B). If produced in an ambiguous compartment (i.e. a compartment not explicitly named in the progeny's model), the progeny is assumed to transfer at a specified rate to the central blood compartment of its characteristic biokinetic model and to follow that model thereafter. The following transfer rates to the central blood compartment are assigned to rhenium, osmium, iridium, and platinum produced in an ambiguous compartment: 1000 d^{-1} if produced in a blood compartment; and at the following element-specific rates if produced in a tissue compartment: rhenium, 0.462 d^{-1}; osmium or platinum, 0.09902 d^{-1}; iridium, 0.0693 d^{-1}.

Table 35.3. Transfer coefficients (d^{-1}) in the biokinetic models for systemic gold.

From	To	Transfer coefficient (d^{-1})
Blood 1	Blood 2	0.1
Blood 1	Kidneys	0.1
Blood 1	Liver	0.1
Blood 1	Other 1	0.18
Blood 1	Other 2	0.1

Blood 1	Urinary bladder content	0.3
Blood 1	Right colon content	0.1
Blood 1	Trabecular bone surface	0.01
Blood 1	Cortical bone surface	0.01
Blood 2	Blood	0.139
Kidneys	Urinary bladder content	0.0693
Liver	Blood 1	0.0693
Other 1	Blood 1	0.0693
Other 2	Blood 1	0.0139
Trabecular bone surface	Blood 1	0.0693
Cortical bone surface	Blood 1	0.0693

35.3. Individual monitoring

35.3.1. ^{195}Au

(653) Measurements of ^{195}Au may be performed by in vivo whole-body measurement technique and by gamma measurement in urine.

Table 35.4. Monitoring techniques for ^{195}Au.

Isotope	Monitoring Technique	Method of Measurement	Typical Detection Limit
^{195}Au	Urine Bioassay	γ-ray spectrometry[a]	0.8 Bq L^{-1}
^{195}Au	Whole-body measurement	γ-ray spectrometry[ab]	270 Bq

[a] Measurement system comprised of Germanium Detectors
[b] Counting time of 20 minutes

35.4. Dosimetric data for gold

Table 35.5. Committed effective dose coefficients (Sv Bq^{-1}) for the inhalation or ingestion of ^{195}Au compounds.

Inhaled particulate materials (5 µm AMAD aerosols)	Effective dose coefficients (Sv Bq^{-1})
	^{195}Au
Type F, — NB: Type F should not be assumed without evidence	1.8E-10
Type M, default	4.1E-10
Type S, elemental gold, gold-labelled Teflon	8.1E-10
Ingested materials	
All forms	1.0E-10

AMAD, activity median aerodynamic diameter

6381 Table 35.6. Dose per activity content of ^{195}Au in total body and in daily excretion of urine (Sv Bq^{-1});
6382 5µm activity median aerodynamic diameter aerosols inhaled by a reference worker at light work.

	Type F		Type M		Type S	
Time after intake (d)	Total body	Urine	Total body	Urine	Total body	Urine
1	3.0E-10	4.6E-09	6.7E-10	1.1E-07	1.3E-09	4.4E-06
2	4.9E-10	6.8E-09	1.2E-09	1.2E-07	2.5E-09	4.8E-06
3	7.9E-10	1.4E-08	2.6E-09	2.4E-07	5.4E-09	9.7E-06
4	1.1E-09	2.4E-08	4.6E-09	4.2E-07	9.6E-09	1.7E-05
5	1.2E-09	3.5E-08	6.0E-09	6.0E-07	1.3E-08	2.5E-05
6	1.3E-09	4.3E-08	6.6E-09	7.2E-07	1.4E-08	3.1E-05
7	1.4E-09	4.8E-08	6.8E-09	7.9E-07	1.4E-08	3.4E-05
8	1.4E-09	5.1E-08	7.0E-09	8.4E-07	1.5E-08	3.7E-05
9	1.5E-09	5.4E-08	7.2E-09	8.8E-07	1.5E-08	3.9E-05
10	1.5E-09	5.7E-08	7.3E-09	9.2E-07	1.5E-08	4.0E-05
15	1.8E-09	7.2E-08	8.0E-09	1.1E-06	1.6E-08	4.9E-05
30	2.8E-09	1.4E-07	9.9E-09	1.6E-06	1.8E-08	7.9E-05
45	4.2E-09	2.4E-07	1.2E-08	2.3E-06	1.9E-08	1.2E-04
60	5.9E-09	4.0E-07	1.4E-08	3.0E-06	2.1E-08	1.5E-04
90	1.1E-08	9.2E-07	1.9E-08	4.5E-06	2.5E-08	2.3E-04
180	4.4E-08	4.7E-06	4.9E-08	1.2E-05	4.1E-08	4.4E-04
365	7.0E-07	7.7E-05	3.2E-07	7.4E-05	1.1E-07	1.3E-03

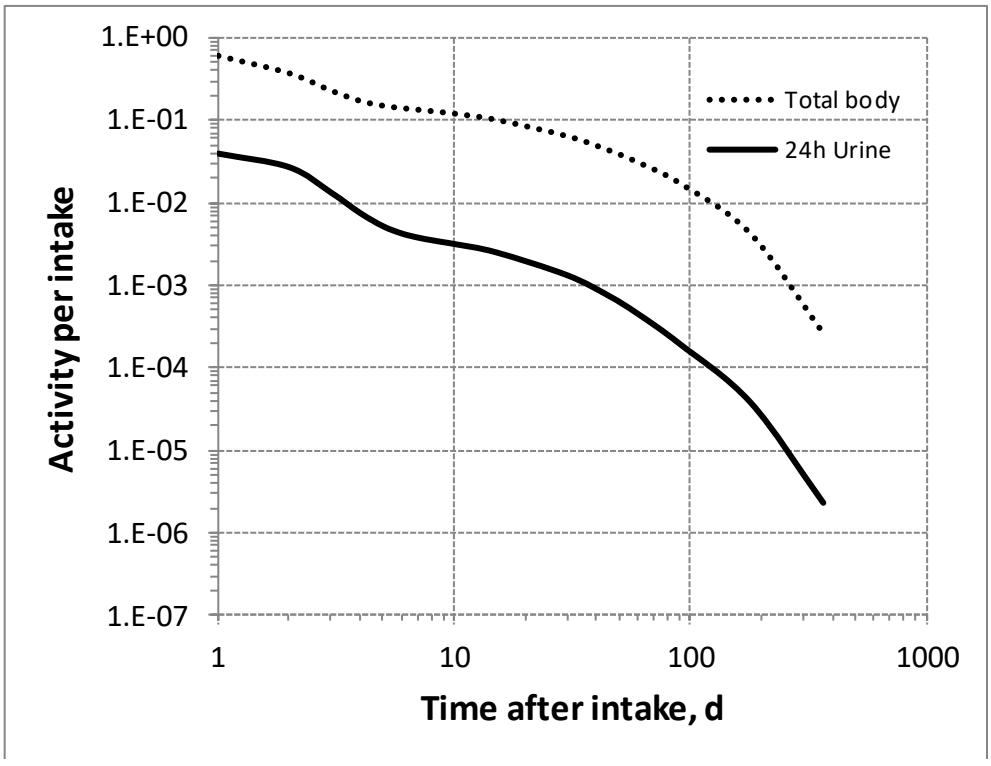

6383
6384 Fig. 35.2. Daily excretion of ^{195}Au following inhalation of 1 Bq Type F.

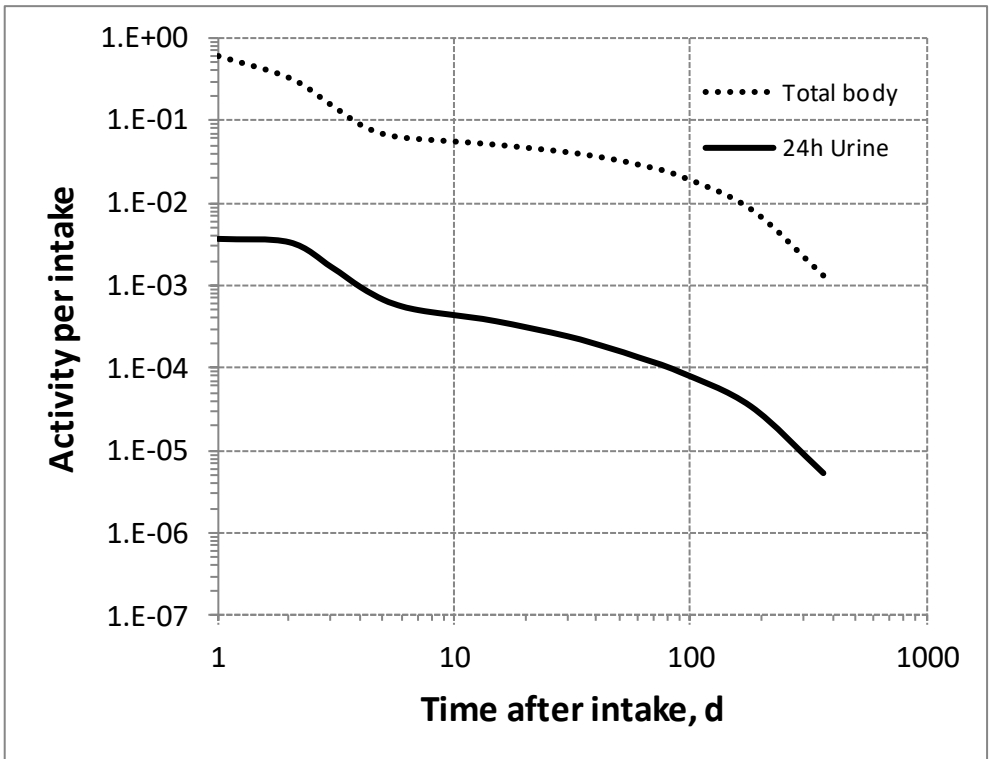

Fig. 35.3. Daily excretion of ^{195}Au following inhalation of 1 Bq Type M.

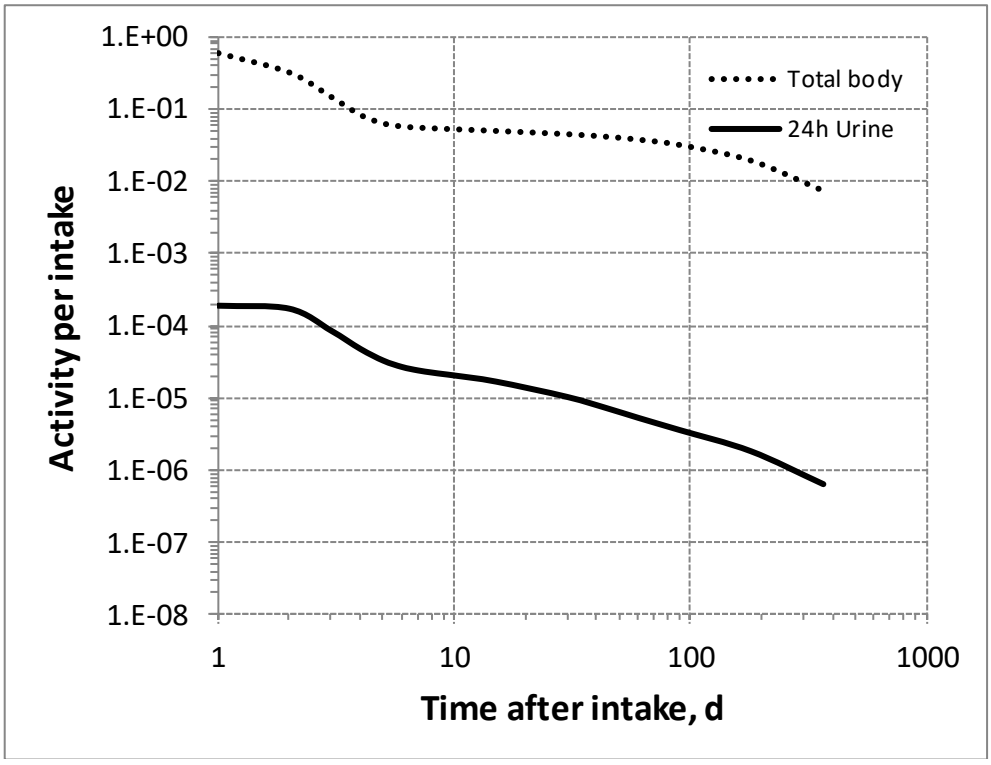

Fig. 35.4. Daily excretion of ^{195}Au following inhalation of 1 Bq Type S.

36. MERCURY (Z=80)

36.1. Isotopes

Table 36.1. Isotopes of mercury addressed in this publication.

Isotope	Physical half-life	Decay mode
^{190}Hg	20.0 min	EC, B+
^{191m}Hg	50.8 min	EC, B+
^{192}Hg	4.85 h	EC
^{193}Hg	3.8 h	EC, B+
^{193m}Hg	11.8 h	EC, B+, IT
^{194}Hg	440 y	EC
^{195}Hg	10.53 h	EC, B+
^{195m}Hg	41.6 h	IT, EC, B+
^{197}Hg	64.94 h	EC
^{197m}Hg	23.8 h	IT, EC
^{199m}Hg	42.66 min	IT
^{203}Hg*	46.612 d	B-

EC, electron-capture decay; B+, beta-plus decay; B-, beta-minus decay; IT, isomeric transition decay.
*Dose coefficients and bioassay data for this radionuclide are given in the printed copy of this publication.
Data for other radionuclides listed in this table are given in the online electronic files on the ICRP website.

36.2. Routes of Intake

36.2.1. Inhalation

36.2.1.1. Absorption types and parameter values

(654) The ICRP Task Group on Lung Dynamics (TGLD, 1966) assigned oxides, hydroxides, halides, nitrates and sulphides of mercury to inhalation class W, and sulphates to class D. This classification was adopted by ICRP in *Publication 30* (ICRP, 1980). In addition, in *Publication 30* it was assumed, based mainly on human studies, that 70% of mercury entering the lung as mercury vapour is deposited there and that following deposition, this fraction is translocated to blood with a biological half-time (T_b) of 1.7 days.

(655) Because of the recognised hazards posed by exposure to mercury, the inhalation toxicology of mercury vapour has been studied extensively. Comprehensive information is available on the behaviour of inhaled mercury vapour from both volunteer experiments and animal studies. Some information is also available from experimental studies of volatile organic compounds and particulate forms. Several studies have been reported following accidental intakes of mercury radioisotopes.

(656) Absorption parameter values and Types, and associated f_A values for gas and vapour forms of mercury are given in Table 36.2 and for particulate forms in Table 36.3. Exposures to both gas/vapour and particulate forms of mercury have occurred, and it is therefore recommended in this series of documents that 50% particulate and 50% gas/vapour should be assumed in the absence of information (ICRP, 2002a).

(657) Reference biokinetic models were used here (i.e. by the Task Group) for the analysis of the data and the determination of absorption parameter values for mercury vapour. Lung retention data were interpreted using the revised HRTM (ICRP, 2015). Mercury in lung tissue

and blood was taken into account in the comparison with experimental data by using the systemic model for mercury described in Section 36.2.3.

36.2.1.2. Gases and vapours

a. Elemental mercury (Hg^0)

(658) Comprehensive information is available on the behaviour of inhaled mercury vapour (Hg^0) from both volunteer and animal experiments. Leggett et al. (2001) carried out a critical review of the literature on the biokinetics of inhaled Hg^0 [See Leggett et al. (2001) for details and references to the papers reviewed.]. They proposed a lung biokinetic model consistent with the results of the review in the framework of the HRTM (ICRP, 1994b). No more recent relevant studies were found in the literature, and therefore the results of the review by Leggett et al. (2001) have been adopted here. Their estimates of total and regional deposition in the respiratory tract are given in Table 36.2: 75% of inhaled Hg^0 depositing in the alveolar-interstitial (AI) region and only 5% in the conducting airways.

(659) With respect to retention, Leggett et al. (2001) concluded that the non-invasive measurements on volunteers who inhaled Hg^0 for short periods indicate that much of the retained Hg is rapidly absorbed to blood and the remainder is removed from the lungs over a period of a few days. However, the more precise data for laboratory animals indicate that most of the deposited Hg^0 is rapidly absorbed to blood, most of the Hg retained in the lungs is removed to blood over a period of hours, and the remainder is removed to blood over a period of days. They represented absorption from the respiratory tract of the deposited Hg^0 by three components: 0.7 absorbed very rapidly (1000 d^{-1}); 0.24 with T_b = 8 hours (clearance rate 2.1 d^{-1}) and 0.06 with T_b = 5 d (clearance rate 0.14 d^{-1}). The very rapid absorption was applied only to the activity deposited in AI. As there was very little faecal excretion of mercury following inhalation of Hg^0, and some of it would have been due to endogenous secretion of mercury after its absorption to blood, Leggett et al. (2001) represented absorption by three 'bound' compartments, from which clearance was only by absorption to blood, with no particle transport to the alimentary tract.

(660) However, in the default implementation of the HRTM (ICRP, 1994b, 2015), there is only one bound compartment. The three-phase absorption described by Leggett et al. (2001) was represented here using the rapid and slow phases of dissolution, and the bound state. Good fits to the lung retention data for guinea pigs and monkeys summarised by Leggett et al. (2001) were obtained using the slow dissolution to represent the intermediate phase and the bound fraction the slow phase, or vice-versa, either:

$$f_r = 0.76;\ s_r = 1000\ d^{-1};\ s_s = 2.1\ d^{-1};\ f_b = 0.06;\ s_b = 0.14\ d^{-1};\ \text{or}$$

$$f_r = 0.94;\ s_r = 1000\ d^{-1};\ s_s = 0.14\ d^{-1};\ f_b = 0.24;\ s_b = 2.1\ d^{-1}$$

(661) In either case, because most of the deposition is in the AI region, from which particle transport is slow, and most of the deposit is absorbed rapidly to blood, there is very little clearance by particle transport, and subsequently to faeces. As discussed below, the results of studies of the distribution of ^{203}Hg after inhalation of ^{203}Hg-labelled mercury vapour or dimethyl mercury are consistent with the assumption that the intermediate phase can be represented by a bound fraction: f_b = 0.24 with s_b = 2.1 d^{-1}; and those parameter values are adopted here. They are assumed to apply throughout the respiratory tract (except region ET_1), and also to particulate forms of mercury.

b. Dimethyl mercury (C_2H_6Hg)

(662) Östlund (1969) followed whole-body retention of ^{203}Hg in mice for 25 days after inhalation of ^{203}Hg-labelled dimethyl mercury. About 80% cleared within 6 hours, by exhalation of dimethyl mercury, and the rest was retained with T_b about 7 days.

(663) Tissue distribution was determined by whole-body autoradiography 20 minutes, 1 and 4 hours and 16 days after inhalation, and at 5 and 20 minutes; 1, 4 and 24 hours; 4 and 16 days after intravenous (IV) injection. No differences in retention or distribution were seen between mice given dimethyl mercury by inhalation or by IV injection. High concentrations of ^{203}Hg in bronchial and nasal mucosa were noted at 5 minutes after IV injection. At 20 minutes and 1 hour the concentrations in nasal and bronchial mucosa were very high; a high activity was also observed in the mucosa of the oral cavity, the pharynx and the oesophagus. At 4 hours the concentration in bronchi was reported to be higher than in fat tissue. At 16 and 24 hours there was a high concentration in nasal mucosa but no accumulation was seen in bronchi. There were few changes in distribution at later times (4 and 16 days).

(664) It was concluded that the initial tissue distribution reflected the volatility and solubility in lipids of dimethyl mercury while subsequent retention was due to formation of metabolic products such as methyl mercury. It was reported that methyl mercury has no specific affinity to the bronchi, which might explain why its retention there was short-lived. It was suggested that the accumulation in nasal mucosa and the oral part of the digestive tract, this might be due to secretion from the nasal mucosa of methyl mercury which is then swallowed.

(665) Although specific parameter values for dimethyl mercury based on in-vivo data could be assessed, they are not adopted here because inhalation exposure to it is so unlikely, and its systemic behaviour is different from that of the model adopted here.

Table 36.2. Deposition and absorption for gas and vapour compounds of mercury.

	Percentage deposited (%)*						Absorption†			
Chemical form/origin	Total	ET_1	ET_2	BB	bb	AI	f_r	s_r (d^{-1})	s_s (d^{-1})	Absorption from the alimentary tract, f_A‡
Mercury Vapour	80	0	2	1	2	75	0.94	1000	0.14	0.094

ET_1, anterior nasal passage; ET_2, posterior nasal passage, pharynx and larynx; BB, bronchial; bb, bronchiolar; AI, alveolar-interstitial.

*Percentage deposited refers to how much of the material in the inhaled air remains in the body after exhalation. Almost all inhaled gas molecules contact airway surfaces, but usually return to the air unless they dissolve in, or react with, the surface lining. The distribution between regions is material specific: 2% ET_2, 1% BB, 2% bb, and 75% AI.

†For mercury, it is assumed that a bound fraction $f_b = 0.24$ with an uptake rate $s_b = 2.1\ d^{-1}$ is applied throughout the respiratory tract except in the ET_1 region.

‡For inhaled material deposited in the respiratory tract and subsequently cleared by particle transport to the alimentary tract, the default f_A values for inhaled materials are applied: i.e. the product of f_r for the absorption type (or specific value where given) and the f_A value for ingested soluble forms of mercury (0.1).

36.2.1.3. Particulate aerosols

a. Mercuric acetate [$Hg(O_2CCH_3)_2$]

(666) Morrow et al. (1968) followed lung retention of ^{203}Hg after inhalation of ^{203}Hg-labelled mercuric acetate by dogs and rats, but few details are given. It was noted that while the acetate is one of the most water soluble forms of mercury it is chemically unstable, particularly around

neutral pH. Following a rapid absorption phase its behaviour was nearly identical to that of mercuric oxide (see below). Behaviour similar to oxide was also observed after intra-muscular injection. Lung retention was described by a two-component exponential function with $T_b = 2.8$ days (55%: clearance rate 0.25 d^{-1}) and 26 days (clearance rate 0.027 d^{-1}). This would be consistent with assignment to Type M, but does not take account of the early rapid phase and Type F cannot be excluded.

b. Mercuric oxide (HgO)

(667) Morrow et al. (1964) followed retention of ^{203}Hg in the 'lower respiratory tract (LRT)' (presumably mainly the alveolar-interstitial, AI, region) for 40 days after inhalation of ^{203}Hg-labelled HgO by dogs. Although chosen partly because of its low solubility, clearance was rapid: on average 45% cleared with T_b less than 24 h, and the rest with $T_b = 33$ days (clearance rate 0.021 d^{-1}). Morrow et al. (1968) reported further studies of ^{203}Hg-labelled HgO inhaled by dogs, but few details are given. Lung retention was described by a two-component exponential function with half-times of 0.5 days (60%: clearance rate 1.4 d^{-1}) and of the order of 10 days (clearance rate ~0.07 d^{-1}).

(668) Newton and Fry (1978) studied the behaviour of ^{203}Hg in two workers for up to about 200 days, starting 3 or 8 days after accidental inhalation of neutron-activated mercuric oxide. In one worker, lung retention was fit by a two-component exponential function with T_b ~2 days (66%) and ~24 d, indicating Type M. However, some clearance would have occurred before measurements started, 3 days after exposure (Lung deposition was lower in the other worker, and measurement of its retention was not attempted.). Excretion (measured in one man only) was predominantly urinary after 40 days, when lung clearance was substantially complete and most of the retained activity was present in the kidneys. Taken with the behaviour of HgO inhaled by dogs, the results are consistent with assignment to Type M.

c. Mercuric nitrate [$Hg(NO_3)_2$]

(669) Izumi et al. (1973) followed the whole-body retention and distribution of ^{203}Hg in two workers for up to about 100 days, starting 10 days after accidental exposure to mercuric nitrate containing ^{197}Hg and ^{203}Hg. Exposure was presumed to have been by inhalation. Measurements of ^{203}Hg in whole body, including scans along the central body axis, and selected sites, were made using external detectors. Whole-body retention showed a T_b of about 30 d for both subjects over the first few weeks. Both radionuclides were deposited mainly in liver and kidneys. The results indicate that a large fraction of the ^{203}Hg retained by the time of the first measurement was systemic, implying Type F or M behaviour.

d. Methyl mercury chloride (CH_3HgCl)

(670) Uchiyama et al. (1976) followed the whole body retention and distribution of ^{203}Hg in two workers for about 6 months, starting about 1 or 2 months after accidental exposure to ^{203}Hg-labelled methyl mercury chloride. Exposure was presumed to have been by inhalation of particles and/or vapour. Measurements of ^{203}Hg in whole body, head, chest and upper abdomen of were made using external detectors. Whole-body retention showed a T_b of about 100 d for both subjects over the first few weeks. Activity in the head was a large percentage (50 – 70%) of that in whole body. The results indicate that a large fraction of the ^{203}Hg retained by the time of the first measurement was systemic, implying Type F or M behaviour.

36.2.1.4. Rapid dissolution rate for mercury

(671) No reliable estimates have been made of the rapid dissolution rate of mercury in particulate form. The general default value of 30 d^{-1} is therefore applied to all Type F forms of mercury.

36.2.1.5. Extent of binding of mercury to the respiratory tract

(672) Evidence was found for binding of mercury to the respiratory tract, mainly from studies of the distribution of ^{203}Hg after inhalation of ^{203}Hg-labelled mercury vapour (Hg^0).

(673) Berlin et al. (1969) measured tissue concentrations of ^{203}Hg immediately, and at 3, 8 and 24 hours, after inhalation of ^{203}Hg-labelled mercury vapour (Hg^0) by guinea pigs. They concluded that a large fraction of the inhaled Hg^0 transferred immediately to blood, and a small fraction deposited in the respiratory tract from which it was slowly absorbed. Lung retention followed an initial T_b of 5 hours (clearance rate 3.3 d^{-1}). Concentrations in samples of trachea and bronchi were several times lower than in the 'peripheral' lung, but the distribution in the lungs did not change during clearance. Autoradiographs of the lung showed concentrations of ^{203}Hg in the bronchial tree peripheral to the lobar bronchi to be higher, but concentrations in the trachea and bronchi to be lower, than in alveolar tissue.

(674) Khayat and Dencker (1983) determined the tissue distribution of ^{203}Hg by whole-body autoradiography immediately, and at 1 and 4 hours after inhalation of ^{203}Hg-labelled mercury vapour (Hg^0) by mice. High concentrations of ^{203}Hg were found in the epithelium of the respiratory tract: nasal mucosa, trachea, bronchi, and lungs. No major differences in the distribution pattern were observed between 0, 1 and 4 hours. However, the lung concentration was lower at 4 h than at 0 and 1 h.

(675) Khayat and Dencker (1984) determined the tissue distribution of ^{203}Hg by whole-body autoradiography immediately after inhalation of ^{203}Hg-labelled mercury vapour (Hg^0) by rats and marmosets. In both species, high concentrations of ^{203}Hg were found in the epithelium of the respiratory tract: nasal mucosa, trachea and bronchial tree. It was attributed to oxidation of Hg^0 to Hg^{2+} in these tissues.

(676) As described above, Östlund (1969) reported a similar pattern of respiratory tract distribution and retention of ^{203}Hg in mice after inhalation of ^{203}Hg-labelled dimethyl mercury. Tissue distribution was also determined by whole-body autoradiography, but over a longer period: up to 16 days after inhalation. High concentrations of ^{203}Hg in bronchial and nasal mucosa were noted up to 1 hour after inhalation. By 16 hours, no accumulation was seen in bronchi, although there was still a high concentration in nasal mucosa. It is plausible that the similarity in behaviour to that of Hg^0 reflects similar properties: high solubility in lipids and rapid oxidation to Hg^{2+} resulting in formation of metabolic products such as methyl mercury.

(677) These results indicate that most of the Hg retained in the respiratory tract (not absorbed immediately into blood) following inhalation of Hg^0 is cleared with a T_b of several hours. The finding that clearance is not faster in the upper respiratory tract, where particle transport to the alimentary tract is relatively rapid, than in the peripheral lungs, is consistent with the assumption that this phase can be represented by a bound fraction which applies throughout the respiratory tract.

(678) As discussed above, following a review of the literature, Leggett et al. (2001) represented absorption from the respiratory tract of the deposited Hg^0 by three components: 0.7 absorbed very rapidly (1000 d^{-1}); 0.24 with T_b = 8 hours (clearance rate 2.1 d^{-1}) and 0.06 with T_b = 5 d (clearance rate 0.14 d^{-1}). The results summarised here are consistent with the assumption that the intermediate phase can be represented by a bound fraction: f_b = 0.24 with

$s_b = 2.1\ d^{-1}$; and those parameter values are adopted here. They are assumed to apply throughout the respiratory tract (except in region ET_1 in which no absorption takes place), and also to particulate forms of mercury.

Table 36.3. Absorption parameter values for inhaled and ingested mercury.

Inhaled particulate materials		Absorption parameter values* f_r	s_r (d^{-1})	s_s (d^{-1})	Absorption from the alimentary tract, f_A
Default parameter values†,‡					
Absorption type	Assigned forms				
F	–	1	30	–	0.1
M§	Mercuric oxide	0.2	3	0.005	0.02
S	–	0.01	3	1×10^{-4}	0.001
Ingested materials¶					
All forms		–	–	–	0.1

*For mercury, it is assumed that a bound fraction $f_b = 0.24$ with an uptake rate $s_b = 2.1\ d^{-1}$ is applied throughout the respiratory tract except in the ET_1 region. The values of s_r for Type F, M and S forms of mercury (30, 3 and 3 d^{-1} respectively) are the general default values.

†Materials (e.g. mercuric oxide) are generally listed here where there is sufficient information to assign to a default absorption type, but not to give specific parameter values (see text).

‡For inhaled material deposited in the respiratory tract and subsequently cleared by particle transport to the alimentary tract, the default f_A values for inhaled materials are applied: i.e. the product of f_r for the absorption type (or specific value where given) and the f_A value for ingested soluble forms of mercury (0.1).

§Default Type M is recommended for use in the absence of specific information on which the exposure material can be assigned to an absorption type (e.g. if the form is unknown, or if the form is known but there is no information available on the absorption of that form from the respiratory tract). For guidance on the use of specific information, see Section 1.1.

¶Activity transferred from systemic compartments into segments of the alimentary tract is assumed to be subject to reabsorption to blood. The default absorption fraction f_A for the secreted activity is the highest value for any form of the radionuclide ($f_A = 0.1$).

36.2.2. Ingestion

(679) Human and animal studies indicate that elemental mercury is virtually unabsorbed, and inorganic salts exhibit absorption in the order of 8–15% (Cooper, 1985; ATSDR, 1999; EFSA, 2012).

(680) The uptake of elemental mercury from the gastrointestinal tract is very limited (Nordberg and Sherfving, 1972) and experiments on rats (Bornmann et al., 1970) suggest that less than 10^{-4} of ingested elemental mercury is absorbed. Reports of human contamination cases also indicate negligible absorption of elemental mercury (Wright et al., 1980; Sue, 1994).

(681) Animal studies of oral administration of inorganic compounds of mercury, mainly as mercuric chloride solutions, provided variable results with fractional absorption averaging in the 10-30% range (Nordberg and Sherfving, 1972; ATSDR, 1999; EFSA, 2012). In humans, the absorption of mercuric chloride and nitrate was evaluated from 2% (EFSA, 2012) to 15% (Rahola et al., 1973; ATSDR, 1999; WHO, 2015) based on limited data. In case of high intake, mercuric chloride may have a disruptive effect on the permeability barriers of the gastrointestinal tract that might raise absorption (EFSA, 2012). Because of water solubility, it is anticipated that the fractional absorption of mercurous [Hg(I)] compounds from the gastrointestinal tract will be less than that of mercuric compounds [Hg(II)] (Nordberg and

Sherfving, 1972). The bioavailability of mercuric sulphide in animals appears to be less than that of mercuric chloride (ATSDR, 1999).

(682) In *Publications 30* and *68* (ICRP, 1980, 1994a), f_1 was taken as 0.02 for all inorganic compounds of mercury. In this publication, a higher value of $f_A = 0.1$ is adopted for all forms when no specific information is available.

36.2.3. Systemic distribution, retention and excretion of mercury

36.2.3.1. Biokinetic data

(683) Mercury (Hg) is ubiquitous in nature. It exists in three general forms: elemental mercury (Hg^0), which may occur as a liquid or vapour; inorganic mercury compounds as monovalent (mercurous) or divalent (mercuric) mercury; and organic mercury compounds as monovalent or divalent mercury. This section summarises biokinetic data and provides biokinetic models for two forms of mercury often encountered in occupational settings: mercury vapour (Hg^0) and divalent inorganic mercury (Hg^{2+}) salts. These two forms initially exhibit distinct kinetics following entry into the systemic circulation, but their systemic behaviours converge over time. The model for systemic Hg^0 is an expansion of the model for Hg^{2+} that adds transfer coefficients depicting the early, distinct behaviour of mercury vapour that reaches blood.

(684) Notable initial differences observed in the systemic behaviours of mercury vapour and divalent mercury salts in human subjects and laboratory animals include much greater uptake by red blood cells (RBC) and brain following inhalation of mercury vapours (Hayes and Rothstein, 1962; Berlin et al., 1969). Over a period of days, the distribution and retention of mercury inhaled as vapour becomes similar to that seen after exposure to divalent inorganic mercury compounds, as mercury vapour is changed to divalent mercury in RBC and tissues (Hayes and Rothstein, 1962; Berlin et al., 1969).

(685) Blood clearance of mercury has been investigated in controlled studies of human subjects who inhaled mercury vapour for a brief period (Hursh et al., 1976, 1980; Cherian et al., 1978; Sandborgh-Englund et al., 1998; Jonsson et al., 1999) and in studies of workers after their removal from chronic exposure to mercury vapour (Barregård et al., 1992; Sallsten et al., 1993). A substantial portion of inhaled vapour moves rapidly into blood, and a smaller portion is oxidised in the lungs and absorbed more slowly. Mercury that enters blood is rapidly taken up by red blood cells (RBC) or tissues, or exhaled (Teisinger and Fiserova-Bergerova, 1965; Magos et al., 1989). The portion entering red blood cells (RBC) and tissues is oxidised to Hg^{2+} (Magos et al., 1989). Data for subjects acutely exposed to mercury vapour under controlled conditions and for workers just removed from exposure to mercury vapour indicate an initial removal half-time of divalent mercury from blood of about 3 d. A second component of retention with a longer half-time (18-45 d) has been observed in workers. Studies of animals administered divalent mercury salts indicate initially rapid disappearance of mercury from blood, but a substantial portion is retained in blood after several hours (Rothstein and Hayes, 1960; Clarkson and Rothstein, 1964).

(686) The kidneys have a high affinity for mercury. In laboratory animals exposed briefly to mercury vapour in inhaled air, the mercury content in the kidneys gradually increased to as much as 25-35% of the initial body burden over a period of days. Apparently, the kidneys took up only a few percent of the mercury vapour absorbed to blood but continued to accumulate divalent mercury that was absorbed more slowly from the lungs to blood or returned from other tissues to blood.

(687) External measurements on human subjects acutely exposed to mercury vapour or inorganic mercury compounds also show considerable accumulation of mercury in the kidneys (Hursh et al., 1976, 1980; Newton and Fry, 1978). Autopsy data on chronically exposed human subjects indicate a higher concentration of mercury in the kidneys than in other tissues.

(688) External measurements on human subjects following brief inhalation of mercury vapour indicate a mean biological half-time of 52 d (range, 35-90 d) for mercury in the kidneys (Hursh et al., 1976, 1980). External measurements on subjects accidentally exposed to aerosols of mercury indicate a mean half-time of 49 d (range, 37-60 d) (Newton and Fry, 1978). These values are reasonably consistent with half-times derived from urinary mercury measurements following exposure to mercury vapour or inorganic mercury compounds. Half-times of 90 d or more derived in some cases at times remote from exposure could result from a long-term component of retention in the kidneys but may also reflect a long-term component in other systemic tissues, since much of the mercury lost from other tissues is accumulated in the kidneys.

(689) In laboratory animals exposed briefly to mercury vapour in air, the liver typically accumulated 3-6% (range, 2-18%) of the initial body burden shortly after intake. The collective data suggest a slight rise in the liver content over the first few days after inhalation of mercury vapour. Higher initial uptake by the liver was seen after intravenous injection with divalent mercury than after inhalation of mercury vapour (Hayes and Rothstein, 1962; Magos et al., 1989). In laboratory animals, mercury is removed from the liver with a half-time of a few days.

(690) Mercury vapour carried in plasma to the brain readily crosses the blood-brain barrier. Mercury vapour that enters the brain is converted to the divalent form, which is trapped because it is more difficult for the divalent form to cross the blood-brain barrier. After acute inhalation of mercury vapour by squirrel monkeys, rats, mice, rabbits, and guinea pigs, the peak mercury content in the brain typically was 1-2% of the initial body burden, which is an order of magnitude greater than uptake of circulating divalent mercury (Berlin et al., 1966, 1969). The pattern of uptake and retention is reasonably consistent across species, despite the large variation in brain size as a fraction of total-body weight. Data for laboratory animals indicate a biological half-time on the order of 10 d for the preponderance of inorganic mercury deposited in the brain. External measurements over the head in human subjects suggest half-times in the range 14-29 d (Hursh et al., 1976, 1980; Newton and Fry, 1978).

(691) More than half of mercury vapour entering blood is deposited in massive soft tissues such as muscle, skin, and fat. Uptake of divalent mercury by massive soft tissues appears to be lower due to relatively greater competition from kidneys and liver. The portion of total-body mercury in the massive soft tissues declines over a period of days or weeks as mercury redistributes to the kidneys and liver. After inhalation of mercury vapour by rats for a period of 5 h, kidneys and liver accounted for about 20% of retained mercury at the end of exposure, 40% after 1 d, 50% after 5 d, and 67% after 15 d (Hayes and Rothstein, 1962). In rats injected with inorganic divalent mercury, kidneys and liver accounted for about 10% of the systemic burden after 4 h, 40% after 1 d, 70% after 6 d, 88% after 15 d, and 91% after 52 d (Rothstein and Hayes, 1960). External measurements on human subjects exposed to inorganic mercury suggest that much of the mercury deposited in soft tissues other than kidneys is lost from soft tissues over a period of a few weeks.

(692) In rats receiving mercury chloride by intravenous or intramuscular injection, a slow phase of excretion with a half-time of at least 90 d was apparent by 2 months after injection, when the body burden was about 17% of the dosage. A component of retention with a half-time on the order of 100 d is also indicated by long-term measurements of urinary mercury following exposure to inorganic mercury.

(693) Urinary mercury appears to originate predominantly from mercury stored in the kidneys (Barregård, 1993; Clarkson, 1997). In human subjects, the peak concentration of mercury in urine occurs 2-3 weeks after short-term inhalation of mercury vapour (Barregård, 1993), in parallel with the peak kidney content.

(694) Following inhalation of mercury vapour, more than half of absorbed inorganic mercury is removed from the body in urine. Initially, the rate of faecal excretion is much higher than that of urinary excretion, but this relation reverses over a few weeks. At times remote from exposure, daily urinary losses are considerably larger than faecal losses (Hursh et al., 1976, 1980; Newton and Fry, 1978; Jonsson et al., 1999). Analysis of excretion data for human subjects who inhaled mercury vapour for a short period (Jonsson et al., 1999) indicate that cumulative faecal excretion represented roughly 25-30% of the initial body burden. Results of animal studies indicate that faecal excretion of mercury may arise from a combination of biliary secretion and secretions across the intestinal wall that are most prominent in the small intestine (Gregus and Klaassen, 1986; Zalups, 1998).

(695) In addition to losses in urine and faeces, mercury is removed from the systemic fluids and tissues by exhalation of mercury vapour, and small amounts are lost through sweat, hair, and other routes. Exhalation of mercury vapour occurs over a period of at least several days, either after administration of mercuric salts or inhalation of mercury vapour (Clarkson and Rothstein, 1964; Hursh et al., 1976; Cherian et al., 1978; Berlin, 1986; Jonsson et al., 1999). Hursh et al. (1976) estimated that approximately 7% of the initial body burden was exhaled in expired air over the first few days after acute inhalation of mercury vapour by human subjects. The rate of exhalation of mercury was highest soon after intake and declined with a half-time of 1-2 d.

36.2.3.2. Biokinetic model for systemic mercury

(696) The biokinetic model for systemic mercury adopted in this publication is designed to address absorption of inorganic mercury to blood either as mercury vapour (Hg^0) or divalent mercury (Hg^{2+}), or as some combination of these two forms. The model depicts initially distinct kinetics of Hg^0 and Hg^{2+} following entry into the systemic circulation but convergence of the kinetics of the two forms over time after conversion of Hg^0 to Hg^{2+} in cells.

(697) The structure of the systemic model for mercury vapour is shown in Fig. 36.1. The same structure, minus Compartment Plasma 0 and its associated arrows, is applied to divalent inorganic mercury.

(698) Transfer coefficients for mercury vapour that enters the systemic circulation are listed in Table 36.4. Transfer coefficients for divalent mercury that enters the systemic circulation are listed in Table 36.5. The transfer coefficients listed in Table 36.5 are a subset of those listed in Table 36.4, representing mercury vapour that is converted to divalent mercury in RBC and tissues. Transfer coefficients are intended to depict the typical (central) behaviour of systemic mercury in human subjects, supplemented where needed with data for laboratory animals, as summarised in the preceding section.

(699) The fraction of inhaled mercury vapour that is rapidly absorbed into blood, $f_r(1-f_b)$, enters the systemic cicrculation as mercury vapour through the Plasma_0 compartment, while the slowly absorbed fraction, $(1-f_r)(1-f_b)$, and the bound fraction, f_b, enter the systemic circulation through the Plasma_1 compartment, as mercury vapour is changed to divalent mercury in the lung tissues.

(700) Blood is divided into three plasma compartments and a fourth compartment representing red blood cells. Two plasma compartments, called Plasma 0 and Plasma 1, are used to account for differences in the rates of disappearance of absorbed mercury vapour and

absorbed divalent mercury from plasma and differences in their initial distributions. Absorbed mercury vapour is assigned to Plasma 0, and absorbed divalent mercury is assigned to Plasma 1. A third compartment, called Plasma 2, is used to account for a relatively long-term component of retention of divalent mercury in plasma associated with binding to plasma proteins.

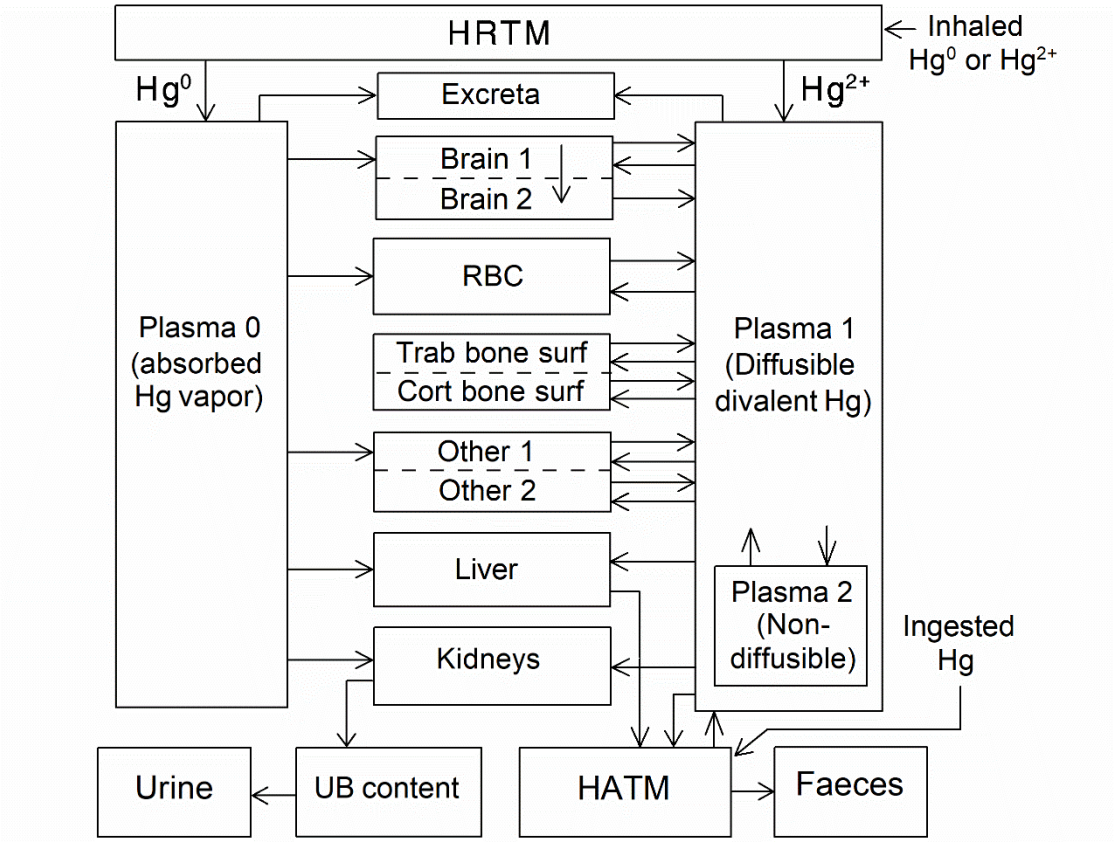

Fig. 36.1. Structure of the biokinetic model for mercury vapour (all compartments and paths) and inorganic divalent mercury (excludes Plasma 0 and associated paths). HRTM = Human Respiratory Tract Model, HATM = Human Alimentary Tract Model, RBC = red blood cells, Trab = trabecular, Cort = cortical, surf = surface, UB = urinary bladder.

36.2.3.3. Treatment of progeny

(701) Progeny of mercury addressed in this publication are radioisotopes of mercury, gold, osmium, and platinum. The models for all four elements as progeny of mercury are expansions of the characteristic models for these elements with added compartments and associated transfer coefficients needed to solve the linked biokinetic models for chains headed by mercury (see Annex B). If produced in an ambiguous compartment (i.e. a compartment not explicitly named in the progeny's model), the progeny is assumed to transfer at a specified rate to the central blood compartment of its characteristic biokinetic model and to follow that model thereafter. The following transfer rates to the central blood compartment are assigned to mercury, gold, osmium, and platinum produced in an ambiguous compartment: 1000 d^{-1} if produced in a blood compartment; and at the following element-specific rates if produced in any other ambiguous compartment: gold, 0.0693 d^{-1}; osmium or platinum, 0.09902 d^{-1}.

6788 Table 36.4. Transfer coefficients in the biokinetic model for systemic mercury vapour.

From	To	Transfer coefficient (d^{-1})
Plasma 0	RBC	100
Plasma 0	Brain 1	20
Plasma 0	Kidneys	100
Plasma 0	Liver	60
Plasma 0	Other 1	650
Plasma 0	Excreta	70
Plasma 1	RBC	0.48
Plasma 1	Plasma 2	2.4
Plasma 1	Kidneys	7.2
Plasma 1	Liver	4.8
Plasma 1	Brain 1	0.048
Plasma 1	Trabecular bone surface	0.024
Plasma 1	Cortical bone surface	0.024
Plasma 1	Other 1	5.184
Plasma 1	Other 2	0.72
Plasma 1	Small intestine content	1.92
Plasma 1	Excreta	1.2
RBC	Plasma 1	0.33
Plasma 2	Plasma 1	0.6
Kidneys	Urinary bladder content	0.0198
Liver	Small intestine content	0.1733
Brain 1	Plasma 1	0.0329
Brain 1	Brain 2	0.00173
Brain 2	Plasma 1	0.00038
Trabecular bone surface	Plasma 1	0.0347
Cortical bone surface	Plasma 1	0.0347
Other 1	Plasma 1	0.0347
Other 2	Plasma 1	0.00693

6789 Table 36.5. Transfer coefficients in the biokinetic model for systemic divalent inorganic mercury.

From	To	Transfer coefficient (d^{-1})
Plasma 1	RBC	0.48
Plasma 1	Plasma 2	2.4
Plasma 1	Kidneys	7.2
Plasma 1	Liver	4.8
Plasma 1	Brain 1	0.048
Plasma 1	Trabecular bone surface	0.024
Plasma 1	Cortical bone surface	0.024
Plasma 1	Other 1	5.184
Plasma 1	Other 2	0.72
Plasma 1	Small intestine content	1.92
Plasma 1	Excreta	1.2
RBC	Plasma 1	0.33
Plasma 2	Plasma 1	0.6
Kidneys	Urinary bladder content	0.0198
Liver	Small intestine content	0.1733
Brain 1	Plasma 1	0.0329
Brain 1	Brain 2	0.00173
Brain 2	Plasma 1	0.00038
Trabecular bone surface	Plasma 1	0.0347
Cortical	Plasma 1	0.0347

Other 1	Plasma 1	0.0347
Other 2	Plasma 1	0.00693

36.3. Individual monitoring

36.3.1. ^{203}Hg

(702) Measurements of ^{203}Hg may be performed by in vivo whole-body measurement technique and by gamma measurement in urine.

Table 36.6. Monitoring techniques for ^{203}Hg.

Isotope	Monitoring Technique	Method of Measurement	Typical Detection Limit
^{203}Hg	Urine Bioassay	γ-ray spectrometry[a]	1.1 Bq L^{-1}
^{203}Hg	Whole-body measurement	γ-ray spectrometry[ab]	45 Bq

[a] Measurement system comprised of Germanium Detectors
[b] Counting time of 20 minutes

36.4. Dosimetric data for mercury

Table 36.7. Committed effective dose coefficients (Sv Bq^{-1}) for the inhalation or ingestion of ^{203}Hg compounds.

	Effective dose coefficients (Sv Bq^{-1})
Inhaled gases or vapours	^{203}Hg
Mercury vapour	1.2E-09
Inhaled particulate materials (5 μm AMAD aerosols)	
Type F, — NB: Type F should not be assumed without evidence	9.7E-10
Type M, mercuric oxide, default	7.9E-10
Type S	8.5E-10
Ingested materials	
All forms	2.3E-10

AMAD, activity median aerodynamic diameter

6802 Table 36.8. Dose per activity content of ^{203}Hg in total body and in daily excretion of urine (Sv Bq^{-1});
6803 5μm activity median aerodynamic diameter aerosols inhaled by a reference worker at light work.

	Mercury vapour		Type F		Type M		Type S	
Time after intake (d)	Total body	Urine	Total body	Urine	Total body	Urine	Total body	Urine
1	1.8E-09	8.1E-07	8.3E-10	5.3E-07	1.1E-09	7.3E-06	1.4E-09	1.9E-04
2	1.8E-09	5.5E-07	1.3E-09	3.3E-07	2.0E-09	3.8E-06	2.6E-09	9.9E-05
3	1.9E-09	5.0E-07	1.9E-09	3.2E-07	4.2E-09	3.5E-06	5.7E-09	9.3E-05
4	2.0E-09	4.8E-07	2.4E-09	3.2E-07	7.1E-09	3.5E-06	1.0E-08	9.2E-05
5	2.1E-09	4.7E-07	2.7E-09	3.2E-07	9.2E-09	3.5E-06	1.4E-08	9.3E-05
6	2.2E-09	4.6E-07	2.9E-09	3.3E-07	1.0E-08	3.5E-06	1.5E-08	9.4E-05
7	2.2E-09	4.6E-07	3.1E-09	3.3E-07	1.1E-08	3.6E-06	1.6E-08	9.5E-05
8	2.3E-09	4.5E-07	3.2E-09	3.4E-07	1.1E-08	3.6E-06	1.7E-08	9.7E-05
9	2.4E-09	4.5E-07	3.4E-09	3.5E-07	1.2E-08	3.7E-06	1.7E-08	9.9E-05
10	2.5E-09	4.5E-07	3.5E-09	3.6E-07	1.2E-08	3.8E-06	1.7E-08	1.0E-04
15	3.0E-09	4.7E-07	4.3E-09	4.1E-07	1.4E-08	4.1E-06	1.9E-08	1.1E-04
30	4.7E-09	5.9E-07	7.2E-09	6.1E-07	2.0E-08	5.6E-06	2.6E-08	1.6E-04
45	7.5E-09	8.0E-07	1.1E-08	9.4E-07	2.7E-08	7.7E-06	3.3E-08	2.3E-04
60	1.2E-08	1.2E-06	1.8E-08	1.5E-06	3.8E-08	1.1E-05	4.3E-08	3.2E-04
90	3.0E-08	2.6E-06	4.6E-08	3.6E-06	7.4E-08	2.1E-05	7.1E-08	6.6E-04
180	4.3E-07	3.8E-05	6.3E-07	5.9E-05	5.2E-07	1.6E-04	3.2E-07	4.5E-03
365	4.7E-05	8.8E-03	6.0E-05	1.2E-02	2.6E-05	8.5E-03	6.6E-06	1.2E-01

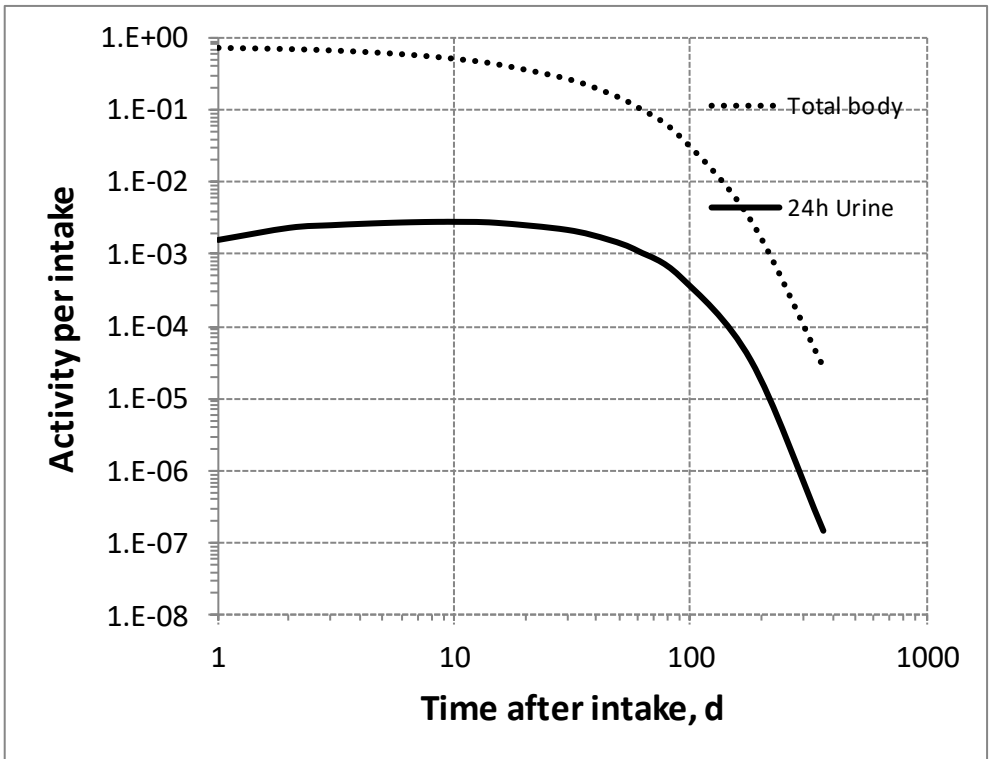

6804
6805 Fig. 36.2. Daily excretion of ^{203}Hg following inhalation of 1 Bq mercury vapour.

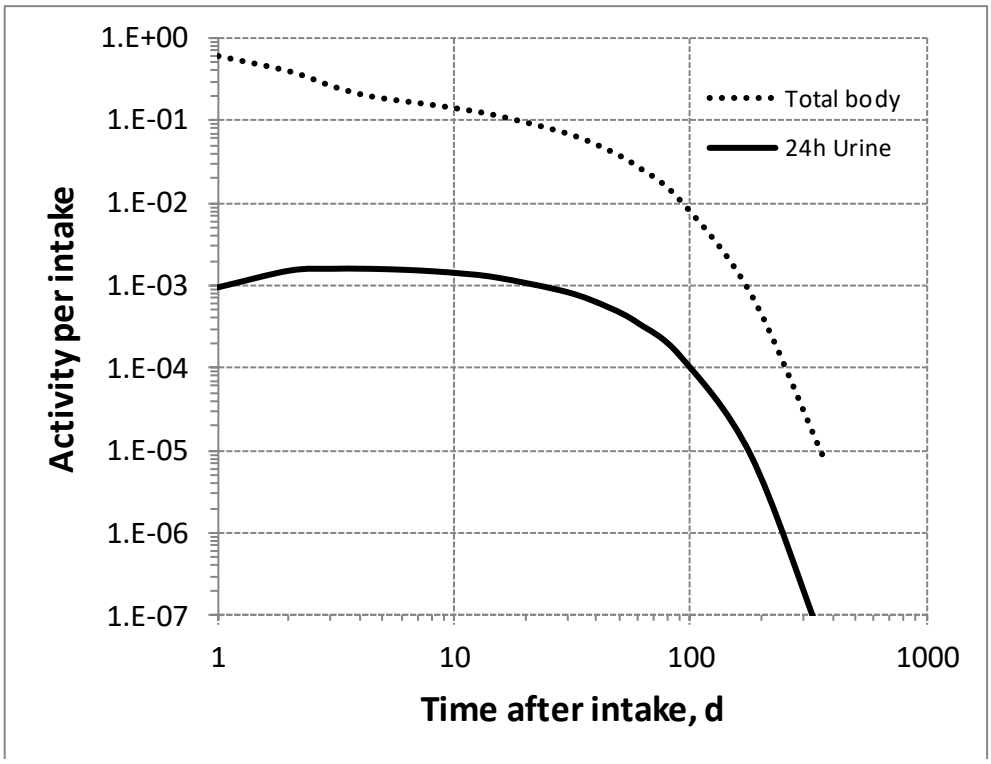

Fig. 36.3. Daily excretion of ^{203}Hg following inhalation of 1 Bq Type F.

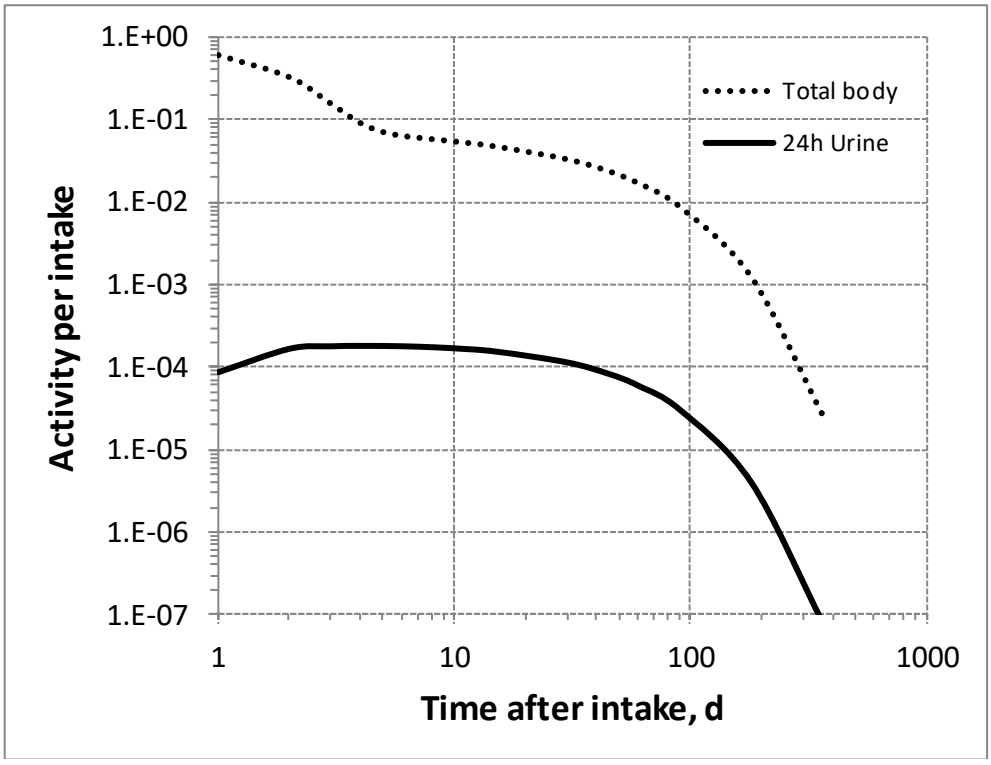

Fig. 36.4. Daily excretion of ^{203}Hg following inhalation of 1 Bq Type M.

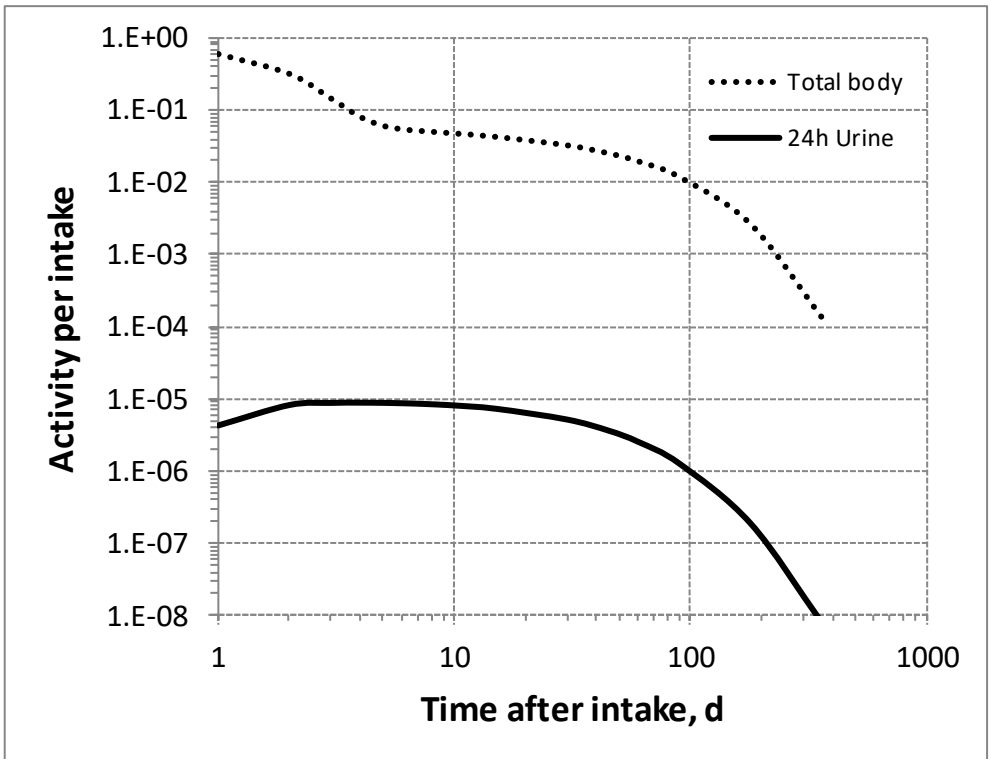

Fig. 36.5. Daily excretion of ^{203}Hg following inhalation of 1 Bq Type S.

37. THALLIUM (Z=81)

37.1. Isotopes

Table 37.1. Isotopes of thallium addressed in this publication.

Isotope	Physical half-life	Decay mode
^{194}Tl	33.0 m	EC, B+
^{194m}Tl	32.8 m	EC, B+
^{195}Tl	1.16 h	EC, B+
^{196}Tl	1.84 h	EC, B+
^{197}Tl	2.84 h	EC, B+
^{198}Tl	5.3 h	EC, B+
^{198m}Tl	1.87 h	EC, B+, IT
^{199}Tl	7.42 h	EC, B+
^{200}Tl*	26.1 h	EC, B+
^{201}Tl*	72.912 h	EC
^{202}Tl*	12.23 d	EC
^{204}Tl	3.78 y	B-, EC

EC, electron-capture decay; B+, beta-plus decay; B-, beta-minus decay; IT, isomeric transition decay.
*Dose coefficients and bioassay data for this radionuclide are given in the printed copy of this publication.
Data for other radionuclides listed in this table are given in the online electronic files on the ICRP website.

37.2. Routes of Intake

37.2.1. Inhalation

(703) For thallium, default parameter values were adopted on absorption to blood from the respiratory tract (ICRP, 2015). Absorption parameter values and types, and associated f_A values for particulate forms of thalium are given in Table 37.2.

37.2.2. Ingestion

(704) Thallium is readily absorbed from the gastrointestinal tract. It has been detected in the urine of exposed humans and animals (U.S. EPA, 2009), implying absorption from environmental sources. Limited quantitative data indicate that thallium is rapidly and extensively (60-100%) absorbed after oral administration of sulphate or nitrate to humans (Barclay et al., 1953), dogs (Shaw, 1933) and rats (Lie et al., 1960; Manzo et al., 1983). However, Sabbioni et al. (1980) observed, 16 h and 8 d after oral administration to rats, about 20 times reduced body retention of dimethyl thallium (III) bromide, compared with that of inorganic thallium. This might indicate a lower absorption of organic compounds.

(705) In *Publications 30* and *68* (ICRP, 1981, 1994a), f_1 was taken as 1 for all compounds of the element. In this publication, $f_A = 1$ is adopted as the default for all chemical forms of thallium ingested at the workplace.

Table 37.2. Absorption parameter values for inhaled and ingested thallium.

	Absorption parameter values*			
Inhaled particulate materials	f_r	s_r (d^{-1})	s_s (d^{-1})	Absorption from the alimentary tract, f_A
Default parameter values†				

Absorption type				
F	1	30	–	1
M‡	0.2	3	0.005	0.2
S	0.01	3	1×10^{-4}	0.01
Ingested materials§				
All forms				1

*It is assumed that the bound state can be neglected for thallium (i.e. $f_b = 0$). The values of s_r for Type F, M and S forms of thalium (30, 3 and 3 d^{-1} respectively) are the general default values.

†For inhaled material deposited in the respiratory tract and subsequently cleared by particle transport to the alimentary tract, the default f_A values for inhaled materials are applied [i.e. the product of f_r for the absorption type and the f_A value for ingested soluble forms of thalium (1)].

‡Default Type M is recommended for use in the absence of specific information on which the exposure material can be assigned to an absorption type (e.g. if the form is unknown, or if the form is known but there is no information available on the absorption of that form from the respiratory tract). For guidance on the use of specific information, see Section 1.1.

§Activity transferred from systemic compartments into segments of the alimentary tract is assumed to be subject to reabsorption to blood. The default absorption fraction f_A for the secreted activity is the highest value for any form of the radionuclide ($f_A = 1$).

37.2.3. Systemic distribution, retention and excretion of thallium

37.2.3.1. Biokinetic data

(706) The biokinetics of thallium has been investigated extensively in human subjects and laboratory animals, due largely to the importance of radio-thallium in nuclear medicine and many occurrences of poisoning with stable thallium (Gettler and Weiss, 1943; Barclay et al., 1953; Lie et al., 1960; Gehring and Hammond, 1967; Potter et al., 1971; Bradley-Moore et al., 1975; Strauss et al., 1975; Atkins et al., 1977; Suzuki et al., 1978; Berger et al., 1983; Nakamura et al., 1985; Gregus and Klaassen, 1986; Krahwinkel et al., 1988; Lathrop et al., 1989; Blanchardon et al., 2005; Thomas et al., 2005). Comparisons of the disappearance of radioisotopes of thallium, potassium, and rubidium from blood and their uptake by tissues of laboratory animals suggest a close relation in the movement of these elements (Gehring and Hammond, 1967; Strauss et al., 1975). These elements are rapidly removed from plasma, and their early distributions are determined largely by the distribution of cardiac output. After entering the cell, thallium is released more slowly than potassium or rubidium, but the mean residence time of thallium in the body is less than that of potassium or rubidium due to a higher rate of clearance from plasma to excretion pathways.

(707) Most reported removal half-times of thallium from the adult human body are in the range 9-13 d (Atkins et al., 1977; Krahwinkel et al., 1988; Blanchardon et al., 2005). Chen et al. (1983) reported two components of retention of thallium: 7d for 63% and 28 d for 37% of the injected amount. It appears that faecal excretion typically represents more than half of cumulative excretion of thallium over a period of weeks following its acute intake, although some relatively short-term human studies have suggested that excretion of thallium is primarily in urine (cf. Barclay et al., 1953; Lathrop et al., 1975; Atkins et al., 1977; Blanchardon et al., 2005).

37.2.3.2. Biokinetic model for systemic thallium

(708) The structure of the biokinetic model for thallium used in this publication is shown in Fig. 37.1. Transfer coefficients are listed in Table 37.3.

(709) It is assumed that thallium leaves the central blood compartment (Plasma) at the rate 200 d^{-1} (corresponding to a half-time of 5 min) and is distributed as follows: 2.5% to red blood cells (RBC), 0.75% to Urinary bladder content, 1.75% to Right colon content, 5% to Kidneys, 5% to Liver, 7.5% to Trabecular bone surface, 7.5% to Cortical bone surface, and 70% to remaining soft tissues (Other). Thallium returns from RBC to Plasma at the rate 3.7 d^{-1} and from tissue compartments to Plasma at the rate 2.5 d^{-1}.

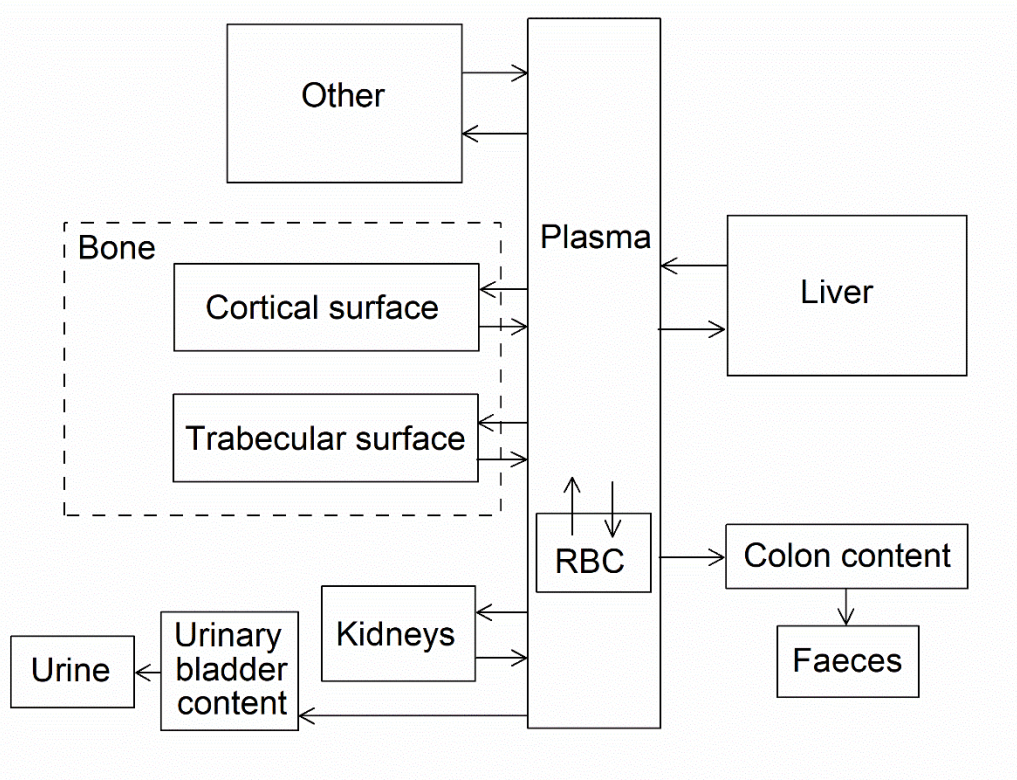

Fig. 37.1. Structure of the biokinetic model for systemic thallium.

37.2.3.3. Treatment of progeny

(710) Progeny of thallium addressed in this publication are isotopes of thallium, mercury, and gold. The model for thallium as a parent is applied to thallium produced by decay of another isotope of thallium. The characteristic models for gold and divalent mercury are applied to these elements as members of chains headed by thallium with added transfer coefficients needed to solve the linked biokinetic models of chains headed by thallium. The following transfer rates to the central blood compartment are added to the characteristic model for mercury or gold: 1000 d^{-1} if produced in a blood compartment not contained in the progeny's model; and at the following element-specific rates if produced in any other ambiguous compartment: mercury, 0.0347 d^{-1}; gold, 0.0693 d^{-1}.

Table 37.3. Transfer coefficients in the biokinetic model for systemic thallium.

From	To	Transfer coefficient (d^{-1})
Plasma	Liver	10
Plasma	Kidneys	10
Plasma	RBC	5
Plasma	Trabecular bone surface	15

Plasma	Cortical bone surface	15
Plasma	Other	140
Plasma	Urinary bladder content	1.5
Plasma	Right colon content	3.5
RBC	Plasma	3.7
Liver	Plasma	2.5
Kidneys	Plasma	2.5
Trabecular bone surface	Plasma	2.5
Cortical bone surface	Plasma	2.5
Other	Plasma	2.5

37.3. Individual monitoring

37.3.1. ^{200}Tl

(711) Measurements of ^{200}Tl in urine may be used to determine intakes of the radionuclide.

Table 37.4. Monitoring techniques for ^{200}Tl.

Isotope	Monitoring Technique	Method of Measurement	Typical Detection Limit
^{200}Tl	Urine Bioassay	γ-ray spectrometry[a]	1 Bq L^{-1}

[a] Measurement system comprised of Germanium Detectors

37.3.2. ^{201}Tl

(712) Measurements of ^{201}Tl in urine may be used to determine intakes of the radionuclide.

Table 37.5. Monitoring techniques for ^{201}Tl.

Isotope	Monitoring Technique	Method of Measurement	Typical Detection Limit
^{201}Tl	Urine Bioassay	γ-ray spectrometry[a]	8 Bq L^{-1}

[a] Measurement system comprised of Germanium Detectors

37.3.3. ^{202}Tl

(713) Measurements of ^{202}Tl in urine may be used to determine intakes of the radionuclide.

Table 37.6. Monitoring techniques for ^{202}Tl.

Isotope	Monitoring Technique	Method of Measurement	Typical Detection Limit
^{202}Tl	Urine Bioassay	γ-ray spectrometry[a]	1 Bq L^{-1}

[a] Measurement system comprised of Germanium Detectors

37.4. Dosimetric data for thalium

Table 37.7. Committed effective dose coefficients (Sv Bq^{-1}) for the inhalation or ingestion of ^{200}Tl, ^{201}Tl and ^{202}Tl compounds.

Inhaled particulate materials (5 µm AMAD aerosols)	Effective dose coefficients (Sv Bq^{-1})		
	^{200}Tl	^{201}Tl	^{202}Tl

Type F, — NB: Type F should not be assumed without evidence	1.3E-10	5.2E-11	3.1E-10
Type M, default	2.0E-10	8.0E-11	2.7E-10
Type S	2.1E-10	8.5E-11	2.6E-10
Ingested materials			
All forms	2.1E-10	7.2E-11	4.5E-10

AMAD, activity median aerodynamic diameter

Table 37.8 Dose per activity content of ^{200}Tl in daily excretion of urine (Sv Bq^{-1}); 5μm activity median aerodynamic diameter aerosols inhaled by a reference worker at light work.

Time after intake (d)	Type F Urine	Type M Urine	Type S Urine
1	2.0E-08	1.7E-07	3.6E-06
2	4.2E-08	2.9E-07	6.2E-06
3	8.4E-08	5.8E-07	1.2E-05
4	1.7E-07	1.2E-06	2.5E-05
5	3.4E-07	2.3E-06	5.0E-05
6	6.8E-07	4.7E-06	1.0E-04
7	1.4E-06	9.4E-06	2.0E-04
8	2.8E-06	1.9E-05	4.0E-04
9	5.6E-06	3.8E-05	8.1E-04
10	1.1E-05	7.6E-05	1.6E-03
15	3.7E-04	2.5E-03	5.3E-02
30	N/A	N/A	N/A
45			
60			
90			
180			
365			

Table 37.9. Dose per activity content of ^{201}Tl in daily excretion of urine (Sv Bq^{-1}); 5μm activity median aerodynamic diameter aerosols inhaled by a reference worker at light work.

Time after intake (d)	Type F Urine	Type M Urine	Type S Urine
1	5.2E-09	4.5E-08	9.8E-07
2	7.2E-09	5.3E-08	1.1E-06
3	9.6E-09	7.0E-08	1.5E-06
4	1.3E-08	9.3E-08	2.0E-06
5	1.7E-08	1.2E-07	2.6E-06
6	2.3E-08	1.6E-07	3.5E-06
7	3.1E-08	2.2E-07	4.6E-06
8	4.1E-08	2.9E-07	6.2E-06
9	5.5E-08	3.9E-07	8.3E-06

10	7.3E-08	5.2E-07	1.1E-05
15	3.1E-07	2.2E-06	4.7E-05
30	2.4E-05	1.6E-04	3.4E-03
45	1.9E-03	1.0E-02	2.4E-01
60	1.5E-01	6.1E-01	N/A
90	N/A	N/A	
180			
365			

Table 37.10. Dose per activity content of ^{202}Tl in daily excretion of urine (Sv Bq^{-1}); 5µm activity median aerodynamic diameter aerosols inhaled by a reference worker at light work.

Time after intake (d)	Type F Urine	Type M Urine	Type S Urine
1	2.6E-08	1.3E-07	2.6E-06
2	3.0E-08	1.3E-07	2.4E-06
3	3.4E-08	1.4E-07	2.7E-06
4	3.8E-08	1.6E-07	3.1E-06
5	4.3E-08	1.8E-07	3.4E-06
6	4.8E-08	2.0E-07	3.8E-06
7	5.4E-08	2.2E-07	4.3E-06
8	6.1E-08	2.5E-07	4.9E-06
9	6.9E-08	2.8E-07	5.5E-06
10	7.8E-08	3.1E-07	6.1E-06
15	1.4E-07	5.6E-07	1.1E-05
30	8.4E-07	3.1E-06	6.2E-05
45	5.0E-06	1.6E-05	3.3E-04
60	3.0E-05	6.9E-05	1.6E-03
90	1.1E-03	8.4E-04	2.0E-02
180	N/A	3.1E-01	N/A
365		N/A	

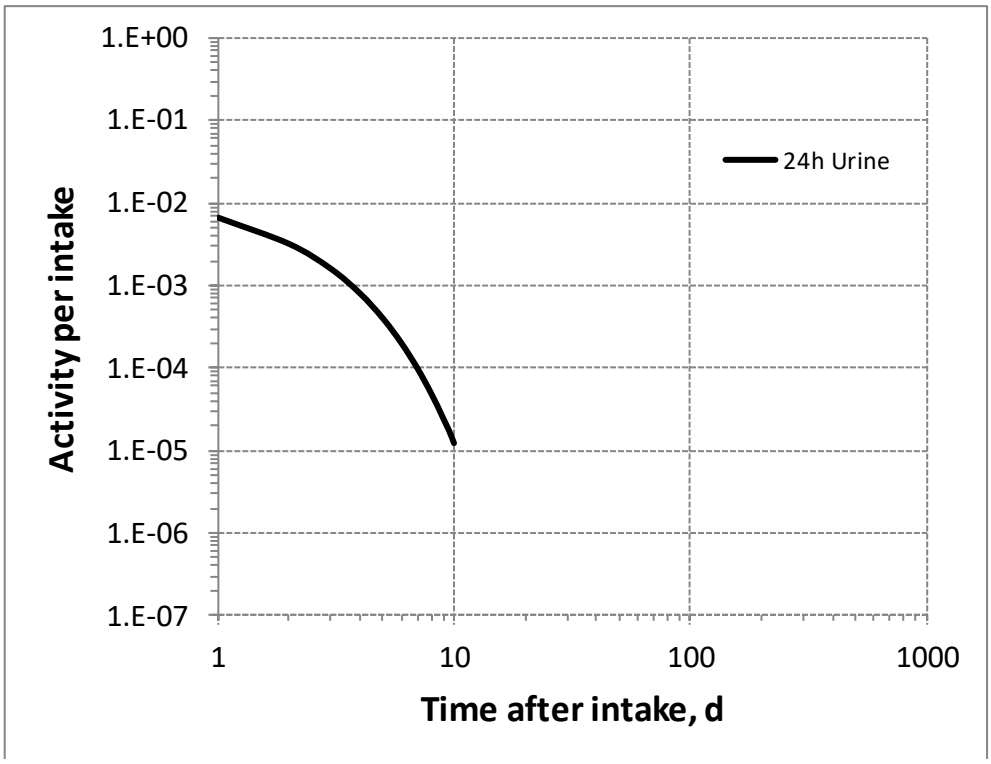

6918

6919 Fig. 37.2. Daily excretion of ^{200}Tl following inhalation of 1 Bq Type F.

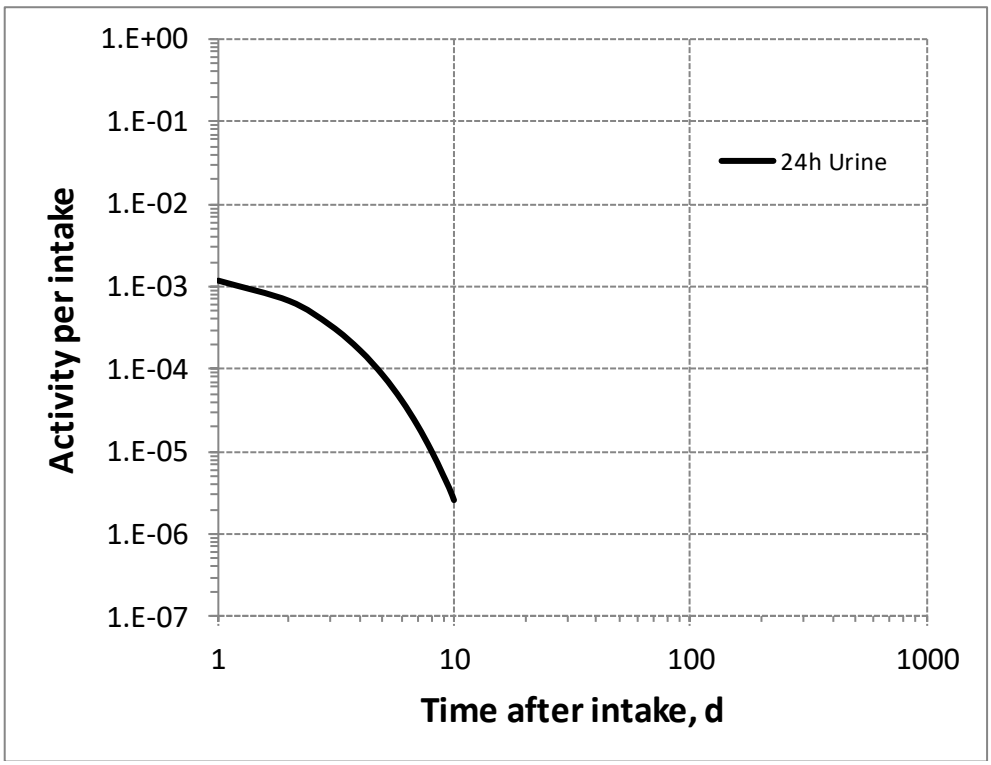

6920

6921 Fig. 37.3. Daily excretion of ^{200}Tl following inhalation of 1 Bq Type M.

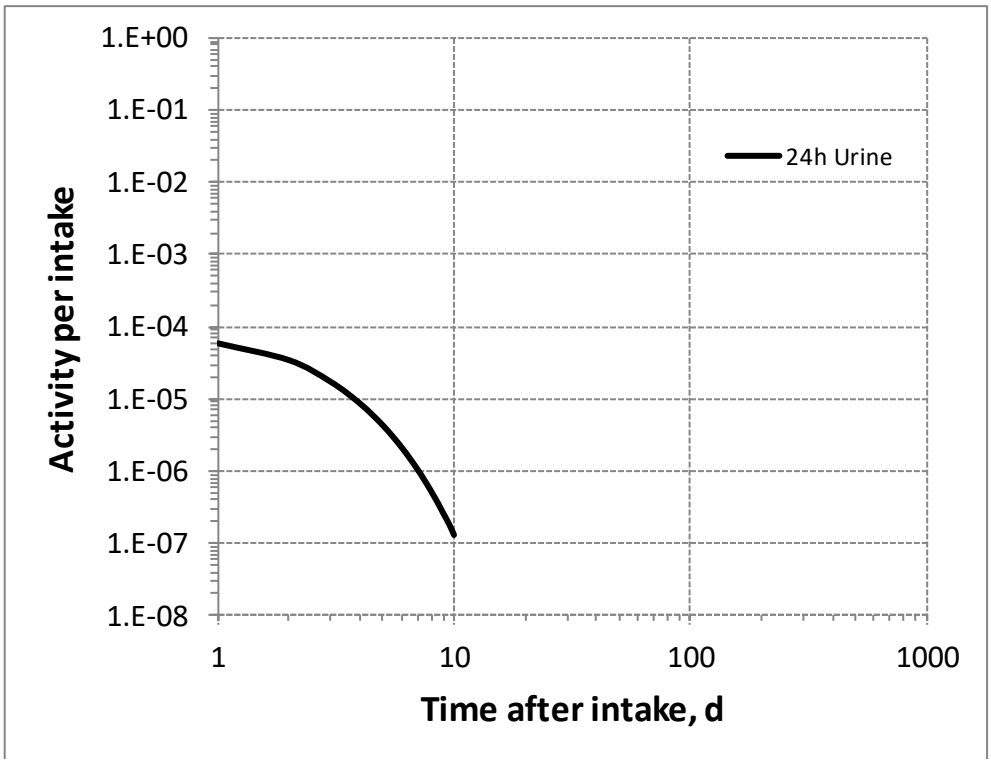

6922

6923 Fig. 37.4. Daily excretion of ^{200}Tl following inhalation of 1 Bq Type S.

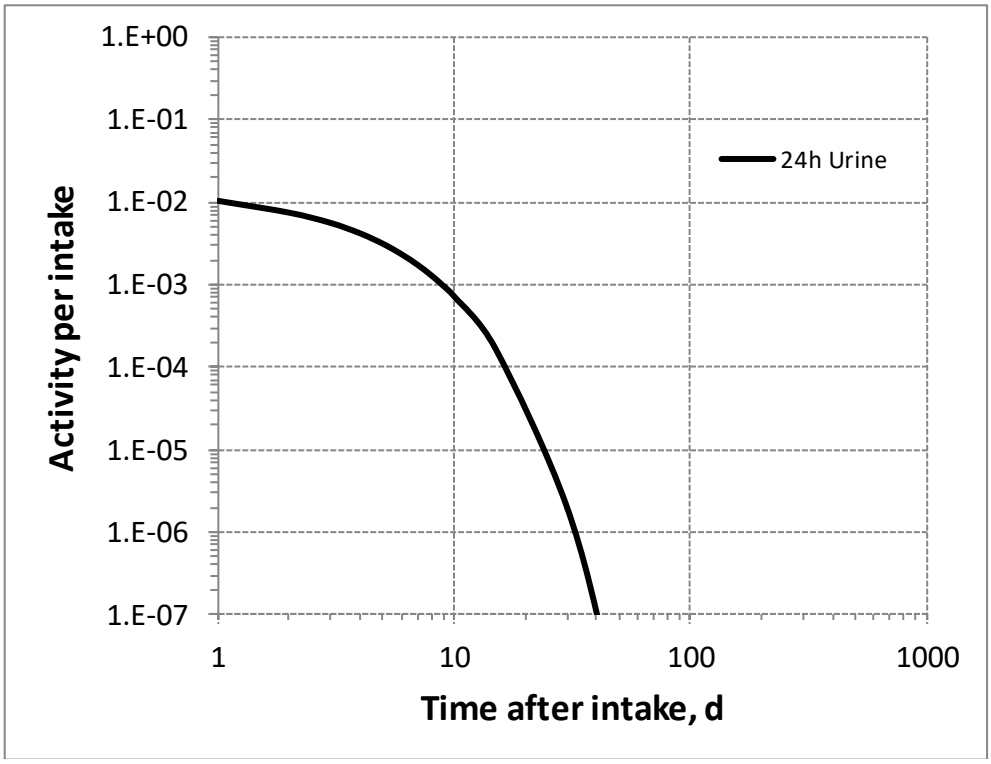

6924

6925 Fig. 37.5. Daily excretion of ^{201}Tl following inhalation of 1 Bq Type F.

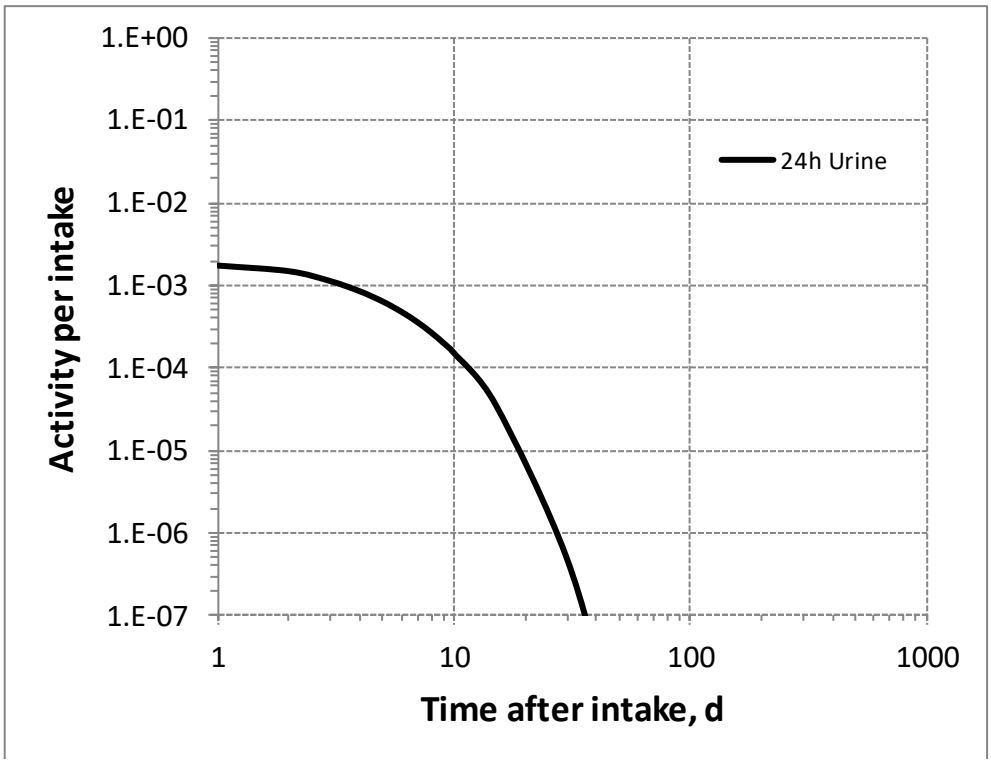

6926

6927 Fig. 37.6. Daily excretion of ^{201}Tl following inhalation of 1 Bq Type M.

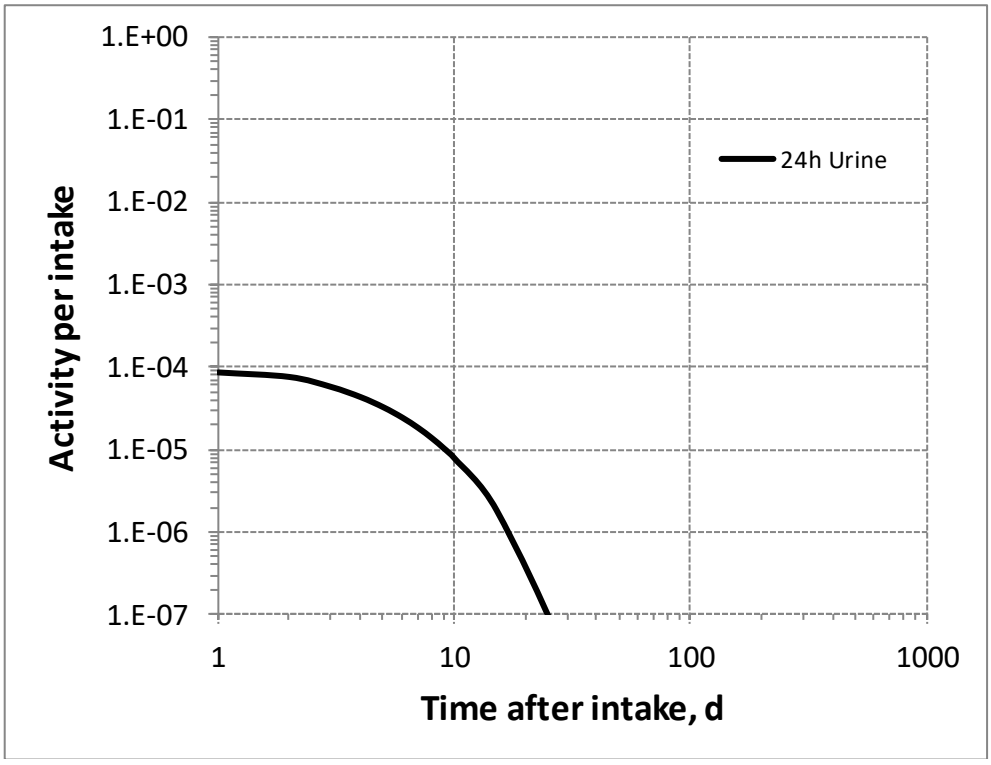

6928

6929 Fig. 37.7. Daily excretion of ^{201}Tl following inhalation of 1 Bq Type S.

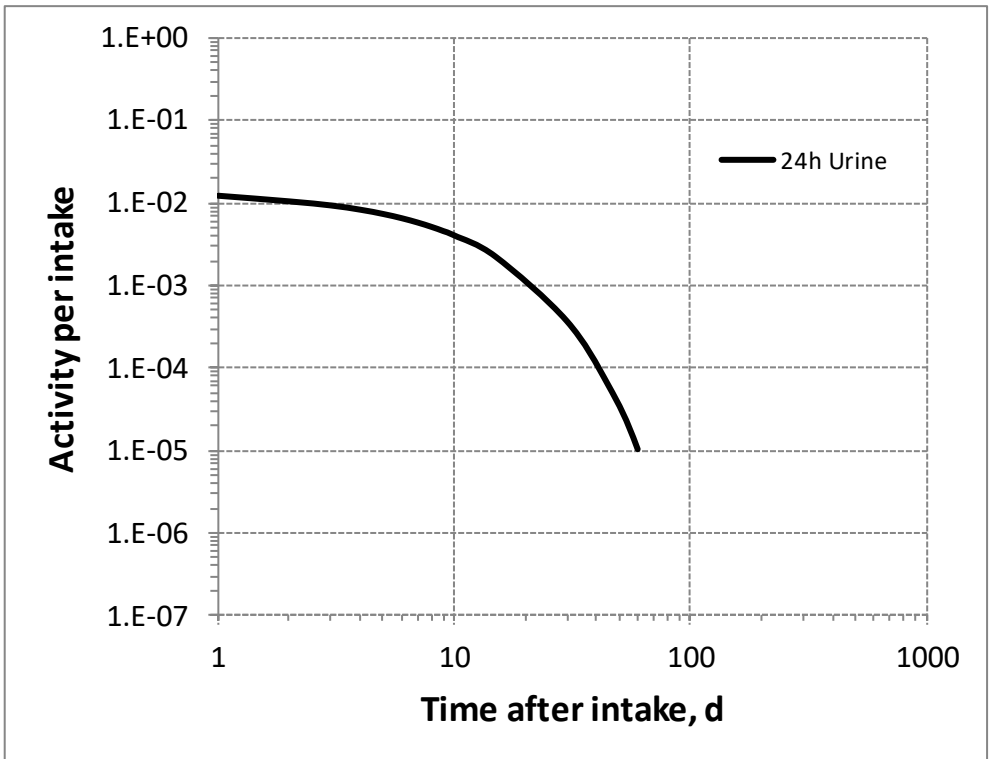

6930

6931 Fig. 37.8. Daily excretion of ^{202}Tl following inhalation of 1 Bq Type F.

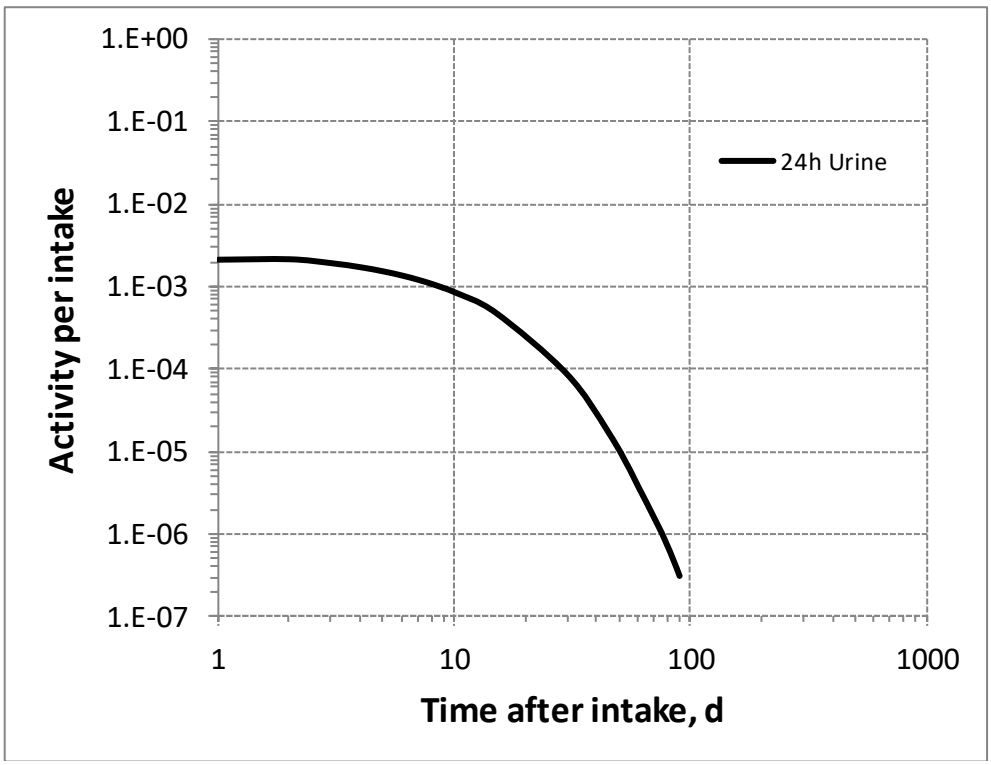

6932

6933 Fig. 37.9. Daily excretion of ^{202}Tl following inhalation of 1 Bq Type M.

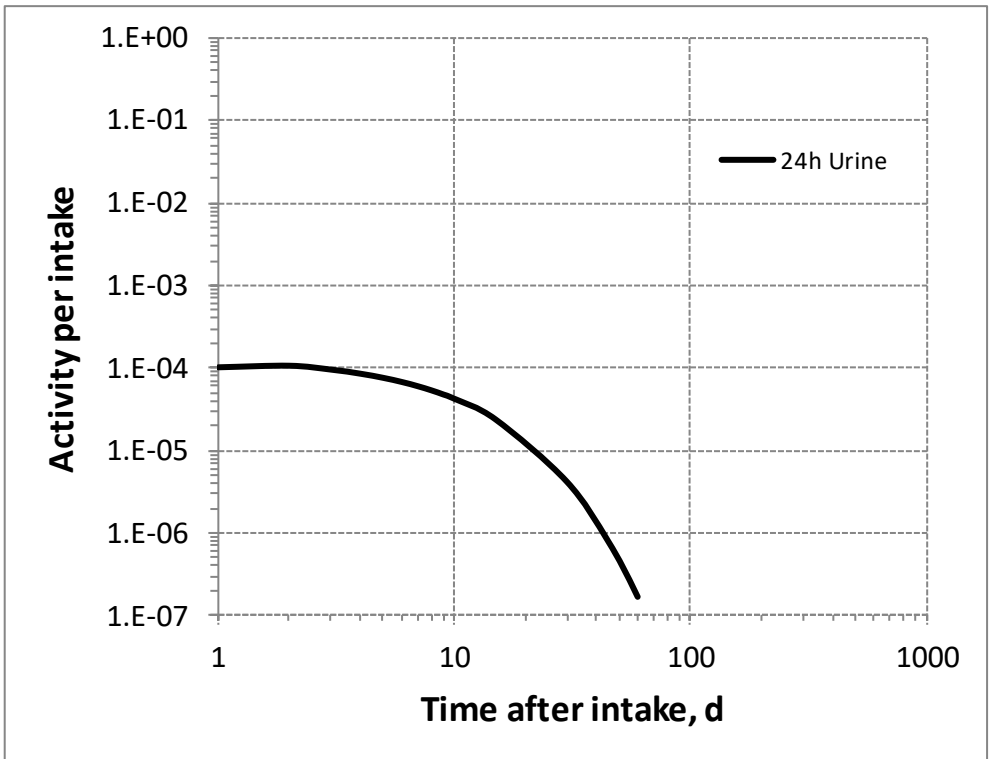

Fig. 37.10. Daily excretion of ^{202}Tl following inhalation of 1 Bq Type S.

38. ASTATINE (Z=85)

38.1. Isotopes

Table 38.1. Isotopes of astatine addressed in this publication.

Isotope	Physical half-life	Decay mode
^{205}At	26.2 min	EC, B+, A
^{206}At	30.6 min	EC, B+, A
^{207}At	1.80 h	EC, B+, A
^{208}At	1.63 h	EC, B+, A
^{209}At	5.41 h	EC, B+, A
^{210}At*	8.1 h	EC, B+, A
^{211}At	7.214 h	ECA

EC, electron-capture decay; B+, beta-plus decay; B-, beta-minus decay; IT, isomeric transition decay; A, alpha decay.
*Dose coefficients and bioassay data for this radionuclide are given in the printed copy of this publication. Data for other radionuclides listed in this table are given in the online electronic files on the ICRP website.

38.2. Routes of Intake

38.2.1. Inhalation

(714) For astatine, default parameter values were adopted for the absorption to blood from the respiratory tract (ICRP, 2015). For astatine, and the other halogens, intakes could be in both particulate and gas and vapour forms, and it is therefore assumed that inhaled astatine is 50% particulate and 50% gas/vapour in the absence of information (ICRP, 2002b). Absorption parameter values and types, and associated f_A values for gas and vapour forms of astatine are given in Table 38.2 and for particulate forms in Table 38.3. By analogy with the halogen iodine, considered in detail in *Publication 137* (ICRP, 2017), default Type F is recommended for particulate forms in the absence of specific information on which the exposure material can be assigned to an absorption type.

Table 38.2. Deposition and absorption for gas and vapour compounds of astatine.

	Percentage deposited (%)*						Absorption†	
Chemical form/origin	Total	ET_1	ET_2	BB	bb	AI	Type	Absorption from the alimentary tract, f_A‡
Unspecified	100	0	20	10	20	50	F	1.0

ET_1, anterior nasal passage; ET_2, posterior nasal passage, pharynx and larynx; BB, bronchial; bb, bronchiolar; AI, alveolar-interstitial.
*Percentage deposited refers to how much of the material in the inhaled air remains in the body after exhalation. Almost all inhaled gas molecules contact airway surfaces, but usually return to the air unless they dissolve in, or react with, the surface lining. The default distribution between regions is assumed: 20% ET2, 10% BB, 20% bb, and 50% AI.
†It is assumed that the bound state can be neglected for astatine (i.e. $f_b = 0$).
‡For inhaled material deposited in the respiratory tract and subsequently cleared by particle transport to the alimentary tract, the default f_A values for inhaled materials are applied [i.e. the product of f_r for the absorption Type (or specific value where given) and the f_A value for ingested soluble forms of astatine (1)].

Table 38.3. Absorption parameter values for inhaled and ingested astatine.

Inhaled particulate materials	Absorption parameter values* f_r	s_r (d^{-1})	s_s (d^{-1})	Absorption from the alimentary tract, f_A
Default parameter values†				
Absorption type				
F‡	1	30	–	1
M	0.2	3	0.005	0.2
S	0.01	3	1×10^{-4}	0.01
Ingested materials§				
All forms				1

*It is assumed that the bound state can be neglected for astatine (i.e. $f_b = 0$). The values of s_r for Type F, M and S forms of astatine (30, 3 and 3 d^{-1} respectively) are the general default values.

†For inhaled material deposited in the respiratory tract and subsequently cleared by particle transport to the alimentary tract, the default f_A values for inhaled materials are applied [i.e. the product of f_r for the absorption type and the f_A value for ingested soluble forms of astatine (1)].

‡Default Type F is recommended for use in the absence of specific information on which the exposure material can be assigned to an absorption type (e.g. if the form is unknown, or if the form is known but there is no information available on the absorption of that form from the respiratory tract). For guidance on the use of specific information, see Section 1.1.

§Activity transferred from systemic compartments into segments of the alimentary tract is assumed to be subject to reabsorption to blood. The default absorption fraction f_A for the secreted activity is the highest value for any form of the radionuclide ($f_A = 1$).

38.2.2. Ingestion

(715) There appears to be no data on the gastrointestinal absorption of astatine. However, as another halogen, it may be expected to be absorbed in proportion close to that of iodine. Injection studies confirm a similar behaviour of astatide and iodide, indicate partial in vivo deastatination of organic compounds, formation of sulphur-astatine bounds with proteins and similar tissue distribution for At^-, At^0 and At^+ (Visser et al., 1981).

(716) In *Publications 30* and *68* (ICRP, 1981, 1994a), f_1 was taken to be 1 for all compounds of astatine by analogy with the lighter halides, chlorine, bromine and iodine. The same value of $f_A = 1$ is used in this publication for all chemical forms of astatine.

38.2.3. Systemic distribution, retention and excretion of astatine

38.2.3.1. Biokinetic data

(717) Astatine (At) is the heaviest member of the halogen group of elements (Group VIIA of the periodic table). The systemic behaviour of astatine resembles that of the next heaviest halogen, iodine, particularly regarding the selective uptake of these two elements by the thyroid gland and stomach wall. Other biological similarities of astatine and iodine include their blood clearance rates and excretion patterns. However, some quantitative differences in the systemic behaviours of astatine and iodine are evident. The level of accumulation of astatine in the thyroid was lower than that of iodine during the first day after administration to human subjects, monkeys, guinea pigs, rats, and mice (Hamilton et al., 1953; Shellabarger and Godwin, 1954; Cobb et al., 1988; Garg et al., 1990). Also, astatine shows longer retention than iodine in the stomach wall and in most other soft tissues (Hamilton et al., 1953; Garg et al., 1990). It is not known whether astatine becomes organically bound in the thyroid, similarly to iodine.

(718) Following parenteral administration to guinea pigs, the thyroidal content and cumulative urinary and faecal excretion at 4 h represented 8.5%, 12%, and 0.8%, respectively, of the administered amount of iodine, and 3.4%, 8.8%, and 0.4%, respectively, of administered astatine (Hamilton and Soley, 1940). Corresponding values at 18 h were 17%, 37%, and 17% for iodine and 5.4%, 36%, and 13% for astatine.

(719) Hamilton et al. (1953) compared the biokinetics of intravenously administered ^{211}At and ^{131}I in rats. Plasma clearance was rapid for both radionuclides, with clearance of ^{131}I slightly faster than that of ^{211}At. At 24 h, plasma contained about 0.9% of injected ^{211}At and 0.6% of injected ^{131}I (after correction for radioactive decay). At 1 h the thyroid and stomach wall contained on average 5.6% and 6.1%, respectively, of injected ^{131}I, and 1.1% and 5.2% respectively, of injected ^{211}At. The stomach content of ^{131}I decreased steadily to about 0.5% of the injected amount at 24 h, while the stomach content of ^{211}At increased to 9.9% of the injected amount at 4 h and then decreased gradually to 5.9% at 24 h. The thyroid content of both radionuclides peaked at 24 h, at which time the thyroid contained about 1.5% of injected ^{211}At and 12% of injected ^{131}I. The ^{211}At content of the thyroid decreased by about a factor of 2 from 24-48 h and showed little if any change from 48-72 d. The ^{131}I content decreased more slowly than that of ^{211}At after 24 h, declining by about one-fourth from 24-72 h. Non-thyroidal tissues generally contained a larger portion of injected ^{211}At than injected ^{131}I from 4-24 h. For example, the mean ^{211}At content (% injected activity) of the liver, kidneys, and muscle were, respectively, about 4.6, 5.6, and 3.6 times the content of ^{131}I.

(720) Hamilton et al. (1953, 1954a,b) observed higher thyroidal accumulation of ^{211}At in limited studies on monkeys and human subjects than was observed in rats. In two monkeys, the thyroid contained 9 and 20% of administered ^{211}At at 24 h. In human subjects with various forms of thyroid pathology, 4.6-17.8% of administered astatine was contained in the thyroid at 24 h, compared with 12-30% of administered ^{131}I (Hamilton et al., 1954).

(721) Harrison and Royle (1984) measured the content of ^{211}At in blood, thyroid, kidneys, and testes of mice over the first 28.5 h after intravenous injection. The blood content (corrected for decay) declined to ~0.5% of the injected amount by ~12 h post injection and remained at that level through 28.5 h. The thyroid content peaked at ~3.5% of the injected amount within 3-4 h post injection, declined to roughly 40% of the peak content by 12-15 h, and remained near that level through 28.5 h. The pattern of uptake and retention by the testes was broadly similar to that of the thyroid. The kidneys contained about 5-6% of the injected amount at 0.5-1 h, 3% at 4-5 h, and 1.0-1.5% from 12-28.5 h.

(722) Larsen et al. (1998) compared the biokinetics of intravenously administered iodide (^{131}I) and astatide (^{211}At) in mice. Activity concentrations were determined in 12 tissues and in blood. High concentrations of ^{131}I were measured in thyroid and stomach at 1 and 4 h, with relatively low concentrations found in other tissues at 4 h. The thyroid showed high concentrations of ^{211}At at 1 and 4 h but only about one-half of that of ^{131}I at 1 h and one-fourth at 4 h. The two radionuclides showed similar uptake by the stomach wall at 1 h. By 4 h the concentration of ^{131}I in the stomach had decreased considerably while the ^{211}At concentration showed little change. On average, the ^{211}At concentration in individual tissues (% dosage g^{-1}) was 2.2 and 3.0 times the ^{131}I concentration at 1 h and 4 h, respectively.

38.2.3.2.Biokinetic model for systemic astatine

(723) The biokinetic model for systemic astatine used in this publication is a modification of the model for iodine adopted in *Publication 137* (2017), based on observed similarities and differences in the systemic behaviours of these elements. Fractional uptake of astatine from plasma to the thyroid is assumed to be one-half the value for iodine. An apparently greater

accumulation of astatine than iodine in tissues other than thyroid is assumed to result from slower return of astatine from these tissues to plasma. The structure of the model for iodine is simplified in some ways for application to astatine (e.g. by representing each of the tissues liver, kidneys, and 'Other' as single rather than multiple compartments), but additional tissues are treated explicitly in the astatine model based on apparent differences of the level of accumulation of iodine and astatine or its progeny in these tissues.

(724) The structure of the biokinetic model for systemic astatine applied in this publication is shown in Fig. 38.1. Transfer coefficients are listed in Table 38.4.

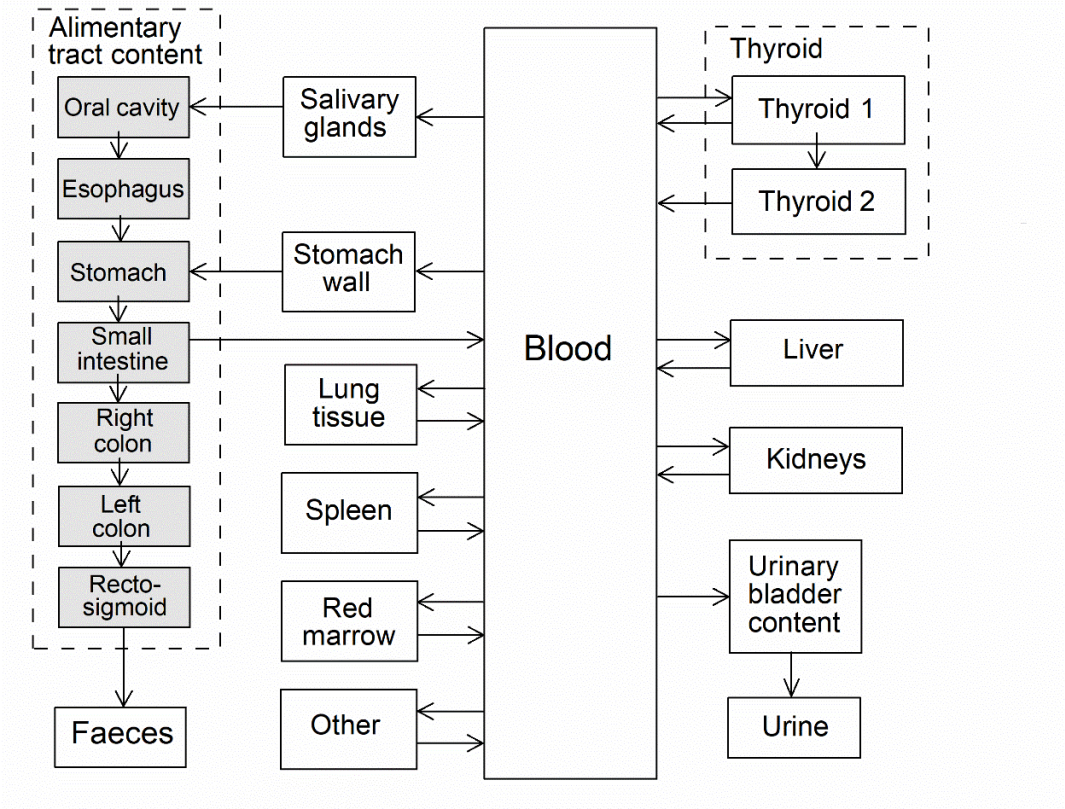

Fig. 38.1. Structure of the biokinetic model for systemic astatine.

38.2.3.3. Treatment of progeny

(725) Progeny of astatine addressed in this publication are radioisotopes of thallium, lead, bismuth, and polonium. The models for these four elements as progeny of astatine are expansions of their models as progeny of lead, described in Section 9.2.3.3 of *Publication 137* (2017). Thyroid, salivary glands, stomach wall, and lung tissue are added to the explicitly identified tissues in the model for polonium as a progeny of lead, and the following transfer rates between blood and the added tissues are assigned: plasma to thyroid, 0.1 d^{-1}; plasma to salivary glands, 0.4 d^{-1}; plasma to stomach wall, 0.2 d^{-1}; plasma to lung tissue, 2.0 d^{-1}; outflow from each of these four tissues to plasma, 0.099 d^{-1}. As in the models for thallium, lead, bismuth, and polonium as progeny of lead, the following transfer rates to a progeny's central blood compartments are assigned when the progeny is produced in a compartment that is not in the progeny's model: 1000 d^{-1} if produced in a blood compartment; at the rate of bone turnover if produced in a bone volume compartment; and at the following element-specific rates if produced in any other compartment: thallium, 2.5 d^{-1}; lead, 7.39 d^{-1}; bismuth, 66.54 d^{-1}; polonium, 0.099 d^{-1}.

7074 Table 38.4. Transfer coefficients in the biokinetic model for systemic astatine.

From	To	Transfer coefficients (d^{-1})
Blood	Thyroid 1	3.63
Blood	Urinary bladder content	11.84
Blood	Salivary glands	5.16
Blood	Stomach wall	8.6
Blood	Kidneys	25
Blood	Liver	45
Blood	Lung tissue	25
Blood	Spleen	25
Blood	Red marrow	25
Blood	Other	500
Thyroid 1	Blood	36
Thyroid 1	Thyroid 2	95
Thyroid 2	Blood	0.0077
Salivary glands	Oral cavity	25
Stomach wall	Stomach content	25
Kidneys	Blood	50
Liver	Blood	50
Lung tissue	Blood	50
Spleen	Blood	50
Red marrow	Blood	50
Other	Blood	100

7075 ## 38.3. Individual monitoring

7076 (726) Information of detection limit for routine individual measurement is not available.

7077 ## 38.4. Dosimetric data for astatine

7078 Table 38.5. Committed effective dose coefficients (Sv Bq^{-1}) for the inhalation or ingestion of ^{210}At
7079 compounds.

	Effective dose coefficients (Sv Bq^{-1})
Inhaled gases and vapours	^{210}At
Unspecified	4.8E-09
Inhaled particulate materials (5 μm AMAD aerosols)	
Type F, default	4.8E-09
Type M	3.4E-09
Type S	4.6E-09
Ingested materials	
All forms	8.6E-09

7080 AMAD, activity median aerodynamic diameter
7081

39. FRANCIUM (Z=87)

39.1. Isotopes

Table 39.1. Isotopes of francium addressed in this publication.

Isotope	Physical half-life	Decay mode
^{212}Fr	20.0 min	EC, B+, A
^{222}Fr	14.2 min	B-
^{223}Fr*	22.00 min	B-, A

EC, electron-capture decay; B+, beta-plus decay; B-, beta-minus decay; A, alpha decay.
*Dose coefficients and bioassay data for this radionuclide are given in the printed copy of this publication.
Data for other radionuclides listed in this table are given in the online electronic files on the ICRP website.

39.2. Routes of Intake

39.2.1. Inhalation

(727) For francium, default parameter values were adopted on absorption to blood from the respiratory tract (ICRP, 2015). Absorption parameter values and types, and associated f_A values for particulate forms of francium are given in Table 39.2.

Table 39.2. Absorption parameter values for inhaled and ingested francium.

	Absorption parameter values*			Absorption from the alimentary tract, f_A
Inhaled particulate materials	f_r	s_r (d^{-1})	s_s (d^{-1})	
Default parameter values†				
Absorption type				
F	1	30	–	1
M‡	0.2	3	0.005	0.2
S	0.01	3	1×10^{-4}	0.01
Ingested materials§				
All forms				1

*It is assumed that the bound state can be neglected for francium (i.e. $f_b = 0$). The values of s_r for Type F, M and S forms of francium (30, 3 and 3 d^{-1} respectively) are the general default values.
†For inhaled material deposited in the respiratory tract and subsequently cleared by particle transport to the alimentary tract, the default f_A values for inhaled materials are applied [i.e. the product of f_r for the absorption type and the f_A value for ingested soluble forms of francium (1)].
‡Default Type M is recommended for use in the absence of specific information on which the exposure material can be assigned to an absorption type (e.g. if the form is unknown, or if the form is known but there is no information available on the absorption of that form from the respiratory tract). For guidance on the use of specific information, see Section 1.1.
§Activity transferred from systemic compartments into segments of the alimentary tract is assumed to be subject to reabsorption to blood. The default absorption fraction f_A for the secreted activity is the highest value for any form of the radionuclide ($f_A = 1$).

39.2.2. Ingestion

(728) There appear to be no data on the gastrointestinal absorption of francium. In *Publications 30* and *68* (ICRP, 1981, 1994a), f_1 was taken to be 1 for all compounds of francium, by analogy with potassium, rubidium and caesium. In this publication, $f_A = 1$ is also applied to all chemical forms of francium.

39.2.3. Systemic distribution, retention and excretion of francium

39.2.3.1. Biokinetic model for systemic francium

(729) Francium is the heaviest member of the alkali metal family, positioned below caesium in the period table. For lack of specific biokinetic data for francium, its systemic behaviour is assumed to be the same as that of caesium. A much simpler model is applied to francium than to caesium (ICRP, 2017), however, in view of the short half-life of francium radioisotopes (≤ 22 min) and the uncertainty in the accuracy of the caesium analogy.

(730) Francium is assumed to leave blood at the rate 200 d^{-1} (half-time ~5 min), with 5% going to the urinary bladder content, 1% going to the right colon content, and 94% uniformly distributed in all tissues. Francium deposited in tissues is assumed to transfer to blood at the rate 0.1 d^{-1}.

(731) Transfer coefficients for francium are listed in Table 39.3.

Table 39.3. Transfer coefficients (d^{-1}) in the biokinetic model for systemic francium.

From	To	Transfer coefficient (d^{-1})
Blood	Other	188
Blood	Urinary bladder content	10
Blood	Right colon content	2
Other	Blood	0.1

39.2.3.2. Treatment of progeny

(732) Progeny of francium addressed in this publication are isotopes of thallium, lead, bismuth, polonium, astatine, radon, or radium. The models for francium progeny produced in systemic compartments are essentially the same as the models applied to these elements as radium progeny in Section 13.2.3.3 of *Publication 137* (2017). As in the models for these elements as progeny of radium, the following transfer rates to a progeny's central blood compartments are assigned when the progeny is produced in a compartment that is not in the progeny's model: 1000 d^{-1} if produced in a blood compartment; at the rate of bone turnover if produced in a bone volume compartment; and at the following element-specific rates if produced in any other compartment: thallium, 2.5 d^{-1}; lead, 7.39 d^{-1}; bismuth, 66.54 d^{-1}; polonium, 0.099 d^{-1}; radium, 6.98 d^{-1}.

39.3. Individual monitoring

(733) Information of detection limit for routine individual measurement is not available.

39.4. Dosimetric data for francium

Table 39.4. Committed effective dose coefficients (Sv Bq^{-1}) for the inhalation or ingestion of ^{223}Fr compounds.

Inhaled particulate materials (5 μm AMAD aerosols)	Effective dose coefficients (Sv Bq^{-1})
	^{223}Fr
Type F, — NB: Type F should not be assumed without evidence	2.1E-10
Type M, default	2.3E-09

Type S	2.9E-09
Ingested materials	
All forms	1.5E-10

AMAD, activity median aerodynamic diameter

REFERENCES

Aamodt, R.L., 1973. Retention and excretion of injected 181W labeled sodium tungstate by beagles. Health Phys 24: 519–524.

Aamodt, R.L., 1975. Inhalation of 181W labeled tungstic oxide by six beagle dogs. Health Phys 28: 733–742.

Abdel-Rahman, M.S., Couri, D. and Bull, R.J., 1982. Metabolism and pharmacokinetics of alternate drinking water disinfectants. Environmental Health Perspectives 46: 19–23.

Abdel-Rahman, M.S., Waldron, D.M. and Bull, R.J., 1983. A comparative kinetics study of monochloramine and hypochlorous acid in the rat. Journal of Applied Toxicology 3(4): 175–179. DOI: 10.1002/jat.2550030403.

Adachi, A., Ogawa, K., Tsushi, Y., et al., 2000. Balance, excretion and tissue distribution of vanadium in rats after short-term ingestion. Journal of Health Science 46(1): 59–62. DOI: 10.1248/jhs.46.59.

Adeyemi, A., Garelick, H. and Priest, N.D., 2010. A biokinetic model to describe the distribution and excretion of arsenic by man following acute and chronic intakes of arsenite/arsenate compounds by ingestion. Human Expl. Toxicol 29: 891–902.

Adler, A.J., Etzion, Z. and Berlyne, G.M., 1986. Uptake, distribution, and excretion of 31silicon in rats. Am. J. Physiol: 251 670– 673.

ATSDR, 1988. Toxicological Profile for Beryllium. Prepared by Syracuse Research Corporation under Contract 68-C8-0004. Agency for Toxic Substances and Disease Registry (ATSDR). Atlanta, Georgia: U.S. Public Health Service.

ATSDR, 1999. Toxicological Profile for Mercury. Agency for Toxic Substances and Disease Registry (ATSDR). Atlanta, Georgia: U.S. Department of Health and Human Services. Public Health Service.

ATSDR, 2002. Toxicological Profile for Beryllium. Agency for Toxic Substances and Disease Registry (ATSDR). Atlanta, Georgia: U.S. Department of Health and Human Services. Public Health Service.

ATSDR, 2003. Toxicological Profile for Selenium. Agency for Toxic Substances and Disease Registry (ATSDR). Atlanta, Georgia: U.S. Department of Health and Human Services. Public Health Service.

ATSDR, 2004. Toxicological Profile for Copper. Agency for Toxic Substances and Disease Registry (ATSDR). Atlanta, Georgia: U.S. Department of Health and Human Services. Public Health Service.

ATSDR, 2005a. Toxicological Profile for Nickel. Agency for Toxic Substances and Disease Registry (ATSDR). Atlanta, Georgia: U.S. Department of Health and Human Services. Public Health Service.

ATSDR, 2005b. Toxicological Profile for Tin. Agency for Toxic Substances and Disease Registry (ATSDR). Atlanta, Georgia: U.S. Department of Health and Human Services. Public Health Service.

ATSDR, 2005c. Toxicological Profile for Tungsten. Agency for Toxic Substances and Disease Registry (ATSDR). Atlanta, Georgia: U.S. Department of Health and Human Services. Public Health Service.

ATSDR, 2007. Toxicological Profile for Arsenic. Agency for Toxic Substances and Disease Registry (ATSDR). Atlanta, Georgia: U.S. Department of Health and Human Services. Public Health Service.

ATSDR, 2008. Toxicological Profile for Perchlorates. Agency for Toxic Substances and Disease Registry (ATSDR). Atlanta, Georgia: U.S. Department of Health and Human Services. Public Health Service.

7190 ATSDR, 2012a. Toxicological Profile for Cadmium. Agency for Toxic Substances and Disease
7191 Registry (ATSDR). Atlanta, Georgia: U.S. Department of Health and Human Services.
7192 Public Health Service.
7193 ATSDR, 2012b. Toxicological Profile for Chromium. Agency for Toxic Substances and
7194 Disease Registry (ATSDR). Atlanta, Georgia: U.S. Department of Health and Human
7195 Services. Public Health Service.
7196 ATSDR, 2012c. Toxicological Profile for Manganese. Agency for Toxic Substances and
7197 Disease Registry (ATSDR). Atlanta, Georgia: U.S. Department of Health and Human
7198 Services. Public Health Service.
7199 ATSDR, 2017. Toxicological Profile for Silica. Agency for Toxic Substances and Disease
7200 Registry (ATSDR). Atlanta, Georgia: U.S. Department of Health and Human Services.
7201 Public Health Service.
7202 Aikawa, J.K., Gordon, G.S. and Rhoades, E.L., 1960. Magnesium metabolism in human beings:
7203 studies with 28Mg. J. Appl. Physiol 15: 503–507.
7204 Alexander, J., Hogberg, J., Thomassen, Y., et al., 1988. Selenium. In: Seiler HG, Sigel H, and
7205 Sigel A (eds) Handbook on Toxicity of Inorganic Compounds. New York: Marcel Dekker,
7206 pp. 581–594.
7207 Alimonti, A., Petrucci, F., Krachler, M., et al., 2000. Reference values for chromium, nickel
7208 and vanadium in urine of youngsters from the urban area of Rome. Journal of Environmental
7209 Monitoring 2(4): 351–354. DOI: 10.1039/b001616k.
7210 Alvioli, L.V. and Berman, M., 1966. 28Mg kinetics in man. J. Appl. Physiol 21(6): 1688–1694.
7211 Amano, R., Enomoto, S., Nobuta, M., et al., 1996. Bone uptake of vanadium in mice
7212 Simultaneous tracing of V, Se, Sr, Y, Zr, Ru and Rh using radioactive multitracer. Journal
7213 of Trace Elements in Medicine and Biology 10: 145–148.
7214 Andersen, J.C.Ø., Cropp, A. and Paradise, D.C., 2017. Solubility of indium-tin oxide in
7215 simulated lung and gastric fluids: Pathways for human intake. Science of the Total
7216 Environment 579: 628–636. DOI: 10.1016/j.scitotenv.2016.11.047.
7217 Andersen, M.E., Gearhart, J.M. and Clewell, H.J., 1999. Pharmacokinetic data needs to support
7218 risk assessment for inhaled and ingested manganese. NeuroToxicology 20: 161–72.
7219 Anderson, R.A., 1997. Chromium as an Essential Nutrient for Humans. Regulatory Toxicology
7220 and Pharmacology 26: 35– 41.
7221 Andersson, L., Hallstadius, L. and Strand, S-E., 1988. Biokinetics and dosimetry for 195Au,
7222 evaluated in an animal model. Eur. J. Nucl. Med 14: 393–399.
7223 Andersson, M., Mattsson, S., Johansson, L., et al., 2017. A biokinetic and dosimetric model for
7224 ionic indium in humans. Physics in Medicine and Biology 62(16): 6397–6407. DOI:
7225 10.1088/1361-6560/aa779f.
7226 Ando, A. and Ando, I., 1986. Distribution of 95Zr and 181Hf in tumor-bearing animals and
7227 mechanism for accumulation in tumor and liver. International Journal of Radiation
7228 Applications and Instrumentation. Part B 13(1): 21–29. DOI: 10.1016/0883-2897(86)90247-
7229 3.
7230 Ando, A. and Ando, I., 1990. Biodistribution of 95Nb and 182Ta in tumor-bearing animals and
7231 mechanisms for accumulation in tumor and liver. Journal of Radiation Research 31(1): 97–
7232 109. DOI: 10.1269/jrr.31.97.
7233 Ando, A. and Ando, I., 1994. Biodistributions of radioactive bipositive metal ions in tumor-
7234 bearing animals. BioMetals 7(2): 185–192. DOI: 10.1007/bf00140490.
7235 Ando, A., Ando, I., Hiraki, T., et al., 1989. Relation between the location of elements in the
7236 periodic table and various organ-uptake rates. International Journal of Radiation
7237 Applications and Instrumentation. 16(1): 57–80. DOI: 10.1016/0883-2897(89)90216-X.

7238 Angelova, M., Asenova, S., Nedkova, V., et al., 2011. Copper in the human organism. Trakia
7239 J. Sci 9: 88–98.
7240 Archimbaud, Y., Grillon, G., Poncy, J.L., et al., 1992. 75Se transfer via placenta and milk,
7241 distribution and retention in fetal, young and adult rat. Radiation Protection Dosimetry 41:
7242 147–151.
7243 Artelt, S., Koch, H., Nachtigall, D., et al., 1998. Bioavailability of platinum emitted from
7244 automobile exhaust. Toxicology Letters 96/97: 163 –167.
7245 Artelt, S., Creutzenberg, O., Kock, H., et al., 1999. Bioavailability of fine dispersed platinum
7246 as emitted from automotive catalytic converters: a model study. Science of the Total
7247 Environment 228: 219 –242.
7248 Asakura, K., Satoh, H., Chiba, M., et al., 2008. Oral toxicity of indium in rats: Single and 28-
7249 day repeated administration studies. Journal of Occupational Health 50(6): 471–478. DOI:
7250 10.1539/joh.l8070.
7251 Atkins, H.L., Budinger, T.F., Lebowitz, E., et al., 1977. Thallium-201 for medical use, 3.
7252 Human distribution and physical imaging properties. J. Nucl. Med 18: 133–140.
7253 Azay, J., Bres, J., Krosniak, M., et al., 2001. Vanadium pharmacokinetics and oral
7254 bioavailability upon single-dose administration of vanadyl sulfate to rats. Fundamental &
7255 Clinical Pharmacology 15(5): 313–324.
7256 Bachler, G., Losert, S., Umehara, Y., et al., 2015. Translocation of gold nanoparticles across
7257 the lung epithelial tissue barrier: Combining in vitro and in silico methods to substitute in
7258 vivo experiments. Particle and Fibre Toxicology 12(1).
7259 Bacso, J., Uzonyi, I. and Dezso, B., 1988. Determination of gold accumulation in human tissues
7260 caused by gold therapy using x-ray fluorescence analysis. Appl. Radiat. Isot 39: 323–326.
7261 Bair, W.J., 1961. Deposition, retention, translocation and excretion of radioactive particles. In:
7262 Davies CN (ed.) Inhaled Particles and Vapours. Oxford: Pergamon Press, pp. 192–208.
7263 Baisch, B.L., Corson, N.M., Wade-Mercer, P., et al., 2014. Equivalent titanium dioxide
7264 nanoparticle deposition by intratracheal instillation and whole body inhalation: The effect of
7265 dose rate on acute respiratory trace inflammation. Particle and Fibre Toxicology 11: 5–16.
7266 Balasubramanian, S.K., Poh, K-W., Ong, C-N., et al., 2013. The effect of primary particle size
7267 on biodistribution of inhaled gold nano-agglomerates. Biomaterials 34(22): 5439–5452.
7268 Ballou, J.E., 1960. Metabolism of 185W in the rat. AEC Research and Development Report
7269 HW‐64112. Durham, NC: Hanford Laboratory.
7270 Barceloux, D.G. and Barceloux, D., 1999. Vanadium. Journal of Toxicology: Clinical
7271 Toxicology 37(2). Taylor & Francis: 265–278. DOI: 10.1081/CLT-100102425.
7272 Barclay, R.K., Peacock, W.C. and Karnofsky, D.A., 1953. Distribution and excretion of
7273 radioactive thallium in the chick embryo, rat, and man. Journal of Pharmacology and
7274 Experimental Therapeutics 107(2): 178–187.
7275 Barnes, J.M. and Stoner, H.B., 1959. The toxicology of tin compounds. Pharmacological
7276 Reviews 11(2, Part 1): 211–231.
7277 Barregård, L., 1993. Biological monitoring of exposure to mercury vapour. Scand. J. Work.
7278 Environ. Health 1: 45–49.
7279 Barregård, L., Sallsten, G., Schutz, A., et al., 1992. Kinetics of mercury in blood and urine after
7280 brief occupational exposure. Arch. Environ. Health 47: 176–184.
7281 Barrett, H.M., Irwin, D.A. and Semmons, E., 1947. Studies on the toxicity of inhaled cadmium.
7282 I. The acute toxicity of cadmium oxide by inhalation. J. Ind. Hyg. Toxicol 29: 279–285.
7283 Baruthio, F., Guillard, O., Arnaud, J., et al., 1988. Determination of manganese in biological
7284 materials by electrothermal atomic absorption spectrometry: A review. Clin Chem 34: 227–
7285 34.

7286 Basse-Cathalinat, B., Blanquet, P., Collignon, G., et al., 1968. Bone scintigraphy with 47Sc and
7287 the scintillation camera. Journal of Nuclear Medicine 9(8): 436–438.
7288 Bau, M. and Dulski, P., 1995. Comparative study of yttrium and rare-earth element behaviors
7289 in fluorine-rich hydrothermal fluids. Contributions to Mineralogy and Petrology 119: 213–
7290 223.
7291 Beamish, M.R. and Brown, E.B., 1974. The metabolism of transferrin-bound 111In and 59Fe
7292 in rat. Blood 43: 693–701.
7293 Becker, K., Schulz, C., Kaus, S., et al., 2003. German Environmental Survey 1998 (GerES III):
7294 Environmental pollutants in the urine of the German population. International Journal of
7295 Hygiene and Environmental Health 206(1): 15–24. DOI: 10.1078/1438-4639-00188.
7296 Begerow, J., Sensen, U., Wiesmüller, G.A., et al., 1999. Internal platinum, palladium, and gold
7297 exposure in environmentally and occupationally exposed persons. Zentralblatt für Hygiene
7298 und Umweltmedizin = International journal of hygiene and environmental medicine 202(5):
7299 411–424.
7300 Begerow, J., Neuendorf, J., Turfeld, M., et al., 1999. Long-term urinary platinum, palladium,
7301 and gold excretion of patients after insertion of noble-metal dental alloys. Biomarkers 4(1):
7302 27–36. DOI: 10.1080/135475099230976.
7303 Bell, M.C. and Sneed, N.N., 1970. Metabolism of tungsten by sheep and swine. In: Mills CF
7304 (ed.) Trace Element Metabolism in Animals. E&S Livingstone. Edinburgh, pp. 70–72.
7305 Bello, D. and Warheit, D.B., 2017. Biokinetics of engineered nano-TiO2 in rats administered
7306 by different exposure routes: Implications for human health. Nanotechnology 11: 431–433.
7307 Benoy, C.J., Hooper, P.A. and Schneider, R., 1971. The toxicity of tin in canned fruit juices
7308 and solid foods. Food and Cosmetics Toxicology 9: 645–656.
7309 Benson, J.M., Cheng, Y-S. and Medinsky, M.A., 1991. Toxicokinetics of 63Ni after inhalation
7310 of nickel sulfatehexahydrate and nickel oxide. In: Inhalation Toxicology Research Institute
7311 Annual Report 1990–1991. Lovelace Biomedical&Environmental Research Institute.
7312 Albuquerque, New Mexico, pp. 42–43.
7313 Benson, J.M., Chang, I-Y., Cheng, Y-S., et al., 1992. Effects of repeated inhalation exposure of
7314 F344/N rats and B6C3F1 mice to nickel oxide and nickel sulfate hexahydrate on lung
7315 clearance. In: Inhalation Toxicology Research Institute Annual Report, 1991–1992. LMF-
7316 138. Albuquerque, New Mexico: Lovelace Biomedical & Environmental Research Institute,
7317 pp. 74–76.
7318 Benson, J.M., Cheng, Y-S., Muggenburg, B.A., et al., 1993. The fate of inhaled nickel
7319 compounds in cynomolgus monkeys. In: Inhalation Toxicology Research Institute Annual
7320 Report 1992–1993. Albuquerque, New Mexico: Lovelace Biomedical & Environmental
7321 Research Institute, pp. 43–44.
7322 Benson, J.M., Barr, E.B., Bechtold, W.E., et al., 1994. Fate of inhaled nickel oxide and nickel
7323 subsulfide in f344/n rats. Inhalation Toxicology 6(2): 167–183. DOI:
7324 10.3109/08958379409029703.
7325 Benson, J.M., Chang, I-Y., Cheng, Y.S., et al., 1995a. Particle clearance and histopathology in
7326 lungs of F344/N rats and B6C3F1 mice inhaling nickel oxide or nickel sulfate. Toxicological
7327 Sciences 28(2). Toxicol Sci: 232–244. DOI: 10.1093/toxsci/28.2.232.
7328 Benson, J.M., Cheng, Y-S., Eidson, A.F., et al., 1995b. Pulmonary toxicity of nickel subsulfide
7329 in F344/N rats exposed for 1-22 days. Toxicology 103(1): 9–22. DOI: 10.1016/0300-
7330 483X(95)03098-Z.
7331 Benson, J.M., Maples, K.R. and Hahn, F.F., 1995c. Species Differences in the Fate of Nickel
7332 Compounds in the Respiratory Tract. In: Inhalation Toxicology Research Institute Final
7333 Report to Nickel Producers Environmental Research Association, Inc (NiPERA).
7334 Albuquerque, New Mexico: Lovelace Biomedical & Environmental Research Institute.

Beresford, N.A., Mayes, R.W., Crout, N.M.J., et al., 1994. Dynamic behavior of 110mAg in sheep tissues. Health Physics 66: 420–426.

Berg, H.F., 1951. Localization of radioactivity of colloidal gold198 (a preliminary report. AMA Arch. Surg 63: 545–553.

Berg, H.F., Christopherson, W.M. and Bryant, J.R., 1954. Time and site study for optimum lymph node concentration of radiogold following intrabronchial injection. Cancer Res 4. Berg, H.F., Christopherson, W.M., Bryant, J.R: 775–779.

Berger, C.D., Lane, B.H. and Hamrick, T., 1983. Clearance of 202Tl contaminate following intravenous injection of 201Tl. Health Phys 45: 999–1001.

Bergstrom, W.H., 1955. The participation of bone in total body sodium metabolism in the rat. J. Clin. Invest 34: 997–1004.

Berlin, M., 1986. Mercury. In: Friberg L, Nordberg GF, and Vouk VB (eds) Handbook of the toxicology of metals. New York: Elsevier, pp. 387–445.

Berlin, M., Jerksell, L.G. and Ubisch, H., 1966. Uptake and retention of mercury in the mouse brain. Arch. Environ. Health 12: 33–42.

Berlin, M., Fazackerley, J. and Nordberg, G., 1969. The uptake of mercury in the brains of mammals exposed to mercury vapour and to mercuric salts. Arch. Environ. Health 18: 719–729.

Berlin, M.H., Nordberg, G.F. and Serenium, F., 1969. On the site and mechanism of mercury vapour resorption in the lung. A study in the guinea pig using mercuric nitrate Hg-203. Arch. Environ. Health 18: 43–50.

Berlyne, G.M., Ben, Ari, J., Knopf, E., et al., 1972. Aluminium toxicity in rats. Lancet 299: 564–568.

Berlyne, G.M., Shainkin-Kestenbaum, R., Yagil, R., et al., 1986. Distribution of 31silicon-labeled silicic acid in the rat. Biol. Trace Elem. Res 10: 159–162.

Bernstein, L.R., 1998. Mechanisms of therapeutic activity for gallium. Pharmacological Reviews 50: 665–682.

Berry, J.P. and Galle, P., 1992. Preferential localization of hafnium in nodular lymphatic cells. Study by electron microprobe. Journal of Submicroscopic Cytology and Pathology 24: 15–18.

Bertinato, J., Plouffe, L.J., Lavergne, C., et al., 2014 Bioavailability of magnesium from inorganic and organic compounds is not affected in rats fed a high phytic acid diet. Magnes Res 27(4): 175–85.

Bettley, F.R. and O'Shea, J.A., 1975. The absorption of arsenic and its relation to carcinoma. British Journal of Dermatology 92: 563–568.

Bianco, A., Bassi, P., Belvisi, M., et al., 1980. Inhalation of a radioactively labelled monodisperse aerosol in rats for the assessment of regional deposition and clearance. Am. Ind. Hyg. Ass. J 41(8): 563–567.

Black, D.A.K., Davies, H.E.F. and Emery, E.W., 1955. The disposal of radioactive potassium injected intravenously. Lancet 265: 1097–1099.

Blanchardon, E., Challeton-de Vathaire, C., Boisson, P., et al., 2005. Long term retention and excretion of 201Tl in a patient after myocardial perfusion imaging. Radiation Protection Dosimetry 113(1): 47–53. DOI: 10.1093/rpd/nch430.

Block, W.D., Buchanan, O.H. and Freyberg, R.H., 1942 Metabolism, toxicity and manner of action of gold compounds used in the treatment of arthritis. IV. Studies of the absorption, distribution and excretion of gold following the intramuscular injection of gold thioglucose and gold calcium thiomalate. J. Pharmacol. Exp. Ther 76: 355–357.

Block, W.D., Buchanan, O.H. and Freyberg, R.H., 1944. Metabolism, toxicity and manner of action of gold compounds used in the treatment of arthritis. V. A comparative study of the

rate of absorption, the retention, and the rate of excretion of gold administered in different compounds. J. Pharmacol. Exp. Ther 82: 391–398.
Bockman, R.S., Boskey, A.L., Blumenthal, N.C., et al., 1986. Gallium increases bone calcium and crystallite perfection of hydroxyapatite. Calcified Tissue International 39(6): 376–381. DOI: 10.1007/BF02555174.
Böckmann, J., Lahl, H., Eckert, T., et al., 2000. Titan-Blutspiegel vor und nach Belastungsversuchen mit Titandioxid. Pharmazie 55: 140–143.
Bogden, J.D., Higashino, H., Lavenhar, M.A., et al., 1982. Balance and tissue distribution of vanadium after short-term ingestion of vanadate. Journal of Nutrition 112: 2279–2285.
Boisset, M., Girard, F., Godin, J., et al., 1978. Cadmium content of lung, liver, and kidney in rats exposed to cadmium oxide fumes. Int. Arch. Occup. Environ. Health 41: 41–53.
Bornmann, G., Henke, G., Alfes, H., et al., 1970. Uber die Enterlae Resorption von Metallischem Quecksilber. Archiv für Toxikologie: 203–209.
Bradley-Moore, P.R., Lebowitz, E., Greene, M.W., et al., 1975. Thallium-201 for medical use, 2 Biologic behavior. J. Nucl. Med 16: 156–160.
Brandt, J.L., Glaser, W. and Jones, A., 1958. Soft-tissue distribution and plasma disappearance of intravenously administered isotopic magnesium with observations on uptake in bone. Metab. Clin. Exp 7: 355–363.
Breiter, K. and Škoda, R., 2017. Zircon and whole-rock Zr/Hf ratios as markers of the evolution of granitic magmas: Examples from the Teplice caldera (Czech Republic/Germany). Mineralogy and Petrology 111(4): 435–457. DOI: 10.1007/s00710-017-0509-z.
Brihaye, C. and Guillaume, M., 1990. 195Au biokinetics and dosimetry. Eur. J. Nucl. Med 16: 369–371.
Brune, D., Nordberg, G. and Wester, P.O., 1980. Distribution of 23 elements in the kidney, liver and lungs of workers from a smeltery and refinery in North Sweden exposed to a number of elements and of a control group. Sci. Total Environ 16: 13–35.
Bryant, J.R., Berg, H.F. and Christopherson, W.M., 1953. Localization of radioactivity in the lung and the lymph nodes. J. Thorac. Surg 26. Bryant, J.R., Berg, H.F., Christophersen, W.M: 221–232.
Brzoska, M.M. and Moniuszko-Jakoniuk, J., 2001. Interactions between cadmium and zinc in the organism. Food Chem. Toxicol 39: 967–980.
Buchet, J.P., Lauwerys, R. and Roels, H., 1981a. Comparison of the urinary excretion of arsenic metabolites after a single oral dose of sodium arsenite, monomethylarsonate, or dimethylarsinate in man. Int. Arch . Occup. Environ. Health 48: 71–79.
Buchet, J.P., Lauwerys, R. and Roels, H., 1981b. Urinary excretion of inorganic arsenic and its metabolites after repeated ingestion of sodium metaarsenite by volunteers. International Archives of Occupational and Environmental Health 48: 111–118.
Bugryshev, P.F., Moskalev, Y.I. and Nozarova, V.A., 1974. Effect of an isotope carrier (9Be) on the distortion of the 7Be in the organs and tissues of rats. Gig. Sanit 6: 43–47.
Bugryshev, P.F., Zaikina, T.I. and Moskalev, I.I., 1984. Absorption of beryllium from the gastrointestinal tract of rats [Vsasyvanie berilliia iz zheludochno-kishechnogo trakta krysy. Meditsina Truda I Promyshlennaya Ekologiya 6: 52–53.
Burch, G.E., Threefoot, S.A. and Ray, C.T., 1955. The rate of disappearance of Rb-86 from the plasma, the biologic decay rates of Rb-86, and the applicability of Rb-86 as a tracer of potassium in man with and without chronic congestive heart failure. J. Lab. Clin. Med 45: 371–394.
Burk, R.F., 2013. Selenium in man. In: Prasad AS (ed.) Essential and toxic elements: Trace elements in human health and disease. Elsevier, pp. 105–133.

7432 Burkstaller, M.A., Weissman, S.H. and Cuddihy, R.G., 1977. Generation of selenious acid
7433 aerosols. In: Inhalation Toxicology Research Institute Annual Report 1976–1977.
7434 Albuquerque, New Mexico: Lovelace Biomedical and Environmental Research Institute, pp.
7435 285–288.
7436 Burrill, M.W., Freeman, S. and Ivy, A.C., 1945. Sodium potassium and chloride excretion of
7437 human subjects exposed to a simulated altitude of eighteen thousand feet. Journal of
7438 Biological Chemistry 157: 297–302.
7439 Byrne, A.R. and Kosta, L., 1978. Vanadium in foods and in human body fluids and tissues.
7440 Science of the Total Environment 10: 17–30.
7441 Calamosca, M. and Pagano, P., 1991. Nasopharyngeal deposition and retention of an insoluble
7442 aerosol by rats. Radiat. Prot. Dosim 38(1/3): 35–39.
7443 Callis, G.E. and Wentworth, R.A., 1977. Tungsten vs. molybdenum in models for biological
7444 system. Bioinorg. Chem 7: 57–70.
7445 Camner, P., Hellström, P.A. and Lundborg, M., 1973. Coating 5µ particles with carbon and
7446 metals for lung clearance studies. Archives of Environmental Health 27: 331–333.
7447 Camner, P.E., Lundborg, M. and Philipson, M.Sc.K., 1977. Lung clearance of 4-µm particles
7448 coated with silver, carbon, or beryllium. Archives of Environmental Health 32(2): 58–62.
7449 DOI: 10.1080/00039896.1977.10667256.
7450 Campbell, B.J., Reinhold, J.G., Cannell, J.J., et al., 1976. The effects of prolonged consumption
7451 of wholemeal bread upon metabolism of calcium, magnesium, zinc and phosphorus of two
7452 young American adults. Pahlavi Medical Journal 7: 1–17.
7453 Cardin, C.J. and Mason, J., 1976. Molybdate and tungstate transfer by rat ileum competitive
7454 inhibition by sulphate. Biochim. Biophys. Acta 455: 937–946.
7455 Caroli, S., Alimonti, A., Petrucci, F., et al., 2001. Assessment of exposure to platinum-group
7456 metals in urban children. Spectrochim Acta Part B 56: 1241 –1248.
7457 Cartwright, G.E. and Wintrobe, M.M., 1964 Copper Metabolism in Normal Subjects. The
7458 American Journal of Clinical Nutrition 14(4). Oxford Academic: 224–232. DOI:
7459 10.1093/ajcn/14.4.224.
7460 Carvalho, S.M. and Ziemer, P.L., 1982. Distribution and clearance of 63Ni administered in the
7461 rat: intratracheal study. Archives of environmental contamination and toxicology 11: 245–
7462 248.
7463 Castronovo, F.P. and Wagner, H.N., 1971. Factors affecting the toxicity of the element indium.
7464 British Journal of Experimental Pathology 52: 543–559.
7465 Castronovo, Jr. F.P. and Wagner, Jr. H.N., 1973. Comparative toxicity and pharmacodynamics
7466 of ionic indium chloride and hydrated indium oxide. Journal of Nuclear Medicine 14(9):
7467 677–682.
7468 Charkes, N.D., Makler, P.T. and Philips, C., 1978. Studies of skeletal tracer kinetics. I. digital-
7469 computer solution of a five-compartment model of [18F] fluoride kinetics in humans. Journal
7470 of Nuclear Medicine 19: 1301–1309.
7471 Chauncey, D.M., Schelbert, H.R., Halpern, S.E., et al., 1977. Tissue distribution studies with
7472 radioactive manganese: A potential agent for myocardial imaging. J Nucl Med 18: 933–6.
7473 Chen, C.T., Lathrop, K.A., Harper, P.V., et al., 1983. Quantitative measurement of long term
7474 in vivo thallium distribution in the human. J. Nucl. Med 24: 50.
7475 Cherian, M.G., Hursh, J.B., Clarkson, T.W., et al., 1978. Radioactive mercury distribution in
7476 biological fluids and excretion in human subjects after inhalation of mercury vapour. Arch.
7477 Environ. Health 33: 109–114.
7478 Chertok, R.J. and Lake, S., 1971a. Availability in the peccary pig of radionuclides in nuclear
7479 debris from the plowshare excavation buggy. Health Phys 20: 313–316.

7480 Chertok, R.J. and Lake, S., 1971b. Biological availability of radionuclides produced by the
7481 plowshare event schooner I. Body distribution in domestic pigs exposed in the field. Health
7482 Phys 20: 317–324.
7483 Chertok, R.J. and Lake, S., 1971c. Biological availability of radionuclides produced by the
7484 plowshare event schooner-II. Retention and excretion rates in peccaries after a single oral
7485 dose of debris. Health Physics 20: 325–330.
7486 Chertok, R.J. and Lake, S., 1971d. Biological availability of radionuclides produced by the
7487 plowshare event schooner-III. Accumulation, excretion rates and body distribution in
7488 peccaries after daily ingestion of debris. Health Physics 20: 577–584.
7489 Cheryan, M., 1980. Phytic acid interactions in food systems. Critical Reviews in Food Science
7490 and Nutrition 13: 297–335.
7491 Chiba, M., Shinohara, A. and Ujiie, C., 1991. Tin concentrations in various organs in humans,
7492 dogs, and mice. Biomed. Trace Element Res 2: 257–258.
7493 Chou, T. and Adolph, W.H., 1935. Copper metabolism in man. Biochem J 29: 476–479.
7494 Christensen, J.M., Holst, E., Bonde, J.P., et al., 1993. Determination of Chromium in Blood and
7495 Serum: Evaluation of Quality Control Procedures and Estimation of Reference Values in
7496 Danish Subjects. Science of the Total Environment 132(1): 11–25.
7497 Christensen, O.B. and Lagesson, V., 1981. Nickel concentration of blood and urine after oral
7498 administration.Ann. Clinical Laboratory Science 11: 119–125.
7499 Christensen, O.B., Moller, H., Andrasko, L., et al., 1979. Nickel concentration of blood, urine
7500 - and sweat after oral administration. Contact Dermatitis 5: 312–316.
7501 Christie, H., MacKay, R.J. and Fisher, A.M., 1963. Pulmonary effects of inhalation of
7502 aluminium by rats and hamsters. Am. Ind. Hyg. J 24: 47–56.
7503 Cima, F., 2011. Tin: Environmental pollution and health effects. In: Nriagu JO (ed.)
7504 Encylopedia of Environmental Health. London: Elsevier, pp. 351–359.
7505 Clarkson, T. and Rothstein, A., 1964. The excretion of volatile mercury by rats injected with
7506 mercuric salts. Health Phys 10: 1115–1121.
7507 Clarkson, T.W., 1997. The toxicology of mercury. Critical Rev. Clin. Lab. Sci 34: 369–403.
7508 Clary, J.J., 1975. Nickel chloride-induced metabolic changes in the rat and guinea-pig.
7509 Toxicology and Applied Pharmacology 31: 55–65.
7510 Coates, G., Gilday, D.L., Cradduck, T.D., et al., 1973. Measurement of the rate of stomach
7511 emptying using Indium-113m and a 10-crystal rectilinear scanner. Canadian Medical
7512 Association Journal 108: 180–183.
7513 Cobb, L.M., Harrison, A. and Butler, S.A., 1988. Toxicity of 211At in the mouse. Human
7514 Toxicol 7: 529–534.
7515 Cochran, K.W., Doull, J., Mazur, M., et al., 1950. Acute toxicity of zirconium, columbium,
7516 strontium, lanthanum, cesium, tantalum and yttrium. Archives of Industrial Hygiene and
7517 Occupational Medicine 1(6): 637–50.
7518 Colombo, C., Monhemius, A.J. and Plant, J.A., 2008. The estimation of the bioavailabilities of
7519 platinum, palladium and rhodium in vehicle exhaust catalysts and road dusts using a
7520 physiologically based extraction test. Science of the Total Environment 389(1): 46–51.
7521 Conklin, A.W., Skinner, S.C., Felten, T.L., et al., 1982. Clearance and distribution of
7522 intratracheally instilled vanadium-48 compounds in the rat. Toxicology Letters 11: 199–203.
7523 Cooper, J.R., 1985. The influence of speciation on the gastrointestinal absorption of elements.
7524 In: Bulman RA and Cooper JR (eds) Speciation of Fission and Activation Products in the
7525 Environment. London: Elsevier, pp. 162–174.
7526 Corsa, L., Olney, J.M., Steenburg, R.W., et al., 1950. The measurement of exchangeable
7527 potassium in man by isotope dilution. J. Clin. Invest 29: 1280–1295.

7528 Costeas, R., Woodard, H.Q. and Laughlin, J.S., 1970. Depletion of 18F from blood flowing
7529 through bone. Journal of Nuclear Medicine 11: 43–45.
7530 Cotzias, G.C., Borg, D.C. and Selleck, B., 1961. Virtual absence of turnover in cadmium
7531 metabolism: 109Cd studies in the mouse. Am. J. Physiol 201: 927–930.
7532 Coudray, C., Rambeau, M., Feillet-Coudray, C., et al., 2005. Study of magnesium
7533 bioavailability from ten organic and inorganic Mg salts in Mg-depleted rats using a stable
7534 isotope approach. Magnesium Research 18(4): 215–223.
7535 Crecelius, E.A., 1977. Changes in the chemical speciation of arsenic following ingestion by
7536 man. Environmental Health Perspectives 19: 147–150.
7537 Cromwell, G.L., 1997. Copper as a nutrient for animals. In: Richardson HW (ed.) Handbook of
7538 Copper Compounds and Applications. New York: Marcel Dekker, pp. 177–202.
7539 Curran, G.L. and Costello, R.L., 1956. Reduction of excess cholesterol in the rabbit aorta by
7540 inhibition of endogenous cholesterol synthesis. Journal of Experimental Medicine 103: 49–
7541 56.
7542 Curran, G.L., Azarnoff, D.L. and Bolinger, R.E., 1959. Effect of cholesterol synthesis inhibition
7543 in normocholesteremic young men. Journal of Clinical Investigation 38: 1251–1261.
7544 Dadachova, E., Bouzahzah, B., Zuckier, L.S., et al., 2002. Rhenium-188 as an alternative to
7545 iodine-131 for treatment of breast tumors expressing the sodium/iodide symporter (NIS.
7546 Nuclear Medicine and Biology 29: 13–18.
7547 Dainty, J.R., 2001. Use of stable isotopes and mathematical modelling to investigate human
7548 mineral metabolism. Nutrition Research Reviews 14: 295–315.
7549 Danish Environmental Protection Agency (DEPA), 2008. Nickel and Nickel Compounds -
7550 Background Document in Support of Individual Risk Assessment Reports of Nickel
7551 Compounds.
7552 Dastur, D.K., Manghani, D.K., Raghavendran, K.V., et al., 1969. Distribution and fate of 54Mn
7553 in the rat, with special reference to the CNS. Q J Exp Physiol 54: 322–31.
7554 Dastur, D.K., Manghani, D.K. and Raghavendran, K.V., 1971. Distribution and fate of 54Mn
7555 in the monkey: Studies of different parts of the central nervous system and other organs. J
7556 Clin Invest 50: 9–20.
7557 Datz, F. and Taylor, A., 1985. The clinical use of radionuclide bone marrow imaging. Seminars
7558 in Nuclear Medicine XV(3).
7559 Davidsson, L., Cederblad, Å., Lönnerdal, B., et al., 1989. Manganese retention in man: a
7560 method for estimating manganese absorption in man. The American Journal of Clinical
7561 Nutrition 49(1). Oxford Academic: 170–179. DOI: 10.1093/ajcn/49.1.170.
7562 Demigné, C., Sabboh, H., Rémésy, C., et al., 2004. Protective effects of high dietary potassium:
7563 Nutritional and metabolic aspects. Journal of Nutrition 134: 2903–2906.
7564 Deutsch, E., Libson, K., Vanderheyden, J.L., et al., 1986. The chemistry of rhenium and
7565 technetium as related to the use of isotopes of these elements in therapeutic and diagnostic
7566 nuclear medicine. Int. J. Rad. Appl. Instrum. B 13: 465–477.
7567 DeVoto, E. and Yokel, R.A., 1994. The biological speciation and toxicokinetics of aluminum.
7568 Environ. Health Prespect 102: 940–951.
7569 Dimond, E.G., Caravaca, J. and Benchimol, A., 1963. Vanadium: Excretion, toxicity, lipid
7570 effect in man. Am J Clin Nutr 12: 49–53.
7571 Doisy, R.J., Streeten, D.H.P., Souma, M.L., et al., 1971. Metabolism of 51Chromium in Human
7572 Subjects / Normal, Elderly, and Diabetic Subjects. In: Newer Trace Elements in Nutrition,
7573 pp. 155–168.
7574 Dorman, D.C., Struve, M.F. and Wong, B.A., 2001. Factors that influence manganese delivery
7575 to the brain. Centers for Health Research. CIIT Activities 21(7–8).

7576 Dorman, D.C., Struve, M.F., Marshall, M.W., et al., 2006. Tissue manganese concentrations in
7577 young male rhesus monkeys following subchronic manganese sulfate inhalation.
7578 Toxicological Sciences 92: 201–10.
7579 Doull, J. and Dubois, K.P., 1949. Metabolism and toxicity of radioactive tantalum, Part 2. In:
7580 Quarterly Progress Report Number Two. University of Chicago Toxicity Laboratory, p. 12.
7581 Downey, H.F. and Bashour, F.A., 1975. Dynamics of tissue distribution of radiopotassium as
7582 affected by simulated differences in regional extraction. Cardiovasc. Res 9: 607–612.
7583 Drake, P.L. and Hazelwood, K.J., 2005. Exposure-related health effects of silver and silver
7584 compounds: A review. Annals of Occupational Hygiene 49: 575–585.
7585 Drasch, G., Muss, C. and Roider, G., 2000. Gold and palladium burden from dental restoration
7586 materials. Journal of Trace Elements in Medicine and Biology 14(2): 71–75.
7587 Ducoff, H.S., Neal, W.B., Straube, R.L., et al., 1948. Biological Studies with Arsenic76 II.
7588 Excretion and Tissue Localization. Proceedings of the Society for Experimental Biology and
7589 Medicine 69(3). SAGE Publications Sage UK: London, England: 548–554.
7590 Ducoulombier-Crépineau, C., Feidt, C. and Rychen, G., 2007. Platinum and palladium transfer
7591 to milk, organs and tissues after a single oral administration to lactating goats. Chemosphere
7592 68: 712–715.
7593 Dudley, H.C. and Levine, M.D., 1949. Studies of the toxic action of gallium. Journal of
7594 Pharmacology and Experimental Therapeutics 95: 487–493.
7595 Dunn, M.A., Green, M.H. and Leach, R.M., 1991. Kinetics of copper metabolism in rats: a
7596 compartmental model. Am. J. Physiol 261:E115-E125.
7597 Durbin, P.W., 1959. Metabolic characteristics within a chemical family. Health Physics 2(3):
7598 225–238. DOI: 10.1097/00004032-195907000-00001.
7599 Durbin, P.W., Scott, K.G. and Hamilton, J.G., 1957. The distribution of radioisotopes of some
7600 heavy metals in the rat. University of California publications in Pharmacology 3(1). Univ.
7601 Calif. Pub. Pharmacol: 1–34.
7602 Edvardsson, K.A., 1971. Case studies of elimination of radioactive contaminants observed at
7603 Studsvik between 1963 and 1970. In: Assessment of Radioactive Contamination in Man.
7604 Proc. Symp. Stockholm 22-26 November 1971, Stockholm, IAEA Vienna, 1971.
7605 Ekman, L., Figueiras, H.D., Jones, B.E.V., et al., 1977. Metabolism of 181W-labelled sodium
7606 tungstate in goats. FOA-C-40070. Sundbyberg, Sweden: Foersvarets Forskningsanstalt.
7607 Elakhovskaya, N.P., 1972. Metabolism of nickel entering the body with drinking water. Gigiena
7608 i Sanitarija 37(6): 20–22.
7609 Elgrabli, D., Beaudouin, R., Jbilou, N., et al., 2015. Biodistribution and clearance of TiO2
7610 nanoparticles in rats after intravenous injection. PLOS One: 13. DOI:
7611 10.1371/journal.pone.0124490.
7612 Elin, R.J., 1987. Assessment of magnesium status. Clinical chemistry 33(11): 1965–1970.
7613 Elinder, C.G., Kjellström, T., Friberg, L., et al., 1976. Cadmium in kidney cortex, liver and
7614 pancreas, from Swedish autopsies. Arch. Environ. Health 31: 292–302.
7615 Elinder, C.G., Friberg, L., Lind, B., et al., 1983. Lead and cadmium levels in blood samples
7616 from the general population Sweden. Environ. Res 30: 233–253.
7617 Elinder, C.G., Ahrengart, L., Lidums, V., et al., 1991. Evidence of aluminium accumulation in
7618 aluminium welders. Br J Ind Med 48: 735–738. DOI: 10.1136/oem.48.11.735.
7619 El-Masri, H.A. and Kenyon, E.M., 2008. Development of a human physiologically based
7620 pharmacokinetic (PBPK) model for inorganic arsenic and its mono- and di-methylated
7621 metabolites. Journal of Pharmacokinetics and Pharmacodynamics 35(1): 31–68. DOI:
7622 10.1007/s10928-007-9075-z.
7623 Emery, E.W., Holmes, R., Davies, H.E., et al., 1955. Renal uptake of radioactive potassium.
7624 Clin. Sci 14: 241–244.

English, J.C., Parker, R.D.R. and Shama, R.P., 1981. Toxicokinetics of nickel in rats after intratracheal administration of a soluble and insoluble form. American Industrial Hygiene Association Journal 42: 486–492.

Ensslin, A.S., Huber, R., Pethran, A., et al., 1997. Biological monitoring of hospital pharmacy personnel occupationally exposed to cytostatic drugs: urinary excretion and cytogenetics studies. International Archives of Occupational and Environmental Health 70: 205 –208.

Erck, A., Sherwood, E., Bear, J.L., et al., 1976. The metabolism of rhodium(II) acetate in tumor-bearing mice. Cancer Res 36: 2204–2209.

EFSA, 2009. Scientific Opinion of the Panel on Food Additives and Nutrient Sources added to Food on choline-stabilised orthosilicic acid added for nutritional purposes to food supplements following a request from the European Commission. EFSA Journal 948: 1–23.

EFSA, 2011 On the evaluation of a new study related to the bioavailability of aluminium in food. EFSA Journal 9(5): 2157.

EFSA, 2012. Scientific Opinion on the risk for public health related to the presence of mercury and methylmercury in food. EFSA Journal 10(12): 2985. DOI: 10.2903/j.efsa.2012.2985.

EFSA, 2013. Scientific Opinion on Dietary Reference Values for manganese. EFSA Journal 11(11): 3419. DOI: 10.2903/j.efsa.2013.3419.

EFSA, 2014. Scientific Opinion on the risks to public health related to the presence of chromium in food and drinking water. EFSA Journal 12(3): 3595.

EFSA, 2015a. Scientific Opinion on Dietary Reference Values for copper. EFSA Journal 13(10): 4253.

EFSA, 2015b. Scientific Opinion on Dietary Reference Values for magnesium. EFSA Journal 13(7): 4186. DOI: doi:10.2903/j.efsa.2015.4186.

EFSA, 2015c. Scientific Opinion on risks for public health related to the presence of chlorate in food. EFSA Journal 13(6): 4135. DOI: 10.2903/j.efsa.2015.4186.

EFSA, 2016. Scientific Opinion on the re-evaluation of titanium dioxide (E 171) as a food additive. EFSA Journal 14(9): 4253.

EFSA, 2018a. Scientific opinion on the re-evaluation of calcium silicate. EFSA Journal 16(8): 5375.

EFSA, 2018b. Scientific Opinion on the re-evaluation of silicon dioxide (E 551) as a food additive. EFSA Journal 16(1): 5088.

Fabian, E., Landsiedel, R., Ma-Hock, L., et al., 2008. Tissue distribution and toxicity of intravenously administered titanium dioxide nanoparticles in rats. Archives of Toxicology 82: 151–157.

Falk, R. and Lindhe, J.C., 1975. Radiation dose received by humans from intravenously administered sodium selenite marked with selenium-75. 31(12): 3360.

Farrar, G., Morton, A.P. and Blair, J.A., 1987. The intestinal absorption and tissue distribution of aluminium, gallium and scandium: a comparative study. Biochemical Society Transactions 15(6): 1164–1165.

Finch, G.L., Mewhinney, J.A., Hoover, M.D., et al., 1990. Clearance, translocation, and excretion of beryllium following acute inhalation of beryllium oxide by beagle dogs. Fundamental and Applied Toxicology 15(2): 231–241. DOI: 10.1016/0272-0590(90)90050-T.

Finley, J.W., 1998. The absorption and tissue distribution of selenium from high-selenium broccoli are different from selenium from sodium selenite, sodium selanate, and selenomethionine as determined in selenium-deficient rats. Journal of Agricultural and Food Chemistry 46: 3702–3707.

Finley, J.W., 1999. Manganese absorption and retention by young women is associated with serum ferritin concentration. Am J Clin Nutr 70: 37–43.

Finley, J.W., Johnson, P.E. and Johnson, L.K., 1994. Sex affects manganese absorption and retention by humans from a diet adequate in manganese. Am J Clin Nutr 60: 949–55.

Firoz, M. and Graber, M., 2001. Bioavailability of US commercial magnesium preparations. Magnesium Research 14: 257–62.

Fleshman, D., Krotz, S. and Silva, A., 1966. The metabolism of elements of high atomic number. UCRL 14739: 69–86.

Fleshman, D.G., Silva, A.J. and Shore, B., 1971. The metabolism of tantalum in the rat. Health Physics 21: 385–392.

Food and Agriculture Organization of the United Nations, World Health Organization, FAO Panel of Experts on Pesticide Residues in Food and the EnvironmentEnvironment, et al., 1989. Bromide ion. In: Pesticide Residues in Food : 1988 [Evaluations], Sponsored Jointly by FAO and WHO with the Support of the International Programme on Chemical Safety (IPCS, Joint Meeting of the FAO Panel of Experts on Pesticide Residues in Food and the Environment and the WHO Expert Group on Pesticide Residues, Geneva, 19-28 September 1988. Part 2., Toxicology. Rome: Food and Agriculture Organization of the United Nations. Available at: https://apps.who.int/iris/handle/10665/38225.

Forbes, G.B. and McCoord, A., 1969. Long-term behavior of radiosodium in bone: comparison with radiocalcium and effects of various procedures. Calc. Tiss. Res 4: 113–128.

Foulkes, E.C. and McMullen, D.M., 1986. On the mechanism of nickel absorption in the rat jejunum. Toxicology 38(1): 35–42. DOI: 10.1016/0300-483x(86)90170-8.

Freed, B.R., Woodard, H.Q. and Laughlin, J.S., 1975. Kinetics of 47Sc generated by decay of 47Ca in vivo. Health Physics 29: 90.

Freyberg, R.H., Block, W.D. and Levey, S., 1942. Metabolism, toxicity and manner of action of gold compounds used in the treatment of arthritis. III. Complete excretion studies and comparison of intravenous and intramuscular administration of some gold salts. Ann. Rheum. Dis 3: 77–89.

Friberg, L., 1984. Cadmium and the kidney. Environ. Health Persp 54: 1–11.

Friberg, L., Piscator, M., Nordberg, G.F., et al., 1974. Cadmium in the Environment. 2nd ed. Boca Raton, Fla: CRC Press.

Fritsch, P., de Saint Blanquat, G. and Derache, R., 1977. Effect of various dietary components on absorption and tissue distribution of orally administered inorganic tin in rats. Food and Cosmetics Toxicology 15: 147–149.

Froment, D.H., Buddington, B., Miller, N.L., et al., 1989. Effect of solubility on the gastrointestinal absorption of aluminum from various aluminum compounds in the rat. Journal of Laboratory and Clinical Medicine 114: 237–242.

Frost, D.V. and Lish, P.M., 1975. Selenium in biology. Annual Review of Pharmacology 15: 259–284.

Fukayama, M.Y., Tan, H., Wheeler, W.B., et al., 1986. Reactions of aqueous chlorine and chlorine dioxide with model food compounds. Environmental Health Perspectives 69: 267–274.

Furchner, J.E. and Drake, G.A., 1976. Comparative metabolism of radionuclides in mammals – XI. Retention of 113Sn in the mouse, rat, monkey and dog. Health Phys 31: 219–224.

Furchner, J.E., Richmond, C.R. and Drake, G.A., 1966. Comparative metabolism of radionuclides in mammals – III. Retention of manganese-54 in the mouse, rat, monkey and dog. Health Phys 12: 1415–23.

Furchner, J.E., Richmond, C.R. and Drake, G.A., 1968. Comparative Metabolism of Radionuclides in Mammals – IV. Retention of silver-110m in the mouse, rat, monkey and dog. Health Physics 15: 505–514.

7722 Furchner, J.E., Richmond, C.R. and Drake, G.A., 1971. Comparative metabolism of
7723 radionuclides in mammals—V. Retention of 192Ir in the mouse, rat, monkey and dog. Health
7724 Physics 20: 375–382.
7725 Furchner, J.E., Richmond, C.R. and London, J.E., 1973. Comparative metabolism of
7726 radionuclides in mammals. VIII Retention of beryllium in the mouse, rat, monkey and dog.
7727 Health Phys 24: 293–300.
7728 Furchner, J.E., London, J.E. and Wilson, J.S., 1975. Comparative metabolism of radionuclides
7729 in mammals-IX. Retention of 7SSe in the mouse, rat, monkey and dog. Health Physics 29:
7730 641–648.
7731 Gabler, W.L., 1968. Absorption of fluoride through the oral mucosa of rats. Archives of Oral
7732 Biology 13: 619–623.
7733 Garcia, F., Ortega, A., Domingo, J.L., et al., 2001. Accumulation of metals in autopsy tissues
7734 of subjects living in Tarragona Country, Spain. J. Environ. Sci. Health A 36: 1767–1786.
7735 Garg, P.K., Harrison, C.L. and Zalutsky, M.R., 1990. Comparative tissue distributio in mice of
7736 the α-emitter 211At and 131I as labels of monoclonal antibody and F(ab')2 fragment. Cancer
7737 Res 50: 3514–3520.
7738 Gehring, P.J. and Hammond, P.B., 1967. The interrelationship between thallium and potassium
7739 in animals. J. Pharmacol. Exp. Ther 155: 187–201.
7740 Geraets, L., Oomen, A., Krystek, P., et al., 2014. Tissue distribution and elimination after oral
7741 and intravenous administration of different titanium dioxide nanoparticles in rats. Particle
7742 and Fibre Toxicology 11: 30.
7743 Gettler, A.O. and Weiss, L., 1943. Thallium poisoning III. Clinical toxicology of thallium.
7744 Amer. J. Clin. Pathol 13: 422–429.
7745 Gillespie, P.A., Kang, G.S., Elder, A., et al., 2010. Pulmonary response after exposure to
7746 inhaled nickel hydroxide nanoparticles: short and long-term studies in mice. Nanotoxicology
7747 4(1): 106–119. DOI: 10.3109/17435390903470101.
7748 Ginsburg, J.M., 1962. Equilibration of potassium in blood and tissues. Digest. Dis. Sci 7: 34–
7749 42.
7750 Ginsburg, J.M. and Wilde, W.S., 1954. Distribution kinetics of intravenous radiopotassium.
7751 Am. J. Physiol 179: 63–75.
7752 Gitelman, H.J., 1995. Aluminum exposure and excretion. Sci Total Environ 163: 129–135.
7753 Gitelman, H.J., Alderman, F.R., Kurs-Lasky, M., et al., 1995. Serum and urinary aluminium
7754 levels of workers in the aluminium industry. Ann Occup Hyg 39: 181–191.
7755 Glaser, U., Kloppel, H. and Hochrainer, D., 1986. Bioavailability indicators of inhaled
7756 cadmium compounds. Ecotoxicol. Environ. Saf 11: 261–271.
7757 Golasik, M., Wrobel, P., Olbert M., et al., 2016a. Does titanium in ionic form display a tissue-
7758 specific distribution? BioMetals 29: 487–494.
7759 Golasik, M., Herman, M., Olbert, M., et al., 2016b. Toxicokinetics and tissue distribution of
7760 titanium in ionic form after intravenous and oral administration. Toxicology Letters 24: 56–
7761 61.
7762 Gongora, G., Roy, M., Gongora, R., et al., 1973. Méthode utilisée pour l'etude de la réparation
7763 de l'épuration pulmonaire chez l'homme normal, après administration d'aérosols radioactifs.
7764 J. Biol. Med. Nucl 102: 19–26.
7765 Gongora, G., Roy, M., Gongora, R., et al., 1974. Techniques de mesure à long terme de
7766 l'épuration pulmonaire chez l'homme et premiers résultats. In: Réactions
7767 bronchopulmonaires aux polluants atmosphériques: compte rendu du colloque tenu les 18 et
7768 19 janvier 1974 à Pont-à-Mousson Paris. Editions INSERM (Institut National de la Santé et
7769 de la Recherche Medicale, pp. 183–192.

7770 Goodman, J.E., Prueitt, R.L., Thakali, S., et al., 2011. The nickel ion bioavailability model of
7771 the carcinogenic potential of nickel-containing substances in the lung. Critical Reviews in
7772 Toxicology 41(2): 142–174. DOI: 10.3109/10408444.2010.531460.
7773 Goodwin, D.A., Goode, R. and Brown, L., 1971. 111-In-labeled transferrin for the detection of
7774 tumors. Radiology 100: 175–179.
7775 Gottlieb, N.L., 1983. Comparison of the kinetics of parenteral and oral gold. Scandinavian
7776 Journal of Rheumatology 12(S51): 10–14.
7777 Graham, L.A., Veatch, R.L. and Kaplan, E., 1971. Distribution of 75Se-selenomethionine as
7778 influenced by the route of administration. Journal of Nuclear Medicine 12: 566–569.
7779 Greger, J.L., 1993. Aluminium metabolism. Annu. Rev. Nutr 13: 43–63.
7780 Gregus, Z. and Klaassen, C.D., 1986. Disposition of metals in rats: A comparative study of
7781 faecal, urinary, and biliary excretion and tissue distribution of eighteen metals. Toxicol. Appl.
7782 Pharmacol 85: 24–38.
7783 Griffiths, N., Stewart, R. and Robinson, M., 1976. The metabolism of seienomethionine in four
7784 women. British Journal of Nutrition 35: 373–383.
7785 Hadley, J.G., Conklin, A.W. and Sanders, C.L., 1980. Rapid solubilization and translocation of
7786 109CdO following pulmonary deposition. Toxicology and Applied Pharmacology 54(1):
7787 156–160.
7788 Hahn, P.F., Rouser, G., Brummitt, H., et al., 1952. The drainage of radioactive silver colloids
7789 by the lymphatics following intrapulmonary administration in dogs. The Journal of
7790 laboratory and clinical medicine 39(4): 624–628.
7791 Hall, L.L., Kilpper, R.W., Smith, F.A., et al., 1977. Kinetic model of fluoride metabolism in
7792 the rabbit. Environmental Research 14: 285–302.
7793 Hambidge, K.M. and Baum, J.D., 1972. Hair Chromium Concentrations of Human Newborn
7794 and Changes During Infancy. The American Journal of Clinical Nutrition 25(4): 376–379.
7795 Hamilton, E.I., Minski, M.J. and Cleary, J.J., 1973. The concentration and distribution of some
7796 stable elements in healthy human tissues from the United Kingdom. An environmental study.
7797 Sci.Total Environ 1: 341–374.
7798 Hamilton, J.G. and Soley, M.H., 1940. A comparison of the metabolism of iodine and of
7799 element 85 (Eka-iodine. Proc 26: 483–489.
7800 Hamilton, J.G., Asling, C.W., Garrison, W.M., et al., 1953. The accumulation, metabolism and
7801 biological effects of astatine in rats and monkeys. University of California Publications in
7802 Pharmacology 2: 283–343.
7803 Hamilton, J.G., Durbin, P.W. and Parrott, M.W., 1954a. Accumulation of 211Astatine by
7804 thyroid gland in man. Exptl. Biol. Med 86: 366–369.
7805 Hamilton, J.G., Durbin, P.W. and Parrott, M.L., 1954b. The accumulation and destructive
7806 action of astatine-211 (eka-iodine) in the thyroid gland of rats and monkeys. J. Clin.
7807 Endocrin. Metab 14: 1161–1178.
7808 Han, S.G., Lee, J.S., Ahn, K., et al., 2015. Size-dependent clearance of gold nanoparticles from
7809 lungs of Sprague–Dawley rats after short-term inhalation exposure. Archives of Toxicology
7810 89(7): 1083–1094.
7811 Hansen, T.V., Aaseth, J. and Alexander, J., 1982. The effect of chelating agents on vanadium
7812 distribution in the rat body and on uptake by human erythrocytes. Archives of Toxicology
7813 50: 195–202.
7814 Hanson, S.R., Donley, S.A. and Linder, M.C., 2001. Transport of silver in virgin and lactating
7815 rats and relation to copper. Journal of Trace Elements in Medicine and Biology 15: 243–253.
7816 Hara, T. and Freed, B.R., 1973. Preparation of carrier-free 47Sc by chemical separation from
7817 47Ca and its distribution in tumor bearing mice. International Journal of Applied Radiation
7818 and Isotopes 24: 373–376.

7819 Haram, E.M., Weberg, R. and Berstad, A., 1987. Urinary excretion of aluminum after ingestion
7820 of sucralfate and an aluminum-containing antacid in man. Scandinavian Journal of
7821 Gastroenterology 22: 615–618.
7822 Harrison, A. and Royle, L., 1984. Determination of absorbed dose to blood, kidneys, testes and
7823 thyroid in mice injected with 211At and comparison of testes mass and sperm number in X-
7824 irradiated and 211At treated mice. Health Phys 46: 377–383.
7825 Harrison, H.E., Buting, H., Ordway, N.K., et al., 1947. The Effects and Treatment of Inhalation
7826 of Cadmium Chloride in the Dog. J. Ind. Hyg. Toxicol 29(5): 302–314.
7827 Harrison, H.N., 1979. Pharmacology of sulfadiazine silver. Its attachment to burned human and
7828 rat skin and studies of gastrointestinal absorption and extension. Archives of Surgery 114:
7829 281–285.
7830 Hart, E.B., Steenbock, J., Waddell, J., et al., 1928. Iron in Nutrition. VII. Copper as a
7831 supplement to iron for hemoglobin building in the rat. The Journal of Biological Chemistry
7832 77: 797-812.
7833 Hawkes, W.C., Alkan, F.Z. and Oehler, L., 2003. Absorption, distribution and excretion of
7834 selenium from beef and rice in healthy North American man. Journal of Nutrition 133: 3434–
7835 3442.
7836 Hawkins, R.A., Sung-Cheng Huang, Y.C., Hoh, C.K., et al., 1992. Evaluation of the skeletal
7837 kinetics of fluorine-18-fluoride ion with PET. Journal of Nuclear Medicine 33: 633–642.
7838 Hayes, A.D. and Rothstein, A., 1962. The metabolism of inhaled mercury vapour in the rat
7839 studied by isotope techniques. J. Pharmacol 38: 1–10.
7840 Heck, J.D. and Costa, M., 1982. Surface reduction of amorphous NiS particles potentiates their
7841 phagocytosis and subsequent induction of morphological transformation in Syrian hamster
7842 embryo cells. Cancer Letters 15: 19–26.
7843 Heisler Weissman, S. and Cuddihy, R.G., 1979. Retention and tissue distribution of inhaled
7844 selenious acid and elemental selenium in beagle dogs. In: Inhalation Toxicology Research
7845 Institute Annual Report 1978–1979. Albuquerque, New Mexico: Lovelace Biomedical and
7846 Environmental Research Institute, pp. 436–441.
7847 Henderson, R.F., Reba, A.H. and Pickrell, J.A., 1979. Early damage indicators in the lung. III.
7848 Biochemical and cytological response of the lung to inhaled metal salts. Toxicol. Appl.
7849 Pharmacol 50: 123–136.
7850 Higgins, E.S., Richert, D.A. and Westerfeld, W.W., 1956. Molybdenum deficiency and
7851 tungstate inhibition studies. The Journal of nutrition 59(4): 539–559.
7852 Hiles, R.A., 1974. Absorption, distribution and excretion of inorganic tin in rats. Toxicology
7853 and Applied Pharmacology 27: 366–379.
7854 Hill, C.H., 1980. Interactions of vitamin C with lead and mercury. Annals of the New York
7855 Academy of Sciences 355: 262–266.
7856 Hiller, M.M. and Leggett, R.W., 2020. A biokinetic model for trivalent or hexavalent chromium
7857 in adult humans. J. Radiol. Prot 40: 19–39.
7858 Hinderling, P.H., 2016. The pharmacokinetics of potassium in humans is unusual. J. Clin.
7859 Pharamcol 56: 1212–1220.
7860 Hindsen, M., Christensen, O.B., Möller, H., 1994. Nickel levels in serum and urine in five
7861 different groups of eczema patients following oral ingestion of nickel. Acta Dermato-
7862 Venereologica 74: 176–178.
7863 Hirano, S., Shimada, T., Osugi, J., et al., 1994. Pulmonary clearance and inflammatory potency
7864 of intratracheally instilled or acutely inhaled nickel sulfate in rats. Archives of Toxicology
7865 68(9): 548–554. DOI: 10.1007/s002040050112.

7866 Hirunuma, R., Endo, K., Yanaga, M., et al., 1997. The use of a multitracer technique for the
7867 studies of the uptake and retention of trace elements in rats. Applied Radiation and Isotopes
7868 48: 727–733.
7869 Hirunuma, R., Endo, K., Enomoto, S., et al., 1999. Study on the distribution of radioactive trace
7870 elements in vitamin D-overloaded rats using the multitracer technique. Applied Radiation
7871 and Isotopes 50: 843–849.
7872 Ho, W. and Furst, A., 1973. Nickel excretion by rats following a single treatment. Proceedings
7873 of the Western Pharmacology Society 16: 245–248.
7874 Hochrainer, D., Oberdoerster, G. and Mihm, U., 1980. Generation of NiO aerosols for studying
7875 lung clearance of Ni and its effect on lung function. In: Aerosols in Science, Medicine and
7876 Technology - Physical and Chemical Properties of Aerosols. Proc. GAeF 8 Conference. (eds
7877 W Stöber and D Hochrainer), 1980, pp. 259–264. Gesellschaft für Aerosolforschung.
7878 Hohl, C., Gerisch, P., Korschinek, G., et al., 1994. Medical application of 26Al. Nucl Instr Meth
7879 Phys Res B 92: 478–482.
7880 Holbrook, D.J.Jr., Washington, M.E., Leake, H.B., et al., 1975. Studies on the evaluation of the
7881 toxicity of various salts of lead, manganese, platinum, and palladium. Environmental Health
7882 Perspectives 10: 95–101.
7883 Hopkins, Jr. L.L., 1965. Distribution in the Rat of Physiological Amounts of Injected Cr51(III)
7884 with time. American Journal of Physiology 209(4): 731–735.
7885 Horak, E. and Sunderman, F.W. Jr., 1973. Fecal nickel excretion by healthy adults. Clinical
7886 Chemistry 19: 429–430.
7887 Hughes, M.F., 2002. Arsenic toxicity and potential mechanisms of action. Toxicol. Lett 133:
7888 1–16.
7889 Hursh, J.B., Clarkson, T.W., Cherian, M.G., et al., 1976. Clearance of mercury (Hg - 197, Hg-
7890 203) vapour inhaled by human subjects. Arch. Environ. Health 31: 302–309.
7891 Hursh, J.B., Greenwood, M.R., Clarkson, T.W., et al., 1980. The effect of ethanol on the fate
7892 of mercury vapour inhaled by man. J. Pharmacol. Exp. Ther 214: 520–527.
7893 ICRP, 1975. Report of the Task Group on Reference Man. ICRP Publication 23. Oxford:
7894 Pergamon Press.
7895 ICRP, 1979a. Limits for intakes of radionuclides by workers, ICRP Publication 30, Part 1.
7896 Annals of the ICRP 2(3/4).
7897 ICRP, 1979b. Limits for intakes of radionuclides by workers, ICRP Publication 30, Supplement
7898 to Part 1. Annals of the ICRP 3(1–4).
7899 ICRP, 1980. Limits for intakes of radionuclides by workers. ICRP Publication 30, Part 2.
7900 Annals of the ICRP 4(3/4).
7901 ICRP, 1981. Limits for intakes of radionuclides by workers. ICRP Publication 30, Part 3.
7902 Annals of the ICRP 6(2/3). Ann.
7903 ICRP, 1988. Limits for intakes of radionuclides by workers: an addendum. ICRP Publication
7904 30, Part 4. Annals of the ICRP 19(4). Ann.
7905 ICRP, 1989. Individual Monitoring for Intakes of Radionuclides by Workers. ICRP Publication
7906 54. Annals of the ICRP 19(1–3).
7907 ICRP, 1993. Age dependent doses to members of the public from intake of radionuclides: Part
7908 2, Ingestion dose coefficients. ICRP Publication 67. Annals of the ICRP 23(3/4).
7909 ICRP, 1994a. Dose coefficients for intake of radionuclides by workers. ICRP Publication 68.
7910 Annals of the ICRP 24(4).
7911 ICRP, 1994b. Human respiratory tract model for radiological protection. ICRP Publication 66.
7912 Annals of the ICRP 24(1–3).
7913 ICRP, 1995a. Age-dependent Doses to Members of the Public from Intake of Radionuclides:
7914 Part 3. Ingestion Dose Coefficients, ICRP Publication 69. Annals of the ICRP 25(1).

7915 ICRP, 1995b. Age-dependent Doses to Members of the Public from Intake of Radionuclides:
7916 Part 4. Inhalation Dose Coefficients, ICRP Publication 71. Annals of the ICRP 25(3/4).
7917 ICRP, 1997. Individual monitoring for internal exposure of workers. ICRP Publication 78.
7918 Annals of the ICRP 27(3/4).
7919 ICRP, 2002a. Basic anatomical and physiological data for use in radiological protection:
7920 reference values. ICRP Publication 89. Annals of the ICRP 32(3–4).
7921 ICRP, 2002b. Guide for the practical application of the ICRP Human Respiratory Tract Model.
7922 Supporting Guidance 3. Annals of the ICRP 32(1/2).
7923 ICRP, 2006. Human alimentary tract model for radiological protection. ICRP Publication 100.
7924 Annals of the ICRP 36(1–2). Oxford: Pergamon Press.
7925 ICRP, 2007. The 2007 Recommendations of the International Commission on Radiological
7926 Protection. ICRP Publication 103. Annals of the ICRP 37(2–4).
7927 ICRP, 2008. Nuclear Decay Data for Dosimetric Calculations. ICRP Publication 107. Annals
7928 of the ICRP 38(3).
7929 ICRP, 2015. Occupational Intakes of Radionuclides: Part 1. ICRP Publication 130. Annals of
7930 the ICRP 44(2).
7931 ICRP, 2016. Occupational intakes of radionuclides: Part 2. ICRP Publication 134. Annals of
7932 the ICRP 45(3/4).
7933 ICRP, 2017. Occupational intakes of radionuclides: Part 3. ICRP Publication 137. Annals of
7934 the ICRP 46(3/4).
7935 ICRP, 2019. Occupational Intakes of Radionuclides: Part 4. ICRP Publication 141. Annals of
7936 the ICRP 48(2/3).
7937 Iinuma, T., Watari, K., Nagai, T., et al., 1967. Comparative studies of Cs- 132 and Rb-86
7938 turnover in man using a double-tracer method. J. Radiat. Res 8: 100–1 15.
7939 IARC, 1990. IARC Monographs on the Evaluation of Carcinogenic Risks to Humans of
7940 Chromium, Nickel, and Welding. International Agency for Research on Cancer (IARC).
7941 Lyon, France: World Health Organization.
7942 International Programme on Chemical Safety, 1991. Environmental Health Criteria 108: Nickel.
7943 Geneva: World Health Orgnization.
7944 Ishimatsu, S., Kawamoto, T., Matsuno, K., et al., 1995. Distribution of various nickel
7945 compounds in rat organs after oral administration. Biological Trace Element Research 49(1):
7946 43–52.
7947 Ishiwata, K., Ido, T., Monma, M., et al., 1991. Potential radiopharmceuticals labeled with
7948 titanium-45. Int. J. Rad. Appl. Instrum A 42: 707–712.
7949 Izumi, Y., Fujita, M., Yabe, A., et al., 1973. Retention and distribution of inorganic mercury-
7950 197 and -203 in the human body after single inhalation. In: Proc. 3rd International Congress
7951 of the International Radiological Protection Association, Washington, 1973, pp. 1384–1389.
7952 Jacobsen, N., Alfheim, I. and Jonsen, J., 1978. Nickel and strontium distribution in some mouse
7953 tissues. Passage through placenta and mammary glands. Research Communications in
7954 Chemical Pathology and Pharmacology 20(3): 571–584.
7955 Jamre, M., Salek, N., Jalilian, A.R., et al., 2011. Development of an in vivo radionuclide
7956 generator by labeling bleomycin with 191Os. J. Radioanal. Nucl. Chem 290: 543–549.
7957 Janghorbani, M., Christensen, M.J., Nahapetian, B., et al., 1982. Selenium metabolism in
7958 healthy adults: Quantitative aspects using the stable isotope 74SeO32-. Am J Clin Nutr
7959 35(4): 647–654.
7960 Janghorbani, M., Kasper, L.J. and Young, V.R., 1984. Dynamics of selenite metabolism in
7961 young men: studies with the stable isotope tracer method. Am J Clin Nutr 40: 208–218.

7962 Jarup, L., Rogenfelt, A., Elinder, C.G., et al., 1983. Biological half-time of cadmium in the
7963 blood of workers after cessation of exposure. Scandinavian Journal of Work, Environment
7964 and Health 9(4): 327–331. DOI: 10.5271/sjweh.2404.
7965 JEFCA, 2001. Cadmium. WHO Food Additives Series No. 46. Geneva, Switzerland: World
7966 Health Organization.
7967 Jeffcoat, M.K., McNeil, B.J. and Davis, M.A., 1978. Indium and iron as tracers for erythroid
7968 precursors. J Nucl Med 19: 496–500.
7969 Jeffrey, M.R., Freundlich, H.F. and Bailey, D.M., 1958. Distribution and excretion of radiogold
7970 in animals. Ann. Rheum. Dis 17: 52–60.
7971 Jellum, E., Munthe, E., Guldal, G., et al., 1980. Fate of the gold and the thiomalate part after
7972 intramuscular administration of aurothiomalate to mice. Ann. Rheum. Dis 39: 155–158.
7973 Jereb, M., Falk, R., Jereb, B., et al., 1975. Radiation dose to the human body from intravenously
7974 administered 75Se-sodium selentite. Journal of Nuclear Medicine 16: 846–850.
7975 Johnson, J.R., 1977. Whole body retention following an intravenous injection of 75Se as
7976 selenomethionine. Health Physics 33: 250–251.
7977 Jones, K., Morton, J., Smith, I., et al., 2015. Human in vivo and in vitro studies on
7978 gastrointestinal absorption of titanium dioxide nanoparticles. Toxicology Letters 233: 95–
7979 101.
7980 Jönsson, B.A., 1991. Biokinetics and localization of some In-111-radiopharmaceuticals in rats
7981 at the macroscopic and microscopic level: an approach towards small scale dosimetry.
7982 [doctoral thesis]. Lund University, Lund, Sweden.
7983 Jonsson, F., Sandborgh-Englund, G. and Johanson, G., 1999. A compartmental model for the
7984 kinetics of mercury vapour in humans. Toxicol. Appl. Pharmacol 155: 161–168.
7985 Jugdaohsingh, R., 2007. Silicon and bone health. J. Nutr. Health Aging 11: 99–110.
7986 Kabe, I., Omae, K., Nakashima, H., et al., 1996. In vitro solubility and in vivo toxicity of indium
7987 phosphide. Journal of Occupational Health 38: 6–12.
7988 Kang, G.S., Gillespie, P.A., Gunnison, A., et al., 2011. Comparative pulmonary toxicity of
7989 inhaled nickel nanoparticles; Role of deposited dose and solubility. Inhalation Toxicology
7990 23(2): 95–103. DOI: 10.3109/08958378.2010.543440.
7991 Kang, G.S., Gillespie, P.A., Gunnison, A., et al., 2011. Long-term inhalation exposure to nickel
7992 nanoparticles exacerbated atherosclerosis in a susceptible mouse model. Environmental
7993 Health Perspectives 119(2): 176–181. DOI: 10.1289/ehp.1002508.
7994 Kato, M., 1963. Distribution and excretion of radiomanganese administered to the mouse. Q J
7995 Exp Physiol 48: 355–69.
7996 Kaye, S.V., 1968. Distribution and retention of orally administered radiotungsten in the rat.
7997 Health Phys 15: 399–417.
7998 Kerger, B.D., Finley, B.L., Corbett, G.E., et al., 1997. Ingestion of Chromium(VI) in Drinking
7999 Water by Human Volunteers: Absorption, Distribution, and Excretion of Single and
8000 Repeated Doses. Journal of Toxicology and Environmental Health 50(1): 67–95.
8001 Kernan, R.P., 1969. Accumulation of cesium and rubidium in vivo by red and white muscles of
8002 the rat. J. Physiol 204: 195–205.
8003 Khayat, A. and Dencker, L., 1983. Whole-body and liver distribution of inhaled mercury vapour
8004 in the mouse: influence of ethanol and aminotriazole pretreatment. J. Appl. Toxicol 3: 66–
8005 74.
8006 Khayat, A. and Dencker, L., 1984. Organ and cellular distribution of inhaled metallic mercury
8007 in the rat and marmoset monkey (Callitrix jacchus): Influence of ethyl alcohol pretreatment.
8008 Acta Pharmacol. et Toxicol 55: 145–152.
8009 Kiesswetter, E., Schäper, M., Buchta, M., et al., 2007. Longitudinal study on potential
8010 neurotoxic effects of aluminium: I. Assessment of exposure and neurobehavioural

performance of Al welders in the train and truck construction industry over 4 years. Int Arch Occup Environ Health 81: 41–67.

Kiesswetter, E., Schäper, M., Buchta, M., et al., 2009. Longitudinal study on potential neurotoxic effects of aluminium: II. Assessment of exposure and neurobehavioral performance of Al welders in the automobile industry over 4 years. Int Arch Occup Environ Health 82: 1191–1210.

Kirman, C.R., Hays, S.M., Aylward, L.L., et al., 2012. Physiologically based pharmacokinetic model for rats and mice orally exposed to chromium. Chemico-Biological Interactions 200(1): 45–64. DOI: 10.1016/j.cbi.2012.08.016.

Kittle, C.F., King, E.R., Bahner, C.T., et al., 1951. Distribution and excretion of radioactive hafnium sodium mandelate in the rat. Proceedings of the Society for Experimental Biology and Medicine 76: 278–282.

Klaassen, C.D., 1979. Biliary excretion of silver in the rat, rabbit, and dog. Toxicology and Applied Pharmacology 50: 49–55.

Kleinsorge, H., 1967. Die Resorption Therapeutisch Anwendbarer Goldsalze und Goldsole. Arzneim-Forsch 17: 100–102.

Klosterkötter, W., 1960. Effects of ultramicroscopic gamma-aluminium oxide on rats and mice. Arch. Indust. Health 21: 458–472.

Knudsen, E., Sandstrom, B. and Solgaard, P., 1996. Zinc, copper and magnesium absorption from a fibre-rich diet. Journal of Trace Elements in Medicine and Biology 10: 68–76.

Kolanz, M.E., 2001. Introduction to beryllium: uses, regulatory history, and disease. Appl. Occup. Environ. Hyg 16: 559–567.

Korst, D.R., 1968. Blood volume and red blood cell survival. In: Wagner HN and Saunders WB (eds) Principles of nuclear medicine. Philadelphia, pp. 429–471.

Krahwinkel, W., Herzog, H. and Feinendegen, L.E., 1988 Paramacokinetics of thallium-201 in normal individuals after routine myocardial scintigraphy. J. Nucl. Med 29: 1582–1586.

Kreiss, K., Day, G.A. and Schuler, C.R., 2007. Beryllium: A modern industrial hazard. Annual Review of Public Health 28: 259–277. DOI: 10.1146/annurev.publhealth.28.021406.144011.

Kreyling, W.G., Hirn, S., Möller, W., et al., 2014. Air-blood barrier translocation of tracheally instilled gold nanoparticles inversely depends on particle size. ACS Nano 8(1): 222–233. DOI: 10.1021/nn403256v.

Kreyling, W.G., Holzwarth, U., Haberl, N., et al., 2017. Quantitative biokinetics of titanium dioxide nanoparticles after intratracheal instillation in rats: Part 3. Nanotoxicology 11(4). Taylor & Francis: 454–464. DOI: 10.1080/17435390.2017.1306894.

Kreyling, W.G., Holzwarth, U., Haberl, N., 2017. Quantitative biokinetics of titanium dioxide nanoparticles after intravenous injection in rats: Part 1. Nanotoxicology 11(4). Taylor & Francis: 434–442. DOI: 10.1080/17435390.2017.1306892.

Kreyling, W.G., Holzwarth, U., Schleh, C., et al., 2017. Quantitative biokinetics of titanium dioxide nanoparticles after oral application in rats: Part 2. Nanotoxicology 11(4). Taylor & Francis: 443–453. DOI: 10.1080/17435390.2017.1306893.

Kreyling, W.G., Möller, W., Holzwarth, U., et al., 2018. Age-dependent rat lung deposition patterns of inhaled 20 nanometer gold nanoparticles and their quantitative biokinetics in adult rats. ACS Nano 12(8): 7771–7790.

Kriegel, H., 1984. Biokinetics and metabolism of radiogallium. Nuklearmedizin. Nuclear Medicine 23(2): 53–57.

Kristiansen, J., Christensen, J.M., Iversen, B.S., et al., 1997. Toxic trace element reference levels in blood and urine: Influence of gender and lifestyle factors. Sci Total Env 204: 147–60.

8059 Kuehn, K. and Sunderman, F.W. Jr., 1982. Dissolution half-times of nickel compounds in water,
8060 rat serum and renal cytosol. Journal of Inorganic Biochemistry 17(1): 29–39.
8061 Kuehn, K., Fraser, C.B. and Sunderman, F.W. Jr., 1982. Phagocytosis of particulate nickel
8062 compounds by rat peritoneal macrophages in vitro. Carcinogenesis 3: 321–326.
8063 Kumana, C.R., Au, W.Y., Lee, N.S.L., et al., 2002. Systemic availability of arsenic from oral
8064 arsenic-trioxide used to treat patients with hematological malignancies. European Journal of
8065 Clinical Pharmacology 58: 521–526.
8066 Kutzner, J. and Brod, K.H., 1971. Studies on absorption and secretion of tin following oral
8067 administration of 113 Sn [Untersuchungen zur Resorption und Ausscheiding von Zinn nach
8068 oraler Gabe mittels 113Sn. NuklearMedizin 10(3): 286–297.
8069 Lachine, E.E., Noujaim, A.A., Ediss, C., et al., 1976. Toxicity, tissue distribution and excretion
8070 of 46ScCl3, and 46Sc-EDTA in mice. International Journal of Applied Radiation and
8071 Isotopes 27: 373–377.
8072 Lange, R.C., Spencer, R.P. and Harder, H.C., 1973. The anti-tumor agent cis-Pt(NH3)2Cl2:
8073 Distribution studies and dose calculations for 193mPt and 195mPt. J. Nucl. Med 14: 191–
8074 195.
8075 Langham-New, S.A. and Lambert, H., 2012. Potassium. Adv. Nutr 3: 820–821.
8076 Larsen, R.H., Slade, S. and Zalutsky, M.R., 1998. Blocking [211At]astatide accumulation in
8077 normal tissues: preliminary evaluation of seven potential compounds. Nucl. Med. Biol 25:
8078 351–357.
8079 Lathrop, K.A., Harper, P.V. and Malkinson, F.D., 1968. Human total-body retention and
8080 excretory routes of 75Se for selenomethionine. Strahlentherapie 67: 436–443.
8081 Lathrop, K.A., Johnston, R.E., Blau, M., et al., 1972. Radiation dose to humans from 75 Se-L-
8082 selenomethionine. Journal of Nuclear Medicine 6(Suppl 6): 7–30.
8083 Lathrop, K.A., Harper, P.V., Gloria, I.V., et al., 1975. Intestinal localization of Tl-201. J. Nucl.
8084 Med 16(545).
8085 Lathrop, K.A., Tsui, B.M.W., Chen, C-T., et al., 1989. Multiparameter extratrapolation of
8086 biodistribution data between species. Health Phys 1: 121–126.
8087 Laval, M., Dumesny, C., Eutick, M., et al., 2018. Oral trivalent bismuth ions decrease, and
8088 trivalent indium or ruthenium ions increase, intestinal tumor burden in ApcΔ14/+ mice.
8089 Metallomics 10: 194–200.
8090 Lawrence, J.S., 1961. Studies with radioactive gold. Ann. Rheum. Dis 20: 341–352.
8091 Lazzara, R., Hyatt, K., Love, W.D., et al., 1963. Tissue distribution, kinetics, and biologic half-
8092 life of 28Mg in the dog. Am. J. Physiol 204: 1086–1094.
8093 Lefevre, M.E. and Joel, D.D., 1986. Distribution of label after intragastric administration of
8094 7Be-labeled carbon to weanling and aged mice. Proceedings of the Society for Experimental
8095 Biology and Medicine 182(1): 112–119.
8096 Leggett, R., 2011. A biokinetic model for manganese. Sci. Total Environ 409: 4179–4186.
8097 Leggett, R. and O'Connell, C., 2018. Biokinetic models for Group VB elements. Journal of
8098 Radiological Protection 38(2): 564–586. DOI: 10.1088/1361-6498/aab1c1.
8099 Leggett, R.W., 1997. A model of the distribution and retention of tungsten in the human body.
8100 Science of the Total Environment 206: 147–165.
8101 Leggett, R.W. and Williams, L.R., 1986. A model for the kinetics of potassium in healthy
8102 humans. Physics in Medicine & Biology 31: 23–42.
8103 Leggett, R.W. and Williams, L.R., 1988. A biokinetic model for Rb in humans. Health Physics
8104 55(4): 685–702. DOI: 10.1097/00004032-198810000-00009.
8105 Leggett, R.W., Munro, N.B. and Eckerman, K.F., 2001. Proposed revision of the ICRP model
8106 for inhaled mercury vapour. Health Phys 81: 450–455.

8107 Leggett, R.W., Williams, L.R., Melo, D.R., et al., 2003. A physiologically based biokinetic
8108 model for cesium in the human body. Sci. Total Environ 317: 235–255.
8109 Levander, O.A., 1987. A global view of human selenium nutrition. Annual Review of Nutrition
8110 7: 227–50.
8111 Leverton, R.M. and Binkley, E.S., 1944. The copper metabolism and requirement of young
8112 women. J. Nutr 27: 43–52.
8113 Lewis, G.P., Coughlin, L., Jusko, W., et al., 1972. Contribution of cigarette smoking to
8114 cadmium accumulation in man. Lancet 1: 291–292.
8115 Lie, R., Thomas, R.G. and Scott, J.K., 1960. The distribution and excretion of thallium-204 in
8116 the rat with suggested MPC's and a bio-assay procedure. Health Physics 2: 334–340.
8117 Lim, T.H., Sargent, T. and Kusubov, N., 1983. Kinetics of trace element chromium(III) in the
8118 human body. American Journal of Physiology-Regulatory, Integrative and Comparative
8119 Physiology 244(4). American Physiological Society: R445–R454. DOI:
8120 10.1152/ajpregu.1983.244.4.R445.
8121 Lindberg, J.S., Zobitz, M.M., Poindexter, J.R., et al., 1990. Magnesium bioavailability from
8122 magnesium citrate and magnesium oxide. Journal of the American College of Nutrition 9:
8123 48–55.
8124 Linder, M.C. and Hazegh-Azam, M., 1996. Copper biochemistry and molecular biology. Am.
8125 J. Clin. Nutr 63(797).
8126 Lindgren, A., Vahter, M. and Dencker, L., 1982. Autoradiographic studies on the distribution
8127 of arsenic in mice and hamsters administered 74As-arsenite or arsenate. Acta Phamacol.
8128 Toxicol 51: 253–265.
8129 Ling, M-P. and Liao, C-M., 2009. A human PBPK/PD model to assess arsenic exposure risk
8130 through farmed tilapia consumption. Bull. Environ. Contam. Toxicol 83: 108–114.
8131 Lippmann, M. and Albert, RE., 1969. The effect of particle size on the regional deposition of
8132 inhaled aerosols in the human respiratory tract. Am. Ind. Hyg. Assoc. J 30: 257–275.
8133 Litterst, C.L., Gram, T.E., Dedrick, R.L., et al., 1976. Distribution and disposition of platinum
8134 following intravenous administration of cis-diamminedichloroplatinum (II) (NSC119875) to
8135 dogs. Cancer Res 36: 2340–2355.
8136 Ljunggren, K.G., Lidums, V. and Sjögren, B., 1991. Blood and urine concentrations of
8137 aluminium among workers exposed to aluminium flake powders. Br J Ind Med 48: 106–109.
8138 Lloyd, R.D., Mays, C.W., McFarland, S.S., et al., 1972. 83Rb AND 137Cs METABOLISM IN
8139 PERSONS AFFECTED BY MUSCLE DISEASE. COO-119-247, 1 January. Utah Univ.,
8140 Salt Lake City. Radiobiology Div. DOI: 10.2172/4600250.
8141 Lloyd, R.D., Mays, C.W., McFarland, S.S., et al., 1973. Metabolism of Rb-83 and Cs-137 in
8142 persons with muscle disease. Radiation Research 54(3). Allen Press: 463–478. DOI:
8143 10.2307/3573739.
8144 Love, W.D. and Burch, G.E., 1953 A comparison of K-42, Rb-86, and Cs-134 as tracers of
8145 potassium in the study of cation metabolism of human erythrocytes in vitro. J. Lab. Clin.
8146 Med 41: 351–362.
8147 Love, W.D., Romney, R.B. and Burch, G.E., 1954. A comparison of the distribution of
8148 potassium and exchangeable rubidium in the organs of the dog, using rubidium. Circ. Res 2:
8149 112–122.
8150 Lown, B.A., Morganti, J.B. and Stineman, C.H., 1980. Tissue organ distribution and behavioral
8151 effects of platinum following acute and repeated exposure of the mouse to platinum sulfate.
8152 Environmental Health Perspectives 34: 203–212.
8153 Luckey, T.D., Venugopal, B. and Hutcheson, D., 1975. Heavy Metal Toxicity,Safety and
8154 Hormonology. Stuttgart: Georg Thieme Publishers.

8155 Mabille, H., Larcan, A., Streiff, F., et al., 1961. Etude de la répartition du rubidium radioactif
8156 chez l'homme (86Rb). In: Comptes rendus des seances de la societe de biologie et de ses
8157 filiales, Paris, France, 1961, p. 571. Masson éditeur.
8158 MacDonald, E. and Bahner, C.T., 1953 Hafnium complexes for biological investigations.
8159 Proceedings of the Society for Experimental Biology and Medicine 83: 801–804.
8160 Magos, L. and Berg, G.G., 1988. Selenium. In: Clarkson TW, Fuberg L, Nordberg GF, et al.
8161 (eds) Biological Monitoring of Toxic Metal. New York: Plenum Press.
8162 Magos, L., Clarkson, T.W. and Hudson, A.R., 1989. The effects of dose of elemental mercury
8163 and first-pass circulation time on exhalation and organ distribution of inorganic mercury in
8164 rats. BBA - General Subjects 991(1): 85–89. DOI: 10.1016/0304-4165(89)90032-9.
8165 Mahoney, J.P. and Small, W.J., 1968. Studies on manganese. 3. The biological half-life of
8166 radiomanganese in man and factors which affect this half-life. The Journal of clinical
8167 investigation 47(3): 643–653. DOI: 10.1172/JCI105760.
8168 Mann, S., Droz, P-O. and Vahter, M., 1996. A physiologically based pharmacokinetic model
8169 for arsenic exposure. II. Validation and application in humans. Toxicology and Applied
8170 Pharmacology 140(2): 471–486. DOI: 10.1006/taap.1996.0244.
8171 Manzo, L., Rade-Edel, J. and Sabbioni, E., 1983. Environmental Toxicology Research on
8172 Thallium: Metabolic and Toxicological Studies in the Rat as Carried out by Nuclear and
8173 Radioanalytical Methods.
8174 Mappes, R., 1977. Experiments on excretion of arsenic in urine. International Archives of
8175 Occupational and Environmental Health 40: 267–272.
8176 Marafante, E. and Vahter, M., 1987. Solubility, retention and metabolism of intratracheally and
8177 orally administered inorganic arsenic compounds in the hamster. Environmental Research
8178 42: 72–82.
8179 Marafante, E., Rade, J. and Sabbioni, E., 1981. Intracellular interaction and metabolic fate of
8180 arsenite in the rabbit. Clin. Toxicol 18: 1335–1341.
8181 Martin, R.F., Janghorbani, M. and Young, V.R., 1989. Experimental selenium restriction in
8182 healthy adult humans: changes in selenium metabolism studied with stable-isotope
8183 methodology. Am J Clin Nutr 49: 854–861.
8184 Mascarenhas, B.R., Granda, J.L. and Freyberg, R.H., 1972 Gold metabolism in patients with
8185 rheumatoid arthritis treated with gold compounds – reinvestigated. Arthritis and
8186 Rheumatism 15: 391–402.
8187 Mashitsuka, S. and Inoue, M., 1998. Urinary excretion of aluminum from antacid ingestion and
8188 estimation of its apparent biological half-time. Trace Elem Electrolytes 15: 132–135.
8189 Mason, J., Mulryan, G., Lamand, M,, et al., 1989. Behavior of [185W] thiotungstates injected
8190 into sheep and the influence of copper: their fate and the effect of the compounds upon
8191 plasma copper. J. Inorg. Biochem: 35,115–126.
8192 Massarella, J.W. and Pearlman, R.S., 1987. Gold disposition in the rat: Studies of its plasma
8193 half-life and its urinary, biliary and faecal elimination pathways. J. Pharmacol. Exp. Ther
8194 243: 247–257.
8195 Maynard, L.S. and Fink, S., 1956. The influence of chelation on radiomanganese excretion in
8196 man and mouse. J Clin Invest 8: 831–6.
8197 McAughey, J., Newton, D., Talbot, R., et al., 1998. Uptake and excretion of inhaled 26Al-
8198 aluminium oxide. AEA Technology Report (AEA-2221).
8199 McIntyre, P.A., Larson, S.M., Eikman, E.A., et al., 1974. Comparison of the metabolism of
8200 iron-labeled transferrin (Fe· TF) and indium-labeled transferrin (In· TF) by the
8201 erythropoietic marrow. Journal of Nuclear Medicine 15(10). Society of Nuclear Medicine:
8202 856–862.

8203 McLaughlin, A.I., Kazantzis, G., King, E., et al., 1962. Pulmonary fibrosis and encephalopathy
8204 associated with the inhalation of aluminium dust. Br J Ind Med 19: 253–263.
8205 McNeely, M.D., Nechay, M.W. and Sunderman, F.W. Jr., 1972. Measurements of nickel in
8206 serum and urine as indices of environmental exposure to nickel. Clinical Chemistry 18(9):
8207 992–995.
8208 McNeil, B.J., Holman, B.L., Button, L.N., et al., 1974. Use of indium chloride scintigraphy in
8209 patients with myelofibrosis. Journal of Nuclear Medicine: Official Publication, Society of
8210 Nuclear Medicine 15(8): 647–651.
8211 McQueen, E.G. and Dykes, P.W., 1969. Transport of gold in the body. Ann. Rheum. Dis 28:
8212 437–442.
8213 Mealey, J., Brownell, G.L. and Sweet, W.H., 1959. Radioarsenic in plasma, urine, normal
8214 tissues, and intracranial neoplasms. A. M. A. Archives Neurol. Psychiatry 81: 310–320.
8215 Medinsky, M.A., Cuddihy, R.G. and Griffith, R.G., 1981. A simulation model describing the
8216 metabolism of inhaled and ingested selenium compounds. Toxicology and Applied
8217 Pharmacology 59: 54–63.
8218 Medinsky, M.A., Cuddihy, R.G. and McClellan, R.O., 1981. Systemic absorption of selenious
8219 acid and elemental selenium aerosols in rats. Journal of Toxicology and Environmental
8220 Health 8: 917–928.
8221 Medinsky, M.A., Benson, J.M. and Hobbs, C.H., 1987. Lung clearance and disposition of 63Ni
8222 in F344/N rats after intratracheal instillation of nickel sulfate solutions. Environmental
8223 Research 43: 168–178.
8224 Meek, S.F., Harrold, G.C. and McCord, C.P., 1943. The physiologic properties of palladium
8225 and its compounds. Industrial Medicine and Surgery 12: 447–448.
8226 Mehard, C.W. and Volcani, B.E., 1975. Similarity in uptake and retention of trace amounts of
8227 31Silicon and 68Germanium in rat tissues and cell organelles. Bioinorg. Chem 5: 107–124.
8228 Melo, D.R. and Leggett, R.W., 2017. A biokinetic model for systemic nickel. Health Physics
8229 112: 18–27.
8230 Mena, I., Marin, O., Fuenzalida, S., et al., 1967. Chronic manganese poisoning. Clinical picture
8231 and manganese turnover. Neurology 17: 128–36.
8232 Meneely, G.R., Auerbach, S.H., Woodcock, C.C., et al., 1953. Transbronchial instillation of
8233 radioactive gold colloid in the lung of the dog. Distribution studies, survival and pathology.
8234 Am. J. Med. Sci 225: 172–177.
8235 Menne, T., Mikkelsen, H. and Solgard, P., 1978. Nickel excretion in urine after oral
8236 administration. Contact Dermatitis 4: 106–108.
8237 Menzel, D.B., Ross, M., Oddo, S.V., et al., 1994. A physiologically based pharmacokinetic
8238 model for ingested arsenic. Environ. Geochem. Health 16: 209–218.
8239 Merritt, K. and Brown, S.A., 1995. Distribution of titanium and vanadium following repeated
8240 injection of high‐dose salts. Journal of Biomedical Materials Research 29(10): 1175‐1178.
8241 DOI: 10.1002/jbm.820291003.
8242 Merritt, K., Margevicius, R.W. and Brown, S.A., 1992. Storage and elimination of titanium,
8243 aluminum, and vanadium salts, in vivo. Journal of Biomedical Materials Research 26: 1503–
8244 1515.
8245 Mertz, W., 1993. Chromium in human nutrition: A review. Journal of Nutrition 123(4): 626–
8246 633.
8247 Mertz, W., Roginski, E.E. and Reba, R.C., 1965. Biological Activity and Fate of Trace
8248 Quantities of Intravenous Chromium(III) in the Rat. American Journal of Physiology 209(3):
8249 489–494.
8250 Miller, H., Munro, D.S. and Wilson, G.M., 1957. The human use of 22Na. Lancet 272(734).

8251 Miller, J.K. and Byrne, W.F., 1970. Comparison of scandium-46 and cerium-144 as
8252 nonabsorbed reference materials in studies with cattle. Journal of Nutrition 100: 1287–1292.
8253 Miller, J.K., Byrne, W.F. and Lyke, W.A., 1972. Comparison of faecal excretions of scandium-
8254 46 tagged sand and soluble cerium-144 by calves. Health Physics 22: 461–465.
8255 Miller, J.K., Madsen, F.C. and Hansard, S.L., 1976. Absorption, excretion and tissue deposition
8256 of titanium in sheep. Journal of Dairy Science 59: 2008–2010.
8257 Miller, M.R., Raftis, J.B., Langrish, J.P., et al., 2017. Inhaled Nanoparticles Accumulate at Sites
8258 of Vascular Disease. ACS Nano 11: 4542 4552.
8259 Milne, D.B., Sims, R.L. and Ralston, N.V.C., 1990. Manganese content of the cellular
8260 components of blood. Clin Chem 36: 450–2.
8261 MIRD, 1973. Summary of current radiation dose estimates to humans from 66Ga, 67Ga, 68Ga,
8262 and 72Ga citrate. J Nucl. Med 14: 755–756.
8263 Miyao, K., Onishi, T., Asai, K., et al., 1980. Toxicology and phase I studies on a novel
8264 organogermanium compound, Ge-132. Curr. Chemother. Infect. Dis 2: 1527–1529.
8265 Mochizuki, H., 2019. Arsenic neurotoxicity in humans. Int. J. Mol. Sci 20(3418): 1–11.
8266 Mole, R.H., 1984. Sodium in man and the assessment of radiation dose after criticality accidents.
8267 Phys. Med. Biol 29: 1307–1327.
8268 Moore, Jr. W., Hysell, D., Crocker, W., et al., 1974. Biological fate of 103Pd in rats following
8269 different routes of exposure. Environmental Research 8(2): 234–240. DOI: 10.1016/0013-
8270 9351(74)90055-3.
8271 Moore, W., Stara, J.F. and Crocker, W.C., 1973. Comparison of 115Cd retention in rats
8272 following different routes of administration. Environ. Res 6: 473–478.
8273 Moore, W., Malanchuk, M., Crocker, W., et al., 1975a. Biological fate of a single administration
8274 of 191Pt in rats following different routes of exposure. Environmental Research 9(2): 152–
8275 158. DOI: 10.1016/0013-9351(75)90059-6.
8276 Moore, W., Hysell, D. and Hall, L., 1975b. Preliminary studies on the toxicity and metabolism
8277 of palladium and platinum. Environmental Health Perspectives 10: 63–71.
8278 Moore, W., Hysell, D., Crocker, W., et al., 1975c. Whole body retention in rats of different
8279 191Pt compounds following inhalation exposure. Environ. Health Persp 12: 35–39.
8280 Morgan, D.L., Shines, C.J., Jeter, S.P., et al., 1997. Comparative pulmonary absorption,
8281 distribution, and toxicity of copper gallium diselenide, copper indium diselenide, and
8282 cadmium telluride in Sprague-Dawley rats. Toxicology and Applied Pharmacology 147(2):
8283 399–410. DOI: 10.1006/taap.1997.8267.
8284 Morris, M.E., Leroy, S. and Sutton, S.C., 1987. Absorption of magnesium from orally
8285 administered magnesium sulfate in man. Clinical Toxicology 25(5): 371–382.
8286 Morrow, P.E., Gibb, F.R. and Johnson, L., 1964. Clearance of insoluble dust from the lower
8287 respiratory tract. Health Phys 10: 543–555.
8288 Morrow, P.E., Gibb, F.R., Davies, H., et al., 1968. Dust removal from the lung parenchyma: an
8289 investigation of clearance stimulants. Toxicology and Applied Pharmacology 12(3): 372–
8290 396. DOI: 10.1016/0041-008X(68)90146-4.
8291 Moser-Veillon, P.B., Reed Mangels, A., Patterson, K.Y., et al., 1992. Utilization of two
8292 different chemical forms of selenium during lactation using stable isotope tracers: an
8293 example of speciation in nutrition. Analyst 117: 559–562.
8294 Mühlbauer, B., Schwenk, M., Coram, W.M., et al., 1991. Magnesium-L-aspartate-HCl and
8295 magnesium-oxide: bioavailability in healthy volunteers. European Journal of Clinical
8296 Pharmacology 40: 437–8.
8297 Mullen, A.L., Stanley, R.E., Lloyd, SR., et al., 1972. Radioberyllium metabolism by the dairy
8298 cow. Health Phys 22: 17–22.

8299 Mullen, A.L., Bretthauer, E.W. and Stanley, R.E., 1976. Absorption, distribution and milk
8300 secretion of radionuclides by the dairy cow - V Radiotungsten. Health Physics 31: 417-
8301 424.
8302 Münker, C., Pfänder, J.A., Weyer, S., et al., 2003. Evolution of planetary cores and the Earth-
8303 Moon system from Nb/Ta systematics. Science 301: 84–87.
8304 Mussi, I., Calzaferri, G., Buratti, M., et al., 1984. Behaviour of plasma and urinary aluminum
8305 levels in occupationally exposed subjects. Int Arch Occup Environ Health 54: 155–161.
8306 Muth, O.H., Oldfield, J.E. and Weswig, P.H. (eds), 1967. Selenium in Biomedicine. Westport
8307 CT, AVI.
8308 Nagata, N., Yoneyama, T., Yanagida, K., et al., 1985. Accumulation of germanium in the
8309 tissues of a long-term user of germanium preparation died of acute renal failure. Journal of
8310 Toxicological Sciences 10(4): 333–341. DOI: 10.2131/jts.10.333.
8311 Nakagawara, S., Goto, T., Nara, M., et al., 1998. Spectroscopic Characterization and the pH
8312 Dependence of Bactericidal Activity of the Aqueous Chlorine Solution. Analytical Sciences
8313 14: 691–698.
8314 Nakamura, K., Nishiguchi, I., Takagi, Y., et al., 1985. Distribution of 201Tl in blood.
8315 Radioisotopes 34: 550–554.
8316 National Research Council (NRC) and Committee on Medical and Biological Effects of
8317 Environmental Pollutants, 1975) Nickel. Washington: National Academy of Sciences.
8318 Nelson, B., Hayes, R.L., Edwards, C.L., et al., 1972. Distribution of gallium in human tissues
8319 after intravenous administration. J. Nucl. Med 13: 92–100.
8320 Neuman, W.F. and Neuman, M.W., 1958. The Chemical Dynamics of Bone Mineral. Chicago:
8321 University of Chicago Press.
8322 Newton, D. and Fry, F.A., 1978. The retention and distribution of radioactive mercuric oxide
8323 following accidental inhalation. Ann Occup. Hyg 21: 21–32.
8324 Newton, D. and Holmes, A., 1966. A case of accidental inhalation of zinc-65 and silver-110m.
8325 Radiation Research 29: 403–412.
8326 Nicolaou, G., Pietra, R., Sabbioni, E., et al., 1987. Multielement determination of metals in
8327 biological specimens of hard metal workers: A study carried out by neutron activation
8328 analysis. J. Trace Elem. Electrolytes Health Dis 1: 73–77.
8329 Nieboer, E., Sanford, W.E. and Stace, B.C., 1992. In: Nieboer E and Nriagu JO (eds) Nickel
8330 and Human Health: Current Perspectives. Wiley series in advances in environmental science
8331 and technology 25. New York, USA: John Wiley, pp. 49–68.
8332 Nielsen, G.D., Søderberg, U., Jørgensen, P.J., et al., 1999. Absorption and Retention of Nickel
8333 from Drinking Water in Relation to Food Intake and Nickel Sensitivity. Toxicology and
8334 Applied Pharmacology 154: 67–75.
8335 NiPERA, 1996. Occupational Exposure Limits: Criteria Document for Nickel and Nickel
8336 Compounds. Washington, DC: Nickel Producers Environmental Research Association.
8337 Nishimura ,Y., Inaba, J., Matusaka, N., et al., 1991. Biokinetics of selenium in rats of various
8338 ages. Biomed Trace Element. Res 2: 11–19.
8339 Nodiya, P.J., 1972. Cobalt and nickel balance in students of an occupational technical school.].
8340 Gigiena i Sanitarija 37: 108–109.
8341 Nomoto, S. and Sunderman, Jr. F.W., 1970. Atomic absorption spectrometry of nickel in serum,
8342 urine, and other biological materials. Clinical Chemistry 16(6): 477–485.
8343 Nordberg, G.F. and Sherfving, S., 1972. Metabolism. In: Mercury in the Environment: An
8344 Epidemiological and Toxicological Appraisal. 3. Pr. Cleveland, Ohio: CRC Press.
8345 Nordberg, G.F., Kjellstrom, T. and Nordberg, M., 1985. Kinetics and metabolism. In: Friberg
8346 L, Elinder CG, and T. K (eds) Exposure, dose, and metabolism. Boca Raton, FL: CRC Press,
8347 pp. 103–178.

8348 Nygren, O. and Lundgren, C., 1997. Determination of platinum in workroom air and in blood
8349 and urine from nursing staff attending patients receiving cisplatin chemotherapy.
8350 International Archives of Occupational and Environmental Health 70: 209 –214.
8351 Oberdoerster, G., Baumert, H.P., Hochrainer, D., et al., 1979. The clearance of cadmium
8352 aerosols after inhalation exposure. Am. Ind. Hyg. Assoc. J 40(6): 443–450.
8353 Oberdörster, G., 1988. Lung clearance of inhaled insoluble and soluble particles. J. Aerosol
8354 Med 1: 289–330.
8355 Oberdörster, G., Oldiges, H. and Zimmermann, B., 1980. Lung deposition and clearance of
8356 cadmium in rats exposed by inhalation or by intratracheal instillation. Zentralbl Bakteriol B
8357 170(1–2): 35–43.
8358 Oberdorster, G., Cox, C. and Baggs, R., 1987. Long term lung clearance and cellular retention
8359 of cadmium in rats and monkeys. J. Aerosol Sci 18(6): 745–748.
8360 O'Dell, G.D., Miller, W.J., Moore, S.L., et al., 1971. Effect of dietary nickel level on excretion
8361 and nickel content of tissues in male calves. Journal of Animal Science 32(4): 769–773.
8362 O'Flaherty, E.J., 1996. A Physiologically Based Model of Chromium Kinetics in the Rat.
8363 Toxicology and Applied Pharmacology 138: 54–64.
8364 O'Flaherty, E.J., Kreger, B.D., Hays, S.M., et al., 2001. A Physiology Based Model for the
8365 Ingestion of Chromium(III) and Chromium(VI) by Humans. Toxicological Sciences 60:
8366 196–213.
8367 Oller, A.R., Kirkpatrick, D.T., Radovsky, A., et al., 2008. Inhalation carcinogenicity study with
8368 nickel metal powder in Wistar rats. Toxicology and Applied Pharmacology 233(2): 262–275.
8369 DOI: 10.1016/j.taap.2008.08.017.
8370 Olsen, I. and Jonsen, J., 1979. Whole-body autoradiography of 63Ni in mice throughout
8371 gestation. Toxicology 12: 165–172.
8372 Olsson, K.A., Söremark, R. and Wing, K.R., 1969. Uptake and Distribution of Rubidium - 86
8373 and Potassium - 43 in Mice and Rats—an Autoradiographic Study. Acta Physiologica
8374 Scandinavica 77(3): 322-332. DOI: 10.1111/j.1748-1716.1969.tb04577.x.
8375 Onkelinx, C., 1977. Compartment analysis of metabolism of chromium (III) in rats of various
8376 ages. American Journal of Physiology 232(5): E478–E484. DOI:
8377 10.1152/ajpendo.1977.232.5.E478.
8378 Onkelinx, C., Becker, J. and Sunderman, Jr. F.W., 1973. Compartmental analysis of the
8379 metabolism of 63Ni(II) in rats and rabbits. Research communications in Chemical Pathology
8380 and Pharmacology 6(2): 663–676.
8381 Oskarsson, A. and Tjälve, H., 1979. The distribution and metabolism of nickel carbonyl in mice.
8382 British Journal of Industrial Medicine 36: 326–335.
8383 Osredkar, J. and Sustar, N., 2011. Copper and zinc, biological role and significance of
8384 copper/zinc imbalance. J Clinic Toxicol S S3(1): 1–18.
8385 Östlund, K., 1969. Studies on the metabolism of methyl mercury in mice. Acta Pharmacol
8386 Toxicol. (Suppl. 1: 27, 5–132.
8387 Owen, C.A., 1965. Metabolism of radiocopper (64Cu) in the rat. Amer. J. Physiol 209: 900–
8388 904.
8389 Palmer, B.F., 2015. Regulation of potassium homeostasis. Renal Physiol 10: 1050–1060.
8390 Paquet, F., Houpert, P., Verry, M., et al., 1998. The gastrointestinal absorption of 63Ni and
8391 95Nb in adult and neonatal rats: effect of the chemical form administered. Radiation
8392 Protection Dosimetry 79: 191–195.
8393 Parker, K. and Sunderman, F.W. Jr., 1974. Distribution of 63Ni in rabbit tissues following
8394 intravenous injection of 63NiC12. Research communications in Chemical Pathology and
8395 Pharmacology (7): 755–762.

8396 Partington, J.R., 1954. In: General and Inorganic Chemistry. London: Macmillan, pp. 834–835.
8397 Patri, A., Umbreit, T., Zheng, J., et al., 2009. Energy dispersive X-ray analysis of titanium
8398 dioxide nanoparticle distribution after intravenous and subcutaneous injection in mice.
8399 Journal of Applied Toxicology 29(8): 662–672. DOI: 10.1002/jat.1454.
8400 Patriarca, M., Lyon, T.D.B. and Fell, G.S., 1997. Nickel metabolism in humans investigated
8401 with an oral stable isotope. Am J Clin Nutr 66(3): 616–621. DOI: 10.1093/ajcn/66.3.616.
8402 Patrick, G. and Stirling, C., 1992. Transport of particles of colloidal gold within and from rat
8403 lung after local deposition by alveolar microinjection. Environ. Health Perspect 97: 47–51.
8404 Patrick, G. and Stirling, C., 1994. The redistribution of colloidal gold particles in rat lung
8405 following local deposition by alveolar microinjection. Eds. Dodgson J and McCallum RI
8406 (eds) Inhaled Particles VII, Proceedings of the Seventh International Symposium on Inhaled
8407 Particles, Edinburgh, United Kingdom, September 17–21, 1991 38(Supplement 1): 225–234.
8408 Patrick, G. and Stirling, C., 1997a. Particle dissolution contributes to long-term alveolar
8409 clearance of colloidal gold in the rat. Eds. Cherry N and Ogden T (eds) Inhaled Particles
8410 VIII, Proceedings of the Eighth International Symposium on Inhaled Particles, Cambridge,
8411 United Kingdom, August 26–30 1996 41(Supplement 1): 601–606.
8412 Patrick, G. and Stirling, C., 1997b. Slow clearance of different-sized particles from rat trachea.
8413 Journal of Aerosol Medicine 10(1): 55–65.
8414 Patten, J.R., Whitford, G.M., Stringer, G.I., et al., 1978. Oral absorption of radioactive fluoride
8415 and iodide in rats. Archives of Oral Biology 23: 215–217.
8416 Patterson, B.H., Levander, O.A., Helzlsouer, K., et al., 1989. Human selenite metabolism: A
8417 kinetic model. American Journal of Physiology 257(3): R556– R567.
8418 Pavelka, S., 2004. Metabolism of bromide and its interference with the metabolism of iodine.
8419 Physiol Res 53(Suppl. 1): 81– 90.
8420 Pechova, A. and Pavlata, L., 2007. Chromium as an essential element: a review. Veterinarni
8421 Medicina 52(1).
8422 Pele, L.C., Thoree, V., Bruggaber, S.F.A., et al., 2015. Pharmaceutical/food grade titanium
8423 dioxide particles are absorbed into the bloodstream of human volunteers. Particle and Fibre
8424 Toxicology 12: 26.
8425 Phalen, R.F. and Morrow, P.E., 1973 Experimental inhalation of metallic silver. Health Physics
8426 24: 509–518.
8427 Phatak, S.S. and Patwardhan, V.N., 1952. Toxicity of nickel. Accumulation of nickel in rats fed
8428 on nickel-containing diets and its elimination. Journal of Scientific and Industrial Research
8429 11B: 173–176.
8430 Philipson, K., Falk, R., Gustafsson, J., et al., 1996. Long–term lung clearance of 195Au–
8431 labelled teflon particles in humans. Env. Lung Res 22: 65–83.
8432 Pierre, F., Baruthio, F., Diebold, F., et al., 1995. Effect of different exposure compounds on
8433 urinary kinetics of aluminium and fluoride in industrially exposed workers. Occup. Environ.
8434 Med 52: 396–403.
8435 Pierre, F., Diebold, F. and Baruthio, F., 1998. Biomonitoring of aluminium in production
8436 workers. In: Priest ND and O'Donnell TV (eds) Health in the Aluminium Industry. London:
8437 Middlesex University Press, pp. 68–89.
8438 Pleban, P.A. and Pearson, K.H., 1979. Determination of manganese in whole blood and serum.
8439 Clin Chem 25: 1915–8.
8440 Poirier, J., Semple, H., Davies, J., et al., 2011. Double-blind, vehicle-controlled randomized
8441 twelve month neurodevelopmental toxicity study of common aluminum salts in the rat.
8442 Neuroscience 193: 338–362.
8443 Polachek, A.A., Cope, C.B., Williard, R.F., et al., 1960. Metabolism of radioactive silver in a
8444 patient with carcinoid. The Journal of laboratory and clinical medicine 56: 499–505.

8445 Pomroy, C., Charbonneau, S.M., McCullough, R.S., et al., 1980. Human retention studies with
8446 74As. Toxicol. Appl. Pharmacol 53: 550–556.
8447 Popplewell, J.F., King, S.J., Day, J.P., et al., 1998. Kinetics of uptake and elimination of silicic
8448 acid by a human subject: A novel application of 32Si and accelerator mass spectrometry.
8449 Journal of Inorganic Biochemistry 69: 177–180.
8450 Potter, G.D., Vattuone, G.M. and McIntyre, D.R., 1971. The fate and implications of ingested
8451 204Tl in a dairy cow and a calf. Health Phys 20: 657–662.
8452 Poulheim, K.F., 1984. Zur retention von 60Co, 58Co/54Mn und 110mAg nach inhalativer
8453 Aufnahme im Menschen. Isotopenpraxis 20: 299–300.
8454 Priest, N.D., 1997. Biokinetics and availability of aluminium in man. Chapter 10. In: Managing
8455 Health in the aluminium Industry (ed. ND Priest), Montreal, Canada, 1997.
8456 Priest, N.D., 2004. The biological behaviour and bioavailability of aluminium in man, with
8457 special reference to studies employing aluminium-26 as a tracer: Review and study update.
8458 Journal of Environmental Monitoring 6: 375–403.
8459 Priest, N.D., Newton, D., Day, J.P., et al., 1995. Human metabolism of aluminium-26 and
8460 gallium-67 injected as citrates. Human Exper. Toxicol 14: 287–293.
8461 Priest, N.D., Talbot, R.J., Austin, J.G., et al., 1996. The bioavailability of 26Al-labelled
8462 aluminum citrate and aluminum hydroxide in volunteers. BioMetals 9(3): 221–228.
8463 Priest, N.D., Newton, D., Talbot, R., et al., 1998. Industry-sponsored studies on the biokinetics
8464 and bioavailability of aluminium in man. In: Priest ND and O'Donnell TV (eds) Health in
8465 the Aluminium Industry. London: Middlesex University Press, pp. 105–129.
8466 Priest, N.D., Talbot, R.J., Newton, D., et al., 1998. Uptake by man of aluminum in a public
8467 water supply. Human and Experimental Toxicology 17(6): 296–301.
8468 Proescher, F., Seil, H.H. and Stillians, A.W., 1917. A contribution to the action of vanadium
8469 with particular reference to syphilis. American Journal of Syphilis 1: 347–405.
8470 Rahola, T., Hattula, T., Korolainen, A., et al., 1973. Elimination of free and protein bound ionic
8471 mercury (203Hg2+) in man. Annals of Clinical Research 5(4): 214–219.
8472 Ranade, V.V. and Somberg, J.C., 2001. Bioavailability and pharmacokinetics of magnesium
8473 after administration of magnesium salts to humans. American Journal of Therapeutics 8:
8474 345–357.
8475 Rauws, A.G., 1983. Pharmacokinetics of bromide ion – an overview. Food and Chemical
8476 Toxicology 21(4): 379–382.
8477 Ray, C.T., Burch, G.E. and Threefoot, S.A., 1952. Biologic decay rates of chloride in normal
8478 and diseased man, determined with long-life radiochlorine, 36Cl. J. Lab. Clin. Med 39: 673–
8479 696.
8480 Reeves, A.L., 1965. The absorption of beryllium from the gastrointestinal tract. Arch. Environ.
8481 Health 11: 209–214.
8482 Refvik, T. and Andreassen, T., 1995. Surface binding and uptake of nickel(II) in human
8483 epithelial kidney cells: modulation by ionomycin, nicardipine and metals. Carcinogenesis
8484 16: 1107–1112.
8485 Reid, A.F., Forbes, G.B., Bondurant, J., et al., 1956. Estimation of Total Body Chlorine in Man
8486 by Radio-Bromide Dilution. J. Lab. Clin. Med 48: 63–68.
8487 Reinhold, J.G., Faradji, B., Abadi, P., et al., 1976. Decreased absorption of calcium, magnesium,
8488 zinc and phosphorus by humans due to increased fiber and phosphorus consumption as wheat
8489 bread. Journal of Nutrition 106: 493–503.
8490 Relman, A.S., 1956. The physiological behavior of rubidium and cesium in relation to that of
8491 potassium. Yale J. Biol. Med 29: 248–262.

8492 Rhoads, K. and Sanders, C.L., 1985. Lung clearance, translocation and acute toxicity of arsenic,
8493 beryllium, cadmium, cobalt, lead, selenium, vanadium and ytterbium oxides following
8494 deposition in rat lung. Environmental Research 36: 359–378.
8495 Richmond, C.R., 1980. Retention and excretion of radionuclides of the alkali metals by five
8496 mammalian species. Health Phys 38: 1111–1153.
8497 Richmond, C.R., Furchner, J.E. and Trafton, G.A., 1960. Metabolism of Zr-95 and ruthenium-
8498 106 in mammals. In: Biological and Medical Research Group (H4) of the Health Division,
8499 Semiannual Report July through December 1959. Los Alamos Scientific Laboratory, pp. 90–
8500 93.
8501 Riihimäki, V., Valkonen, S., Engström, B., et al., 2008. Behavior of aluminum in aluminum
8502 welders and manufacturers of aluminum sulfate–impact on biological monitoring. Scand J
8503 Work Environ Health 34: 451–462.
8504 Robinson, J.R., Robinson, M.F., Levander, O.A., et al., 1985. Urinary excretion of selenium by
8505 New Zealand and North American human subjects on differing intakes. Am J Clin Nutr 41:
8506 1023–1031.
8507 Robinson, M., Rea, H., Friend, G., et al., 1978. On supplementing the selenium intake of New
8508 Zealanders. British Journal of Nutrition 39: 589–600.
8509 Rodushkin, I., Engström, E., Sörlin, D., et al., 2011. Uptake and accumulation of anthropogenic
8510 Os in free-living bank voles (Myodes glareolus). Water, Air, and Soil Pollution 218(1–4):
8511 603–610.
8512 Roels, H., Meiers, G. and Delos, M., 1997. Influence of the route of administration and the
8513 chemical form (MnCl2, MnO2) on the absorption and cerebral distribution of manganese in
8514 rats. Archives of Toxicology 71: 223–230.
8515 Röllin, H.B., Theodorou, P. and Kilroe-Smith, T.A., 1991. Deposition of aluminium in tissues
8516 of rabbits exposed to inhalation of low concentrations of Al2O3 dust. Br J Ind Med 48: 389–
8517 391.
8518 Röllin, H.B., Theodorou, P., Nogueira, C.M.C.A., et al., 2001. Aluminium uptake and excretion
8519 in potroom workers of a new primary aluminium smelter during the construction stage.
8520 Journal of Environmental Monitoring 3: 560–564.
8521 Rosenfeld, G., 1954. Studies of the metabolism of germanium. Archives of Biochemistry and
8522 Biophysics 48: 84–94.
8523 Roshchin, A., Ordzhonikidze, E. and Shalganova, I., 1980. Vanadium–toxicity, metabolism,
8524 carrier state. Journal of Hygiene, Epidemiology, Microbiology, and Immunology 24: 377–
8525 383.
8526 Rosoff, B., Siegel, E., Williams, G.L., et al., 1963. Distribution and excretion of radioactive
8527 rare-earth compounds in mice. International Journal of Applied Radiation and Isotopes 14:
8528 129–135.
8529 Rosoff, B., Spencer, H., Cohn, S.H., et al., 1965. Metabolism of scandium-46 in man.
8530 International Journal of Applied Radiation and Isotopes 16: 479–485.
8531 Roth, P. and Werner, E., 1979. Intestinal absorption of magnesium in man. International Journal
8532 of Applied Radiation and Isotopes 30: 523–526.
8533 Rothstein, A. and Hayes, A.D., 1960. The metabolism of mercury in the rat studied by isotope
8534 techniques. J. Pharmacol. Exp. Ther 130: 166–176.
8535 Rubin, M., Sliwinski, A., Photias, M., et al., 1967. Influence of chelation on gold metabolism
8536 in rats. Proc. Soc. Exp. Biol. Med 124: 290–296.
8537 Rubow, S., Klopper, J. and Scholtz, P., 1991. Excretion of gallium 67 in human breast milk and
8538 its inadvertent ingestion by a 9-month-old child. European Journal of Nuclear Medicine
8539 18(10): 829–833.

8540 Ruoff, W., 1995. Relative bioavailability of manganese ingested in food or water. In:
8541 Proceedings, Lexington, MA, 1995, pp. 65–75. Eastern Research Group, Inc.
8542 Rusch, G.M., O'Grodnick, J.S. and Rinehart, W.E., 1986. Acute inhalation study in rat of
8543 comparative uptake, distribution and excretion of different cadmium containing materials.
8544 Am. Ind. Hyg. Assoc 47: 754–763.
8545 Russell, M.A., King, L.E. and Boyd, A.S., 1996 Lichen planus after consumption of a gold
8546 containing liquor. New England Journal of Medicine 334(9): 603.
8547 Ryan, J.W., Harper, P.V., Stark, V.S., et al., 1985. Radiation absorbed dose estimate for
8548 rubidium-82 determined from in vivo measurements in human subjects. Shalafke-Stelson
8549 AT and Watson EE (eds) Radiopharmaceutical Dosimetry Symposium CONF–85113.
8550 Springfield, VA: NTIS: 346–358.
8551 Rydzynski, K. and Pakulska, D., 2012. Vanadium, Niobium, and Tantalum. In: Bingham E and
8552 B C (eds) Patty's toxicology. Hoboken, N.J: Wiley-Blackwell, p. 6.
8553 Sabatier, M., Pont, F., Arnaud, M.J., et al., 2003. A compartmental model of magnesium
8554 metabolism in healthy men based on two stable isotope tracers. American Journal of
8555 Physiology - Regulatory Integrative and Comparative Physiology 285(3 54-3): R656–R663.
8556 DOI: 10.1152/ajpregu.00749.2002.
8557 Sabatier, M., Arnaud, M.J. and Turnlund, J., 2003. Magnesium absorption from mineral water.
8558 European Journal of Clinical Nutrition 57: 801–802.
8559 Sabbioni, E., Marafante, E., Amantini, L., et al., 1978. Similarity in metabolic patterns of
8560 different chemical species of vanadium in the rat. Bioinorganic Chemistry 8: 503–515.
8561 Sabbioni, E., Loetz, L., Maravante, E., et al., 1980. Metabolic fate of different inorganic and
8562 organic species of thallium in the rat. Science of the Total Environment 15: 123–125.
8563 Sabbioni, E., Marafante, E., Rade, J., et al., 1981. Biliary excretion of vanadium in rats.
8564 Toxicological European Research 3: 93–98.
8565 Sallsten, G., Baregard, L. and Schutz, A., 1993. Decrease in mercury concentration in blood
8566 after long term exposure: a kinetic study of chloralkali workers. Brit. J. Ind. Med 50: 814–
8567 821.
8568 Sandborgh-Englund, G., Elinder, C-G., Johanson, G., et al., 1998. The absorption, blood levels,
8569 and excretion of mercury after a single dose of mercury vapour in humans. Toxicol. Appl.
8570 Pharmacol 150: 146–153.
8571 Santucci, B., Manna, F., Cannistraci, C., et al., 1994. Serum and urine concentrations in nickel-
8572 sensitive patients after prolonged oral administration. Contact Dermatitis 30: 97 –101.
8573 Sargent, T., Lim, T.H. and Jenson, R.L., 1979. Reduced chromium retention in patients with
8574 hemochromatosis, a possible basis of hemochromatotic diabetes. Metabolism 28(1): 70–79.
8575 DOI: 10.1016/0026-0495(79)90171-9.
8576 Sarmiento-Gonzalez, A., Encinar, J.R., Marchante-Gayon, J.M., et al., 2009. Titanium levels in
8577 the organs and blood of rats with a titanium implant, in the absence of wear, as determined
8578 by double-focusing ICP-MS. Analytical and Bioanalytical Chemistry 393: 335–343.
8579 Sauer, F., Laughland, D.H. and Davidson, W.M., 1959. The silica content of guinea pig tissues
8580 as determined by chemical and isotopic techniques. Can. J. Biochem. Physiol 37: 1173–1181.
8581 Sayato, Y., Nakamuro, K., Matsui, S., et al., 1980. Metabolic Fate of Chromium Compounds.
8582 I. Comperative Behavior of Chromium in Rat Administered with Na251CrO4 and 51CrCl3.
8583 Journal of Pharmacobio-Dynamics 3: 17–23.
8584 Sayle, B.A., Helmer, E. and Birdsong, B.A., 1982. Bone marrow imaging with indium-111
8585 chloride in aplastic anemia and myelofibrosis: Concise communication. J Nucl Med:
8586 23,121–125.
8587 Scaffidi-Argentina, F., Longhurst, G.R., Shestakov, V., et al., 2000. Beryllium R&D for fusion
8588 applications. Fusion Engineering and Design 51–52: 23–41.

8589 Scansetti, G., 1992. Exposure to metals that have recently come into use. Sci. Total Environ
8590 120: 85–91.
8591 Schauss, A.G., 1991. Nephrotoxicity in humans by the ultratrace element germanium. Renal
8592 Failure 29: 267–280.
8593 Schiepers, C., Nuyts, J., Bormans, G., et al., 1997. Fluoride kinetics of the axial skeleton
8594 measured in vivo with fluorine- 18-fluoride PET. Journal of Nuclear Medicine 38(12): 1970–
8595 1976.
8596 Schinohara, N., Danno, N., Ichinose, T., et al., 2014. Tissue distribution and clearance of
8597 intravenously administered titanium dioxide (TiO2) nanoparticles. Nanotoxicology 8: 132–
8598 141.
8599 Schleh, C., Semmler-Behnke, M., Lipka, J., et al., 2012. Size and surface charge of gold
8600 nanoparticles determine absorption across intestinal barriers and accumulation in secondary
8601 target organs after oral administration. Nanotoxicology 6(1): 36–46. DOI:
8602 10.3109/17435390.2011.552811.
8603 Schleh, C., Holzwarth, U., Hirn, S., et al., 2013. Biodistribution of inhaled gold nanoparticles
8604 in mice and the influence of surfactant protein D. Journal of Aerosol Medicine and
8605 Pulmonary Drug Delivery 26(1): 24–30.
8606 Schönholzer, K.W., Sutton, R.A.L., Walker, V.R., et al., 1997. Intestinal absorption of trace
8607 amounts of aluminum in rats studied with 26aluminum and accelerator mass spectrometry.
8608 Clinical Science 92(4): 379– 383.
8609 Schroeder, H.A. and Balassa, J.J., 1967. Abnormal trace metals in man: germanium. Journal of
8610 Chronic Diseases 20: 211–224.
8611 Schwartz, R., Spencer, H. and Wentworth, R.A., 1978. Measurement of magnesium absorption
8612 in man using stable 26Mg as a tracer. Clinica Chimica Acta 87: 265–273.
8613 Scott, J.K., Neuman, W.F. and Allen, R., 1950. The effect of added carrier on the distribution
8614 and excretion of soluble 7Be. J. Biol. Chem 182: 291–298.
8615 Scott, K.C. and Turnland, J.R., 1994. Compartmental model of copper metabolism in adult men.
8616 J. Nutr. Biochem 5: 342–350.
8617 Scott, K.G., 1952. The metabolic properties of various metals. USAEC, pp. 7–11.
8618 Scott, K.G. and Hamilton, J.G., 1950. The metabolism of silver in the rat with radio-silver used
8619 as an indicator. University of California publications in Pharmacology 2: 241–262.
8620 Semmler-Behnke, M., Kreyling, W.G., Lipka, J., et al., 2008. Biodistribution of 1.4- and 18-
8621 nm gold particles in rats. Small 4: 2108–2111.
8622 Serita, F., Kyono, H. and Seki, Y., 1999. Pulmonary clearance and lesions in rats after a single
8623 inhalation of ultrafine nickel at dose levels comparable to the Threshold Limit Value.
8624 Industrial Health 37(4): 353–363.
8625 Setyawati, I.A., Thompson, K.H., Yuen, V.G., et al., 1998. Kinetic analysis and comparison of
8626 uptake, distribution, and excretion of 48V-labeled compounds in rats. Journal of Applied
8627 Physiology 84(2): 569–575.
8628 Sharma, R.P., Oberg, S.G. and Parker, R.D.R., 1980. Vanadium retention in rat tissues
8629 following acute exposures to different dose levels. Journal of Toxicology and Environmental
8630 Health 6(1): 45–54. DOI: 10.1080/15287398009529829.
8631 Sharma, R.P., Flora, S.J., Drown, D.B., et al., 1987. Persistence of vanadium compounds in
8632 lungs after intratracheal instillation in rats. Toxicology and Industrial Health 3: 321–329.
8633 Shaw, P.A., 1933. Toxicity and deposition of thallium in certain game birds. Journal of
8634 Pharmacology and Experimental Therapeutics 48: 478–487.
8635 Sheehan, R.M. and Renkin, E.M., 1972. Capillary, interstitial, and cell membrane barriers to
8636 blood-tissue transport of potassium and rubidium in mammalian skeletal muscle. Circulation
8637 research 30(5): 588–607. DOI: 10.1161/01.RES.30.5.588.

8638 Shellabarger, C.J. and Godwin, J.T., 1954. Studies of the thyroidal uptake of astatine in the rat.
8639 J. Clin. Endocrin. Metab 14: 1149–1160.
8640 Shelley, W.B., 1973. Chondral dysplasia induced by zirconium and hafnium. Cancer Research
8641 33: 287–292.
8642 Shi, H., Magaye, R., Castranova, V., et al., 2013. Titanium dioxide nanoparticles: A review of
8643 current toxicological data. Particle and Fibre Toxicology 10(1): 15.
8644 Shinogi, M., Masaki, T. and Mori, I., 1989. Determination and biokinetics of germanium in
8645 mouse tissues by atomic absorption spectrometry with electrothermal atomization. J. Trace
8646 Elem. Electrolytes Health Dis 3: 25–28.
8647 Silva, A.J., Fleshman, D.G. and Shore, B., 1973. The effects of penicillamine on the body
8648 burdens of several heavy metals. Health Physics 24: 535–539.
8649 Simonsen, J.A., Braad, P.E., Veje, A., et al., 2009. 111Indium-transferrin for localization and
8650 quantification of gastrointestinal protein loss. Scand. J. Gastroenterol 44: 1191–1197.
8651 Sivulka, D.J., 2005. Assessment of respiratory carcinogenicity associated with exposure to
8652 metallic nickel: A review. Regulatory Toxicology and Pharmacology 43: 117–133.
8653 Sjodin, R.A., 1959. Rubidium and cesium fluxes in muscle as related to the membrane potential.
8654 J. Gen. Physiol 42: 983–1003.
8655 Sjögren, B., Lidums, V., Håkansson, M., et al., 1985. Exposure and urinary excretion of
8656 aluminum during welding. Scand J Work Environ Health 11: 39–43.
8657 Sjögren, B., Elinder, C.G., Lidums, V., et al., 1998. Uptake and urinary excretion of aluminium
8658 amongst welders. Int. Arch Occup. Environ. Health 60: 77–79.
8659 Skalsky, H.L. and Carchman, R.A., 1983. Aluminum Homeostasis in Man. International
8660 Journal of Toxicology 2(6): 405–423. DOI: 10.3109/10915818309140728.
8661 Smilay, M.G., Dahl, L.K., Spraragen, S.C., et al., 1961. Isotopic sodium turnover studies in
8662 man: evidence of minimal sodium (22Na) retention 6 to 11 months after administration. J.
8663 Lab. Clin. Med 58: 60–66.
8664 Smith, G.A., Thomas, R.G. and Scott, J.K., 1960. The metabolism of indium after
8665 administration of a single dose to the rat by intratracheal, subcutaneous, intramuscular and
8666 oral injection. Health Physics 4: 101–108.
8667 Smith, J.C. and Hackley, B., 1968. Distribution and excretion of nickel-63 administered
8668 intravenously in rats. Journal of Nutrition 95: 541–546.
8669 Smith, J.R.H., Bailey, M.R., Etherington, G., et al., 2007. Further study of the effect of particle
8670 size on slow particle clearance from the bronchial tree. Radiat. Prot. Dosim 127: 35–39.
8671 Smith, J.R.H., Bailey, M.R., Etherington, G., et al., 2008. Effect of particle size on slow particle
8672 clearance from the bronchial tree. Exp. Lung Res 34: 287–312.
8673 Smith, P.H.S. and Taylor, D.M., 1974. Distribution and retention of the antitumor agent
8674 195mPt-cis-dichlorodiammine platinum (II) in man. J. Nucl. Med 15: 349–351.
8675 Sollenberger, D.M., 1981. The fate of intragastrically or intratracheally administered or inhaled
8676 vanadium-48 oxydichloride in juvenile and mature rats. Ph.D. dissertation. Purdue
8677 University, West Layfayette, IN.
8678 Solomons, N.W., Viteri, F., Shuler, T.R., et al., 1982. Bioavailability of nickel in man: effects
8679 on foods and chemically-defined dietary constituents on the absorption of inorganic nickel.
8680 Journal of Nutrition 112: 39–50.
8681 Söremark, R., 1960a. Excretion of bromide ions by human urine. Acta Physiologica
8682 Scandinavica 50: 306–310.
8683 Söremark, R., 1960b. The biological half-life of bromide ions in human blood. Acta Physiol.
8684 Scand 50: 119–123.

8685 Spencer, H., Norris, C. and Williams, D., 1994. Inhibitory effects of zinc on magnesium balance
8686 and magnesium absorption in man. Journal of the American College of Nutrition 13: 479–
8687 484.
8688 Sripanyakorn, S., Jugdaohsingh, R., Elliott, H., et al., 2004. The silicon content of beer and its
8689 bioavailability in healthy volunteers. British Journal of Nutrition 91: 403–409.
8690 Sripanyakorn, S., Jugdaohsingh, R., Dissayabutr, W., et al., 2009. The comparative absorption
8691 of silicon from different foods and food supplements. British Journal of Nutrition 102: 825–
8692 834.
8693 Stahlhofen, W., Gebhart, J. and Heyder, J., 1980. Experimental determination of the regional
8694 deposition of aerosol particles in the human respiratory tract. Am. Ind. Hyg. Assoc. J 41:
8695 385–398.
8696 Stahlhofen, W., Gebhart, J., Heyder, J., et al., 1981. Intercomparison of regional deposition of
8697 aerosol particles in the human respiratory tract and their long term elimination. Exp. Lung.
8698 Res 2: 131–139.
8699 Stahlhofen, W., Gebhart, J., Rudolf, G., et al., 1986a. Clearance from the human airways of
8700 particles of different sizes deposited from inhaled aerosol boli. Aerosols: Formation and
8701 Reactivity. Second International Aerosol Conference, West. Berlin, Germany: 192–196.
8702 Stahlhofen, W., Gebhart, J., Rudolf, G., et al., 1986b. Measurement of lung clearance with
8703 pulses of radioactively labelled aerosols. J. Aerosol Sci 17: 333–336.
8704 Stahlhofen, W., Gebhart, J., Rudolf, G., et al., 1987. Human lung clearance of inhaled
8705 radioactively labelled particles in horizontal and vertical position of the inhaling person. J.
8706 Aerosol Sci 18: 741–744.
8707 Stahlhofen, W., Koebrich, R., Rudolf, G., et al., 1990. Short term and long term clearance of
8708 particles from the upper respiratory tract as a function of particle size. J. Aerosol Sci 21
8709 Suppl. 1: 407– 410.
8710 Stanek, E.J., Calabrese, E.J., Barnes, R.M., et al., 2010. Bioavailability of arsenic in soil: Pilot
8711 study results and design considerations. Human and Experimental Toxicology 29(11): 945–
8712 960.
8713 Steinhagen, W.H., Cavender, F.L. and Cockrell, B.Y., 1978. Six month inhalation exposures of
8714 rats and guinea pigs to aluminum chlorhydrate. Journal of Environmental Pathology and
8715 Toxicology 1: 267–277.
8716 Steinhausen, C., Kislinger, G., Winklhofer, C., et al., 2004. Investigation of the aluminum
8717 biokinetics in humans: A 26Al tracer study. Food and Chemical Toxicology 42(3): 363–371.
8718 Sterns, R.H., Feig, P.U., Pring, M., et al., 1979. Disposition of intravenous potassium in anuric
8719 man: A kinetic analysis. Kidney International 15(6): 651–660. DOI: 10.1038/ki.1979.85.
8720 Stiefel, T., Schulze, K., Zorn, H., et al., 1980. Toxicokinetic and toxicodynamic studies of
8721 beryllium. Arch. Toxicol 45: 81–92.
8722 Stone, C.J., McLaurin, D.A., Steinhagen, W.H., et al., 1979. Tissue deposition patterns after
8723 chronic inhalation exposures of rats and guinea pigs to aluminum chlorhydrate. Toxicol Appl
8724 Pharmacol 49: 71–76.
8725 Strain, W.H., Berliner, W.P., Lankau, C.A., et al., 1964. Retention of radioisotopes by hair,
8726 bone and vascular tissue. Journal of Nuclear Medicine 5: 664–674.
8727 Strauss, H.W., Harrison, K., Langan, J.K., et al., 1975. Thallium-201 for myocardial imaging.
8728 Circulation 51: 641–645.
8729 Sue, Y-J., 1994. Mercury. In: Goldfrank LR, Flomenbaum NE, and Lewin NA (eds)
8730 Goldfrank's Toxicologic Emergencies, Fifth Edition. Fifth Edition. Norwalk, Connecticut:
8731 Appleton and Lange.
8732 Sugawa-Katayama, Y., Koishi, H. and Danbara, H., 1975. Accumulation of gold in various
8733 organs of mice injected with gold thioglucose. J. Nutr 105: 957–962.

8734 Sunderman, F.W., 1993. Biological monitoring of nickel in humans. Scandinavian Journal of
8735 Work, Environment & Health 19(Suppl 1): 34–38.
8736 Sunderman, F.W., 2004. Nickel. In: Merian E, Anke M, Ihnat M, et al. (eds) Elements and Their
8737 Compounds in the Environment - Occurrence, Analysis, and Biological Relevance. New
8738 York: John Wiley, pp. 841–865.
8739 Sunderman, F.W., Hopper, S.M., Sweeney, K.R., et al., 1989. Nickel absorption and kinetics in
8740 human volunteers. Proceedings of the Society for Experimental Biology and Medicine 191:
8741 5–11.
8742 Sunderman, F.W. Jr. and Selin, C.E., 1968. The metabolism of nickel-63 carbonyl. Toxicology
8743 and Applied Pharmacology 12: 207–218.
8744 Sunderman, F.W. Jr., Shen, S.K., Mitchell, J.M., et al., 1978. Embryotoxicity and fetal toxicity
8745 of nickel in rats. Toxicology and Applied Pharmacology 43: 381 – 390.
8746 Sunderman, Jr. F.W., Dingle, B., Hopfer, S.M., et al., 1988. Acute Nickel Toxicity in
8747 Electroplating Workers Who Accidently Ingested a Solution of Nickel Sulfate and Nickel
8748 Chloride. American Journal of Industrial Medicine 14: 257–266.
8749 Suttie, J.W. and Phillips, P.H., 1959. The effect of age on the rate of fluorine deposition in the
8750 femur of the rat. Archives of Biochemistry and Biophysics 83: 355–359.
8751 Suzuki, M., Morikawa, M., Tomita, K., et al., 1978. Thallous chloride-201Tl – Fundamental
8752 studies on its behavior and clinical evaluation. Kaku Igaku. Japanese J. Nucl. Med 15: 27–
8753 40.
8754 Swanson, C.A., Reamer, D.C., Veillon, C., et al., 1983. Quantitative and qualitative aspects of
8755 selenium utilization in pregnant and non-pregnant women: an application of stable isotope
8756 methodology. Am J Clin Nutr 38: 169–180.
8757 Takahashi, S., Moriguchi, K., Kubota, Y., et al., 1989. The deposition pattern of insoluble
8758 particles with different sizes in the rat trachea. Hoken Butsuri 24: 19–24.
8759 Takenaka, S., Karg, E., Moller, W., et al., 2000. A morphologic study on the fate of ultrafine
8760 silver particles: Distribution pattern of phagocytized metallic silver in vitro and in vivo.
8761 Inhalation Toxicology 12(SUPPL. 3): 291–299.
8762 Takenaka, S., Karg, E., Roth, C., et al., 2001. Pulmonary and systemic distribution of inhaled
8763 ultrafine silver particles in rats. Environmental Health Perspectives 109(SUPPL. 4): 547–
8764 551.
8765 Takenaka, S., Karg, E., Kreyling, W., et al., 2006. Distribution pattern of inhaled ultrafine gold
8766 particles in the rat lung. Inhalation Toxicology 18(10): 733–740.
8767 Talbot, R.J., Newton, D., Priest, N.D., et al., 1995. Inter-subject variability in the metabolism
8768 of aluminium following intravenous injection as citrate. Human Exper. Toxicol 14: 595–599.
8769 Tam, G.K.H., Charbonneau, S.M., Bryce, F., et al., 1982. Excretion of a single oral dose of fish-
8770 arsenic in man. Bulletin of Environmental Contamination and Toxicology 28: 669–673.
8771 Tanaka, I., Ishimatsu, S., Matsuno, K., et al., 1985. Biological half time of deposited nickel
8772 oxide aerosol in rat lung by inhalation. Biological Trace Element Research 8(3): 203–210.
8773 DOI: 10.1007/BF02917459.
8774 Tanaka, I., Ishimatsu, S., Haratake, J., et al., 1988. Biological half-time in rats exposed to nickel
8775 monosulfide (amorphous) aerosol by inhalation. Biological Trace Element Research 17(1):
8776 237–246. DOI: 10.1007/BF02795460.
8777 Tao, S-H. and Bolger, P.M., 1997. Hazard assessment of germanium supplements. Regulatory
8778 Toxicology and Pharmacology 25: 211–219.
8779 Task Group on Lung Dynamics (TGLD), 1966. Deposition and retention models for internal
8780 dosimetry of the human respiratory tract. Health Physics 12: 173–207.
8781 Taylor, D.M., 1966. The metabolism of scandium-47 produced by the decay of calcium 47 in
8782 vivo. British Journal of Radiology 39: 620–622.

8783 Taylor, D.M., Lehmann, M., Planas-Bohne, F., et al., 1983. The metabolism of radiohafnium
8784 in rats and hamsters: a possible analog of plutonium for metabolic studies. Radiation
8785 Research 95: 339–358.
8786 Taylor, D.M., Seidel, A. and Doerfel, H., 1985. The metabolism of radiohafnium in marmosets
8787 and hamsters. International Journal of Nuclear Medicine and Biology 12(5): 387–391. DOI:
8788 10.1016/S0047-0740(85)80009-7.
8789 Taylor, T.P., Ding, M., Ehler, D.S., et al., 2002. Beryllium in the environment: a review. J.
8790 Environ. Sci. Health A 38: 439–469.
8791 Tedeschi, R.E. and Sunderman, F.W., 1957. Nickel poisoning. V. The metabolism of nickel
8792 under normal conditions and after exposure to nickel carbonyl. A. M. A. archives of
8793 industrial health 16(6): 486–488.
8794 Teisinger, J. and Fiserova-Bergerova, V., 1965. Pulmonary retention and excretion of mercury
8795 vapours in man. Ind. Med. Surg 34: 580–584.
8796 Templeton, D.M., Sunderman, F.W. Jr. and Herber, R.F.M., 1994. Tentative reference values
8797 for nickel concentrations in human serum, plasma, blood and urine: Evaluation according to
8798 the TRACY protocol. Science of the Total Environment 148: 243–251.
8799 Tepperman, K., Finer, R., Donovan, S., et al., 1984. Intestinal uptake and metabolism of
8800 auranofin, a new oral gold-based antiarthritis drug. Science 225(4660): 430–432. DOI:
8801 10.1126/science.6429854.
8802 Teraoka, H., 1981. Distribution of 24 elements in the internal organs of normal males and the
8803 metallic workers in Japan. Arch Environ Health 36: 155–165.
8804 Thomas, R.G. and Archuleta, R.F., 1980. Titanium retention in mice. Toxicology Letters 6:
8805 115–118.
8806 Thomas, S.R., Stabin, M.G. and Castronovo, F.P., 2005. Radiation-absorbed dose from 201Tl-
8807 thallous chloride. J. Nucl. Med 46: 502–508.
8808 Thomassen, P.R. and Leicester, H.M., 1964. Uptake of radioactive beryllium, vanadium,
8809 selenium, cerium, and yttrium in the tissues and teeth of rats. Journal of Dental Research 43:
8810 346–352.
8811 Thomson, C.D. and Robinson, M.F., 1986. Urinary and fecal excretions and absorption of a
8812 large supplement of selenium: superiority of selenate over selenite. Am J Clin Nutr 44: 659–
8813 663.
8814 Thomson, C.D. and Stewart, R.D.H., 1973. Metabolic studies of [75Se]selenomethionine and
8815 [75Se]selenite in the rat. British Journal of Nutrition 30: 139–147.
8816 Thomson, C.D. and Stewart, R.D.H., 1974. The metabolism of 75Se selenite in young women.
8817 British Journal of Nutrition 32: 303–323.
8818 Thorne, M.C., Jackson, D. and Smith, A.D., 1986. Pharmacodynamic Models of Selected Toxic
8819 Chemicals in Man. Review of metabolic data. Lancaster: MTP Press Limited.
8820 Threefoot, S., Burch, G. and Reaser, P., 1949. The biologic decay periods of sodium in normal
8821 man, in patients with congestive heart failure and in patients with the nephrotic syndrome as
8822 determined by 22Na as the tracer. J. Lab. Clin. Med 34: 1–13.
8823 Tipton, I., Stewart, P. and Martin, P., 1966. Trace elements in diet and excreta. Health Physics
8824 12: 1683–1689.
8825 Tompsett, S.L., 1934. The excretion of copper in urine and faeces and its relation to the copper
8826 content of the diet. Biochem J 28: 2088–2091.
8827 Tompsett, S.L., 1935. The copper and “inorganic” iron contents of human tissues. Biochem J
8828 29: 480–486.
8829 Toohey, R.E., Essling, M.A. and Huff, D.R., 1979. Retention and gross distribution of 75Se
8830 following intravenous injection of 75Se-selenomethionine. Health Physics 37: 395–397.

TERA, 1999. Toxicological review of soluble nickel salts - Prepared for: Metal Finishing Association of Southern California, Inc., US Environmental Protection Agency and Health Canada. Prepared by Toxicology Excellence for Risk Assessment (TERA) under subcontract in part with Science Applications International Corporation (SAIC).

Turner, A. and Price, S., 2008. Bioaccessibility of platinum group elements in automotive catalytic converter particulates. Environmental Science & Technology 42: 9443–9448.

Turnland, J.R., 1998. Human whole-body copper metabolism. Am. J. Clin. Nutr.(suppl 67(960).

Uchiyama, M., Akiba, S., Ohmomo, Y., et al., 1976. 203Hg-labelled methyl mercury chloride retention in man after inhalation. Health Phys 31: 335–342.

Udensi, K.U. and Tchounwou, P.B., 2017. Potassium homeostasis, oxidative stress, and human disease. Int. J. Clin. Exp. Physiol 4: 111–122.

Underwood, E.J., 1977. Trace Elements in Human and Animal Nutrition (Fourth Edition). Underwood EJ (ed.). London: Academic Press. DOI: 10.1016/B978-0-12-709065-8.50005-5.

United Nations Environment Programme (UNEP), International Labour Organization and World Health Organization (eds), 1982. Titanium. Environmental Health Criteria 24. Geneva: World Health Organization.

United Nations Environment Programme (UNEP), International Labour Organization and World Health Organization (eds), 1988., Vanadium. Environmental Health Criteria 81. Geneva: World Health Organization. Available at: http://hdl.handle.net/20.500.11822/29388.

U.S. EPA, 2001. Toxicological review of bromate in support of Integrated Risk Information System (IRIS). Washington, DC: United States Environmental Protection Agency (EPA).

U.S. EPA, 2009. IRIS Toxicological review of thallium and compounds (Final report). EPA/635/R-08/001F. Washington, DC: United States Environmental Protection Agency (EPA).

U.S. EPA, 2012. Compilation and review of data on relative bioavailablity of arsenic in soil. Washington, DC: United States Environmental Protection Agency (EPA). Available at: http://www.epa.gov/superfund/bioavailability/pdfs/Arsenic%20Bioavailability%20SCIENCE%20Report_.

Usuda, K., Kono, R., Ueno, T., et al., 2014. Risk assessment visualization of rubidium compounds: comparison of renal and hepatic toxicities, in vivo. Biological Trace Element Research 159: 263–268.

Vacher, J. and Stoner, H.B., 1968. The removal of injected beryllium from the blood of the rats. The role of the reticulo-endothelial system. Brit. J. Exper. Pathol 49: 315–323.

Vahter, M., 2002. Mechanisms of arsenic biotransformation. Toxicology 182: 211–217.

Vahter, M. and Marafante, E., 1985. Reduction and binding of arsenate in marmoset monkeys. Arch. Toxicol 57: 119–124.

Vahter, M. and Norin, H., 1980. Metabolism of 74As-labeled trivalent and pentavalent inorganic arsenic in mice. Environ. Res 21: 446–467.

Valberg, L.S., Flanagan, P.R., Haist, J., et al., 1981. Gastrointestinal metabolism of gallium and indium: Effect of iron deficiency. Clinical and Investigative Medicine 4: 103–108.

Valentine, R. and Fisher, G.L., 1984. Pulmonary clearance of intratracheally administered 63Ni3S2 in strain A/J mice. Environmental Research 34: 328–334.

Van Cleave, C.D. and Kaylor, C.T., 1953. Distribution and retention of carrier-free radioberyllium in the rat. AMA Arch. Ind. Hyg. Occup. Med 7: 367–375.

Van Cleave, C.D. and Kaylor, C.T., 1955. Distribution, retention, and elimination of 7Be in the rat after intratracheal injection. AMA Arch. Ind. Hyg. Occup. Med 11: 375–392.

8879 Van Hulle, M., De Cremer, K., Vanholder, R., et al., 2005. In vivo distribution and fractionation
8880 of indium in rats after subcutaneous and oral administration of [114mIn]InAs. Journal of
8881 Environmental Monitoring 7: 365–370.
8882 Van Paemel, M., Dierick, N., Janssens, G., et al., 2010. Selected trace and ultratrace elements:
8883 Biological role, content in feed and requirements in animal nutrition – Elements for risk
8884 assessment. Technical report submitted to EFSA (Question No EFSA-Q-2008-04990).
8885 Technical report. Ghent, Belgium: Ghent University. Available at: DOI:
8886 10.2903/sp.efsa.2010.EN-68.
8887 Veall, N., Fisher, A.J., Browe, J.C., et al., 1955. An improved method for clinical studies of
8888 total exchangeable sodium using 22Na and a whole-body counting technique. Lancet 1: 419–
8889 422.
8890 Velasquez, D.J. and Morrow, P.E., 1984. Estimation of guinea pig tracheobronchial transport
8891 rates using a compartment model. Exp. Lung Research 7: 163–176.
8892 Velikyan, I., Antoni, G., Sörensen, J., et al., 2013. Organ biodistribution of germanium-68 in
8893 rat in the presence and absence of [68Ga]Ga-DOTA-TOC for the extrapolation to the human
8894 organ and whole-body radiation dosimetry. Am. J. Nucl. Med. Mol. Imaging 3: 154–165.
8895 Vendeland, S.C., Deagen, J.T. and Whanger, P.D., 1992. Uptake of selenotrisuflides of
8896 glutathione and cysteine by brush border membranes from rat intestines. Journal of Inorganic
8897 Biochemistry 47: 131–140.
8898 Vendeland, S.C., Deagen, J.T., Butler, J.A., et al., 1994. Uptake of selenite, selenomethionine
8899 and selenate by brush border membrane vesicles isolated from rat small intestine. BioMetals
8900 7: 305–312.
8901 Vennart, J., 1963. External Counting. In: Diagnosis and Treatment of Radioactive Poisoning,
8902 Vienna, Austria, 1963, pp. 3–22. International Atomic Energy Agency (IAEA).
8903 Verhas, M., Gueronniere, V., Grognet, J-M., et al., 2002. Magnesium bioavailability from
8904 mineral water. A study in adult men. Eur. J. Clin. Nutr 56: 442–447.
8905 Versieck, J. and Cornelis, R., 1980. Normal levels of trace elements in human blood plasma or
8906 serum. Analytica Chimica Acta 116: 217–54.
8907 Versieck, J., Vanballenberghe, L. and De Kesel, A., 1988. More on determination of manganese
8908 in biological materials. Clin Chem 34: 1659–60.
8909 Veterans Administration Hospital and Hines IL, 1976. Metabolism of 90Sr and of other
8910 elements in man. Nuclear Sciences Abstract 33(8): 1791.
8911 Visser, G.W.M., Diemer, E.L., Vos, C.M., et al., 1981. The biological behaviour of bome
8912 organic astatine compounds in rats. International Journal of Applied Radiation und Isotopes
8913 32: 913–917.
8914 Vormann, J., 2003. Magnesium: nutrition and metabolism. Molec. Aspects Med 24: 27–37.
8915 Wagner, M.J., 1962. Absorption of fluoride by the gastric mucosa in the rat. Journal of Dental
8916 Research 41: 667– 674.
8917 Walker, A.F., Marakis, G., Christie, S., et al., 2003. Mg citrate found more bioavailable than
8918 other Mg preparations in a randomized, double-blind study. Magnesium Research 16(3):
8919 183–191.
8920 Wase, A.W., 1956. Absorption and distribution of radio ‐ tungstate in bone and soft tissues.
8921 Arch. Biochem. Biophys 61: 272‐277.
8922 Watanabe, K., Shima, S., Tachikawa, S., et al., 1985. Biotoxicity and beryllium distribution in
8923 organs by oral administration of beryllium compounds for long periods II. Experimental
8924 study on oral administration of beryllium compounds. Rodo Kagaku 61: 235–246.
8925 Watson, W.S., Hilditch, T.E., Horton, P.W., et al., 1979. Magnesium metabolism in blood and
8926 the whole body in man using 28Mg. Metab. Clin. Exp 28: 90–95.

8927 Weber, H., 1983. Long-Term Study of the Distribution of Soluble Chromate-51 in the Rat After
8928 a Single Intratracheal Administration. Journal of Toxicology and Environmental Health 11:
8929 749–764.
8930 Weberg, R. and Berstad, A., 1986. Gastrointestinal absorption of aluminium from single doses
8931 of aluminium containing antacids in man. European Journal of Clinical Investigation 16(5):
8932 428–432.
8933 Wehner, A.P. and Craig, D.K., 1972. Toxicology of inhaled NiO and CoO in Syrian golden
8934 hamsters. American Industrial Hygiene Association Journal 33: 146–155.
8935 Weininger, J., Issachar, D., Lubin, E., et al., 1990. Influence of PH adjustment agents on the
8936 biologic behavior of osmium-191 impurity in iridium-191m generator eluates. J. Nucl. Med
8937 31: 523–525.
8938 Weissman, S., Cuddihy, R.G. and Medinsky, M.A., 1983. Absorption, distribution and retention
8939 of inhaled selenious acid and selenium metal aerosols in beagle dogs. Toxicology and
8940 Applied Pharmacology 67: 331–337.
8941 Welsh, L.W. and Welsh, J.J., 1963. Laryngeal lymphatics, human in vivo studies. Am. Acad.
8942 Opthalmol. Otolaryngol 67: 524–529.
8943 West, B. and Wyzan, H., 1963. Investigations of the possible absorption of titanium dioxide
8944 from the gastrointestinal tract. In: FAO/WHO (1970) Toxicological Evaluation of Some
8945 Food Colours, Emulsifiers, Stabilizers, Anti-Caking Agents and Certain Other Substances,
8946 pp. 55–56.
8947 Wester, P.O., 1973. Trace elements in serum and urine from hypertensive patients before and
8948 during treatment with chlorthalidone. Acta Med. Scand 194: 505–512.
8949 Wester, P.O., 1974. Trace element balances in relation to variations in calcium intake.
8950 Atherosclerosis 20: 207–215.
8951 Whanger, P.D., Pedersen, N.D., Hatfield, J., et al., 1976. Absorption of selenite and
8952 selenomethionine from ligated digestive tract segments in rats. Proceedings of the Society
8953 for Experimental Biology and Medicine 153: 295–297.
8954 Whitford, G.M., 1994. Intake and metabolism of fluoride. Advances in Dental Research 8: 5–
8955 14.
8956 Wiegmann, T.B., Day, H.D. and Patak, R.V., 1982. Intestinal absorption and secretion of
8957 radioactive vanadium (48VO3–) in rats and effect of Al(OH)3. Journal of Toxicology and
8958 Environmental Health 10: 233–245.
8959 Wilhelm, M., Zhang, X-J., Hafner, D., et al., 1992. Single-dose toxicokinetics of aluminum in
8960 the rat. Archives of Toxicology 66: 700–705.
8961 Willard, D.H. and Bair, W.J., 1961. Behaviour of 131I following its inhalation as a vapour and
8962 as a particle. Acta Radiologica 55: 486–496.
8963 Williams, R.H., Maturen, A. and Sky-Peck, H.H., 1987. Pharmacologic role of rubidium in
8964 psychiatric research. Comprehensive Therapy 13: 46–54.
8965 Wiseman, G., 1964. Absorption from the Intestine. London: Academic Press.
8966 Wootton, R., 1974. The single passage extraction of 18F in rabbit bone. Clinical Science and
8967 Molecular Medicine 47: 73–77.
8968 WHO, 1990. Environmental Health Criteria 106: Beryllium. Geneva: World Health
8969 Organization.
8970 WHO (ed.), 1996. Trace Elements in Human Nutrition and Health. Geneva: World Health
8971 Organization.
8972 WHO, 2000. Chapter 6.1 Arsenic. In: WHO Air Quality Guidelines. 2nd ed. Copenhagen,
8973 Denmark: World Health Organization Regional Office for Europe.

WHO, 2011a. Cadmium in drinking-water. Background document for development of WHO Guidelines for Drinking-water Quality. WHO/SDE/WSH/03.04/80/Rev/1. Geneva, Switzerland: World Health Organization.

WHO, 2011b. Copper in drinking-water. Background document for development of WHO Guidelines for Drinking-water Quality. WHO/SDE/WSH/03.04/88. Geneva, Switzerland: World Health Organization.

WHO, 2015. Mercury in drinking-water. Background Document for development of WHO guidelines for drinking-water quality. WHO/SDE/WSH/05.08/10. Geneva, Switzerland: World Health Organization.

Wright, N., Yeoman, W.B. and Carter, G.F., 1980. Massive oral ingestion of elemental mercury without poisoning [letter. Lancet 1(8161): 206.

Wright, P.L. and Bell, M.C., 1966. Comparative metabolism of selenium and tellurium in sheep and swine. American Journal of Physiology 211: 6–10.

Wu, X., Li, J., Hu, J-N., et al., 2012. The effects of glutamate and citrate on absorption and distribution of aluminum in rats. Biol. Trace Elem. Res 148: 83–90.

Xie, G.P., Wang, C., Sun, J., et al., 2011. Tissue distribution and excretion of intravenously administered titanium dioxide nanoparticles. Toxicology Letters 205: 55–61.

Yamauchi, H., Takahashi, K., Yamamura, Y., et al., 1992. Metabolism of subcutaneous administered indium arsenide in the hamster. Toxicol. Appl. Pharmacol 116: 66–67.

Yanaga, M., Enomoto, S., Hirunuma, R., et al., 1996. Multitracer study on uptake and excretion of trace elements in rats. Applied Radiation and Isotopes 47(2): 235–240. DOI: 10.1016/0969-8043(95)00279-0.

Yoakum, A.M., Steward, P.L. and Sterrett, J.E., 1975. Method development and subsequent analysis of biological tissues for platinum, lead and manganese content. Environ. Health Persp 10: 85–93.

Yokel, R.A., 2002. Brain uptake, retention, and efflux of aluminum and manganese. Environmental Health Perspectives 110(SUPPL. 5): 699–704.

Yokel, R.A. and Florence, R.L., 2006. Aluminum bioavailability from the approved food additive leavening agent acidic sodium aluminum phosphate, incorporated into a baked good, is lower than from water. Toxicology 227: 86–93.

Yokel, R.A. and McNamara, P.J., 1988. Influence of renal impairment, chemical form, and serum protein binding on intravenous and oral aluminum kinetics in the rabbit. Toxicology and Applied Pharmacology 95(1): 32–43.

Yokel, R.A. and McNamara, P.J., 2001. Aluminium Toxicokinetics: An Updated MiniReview. Pharmacology & Toxicology 88(4): 159–167. DOI: 10.1111/j.1600-0773.2001.880401.x.

Yu, D.H., 1999. A pharmacokinetic modeling of inorganic arsenic: a short‐term oral exposure model for humans. Chemosphere 39: 2737‐2747.

Yu, Y-Q. and Yang, J-Y., 2019. Oral bioaccessibility and health risk assessment of vanadium(IV) and vanadium(V) in a vanadium titanomagnetite mining region by a whole digestive system in-vitro method (WDSM). Chemosphere 215: 294–304.

Zafar, T.A., Weaver, C.M., Martin, B.R., et al., 1997. Aluminum (26Al) Metabolism in Rats. Proceedings of the Society for Experimental Biology and Medicine 216(1). SAGE Publications: 81–85. DOI: 10.3181/00379727-216-44159.

Zalikin, G.A., Tronova, I.N. and Denisov, I.I., 1969. Distribution of scandium-46 in the body of rats for different paths of administration. In: Radioaktivonye Izotopy i Organizm. Izdatel' stvo Meditsina. Moscow, Russia.

Zalups, R.K., 1998. Intestinal handling of mercury in the rat: implication of intestinal secretion of inorganic mercury following biliary ligation or cannulation. J. Toxicol. Environ. Health 53: 615–636.

9023 Zheng, W., Winter, S.M., Kattnig, M.J., et al., 1994. Tissue distribution and elimination of
9024 indium in male fischer 344 rats following oral and intratracheal administration of indium
9025 phosphide. Journal of Toxicology and Environmental Health 43: 483–494.
9026 Zheng, W., Kim, H. and Zhao, Q., 2000. Comparative toxicokinetics of manganese chloride
9027 and methylcyclopentadienyl manganese tricarbonyl (MMT) in Sprague-Dawley rats.
9028 Toxicological Sciences 54: 295–301.
9029 Zheng, Y., Wu, J., Ng, J.C., et al., 2002. The absorption and excretion of fluoride and arsenic
9030 in humans. Toxicology Letters 133(1): 77–82.
9031 Zhu, H., Wang, N., Zhang, Y., et al., 2010. Element contents in organs and tissues of Chinese
9032 adult men. Health Physics 98: 61–71.
9033 Zuckier, L.S., Dohan, O., Li, Y., et al., 2004. Kinetics of perrhenate uptake and comparative
9034 biodistribution of perrhenate, pertechnetate, and iodide by NaI symporter-expressing tissues
9035 in vivo. Journal of Nuclear Medicine 45: 500–507.
9036

ANNEX A. TREATMENT OF OCCUPATIONAL EXPOSURE BY SUBMERSION

A.1. Introduction

(A.1) Airborne radioisotopes can irradiate workers by the submersion pathway. The exposure conditions differ from the semi-infinite geometry assumed for environmental exposures as the emitted radiations scatter off the walls and ceilings thus altering the incident energy and angular spectrum. The emitted electron and photon radiations deliver a dose to the skin and organs of body.

(A.2) Effective dose rate coefficients for occupational exposure to airborne noble gases by submersion were tabulated in *Publications 30* and *68* (ICRP, 1979, 1994). Veinot et al. (2017) have derived effective dose rate coefficients for the noble radioisotopes using the ICRP reference phantoms of *Publication 110* (ICRP, 2009) positioned in rooms representative of an office, laboratory, and warehouse. These coefficients assume the tissue weighting factors of *Publication 103* (ICRP, 2007).

A.2. Monte Carlo Calculations

(A.3) The Monte Carlo calculations for these submersion exposures were carried out using the MCNP-6.1 Monte Carlo code (Pelowitz, 2013). The reference phantoms of *Publication 110* were used for all organ and tissue calculations except for skin. These phantoms are within rectangular prisms consisting of voxels. The male phantom consists of about 7.2 million voxels of which about 2 million represent tissue. The female phantom consists of about 14 million voxels of which about 3.9 million are tissue. Monte Carlo calculations were carried out for monoenergetic electrons and photons emitted uniformly distributed within a) the volume of the room minus the rectangular prism, and b) the non-tissue voxels of the rectangular prism. These two data sets were combined to represent the absorbed dose rate in the tissues per unit airborne concentration of the monoenergetic emitter.

(A.4) The room dimensions and their assumed construct is described in Table A.1. The room sizes were office (100 m^3), laboratory (600 m^3) and warehouse (1200 m^3). The rooms had a concrete floor with concrete and sheet rock walls and ceilings. The elemental composition and densities of the room materials were taken from the McCoon Jr. et al. compendium (2011).

(A.5) The skin dose coefficients were calculated in the basal cells lying within 50 to 90 microns of the skin surface (ICRP, 2007) using a mathematical representation of the body. For most radionuclides the skin dose is a minor contributor to the effective dose due to its tissue weighting factor of 0.01 (ICRP, 2007). However for pure beta emitters, the skin dose it is the dominant contributor to the effective dose.

A.3. Results

(A.6) The effective dose rate coefficient for monoenergetic electrons (negatrons), photons, and positrons are shown graphically in Figs A.1, A.2 and A.3, respectively. Effective dose rate coefficients for the noble gas nuclides of *Publication 107* (ICRP, 2008) in the three rooms are shown in Table A.2. The coefficients in the right most column of Table A.2 are from *Publication 144* (ICRP, 2020) for an semi-infinite environmental exposure geometry and the phantom positioned at the air-ground interface.

(A.7) The effective dose rate coefficients for ^{39}Ar, ^{42}Ar, and ^{83m}Kr in the occupational setting exceed those of the semi-infinite environmental of *Publication 144* (ICRP, 2020). This is a consequence to greater bremsstrahlung production in the floor, ceiling and walls of the rooms instead of the soil and air in the environment. In addition, the skin target region was modelled in a different manner. In *Publication 144* the skin dose is computed in tissue at depths of 50 to 100 microns modelled using a polygon mesh. Veinot et al. used a mathematical phantom with the target region being 50 to 90 microns.

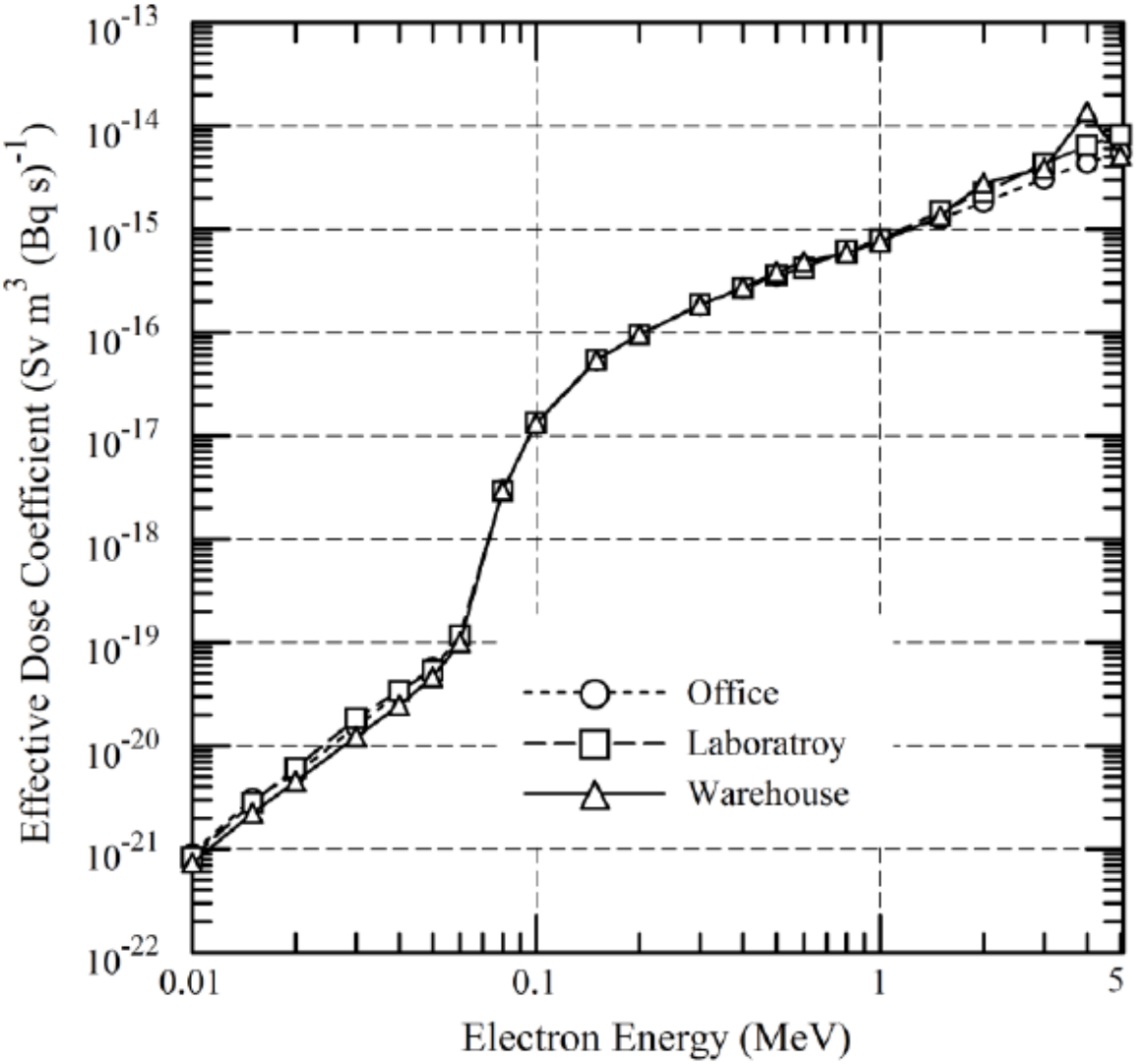

Fig. A.1. Effective dose rate coefficient for submersion exposure – electrons.

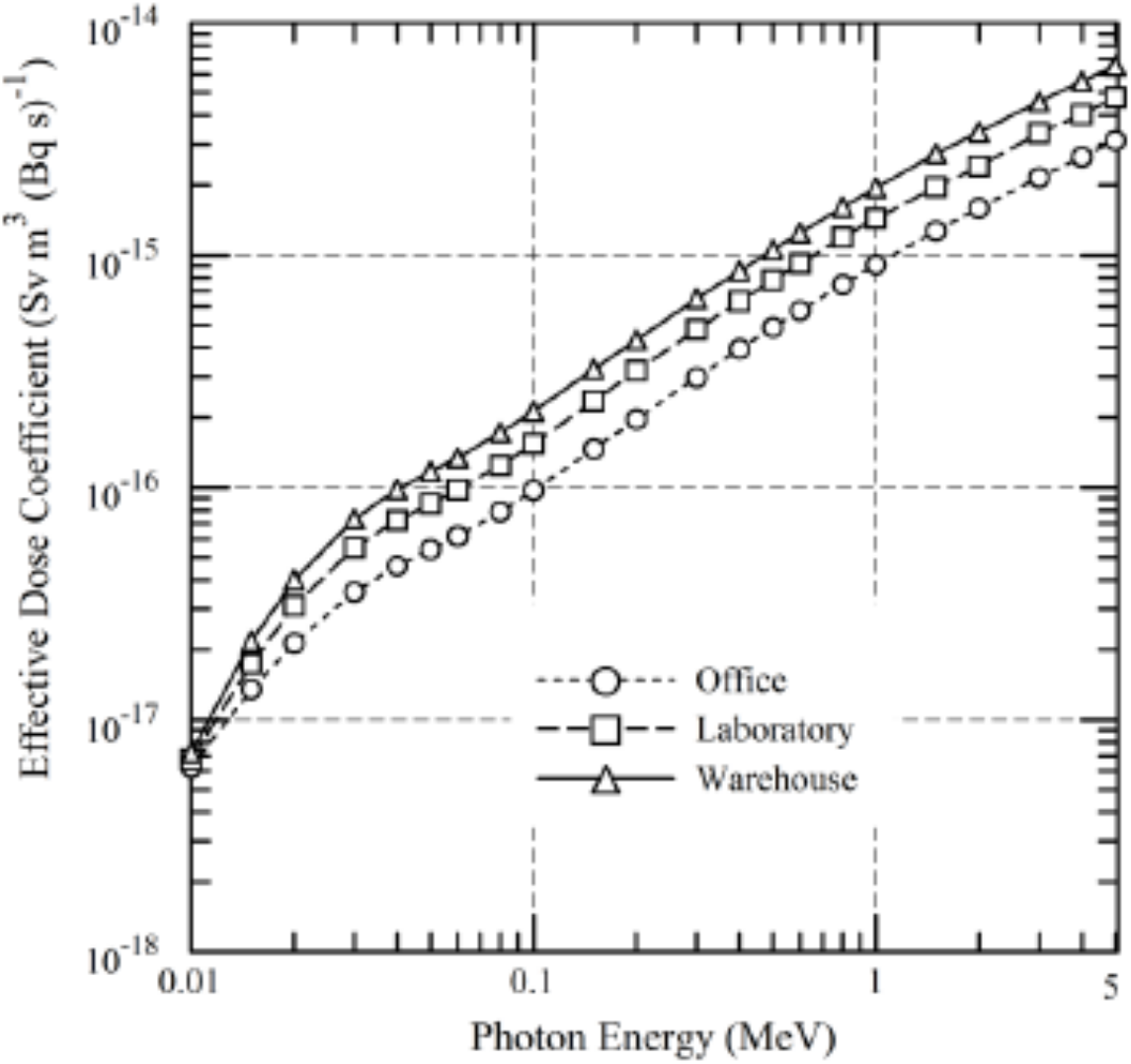

Fig. A.2. Effective dose rate coefficient for submersion exposure – photons.

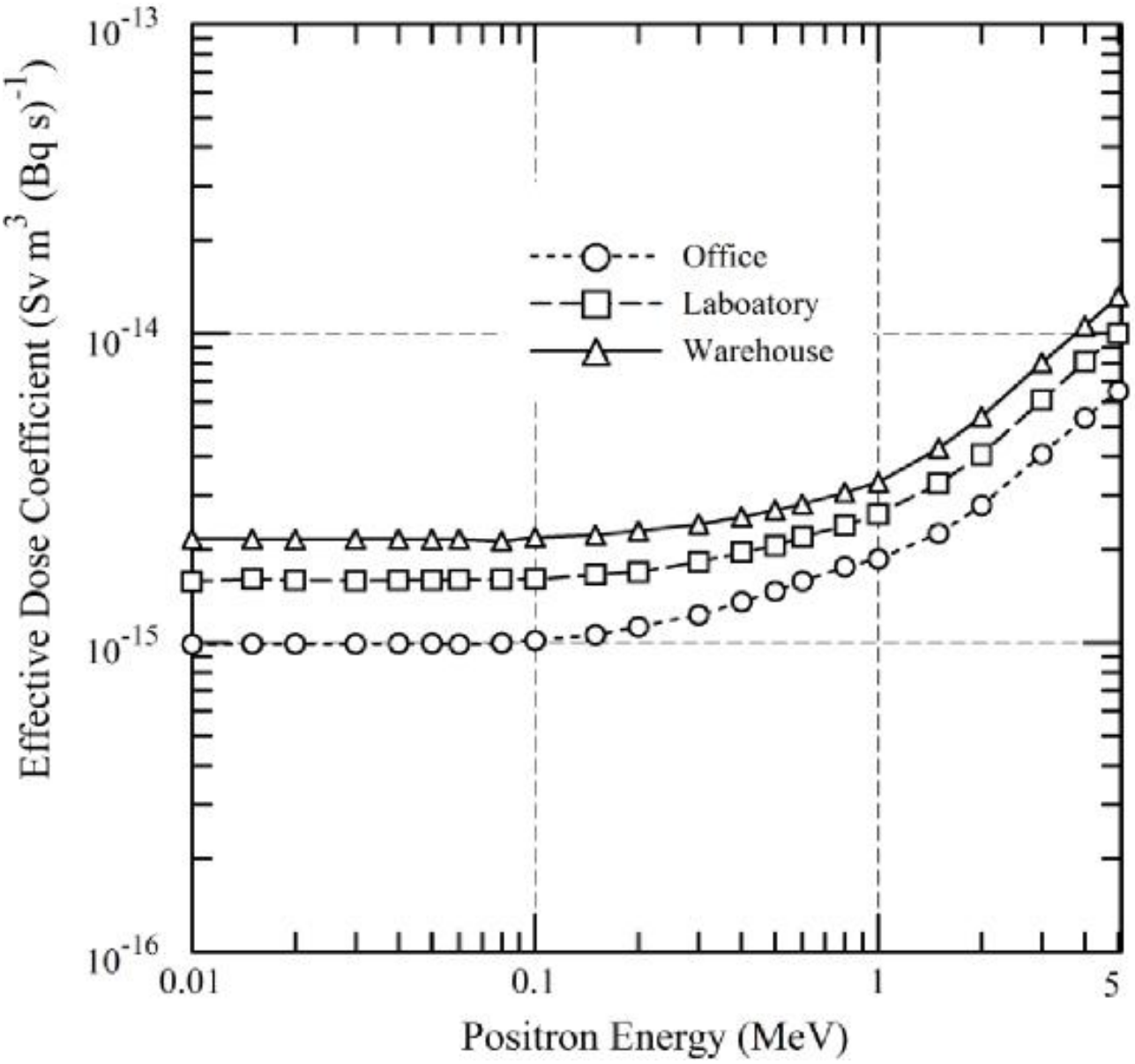

Fig. A.3. Effective dose rate coefficient for submersion exposure – positrons.

Table A.1. Room Dimensions and Geometry.

Room	Dimension (m)	Volume (m^3)	Composition
Office	5.8 x 5.8 x 3.0	100.92	Walls and ceiling – 2.54 cm (1 inch) concrete with 1.27 cm (1/2 inch) sheet rock Floor – 30 cm concrete
Laboratory	10 x20 x 3.0	600	Walls and ceiling – 2.54 cm (1 inch) concrete with 1.27 cm (1/2 inch) sheet rock Floor – 30 cm concrete
Warehouse	15 x 15 x 5.3	~1192	Walls and ceiling- 20.32 cm (8 inch) concrete Floor- 30 cm concrete

Table A.2. Submersion Dose Rate Coefficients for Airborne Isotopes.

Isotope	$T_{1/2}$	Decay Mode	Effective Dose Rate Coefficient (Sv m^3 Bq^{-1} s^{-1})			
			Office	Laboratory	Warehouse	Environment*
Ne-19	17.22 s	EC, B+	1.83E-15	2.60E-15	3.36E-15	4.33E-14
Ne-24	3.38 m	B-	1.15E-15	1.51E-15	1.78E-15	2.33E-14
Ar-37†	35.04 d	EC	0	0	0	0
Ar-39	269 y	B-	1.19E-16	1.21E-16	1.22E-16	9.89E-17
Ar-41	109.61 m	B-	1.44E-15	2.06E-15	2.73E-15	6.08E-14
Ar-42	32.9 y	B-	1.30E-16	1.32E-16	1.35E-16	1.09E-16
Ar-43	5.37 m	B-	2.51E-15	3.53E-15	4.47E-15	7.50E-14
Ar-44	11.87 m	B-	2.00E-15	2.88E-15	3.87E-15	9.31E-14
Kr-74	11.50 m	EC, B+	1.55E-15	2.23E-15	2.90E-15	4.33E-14
Kr-75	4.29 m	EC, B+	2.63E-15	3.85E-15	5.07E-15	5.53E-14
Kr-76	14.8 h	EC	4.19E-16	6.70E-16	9.08E-16	1.68E-14
Kr-77	74.4 m	EC, B+	1.60E-15	2.29E-15	2.98E-15	4.25E-14
Kr-79	35.04 h	EC, B+	2.59E-16	4.04E-16	5.44E-16	1.03E-14
Kr-81	2.29E+5 y	EC	5.53E-18	6.88E-18	8.36E-18	3.72E-17
Kr-81m	13.10 s	IT, EC	1.53E-16	2.31E-16	3.05E-16	4.86E-15
Kr-83m	1.83 h	IT	1.58E-18	1.92E-18	2.31E-18	1.86E-18
Kr-85	10.756 y	B-	1.48E-16	1.51E-16	1.58E-16	2.16E-16
Kr-85m	4.480 h	B-, IT	3.09E-16	4.03E-16	5.00E-16	5.92E-15
Kr-87	76.3 m	B-	1.83E-15	2.48E-15	2.93E-15	3.94E-14
Kr-88	2.84 h	B-	1.83E-15	2.70E-15	3.64E-15	9.58E-14
Kr-89	3.15 m	B-	2.83E-15	4.05E-15	5.23E-15	9.44E-14
Xe-120	40 m	EC, B+	3.95E-16	6.25E-16	8.44E-16	1.54E-14
Xe-121	40.1 m	EC, B+	1.79E-15	2.66E-15	3.55E-15	6.69E-14
Xe-122	20.1 h	EC	7.22E-17	1.14E-16	1.53E-16	1.97E-15
Xe-123	2.08 h	EC, B+	7.44E-16	1.10E-15	1.47E-15	2.69E-14
Xe-125	16.9 h	EC, B+	2.79E-16	4.40E-16	5.95E-16	9.72E-15
Xe-127	36.4 d	EC	2.90E-16	4.59E-16	6.19E-16	1.00E-14
Xe-127m	69.2 s	IT	2.04E-16	3.05E-16	4.02E-16	5.47E-15
Xe-129m	8.88 d	IT	1.26E-16	1.59E-16	1.91E-16	7.89E-16
Xe-131m	11.84 d	IT	6.85E-17	8.23E-17	9.40E-17	2.97E-16
Xe-133	5.243 d	B-	8.07E-17	1.09E-16	1.38E-16	1.12E-15
Xe-133m	2.19 d	IT	1.35E-16	1.60E-16	1.85E-16	1.13E-15
Xe-135	9.14 h	B-	4.44E-16	5.94E-16	7.44E-16	9.92E-15
Xe-135m	15.29 m	ITB-	4.83E-16	7.30E-16	9.70E-16	1.76E-14
Xe-137	3.818 m	B-	1.73E-15	2.27E-15	2.54E-15	1.11E-14
Xe-138	14.08 m	B-	1.45E-15	2.02E-15	2.59E-15	5.36E-14

*Semi-infinite submersion coefficients from *Publication 144*.

†Ar-37 emits no radiations of energy 10 keV and higher.

A.4. References

ICRP 1979. Limits for Intakes of Radionuclides by Workers, ICRP Publication 30. Pergamon Press, Inc., Elmsford, New York.

ICRP 1994. Dose Coefficient for Intake of Radionuclides by Workers. ICRP Publication 68, Ann. ICRP 24(4).

ICRP 2007. The 2007 Recommendations of the International Commission on Radiological Protection, ICRP Publication 103. Ann. ICRP 37 (2-4).

ICRP 2008. Nuclear Decay Data for Dosimetric Calculations, ICRP Publication 107. Ann. ICRP 38 (3).
ICRP 2009. Adult Reference Computational Phantoms, ICRP Publication 110. Ann. ICRP 39 (2).
ICRP 2020. Dose Coefficients for External Exposure to Environmental Sources, ICRP Publication 144, Ann. ICRP.
McConn, R.J. Jr., Gesh, C.J. Pagh, R.T., et al., 2011. Compendium of Material Composition Data for Radiation Transport Modeling PIET-43741-TM-963/PNNL-15870, Rev. 1. Pacific Northwest National Laboratory.
Pelowitz, D. B. Ed., 2013. MCNP6 USER'S MANUAL Version 1.0, LA-CP-13-00634 Rev. 0, Los Alamos National Laboratory Los Alamos, New Mexico.
Veinot, K.G., Dewji, S.A., Hiller, M.M., et al., 2017. Organ and Effective Dose Rate Coefficients For Submersion Exposure in Occupational Settings, *Radia Environ Biophys* 56: 453-472.

ANNEX B. SYSTEMIC BIOKINETIC MODELS FOR PROGENY

B.1. Description of systemic biokinetic models for progeny

(B.1) A dose coefficient for an internally deposited radionuclide includes the contribution to dose from progeny produced in the body following intake of the radionuclide. The dose coefficient may depend strongly on assumptions concerning the biokinetics of the progeny. The default assumption in *Publications 30* and *68* (ICRP, 1979, 1994b), was that chain members produced in systemic compartments follow the biokinetic model of the parent (the assumption of 'shared kinetics'). The alternative assumption of independent kinetics of chain members was made in *Publication 68* for selected parent radionuclides; that is, the systemic behaviour of progeny produced *in vivo* was assumed to be determined by biological properties of the progeny themselves rather than those of the parent.

(B.2) The assumption of independent kinetics of chain members generally is applied in this publication series to radionuclides produced in, or absorbed into, systemic compartments. This assumption is based on published data from experimental and occupational studies of the systemic behaviour of progeny produced in the body (Leggett et al., 1984). The data indicate that progeny produced in soft tissues or on bone surface generally migrate from preceding chain members and follow their characteristic biological behaviour, while most radionuclides produced in bone volume tend to remain with the parent radionuclide in bone.

(B.3) The 'characteristic biological behaviour' of a radionuclide refers in this publication series to its systemic behaviour following its direct intake the body.

(B.4) The term 'characteristic biokinetic model' or 'characteristic model' of an element refers to the biokinetic model used in this publication series to describe the element's systemic behaviour after it is taken directly into the body.

(B.5) The implementation of the assumption of independent kinetics for a given chain of radionuclides is straightforward in the case that the characteristic models for all chain members have a common model structure, including the same identifiers (names) of compartments. In such cases a progeny is assumed to follow its characteristic biokinetic model from its time of production in a systemic compartment or absorption into the systemic circulation.

(B.6) The implementation of independent kinetics of chain members requires additional modelling in the frequently occurring situation that the characteristic biokinetics models for different chain members have different model structures. For example, the models for different chain members may include different explicitly identified source regions, resulting in the situation that a chain member Y is produced in an explicitly identified source region in the characteristic model for a preceding chain member that is not an explicitly designated region in Y's characteristic model. When this happens, the rate of removal of Y from its point of origin and the destination of the removed activity must be specified before the model can be solved. This issue is addressed in this publication series by expanding the characteristic biokinetic model for each member of a chain excluding the parent as needed so that any source region explicitly depicted in the model for a chain member is also explicitly depicted in the model for all lower chain members. The transfer coefficients describing uptake and retention of Y by an added source region are based where feasible on the same data sets used to develop the characteristic model of Y. In the absence of specific information on uptake and retention of Y by a given source region, the transfer coefficients are based on the kinetics of Y in Other (the collective tissues of the body not named explicitly in the model for Y), considering that the added source region is implicitly contained in Other in the characteristic model for Y.

(B.7) Another complicating factor that arises frequently in implementation of independent kinetics of progeny is that a source region R that is addressed explicitly in the characteristic models of successive chain members X and Y is compartmentalised differently in the characteristic models for X and Y. As a hypothetical example, the spleen may be addressed explicitly in the characteristic models for both X and Y but treated as a single compartment named 'Spleen' in the model for X and as two compartments named Spleen 1 and Spleen 2 in the model for Y. In such a case, the compartments of R in the model for X that are ambiguous regarding the outflow rate and destination of Y ('Spleen' in the hypothetical example above) are added to the characteristic model for Y and are assumed to empty into the central blood compartment of the characteristic model for Y. The assigned rates of transfer from ambiguous tissues to the central blood compartment of Y generally are based on some combination of default values and element-specific values. Virtually instantaneous outflow from an ambiguous compartment is represented by a transfer coefficient of 1000 d^{-1} (half-time of 1 min). The rate 1000 d^{-1} is used as a default value for transfer of a progeny produced in an ambiguous blood compartment to the progeny's central blood compartment. This value is also applied to some element and tissue combinations for which rapid loss is expected. The reference rate of bone turnover for the indicated bone type generally is used as a default value for progeny produced in ambiguous bone volume compartments. For an ambiguous compartment representing bone surface or a soft tissue, the assigned transfer rate to Y's central blood compartment usually is selected from the rate(s) of loss of Y from Y's 'Other'. If Other consists of a single compartment, the transfer rate from Other to Y's central blood compartment is assigned. If Other consists of multiple compartments, the highest rate of transfer from a compartment of Other to blood usually is applied, but the outflow rate from another compartment of Other is applied to some elements that are known or presumed to have relatively low mobility under most circumstances.

B.2. References

ICRP, 1979. Limits for intakes of radionuclides by workers, ICRP Publication 30, Part 1. Annals of the ICRP 2(3/4).

ICRP, 1994. Dose coefficients for intake of radionuclides by workers. ICRP Publication 68. Annals of the ICRP 24(4).

Leggett, R. W., Dunning, D. E., Eckerman, K. F., 1984. Modelling the behaviour of chains of radionuclides inside the body. Radiation Protection Dosimetry 9(2), 77–91.

ACKNOWLEDGEMENTS

Publication 130 (ICRP, 2015) was the first in a series of 'Occupational Intakes of Radionuclides' (OIR) publications replacing the *Publication 30* series (ICRP, 1979b, 1980a, 1981, 1988b) and *Publication 68* (ICRP, 1994a) to provide revised dose coefficients for occupational intakes of radionuclides by inhalation and ingestion. It provided an introduction to the series of publications, and included sections on control of occupational exposures, biokinetic and dosimetric models, monitoring methods, monitoring programmes, and retrospective dose assessment.

The current publication, the fifth and the last in the OIR series, provides data on individual elements and their radioisotopes, including a list of principal radioisotopes and their physical half-lives and decay modes, the parameter values of the reference biokinetic models, and data on monitoring techniques for the radioisotopes most commonly encountered in workplaces. For most of the elements, reviews of data on inhalation, ingestion and systemic biokinetics are also provided.

Dosimetric data provided in the printed publications of the series include tables of committed effective dose per intake (Sv Bq^{-1}) for inhalation and ingestion, tables of committed effective dose per content (Sv Bq^{-1}) for inhalation, and graphs of retention and excretion data per Bq intake for inhalation. These data are provided for all absorption types and for the most common isotope(s) of each element section.

The electronic annex that accompanies this series of publications contains a comprehensive set of committed effective and equivalent dose coefficients, committed effective dose per content functions, and reference bioassay functions for inhalation, ingestion and for direct input to the blood.

The new biokinetic and dosimetric models, dose coefficients and bioassay data presented and used in this OIR series of publications supersede those applied in the *Publication 30* series, the first volumes of which were published almost 40 years ago. Since that time, ICRP has made modifications to the radiation and tissue weighting factors used in the calculation of effective dose (*Publications 60* and *103*), updated some characteristics of the Reference male and female (*Publication 89*), updated radionuclide decay data (*Publication 107*), adopted new anthropomorphic phantoms (*Publication 110*) and revised biokinetic models for inhalation, ingestion and systemic distribution of radionuclides (*Publication 130* and this publication). All of these changes ensure that the ICRP dose coefficients make appropriate use of scientific knowledge and reduce the uncertainties associated with the calculation of doses after internal contamination.

This fifth and last publication in the series provides the above data for the following elements : beryllium (Be), fluorine (F), sodium (Na), magnesium (Mg), aluminium (Al), silicon (Si), chlorine (Cl), potassium (K), scandium (Sc), titanium (Ti), vanadium (V), chromium (Cr), manganese (Mn), nickel (Ni), copper (Cu), gallium (Ga), germanium (Ge), arsenic (As), selenium (Se), bromine (Br), rubidium (Rb), rhodium (Rh), palladium (Pd), silver (Ag), cadmium (Cd), indium (In), tin (Sn), hafnium (Hf), tantalum (Ta), tungsten (W), rhenium (Re), osmium (Os), platinium (Pt), gold (Au), mercury (Hg), thallium (Tl), astatine (At) and francium (Fr). Additional dosimetric data for exposure from submersion in a cloud of gas are given in the annex for the noble gases neon (Ne), argon (Ar), krypton (Kr) and xenon (Xe).

ICRP thanks all those involved in the development of this publication for their hard work and dedication over many years. The numerous and constructive suggestions raised during the public consultation of this publication are gratefully acknowledged.

The work of the authors was aided by significant contributions from K.Eckerman, S. Lamart, M. A. Lopez, A Giussani, D.W. Jokisch and all the other IDC members.

Task Group 95 members *(2014-2020)*

F. Paquet (Chair)	G. Etherington	J. Marsh
M. R. Bailey	T. Fell	D. Melo
V. Berkovski	A. Giussani	D. Noβke
L. Bertelli	D. Gregoratto	G. Ratia
E. Blanchardon	S. Lamart	T. Smith
E. Davesne	R. W. Leggett	

Main commission critical reviewers

M. Kai S. Romanov

Editorial members

C.H. Clement (Scientific Secretary & Annals of the ICRP Editor-in-Chief)
H. Fujita (Assistant Scientific Secretary & Annals of the ICRP Associate Editor)

Committee 2 members during preparation of this publication

(2017-2021)

J.D. Harrison (Chair)	A. Giussani	T. Sato
F. Paquet (Vice-Chair)	D. Jokisch	T. Smith
W.E. Bolch (Secretary)	C.H. Kim	A. Ulanowski
M. Antonia Lopez	R. Leggett	F. Wissmann
V. Berkovski	J. Li	
E. Blanchardon	N. Petoussi-Henss	

Emeritus Member

K. Eckerman

Main Commission members at the time of approval of this publication

Chair: C. Cousins, *UK*
Vice-Chair: J. Lochard, *France*
Scientific Secretary: C.H. Clement, *Canada*; sci.sec@icrp.org *

K.E. Applegate, *USA*	S. Liu, *China*	**Emeritus Members**
S. Bouffler, *UK*	S. Romanov, *Russia*	R.H. Clarke, *UK*
K.W. Cho, *Korea*	W. Rühm, *Germany*	F.A. Mettler Jr., *USA*
D.A. Cool, *USA*		R.J. Pentreath, *UK*
J.D. Harrison, *UK*		R.J. Preston, *USA*
M. Kai, *Japan*		C. Streffer, *Germany*
C.-M. Larsson, *Australia*		E. Vaño, *Spain*
D. Laurier, *France*		

* Although formally not a member since 1988, the Scientific Secretary is an integral part of the Main Commission.